Analysis of Selected Pharmaceuticals and Endocrine Disrupting Compounds and their Removal by Granular Activated Carbon in Drinking Water Treatment

by

Zirui Yu

A thesis
presented to the University of Waterloo
in fulfillment of the
thesis requirement for the degree of
Doctor of Philosophy
in
Civil Engineering

Waterloo, Ontario, Canada, 2007

AUTHOR'S DECLARATION

I hereby declare that I am the sole author of this thesis. This is a true copy of the thesis, including any required final revisions, as accepted by my examiners.

I understand that my thesis may be made electronically available to the public.

Abstract

Over the last decade, endocrine disrupting compounds (EDCs) and pharmaceutically active compounds (PhACs) have been detected in drinking water at very low levels, mostly ng/L concentrations, suggesting that these compounds resisted removal through water treatment processes. Concerns have been raised regarding the effectiveness of common drinking water treatment technologies to remove these emerging contaminants. Adsorption processes were suggested to play an important role in the removal of PhACs and EDCs, based on the assumption that these compounds are similar to other conventional micropollutants such as pesticides in both physicochemical properties and concentration levels present in water. However, this remains to be demonstrated since the availability of adsorption data for PhACs and EDCs is extremely limited and their environmental concentrations are typically much lower than the ones for pesticides. The primary objective of this research was to evaluate in detail the removal of representative EDCs and PhACs at environmentally relevant concentrations by granular activated carbon (GAC) adsorption.

In the first stage of this study, EDCs (15) were screened separately from the PhACs (86) with two different sets of assessment criteria due to the different nature and the availability of information for these two groups of compounds. As a result, 6 EDCs and 12 PhACs were selected for further evaluation. Subsequently, a multi-residue analytical method based on gas chromatography/mass spectrometry (GC/MS) was developed for the simultaneous determination of the selected PhACs and EDCs. Two key analytical steps - solid phase extraction and derivatization - were systematically optimized using full factorial design and a central composite design, respectively. The statistical experimental design in combination with the concept of the total desirability was demonstrated to be an effective tool for developing a multi-residue analytical method. The application of the developed method to Grand River water, a local raw water source, and finished drinking water from this source indicated that PhACs such as naproxen, carbamazepine, salicylic acid, ibuprofen, and gemfibrozil, and EDCs such as estrone (E1) and nonylphenol mono-ethoxy carboxylate (NP1EC) were the most common contaminants. Based on these results, the quality of the analytical data, and the physicochemical properties relevant to the adsorption on activated carbon, two PhACs (naproxen, carbamazepine) and one EDC (nonylphenol (NP)) were finally chosen for the adsorption studies.

Adsorptions of the selected target compounds were evaluated on two types of activated carbon (coal-based Calgon Filtrasorb® 400 (F400) and coconut shell-based PICACTIF TE (PICA) by first investigating their isotherms at environmentally relevant concentrations (equilibrium liquid phase concentration ranging from 10 to 1000 ng/L). The single-solute isotherm data determined for both

carbons showed that the relative adsorbabilities of the three target compounds were not in agreement with expectations based on their log K_{ow} values. Overall, in this low concentration range, carbamazepine was most easily removed, and NP was least adsorbable. The adsorption of naproxen was negatively influenced by its dissociation in water. Comparison of single-solute isotherms on F400 carbon for the target compounds to those for other selected conventional micropollutants showed that naproxen and carbamazepine have generally comparable isotherms to 2-methylisoborneol (MIB) and geosmin. The isotherm tests in a post-sedimentation (PS) water from a full-scale plant demonstrated that the presence of background natural organic matter (NOM) significantly reduced the adsorption of all three target compounds, among which.NP was the least impacted compound. Based on the quantification of the direct competition using the ideal adsorbed solution theory (IAST) in combination with the equivalent background compound (EBC) approach, the minimum carbon usage rates (CURs) for removing 90% of the target compounds in PS water were calculated at two environmentally relevant concentrations (50 and 500 ng/L). This work confirmed that the percentage removal of the trace level target compound at a given carbon dosage was independent of the initial target compound concentration.

Isotherm experiments were conducted for the target compound on GACs preloaded with PS water for various time intervals (up to 16 weeks) at the Mannheim Water Treatment Plant (Region of Waterloo, ON, Canada). The results indicated that the adsorption of all target compounds were subject to significant negative impacts from preloading of NOM, albeit to different extents. Among the three target compounds, reduction in adsorption capacity for naproxen was most severe, followed by carbamazepine and then NP. The three target compounds followed quite different patterns of decrease in adsorption capacity with increasing preloading time, thus revealing different competitive mechanisms at work for the different compounds. For naproxen, the change in heterogeneity of the carbons due to preloading suggests that some pre-adsorbed NOM could not be replaced by naproxen. However, both direct competitive and pore blockage mechanisms could successfully explain the adsorption performance of naproxen and carbamazepine. The removal of NP even at prolonged preloading times could be explained by absorption or partitioning in the NOM matrix on the surface of, or inside the carbons.

The kinetic parameters for each target compound-virgin carbon pair were determined using the short fixed bed (SFB) approach based on the pore and surface diffusion model (PSDM). The SFB results and sensitivity analyses indicated that, under the very low influent concentration conditions, film diffusion (indexed as β_L) exerts a much greater effect on breakthrough profiles than internal

diffusion. The SFB tests on preloaded GACs showed that mass transport of all the target compounds decreased with increasing preloading time. Similar to the impact of preloading on adsorption capacity, naproxen was subject to the most deteriorative effect, followed by carbamazepine and then NP. In addition, potential mechanisms for the decay of the film diffusion coefficient with increased preloading time were discussed based on scanning electron microscope (SEM) images of virgin and preloaded GAC. Electrostatic interactions between the NOM/bio film formed on the preloaded carbon and dissociated naproxen may have contributed to the enhanced reduction in its film diffusion. Sensitivity analyses and subsequent calculations of the Biot numbers confirmed that film diffusion was also the predominant mechanism controlling the mass transport on preloaded carbon, in particular for naproxen. This suggests that the early breakthrough prediction of the target compounds at their environmentally relevant concentrations could be further simplified by only considering film diffusion and adsorptive capacity.

Kinetic and isotherm parameters were used as input for modeling using time-variable PSDM. It was found that the varying trends for Freundlich K_F and 1/n, and β_L could be generally depicted by a corresponding empirical model. Pilot scale treatability tests were performed for the target compounds which subsequently validated the time-variable PSDM results thus demonstrating its effectiveness and robustness to model GAC adsorber performance for PhAC and EDC removal at environmentally relevant concentrations. The time-variable approach was further improved by adjusting for NOM surface loading differences between the preloading and the pilot columns, which successfully compensated for the prediction errors at the early phase.

The validated NOM surface loading associated time variable PSDM was used to predict performances of hypothetical F400 and PICA full-scale adsorbers. Both adsorbers were expected to provide satisfactory performance in achieving 90% removals for the neutral target compounds (carbamazepine and NP). Naproxen was predicted to break through fast since both, capacity and kinetic parameters decay quickly due to carbon fouling by NOM and the physicochemical properties of this compound. Initial recommendations on the choice of adsorption process (GAC vs. PAC) for removing EDCs and PhACs can be made based on the comparison of carbon usage rates (CUR) which were calculated for a GAC adsorber using the validated improved PSDM and for PAC using the minimum applied dosages predicted by the IAST-EBC model.

Acknowledgements

I would like to express my sincerest gratitude to my supervisor Dr. Peter M. Huck for his offer to support this tough but exciting research and for his expert guidance throughout. I would like to give my sincerest thanks to my co-supervisor Dr. Sigrid Peldszus for her willingness to supervise my research, for her patience and encouragement, and for her leadership on this project.

I am grateful to all the members of the NSERC Chair in Water Treatment that has provided me an amenity of intelligence and friendliness. I would specially thank Dr. William B. Anderson for his valuable suggestions to set up experimental facilities at the Mannheim Water Treatment Plant.

I would like to acknowledge the NSERC Chair in Water Treatment and its partners, and give my special thanks to Olga Vrentzos from the Region of Waterloo for providing access to the Mannheim Water Treatment Plant. I would also like to thank Tim Walton, Frank Smith, and Lane Stevens from the Region of Waterloo for their support and effort in coordinating the preloading and pilot-scale experiments. I also gratefully acknowledge PICA USA Inc. and Calgon Carbon Corporation for their donation of activated carbon.

My thanks also go to Bruce Stickney and Mark Sobon for their assistance with conducting experiments in our research laboratory. I would like to thank Bob McPhail for his willingness to help me conduct the tedious kinetic tests and to share with me his interest in music as well. Thanks are also given to my friend Yong Yin for his suggestions for dealing with the program codes. Many thanks to my friends and fellow grad students: Peter Knappet, Lawrence Lee, Quinn Crosina, Guo Liu, Jianping Zhang, Xiuyuan Xu, Cynthia Guay, Jeff Deloyde, and Shawn Cleary (to name a few) for all of their shared laughter and support.

Finally, I would like to express my deepest gratitude to my family, especially to my parents, Yuxiang Yu and Zunxiu Gao, and my wife, Suhua Ni, for their unwavering love and support.

Table of Contents

List of Figures

List of Tables

CHAPTER 1
INTRODUCTION

1.1 Background

Over the last decade, endocrine disrupting compounds (EDCs) and pharmaceutically active substances (PhACs) have been frequently detected in the environment. Their presence and related consequences have become a topic of intense research activities. EDCs such as alkylphenol exothylates (APEO), bisphenol A (BPA) and phthalates originate largely from industrial production and product consumption (Ying *et al.*, 2002; Birkett, 2003), while steroid hormones are mostly excreted by humans and animals (Blok and Woston, 2000). EDCs may be released into the aquatic environment through wastewater effluent, or surface run-off, and can be consequently found at trace levels in surface water and sometimes ground water (Kolpin *et al.*, 2002; Staples *et al.*, 2000). PhACs for human use and their metabolites, as well as veterinary drugs and their metabolites, are excreted via urine and feces, and can subsequently enter into the aquatic environment albeit by different pathways (Daughton and Ternes, 1999). Some of these contaminants have even been detected in drinking water at low levels.

The interest in EDCs and PhACs has largely been facilitated by recent developments in analytical instrumentation and methods. However, development of a method suitable for extremely low concentrations (ng/L-µg/L) and a wide variety of EDCs and PhACs still presents a challenge to analysts. The most common analytical methods consist of extraction, chromatographic separation and detection. These techniques vary greatly in sophistication, sensitivity, reliability and cost. Due to sub-µg/L concentrations of most EDCs and PhACs in water, extraction procedures are generally applied to concentrate the compounds of interest from the aqueous matrix. Various types of analytical instrumentation may be used to measure target compounds in their extracts. However, mass spectrometry (MS) or tandem MS following gas chromatography (GC) or liquid chromatography (LC) are becoming the most commonly used instrumentation for the analysis of these trace contaminants. The analysis of EDCs and PhACs on GC-MS/ tandem MS often requires additional derivatization steps following extraction in order to make the target compounds less polar and/or more volatile. In general, the published multi-residue analytical methods (Ternes *et al.*, 1998; Lopez *et al.*, 1998) were either focusing on a group of specific compounds with similar properties or utilized complex sample preparation schemes often including sequential elution and separate derivatization of different groups

of compounds. Experimental conditions in these studies were investigated separately for different groups of compounds with different properties in order to increase detection sensitivity. Therefore, if the multi-residue analytical method can be developed systematically based on a statistically experimental design for all the target compounds which can be analyzed on GC-MS, the efficiency and accuracy of the determinations are expected to be improved simultaneously.

Although survey campaigns have confirmed that the presence of trace level EDCs and PhACs can have chronic, subtle effects on the development, reproduction, and behavior of a number of animal species in aquatic environments (Vethaak and Rijs, 2002; Cleuvers, 2003, Pomati *et al.*, 2004), the effects on human beings remain uncertain and disputable. However, uncertainty should not be the excuse for allowing these groups of environmental contaminants to remain in drinking water supplies. Although EDCs and PhACs are not currently regulated, it would be prudent to apply precautionary measures in order to reduce the levels of these compounds in drinking water as much as possible. In 1996, the United States Environmental Protection Agency (US EPA) received a mandate from US congress to implement a program in which pesticides and chemicals found in drinking water sources were screened for their endocrine disrupting potential (Parrott *et al.*, 2001). The Canadian Environmental Protection Act (CEPA, 1999) makes research on EDCs a ministerial duty for both Environment Canada and Health Canada (Hewitt and Servos, 2001).

Among existing treatment options in drinking water treatment plants (WTPs), activated carbon is frequently used to remove micropollutants such as various pesticides and taste and odorous compounds (e.g. Sontheimer *et al.*, 1988). Predictions regarding the removal of EDCs and PhACs are largely based on the assumption that these compounds are similar to pesticides in both physical and chemical properties as well as concentration levels present in the water matrix (Janex *et al.*, 2003; US EPA 2003; Jones *et al.*, 2005). However, to date, only limited studies on adsorption of EDCs and PhACs have been carried out, and this assumption remains to be confirmed. In addition, surveys showed that several EDCs and PhACs were found in drinking waters produced by the plants equipped with an adsorption process (Janex *et al.*, 2002; Boyd *et al.,* 2003; Stackelberg *et al.*, 2004), suggesting that some compounds are resistant to the adsorption. Compared to intensive studies on removing conventional micropollutants by activated carbon, extremely limited research has been done on PhACs and EDCs. Although a few isotherm data on EDCs and PhACs were documented (Walker, 2000; Ternes *et al.*, 2002; Yoon *et al.*, 2003; Choi *et al.*, 2005), they were all at microgram-per-liter, or higher equilibrium concentrations, which is well above those found in raw water for drinking water production. Furthermore, in these studies, the competition between EDCs or PhACs and background

organic matters (including natural organic matters (NOM) and possible effluent organic matter (EfOM)[†]) has not been well documented, and thus does not reflect the removals under real conditions.

Granular activated carbon (GAC) adsorbers have been employed either as the primary treatment step for the control of micropollutants or as a secondary barrier for the removal of micropollutants which escaped previous treatment, such as powder activated carbon (PAC), primary chlorination, or ozonation. In general, adsorption processes are recognized as effective. In practice, WTPs typically operate their GAC adsorbers on a continuous basis, which leads to problems caused by the background NOM present in the raw water. Background NOM profoundly affects the removal efficiency of GAC adsorbers for eliminating micropollutants because it is present at significantly higher concentrations, and has a much longer mass transfer zone (MTZ) than micropollutants, leading to strong competitive effects.

The presence of background NOM can affect the removal of a micropollutant to different extents in different ways, depending on the compositions of background NOM, properties of target compounds, and characteristics of the GAC (Newcombe *et al.*, 1997, 2002a, b; Pelekani and Snoeyink, 1999; Karanfil *et al.*, 2006). When both background NOM and micropollutants are present and adsorbing simultaneously during the early stages of operation, background NOM can compete with the micropollutants for available adsorption sites directly. In addition, background NOM molecules will deposit on the carbon over time and hence pre-occupy adsorption sites. Furthermore, large NOM molecules may block the meso/micro pores on activated carbon thus preventing access of the micropollutant molecules to adsorption sites. EDCs and PhAC,s as a new group of micropollutants, are typically detected at lower concentrations in water than conventional micropollutants. Thus it is expected that they will be influenced to a higher degree by the competitive effects. Unfortunately, investigations in this field are lacking.

If the decision of regeneration frequency of GAC adsorbers is determined by the GAC's removal efficiency for EDCs and PhACs, it would be beneficial to have a mathematical model which is capable of predicting the breakthrough profile and the remaining life of the adsorbers. However, the competitive effects from background NOM make the modeling challenging. Therefore, to ensure

[†] If a water treatment plant is located downstream a wastewater treatment plant, it is possible that backgrounds of raw water contain large amount of EfOM. However, since two types of OMs can not be distinguished with respect to competitive effects, only background NOM is used in the thesis in order to be consistent to the common name in other literature.

adequate predictions by a mathematical model, the impacts of the competitive effects on target compound adsorption must be understood and taken into account.

This research project was designed: to understand the adsorption characteristics of selected EDCs and PhACs under ideal and real conditions; to evaluate the performance of GAC adsorbers; and to further provide guidance in choice, design and operation of GAC adsorbers.

1.2 Objectives

The primary objective of this research was to evaluate the removal of selected EDCs and PhACs at environmentally relevant concentrations in GAC adsorption processes.

Specifically, the main objectives were:

1) Determine equilibrium parameters for adsorption of selected EDCs and PhACs at environmentally relevant concentrations onto selected virgin GAC, and compare the adsorption capacities among the target compounds and with other conventional micropollutants.

2) Understand mass transport mechanisms of selected EDCs and PhACs through determining their mass transport rates onto two types of GAC at environmentally relevant concentrations.

3) Investigate the reduction of adsorption capacity caused by the competitive adsorption in the presence of background NOM by determining the direct competitive effect on adsorptive capacity.

4) Determine the effect of preloading from background NOM on the GAC adsorption rates of selected EDCs and PhACs.

5) Model the breakthrough of selected EDCs and PhACs in GAC columns, and try to predict full-scale GAC adsorber performance in removing the selected EDCs and PhACs.

To support the major objectives in this project, additional objectives were as follows:

6) Develop protocols for prioritizing the EDCs and PhACs for general purpose of treatment, and subsequently select target compounds that are most representative for the adsorption study.

7) Develop a multi-residue analytical method for simultaneously determining the selected target compounds with GC/MS, (i.e. instrumentation available in lab).

A more detailed discussion of the specific objectives will be presented in Chapter 2, following a comprehensive literature review on relevant information regarding EDCs and PhACs as well as on theoretical and experimental investigation in the area of GAC adsorption.

CHAPTER 2
LITERATURE REVIEW

2.1 Occurrence of PhACs and EDCs in the Environment

2.1.1 Definition and Introduction

Over the last five decades, endocrine disrupting compounds (EDCs) have been receiving more and more public attention. A growing body of scientific research indicates that natural and man-made chemicals may interfere with the normal functioning of both wildlife and human endocrine systems. In 1999, the Canadian Environmental Protection Act (CEPA, 1999), defined an EDC as "a substance that has the ability to disrupt the synthesis, secretion, transport, binding, action or elimination of hormones in an organism, or its progeny, that is responsible for the maintenance of homeostasis, reproduction, development or behaviour of an organism." EDCs can be classified according to their structure and use (Ghijsen and Hoogenboezem, 2002): natural and synthetic hormones, organochlorine pesticides (OCPs), polychlorinated biphenyls (PCBs), dioxins, alkylphenol polyethoxylates (APEOs) and their metabolites, phthalates, some individual compounds like bisphenol A (BPA), and fire retardants. Although many investigations have demonstrated the relationship between the presence of certain EDCs and developmental changes in a number of animal species in the aquatic environment, the effects on human beings is largely uncertain and disputable. However, from a conservative perspective, it does not mean that long term exposure would not cause any adverse effect to humans. Therefore, Canada (Hewitt and Servos, 2001), the United States (Parrott *et al.*, 2001), and the European Union (Janex *et al.*, 2003) all launched research campaigns on both scientific and managerial levels.

The presence of pharmaceutically active compounds (PhACs) in the environment has emerged as an environmental issue of concern in the 1990s. PhACs mainly come from pharmaceuticals that are used in large amounts for diagnosis, treatment, alteration, or prevention of human disease, health condition, or structure/function of the human body, and similarly through veterinary uses, throughout the world. Daughton and Ternes (1999) estimated that the quantity of pharmaceuticals entering the environment annually was about equal to the amount of pesticides used each year. PhACs can be introduced into the environment after human excretion via sewage treatment plants (STPs) and via run off from agricultural fields after use in livestock productions. In general, PhACs are classified

according to their therapeutic effects in order to trace their sources and possible effects. However, in most survey and treatment studies, PhACs are largely grouped based on their structure and physicochemical properties. To date, still little is known about the effects of PhACs on human beings at environmentally relevant concentration levels (i.e. ng/L to low μg/L). Nevertheless, individual, synergistic/antagonistic and possible mixture effects at trace level concentrations of PhACs over an extended period of time should be an issue of concern based on the precautionary principle (Daughton and Ternes, 1999; Jones *et al.*, 2002; Jones *et al.*, 2005;). Moreover, an increasing number of studies have found possible negative effects of PhACs on animals or human beings. For example, Cleuvers (2003) evaluated the ecotoxicological potential of ten prescription drugs and found their combinations had stronger effects than did the individual drugs. Recently, Pamati *et al.* (2006) have proven the positively inhibitive effect of mixtures of PhACs at environmental levels on human cells. The American Water Works Association Research Foundation (AWWARF) set up a workshop that focused on PhACs in drinking water in 2001. In 2002, Health Canada and Environment Canada sponsored a multi-stakeholder scientific workshop to begin studies on environmental impacts of therapeutic products (Queen's Landing Inn, 2002).

Since some EDCs such as OCPs, PCBs, and dioxins have been extensively studied before, in this research, only EDCs, such as steroid hormones, APEOs and their metabolites, phthalates and BPA, which gained interest only recently, and frequently reported PhACs, were reviewed in order to select the representative target compounds.

2.1.2 Occurrence in Surface and Ground Water

Steroid hormones, such as 17α-ethynyl estradiol (EE2), 17β-estradiol (E2), estrone (E1), and estriol (E3), were reported to be present in the effluent from STPs and surface water. The concentrations ranged from limit of detection (LOD) to 15 ng/L in STPs effluent, and from LOD to 73 ng/L in surface water, respectively, in European countries (Bruchet *et al.*, 2002; Alda and Barcelo, 2001; Kuch and Ballschmiter, 2001; Blok and Wonsten, 2000), US (Kolpin *et al.*, 2002), and Canada (Servos *et al.*, 2003).

APEOs are nonionic surfactants which have been found in widespread use as detergents, emulsifiers, defoamers, lubricants, and pesticide formulations, etc, consequently, APEOs and their metabolites have been found to be widely present in the environment from LOD to 10,000 ng/L, depending on the type of water. Bennie (1997) surveyed the occurrence of alkylphenols and their mono- and di-ethoxylates in waters of the Laurentian Great Lakes basin and the upper St. Lawrence

River in Canada. The concentrations of nonylphenol (NP), octylphenol (OP), nonylphenol mono-ethoxylate (NP1EO) and nonylphenol di-ethoxylate (NP2EO) were <10-920, <5-84, <20-7800 and <20-10,000 ng/L in receiving water, respectively. In Toronto, the survey results showed that the concentrations of NP and NPEOs in the samples generally exceeded the City of Toronto By-Law (No.457-2000) limit, which are 1 ng/L for NP and 10ng/L for NPEOs. Ying *et al.* (2002) indicated that NPEC, which is the product of degraded NPEOs, were relatively water-soluble so that the concentrations of NPECs in river water were typically higher than those of the NPEOs or NP.

BPA is widely used in households and industry. It is therefore expected to be present in raw sewage, wastewater, and receiving surface waters. Generally, BPA was not found in high concentration in surface water or ground water due to its relatively easy degradation. Kuch and Ballschmiter (2001) reported that, in Germany, the mean concentrations in STP effluent, river water and drinking water were 16, 4.7, 1.1 ng/L, respectively. The median concentrations of BPA were found to be 13.5 and 17.5 ng/L in Meuse and Rhine rivers, respectively, by Ghijsen and Hoogenboezem (2002) in the Netherlands. In the USGS national reconnaissance report (Kolpin *et al.*, 2002), the median concentration in surface water was reported as 0.14 μg/L and BPA was detected in 41.2% out of 85 samples with a maximum concentration of 12 μg/L.

Similar to BPA, phthalates are also released into the environment during manufacturing processes and from the final products. Since commercial phthalate esters (PAEs) are diverse, only three of them, namely di(2-ethylhexyl) phthalate (DEHP), dibutyl phthalate (DBP) and butylbenzyl phthalate (BBP), were considered in this research, largely based on their consumption volumes and reported estrogenicity. The survey data published by Ghijsen and Hoogenboezem (2002) showed that many types of PAEs were found in the Meuse and Rhine River, with combined concentrations ranging from 95 to 21220 ng/L, in which DBP was one of the most frequently detected PAEs. DEHP existed in waters at relatively higher concentrations compared to other PAEs in Canada. It was reported with a mean concentration of DEHP 38.48 ng/L in Niagara-on-the-lake. In Albert, the average concentrations of DEHP in surface water and groundwater were 3.0 and 2.0 μg/L, respectively. However, DEHP was not detected in 22 samples of raw drinking water supplies from 11 municipalities in Quebec (CEPA, 1999b).

Survey campaigns in the 1990's in Europe and the U.S. provided evidence of existence of PhACs in surface and ground waters. Halling-Sorensen *et al.* (1998) and Daughton and Ternes (1999) comprehensively reviewed environmental origin, occurrence, fate, and possible effects of PhACs, drawing more attention to the issue in the environmental science community thereafter. As

summarized in the study by Daughton and Ternes (1999), a total of 118 PhACs, mostly from human sources, were reported to have been found in sewage, surface water, and ground water. Almost all the studies to date agree that PhACs are ubiquitous and pseudo-persistent contaminants in the environment, since they are continuously released, in particular, from sewage and improper disposal (Doerr-MacEwen and Haight, 2006).

In the U.S., both veterinary and human drugs were monitored systematically in various streams across the country during 1999 and 2000 (Kolpin *et al.*, 2002), and it was found that antibiotics and other prescription drugs were detected at relatively similar frequencies. However, non-prescription drugs were detected more frequently partially due to their greater annual use. Amongst all classes of drugs, antibiotics are of special concern because they may contribute to an increase in antibiotic resistant microorganism. Furthermore, many antibiotics have low elimination rates during wastewater treatment. Surveys on antibiotics have been carried out in Germany (Hirsch *et al.*, 1999), Italy (Zuccato *et al.*, 2002), Switzerland (Alder *et al.*, 2001), the U.S. (Kolpin *et al.*, 2002), and Canada (Metcalfe *et al.*, 2003). In general, the major antibiotics can be classified into several groups including macrolides, quinolones, sulfonamides, β-lactams and tetracyclines. Many antibiotics in the first three classes such as erythromycin, ciprofloxacin, and sulfamethoxazole, etc, have been found up to the low μg/L-level in sewage and between ten to several hundred ng/L in surface water and ground water.

The estrogenic drugs are used by humans for estrogen-replacement therapy, as oral contraceptives, and to enhance athletic performance, whereas in veterinary medicine they are used as growth promoters (Daughton and Ternes, 1999). 17β-estradiol has been found in STPs effluent, surface water and even finished drinking water at the low ng/L range (Heberer 2002; Souali *et al.*, 2003; Belfroid *et al.*, 1999; Kolpin *et al.*, 2002; Blok and Wosten, 2000). Ternes *et al.* (1999) reported less than LOD to 9 ng/L 17β-estradiol in Canadian wastewater effluents.

Anti-inflammatory drugs under investigation include ibuprofen, diclofenac, acetylsalicylic acid, acetaminophen, naproxen, and others, most of which have acidic characteristics. Ternes (1998) reported their occurrence in German sewage and surface water at concentrations ranging from μg/L to ng/L. Stan and Heberer (1997) found ibuprofen and diclofenac to be present in the groundwater at concentrations up to 380 ng/L. Acetylsalicylic acid has not been reported in the environment partially due to its biodegradability (Stuer-Lauridsen *et al.*, 2000). In Canada, a survey conducted by Metcalfe *et al.* (2003b) in the lower Great Lakes region found that ibuprofen, naproxen, and diclofenac presented in the all examined STP effluent, and thus were detected in some surface waters adjacent to

the STP discharges. A study performed by Lissemore *et al.* (2006) revealed that the naproxen residue was greatly prevalent in a river downstream from a large urban area in Southern Ontario.

Blood lipid regulators such as clofibrate, bezafibrate and gemfibrozil, are heavily used in developed countries. Clofibric acid, which is the active metabolite of the lipid regulators clofibrate, etofyllinclofibrate and etofibrate, is one of the more ubiquitous and persistent PhACs in Europe. It has been detected frequently in surface and ground waters (Heberer *et al.*, 2002; Ternes *et al.*, 2003; Ternes, 1998; Ferrari *et al.*, 2003; Stan and Heberer, 1997, Halling-Sorensen *et al.*, 1998. Ternes, 2001). The prevalence of gemfibrozil was confirmed in river water sampled downstream from a large urban area in Southern Ontario (Lissemore *et al.*, 2006). Although clofibric acid is of great importance to European countries, it is not prescribed in Canada and should therefore not be detected in Canadian waters. Alternatively, newer blood lipid regulators such as atorvastatin and simvastatin are ranked among the top 50 prescribed drugs in Canada (http://www.imshealthcanada.com/). Atorvastatin was reported to be found from non-detected to low ng/L in STP effluents and their corresponding receiving surface waters (Metcalfe *et al.*, 2003b).

The antiepileptic, carbamazepine has been found frequently in STPs effluent (Ternes, 1998; Ferrari *et al*,. 2003; Metcalfe *et al.*, 2003b, Brun *et al.*, 2006) and surface water (Ternes, 1998; Heberer, 2002; Furlong *et al.*, 2003; Metcalfe *et al.*, 2003b; Brun *et al.*, 2006). The typical reported concentrations in surface water ranged from 50 to 1,000 ng/L (Heberer *et al.*, 2002). Its ubiquitous occurrence resulted from its very low removals in STPs, which was reported to be as low as 7% removal by Ferrari *et al.* (2003). As a result, the study carried out in Southern Ontario by Kormos *et al.* (2006) found that the carbamazepine levels in river waters were greatly impacted by the location of STPs, and approximately ranged from 10 – 1900 ng/L. The persistence of carbamazepine residue in the river downstream from a STP plant was also confirmed by Brun *et al.* (2006) in Atlantic Canadian area. In addition, it has been reported that carbamazepine and its metabolites were not effectively removed during wastewater treatments (Miao *et al.*, 2005). Hence, it can be expected that this group of contaminants would be frequently detected in the surface waters, which are influenced by STP discharges.

The occurrences of other classes of PhACs such as beta-blockers, antineoplastic agents, anti-depressants, tranquilizers and anti-hypertensive agents, etc. were all reported widely in the literature. The selection of the target PhACs was based on a review of occurrence data collected from the literature up to late 2003. Although some new data after 2003 were documented above, they were not considered anymore after the target compounds were selected.

In conclusion, the detected concentrations of EDCs and PhACs of interest are in general in the ng/L to low μg/L range. The presence of EDCs and PhACs in surface water or ground water is of concern since these water may serve as a source water for drinking water production. Noting that the distribution of these compounds is country and region specific, it is important to target the typical compounds occurring in the local watershed for further treatment research. In addition, this information is important for defining the concentration range in further treatment studies because most treatment techniques are sensitive to the concentrations of the compounds to be removed. The selection of target compounds will be discussed further in Chapter 3.

2.1.3 Occurrence in Drinking Water

Compared to the intensive survey work carried out for wastewater and surface water, only limited studies have been conducted concerning the occurrence of residual EDCs and PhACs in finished drinking water. Note that there is currently no regulatory requirement for monitoring these compounds in drinking water. Based on the limited data published (Table 2-1), some EDCs and PhACs have been detected in drinking water at concentrations generally in the ng/L range, suggesting that these compounds can resist removal through water treatment processes.

Table 2-1 Concentrations of selected EDCs and PhACs reported in finished drinking water

Compounds	Concentration (ng/L)	Frequency (%)	Location	reference
		EDCs		
17β-estradiol	0.2 – 0.6	50	Germany	Kuch and Ballschmiter, 2001
17α-ethynyl estradiol	0.2 – 4	NR[§]	Netherlands	Blok and Wosten, 2000
	0.15 – 0.5	40	Germany	Kuch and Ballschmiter, 2001
estrone	0.4	40	Germany	Kuch and Ballschmiter, 2001
nonylphonel	100 - 330	NR	Spain	Díaz *et al.*, 2002
	25 – 90	100	Spain	Petrovic *et al.*, 2003
	2.5 – 16	100	Germany	Kuch and Ballschmiter, 2001
	92	> 25	USA	Stackelberg *et al.*, 2007
BPA	0.5 – 2.0	100	Germany	Kuch and Ballschmiter, 2001
	420[*]	NR	USA	Stackelberg *et al.*, 2004
		PhACs		
Diclofenac	1 – 6	NR	Germany	Stumpf *et al.*, 1996
Gemfibrozil	0.7 – 2.4	NR	Canada	Servos *et al.*, 2004
	ND[†] – 4	NR	Canada	Kormos *et al.*, 2006
Clofibric acid	3.2 – 5.3	NR	Italy	Zuccato *et al.*, 2000
Naproxen	8.7	NR	Canada	Servos *et al.*, 2004
Carbamazepine	ND – 1400	NR	Canada	Kormos *et al.*, 2006
	258[*]	NR	USA	Stackelberg *et al.*, 2004
	10 – 30	NR	Germany	Ternes *et al.*, 2003
	29	>25	USA	Stackelberg *et al.*, 2007

* *maximum concentration*
† *not detected*
§: not reported

As shown in Table 2-1, the occurrence of the hormone residuals in drinking water was reported in Europe mostly at low ng/L concentrations. However, though no direct evidence indicates potential effects of these hormones on human, *in vitro* studies suggested that feminization in some wild male fish may be provoked at 0.1 – 0.5 ng/L of 17α-ethynyl estradiol (Purdom *et al.*, 1994).

Clofibric acid gained much attention in Europe because it is not effectively removed by STPs nor by WTPs (Patterson *et al.*, 2002; Ternes *et al.*, 2002). As a result, it has been detected frequently in surface, ground and even drinking water (Heberer *et al.*, 2002; Ternes *et al.*, 2003; Ternes, 1998; Ferrari *et al.*, 2003; Zuccato *et al.*, 2000; Halling-Sorensen *et al.*, 1998). However, this drug is not prescribed in Canada and consequently not expected to be detected in Canadian waters. In a North American drinking water survey, Stackelberg *et al.* (2004) reported almost 100% detection frequency of carbamazepine with a maximum concentration of 258 ng/L. They also detected other PhACs, such as acetaminophen and dehydronifedipine, etc. in more than 50% of drinking water samples analyzed. It should be noted that the margin between potential indirect daily exposure via drinking water and daily therapeutic dosage is at least three orders of magnitude. However, little is known about long-term chronic health effects associated with exposure to multiple compounds at sub-therapeutic low concentrations. A recent study by Pomati *et al.* (2006) demonstrated that a mixture of pharmaceuticals at typical environmental levels (ng/L levels) can lead to physiological and morphological effects on human embryonic cells. Therefore, from a conservative perspective, drinking water should be as clean as possible. The current water treatment technologies should be re-evaluated for their capability to remove low concentrations of EDCs and PhACs.

2.2 Methods for Analysis of PhACs and EDCs in Waters

While the analysis of EDCs and PhACs is highly challenging due to their very low environmental concentrations (ng/L-µg/L) and their wide range of properties, current analytical methodology has progressed rapidly over the last decade or so and surveys have been undertaken world wide. In general, identification and quantification of EDCs and PhACs compounds in water include extraction from the water of interest, chromatographic separation and final detection. Techniques utilized vary greatly in sophistication, sensitivity, reliability and cost. Due to sub-µg/L concentrations of most EDCs and PhACs in water, extraction procedures are generally applied to concentrate the compounds of interest from the aqueous matrix. Various types of analytical instrumentation may be used to measure target compounds in their extracts. However, mass spectrometry (MS) or tandem MS following gas chromatography (GC) or liquid chromatography (LC) are becoming the most commonly used instrumentation for the analysis of these trace contaminants. LC-MS/MS has demonstrated to be a versatile technique which is mostly applied to polar or thermolabile EDCs or PhACs (e.g. antibiotics). Nevertheless, LC-MS/MS is still relatively costly. Compared to LC, the analysis of EDCs and PhACs on GC-MS, while more limited in scope, still provides a useful and sensitive for their determination and is much more affordable for most labs.

However, it often requires additional derivatization steps following extraction in order to make the target compounds less polar and/or more volatile. The general steps in analyzing EDCs and PhACs by GC-MS are sampling, extraction, derivatization, and finally identification and quantification.

Before sampling, all glassware and equipment that comes into contact with samples should be solvent rinsed and baked to avoid introducing contaminants (Snyder *et al.*, 2002). In addition, some researchers recommended using a 10% dimethyldichlorosilane solution in dichloromethane (Hilton and Thomas, 2003; Xiao *et al.*, 2001) or in toluene (Belfroid *et al.*, 1999) to silanise glassware in order to minimize the surface adsorption and therefore minimize irreproducible losses of the target compounds.

As for extraction, solvent sublation, steam distillation and liquid-liquid extraction methods have been replaced by more efficient and versatile solid-phase extraction (SPE) and solid-phase micro extraction (SPME) techniques. Today SPE, employing both disks and disposable cartridges are frequently used. In the analysis of EDCs and PhACs, octadecyl (C18) bonded silica cartridges have been most widely employed for extraction (Mouatassim-Souali *et al.*, 2003; Kelly *et al.*, 2000; Jeannot *et al.*, 2002). Other SPE materials such as graphitized carbon black (GCB) (Ding and Chen, 1999), ethinylbenzene-divinylbenzene copolymer (Bolz *et al.*, 2000), and polystyrene divinylbenzene (SDB) (Belfroid *et al.*, 1999) are also used. Different SPE materials may have very different extraction efficiencies for specific target compounds. For example, compared to C18 and GCB cartridges, SDB was not suitable for quantitative extraction of relatively polar compounds due to their low retention and thus early breakthrough (Petrovic *et al.*, 2002). When a single step is not suitable for extracting a wide range of compounds with different polarities, sequential SPE procedures may be employed. Recently, the Oasis HLB sorbent, consisting of polystyrene-divinylbenzene-N-vinylpyrrolidone terpolymer (Tixier *et al.*, 2003), was widely applied and seems to be accepted as a standard SPE phase for EDC and PhAC extraction. The adsorbent in the cartridges exhibits both hydrophilic and lipophilic retention characteristics (Rodriguez *et al.*, 2003), thus interacting with both acidic and basic functional groups in EDCs and PhACs molecules. These properties can eliminate the need for sequential extractions to achieve the selectivity required for sample preparation. In addition, this material has excellent wetting properties thus providing the advantage of no negative "running dry" effects on analyte recovery (Ollers *et al.*, 2001).

After extraction using SPE, it is also important to apply solvents of different polarities and selective desorption potentials to elute the target compounds from the resin. Ethyl acetate alone or in combination with acetone is the most common solvent used to desorb neutral and less polar

compounds. For example, Xiao *et al.* (2001) use ethyl acetate to elute steroid hormones from Oasis HLB SPE cartridges. However, the choice of elution solvent and volume depends largely on the analytes of interest and the SPE materials. Solvent ratio, volume and elution rate should be determined experimentally. The use of various extraction methods were summarized in Table 2-2.

Derivatization converts the analyte into a product with greater stability, superior chromatographic properties or much better response. It is a very important step in the analysis of EDCs and PhACs by GC, because most of the target compounds containing hydroxyl, carboxyl or ammonia groups have high polarities and are not volatile. Off-line derivatization to corresponding trimethylsilyl ethers, methyl ethers, acetyl esters, and pentafluorobenzoyl esters, was applied in numerous studies (see Table 2-2). In terms of derivatization of EDCs and PhACs, the most commonly used derivatization reagents are bis (trimethyl-silyl)trifluoroacetamide (BSTFA), *N*-methyl-*N*-*tert.*-butyldimethylsilyl-trifluoroacetamide (MTBSTFA), diazomethane, *N*-methyl-*N*-(trimethylsilyl)trifluoroacetamide (MSTFA) and pentaflurobenzyl bromide (PFBBr). The use of diazomethane for the methylation of a wide variety of acidic substances is rapid and produces minimal by-products. Major disadvantages of this reagent are its toxicity and potential dangers in its preparation coupled with a very limited reagent storage time (Wells, 1999). Diazomethane was reported to derivatize acidic drugs such as ibuprofen, diclofenac, ketoprofen, naproxen and clofibric acid (Ollers *et al.*, 2001). BSTFA, MTBSTFA and MSTFA are all silylation agents. They differ in their reactivity towards different functional groups (i.e. aromatic and aliphatic hydroxyl groups, carboxyl and amino groups) and in the stability of their derivatives. BSTFA is the most popular silylation reagent, and produces trimethylsilyl (TMS) derivatives. BSTFA was reported to react rapidly and quantitatively with a variety of hydroxyl compounds under moderate conditions. The stability of the BSTFA derivatives for long-term storage can be ensured by hydrolysing excess derivatising reagent with water followed by dehydration using anhydrous sodium sulphate (Li *et al.*, 2001). Reaction rates of BSTFA derivatizations are solvent dependent. Acetone was reported to be very suitable for silyl derivatization of alkyl phenols (Li and Park, 2001). The disadvantage of using BSTFA is its high sensitivity to moisture. Compared to BSTFA, MTBSTFA was preferred in some studies because of the greater thermal and hydrolytic stability of the *tert.*-butyldimethylsilyl (TBS) derivatives, and also because it was expected to improve the chromatographic separation and MS detection (Rodriguez *et al.*, 2003). PFBBr was used for the derivatization of acidic herbicides with carboxyl and phenol groups (Rompa *et al.*, 2003). Lerch and Zinn (2003) reported that the best derivatization yields of steroids by PFBBr were achieved in acetone with K_2CO_3 added as a base. MBTFA can be used to derivatize primary and secondary amines. Paterson *et al.* (2000) used MSTFA

and N-methyl-bis-trifluoroacetamide (MBTFA) sequentially to derivatize the hydroxyl groups and amino groups on drugs found in urine.

Different derivatization reagents have a significant effect on the quality of the quantification. Lerch and Zinn (2003) recommended that the following criteria be considered when choosing the appropriate derivatization reagent: 1) completeness of derivatization; 2) conversion of all target functional groups; and 3) as few by-products as possible. It is important to note that many EDCs and PhACs, such as EE2 and acetaminophen, have more than one different polar group requiring derivatization. Incomplete derivatization leads to low peak response and thus a high detection limit. For example, the incomplete derivatization by PFBBr could happen when more than one aliphatic hydroxyl group is present in the molecule (Lerch and Zinn, 2003). Another reason for incomplete derivatization may come from sterically hindered groups. Kelly's experiments (2000) showed that the aliphatic hydroxyl group in EE2 could not be derivatized by MTBSTFA due to the ethinyl group on the same carbon atom. However, MSTFA could derivatize all the hydroxyl groups in EE2 (Quintana *et al.*, 2004). Besides the choice of derivatization reagent, other factors such as reaction time, temperature, derivatization reagent dosage, presence of catalyst, and nature of solvent may also be of importance to the yield of the derivatized analyte. In order to increase yield and therefore detection sensitivity, the above experimental conditions are typically optimized separately in most studies. However, if multiple factors can be analyzed simultaneously and systematically based on a statistical experimental design, the efficiency and accuracy of the determination are expected to be improved simultaneously. For instance, Quintana *et al.* (2004) evaluated a range of factors when optimizing the derivatization of steroid hormones with MSTFA. A central composite design was applied to optimize the derivatization of acidic drugs by Rodrigues *et al.* (2003).

Separation and quantification of the target compounds are accomplished using either LC-MS or GC-MS. In terms of GC-MS quantification, the quality of the analysis depends on the condition of the instrument, the instrument parameters and programs used to separate and detect the mixture, in addition to previous treatment steps such as extraction and derivatization. In general, to analyze low concentration environmental samples on GC/MS, selected ion mode (SIM) are used in order to suppress background interference and increase sensitivity.

A comprehensive review of methods for analyzing pharmaceuticals in aqueous samples was provided by Ternes (2001). Therefore, Table 2-2 summarizes a number of methods developed and published since then.

Table 2-2 Published methods for analyzing EDCs and PhACs in aqueous matrices

Compound	Sample preparation (extraction, elution, sample volume)	Derivatization	Internal standard/ surrogate standard	Detection	LOD and LOQ (ng/L), matrix	Reference
E1, E2, E3, EE2	Octadecyl-bonded silica C18; acetonitrile in water; 200 mL sample	N/A	N/A	LC-UV	LOD: 10-15, in waste water	Alder and Barcelo, 2001
E1, E2, E3, EE2 and their conjugates	Speeddisk-C18; water-acetone (4:1) and acetate; 2 L sample	50 µL Pentafluoropropionic acid anhydride (PFPA)	N/A	GC-MS	LOQ: 0.04-0.32 , in waste water	Mouatassim-Souali *et al.*, 2003
E1, E2, EE2, NP, 4-t-OP	LiChrolut EN; acetone and methanol; 1 L sample	Pentafluorobenzoyl chloride (PFBCl)	1,4-bispentafluorobenzylbenzene (BPFBB) as internal standard	HRGC/NCI-MS and GC-ECD	LOD: 0.05-0.1 in surface water	Kuch and Ballschmitter, 2001
E1, E2, EE2	C_{18} disk; methanol-water; 2.5L sample	MTBSTA containing 1% TBDMCS in acetonitrile	Deuterated analytes	GC/MS and GC/MS-MS	N/A	Kelly, 2000
E1, E2, EE2	LL extraction with CH_2Cl_2 at ambient pH	Trimethylsilyl (TMS)	E2-d_4 and cholesterol-d_4	GC/MS	N/A	Kolpin *et al.*, 2002
E1, E2, 17α-estradiol, EE2	SDB-XC disk ; methanol; 1L sample	dimethyldichlorocilane (SILA) in toluene	PCB 103	GC/MS-MS	LOD: 0.1-0.6 in surface water	Belfroid *et al.*, 1999
NP, OP, E1, E2, E3 and EE2[a]	N/A	anhydrides HFBA and TFAA in toluene	N/A	GC/CI-MS	NR	Lerch and Zinn, 2003
E1, E2,E3,EE2, and mestranol	Oasis C18 cartridge; ethyl acetate	MSTFA in ethyl acetate	Deuterated E2	GC/MS or GC/MS-MS	LOQ: 3-5 in waste water	Quintana *et al.*, 2004
NP, NP1EO, NP2EO, NP3EO, NP1EC, NP2EC	Bond Elut C18-HF cartridge; methyl acetate	N,O-bis(trimethysilyl)acetamide (BSA) in methyl acetate	OP-d, OP1EO-d, and OP1EC-d as surrogates; phenanthrene-d_{10} and pyrene-d_{10} as internal standards	GC/MS-MS	LOD: 2.5-9.5 in MilliQ water	Hoai *et al.*, 2003
t-NP, BPA, EE2	In-sample SPME	N/A	4n-NP, β-estradioldiacetate and [$^2H_{14}$]BPA	GC-MS	LOQ: 120-3000 in waste water	Braun *et al.*, 2003
4-n-NP, 4-n-OP, BPA	SPME	BSTFA	N/A	GC-MS	LOD: 10-100 in MilliQ water	Helaleh *et al.*, 2001
NP, NP1EO, NP2EO	LL extraction, pentane	N/A	$^{13}C_6$-NPnEO	HRGC/MS	LOD: 4-2122 in waste water	Planas *et al.*, 2002
NP, NP1EO, NP2EO, NP1EC, NP2EC	SPME	Dimethyl sulphate (DMS)	n-nonyoxylbenzoic methyl ester	GC-MS	LOD: 20-1500 in MilliQ water	Diaz and Ventura, 2002

Table 2-2 *continued*

Compound	Sample preparation (extraction, elution, sample volume)	Derivatization	Internal standard/ surrogate standard	Detection	LOD and LOQ (ng/L), matrix	Reference
NP, NP1EO, NP2EO, NP1EC, NP2EC	SPME	Dimethyl sulphate (DMS)	n-nonyoxylbenzoic methyl ester	GC-MS	LOD: 20-1500 in MilliQ water	Diaz and Ventura, 2002
4-t-OP, 4-NP, BPA	C18 and polystyrene copolymer ENV+; acetone; 1L sample	phenyltrimethylammoniumhy -oxide	biphenyl	GC-MS	LOQ: 4-t0.02-0.05 in MilliQ water	Bolz *et al.*, 2000
4-NP, 4-t-OP, BPA, E1, E2, E3, EE2	C18 cartridge; hexane-dichloromethane (90:10), methanol-dichloromethane (90:10); Oasis HLB; methanol-diethylether (10:90); 1L sample	BSTFA	BPA-d_{16}	GC-MS	LOQ (HLB extraction): 2-10 in MilliQ water	Jeannot, 2002
Carbamazepine, clofibric acid, diclofenac, ibuprofen, ketoprofen, naproxen	Waters oasis HLB; 1L sample	diazomethane	Mecoprop-d3, dihydrocarbamazepine	GC-MS	NR	Tixier, 2003
Carbamazepine, ibuprofen, diclofenac, ketoprofen, naproxen, clofibric acid, bezafibrate, gemfibrozil, diazepam	RP-C_{18} cartridge; 4mL acetone; 1L sample,	PFBBr in cyclohexane with triethylamine at 100^{o}C for 2h	2,3-dichlorophenoxyacetic (2,3-D) as surrogate standard	GC/MS	LOQ: 13-32 in ground water	Sacher, 2001
Ibuprofen, naproxen, ketoprofen, tolfenamic acid, diclofenac	oasis HLB cartridge; ethyl acetate; 500mL sample	MTBSTFA	Meclofenaic acid as surrogate standard. PCB-30 as internal standard	GC-MS	LOQ: 20-50 in surface water	Rodriguez, 2003
Carbamazepine, ibuprofen, diclofenac, ketoprofen, naproxen, clofibric acid	Oasis HLB; ethyl acetate - acetone (50/50); 1L sample	diazomethane	[$^{13}C_6$]metolachor, atrazine-d_3, MCPA-d_3, dimethenamide-d_3, Mecoprop-d_3, dihydrocarbamazepine	GC-MS	LOD: 0.3-4.5 in surface water	Ollers., 2001
51 EDCs and PhACs	Oasis HLB; methanol and methanol/MTBE (10:90), and DCM	N/A	Related deuterated compounds	GC-MS/MS; LC-MS/MS	LOD: 1-10 in surface water	Trenholm *et al.*, 2006

Table 2-2 *continued*

Compound	Sample preparation (extraction, elution, sample volume)	Derivatization	Internal standard/ surrogate standard	Detection	LOD and LOQ (ng/L), matrix	Reference
Diclofenac, ibuprofen, clofibric acid, phenazone, propyphenazone	C_{18} cartridge; 2.5mL methanol; 1L sample	200 µL PFBBr and 5 µL trimethyamine in toluene, 110°C, 1h	3,4-D as surrogate standard; 2,4-dichlorobenzoic acid as internal standard	GC/ITD-MS	LOQ: 1.6-60 in wastewater	Koutsouba et al., 2003
21 prescription and non-prescription drugs	Oasis HLB; CH_3OH and mixture of CH_3OH and $C_2HCl_3O_2$	N/A	C_{13}-phenacetin as surrogate standard	HPLC	NR	Kolpin *et al.*, 2002
Naproxen, ibuprofen, E1, E2, BPA, clorophene, triclosan, fluoxetine, clofibric acid, acetaminophen	SDB-XC Empore disk; methanol, dichloromethane and methane	BSTFA	Phenanthrene-d_{10} as internal standard; acetaminophen-d4, BPA-d16, and E1-d4 as surrogate standard	GC-MS	LOD: 0.1-25.8 in surface water	Boyd *et al.*, 2003
21 endocrine disrupting phenols and acidic PhACs	Oasis MAX SPE; methanol and formic acid in methanol (2:98)	EDCs by pentafluoropropionic acid anhydride (PFPA); acidic PhACs by MTBSTFA	Deuterated E2, BPA for EDCs; 2,3-D for acidic drugs	GC-MS	LOD: 10-100 in waste water	Lee *et al.*, 2005
Clofibric acid, ibuprofen, carbamazepine, naproxen, ketoprofen, diclofenac	Oasis HLB; methanol	Tetrabutylammonium hydrogen sulphate (TBA-HSO_4)	Deuterated chrysene	GC-MS	LOD: 1.0-8.0 in drinking water	Lin *et al.*, 2005
Nine acidic pharamaceuticals	LiChrolut 100 RP-18; methanol; 500 mL sample	N/A	N/A	LC - tandem MS	LOD: 5 – 20 in STP effluent	Miao *et al.*, 2002

N/A: not application; NR: not reported

2.3 PhACs and EDCs Removal in Drinking Water Treatment

Conventional water treatment processes for surface water consist of coagulation/flocculation, sedimentation, filtration, and disinfection. A number of processes may be effective at removing certain EDCs and PhACs. Removal efficiencies of these conventional processes may be a joint function of the compound's structure and the treatment technology employed. Yoon *et al.* (2002) reviewed the potential removal of EDCs and PhACs from drinking water by different treatment processes based on studies published before 2002. Since then, more attention has also been paid to advanced drinking water treatment technologies including advanced oxidation process (AOP) and membrane filtration. This section briefly summarizes recently published studies.

Coagulation/flocculation, which removes only hydrophobic compounds associated with particle or colloidal material with high organic carbon content, is expected not to be an efficient way of removing most EDCs and PhACs because most of these compounds are fairly polar and hydrophilic. This point is supported by studies by Adams *et al.* (2002) who found that coagulation/flocculation/sedimentation with alum or iron salts had poor removals of the selected antibiotics. Ternes and his colleagues (2002) confirmed that iron chloride coagulation led only to insignificant removals of carbamazepine, clofibric acid and diclofenac based on the results from lab scale and full-scale experiments. The acidic PhAC naproxen was poorly removed from river water by this process in a survey at a full-scale drinking water treatment plant (Boyd *et al.*, 2003). Jar tests over a range of ferric chloride dosages and pH conditions showed that coagulation under these conditions was ineffective at removing estrone in water (Chang *et al.*, 2004). Westerhoff and his colleagues (2005) comprehensively examined the removal of 62 different EDCs and PhACs, and concluded that, except for some polyaromatic hydrocarbons (PAHs), alum sulfate and ferric chloride coagulants generally removed less than 25 % of most EDCs and PhACs. Nevertheless, the presence of natural organic matters (NOM) in water may have some positive effects on the removal of specific PhACs and EDCs with high molecular weights (MW) and low charge densities by coagulation. Lindquist *et al.* (2003) studied the effects of target compound properties, NOM in raw water, types of coagulant and pH on removal efficiencies and reported that, under optimized conditions, almost 30% of diclofenac was removed by ferric sulphate and up to 80% removal was achieved by adding humic substances. Compared to ferric salt, the alum salt coagulation had a much lower removal efficiency.

Adsorption using activated carbon could play an important role in the removal of EDCs and PhACs, based on the assumption that these groups of compounds are similar to some pesticides in

both physicochemical properties and concentration levels present in the water matrix (Janex *et al.*, 2002; USEPA, 2001). Hydrophobic interactions are the dominant mechanism in activated carbon adsorption of organic compounds (Yoon *et al.*, 2002). Therefore, the EDCs and PhACs with higher octanol-water partition coefficient (K_{ow}) are expected to be conducive to removal by activated carbon. However, the performance of activated carbon in natural water is significantly impacted by background NOM in the water. As a result, studies in pure water may overestimate the efficacy of activated carbon when it is used in natural water. This discrepancy was confirmed by Stackelberg *et al.* (2004) who found that carbamazepine persisted through a granular activated carbon (GAC) filter while it was reported to be effectively removed in the study by Ternes *et al.* (2002). Another example is that, even though the addition of 10-20 mg/L of powdered activated carbon (PAC) efficiently removed seven antibiotics from distilled water, removals decreased 10 - 20% in river water (Snyder *et al.*, 2003). In general, studies on removals of EDCs and PhACs by GAC is lacking in details compared to PAC. However, PAC is only added seasonally or event specific at many conventional drinking water treatment facilities to remove trace organic compounds (Yoon *et al.*, 2002). Since EDCs and PhACs are released more or less continuously into the environment, they can be regarded as persistent contaminants. Hence, GAC adsorbers would be a more suitable treatment option for reducing these compounds. However, neither the competitive effects from background NOM nor the performance of GAC adsorbers has been well documented. Since the adsorption is the main topic in this study, it will be discussed in more detail in Section 2.4.

Free chlorine, which is also a strong oxidant, is commonly used for disinfection. It is therefore possible that EDCs and PhACs undergo reactions with free chlorine during water treatment. Free chlorine also reacts with ammonia or organic amine to produce chloramines, which are weaker oxidizing agents. The available data suggests that chloramines are much less reactive than free chlorine with EDCs and PhACs (Pinkston and Sedlak, 2003). Chlorine has been proven to react rapidly with E2, with almost 100% of E2 having disappeared after a 10 min reaction period (Hu *et al.*, 2003). Similarly, BPA was also eliminated completely within 5 min of chlorination under a dosage of 10.24 mg/L (Yamamoto and Yasuhara, 2002). 50-90% removal of seven common antibiotics by chlorination under typical water treatment conditions was reported by Adam *et al.* (2002). In a pre-chlorination study of NPEOs in drinking water, the elimination of NPEOs and NP were in part due to the transformation into halogenated nonylphenolic compounds or brominated acidic metabolites (Petrovic *et al.*, 2003). Westerhoff *et al.* (2005) investigated that a number of EDCs and PhACs compounds were chlorinated at pH 5.5 at bench scale, and reported that the elimination efficiency ranged from <10% to >90% depending on the structures of the compounds. Similarly, ClO_2 applied in

water treatment only acts as a partial barrier for pharmaceuticals. Even though ClO_2 is relatively effective in oxidizing antibiotics and estrogens, carbamazepine, naproxen and ibuprofen could not be adequately reduced by ClO_2 (Huber *et al.*, 2005).

Recently, more attention has been paid to the formation of disfection by-products (DBPs) during chlorination of EDCs and PhACs. The formation of DBPs makes the desired reduction in toxicity more complex because some DBPs pose a more serious health risk while others have a lower risk than their parent compounds (Westerhoff *et al.*, 2005). Changes in estrogenicity were investigated when studying the chlorination of EDCs. Hu and his colleagues conducted chlorination experiments on EDCs such as 4-NP (Hu *et al.*, 2002), E2 (Hu *et al.*, 2003) and BPA (Hu *et al.*, 2002b) in drinking water. By using GC/MS and LC/MS, thirteen by-products of BPA, and seven by-products of 4-NP and E2 were identified in the chlorinated drinking water. The estrogenic activities of the chlorinated water at different reaction times were assessed by a yeast two-hybrid system, a human estrogen receptor and a coactivator. BPA by-products exhibited greater estrogenic activities than the parent BPA, while chlorinated E2 elicited the same estrogenicity as E1 and the chlorinated 4-NP solution showed anti-estrogenic activities. DPBs were also observed in chlorination of naproxen (Boyd *et al.*, 2005).

Ozone is used in water treatment as both a disinfectant and an oxidant. In general, ozone reacts with organic compounds found in water via two different pathways: direct molecular destruction and indirect radical chain type reaction with OH radicals. Contributions of these two pathways to the destruction of a compound depend upon pH and composition of water. It is expected that the more selective molecular ozone is the major oxidant at acidic pH, whereas less selective and faster radical oxidation (mainly hydroxyl radical) becomes dominant at pH>7 as a consequence of OH radical accelerated ozone decomposition (Balcioglu and Otker, 2003). AOPs, such as UV/H_2O_2, O_3/H_2O_2 and UV/O_3, can increase the concentration of hydroxyl radicals which exhibit higher oxidation potential than ozone and in many cases micropollutant removal is improved.

Ozonation was reported to be an effective way to remove steroid hormones and the related estrogenicity in water treatment processes. The main reason stated was that changes in the number of functional groups and in the molecule's polarity by ozonation led to the disappearance of the original medicinal modes (Ternes *et al.*, 2003). For water treatment conditions (pH 7-8, O_3=1mg/L), the reported half-lives for EE2, carbamazepine, roxithromycin, diclofenac and sulfamethoxazole were all less than 0.5 s (Huber *et al.*, 2003). Adams *et al.* (2002) concluded from their experimental results that ozone concentrations even below typical water treatment dosage were still effective at achieving

oxidation of antibiotics to levels below detection limits. However, the efficiency of the ozonation process for the removal of PhACs turned out to be very compound specific (Ternes *et al.*, 2002).

The kinetics of ozonation and AOPs are currently under extensive study. The reaction constants k_{O3} and k_{OH} for EDCs and PhACs can be determined in bench scale experiments (Yoon *et al.*, 2002; Andreozzi *et al.*, 2003; Vogna *et al.*, 2004; Huber *et al.*, 2003). In general, the structure of the target compounds and water quality parameters such as dissolved organic carbon (DOC), alkalinity, pH and temperature, are the most influential factors. For example, the amino groups present in bezafibrate and diclofenac are probable reactive sites for molecular ozone. This is supported by the fact that diclofenac could be degraded more readily than ibuprofen and clofibric acid by ozonation (Zwiener and Frimmel, 2000). pK_a is also important in ozonation. Generally, deprotonated species react faster with the electrophilic ozone because they are stronger nucleophiles. Rate constants for EE2 and roxithromycin depend strongly on pH. The deprotonated phenolic group of EE2 and the nonprotonated amine of roxithromycin react many orders of magnitude faster than their protonated forms (Huber *et al.*, 2003). In ozonation, the oxidation of low rate constant pharmaceuticals such as diazepam, ibuprofen and iopromide is mainly due to OH radicals originating from ozone decay. In this case, the oxidation of these compounds is largely influenced by DOC in the water matrix. The oxidation efficiencies increased with increasing DOC and decreased with increasing alkalinity. An increased DOC leads to an enhanced rate of ozone transformation into OH radicals, whereas alkalinity stabilizes ozone by scavenging OH radicals (Huber *et al.*, 2003).

Similar to chlorination, it should be noted that some by-products may be formed during ozonation. For example, McDowell *et al.* (2005) reported that several ozonation products containing quinazoline-based function groups were found during the ozonation of carbamazepine at bench-scale experiments and in real waterworks. Therefore, for the precautious perspective, the risk assessment should also be performed for post-ozonation waters.

Most EDCs and PhACs range from 150 to 500 Daltons in molecular size. Therefore, they are expected to be removed by reverse osmosis (RO) and tight nanofiltration (NF), but not by ultrafiltration (UF). A survey conducted by Kim et al. (2007) in a full-scale WTP demonstrated that UF process contributed little to the removals of EDCs and PhACs found in raw water, while RO and NF processes showed excellent removal rates (>95%). Snyder *et al.* (2003) showed that loose nanofiltration led only to minor removals of PhACs while tight nanofiltration had moderate to good removals. Polar or charged compounds that interact with the membrane surface are expected to be better removed than less polar or neutral compounds (Yoon *et al.*, 2002). Based on these principles,

some EDCs and PhACs are also expected to be removed during membrane filtration with looser membranes. The high rejection observed for some negatively charged EDCs and PhACs compounds using polyamide NF was due to electrostatic repulsion (Kimura *et al.*, 2003). With respect to neutral/uncharged EDCs and PhACs compounds, Kimura *et al.* (2004) reported that retentions varied depending on molecular size, polarity and membrane materials, ranging from 57% to 91% with better performance on polyamide NF than on cellulose NF. In other studies, removal of antibiotics using a low-pressure RO system with a cellulose acetate membrane was examined by Adams *et al.* (2002). The rejection rate for the antibiotics averaged around 90% from distilled water and river water with rejection rates as high as 99 and 99.9% achieved with two and three RO units in series, respectively (Adams *et al.*, 2002). Wintgens *et al.* (2002) tested eleven different nanofiltration membranes in a laboratory set-up and found that the observed retentions for NP and BPA ranged between 70% and 100%.

In summary, chemical coagulation/flocculation/sedimentation were demonstrated to be of less significance in removing EDCs and PhACs, though they are expected to remove some hydrophobic compounds associated with NOM particles. Activated carbon is recommended as a good option for the removal of some EDCs and PhACs in drinking water treatment. However, studies of PhACs removal by adsorption mostly focused on overall treatment efficiencies and to a lesser degree on underlying mechanisms, thus detailed adsorption characteristics in pure water and natural water have not been well documented. The studies on ozone and AOP related treatments are extensively under going, in which the mechanisms of oxidation of EDCs and PhACs have been interpreted. Oxidation processes such as chlorination, ozonation and AOP can effectively destroy many EDCs and PhACs depending on the compound and water quality parameters. However, by-products formed during oxidation may be of concern. Removal efficiencies should therefore be evaluated based on total mineralization or a toxicity assessment of the treated water. Membranes may provide satisfactory results for the removal of EDCs and PhACs by acting as physical barriers and/or electrostatic repulsion of the contaminants. However, the mechanism of retention varies according to physicochemical properties of target compounds and the characteristics of membrane materials. Therefore, a more fundamental understanding of EDCs and PhACs rejection by membrane requires further investigations.

2.4 Adsorption of PhACs and EDCs by Activated Carbon

Since adsorption by activated carbon was recommended as a potentially effective treatment for removing trace level EDCs and PhACs based on its capability in reducing pesticides (i.e. DDT, methoxychlor) in water (USEPA, 2001), several studies have been carried out to investigate the removal of EDCs and PhACs in ultrapure and natural water. Typically, the adsorption capacity determined in ultrapure water is a starting point, by which the characteristics of both adsorbent and adsorbate can be well defined and compared. However, in real drinking water treatment situations, adsorption would be influenced by water quality parameters, and operation conditions. In this section, the most relevant studies to date are summarized.

Adam *et al.* (2002) investigated the removal of seven antibiotics using PAC – Calgon WPH Pulv. in ultrapure water and river water. The percent removal of each of the antibiotics for PAC dosages of 10 and 20 mg/L ranged from 57% to 97% and 81% to 98% in ultrapure water and from 49% to 73% and 65% to 100% in river water. Surprisingly, the statistical comparison at 5% significance level indicated no difference in removals between the two water matrices. A possible reason may be the high initial contaminant concentrations (50 μg/L) applied in this study.

As a part of the European project "POSEIDON", which was launched in 2001, in order to evaluate technologies for the removal of PhACs and personal care products (PPCPs), Janex-Habibi and Bruchet (2004) carried out isotherm and kinetic tests on selected PPCPs with varied initial concentrations between 10-100 μg/L using PAC. The 8 PPCPs were divided into 2 groups according to their K_{ow}. It was found that the group with high K_{ow} easily achieved 99% removal by applying less than 0.2 mg/L PAC while the other group needed much higher dosages to achieve the same removals. The impact of background NOM in natural water was identified in this study. Adsorptive capacities decreased in natural water and the difference in affinities between different groups of compounds became less pronounced in natural water compared to in ultrapure water (Janex-Habibi and Bruchet, 2004).

The isotherms of carbamazepine, bezafibrate, clofibric acid and diclofenac were determined by Ternes *et al.* (2002) in ultrapure and ground water with equilibrium liquid concentrations ranging from 0.1 -100 μg/L using a pulverized granular activated carbon (PGAC). Among the four selected PhACs, carbamazepine, a neutral drug, showed the highest affinity to PGAC in ultrapure water. A reduction of adsorptive capacities of the PGAC for the four compounds was also observed in groundwater, suggesting that lower capacities were to be expected in a pilot fixed bed adsorber, for which groundwater was used as influent (Ternes *et al.*, 2002). However, in the pilot study,

carbamazepine did not show a significantly higher removal profile compared to bezafibrate and diclofenac, which had lower adsorptive affinities than carbamazepine in isotherm tests. This may lie in the fact that the reported pilot results only achieved 20% breakthrough, and hence, differences in the adsorption of these compounds may not have been pronounced. This study also examined a range of other drinking water treatment technologies such as coagulation/flocculation, biofiltration, and ozonation. Although this study represents a good starting point for evaluating treatability of different treatment technologies for EDC and PhACs removal, no further follow-up studies were available.

Similarly, a study on several water treatment technologies including PAC adsorption on 49 different EDCs and PPCPs, was carried out by Westerhoff *et al.* (2005). In this bench-scale study, only one dosage (5 mg/L) of two PAC with different characteristics were spiked into a cocktail of 49 target compounds in four natural waters. They applied low initial concentrations from 50 to 250 ng/L, which were considered to be close to environmentally relevant concentrations. The results showed that PAC was capable of partially removing all EDCs and PPCPs in all four source waters (Westerhoff *et al.*, 2005). For these target compounds, the average percentage removals of carbamazepine and naproxen at a 5 mg/L PAC were reported as 52% and 74%, respectively. Notably, a good linear relationship was found between log K_{ow} and the percentage removals of most target compounds (Westerhoff *et al.*, 2005). In subsequent research conducted by the same group (Snyder *et al.*, 2007), removal of 29 EDCs and PhACs by PAC were evaluated at bench scale. Interestingly, nonylphenol, which has a higher log K_{ow}, was found to have the least average removal (50%) under the same conditions as in the study by Westerhoff *et al.* (2005). The removals of the same group of target compounds were also examined with GAC using bench-scale rapid small scale column tests (RSSCT) and in two full-scale utilities. The published data demonstrated that GAC was capable of removing nearly all compounds by greater than 90%; however, its efficacy was greatly reduced by NOM (Snyder *et al.*, 2007). The observation of a more rapid breakthrough of more hydrophilic contaminants on GAC again proved the general relationship between log K_{ow} and removal efficiencies (Snyder *et al.*, 2007). In addition, the observation on two full-scale GAC adsorbers showed the regeneration of the used GAC restored some capacity in removing the investigated compounds (Snyder *et al.*, 2007).

Two studies on adsorption of steroid hormones, 17β-estradial and estrone, by activated carbon were carried out by Chang *et al.* (2004) and Zhang and Zhou (2005), respectively. In the first study, adsorption isotherm and kinetics on deuterated estrone in the range from 1 to 20 ng/L were investigated in ultrapure water and secondary wastewater effluent. It is interesting to note that the

isotherm obtained for estrone in a very dilute solution demonstrated a linear adsorption. The competitive effect was confirmed through the observation that the adsorption capacity in wastewater treatment effluent was reduced, but this was not further quantified (Chang *et al.*, 2004). The detailed adsorption kinetic parameters were determined on PAC at extremely low concentration of estrone (i.e. 50 ng/L), based on a homogeneous surface diffusion model (HSDM). It was found that both film diffusion and internal surface diffusion controlled the adsorption of estrone under the conditions used (Chang *et al.*, 2004). In contrast, the adsorption capacities and kinetics of 17β-estradiol and estrone were studied by Zhang and Zhou (2005) by means of the adsorption constant K_D, which was used as an index of adsorption capacity. It was concluded that the activated carbon studied had good removals for both 17β-estradiol and estrone, however, the presence of surfactant and humic acid resulted in a reduced adsorption constant for activated carbon (Zhang and Zhou, 2005).

Bautista – Toledo *et al.* (2005) studied the behaviour of two activated carbons in the adsorption of BPA by determining the textural and chemical characteristics of carbon (i.e. surface area, pore size distribution, mineral matter content, and pH of the point of zero charge, etc.). The adsorptive capacity of BPA was determined based on the Langmuir model at fairly high initial concentrations of 50 – 350 mg/L. As a result, the most favourable adsorption was achieved at the experimental conditions of zero net charge density on carbon and BPA in neutral form (Bautista – Toledo *et al.*, 2005).

Removal of BPA and NP was investigated with three GAC, including Calgon F400, made from different materials in both bench-scale isotherm and GAC column tests by Choi *et al.* (2005). The experiments were conducted at relatively high concentration levels of the target compounds (10 – 1000 μg/L equilibrium liquid concentrations for isotherm tests and 200-500 μg/L in influents for column tests) compared to their environmentally occurring concentrations in surface and ground water. Overall, all carbons could effectively adsorb the two compounds with better performance on coal-based F400 due to its larger pore volume (Choi *et al.,* 2005). With respect to the adsorption capacity of the compounds studied, the pore volume was found to be more important than the specific area, but the surface charge was also important due to electrical interactions (Choi *et al.,* 2005). The preloading effect on GAC was investigated, revealing that the adsorption capacity was reduced with increasing operation time, and the extent of the reduction depended on the carbon type and the preloading time (Choi *et al.,* 2005). However, preloading mechanisms were not further investigated.

Tanghe and Verstraete (2000) also carried out an investigation on the adsorption of NP onto Chemviron (Calgon) F300 carbon. Similar to the study by Choi *et al.* (2005), the concentration levels

in this study ranged from 100 to 10,000 μg/L. Based on the adsorption capacity obtained with batch isotherm tests in ultrapure water and humic acid spiked water, it was concluded that a full-scale GAC filter should be capable to remove environmentally relevant NP concentrations of 10 μg/L (Tanghe and Verstraete, 2000). However, neither competitive nor fouling effects were considered in this study.

The results of all of the above studies suggest that adsorption by activated carbon is a promising technology for removing EDCs and PhACs in waters. In addition, activated carbon has been widely applied in Canada and the United States, which makes it amenable to most drinking water utilities in order to address the issue of EDCs and PhACs. However, according to this review, more detailed studies of the adsorption characteristics of EDCs and PhACs are lacking. Adsorption isotherms and kinetics, which are important factors for the design of adsorption processes in drinking water treatment, have not been well studied. It should be emphasized that environmentally relevant concentrations of most EDCs and PhACs are much lower than other synthetic organic compounds (SOCs) such as TCE and atrazine, etc, which is an important factor to consider in adsorption related studies. In addition, in order to implement the adsorption under realistic conditions, the effect caused by background NOM such as competitive and preloading effect should be investigated in detail.

In summary, PAC adsorption provides a viable means for treating the EDCs and PhACs, and thus under more investigations. However, PAC is typically used event specific for only a portion of the year; therefore, extended PAC usage, which may be needed to remove the pseudo-persistent EDCs and PhACs, would increase operating costs correspondingly. Therefore, continuously operated GAC adsorbers would be a better option. However, there is only limited data available for adsorption performances and mechanisms of GAC adsorbers in the removal of EDCs and PhACs to date.

2.5 Direct Competitive Effect in Adsorbing Micropollutants in Natural Water

It has been shown in many studies that the presence of background NOM in natural water reduces the adsorptive capacity of activated carbon when removing micropollutants due to competitive effects (Sontheimer *et al.*, 1988). The mechanisms of competitive effects can be generally explained as: 1) direct competition, in which small NOM molecules simultaneously compete with target compound molecules for access to the adsorption sites on activated carbon; and 2) pore blockage by NOM, in which large NOM molecules accumulate and block the openings of small pores, preventing target compound molecules from accessing adsorption sites. In the application of PAC, the reduction of adsorptive capacity is mainly attributed to direct competition rather than pore blocking due to short contact time (Matsui *et al.*, 2003). However, the pore blockage effect is

predominant when the carbon is preloaded with NOM, which is likely to happen in GAC filter adsorbers since they are operated over long periods of time (Knappe *et al.*, 1999). This section only focuses on the direct competition, while the preloading effect on GAC will be reviewed in a later section.

2.5.1 Studies on the Direct Competitive Effect

While the focus of many studies in the 1980's was on competitive effects in known mixtures, interests shifted to the impact on the adsorption of specific compounds in unknown mixtures, namely natural waters in the mid 1980's (Andrews, 1990). This is of great significance because, for practical uses of activated carbon in water treatment, the major impact on adsorptive capacities is from the difficultly defined background NOM in natural water.

Since then, the competitive effect on many micropollutants has been investigated in natural water. Najm *et al.*, (1990) evaluated the reduction in PAC adsorptive capacity resulting from background NOM in groundwater for 2,4,6–trichlorophenol (TCP) and found a 50% reduction after 20 minutes of contact time. Andrews (1990) investigated competitive effects on trihalomethanes by defining the hypothetical component (HC), which represented the background NOM, in four water matrices. Competition between background NOM and trichloroethylene (TCE) on GAC was also determined through two different isotherm testing approaches (Carter *et al.*, 1992). The concept of a single equivalent background compound (EBC), which is assumed to present a portion of background NOM that only directly competes for adsorption sites with the target compound in natural water, was introduced by Najm *et al.* (1991) in a study of competitive effects on TCP (more discussion in Section 2.5.3). EBC was derived based on the ideal adsorbed solution theory (IAST) in combination with an appropriate adsorption isotherm model (e.g. Freundlich isotherm equation), and thereafter the concept of IAST-EBC was widely accepted and applied in describing the direct competitive effect observed in PAC–natural water systems because it is very applicable for engineering uses (see Section 2.5.2 for more introduction of the IAST). Knappe (1996), in his dissertation, successfully applied the concept of IAST-EBC to predict the adsorption of atrazine in natural water, and found the percentage removal of atrazine at a given PAC dosage was essentially constant at different initial atrazine concentrations. This observation was confirmed lately by a study looking at 2-methyl-isoborneol (MIB) adsorption in natural water (Gillogly, 1998). Based on these observations, the IAST-EBC was further simplified (Knappe *et al.*, 1998), though the three assumptions on which the simplifications based were needed further justification. Graham *et al.* (2000) modelled equilibrium adsorption of MIB and geosmin, applying the IAST-EBC model to four natural waters, finding that

the ratio of initial EBC concentration to TOC of natural water was constant for a specific compound, when adsorption characteristics (Freundlich K_F and 1/n) and molecular weight of the EBC were fixed when calculating the EBC initial concentrations for all natural waters. The study also confirmed that the impact of interactions between different micropollutants was negligible compared to the strong competitive effect from background NOM (Graham *et al.*, 2000). Since the concept of EBC had been introduced, further efforts were made towards understanding the mechanism of direct competition. The studies conducted by Newcombe *et al.* (2002b) and Hepplewhite *et al.* (2004) demonstrated that the low-molecular-weight fraction of NOM, which participated in direct competition with MIB for adsorption sites, had the most competitive potential. However, the competing background NOM fraction was found to vary with different micropollutants. A study of three herbicides (simazine, simetryn, and asulam) indicated that the NOM fraction competing with weakly adsorbed herbicide constituted a larger percentage of the total NOM than that competing with the strongly adsorbed herbicides (Matsui *et al.*, 2003). In the same study, the adsorptive kinetics were investigated under competitive conditions; and it was found that the background NOM had only a negligible effect on pore diffusion, which was determined to be as the dominant internal diffusion mechanism for micropollutant adsorption in natural water. This suggested that direct competition rather than pore blockage was the main mechanism to reduce the adsorptive capacity of PAC for micropollutants (Matsui *et al.*, 2003). In contrast, Ebie *et al.* (2001) stated that, other than direct competition, pore blockage also contributed to the reduction of adsorptive capacity for micropollutants, depending on the type of activated carbon, the micropollutants, and equilibrium concentrations. In general, the deviation caused by pore blockage would typically be found with less adsorbable micropollutants at high equilibrium concentrations (Ebie *et al.*, 2001). The reduction of adsorptive capacity of PAC due to pore blockage in addition to direct competition from background NOM was confirmed by Li *et al.* (2003), who stated that the pore blockage effect on aged PAC in a system such as PAC/membrane reactor could not be ignored. However, in general, the IAST-EBC can successfully describe the reduction of adsorptive capacity in short-contact-time PAC systems due to the direct competitive effect. Recently, the justification of the three assumptions of the simplified IAST-EBC by Qi *et al.* (2007) made this concept even more acceptable and practicable for engineering.

As outlined above, to determine the direct competitive effect from background NOM, accurate measurements of isotherms of target compounds in ultrapure water are required as the first step. As discussed in the last section, the lack of detailed information on isotherms of EDCs and PhACs at the environmentally relevant concentration ranges would impede the design of both PAC and GAC processes. Furthermore, although a reduction in adsorptive capacity of selected EDCs and PhACs was

demonstrated in certain studies (Janex-Habibi and Bruchet, 2004; Chang *et al.*, 2004; Zhang and Zhou, 2005), the competition from background NOM in such studies were not further quantified. Therefore, although the fundamental understanding of capacity reduction in adsorbing other micropollutants attributable to direct competition from background NOM, has progressed in recent years, it has not been applied for predicting removal of PhACs and EDCs in drinking water treatment applications.

2.5.2 The Ideal Adsorbed Solution Theory

An initial study of competitive adsorption was conducted in bi-solute solutions, and the first model derived from the Langmuir model was developed by Butler and Ockrent (Sontheimer *et al.*, 1988). The modified Langmuir model may lead to unsatisfactory results, however, if some parts of the adsorption are non-competitive. The model proposed by Jain-Snoeyink overcomes this difficulty after taking into consideration the non-competitive adsorption on the adsorbent surface (Sontheimer *et al.*, 1988). Other models for competitive adsorption in multicomponent systems were developed on the base of empirical data, such as the multicomponent isotherm of Frits and Schlunder (1981). However, these models involve only competitive interactions attributable to known mixtures, and therefore they require a great deal of multicomponent data to accurately define the adjustable parameters.

The IAST was originally developed by Myers and Prausnitz (1965) and then modified to predict competitive adsorption in dilute aqueous mixtures by Radke and Prausnitz (1972). An advantage of the IAST is that any single-solute isotherm equation that best describes the equilibrium data can be incorporated into the IAST to describe the multicomponent competition. Therefore, to calculate multicomponent adsorption in solutions, only single-solute isotherm data are needed, and the predictive modeling can consequently be simplified.

The IAST model is based on the thermodynamic equivalence of the spreading pressure of each solute at equilibrium. Spreading pressure, π, related to the free energy change resulting from adsorption, is defined as the difference between the interfacial tension of the pure solvent-solid interface and that of the solution-solid interface at the same temperature. According to Raoult's law, the spreading pressure of a component, i, in single solute solution, π_i, is set to equal that of the multicomponent solution, π_m. As summarized by Crittenden *et al.* (1985) and Sontheimer *et al.* (1988), the following five basic equations are used in IAST to predict multicomponent behavior:

$$q_T = \sum_{i=1}^{N} q_i \qquad \textbf{2.1}$$

$$y_i = q_i / q_T \quad (i=1 \text{ to } N) \qquad \textbf{2.2}$$

$$C_i = y_i C_i^o \quad (i=1 \text{ to } N) \qquad \textbf{2.3}$$

$$1/q_T = \sum_{i=1}^{N} y_i / q_i^o \qquad \textbf{2.4}$$

$$\frac{\pi_m A}{RT} = \int_0^{q_i^o} \frac{d(\ln C_i^o)}{d(\ln q_i^o)} dq_i^o = \frac{\pi_i^o A}{RT} = \ldots. \ (i=1 \text{ to } N) \qquad \textbf{2.5}$$

Equation 2.1 and 2.2 define the total surface loading where:

q_T = *total solid-phase concentration*

q_i = *solid-phase concentration for component i*

y_i = *molar fraction of component i on the surface of adsorbent*

N = *number of components in mixture*

Equation 2.3 is derived based on Raoult's law where:

C_i^o = *equilibrium liquid phase concentration in single-solute system with the identical temperature and spreading pressure,* π_m*, as the mixture*

C_i = *equilibrium liquid phase concentration*

Equation 2.4 relates the total solid-phase concentration to the single-solute equilibrium concentration with the meaning of zero area change upon mixing from the single-solute isotherm at the spreading pressure of the mixture where:

q_i^o = *the single-solute, solid-phase concentration in equilibrium with* C_i^o

Equation 2.5 comes from the conclusions that the change in spreading pressure is related to the amount adsorbed, and the spreading pressure of the mixture is equal to that occurring in the single-solute system, where:

π_m = *spreading pressure of the mixture*

A = the adsorption area per mass unit of adsorbent

R = ideal gas law constant

T = absolute temperature

π_i^o *= spreading pressure of single solute component*

If the Freundlich isotherm (Equation 2.6), which has typically been used to describe single-solute isotherms in engineering, is applied in combination with the IAST, a simpler relationship for predicting multicomponent adsorption can be derived as shown in equations 2.7 and 2.8.

$$q_i = K_{Fi} C_i^{1/n_i} \qquad \textbf{2.6}$$

in which K_{Fi} *and* $1/n_i$ *are Freundlich constants for component i*

$$\frac{d(\ln C_i^o)}{d(\ln q_i^o)} = n_i \qquad \textbf{2.7}$$

$$n_1 q_1^o = ... = n_j q_j^o \qquad (j = 2 \text{ to } N) \qquad \textbf{2.8}$$

where n_i *and* n_j *in these equations denote the inverse Freundlich exponents of component i and j, respectively.*

Equation 2.8 comes from a combination of Equation 2.5 and 2.7.

Combining Equations from 2.1 to 2.8, yields the following equation (Equation 2.9):

$$C_i = y_i \left[\frac{\sum_{j=1}^{N} n_j q_j}{n_i K_i} \right]^{n_i} \quad (i = 1 \text{ to } N) \qquad \textbf{2.9}$$

Equation 2.9 can be combined with the following equilibrium mass balance equation (Equation 10) to eliminate liquid-phase concentration and, consequently, yield the Equation 2.11

$$q_i = (C_{io} - C_i) V/M \qquad \textbf{2.10}$$

in which C_{io} *is the initial concentration of component i, V is the bottle volume and M is the mass of the carbon added to the bottle.*

$$F_i(q_1, q_2 .... q_i) = 0 = C_{io} - \frac{M}{V} q_i - \frac{q_i}{\sum_{j=1}^{N} q_j} \left[\frac{\sum_{j=1}^{N} n_j q_j}{n_i K_{Fi}} \right]^{n_i} \quad (i = 1 \text{ to } N) \qquad \textbf{2.11}$$

Equation 2.11 is valid for all components, so that IAST predictions for bottle point isotherms only require the single solute isotherm parameters (e.g. Freundlich parameters in Equation 2.11), initial concentration for each component, and the activated carbon dosage.

It should be noted that the Freundlich exponent 1/n changes with liquid phase concentration, and can only be considered as constant in a limited liquid phase concentration range (Sontheimer *et al.,* 1988). Consequently, the use of only one Freundlich equation in combination with the IAST to predict competition for wide concentration ranges may lead to errors. Therefore, the application of the IAST should be limited to the investigated concentration range where the single-solute isotherm is determined, or as suggested by Sontheimer *et al.* (1988), incorporating an integration constant into calculating the spreading pressure corresponding to the change in the Freundlich isotherm parameters in different concentration regions.

The combination of the IAST and the Freundlich isotherm has been widely accepted and successfully applied for predicting competitive adsorption equilibria (e.g. Crittenden *et al.*, 1985; Andrews, 1990, Najm *et al.*, 1991; Knappe *et al.*, 1993). It is important to being precise in determining single solute isotherm data (Luft, 1984 cited by Andrews, 1990). However, even so, systematic divergences between experimental data and predicted values of multicomponent adsorption by IAST may be observed. For example, Crittenden et al. (1985) used the approach of an average percentage error (APE) to evaluate IAST prediction. Overall, APEs of 29% and 16% for C_i and q_i, respectively, were reported for 256 multicomponent isotherm data points. The systematic deviation may be attributed to divergences from the ideal scenario under the actual adsorption circumstance, the assumption of constant Freundlich parameters over large concentration range, or the assumption that all of the surface area is available for adsorption.

2.5.3 Application of the IAST for Adsorption in Unknown Mixtures

Prediction of the removal of micropollutants in natural water, which is often carried out for drinking water treatment, can be solved using the IAST. This is complicated in natural waters by presence of other substances, of which the greatest portion consists of NOM. The adsorption behaviour of NOM differs considerably depending on source and fractions from easily adsorbable to

poorly or nearly non-adsorbable. Because of the poorly defined characteristics of NOM, it is difficult to quantify the competition between target compounds and different NOM fractions. The solution to determining the competitive effect of unknown NOM background is to represent it by several "fictive" or "hypothetical" components (HC). Consequently, the adsorptive properties of NOM can be obtained without understanding the composition of NOM. The HC parameters (i.e. Freundlich K_F and 1/n, and initial concentration C_o if the Freundlich equation is being used) represent the competitive strengths of all unknown components in the mixture, and can be used in combination with single solute isotherm parameters for a given compound to predict competitive adsorption equilibria for that compound in an unknown background matrix (Andrews, 1990). An adsorption analysis procedure based on tracer tests proposed by Sontheimer *et al.* (1988) can be used to help determine the HC parameters by fitting the experimental data of weakly adsorbable tracer compounds in their single-solute and mixture solutions using the IAST in conjunction with a specific isotherm model. The use of the IAST with the Freundlich equation (Equation 2.11) was recommended by Sontheimer *et al.* (1988) because this model is simple to use and the adjustable parameters can compensate for errors in the IAST. The advantage of the adsorption analysis is that, once the background NOM in certain water has been described adequately, only single-solute isotherm parameters of target compounds are needed to predict the adsorption equilibria in the natural water.

Based on the understanding of the IAST and HC, Najm *et al.* (1991) further simplified the adsorption analysis procedure by introducing the concept of EBC, which was defined to present a portion of background NOM that only competes for adsorption sites simultaneously with the target compound in natural water, thus forming a pseudo-bisolute system. Consequently, equation 2.12 and 2.13, namely the IAST-EBC model, were derived from equations 2.11 to describe the competition between target compound and EBC in pseudo-bisolute system.

$$C_{1,0} - q_{1,eq}D - \frac{q_{1,eq}}{q_{1,eq}+q_{2,eq}}\left(\frac{n_1 q_{1,eq} + n_2 q_{2,eq}}{n_1 K_{F1}}\right)^{n_1} = 0 \qquad \textbf{2.12}$$

$$C_{2,0} - q_{2,eq}D - \frac{q_{2,eq}}{q_{1,eq}+q_{2,eq}}\left(\frac{n_1 q_{1,eq} + n_2 q_{2,eq}}{n_2 K_{F2}}\right)^{n_2} = 0 \qquad \textbf{2.13}$$

D = carbon dosage

$C_{1,0}$, $C_{2,0}$ = initial concentration of component 1 (target compound) and 2 (EBC)

$q_{1,eq}$, $q_{2,eq}$ = equilibrium solid phase concentrations of component 1 and 2 in a bi-solute system

K_{F1}, K_{F2}, n_1, n_2 = Freundlich parameters of component 1 and 2 obtained from single solute system

Therefore, knowing the single-solute isotherm, the EBC characteristics can be determined by fitting equations 2.12 and 2.13 with the isotherm of a given compound in natural water. Using this method, Najm *et al.* (1991) successfully predicted adsorption equilibria of TCP in different natural water. Knappe *et al.* (1993) and Qi *et al.* (1994) also successfully applied this model for predicting atrazine removal in natural water. It should be noted that, though the EBC approach is easily applied, the determined EBC parameters are highly specific to the target compound as well as raw water and activated carbon characteristics (Ebie *et al.,* 2001; Graham *et al.*, 2000). In other words, the EBC parameters need to be determined for each pair of target compound and activated carbon of interest for a specific water matrix.

Further studies on adsorption of micropollutants in natural water have revealed that, if the equilibrium liquid phase concentration is expressed as a percentage of the initial concentration of the target micropollutant, namely as percentage removal, it is independent of initial concentration at a given PAC dosage (Knappe, 1996; Knappe *et al.*, 1998; Graham *et al.*, 2000, Matsui *et al.*, 2003). This trend was also confirmed by Westerhoff *et al.* (2005) who found that the percentage removal of 17β-estradiol at different initial concentrations (135 – 1360 ng/L) in natural water kept constant when 1 mg/L PAC was applied.

Knappe *et al.* (1998) tried to justify the observations by further simplifying the IAST-EBC model. If assuming Freundlich exponents (1/n) of EBC are comparable to that of target micropollutant, and $q_{1,eq} << q_{2,eq}$, equation 2.12 can be simplified to equation 2.14:

$$q_{1,eq} = \frac{C_{1,0}}{D + \frac{1}{q_{2,eq}}\left(\frac{n_2 q_{2,eq}}{n_1 K_1}\right)^{n_1}} \qquad \textbf{2.14}$$

Combining the mass balance for the target compound ($C_{1,0} = C_{1,eq} + q_{1,eq}D$) with the above equation, equation 2.15 is obtained:

$$C_{1,eq} = \left(\frac{q_{1,eq}}{q_{2,eq}}\right)\left(\frac{n_2 q_{2,eq}}{n_1 K_1}\right)^{n_1} \qquad \textbf{2.15}$$

At large activated carbon dosages, the result from the IAST calculation showed that the solid phase concentration of EBC is approximately equal to a constant as shown below:

$$q_{2,eq} \cong \frac{C_{2,0}}{D} \qquad \textbf{2.16}$$

Combination of equations 2.14 and 2.15, equation 2.17 is obtained:

$$\frac{C_{1,eq}}{C_{1,0}} = \frac{\frac{1}{q_{2,eq}}\left(\frac{n_2 q_{2,eq}}{n_1 K_1}\right)^{n_1}}{D + \frac{1}{q_{2,eq}}\left(\frac{n_2 q_{2,eq}}{n_1 K_1}\right)^{n_1}} \qquad \textbf{2.17}$$

Substituting equation 2.16 into 2.17, equation 2.18 is derived:

$$\frac{C_{1,eq}}{C_{1,0}} = \frac{\frac{1}{C_{2,0}}\left(\frac{n_2 C_{2,0}}{n_1 K_1}\right)^{n_1}}{D^{n_1}} \qquad \textbf{2.18}$$

The equation 2.18 suggests that, at a given high activated carbon dosage, the percent removal is independent of initial concentrations of the target micropollutant. In other words, the log-log plot of $C_{1,eq}/C_{1,0}$ versus activated carbon dosage should be a straight line with slope of n_1 (Knappe *et al.*, 1998). It should be noted that all the above derivations are based on an important assumption that the initial concentration of target micropollutant should be much lower than that of EBC. Although this condition is typically satisfied in cases of drinking water treatment, to take a conservative approach, the investigators recommended that the maximum initial concentration of target micropollutant satisfying the proportional relationship should be determined (Knappe *et al.*, 1998). Combining the IAST and the pore surface diffusion model (PSDM), Matsui *et al.* (2003) further validated the independence of percentage removal on micropollutant initial concentrations at a given PAC dosage. However, it was also observed that, for strongly adsorbing micropollutants, the independence rule was only valid at lower initial micropollutant concentrations (Matsui *et al.*, 2003). Recently, the requirement of the proper use of the simplified IAST-EBC was developed and experimentally justified by Qi *et al.* (2007). It was stated that, for a target trace compound with the Freundlich $1/n_1$ in the range of 0.3-1, the minimum molar ratio of EBC to trace compound should be around 20 if n_1/n_2 is less than 1 (Qi *et al.*, 2007).

Although the IAST-EBC model was successfully applied in many cases, it should be emphasized that the IAST-EBC model has limitations due to the assumptions that the Freundlich parameters stay constant and all surface area is available for adsorption. However, as mentioned in the previous section, under realistic adsorption conditions, pore blockage attributable to large molecular weight NOM leads to a deviation of the actual isotherm of the target micropollutant from the IAST-EBC prediction in natural water. This was observed by Pelekani and Snoeyink (1999) and Ebie *et al.* (2001). The effect of pore blockage tends to be more pronounced when the contact time increases (Li *et al.*, 2003) or the applied dosage is insufficient (Ebie *et al.*, 2001). Since the mass transfer zone (MTZ) of background NOM moves much faster than that of the target trace compound through GAC filter adsorbers, the effect of pore blockage is expected to be much more pronounced than in case for PAC applications. Therefore, the implementation of the IAST-EBC will be limited in the case of GAC adsorbers.

2.5.4 Factors Influencing Direct Competitive Effect by Background NOM

Over the last decade, a number of studies have been focusing on understanding the mechanisms of the competitive effects including direct competition and pore blockage. This is of great significance because a better understanding of the competitive processes should contribute to improved model predictions and appropriate selection of activated carbons for treating specific contaminants of interest.

There is no doubt that the physicochemical properties of activated carbon, target micropollutant, and background NOM interact with each other to influence the adsorption efficiency of the target micropollutant in the presence of background NOM. In general, the target micropollutans with higher hydrophobicity show a stronger trend to adsorb onto activated carbons (Hu *et al.*, 1998; Westerhoff *et al.*, 2005). In natural water, it was observed that the NOM fraction competing with weakly adsorbing micropollutants was larger in the percentage of total NOM than the fraction competing with strongly adsorbing micropollutans (Matsui *et al.*, 2003). Activated carbon hydrophobicity can also serve as a general index for adsorption. It was proven that hydrophobic carbons were more effective adsorbents for both hydrophobic and hydrophilic micropollutants regardless of the absence or presence of background NOM (Quinlivan *et al.*, 2005). Moreover, the same study reported that the chemical characteristics of activated carbon (i.e. O+N contents of carbons) did not significantly affect percentage reduction of adsorption capacities for both hydrophilic and hydrophobic micropollutants (Quinlivan *et al.*, 2005). In addition, the effect from electrostatic surface properties of activated carbons was found to be insignificant in terms of NOM uptake (Fairey *et al.*, 2006).

Many studies have shown that size effects, including molecular sizes of micropollutants, molecular size distribution of background NOM molecules, and pore size distribution of activated carbons are predominant factors influencing the competitions between micropollutants and background NOM.

The micropore region on activated carbons is important in terms of adsorbing target micropollutants in water. Micropollutant molecules tend to be adsorbed into micropores of similar sizes (Pelekani and Snoyeyink, 1999; Quinlivan *et al.*, 2005; Karanfil *et al.*, 2006). For example, the optimum pore size region for adsorption of TCE (molecular dimensions 6.6 x 6.2 x 3.6 Å) is 5 – 8 Å and for atrazine (molecular dimensions 11.5 x 10.9 x 6.7 Å) is 8 – 20 Å (Karanfil *et al.*, 2006). Therefore, it is suggested that TCE and atrazine are adsorbed in the primary micropores (< 8 Å) and secondary micropores (8 – 20 Å), respectively.

The molecular size distribution of background NOM is another main factor influencing the competition. It was determined, by using different fractions of NOM obtained through ultrafiltration fractionation, that the low-molecular-weight NOM (<500 Da), which had most similar size to MIB, was the most competitive NOM fraction due to the direct competition of this fraction with MIB (Newcombe *et al.*, 1997b; Newcombe *et al.*, 2002b). At the same time, it was indicated that the large-molecular-weight NOM fraction (> 30,000 Da) had little impact on adsorptive capacity of MIB (Newcombe *et al.*, 1997b). Li *et al.* (2003), based on experiments with atrazine using model NOM compounds, confirmed that the low-molecular-weight NOM was mainly responsible for direct competition, while the large-molecular-weight NOM mostly influenced the kinetics. Therefore, it can be concluded that background NOM with molecular sizes similar to that of the target micropollutants contributes the most to the reduction in adsorptive capacity due to direct competition (Quinlivan *et al.*, 2005). The fractionation analysis of background NOM in natural water indicated that the fraction of low-molecular-weight NOM is only a small portion (< 30%) of total NOM (expressed as DOC) (Newcombe *et al.*, 1997a; Newcombe *et al.*, 2002a). It would be expected that this fraction has most contribution to the EBC.

The pore size distribution of activated carbons is of great importance in the competition between target micropollutants and background NOM. It has been proven that the majority of NOM molecules cannot access the pores smaller than 10 Å (Pelekani and Snoeyink, 1999; Dastgheib *et al.*, 2004; Quinlivan *et al.*, 2005; Karanfil *et al.*, 2006). That means, if target micropollutants are mainly adsorbed in primary micropores, the activated carbon with a very uniform and small pore size distribution less than 10 Å will act as a molecular sieve for NOM molecules, thus preventing direct

competition (Karanfil *et al.*, 2006). However, if target micropollutants can only be adsorbed in secondary micropores (10 – 20 Å), which the competing NOM can also access, the only way to reduce competition between micropollutants and background NOM is to choose the activated carbon with a wide pore size distribution, including secondary micropores and small mesopores (20 – 50 Å) (Ebie *et al.*, 2001; Quinlivan *et al.*, 2005; Karanfil *et al.*, 2006). Although this type of activated carbon cannot reduce the direct competition, it can be expected to alleviate the pore blockage effect caused by large-molecular-weight NOM, despite the fact that more NOM is taken up (Pelekani and Snoeyink, 1999; Karanfil *et al.*, 2006).

2.6 Removal of Micropollutants in Granular Activated Carbon (GAC) Adsorbers

2.6.1 Introduction to GAC Adsorbers – Configuration, Design, and Operation

While the application of PAC has existed for more than 70 years, the implementations of GAC systems increased considerably in North America in the 1980's (Sontheimer *et al.*, 1988; Clark and Lykins, 1989). For surface water, the primary purpose of GAC was initially to control taste and odor. In many cases, GAC adsorbers offered effective solutions for taste and odor control with long service life time (Sontheimer et al., 1988). Later on, GAC filters were used for the removal of a broader range of SOCs from water, such as pesticides. Reduction of disinfection by-products (DBPs) was achieved by removing its precursors, i.e. DOC in water. Given these new focuses, it is expected that the service life of a GAC adsorber would decrease because these compounds usually have higher concentrations than taste and odor compounds. Removal of SOCs and DBP precursors is one of the crucial uses of GAC adsorbers in many waterworks, it has therefore been extensively studied over the past two decades. Discovery of EDCs and PhACs in source water and finished drinking water made the micropollutant database larger and more complex. Although there is considerable knowledge about removal of µg/L level pesticides by GAC, the removal capacity of GAC adsorbers for ng/L level EDCs and PhACs is largely unknown, and presents a new challenge to the implementation of GAC adsorbers in waterworks.

A GAC adsorption system typically consists of a number of GAC reactors. Down-flow patterns are typically used in drinking water treatment (Snoeyink, 1990). If a single adsorber is chosen (usually not the case in full-scale water treatment plants), the GAC needs to be replaced or regenerated once the effluent concentrations of micropollutants reach the maximum permissible concentrations. A single adsorber is typically selected when primarily studying breakthrough characteristics. In practice, multi-down-flow GAC adsorbers are generally operated in series or in

parallel mode. In a series configuration, the first adsorber can be operated until being fully breakthrough, if the effluent from the subsequent adsorbers can still meet the requirements of maximum permissible concentrations (Knappe, 1996). This configuration provides high carbon usage efficiency if being appropriately designed. Although in some cases down-flow GAC adsorbers are used for turbidity removal, it is generally thought that this application cannot make full use of the adsorptive advantages of GAC due to more frequent backwashing and short empty bed contact time (EBCT), which are typically implemented for only filtration purpose (Graese *et al.*, 1987 cited by knappe, 1996). In particular, when a down-flow mode is applied for GAC adsorbers under high turbidity situations, it is important that the GAC adsorber be preceded by sand filtration to reduce backwashing (Clark and Lykins, 1989). In contrast with down-flow configuration, the up-flow or moving bed configuration is appropriate for influents with either high or low turbidity. (Clark and Lykins, 1989).

The first consideration in the design of GAC adsorbers is to choose the appropriate activated carbon. Selection depends on the capability of a given GAC to remove the micropolluant of concern, and to meet other requirements regarding head loss, carbon transport, and regeneration (Clark and Lykins, 1989).

EBCT and breakthrough are two important variables in the design of GAC adsorbers. At a given bed depth, EBCT influences the breakthrough profile, thus altering time intervals between backwashing or regeneration. When designing a GAC adsorber with a given output in volume, EBCT can be varied by either changing the bed depth at a constant flow or by enlarging the cross sectional area of the adsorbers. In addition to delaying breakthrough at longer EBCT, carbon usage rate (CUR) improves as EBCT increases (Clark and Lykins, 1989). For example, Knappe (1996) summarized the effect of EBCT on the removal of atrazine and showed that CUR significantly decreased after increasing EBCT from 3 to 9 minutes; however, further increase in EBCT had little beneficial effect. That means there is an optimum bed depth or bed volume when cost is considered during filter design (Clark and Lykins, 1989).

Breakthrough profiles are important in the design of GAC adsorbers. Their characteristics depend on water quality of the influent, the target micropolluants, and the carbon system, including the physicochemical properties of the activated carbon utilized. When configuration and operation parameters are given, breakthrough profiles can be described mathematically by modeling. In addition to being helpful in designing GAC adsorbers, breakthrough curves can also be used for estimating the minimum reactivation rate (Clark and Lykins, 1989). If only one GAC adsorber is

considered, given the treatment objective, the regeneration time interval can be obtained directly with its breakthrough curve. However, the breakthrough profile predicted under ideal conditions may severely overestimate the capacity of the GAC adsorber due to influences from NOM in raw water and other operational factors, such as backwashing (e.g. Sontheimer *et al.*, 1988). Many studies (e.g. Sontheimer *et al.*, 1988; Carter *et al.*, 1993; Knappe, 1996; Gillogly, 1998; Kilduff and Wigton, 1999) have indicated that the GAC capacity for removing various micropolluants is greatly decrease after being fouled by background NOM from the influent. The fouling by background NOM changes the equilibrium constant as well as the rate constant for adsorption, hence changing the predicted breakthrough profile. Therefore, the detrimental effects should be taken into account during modeling. This preloading effect will be discussed in Section 2.6.4. In addition, periodic backwashing of GAC adsorbers can reduce the removal efficiency because the activated carbon particles are mixed during the first several backwashing and stratified afterwards (Sontheimer *et al.*, 1988). If a sand filtration process is designed upstream of GAC adsorber to remove suspended particles, GAC adsorbers can be expected to run for a long time without backwashing (Sontheimer *et al.*, 1988; Clark and Lykins, 1989).

2.6.2 Prediction of Fixed-bed GAC Adsorbers Performance

In general, two different approaches have been widely used for predicting the performance of full-scale GAC adsorbers. The first approach is to directly use fixed-bed models including the equilibrium column model (ECM) and mass transfer models. The second method is the rapid small-scale column test (RSSCT), which operates smaller columns with smaller GAC particles for shorter periods of short time to simulate long term full-scale GAC adsorber performance.

The RSSCT method scales down the full-scale or pilot scale adsorber to a small column based on a dimensional analysis of a mass transfer model, and therefore maintains the similarity between the performances of the adsorbers (Sontheimer *et al.*, 1988). Overall, the RSSCT well simulates the breakthrough curves for DOC by using the proportional diffusivity design (Crittenden *et al.*, 1991) as well as the removal of micropolluant in organic-free water using the constant diffusivity design (Sontheimer *et al.*, 1988). However, through summarizing previous results simulated by the RSSCT in natural water, an overestimation by the RSSCT, compared to pilot-scale data, was found in the low concentration range of target micropolluants probably due to the impact of background NOM (Sontheimer *et al.*, 1988). Speth and Milter (1989) also observed a significant difference between the breakthroughs obtained with the RSSCT and their pilot column, and attributed the difference to insufficient consideration of NOM fouling in the scale-up method. In a study by Summers *et al.*

(1989), large differences were still observed even when the NOM was preloaded onto small GAC particles using scale-up approach. Knappe *et al.* (1997) found that the RSSCT successfully simulated atrazine breakthrough in river water for the first five months; however, this approach failed to predict atrazine removal over longer periods of time. Therefore, caution should be taken when employing the RSSCT to predict micropolluants removal in the presence of background NOM. The NOM preloading effects on micropolluant removal need to be well understood before employing RSSCT and the scale-up method.

ECM was developed to predict multicomponent adsorption in GAC columns by assuming that different zones develop in GAC bed with each zone containing a unique combination of components. The total liquid-phase concentration is given by the sum of the individual components. There is no mass transfer resistance considered in the ECM, thus only wavefronts of micropolluants are expressed in the breakthrough profile. Consequently, it predicts the longest possible bed life, the largest overshoot concentration, and the elution order of the adsorbates (Sontheimer *et al.*, 1988). The ECM arbitrarily divides a GAC bed into a number of zones that equals the number of target adsorbates. Each zone contains a number of adsorbates. The closer the zone to the influent, the more adsorbates it contains. Thus, the last zone only contains the least adsorbable solute. The location and length of each zone depends on the relative adsorbability of the solutes in that zone (Andrews, 1990). The IAST is used to describe the competition among and the equilibrium concentrations of the micropolluants in the ECM. To complete the simulation, the ECM only requires the adsorbate influent concentration, single solute Freundlich parameters, the superficial velocity of the feed, the bed density, and the void fraction (Hand *et al.*, 1997). In order to consider competition from background NOM, hypothetic components (HCs) should be formed to represent direct competition. The effect of carbon fouling is taken into consideration using isotherm parameters determined with preloaded carbons for various time (Andrews, 1990). The ECM in combination with the methodologies of HC and varied isotherm parameters was found useful in predicting the breakthroughs of trihalomethanes in Andrews' studies (1990). However, since the ECM ignores mass transfer resistances, the model cannot produce the typical 'S' shape breakthrough profile, and thus cannot be used to predict the time to reach the maximum permissible concentrations. Therefore, it has been recommended to be used only for preliminary design calculations (Hand *et al.*, 1997).

Generally, the mass transfer models applied in predicting the performances of GAC adsorbers are based on the understanding of fundamental mass transfer mechanisms on GAC particles, and also on the consideration of advective flow as well as axial dispersion in some cases. Mass transfer

processes on GAC particles include film diffusion, surface diffusion, pore diffusion, and local equilibria between solutes and adsorption sites on GAC. Sontheimer *et al.* (1988) summarized the models commonly used for describing adsorption in GAC adsorbers (Table 2-3). As shown in Table 2-3, the main difference among the models comes from focusing on different internal diffusion mechanisms. The DFPSDM, however, is the most comprehensive mass transfer model. It should be noted that CPHSDM is only used for strong adsorption which leads to a constant shape of mass transfer zone (Sontheimer *et al.*, 1988).

Table 2-3 Fixed-bed models describing adsorber dynamics and their specific mass transfer mechanism (adapted from Sontheimer *et al.*, 1988)

Model		Mass transfer mechanisms			
Abbreviation	Full Name	Film Transfer	Dispersion	Surface Diffusion	Pore Diffusion
PFHSDM	Plug-flow homogeneous surface diffusion model	X		X	
CPHSDM	Constant-pattern homogeneous surface diffusion model	X		X	
DFHSDM	Dispersed-flow homogeneous surface diffusion model	X	X	X	
PFPDM	Plug-flow pore diffusion model	X			X
PFPSDM	Plug-flow pore and surface diffusion model	X		X	X
DFPSDM	Dispersed-flow pore and surface diffusion model	X	X	X	X
ECM	Equilibrium column model	Negligible mass transfer resistance			

It has been proven that the dispersion effects in GAC adsorbers can be negligible due to high surface loading rate usually used in water treatment applications (Weber and Liu, 1980; Sontheimer *et al.*, 1988; Smith and Weber, 1989); however, it was stated by Carter and Weber (1994) that the dispersion effects could not be ignored in bench-scale column experiments, possibly due to the slow flow rate applied. Nevertheless, in practice, two of the most commonly used mass transfer models, which are PFHSDM and PFPSDM, consider only the plug flow situation. The PFHSDM has been successfully employed to simulate the removal of various micropolluants from GAC adsorbers in organic-free and natural water (Weber and Liu, 1980; Sontheimer *et al.*, 1988; Smith and Weber,

1989; Lo and Alok, 1996; Knappe *et al.*, 1999). Many studies have also demonstrated that the PFPSDM is effective in predicting GAC adsorbers' performance in adsorbing micropollutants such as TCE and atrazine (Carter and Weber, 1994; Matsui *et al.*, 2002; Jarvie *et al.*, 2005). However, it was noted that in some of the studies mentioned above, the PSDM was ultimately reduced to the PDM. The difference between the SDM and the PDM lies in which internal mass transfer mechanism is dominant under the experimental conditions of interest. With respect to small-molecular-weight micropolluants in the presence of background NOM, Sontheimer *et al.* (1988) suggested that PFPDM was more appropriate because the preloading of background NOM appeared to shut off surface diffusion for small molecules. However, Sontheimer *et al.* (1988) also thought that in multicomponent systems strongly adsorbing components might follow surface diffusion, displacing the preadsorbed weakly adsorbing components in GAC adsorbers (Sontheimer *et al.*, 1988). Therefore, it is difficult to decide which model is most appropriate.

Since the DFPSDM is the most comprehensive model that includes all the mass transfer mechanisms, it was chosen to simulate the GAC performance in removing the selected PhACs and EDCs in this study. More details about underlying mechanisms and model formulation are discussed in the following section.

2.6.3 The Pore and Surface Diffusion Model (PSDM)

Mechanisms of Mass Transports and Basic Equations of the PSDM

The PSDM for GAC adsorbers and PAC particles considers mass transfer of solutes on and into the activated carbon particles, whereas mass transfer in the axial direction is only relevant for GAC columns. More specifically, as shown in Figure 2-1, a solute molecule contained in the bulk solution in the GAC column migrates from the bulk solution to a hypothetical film surrounding the GAC particle, i.e. the boundary layer. It then diffuses through the boundary layer to the outside surface of the GAC particle via film diffusion. Subsequently, the molecule is transported in the liquid phase within the pores of the GAC particle via pore diffusion, or along the wall of the pores by means of surface diffusion. Finally, the solute molecule, arriving at the adsorption site, attaches onto the carbon, a process that can be described by an adsorption isotherm. Although the PSDM has been proven to well capture the thermodynamics of adsorption and the physics of mass transports of the solute in GAC adsorbers, it should be noted that some assumptions were made in the construction of the model, (Sontheimer *et al.,* 1988). Significant deviation from the assumed ideal conditions may lead to errors in the prediction.

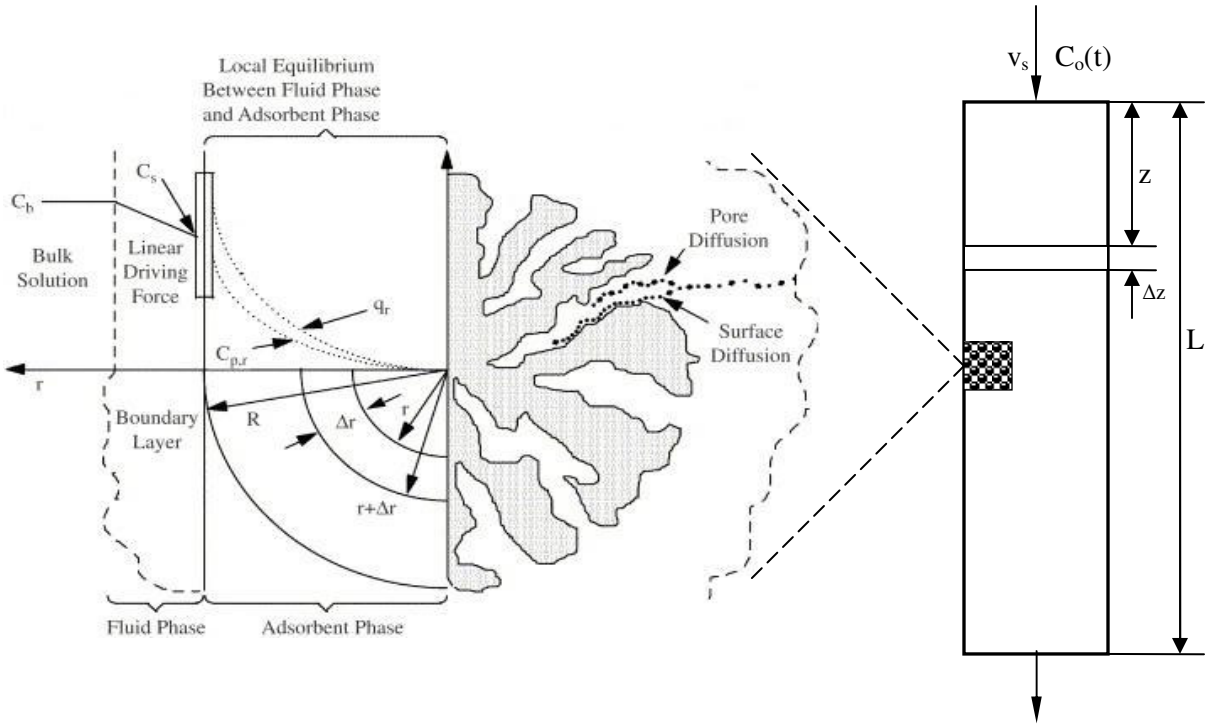

Figure 2-1 Mass transfer mechanisms in GAC adsorbers (adapted from Jarvie *et al.*, 2005)

The assumptions are as follows (Sontheimer *et al.*, 1988):

a) adsorption of solute onto activated carbon follows isothermal conditions and is reversible;

b) the attachment rate of solute onto activated carbon is negligible compared to mass transfer rates;

c) activated carbon particles are spherical and isotropic;

d) the bulk solution near a given GAC particle is completely mixed;

e) no radial direction dispersion happens inside the GAC column/adsorber, i.e. concentration gradients only exist in the direction of the flow (axial direction);

f) GAC particles are small enough, therefore, the bulk solution surrounding particles is homogeneous.

Crittenden *et al.* (1986) and Sontheimer *et al.* (1988) described the mathematical forms for the PSDM in a soil column and in GAC adsorbers, respectively. They are essentially same and presented as follows:

To describe the film diffusion, the model assumes a linear concentration driving force across the film surrounding the round GAC particles, as shown in Equation 2.19:

$$\varepsilon \frac{dC_b(t,z)}{dt} = \frac{3\beta_L(1-\varepsilon)}{R}(C_b(t,z) - C_s(t,z)) \qquad \textbf{2.19}$$

in which, C_b is the concentration in bulk solution, C_s is the liquid phase concentration on the surface of the particle, β_L is the film diffusion coefficient, ε is the GAC bed porosity, R is the radius of the particle, and t and z are the time and spatial variables, respectively .

Note that β_L is related to the free liquid diffusivity and film thickness surrounding the GAC particle (Knappe, 1996), and therefore depends on the properties of the solute molecule and the hydrodynamics of the system. Among the physical properties of the solute, the molecular size is probably the most important for defining the free liquid diffusivity (Sontheimer *et al.*, 1988). Factors such as particle topography and size (Robert *et al.*, 1985; Weber and Wang, 1987), solution viscosity, and surface loading rate for a certain system (Sontheimer *et al.*, 1988) significantly influence the hydrodynamics around the GAC particle.

Incorporation of Equation 2.19 with the mass balance in the mobile phase (axial direction) leads to Equation 2.20:

$$\frac{\partial C_b(z,t)}{\partial t} = D_z \frac{\partial^2 C_b(z,t)}{\partial z^2} - v\frac{\partial C_b(z,t)}{\partial z} - \frac{3(1-\varepsilon)\beta_L}{\varepsilon R}\left[C_b(z,t) - C_p(r=R,z,t)\right] \qquad \textbf{2.20}$$

The initial condition for axial direction is:

$$C_b(z>0, t=0) = 0 \qquad \textbf{2.21}$$

The first boundary condition (Equation 2.22) is obtained by setting the net solute mass flux into the column equal to the rate of accumulating mass in the column:

$$v\left[C_I(t) - C_b(z=L,t)\right] = \frac{\partial}{\partial t}\int_0^L \left[C_b(z,t) + \frac{3(1-\varepsilon)}{R^3\varepsilon}\int_0^R \left[\varepsilon_p C_p(r,z,t) + \rho_p q(r,z,t)\right] r^2 \partial r \right] \partial z \qquad \textbf{2.22}$$

The second boundary conditions (Equations 2.23 and 2.24) are as follows:

$$\frac{\partial^2 C_b(z=L,t)}{\partial t \partial z} = 0 \qquad \textbf{2.23}$$

$$\frac{\partial C_b(z=L,t=0)}{\partial z}=0 \qquad \textbf{2.24}$$

where D_z is the axial diffusion coefficient, C_p is liquid phase concentration in the pores of particles, q is the solid phase concentration on the surface of the pores in GAC particles, C_I is the influent concentration, v is the average interstitial velocity in the pores of the GAC bed, equal to v_s/ε, v_s is surface loading, L is the length of the GAC bed, ε_p is the porosity of GAC particles, ρ_p is the GAC particle density, and r is the radial position variable.

As mentioned previously, D_z is in general negligible under the conditions faced in drinking water applications. If the term for dispersed flow in Equation 2.20 is dropped, the DFPSDM changes into the PFPSDM.

The PSDM accounts for pore diffusion, surface diffusion, and solute mass accumulation in GAC particles in the stationary phase (radial direction). Combining the two parallel internal mass transfers with the mass balances in solid phase and liquid phase yields the following equation (Equation 2.25):

$$\frac{D_p\varepsilon_p}{r^2}\frac{\partial}{\partial r}\left[r^2\frac{C_p(r,z,t)}{\partial r}\right]+\frac{D_s\rho_p}{r^2}\frac{\partial}{\partial r}\left[r^2\frac{\partial q(r,z,t)}{\partial r}\right]=\varepsilon_p\frac{\partial C_p(r,z,t)}{\partial t}+\rho_p\frac{\partial q(r,z,t)}{\partial t} \qquad \textbf{2.25}$$

in which D_s and D_p are the surface diffusion coefficient and the pore diffusion coefficient, respectively.

For fresh GAC grains, Equation 2.26 expresses the initial condition for Equation 2.25,

$$C_p(r,z,t=0)=0 \qquad \textbf{2.26}$$

The first boundary condition (Equation 2.27) results from symmetry at the center of the GAC particle, which also follows the assumption previously mentioned,

$$\frac{\partial C_p(r=0,z,t)}{\partial r}=0 \qquad \textbf{2.27}$$

The second boundary (Equation 2.28) is based on the equivalence between the rate of liquid phase mass transfer and the accumulation of solute mass within the GAC particle, assuming that no accumulation of solute happens on the surface of the particle.

$$\beta_L R^2\left[C_b(z,t)-C_p(r=R,z,t)\right]=\frac{\partial}{\partial t}\int_0^R\left[\varepsilon_p C_p(r,z,t)+\rho_p q(r,z,t)\right]r^2\partial r \qquad \textbf{2.28}$$

Adsorption onto the activated carbon surface is described by a local adsorption equilibrium, which relates C_p and q through an isotherm equation. In this study, the Freundlich equation is used as Equation 2.29.

$$q(r,z,t) = K_F C_p(r,z,t)^{1/n} \qquad \textbf{2.29}$$

where K_F and 1/n are the Freundlich constants.

Dimensionless Formulas of the PSDM

Several dimensioned parameters in the equations for the PSDM can be combined into dimensionless groups by defining relationships among different mass transfer mechanisms and partition relationships of the solutes. Furthermore, the dimensionless forms of the equations have the advantage of simplifying the model equations. Therefore, the de-dimensionalization is commonly carried out before solving the partial differential equations (PDEs).

The basic PDEs (Equations 2.20-2.29) of the PSDM shown in the last section were de-dimensionlized (Equation 2.30 – 2.39) by Crittenden *et al.* (1986). Some dimensionless groups used to convert the dimensioned model as well as their physical meanings are shown in Table 2-4.

Mass transport in axial direction (in the GAC column):

$$\frac{1}{(D_g+1)}\frac{\partial \overline{C}_b(\bar{z},T)}{\partial T} = \frac{1}{P_e}\frac{\partial^2 \overline{C}_b(\bar{z},T)}{\partial \bar{z}^2} - \frac{\partial \overline{C}_b(\bar{z},T)}{\partial \bar{z}} - 3St\left[\overline{C}_b(\bar{z},T) - \overline{C}_p(\bar{r}=1,\bar{z},T)\right] \qquad \textbf{2.30}$$

Initial condition:

$$\overline{C}_b(0 < \bar{z} \le 1, T=0) = 0 \qquad \textbf{2.31}$$

Boundary conditions:

$$\overline{C}_I(T) - \overline{C}_b(\bar{z}=1,T) = \frac{1}{(D_g+1)}\frac{\partial}{\partial T}\left\{\int_0^1\left[\overline{C}_b(\bar{z},T) + 3D_g\int_0^1 \overline{X}(\bar{r},\bar{z},T)\bar{r}^2\partial\bar{r}\right]\partial\bar{z}\right\} \qquad \textbf{2.32}$$

$$\frac{\partial^2 \overline{C}_b(\bar{z}=1,T)}{\partial T \partial \bar{z}} = 0 \qquad \textbf{2.33}$$

$$\frac{\partial \overline{C}_b(\bar{z}=1,T=0)}{\partial \bar{z}}=0 \qquad \textbf{2.34}$$

Mass transport in radial direction (within GAC particles):

$$\frac{D_g}{D_g+1}\frac{\partial \overline{X}(\bar{r},\bar{z},T)}{\partial T}=\frac{1}{\bar{r}^2}\frac{\partial}{\partial \bar{r}}\left\{\bar{r}^2\left[\left(Ed_p-\frac{D_{gp}}{D_{gs}}Ed_s\right)\frac{\partial \overline{C}_p(\bar{r},\bar{z},T)}{\partial \bar{r}}+\left(Ed_s-\frac{D_{gp}}{D_{gs}}Ed_s\right)\frac{\partial \overline{X}(\bar{r},\bar{z},T)}{\partial \bar{r}}\right]\right\} \qquad \textbf{2.35}$$

Initial condition:

$$\overline{C_p}(\bar{r},\bar{z},T=0)=0 \qquad \textbf{2.36}$$

Boundary conditions:

$$\frac{\partial \overline{C_p}(\bar{r}=0,\bar{z},T)}{\partial \bar{r}}=0 \qquad \textbf{2.37}$$

$$\frac{(D_g+1)}{D_g}St\left[\overline{C_b}(\bar{z},T)-\overline{C_p}(\bar{r}=1,\bar{z},T)\right]=\frac{\partial}{\partial T}\int_0^1 \overline{X}(\bar{r},\bar{z},T)\bar{r}^2 d\bar{r} \qquad \textbf{2.38}$$

Binding to adsorption site as described by Freundlich adsorption equilibrium:

$$\overline{X}(\bar{r},\bar{z},T)=\frac{D_{gp}}{D_g}\overline{C}_p(\bar{r},\bar{z},T)+\frac{D_{gs}}{D_g}\overline{C}_p(\bar{r},\bar{z},T)^{1/n} \qquad \textbf{2.39}$$

In the above equations, $\overline{C}_b = C/C_o$, *C_o is the maximum influent concentration;* $\overline{C}_p = C_p/C_o$; $\overline{C}_I = C_I/C_o$; $\overline{X}=(\varepsilon_p C_p+\rho_p q)/(\varepsilon_p C_o+\rho_p q_e)$, *$q_e$ is the solid phase concentration equilibrated with C_o;* $\bar{z}=z/L$; $\bar{r}=r/R$; *throughput* $T=tv/L(1+D_g)$.

Table 2-4 Dimensionless parameters for PSDM

Name	Mathematical expression	Physical meaning
Peclet number (P_e)	vL/D_z	ratio of mass transfer by advection to by axial dispersion
Stanton Number (St)	$(1-\varepsilon)\beta_L L/(\varepsilon vR)$	ratio of mass transfer by film diffusion to by advection
Surface diffusion module (Ed_s)	$LD_p D_{gp}/vR^2$	ratio of mass transfer by surface diffusion to by advection
Pore diffusion module (Ed_p)	$LD_s D_{gs}/vR^2$	ratio of mass transfer by pore diffusion to by advection
Liquid phase solute distribution ratio (D_{gp})	$(1-\varepsilon)\varepsilon_p/\varepsilon$	ratio of solute mass in the liquid in the pores to in the bulk solution at equilibrium with C_o
Solid phase solute distribution ratio (D_{gs})	$(1-\varepsilon)\rho_p q_e/(\varepsilon C_o)$	ratio of solute mass on the adsorbent surface to in the bulk solution at equilibrium with C_o
Solute distribution ratio (D_g)	$D_{gp}+D_{gs}$	ratio of solute mass in the adsorbent particle to in the bulk solution at equilibrium with C_o

Solutions of the PSDM

The dimensionless PDEs presented above can be solved analytically based on simplifications or numerically. Although the PSDM can be simplified and the approximate analytical solutions can consequently be obtained (Crittenden *et al.*, 1986), they are valid only under certain specified conditions. The numerical simulations of adsorption systems have advanced considerably, including the implementation of the finite difference scheme (Sun and Meuneir, 1991; Smith, 1991), the finite element method (Hossain and Young, 1992), and the orthogonal collocation method (Kim *et al.*, 1978; Raghavan and Ruthven, 1983; Crittenden *et al.*, 1986; Gierke *et al.*, 1990; Roy *et al.*, 1992; Carter, 1993).

The orthogonal collocation method has been used increasingly for discretizing PDEs in the HSDM (Kim *et al.*, 1978; Raghavan and Ruthven, 1983; Roy *et al.*, 1992) and the PSDM (Crittenden *et al.*, 1986; Gierke *et al.*, 1990; Carter, 1993). As a result, ordinary differential equations (ODEs) were obtained for activated carbon systems. The orthogonal collocation method was developed by Villadsen and Stewart (1967) based on a combination of the collocation method and the finite

difference method, using orthogonal polynomial expansions fitted by collocation techniques. In this method, sets of orthogonal polynomials are chosen by a trial-function. The roots of the polynomials are orthogonal collocation (OC) points. In the applications, the PDEs can be solved only by obtaining the solutions at only a few OC points. This reduces the complexity of the solutions compared to the finite element method (Villadsen and Michelsen, 1978). In addition, the orthogonal collocation method is known to be more accurate than the finite difference method especially when a large number of OC points are used (Abdel-Jabbar *et al.*, 2001). Compared to other numerical methods, this method does not need to start from the initial conditions for each time step (Kim *et al.*, 1977). This leads to its major advantage that it is very amenable when the parameters in functions are changing with both spatial and time factors. Therefore, the adsorption and kinetic parameters that vary with time and depth in adsorbers can easily be considered and applied in the model (Carter, 1993).

More details about the orthogonal collocation method and its discretization of PDEs in PSDM were presented by Carter (1993). The resulting ODEs for PSDM are included in the Appendix A

Determination of Mass Transfer Rates

Calculation of the film diffusion coefficient by empirical correlation

As a starting point, the film diffusion coefficient (β_L) in mass transfer models can usually be calculated by correlations of dimensionless groups. In general, as in Equation 2.40, the β_L is incorporated in the dimensionless Sherwood number, Sh, which is predicted as a function of Reynolds number, Re, and the Schmidt number, Sc, respectively (Sontheimer *et al.*, 1988; Robert *et al.*, 1985).

$$Sh = A + B \cdot \mathrm{Re}^{m}\, Sc^{n} \qquad \textbf{2.40}$$

in which A, B, m, and n are correlation constants.

The Sherwood number considers laminar and turbulent contributions to transport in flow. Several groups of correlation constants were summarized and compared to the experimentally determined film diffusion coefficients by Robert *et al.* (1985) and Sontheimer *et al.* (1988). As a result, the Gnielinski correlation was found to generally achieve the best fitting over a wide Re range. Thus, it has been used widely for dilute solution conditions, which is typical for drinking water

applications (Hand *et al.*, 1997). Javrie *et al.* (2005) presented a simplified expression of the Gnielinski correlation (Equation 2.41) used for laminar flow.

$$\beta_L = \frac{(1+1.5(1-\varepsilon)\phi D_L)}{2R}(2+0.644\,\mathrm{Re}^{1/2}\,Sc^{1/3}) \qquad \textbf{2.41}$$

$$\mathrm{Re} = \frac{2\rho_L R v_s}{\varepsilon \mu_L} \qquad \textbf{2.42}$$

$$Sc = \frac{\mu_L}{\rho_L D_L} \qquad \textbf{2.43}$$

$$D_L = \frac{13.26\times10^{-5}}{\mu_L^{1.14} V_b^{0.589}} \qquad \textbf{2.44}$$

in which, ρ_L is the density of water; μ_L is the viscosity of water; V_b is the molal volume of the solute at the normal boiling point temperature; D_L is the free liquid diffusivity of the micropollutant; Φ is the GAC particle shape correction factor (1 for the particle diameter obtained from sieve analysis).

The molal volume at the normal boiling point (V_b) can be estimated using the additive-volume increments of Schroeder or Le Bas or from the critical volume (V_c) using the Tyn and Calus method. The two approaches were summarized and published by Reid *et al.* (1977).

It is important to point out that caution should be exercised when using the film diffusion coefficients estimated by this correlation because differences were observed between correlated values and experimentally determined values for film diffusion coefficients. Roberts *et al.* (1985) attributed these differences to the deviations of the real GAC particles from the spherical GAC particles assumed in the correlation method. A difference of approximately a factor of two was found between correlated and experimentally determined β_L values in this study. Moreover, it was found that the deviations from the correlations for crushed GAC were larger than for non-crushed GAC, probably due to more angular grains produced in the crushing process (Roberts *et al.*, 1985). However, a linear relationship between particle size and experimentally determined β_L was reported by Weber and Wang (1987), suggesting that the crushing process might not significantly change the particle topography. Nonetheless, it is recommended that the diffusion parameters, including β_L, should be determined by using experimental approaches, such as the short fixed-bed technique (SFB).

Determination of mass transfer parameters using experimental approaches

With respect to determination of film and internal mass transfer parameters, the experimental approaches, such as completely mixed batch (CMB) reactors, differential column batch (DCB) reactors, and short fixed bed (SFB) reactors were summarized by Sontheimer *et al.* (1988).

In the CMB reactor, activated carbon particles are completely mixed and mass transfer parameters can be obtained by fitting the appropriate mass transfer model (i.e. HSDM or PSDM) to the concentration decay data in the bulk solution. This approach is usually used for PAC systems if similar hydrodynamic conditions are applied in the tests. However, the mass transfer parameters determined in CMB reactors are not recommended to determine the kinetic parameters for fixed-bed systems, because different particle sizes and hydrodynamic conditions are usually applied in fixed-bed systems (Sontheimer *et al.*, 1988, Smith *et al.*, 1989).

In order to create hydrodynamic conditions similar to those used in large adsorbers, the DCB reactor was developed based on the CMB reactor. The solution recirculates through a thin layer of activated carbon fixed in a column, resulting in influent and effluent concentrations that are the same. Similarly, the mass transfer parameters are also determined using the concentration decay profile of the bulk solution. This system was applied for determining mass transfer parameters for three pesticides and phenols by Jaffre *et al.* (2000) and Furuya *et al.* (1996), respectively. Although this system overcomes the hydrodynamic differences, the concentration decay in the bulk solution may lead to an inaccurate determination of the internal diffusion coefficients (in particular, the surface diffusion coefficient) because they are both influenced by the solute concentration. Furthermore, this approach can not be applied in this study because large sample volumes used to determine solute concentrations would significantly influence the total solute mass in the bulk solution, thus leading to inaccuracies.

The third method used to determine mass transfer parameters uses a SFB reactor, which is also called as a short bed adsorber (SBA). This technique was developed by Weber and Liu (1980) for single solute solutions, and then was proven to also be an effective technique in multicomponent systems (Liang and Weber, 1984). Moreover, the SFB reactor has shown its effectiveness in evaluating the adsorption kinetics of lindane in the presence of a model humic substance using the HSDM in combination with the IAST (Smith *et al.*, 1987). Subsequently, the adsorption of two SOCs (TCE and DCB) in the presence of uncharacterized background NOM was successfully evaluated using the SFB technique, though, as stated by the authors, the impact of long preloading times was not considered (Smith and Weber, 1989). Nevertheless, the SFB technique has been demonstrated to

be an effective tool for determining mass transfer parameters of preloaded activated carbon, which were subsequently used in the evaluation of the preloading effect of background NOM on specific micropollutant, such as TCE, MIB, and atrazine using the HSDM or PSDM (Carter and Weber, 1994; Gillogly, 1998; Knappe *et al.*, 1999).

The SFB reactor is a small column filled with a short bed of the GAC of interest. The GAC bed is located between two layers of glass beads which are similar in size to the GAC particles. The bed depth is short enough to achieve an immediate breakthrough of the solute and the initial breakthrough ratio should be between 0.2 and 0.5. The bed is continuously fed with a solution of constant concentration with the hydraulic loading rate of interest. The breakthrough curves are recorded and used to determine film and internal diffusion coefficients. Generally, as shown in Figure 2-2, at the initial stage of breakthrough, the mass transfer process is controlled by film diffusion. In this case, the β_L value can be determined independently based on the breakthrough data in the initial stage (Weber and Liu, 1980; Carter and Weber, 1994). The late breakthrough profiles express the predominant types of controls, which may be film diffusion or one of the internal diffusions independently or all mechanisms taking effect simultaneously. One advantage of this method is that it is more sensitive to changes in film diffusion and internal diffusions coefficients than a long adsorber (Weber and Liu, 1980). The advantage of the SFB technique over the two reactors is that it can simulate the characteristic hydrodynamic conditions and associated solute removal patterns of large adsorbers in small reactors. Given these advantages of the SFB technique, it was applied for determining kinetic parameters of the target compounds with the selected GACs. More details on the design of the SFB reactor are presented in Chapter 5.

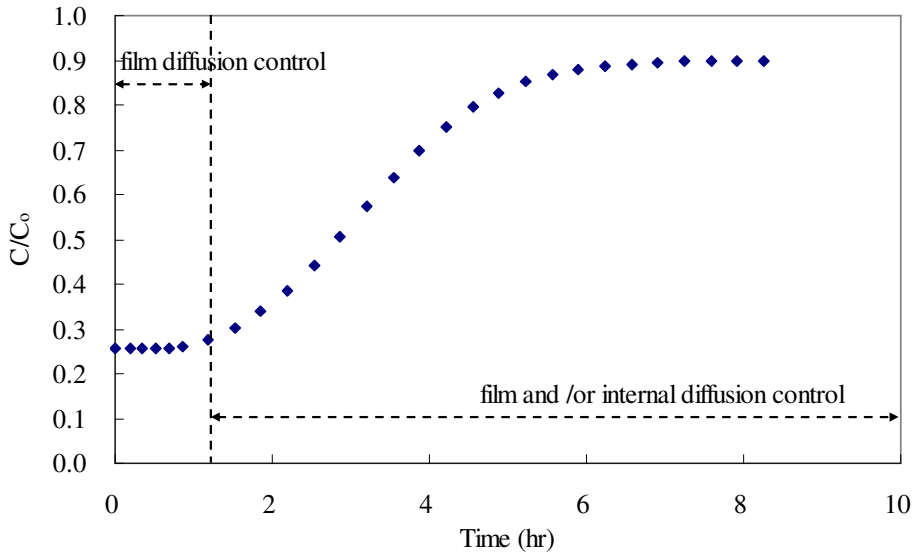

Figure 2-2 Hypothetical breakthrough curve of SFB reactor

However, a study by Carter (1993) found that the coefficients for surface diffusion (D_s) and pore diffusion (D_p) in the PSDM could not be determined simultaneously by fitting SFB experimental data because the two mechanisms acted in parallel. Therefore, the pore diffusion coefficient and surface diffusion coefficient were calibrated individually by setting the other one as zero. The calibration was first carried out for D_p; if the estimated D_p value is larger than the free diffusivity (D_L) of the target compound, this would suggest that the surface diffusion is dominant (Carter, 1993). This methodology was found satisfying in modeling TCE breakthrough on GAC columns in both the absence and presence of background NOM (Carter, 1993). Matsui *et al.* (2003) in their study for adsorption of three pesticides onto PAC in natural water calibrated D_p and D_s seperately. However, different from Carter's approach, the calibration started from D_p equal to D_L. If the good fit could not achieve until D_p decreased to $0.25D_L$, D_s was introduced into model for further calibration by fixing D_p at $0.25D_L$ (Matsui *et al.*, 2003).

2.6.4 GAC Fouling – Long-time Preloading Effect

In a fixed-bed GAC adsorber, the MTZ of background NOM usually moves far beyond the MTZ of the target micropollutant because the background NOM is present at much higher concentrations and it usually has an adsorbability lower than the target micropollutant. As a result, the adsorber is fouled (or preloaded) prior to micropollutant adsorption. In addition, the preloaded background NOM is usually not desorbed from activated carbons (Summer and Robert, 1987) and not replaced by most

micropollutants (Kilduff and Wigton, 1999), thus it is expected that the reduction in capacity for micropollutants in fixed-bed adsorbers is mostly attributed to the preloading and not the direct competition from background NOM. This point of view has been confirmed in the studies for atrazine by Knappe *et al.* (1999) and for MIB by Gillogly (1998) on preloaded carbons.

Effects on Adsorption Capacity

It has been shown in many studies that the preloading of background NOM can significantly reduce the equilibrium capacity of GAC for micropollutants (e.g. Sontheimer *et al.*, 1988; Carter and Weber, 1994; Kilduff *et al.*, 1998; Knappe *et al.*, 1999).

In terms of interpreting the mechanism behind capacity reduction of target micropollutant by the preloading effect, it is commonly accepted that the background NOM first take up the high energy sites and also block the pores through which the micropollutant molecules access adsorption sites. Newcombe *et al.* (2002b) explained that low-molecular-weight NOM larger than MIB molecules diffuses into mesopores and is subsequently adsorbed onto secondary micropores, thus totally blocking access to adsorption sites within the micropores. Meanwhile, the high-molecular-weight NOM adsorbs only at or near the external carbon surface and does not affect the adsorption of MIB significantly (Newcombe *et al.*, 2002b). Kilduff *et al.* (1998) found that preloading with NOM <3K Da exerted a marked influence on the capacity reduction for TCE, while, similar to the conclusions made by Newcombe *et al.* (2002b), preloading with the 10-30K Da fraction of NOM onto GAC did not have any effect in terms of a capacity reduction. No direct competition between atrazine and background NOM was identified in the study by Knappe *et al.* (1999) on the GAC preloaded for five months, suggesting that the available sites on preloaded GAC were accessible to atrazine molecules but not to background NOM after the GAC was fully preloaded. However, the adsorptive capacity continuously reduced on GAC preloaded for 20 and 25 months, even after the GAC was totally exhausted after 5 months (Knappe *et al.*, 1999). Two possible mechanisms may contribute to this observation. First, the weakly adsorbed NOM was replaced by more strongly adsorbed NOM (Roberts and Summers, 1982), therefore further reducing the adsorption sites for the target compound. Second, the adsorbed NOM became reoriented in the GAC particles, hence blocking more pores. The latter was hypothesized by Summers *et al.* (1989) in the explanation of the change of mass transfer rates on preloaded GAC. However, a verification of these two mechanisms has not been presented to date.

When the Freundlich isotherm is used to describe the equilibrium capacity of preloaded GAC, it was found that the Freundlich K_F is a function of preloading time (e.g. Sontheimer *et al.*, 1988; Carter and Weber, 1994; Kilduff *et al.*, 1998; Knappe *et al.*, 1999). Sontheimer *et al.* (1988) recommended a time-variable function representing the reduction of the Freundlich K_F (Equation 2.45):

$$\frac{K_F(t)}{K_{F0}} = 0.01 \times [A1 - A2 \times t + A3 \times \exp(-A4 \times t)] \qquad \textbf{2.45}$$

in which $K_F(t)$ is the Freundlich K_F at time t; K_{F0} is the Freundlich K_F on virgin GAC; A1, A2, A3, and A4 are the empirical kinetic constants specific to a given micropollutant, water matrix, and GAC.

Carter and Weber (1994) adopted a simpler expression (Equation 2.46) to simulate the capacity reduction of TCE on preloaded GAC.

$$K_F(t) = A1 + A2 \exp(A3 \times t) \qquad \textbf{2.46}$$

However, the fundamental physical meanings of the parameters have not been defined; and thus a general expression has yet to be developed.

The observations of the change in the Freundlich 1/n are contradictory. A similar Freundlich 1/n was observed by many investigators such as Sontheimer *et al.* (1988), Summers *et al.* (1989), and Crittenden *et al.* (1991) regardless of time. In contrast, other studies (Carter and Weber, 1994; Kilduff *et al.*, 1998) have demonstrated that the Freundlich 1/n was also a preloading time variable. Carter *et al.* (1995) further investigated the impact of preloading on site energy distributions in GAC particles. Their analysis proved that preloading by a non-desorbable solute resulted in a loss of surface heterogeneity, which was indexed by the Freundlich 1/n (Carter *et al.* 1995). Kilduff *et al.* (1998) confirmed that the site energy distribution shifted to even lower energy sites, reducing average site energy and adsorption capacity at higher preloading levels. Assuming these judgements are true, the Freundlich 1/n, which is the index of the heterogeneity of activated carbons, would be approaching one. Also, it would be influenced only by the low-molecular-weight NOM, which can access the adsorption sites of activated carbon. If no more background NOM is adsorbed after the GAC is exhausted or no reorientation of the adsorbed NOM on GAC particles occurs, the Freundlich 1/n would be constant.

Determination of the capacity of preloaded GAC is typically carried out by using preloaded original size GAC or crushing the preloaded GAC into pulverized GAC (PGAC). Qi (1992)

compared atrazine capacities on uncrushed GAC and PGAC in natural water and found that PGAC showed an artificially high capacity, probably due to the fact that the equilibrium was not achieved in uncrushed GAC. However, both Carter *et al.* (1992) and Knappe *et al.* (1999) demonstrated that the use of PGAC led to overestimation of remaining capacities for TCE and atrazine, respectively. These differences resulted because the crushing process opened the pores blocked by background NOM and made more heterogeneous sites available (Carter *et al.*, 1992). Since the preloading effect has been proven to be independent of particle size (e.g. Summers *et al.*, 1989; Gillogly 1998), it is recommended that the determination of the remaining capacity of preloaded GAC should be conducted on small size, uncrushed preloaded GAC.

Effects on Mass Transfer Rates

Theoretically, the film diffusion should be constant when hydrodynamic conditions do not change in a certain GAC adsorber system. Surprisingly, some studies (Carter and Weber, 1994; Knappe *et al.*, 1999; Schideman *et al.*, 2006a) showed that the film diffusion coefficient (β_L) decreased as preloading time increased. For TCE adsorption from river water, Carter and Weber (1994) showed that the β_L on virgin GAC was 2.5 times larger than that on GAC preloaded for three weeks. It was also found that the β_L determined for adsorbing atrazine on GAC preloaded for five months dramatically decreased compared to that on virgin GAC; however, longer preloading times only had a slight effect on β_L (Knappe *et al.*, 1999). The exact reasons and mechanisms for decreasing β_L values due to preloading have not been clarified to date. However, Carter and Weber (1994) suggested two possible reasons. 1) The local viscosity of the film surrounding a GAC particle increased due to preloading, resulting in decreased diffusion rates of micropollutant molecules across the hydrodynamic boundary layer. 2) Some effective area for mass transfer flux into the carbon particle is blocked by preloaded background NOM, leading to reduced film diffusion flux. Recently, a relationship between the time and spatial variable β_L and the NOM surface loading on GAC particles was suggested by Schideman *et al.* (2006a), which consequently made it possible to account for time and spatial variations of the film diffusion coefficient in model predictions using a more general NOM surface loading parameter. Nevertheless, the influence of a decreasing β_L on the predictions made by mass transfer models and actual GAC adsorber breakthrough is thought to be negligible compared to the reduction of internal diffusion flux during preloading (Carter and Weber, 1994). However, a recent publication (Schideman *et al.*, 2006b) demonstrated that the reduction in film diffusion was most pronounced at early breakthrough phases and in GAC adsorbers with longer EBCTs.

The impact of preloaded NOM on the internal diffusions has been widely reported (e.g. Sontheimer *et al.*, 1988; Carter and Weber, 1994; Gillogly, 1998; Knappe *et al.*, 1999; Ebie *et al.*, 2001, Schideman *et al.*, 2006b) and attributed to the limited channel access to the adsorption sites caused by preloaded large-molecular-size NOM. Some of these studies expressed the reduction of internal diffusion in terms of a decrease in the surface diffusion coefficient (Gillogly, 1998; Knappe *et al.*, 1999; Ebie *et al.*, 2001, Schideman *et al.*, 2006b). However, Sontheimer *et al.* (1988) stated that the surface diffusion flux is significantly reduced on preload carbons, and thus pore diffusion contributed mostly to the internal diffusion flux. Carter and Weber (1994) utilized time-variable pore diffusion to predict TCE breakthrough in natural water. Interestingly, no matter which internal diffusion mechanism was used, the simulation results were generally all satisfying, probably because the two internal diffusion mechanisms mutually compensated for each other in the calibration using the bench-scale kinetic experimental data. Nevertheless, if the pore diffusion coefficient (D_p) is defined as the relationship between the liquid free diffusivity (D_L) and the tortuosity of the pores in carbon particles, as shown in Equation 2.47, then the τ_p can increase, accounting for the preloading effect.

$$D_p = \frac{D_L}{\tau_p} \qquad \textbf{2.47}$$

in which τ_p is the particle tortuosity.

It has been generally observed that the τ_p is equal to 1 when the adsorbers are operated for less than 70 days, and it increases linearly with preloading time (Jarvie *et al.*, 2005), as shown in Equation 2.48.

$$\tau_p = 0.334 + 6.61\times10^{-6}\times t \qquad \textbf{2.48}$$

where t is preloading time in minutes.

However, the proposed linear relationship (Equation 2.48) between the τ_p and preloading time should have a maximum value because the loading of NOM on GAC would decrease and eventually stop when the adsorbers are saturated with NOM. Carter and Weber (1994) found that Equation 2.49 could fit best for the experimentally determined τ_p.

$$\tau_p = A - B\times\exp(C\times t) \qquad \textbf{2.49}$$

in which t is time in weeks, and A, B, and C are the fitted parameters.

Although the application of time-variable internal diffusion coefficients increased the accuracy of model predictions, it should be noted that time-variable functions are empirical and thus adsorption system specific.

2.7 Research Gaps and Objectives

As summarized in the previous review, EDCs and PhACs are detected in surface and ground water worldwide, generally in the ng/L - low μg/L range. Consequently, an increasing number of studies, though still limited, found the occurrence of the EDCs and PhACs in the finished drinking water. Although drinking water standards do not yet exist for these substances, a recent study by Pomati *et al.* (2006) demonstrated that a mixture of pharmaceuticals at typical environmental levels (ng/L level) can lead to physiological and morphological effects on human embryonic cells. Therefore, it is imperative for the water treatment industry to move forward to investigate the removal of EDCs and PhACs, which may be present in their source water. However, there are numerous EDCs and PhACs, and the distribution of these compounds is country and region specific; therefore, it is important to develop an evaluation protocol for selecting representative compounds for further treatment research.

In order to characterize the occurrence of EDCs and PhACs of interest, an analytical method based on GC/MS, the instrument available in our research lab, should be developed. In general, previously published multi-residue analytical methods (Ternes *et al.*, 1998; Lopez *et al.*, 1998) either focused on a group of specific compounds with similar properties or utilized complex sample preparation schemes that often included sequential elution as well as separate derivatization of different groups of compounds. Experimental conditions in these studies were investigated separately for different group of compounds in order to increase detection sensitivity. Therefore, it is desirable to develop a multi-residue analytical method which covers most of the selected PhACs and EDCs. This should be approached systematically based on a statistical experimental design, so that both the efficiency and accuracy of the determination may be improved simultaneously.

In terms of the current drinking water treatment techniques available for removing EDCs and PhACs, activated carbon is recommended as a promising option. The prediction of the removal of EDCs and PhACs is largely based on the assumption that they are similar to pesticides in both physicochemical properties and concentration levels present in the water matrix, and thus they are expected to be efficiently removed by activated carbon (Janex *et al.*, 2003; USEPA 2003; Jones *et al.*, 2005). However, these assumptions are not generally applicable since PhACs and EDCs are usually

present in lower concentrations (low μg/L to ng/L) than pesticides. In addition, PhACs and EDCs tend to be more polar and hydrophilic than most pesticides. Studies investigating the removal of EDCs and PhACs by adsorption mostly focused on documenting treatment efficiencies and to a lesser degree on underlying mechanisms Thus, detailed adsorption characteristics in pure water and natural water in the form of isotherms have not been well documented for PhACs and EDCs at sub μg/L concentrations. PAC is expected to provide an option for removing the EDCs and PhACs, and therefore PAC has been under more investigations. However, it seems that lack of understanding of the direct competition between background NOM and target PhACs and EDCs. Note that in practice PAC is usually applied for seasonal events such as taste and odor problems. When treating persistent or pseudo-persistent compounds such as PhACs and EDCs, a continuous process such as a GAC adsorber would be preferred over PAC for operational and cost reasons. However, there are no detailed studies to date with respect to sub μg/L removal of PhACs and EDCs by GAC. Although many investigations have demonstrated that various mathematical models are capable of predicting the performance of GAC adsorbers in removing a number of micropollutants, their applicability for the lower concentration levels of EDCs and PhACs should be evaluated. A thorough understanding of specific thermodynamic and rate mechanisms, including the consideration of preloading effects from background NOM, would facilitate more reliable predictions of EDC and PhAC removals utilizing the GAC adsorber models. Furthermore, detailed mechanistic information based on the a validated model would provide guidance in the design of GAC adsorbers with respect to removing EDCs and PhACs.

Given the knowledge gaps summarized above, the following objectives were developed:

1) Develop protocols for screening the wide variety of EDCs and PhACs and for selecting target compounds that are most representative for a GAC adsorption study. The evaluation criteria should consider the occurrence of EDCs and PhACs in wastewater effluent, surface, ground, and drinking water, as well as their reported or possible toxicity. In addition, the selection should take into account local occurrence data and analytical capabilities.

2) Develop a multi-residue analytical method for simultaneous determination of the selected target compounds with GC/MS. Special attention is to be put on optimization of enrichment and derivatization steps by using a multi-factorial experimental design. In addition, the stability of the target compounds is to be investigated in order to select a suitable preservation method. Using the developed analytical method, the occurrence of target

compounds in local river and drinking water is to be surveyed briefly in order to aid in compound selection.

3) Determine equilibrium and kinetic parameters for adsorption of selected EDCs and PhACs onto selected virgin GAC and understand the mechanisms of EDCs and PhACs adsorption. It is important to first understand the isotherms and mass transfer mechanisms for adsorption at the low concentration levels (low μg/L to ng/L) of EDCs and PhACs. The analysis on isotherm and kinetic parameters in ultrapure water will provide an opportunity to compare the adsorption characteristics of the EDCs and PhACs to those of other micropollutants.

4) Investigate the reduction of adsorption capacity caused by direct competitive adsorption in the presence of background NOM in the natural water of concern, namely the Grand River. Potential removal of the selected compounds by PAC will be estimated based on the application of the IAST-EBC model.

5) Determine the preloading effect from background NOM on the capacity and on the mass transfer rates of adsorption of selected EDCs and PhACs onto the selected GAC. Preloading effect will be studied as a function of time over a period of several month in order to simulate conditions experienced during full-scale application of GAC adsorbers. The intent is to understand which factors in a preloaded system are influencing the GAC adsorption behaviors of the selected EDCs and PhACs at low concentration levels. Parameters such capacities and mass transfer rates which will be determined for GAC preloaded for different times will also be used as input for a predictive GAC adsorber model.

6) Predict the breakthrough of selected EDCs and PhACs in pilot GAC adsorbers. The validity of the predictive model will be examined using pilot data obtained under real water treatment conditions. Recommendations for choosing a better adsorption processes (PAC or GAC) as well as designing full-scale GAC adsorbers will be made based on the modeling results. The modeling results will also offer an opportunity to make recommendations for removing other trace level PhACs and EDCs in larger adsorbers.

CHAPTER 3
SELECTION OF TARGET COMPOUNDS

3.1 General Considerations

Since a great amount of survey pertaining to EDCs and PhACs has been reported in the scientific literature, the very first task in this study was the prioritization of the EDCs and PhACs of concern. The list of candidate EDCs and PhACs was determined based on a literature review. As for EDCs, only natural and synthetic steroid hormones, some alkylphenol polyethoxylates (APEOs) and their metabolites, phthalates such as DBP and BBP, as well as bisphenol A (BPA) were considered, partially because they were of great interest when this project was initialized. In addition, numerous conventional contaminants such as pesticides or industrial chemicals are also known or suspected EDCs. However, these compounds have already been studied in detail in a drinking water treatment context and they were therefore not considered in this study. With respect to PhACs, the preliminary screening focused only on pharmaceuticals used mainly for human treatment. The PhACs studied in the environmental field in the reviewed literature and the top 50 most prescribed pharmaceuticals in Canada were included in the preliminary candidates list.

The selection of the target compounds for the adsorption study involved three stages, including preliminary prioritization for a general purpose of drinking water treatment studies, then screening compounds in combination with a local survey, and final decision making based on adsorption properties. In the first stage, the preliminary list of EDC and PhAC candidates was identified as previously described. In order to generate the list of target compounds, two issues were generally considered. The first consideration was occurrence in water, including STPs effluent, as well as surface, ground and drinking waters. The second consideration was possible toxicities of the candidate compounds in order to link the occurrence or data of consumed amount to a health effect. Then, the assessment factors were developed to prioritize the chemicals. Since EDCs and PhACs have different data availability with respect to their occurrence and toxicity (estrogenicity to EDCs), the screening processes for EDCs and PhACs were different. As a result, more than one hundred EDCs and PhACs were narrowed down to 18 target compounds with a variety of physicochemical properties. The goal of the second stage was to screen the target compound candidates on the priority list in combination with their occurrence in local waters. Accordingly, an analytical method based on GC/MS was developed to support subsequent limited survey work. One significance of this work was

to promote the relevance of subsequent treatment study to the local situations. In the last stage, only three compounds, which were considered as most representative, were chosen for the GAC study, mainly based on the survey data and their physicochemical properties related to the adsorption study. This chapter only presents the results from the first and third stages. The development of the analytical method and the results of the survey will be discussed in Chapter 4.

3.2 Evaluation and Selection of the Target EDCs

Prior to the discussion, it should be noted that the data being considered in this section were collected only until late 2003, the time when compounds were selected for further study. Since then, more data on environmental concentrations and toxicity (or estrogenicity) have been published. It is expected that the addition of more recently published data into the database might have some influence on the decisions, which will be discussed later in this section. However, the assessment process considers multiple factors which should therefore minimize the unreliability of the evaluation results. Furthermore, the same assessment approaches can be recommended when re-evaluating the candidate EDCs and PhACs when new data are available.

3.2.1 Evaluation Criteria

The information used for evaluating the EDCs were $\log K_{ow}$, estrogenic activity, reported concentration range in surface water and drinking water, and information which was available on drinking water and wastewater treatment processes at the time when performing these evaluation.

$\text{Log}K_{ow}$ was considered because it is an important physicochemical parameter used for predicting the tendency of a chemical to partition between water and solid organic matter. Generally, a $\log K_{ow}$ of less than 2.5 demonstrates a low sorption potential, and log K_{ow} greater than 4 shows a high sorption potential (Voulvoulis and Scrimshaw, 2003). Therefore, it can be predicted that chemicals with lower $\log K_{ow}$ would have a greater tendency to be present in STP effluents and consequently in receiving surface water. Since only the occurrences of EDCs in water were of concern for this project, the focus was on the more hydrophilic compounds.

As defined by World Health Organization (WHO, 2002), EDCs are a group of exogenous chemicals that exhibit biological hormonal activity. Nevertheless, most toxicological studies on EDCs were focused only on their estrogenic activity. Therefore, the estrogenic activity of each EDC was evaluated by estradiol equivalent factors (EEF), which utilizes the estrogenic activity of E2 as a reference point and is accordingly set to 1. Accordingly, the EDC with relatively lower estrogenic

activity than E2 would have an EEF value less than one. The EEF of each EDC was calculated mainly based on literature values for estrogenicity assays such as the estrogen receptor-mediated, chemical-activated luciferase reporter gene-expression (ER-CALUX) assay (Legler *et al.*, 1999). No observed effect concentration (NOEC) for E2 with the ERC assay was reported to be 0.3 ng/L (Ghijsen and Hoogenboezem, 2000). Correspondingly, the NOEC values of the other compounds were calculated by dividing 0.3 ng/L by the reported or derived EEF of the compounds, thus suggesting that the EDC with a low EEF value would have a NOEC value larger than 0.3 ng/L. It should be noted that the EEF values of NP1EO, NP2EO, NP1EC and NP2EC (Table 3-1) are derived on the assumption that the estrogenic activities of these compounds are similar to NP (Fawell and Chipman, 2001; Bennie, 1999). Therefore, once experimentally determined EEF values become available and are different from the above assumption, then the assessment results presented in this thesis should be re-examined.

The reported environmental concentrations of the candidate EDCs were also of importance in selecting the target compounds. The reported data in Canadian surface water was highlighted separately in order to emphasize the Canadian context in the evaluation. Both concentrations in the environment and potential health effect as indicated by NOEC values were combined when judging the overall significance of a compound. Therefore, it was expected that an EDC with either high environmental concentration or low NOEC value might present high potential of risk and thus possibly be selected.

In addition, information regarding treatment studies for the target compounds available at the time of this assessment was considered. In this case, the compounds, which are less studied or have been found to be poorly removed in the studied treatment processes, are given a higher rank. In addition, less studied processes for the candidate compounds were of higher interest, as they were indicative of any research gaps.

Information such as $\log K_{ow}$, estrogenic activity, reported concentration ranges in surface water and drinking water and, treatment process studies available at the time of assessment were collected and summarized in Table 3-1.

The collected information was evaluated with the different factors discussed. Each factor was assigned a weight and five levels (grades) were used for each factor (Table 3-2). It should be noted that the factor of the reported concentrations were evaluated using the quotient of the actually determined concentration (ADC) and the no observed effect concentration (NOEC) (Ghijsen and Hoogenboezem, 2000). More specifically, the ADC in the calculation was the maximum reported

concentration found in the reviewed references, and the NOEC values were calculated according to the method discussed before. This method could reasonably relate the determined concentrations to a possible toxicological risk to human health based on the argument that water which is safe for the aquatic ecology is safe for the preparation of drinking water with conventional techniques (Ghijsen and Hoogenboezem, 2000). The application of this method presumably went over some limitations in the risk assessment, such as shortage of toxicological data on humans and compatibility of toxicological data on aquatic organism with on humans.

Consequently, for each candidate compound, a value – Σ (grade * weight) was calculated. Because the grade and weight were set somewhat arbitrarily, to achieve a robust evaluation, the weights for each factor were changed six times (Table 3-3), and accordingly, six values of Σ (grade * weight) were assayed together and assigned a final grade, on which the EDC selection was based.

Table 3-1 Summary of EDCs candidates

Name	Group	Log K_{ow}	Estrogenic activity		Concentration in surface water (ng/L)[b]	Concentration in surface water (ng/L) (Canada) [c]	Concentration in drinking water (ng/L) [d]	Removal treatment [e]
			EEF [a]	NOEC (ng/L)				
E2	Steroid hormones	3.94	1	0.3	0.6-9	Detected	0.3-0.7	PAC, GAC;UV; Cl_2, O_3
E3		2.81	0.002	150	19	NR	0.35	PAC, GAC;UV
E1		3.43	0.058	5.2	0.7-27	Detected	0.4	PAC, GAC;UV
EE2		4.15	0.81	0.37	0.2-73	NR	0.35,<5	PAC, GAC;UV;Cl_2, O_3
NP	APEOs and their metabolites	4.48	$3.8*10^{-5}$	7894	10-180000	$1.1*10^{4}$-$2.6*10^{6}$	ND-140	STPs; ***GAC, coagulation***
NP1EO		4.17	~$3.8*10^{-5}$	7894	20-69000	<LOD-7800	ND-1100	STPs; ***Sand filtration; GAC and coagulation***
NP2EO		4.21	~$3.8*10^{-5}$	7894	20-32000	<LOD-10000	ND-250	STPs; ***Sand filtration; GAC and coagulation***
NP1EC		1.34	~$3.8*10^{-5}$	7894	NR	NR	NR	NR
NP2EC		1.34	~$3.8*10^{-5}$	7894	2000-71000	NR	164	NR
4-OP		4.12	$1.4*10^{-6}$	214258	5-3000	<5-84	10	NR
OP1EO		4.10	NR[b]	NA	NR	NR	NR	NR
OP2EO		4.00	NR	NA	NR	NR	2	NR
BPA	BPA	3.4	$7.8*10^{-6}$	64000	0.5-776	NR	1.1	STPs; ***UV***
DBP	Phthalate esters	3.74-5.15	$1.8*10^{-8}$	$1.7*10^{7}$	500-13500	NR	NR	STPs
BBP		3.57-4.91	NR	NR	500-2000	NR	NR	STPs

NR: not reported; Detected: reported to be detected but no data shown; ND: not detected; NA: not applicable

a. Most EEF values are calculated based on ERC values from Ghijsen and Hoogenboezem's report (2000). EEF of E3 comes from YTHS (yeast two-hybrid system screen) (Saito et al., 2002). EEF of NP1EO, NP2EO, NP1EC and NP2EC are derived on the assumption that the estrogenic activities of these compounds are similar to NP. (Fawell and Chipman, 2001; Bennie, 1999).

b. From references Bruchet et al., 2002; Alda and Barcelo, 2001; Kolpin et al., 2002; Servos, 2003; Ying et al., 2002b; Blok and Wosten, 2000; Kuch and Ballschmiter, 2001; Ghijsen and Hoogenboezem, 2002; Bennie, 1999; Ying et al., 2002a; Heemken et al., 2001; Fromme et al., 2001; Belfroid et al., 2002; Yuan et al., 2002

c. From references Servos et al., 2003; Bennie et al., 1997; Bennie, 1999; Ying et al., 2002a; CEPA, 1999

d. From references Ying et al., 2002b; Kuch and Ballschmiter, 2001; Petrovic et al., 2002; Bennie, 1999; Ghijsen and Hoogenboezem, 2002

e. Bold font: drinking water treatment studies. Regular font: wastewater treatment studies.From references Walker, 2000; Blok and Wosten, 2000; Fawell et al., 2001; Ying et al., 2002a, Ahel et al., 1994; Tanghe and Verstraete, 2001; Ahel et al., 1996; Furhacker et al., 2000; Staples et al., 1998; Kang and Kondo, 2002; Fukanori et al., 2003; Marttinen et al., 2003; Gavala et al., 2003; Staples et al., 1997

Table 3-2 Evaluation standards for EDC assessment

Weight[1] / Grade[2]	10% Log K_{ow}	20% Estrogenic activity[a]	10% Concentration in surface water[b]	20% Concentration in Canadian surface water[b]	20% Concentration in drinking water[c]	20% Removal treatment
0		No data reported or no estrogenic effect				Intensive studies in drinking water treatment reported, no more research needed
3	$LogK_{ow} \geq 4$, high potential for removal during STPs, possibly no occurrence in surface water, and might be removed by coagulation or filtration	$EEF \leq 10^{-6}$	ADC/NOEC < 0.001	ADC/NOEC < 0.001	ADC/NOEC<0.001	No or only few studies done in drinking water treatment, but much research done on wastewater treatment, good removal reported
5	No Survey Data Reported					
6	$2.5<LogK_{ow}<4$	$10^{-6}<EEF<10^{-3}$	$0.001 \leq$ ADC/NOEC < 0.01	$0.001 \leq$ ADC/NOEC < 0.01	$0.001 \leq$ADC/NOEC<0.01	No or only few studies done in drinking water treatment, but much research done on wastewater treatment, poor removal reported
9	$LogK_{ow} \leq 2.5$, soluble in water, possibly get through STPs, occur in surface water	$EEF \geq 10^{-3}$	ADC/NOEC $\geq$ 0.01	ADC/NOEC $\geq$ 0.01	ADC/NOEC<0.01	No treatment technique reported or poor removal

0 = no importance; 3 = minor importance; 6 = important; 9 = very important

ADC: The actually determined concentration. Maximum actually reported concentration in literature was assumed as ADC from conservative perspective.

NOEC: No observed effect concentration.

a The level of E2 which could cause estrogenic effect is 0.3 ng/L. Therefore, if $EEF \geq 10^{-3}$, ng/L level could lead to estrogenic effect; if $10^{-6} < EEF < 10^{-3}$, μg/L level could lead to estrogenic effect.

b A safty factor of 1000 was used based on the standards from the Priority Substances List Assessment Report (CEPA, 1999), ×10 for interspecies variation, ×10 for intraspecies variation and x10 for potential teratogenicity.

c Standard of drinking water should be more stringent than for surface water. In this table, the same factor is still in use because no criterion about how to evaluate the possible risk to human health from EDCs in drinking water has been reported.

3.2.2 Results and Discussion

In the evaluation, each EDC was assigned to a significant level according to its mean value. The evaluation approach and results are shown in Table 3-3. If a candidate EDCs with a 'neutral significance' or higher significant level was chosen, 12 compounds (i.e. E2, E1, EE2, E3, NP, NP1EO, NP2EO, NP1EC, NP2EC, OP, OP1EO and OP2EO) were selected into the priority list. However, considering the availability of standards in further analytical work and possible similarity between NP1EO and NP2EO, and also between NP1EC and NP2EC, the latter ones of these two groups were taken off the list. OP1EO and OP2EO were also removed because of their similarity to NP1EO and NP2EO.

When looking at Table 3-3 in detail. It is not surprising that all the steroid hormones were given very high significant levels mainly due to their high estrogenicity and corresponding low NOEC values, though they were all found at extremely low concentrations in the environment. For example, the NOEC of the synthetic hormone EE2 is 0.37 ng/L, while the detected maximum concentrations in surface water and drinking water were 73 and 0.35 ng/L, respectively, thus leading to the ratio of ADC to NOEC substantially larger than 0.01. As a matter of fact, most analytical methods developed for detecting EE2 in water matrices have their limits of detection (LODs) ranging from 0.32 – 20 ng/L (Belfroid *et al.*, 1999; Quintana *et al.*, 2004; Soliman *et al.*, 2004; Yu *et al.*, 2007). This suggests that once EE2 is detected, it should be of great concern. Additionally, although steroid hormones have moderate $\log K_{ow}$, which means that they may be removed during STPs, the concentrations of free steroid hormones in STP effluent may be higher than in STP influent due to the deconjugation effect by microorganisms in the activated sludge (e.g. D'Ascenzo *et al.*, 2003). Since all the steroid hormones were of high priority, to ease the analytical burden, only natural E1 and synthetic EE2 were considered in the development of the analytical method. In addition, it should be noted that E1 is partially formed by the degradation of E2 during the sewage treatment (Ying *et al.*, 2002a). Thus the detection of E1 suggests the potential occurrence of E2.

With respect to NP and its mono- or di- ethoxylates, the high $\log K_{ow}$ values generally indicate the tendency of high removal during STP process due to the adsorption on the sludge. Nonetheless, their potential risks are still considerable because it has been reported occurring widely at high concentrations in the aquatic environment. Consequently, their ADC/NOEC values are at high ranking, though their NOECs are much higher than four steroid hormones. The overall grades for the metabolites (NP1EC and NP2EC) are of great significance mainly attributable to the high solubility

and to knowledge gaps of treatment technologies. STPs are considered as the main sources of short chain NPEOs and their metabolites entering into the environment, though STPs are the main way to remove the long chain NPEO discharged by industries and residents. It has been proven that NP, short chain NPEOs and NPECs are formed as the metabolites of long-chain NPEOs during STPs process (CEPA, 1999c, Ahel *et al.*, 1994; Bennie *et al.*, 1999). In addition, short chain NPEOs and NPECs formed in the primary biodegradation can not be ultimately biodegraded due to the presence of the highly branched alkyl group on the phenolic ring (Voulvoulis *et al.*, 2003). Compared to short chain NPEOs, corresponding NPECs are more soluble, thus tends to present in STP effluent. Therefore, all of these factors possibly contribute to their high occurrence in the environment.

The exclusion of BPA, DBP and BBP were mainly due to their high treatability during STPs, and relatively low estrogenic activities. In general, since their ADC/NOEC values are much lower than other candidates, it is unlikely that they impose a risk for human health. Furthermore, BPA has been proven to be easily degraded in STP processes and river systems (Furhacker *et al.*, 2000; Kang and Kondo, 2002). This feature may keep it from being persistent in the environment.

It should be noted that, when this assessment was carried out, the reported concentrations in Canadian waters were very limited. This may contribute to the uncertainty in the judgment, while reducing the Canadian representativeness. In addition, most treatment technologies in terms of drinking water had yet to be studied in detail. Following this reasoning, a limited survey of prioritized compounds in raw and finished drinking water would aid in the final decision.

Table 3-3 Evaluation results for EDCs

Compounds	K_{ow}	Estrogenic Activity	Concentration in surface water	Concentration in Canadian surface water	Concentration in drinking water	Removal Treatment	Total						Mean	Final Grade
							1	2	3	4	5	6		
E2	6	9	9	6	9	6	75	78	76.5	76.5	72	73.5	75	++
E3	6	9	9	5	6	6	67	71	69.5	69.5	68	66.5	69	+
E1	6	9	9	6	9	6	75	78	76.5	76.5	72	73.5	75	++
EE2	6	9	9	5	9	6	73	77	75.5	75.5	71	72.5	74	+
NP	3	6	9	9	9	3	66	63	60	60	54	57	60	O
NP1EO	3	6	9	9	9	3	66	63	60	60	54	57	60	O
NP2EO	3	6	9	9	9	3	66	63	60	60	54	57	60	O
NP1EC	9	9	5	5	5	9	70	74	76	76	78	76	75	++
NP2EC	9	6	9	5	9	9	76	77	77	77	80	80	78	++
4-OP	3	6	9	3	3	9	54	57	57	60	66	63	60	O
OP1EO	3	6	5	5	5	9	58	59	61	64	66	67	63	O
OP2EO	3	6	5	5	3	9	54	55	57	60	64	63	59	O
BPA	6	6	9	3	5	3	49	52	49	47.5	47	44.5	48	-
DBP	3	3	3	5	5	3	38	36	36	36	34	36	36	--
BBP	3	6	6	5	5	3	47	48	46.5	46.5	43	43.5	46	-
Weights Distribution														
Total-1	10%	20%	10%	20%	20%	20%	++ (≥ 75): very high significance;							
Total-2	10%	30%	10%	10%	20%	20%	+ (65 – 75): high significance;							
Total-3	10%	30%	5%	10%	20%	25%	O (55 – 65): neutral significance;							
Total-4	5%	30%	5%	10%	20%	30%	- (45 – 55): minor significance;							
Total-5	10%	20%	10%	10%	10%	40%	-- (< 45): no significance							
Total-6	5%	20%	5%	10%	20%	40%								

3.3 Evaluation and Selection of the Target PhACs

Because a very broad spectrum of pharmaceuticals are used and eventually possibly occur in the environment, the list of candidate PhACs was determined based on literature reviews and the top 50 prescribed drugs in Canada in 2002 (http://www.imshealthcanada.com). As a result, 86 pharmaceuticals were short listed. Subsequently, a review of concentrations reported in literature until late 2003 was conducted. The collected concentration data were organized into classes such as STPs effluent, surface water, ground water and drinking water. The 86 pharmaceuticals belonged to 23 categories based on their therapeutical effects. The numbers of drugs detected in the different water matrices (STP effluent, surface water, ground water, drinking water) were 31, 45, 9, and 12, respectively. In general, the residuals of short-listed pharmaceuticals in STP effluents ranged from ng/L to μg/L, while drug residuals in the other three water matrices were all between lower than the LOQ and tens of ng/L.

To provide insights into the potential human health impacts of pharmaceuticals, the toxicity assessment data for sub-prescription dosage would be necessary. However, these data was extremely limited or non existent. For this reason, the PBT (environmental persistence, bioconcentration potential, and aquatic toxicity) profiler, which was developed by the US EPA, was applied for evaluating the toxicity of the candidate pharmaceuticals. The PBT pollutants are defined as the chemicals that are persistent in the environment, bioaccumulate in food chains and are toxic, thus potentially posing a risk to human health and ecosystems. The PBT profiler estimates the fish chronic value (ChV), which is the index of the aquatic toxicity, by using the Ecological Structure Activity Relationships (ECOSAR) program. More information can be obtained on http://www.pbtprofiler.net. The ChVs estimated by the PBT profiler were used as an indicator for toxicity in the evaluation, assuming there would be the potential for long-term exposure to pharmaceutical residuals if they are regarded as persistent chemicals. However, it should be noted that ChVs estimated based on quantitative structure activity relationships (QSARs) could induce some uncertainties, thus should be verified if experimental data is available (http://www.pbtprofiler.net). In addition, it remains a debate as to whether or not the potential human health risks from exposure to pharmaceuticals in the environment are negligible compared to the therapeutic dosage (Schwab *et al.*, 2005). Nevertheless, the sub-therapeutic dosage may lead to adverse effects through a mechanistic pathway different from that producing the therapeutic effect in a long run (Bruce *et al.*, 2006). Furthermore, synergistic/antagonistic and possible mixture effects at trace level concentrations of PhACs over an extended period of time should be an issue of concern, especially to the sensitive population groups,

based on precautionary principles (Daughton and Ternes, 1999; Jones *et al.*, 2002). Follow this reasoning and due to the lack of toxicity data, it was assumed that the compound with high potential long-term risk to aquatic animals (indexed as ChV herein) would pose a high potential risk to humans.

Meanwhile, overall drug consumption data in Canada on a mass basis were obtained from Environment Canada through Dr. Mark Servos. This provided a chance to preliminarily examine the potential impact of the consumed drugs on the Canadian ecosystem and population based on consumption mass. However, it should be indicated that no other factor such as transformation of the drug in the human body and degradation in the environment were considered.

Generally, the prioritization of the candidate PhACs was carried out in two steps including first prescreening and late considerations of potential health effects and prescription volumes. The objective of the first step was to rule out drugs of minor significance from the large candidate pool. The selection criteria were as follows:

a) Having a reported concentration in surface water, groundwater or drinking water

b) Being listed in the top 50 most prescribed drugs in Canada

c) The ChV was lower than 10 mg/L, which indicates the drug has potentially moderate toxicity to fish.

When a candidate pharmaceutical satisfied two of the above criteria, it was preliminarily selected. In consequence, 28 pharmaceuticals out of 86 candidates were identified for further assessment in the second step. In step two, the ChV values of the 28 pharmaceuticals were calculated using the PBT profiler; and the quotient of overall consumption weight (OCW) divided by the corresponding ChV value was used to assess the potential impact on ecosystems and humans, and thus to screen out insignificant compounds. If the screening criterion was arbitrarily set to 100, as shown in Table 3-4, 22 pharmaceuticals would be chosen.

Among the 22 drugs with OCW/ChV larger than 100, EE2 and estrogen were removed because they have already been included in the list of EDCs. Tetracycline and acetylsalicylic acid were reported to be easily degraded in the environment (Heberer, 2002; Stuer-Lauridsen *et al.*, 2000), therefore, were not considered as persistent contaminants. Accordingly, they were deleted from the list. Furthermore, three antibiotics such as sulfamethoxazole, clarithromycin and erythromycin were excluded because they are also widely applied for veterinary treatment (*Hirsch et al.*, 1999) and should be analyzed on LC/MS which was not available in the lab; thus they might be studied independently. Simvastatin, warfarin, and amlodipine were eliminated from the list after also

considering the limitations of the instrumentation. Nevertheless, the ranking of these three pharmaceuticals are high in Table 3-4 because of their low ChVs. Thus, they should be of further concern if appropriate instruments (such as LC/MS) were available. As a result, 12 pharmaceuticals were finally chosen as target compounds. Chapter 4 describes the development of the analytical method based on the GC/MS for the selected EDCs and PhACs.

Information on the selected EDCs and PhACs are shown in Appendix B.

3.4 Final Selection of Target Compounds for Adsorption Study

It was generally considered that the compounds selected in the first stage all warrant further study with respect to their removal during drinking water treatment processes. However, due to limitations on time and maximum workload, the number of target compounds needed to be further reduced according to certain requirements. Therefore, the final selection was based on the analytical quality (Table 4-2), one-time survey results in Grand River and local tap water (Table 4-6), and the consideration of representiveness in terms of the adsorption on activated carbons.

To facilitate further GC/MS analytical work, the final target compounds should have LODs in drinking water and surface water less than 5 ng/L and good chromatographic performance. At the same time, in order to promote the significance of this study, the selection focused only on those compounds detected in the local area. As for choosing representative compounds for the adsorption study, the target compounds' physicochemical properties should cover a range from hydrophilic to hydrophobic, namely $\log K_{ow}$ from <2.5 to >4, with acidic or neutral properties in water.

According to above criteria, ibuprofen, naproxen, carbamazepine and nonylphenol were chosen for adsorption studies. However, in subsequent isotherm studies using bottle point method showed that ibuprofen sharply degraded after 6 days even in the ultrapure water due to unclear reasons (Yu *et al.*, 2005). Therefore, it was not further investigated because of difficulties in controlling the experimental data quality.

Section 5.1 will present the properties of the selected target compounds in detail.

Table 3-4 Simple risk assessment of candidate pharmaceuticals

Compound Name	OCW (kg)[†]	ChV (mg/L)[§]	OCW/ChV (x10^6 L)
CODEINE	52,827.62	0.06	880,460.33
ACETAMINOPHEN	735,093.35	1.1	668,266.68
IBUPROFEN	180,216.30	5.5	32,766.60
SIMVASTATIN	1,745.29	0.056	31,165.89
TRICLOSAN	617.04	0.022	28,047.27
NIFEDIPINE	3,294.61	0.17	19,380.06
SALICYLIC ACID	24,710.41	550	19,008.01
WARFARIN	425.82	0.027	15,771.11
TETRACYCLINE	8,646.50	0.84	10293.45
SULFAMETHOXAZOLE	24,062.71	3.9	6,169.93
ETHINYLESTRADIOL	234.32	0.04	5,858.00
ESTROGEN (CONJUGATED)	209.06	0.044	4751.36
CLARITHROMYCIN	16,106.38	4.1	3,501.39
DILTIAZEM	14,594.26	20	2,702.64
AMLODIPINE	862.82	0.34	2,537.71
CARBAMAZEPINE	19,181.30	14	1,370.09
NAPROXEN	25,139.28	24	1,047.47
GEMFIBROZIL	967.80	0.93	1040.65
PROPRANOLOL	2,497.61	3.5	731.60
DICLOFENAC	3,476.63	530	709.52
ERYTHROMYCIN	11,774.17	17	692.60
ACETYLSALICYLIC ACID	263,490.64	550	479.07
LEVOTHYROXINE	45.35	1.0	45.35
FUROSEMIDE	6,861.44	170	40.36
ENALAPRIL	1,333.23	93	14.34
CIPROFLOXACIN	12,731.14	1600	7.96
HYDROCHLOROTHIAZIDE	7,824.96	1900	4.12
PRIMIDONE	1,077.38	270	3.99
DIGOXIN	13.51	4.4	3.07

OCW: Overall consumption in weight
ChV: Fish chronic value
†. Source from "Overall drug consumption in Canada based on IMS data (2001)"
§. ChV from http://www.pbtprofiler.net

CHAPTER 4
ANALYTICAL METHOD FOR SELECTED COMPOUNDS

4.1 Introduction

In order to characterize the occurrence of the EDCs and PhACs in local waters and determine the target compounds in the further research project on adsorption, a trace analytical method with high precision and proficiency was required for simultaneously determining most of the selected PhACs and EDCs. As discussed in the literature review, although several papers describe multi-residue analytical methods for determining micro-pollutants in water with GC/MS (Bucheli *et al.*, 1997; Ternes *et al.*, 1998; Lopez *et al.*, 1998), none of them were suitable for the selected compounds. The published methods were either focusing on a group of specific compounds with similar properties or they utilized complex sample preparation schemes often including sequential elution and separate derivatization of different groups of compounds. Therefore, the aim of this study was to develop a fairly simple method which could quantify the selected neutral and acidic target compounds while building on work published by others. This was approached systematically by using a multi-factorial experimental design and statistical analyses thus identifying and optimizing the significant experimental factors. Although this approach has not been used very frequently in analytical method development, it has been employed successfully to optimize the derivatization of a group of acidic drugs by Rodríguez *et al.* (2003). However, this study focuses on optimizing not only the derivatization step for the selected compounds but also looks at extraction issues such as cartridge capacity and elution of analytes. In addition, a stability test was conducted to seek out a suitable preservation conditions. And finally, the developed analytical method was used to determine the occurrence of target compounds in river and tap water thus aiding in compound selection for the subsequent adsorption studies.

This chapter is mainly adapted from the manuscript submitted for publication in the *Journal of Chromatography A* (Yu *et al.*, 2007).

4.2 Experimental

4.2.1 Reagents

HPLC grade methanol and GC grade acetone and toluene were purchased from EMD (Darmstadt, Germany). The silylation reagent – dichlordimethylsilane (DCDMS) was obtained from Aldrich (Milwaukee, WI, USA). The derivatization reagents – MTBSTFA + 1% *tert.*-dutyl-dimethylchlorosilane (TBDMCS) and BSTFA + 1% trimethylchlorosilane (TMCS), were supplied in ampoules by Pierce (Rockford, IL, USA). Oasis HLB solid phase extraction cartridges (3 mL, 60 mg) were purchased from Waters (Milford, MA, USA), and cellulose filtration paper (0.45 µm pore size, 47 mm diameter) was obtained from Pall (Ann Arbor, MI, USA).

The target compounds ibuprofen, salicylic acid, 4-OP, 4-n-NP, gemfibrozil, acetaminophen, naproxen, triclosan, propranolol, diclofenace, carbamazepine, nifidipine, codeine, E1, EE2 and diltiazem were all purchased from Sigma-Aldrich (St. Louis, MO, or Milwaukee, WI, USA; or Steinheim, Germany). Target compounds –NP1EO and NP1EC were initially obtained from Environment Canada. Internal standard (I.S.) 1,4- bis(pentafluorobenzoyl)benzene (BPFBB) and surrogates dihydrocarbamazepine (DCH) and meclofenamic acid were obtained from Sigma-Aldrich (St. Louis, MO, or Milwaukee, WI, USA). [$^2H_3$] Mecoprop (mecoprop – d3) was purchased from Dr. Ehrenstorfer (Augsbury, Germany) and [$^2H_4$] estrone (E1-d4) from CDN isotope (Quebec, Canada).

Except for codeine which was purchased as a 1000 µg/mL stock solution in methanol, all stock solutions (1000 µg/mL) were prepared in acetone and stored at 4 °C in a refrigerator for a maximum of 6 months.

4.2.2 Instrumentation

The derivatized analytes were analyzed on a GC-MS system consisting of a HP 5890, a MD 5791 and an auto-sampler HP 7673 (Agilent Technologies). Helium was used as the carrier gas (constant flow at 1.2 mL/min). A fused-silica column (DB 1701, 30 m x 0.25 mm, 0.25 µm) connected to a length of deactivated guard column was installed in the system. Injection of a 4 µL sample was performed with a split/splitless injector at a temperature of 220 °C and held splitless for 60 s. Derivatized samples were kept at 4 °C on the auto-sampler tray equipped with a cooling system in order to inhibit potential continuation of derivatization reaction.

The GC oven was programmed as follows: 3 min at 45 °C, first ramp 20 °C/min to 200 °C, 5 min at 200 °C, second ramp 10 °C/min to 250 °C, 5 min at 250 °C, third ramp 5 °C/min to 300 °C, 5 min at

300 °C. The total analysis time was approximately 41 min. The GC/MS interface temperature was set at 300 °C. Mass spectra were obtained using electron impact ionization (70 eV) in full scan mode (scanning m/z ranging from 50 to 550) in preliminary experiments, and later on in selected ion mode (SIM).

4.2.3 Glassware Preparation

All glassware was silanized with DCDMS (10 % (v/v) in toluene) in order to minimize the adsorption of trace level target compounds on the glass walls. First the glassware was rinsed with the silylation reagent, cleaned 3 times with toluene followed by 3 times with acetone, and then heated to 150 °C for at least 12 h.

4.3 Sampling and Preservation

4.3.1 Experimental

Possible factors leading to loss during sampling, transportation and storage are microbiological activity and hydrolysis. Considering that low solution pH might increase the degradation rates of compounds subject to acid-catalyzed hydrolysis (e.g. Winslow *et al.*, 2001), and also enhance the adsorption of target compounds on NOM, preservation by acidification was not investigated. Instead, stability tests were conducted by adding 0.01 % (w/v) sodium azide into spiked river water (50 ng/L of each analyte). Samples were stored at 4 °C and at room temperature for predetermined time intervals after which they were processed and analyzed in duplicate.

4.3.2 Results

The results shown in Figure 4-1 suggest that most target compounds (carbamazepine, naproxen, diclofenac, triclosan, E1, NP1EO) were stable at room temperature and at 4 °C. However, concentrations decreased over time for a number of compounds albeit at different rates. EE2 and ibuprofen concentrations declined more slowly i.e. after 5 days of storage whereas gemfibrozil, NP and OP decreased steadily within 2 days of storage. Only salicylic acid showed rapid degradation after only one day which was similar to results observed by Servos *et al.* (2006). In contrast, NP1EC concentrations increased in the first few days, and then leveled off thereafter. One possible reason for this increase may be the degradation of nonylphenolethoxylates (NPEOs), the parent compounds, which may have been present in the river water. However, no corresponding increase of NP1EO was

observed. Note that longer chain NPEOs were not routinely monitored in our lab and hence, no further investigations have been carried out.

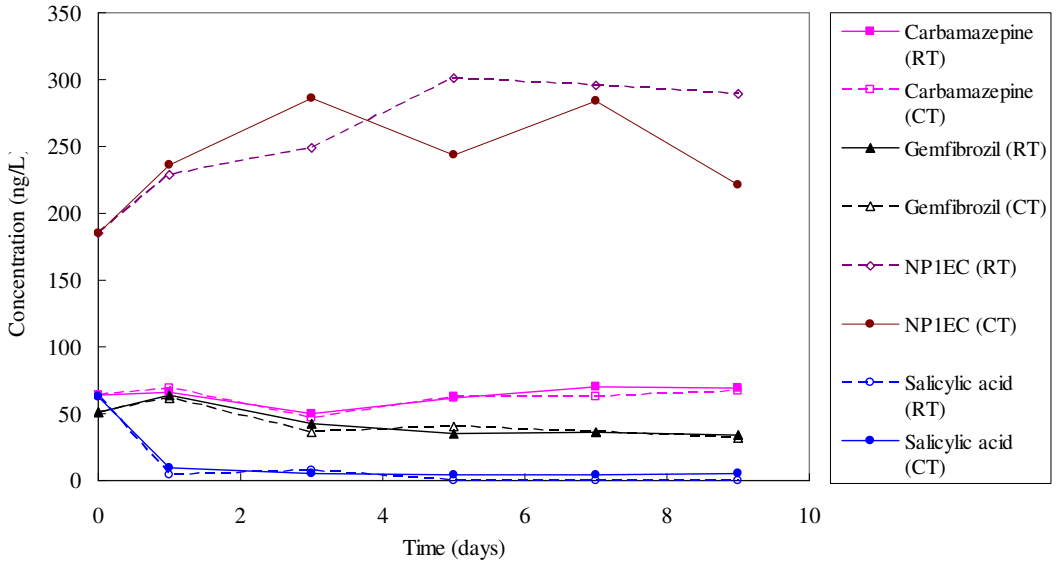

Figure 4-1 Stability test at room temperature (RT) and 4 °C (CT) (Only selected compounds shown for better visual presentation, more details shown in Figure 1&2 in Appendix C)

Although preservation by azide addition worked well for a number of compounds, overall it is recommended to extract samples within 24 h of sampling to avoid losses of some target compounds. Samples to be analyzed for salicylic acid or NP1EC need to be extracted immediately after sampling since sample storage would lead otherwise to unreliable analytical results. Note also that interestingly there was no substantial difference observed for storing samples at room temperature or at 4 °C when azide was added (Figure 4-1).

Therefore, the general sampling approach applied for waters in the environment is as follows: surface and drinking water samples are collected in 1 L and 2 L Teflon bottles. Solid sodium azide (0.01 %, w/v) is added to samples in order to inhibit biological activity. After collecting the sample, the bottles are capped and agitated by hand until the preservative is dissolved. To post chlorinated water, 2-3 drops of 3 % $Na_2S_2O_3$ solution may be added in order to eliminate residual chlorine. Samples are cooled during shipment not exceeding 10 °C, and then stored in the lab at 4 °C in darkness. Samples are extracted as soon as possible i.e. within 24 h. If sample processing has to be interrupted, it was done by storing the dried extraction cartridge prior to elution below -5 °C.

4.4 Optimization of Derivatization

4.4.1 Selection of Derivatization Reagent

Most of the target compounds contain hydroxyl and/or carboxyl groups and have therefore a high polarity and a low volatility. Derivatization will usually decrease the polarity and increase the volatility of the analytes thus making them accessible to GC analysis. Preliminary experiments explored the alkylation of carboxyl groups with PFBBr. But numerous by-products were formed hence requiring an additional clean-up step. Derivatization with PFBBr was therefore not pursued further. Silylation reagents will derivatize both hydroxyl and carboxyl groups. BSTFA and MTBSTFA are commonly used for silylation and were evaluated according to the following criteria: 1) completeness of the derivatization; 2) conversion of all polar groups; 3) by-product formation (Lerch *et al.*, 2003); and 4) response of the derivatized product. Preliminary experiments showed that generally, both reagents reacted well with the hydroxyl and carboxyl groups in the target compounds. However, the performance of the derivatization reagents varied especially for compounds with sterically hindered functional groups which made the evaluation more complex. MTBSTFA reacted selectively with the aromatic hydroxyl group in EE2 resulting in only one peak namely TBS-EE2, whereas derivatization with BSTFA lead to the formation of mono- and di-TMS-EE2. In this case BSTFA was able to react with the aromatic hydroxyl group but only partially with the aliphatic hydroxyl group in EE2 (refer to structures in Appendix B). In addition, EE2 was found to partially break down into E1 during derivatization with MTBSTFA (24 – 30 % under optimized derivatization conditions), whereas this was not observed during BSTFA derivatization. Shareef *et al.* (2004; 2006) found almost 100 % of EE2 converted into E1 when using MTBSTFA, while about 42 % of EE2 was degraded into E1 when derivatizing with BSTFA. The different conversion ratios between Shareef's and this study may be due to different experimental conditions. Codeine was found to yield a single and therefore larger peak by BSTFA derivatization whereas the incomplete reaction with MTBSTFA led to two smaller peaks. Although MTBSTFA and BSTFA both improve chromatographic performance through derivatization of polar functions, in preliminary experiments it was found that for most acidic drugs TBS derivatives (from MTBSTFA) had a higher response than TMS derivatives (from BSTFA). In addition, TBS derivatives are of greater thermal and hydrolytic stability (Rodríguez *et al.*, 2003), which is beneficial for storage. Further choice of the derivatization reagent and reaction conditions were approached systematically through a factorial experimental design as described in the next sections.

4.4.2 Scheme of Central Composite Design

Factors in Experimental Design – Time, Temperature, and Dosage

Obviously, derivatization reactions are affected by many possible factors, such as solvent, time, temperature, and reagent dosage. The reaction may be at sub-optimal settings if the effects are unknown, and if factors (i.e. parameters) are not optimized. Therefore, the objectives were to use a multi-factorial experimental design to first identify significant factors and factor interactions, and then to identify settings of these factors which showed an increased yield of the desired derivative, while yields of the undesirable derivative were decreased if more than one derivative was found.

Factors investigated for each derivatization reagent were time, temperature and dosage. Experimental domain points (= range for each factor) were selected according to conditions reported in the literature. The reaction times for BSTFA and MTBSTFA were reported to vary largely from 15 to 60 min (Boyd *et al.*, 2003; Shareef *et al.*, 2004; Jeannot *et al.*, 2002). The variation might be caused by structural differences in the target compounds and also by interactions with other factors such as reagent dosage and temperature. Considering that 16 target compounds with quite different properties were to be derivatized simultaneously, the central point was set to 60 min. With respect to the reaction temperature, 60-80 ^{o}C was commonly used (Kelly, 2000; Boyd *et al.*, 2003; Jeannot *et al.*, 2002), and the central point was chosen at 80 ^{o}C. The dosage of the derivatization reagent (ranging from 100-200 µL) was reported as having the most significant effect on the derivatization of several acidic drugs (Rodríguez *et al.*, 2003). To ensure the complete reaction of all target compounds, the central point was set to 130 µL while keeping the overall volume at 200 µL through the addition of either acetone for experiments with BSTFA and ethylacetate for experiments with MTBSTFA. Acetone was reported to be a favourable solvent for BSTFA derivatization (Rompa *et al.*, 2003), and ethylacetate was to be most suitable for MTBSTFA derivatization (Rodríguez *et al.*, 2003). In the experiments, the target compound concentrations were set to 4 µg/200 µL in order to obtain a good response on the GC/MS.

Central Composite Design

The effects of reaction time, temperature, and dosage as well as derivatization reagents on the final derivatization output were investigated systematically by employing a factorial experimental design. In order to find the optimal setting for derivatization, a central composite design, which is a type of factorial experimental design, was applied for this study.

A factorial experimental design is a statistical experimental design in which each of the independent variables (i.e. factors) is investigated at two or more levels (typically high vs. low). This is done by performing a series of tests in the lab (= runs) with different high and low settings. In a full factorial design, all possible combinations of high and low settings are investigated; in a fractional factorial design, a subset of combinations is investigated. The designed experimental results are then statistically evaluated. This approach has the advantage over the often employed one-at-a time optimization that it identifies the effect of each independent variable acting on its own, in addition to determining the interactions among two or more factors. Factorially designed experiments are also less time consuming than the one-at-a-time approach since they require a much smaller number of individual experimental runs (US NIST, 2006).

A central composite design is a type of factorial design where, besides factorial points, more star points and central points are considered in order to investigate the response surface corresponding to the main effects and the multi-factor interactions. The star points are determined by the value of α, which indicates the relative distance from the central point to the star point and depends on the number of experimental runs in the factorial portion of the central composite design (US NIST, 2006). In this study, the circumscribed central composite design with $\alpha = 1.682$ (Table 4-1) was based on the factors and experimental domains as described in the previous section. A brief flow chart of the overall optimization process is presented in Figure 4-2.

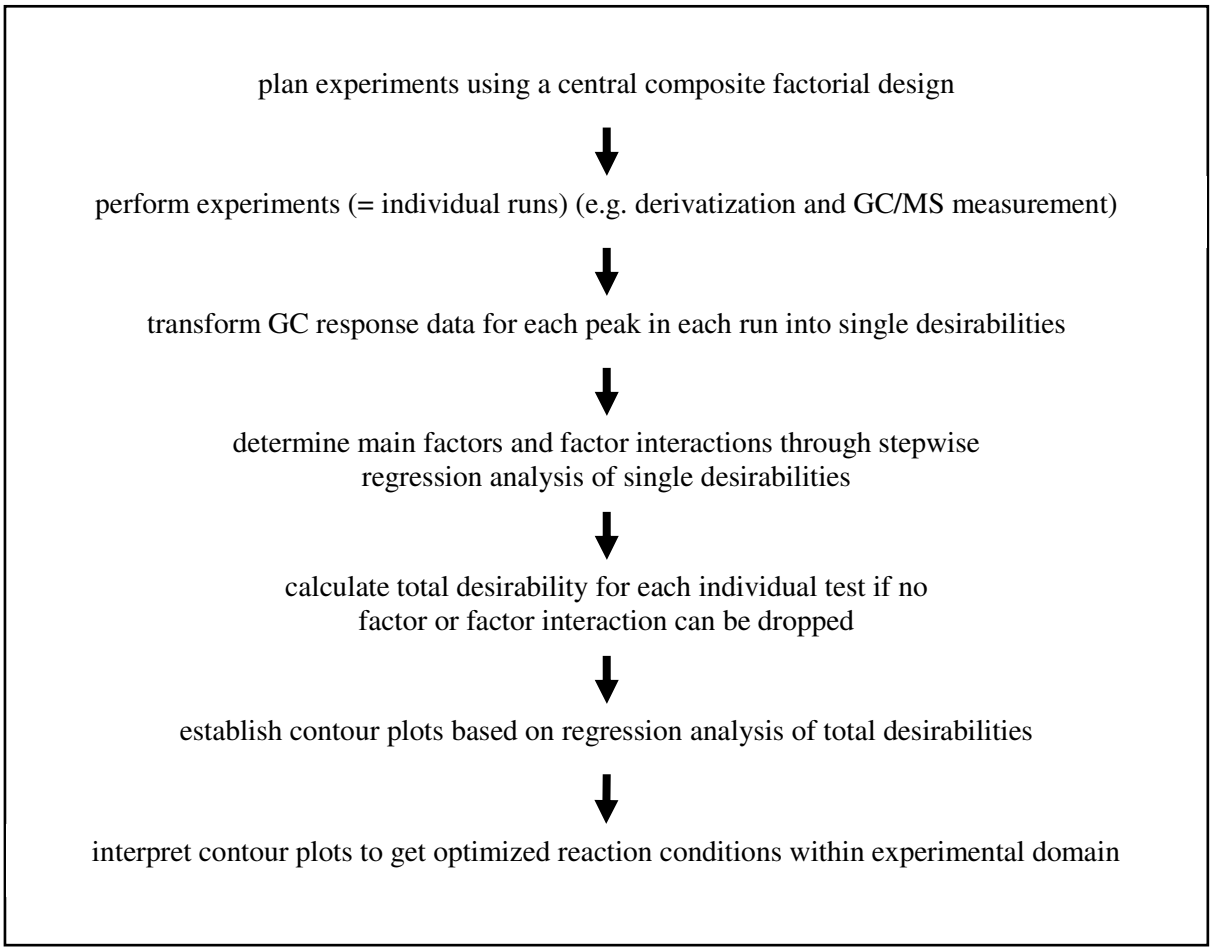

Figure 4-2 Scheme of the optimization process for derivatization

In total, this optimization study required 40 individual runs including 6 replicates at the central point for each derivatization reagent. The test order was randomized in order to eliminate time and other block effects (as shown in Table 4-1). Because it was not feasible to perform all runs within one day, the study was divided into two blocks i.e. experiments were performed on 2 consecutive days. Immediately after reaction, the samples were stored at -15 ^{o}C until being analyzed by GC/MS thus suppressing any continuing reaction. Preliminary experiments showed that there was no substantial difference in responses between the same sample analyzed immediately and after storage at -15 ^{o}C for 48 h. BPFBB was chosen as the I.S. since it did not react with either derivatization reagent. The SIM was used to detect each compound and the I.S. The quantifier ions were mostly the ion peaks with the largest abundance (Table 4-2). The area ratio of the quantifier ion peak for each target compound to that of the I.S. was calculated as the response for each compound in each of the 40 runs.

Table 4-1 Central composite design for derivatization

Std. No.	Run No.	Block[a]	Point Type[b]	Time (min)	Temperature(°C)	Dosage(μL)	Reagent Type
1	23	Block 1	Corner	30	60	60	BSTFA
2	21	Block 1	Corner	90	60	60	BSTFA
3	22	Block 1	Corner	30	100	60	BSTFA
4	7	Block 1	Corner	90	100	60	BSTFA
5	3	Block 1	Corner	30	60	200	BSTFA
6	24	Block 1	Corner	90	60	200	BSTFA
7	1	Block 1	Corner	30	100	200	BSTFA
8	5	Block 1	Corner	90	100	200	BSTFA
9	19	Block 1	Center	60	80	130	BSTFA
10	17	Block 1	Center	60	80	130	BSTFA
11	13	Block 1	Center	60	80	130	BSTFA
12	16	Block 1	Center	60	80	130	BSTFA
13	37	Block 2	Star	9.5	80	130	BSTFA
14	26	Block 2	Star	110.5	80	130	BSTFA
15	39	Block 2	Star	60	46.4	130	BSTFA
16	36	Block 2	Star	60	113.6	130	BSTFA
17	31	Block 2	Star	60	80	12.3	BSTFA
18	29	Block 2	Star	60	80	247.7	BSTFA
19	27	Block 2	Center	60	80	130	BSTFA
20	35	Block 2	Center	60	80	130	BSTFA
21	11	Block 1	Corner	30	60	60	MTBSTFA
22	20	Block 1	Corner	90	60	60	MTBSTFA
23	4	Block 1	Corner	30	100	60	MTBSTFA
24	8	Block 1	Corner	90	100	60	MTBSTFA
25	18	Block 1	Corner	30	60	200	MTBSTFA
26	9	Block 1	Corner	90	60	200	MTBSTFA
27	2	Block 1	Corner	30	100	200	MTBSTFA
28	10	Block 1	Corner	90	100	200	MTBSTFA
29	14	Block 1	Center	60	80	130	MTBSTFA
30	6	Block 1	Center	60	80	130	MTBSTFA
31	12	Block 1	Center	60	80	130	MTBSTFA
32	15	Block 1	Center	60	80	130	MTBSTFA
33	38	Block 2	Star	9.5	80	130	MTBSTFA
34	25	Block 2	Star	110.5	80	130	MTBSTFA
35	30	Block 2	Star	60	46.4	130	MTBSTFA
36	34	Block 2	Star	60	113.6	130	MTBSTFA
37	32	Block 2	Star	60	80	12.3	MTBSTFA
38	28	Block 2	Star	60	80	247.7	MTBSTFA
39	33	Block 2	Center	60	80	130	MTBSTFA
40	40	Block 2	Center	60	80	130	MTBSTFA

a: Block 1 was performed on the 1st and block 2 on the 2nd day.
b: star point level α = 1.682

Table 4-2 Analysis and quality parameters of analytical method

Name	Retention time (min)	Molecular weight after derivatization	Quantitation and qualification ion (m/z) [3]	Drinking water			Surface water		
				Instrument precision[4]	Recovery (±RSD)(%)	LOD (ng/L)	Instrument precision[4]	Recovery (±RSD)(%)	LOD (ng/L)
Ibuprofen	14.66	320.6	161, *263*	3.0	85.7 (12.5)	1.0	4.9	60.5 (4.6)	3.6
Mecoprop –d3[1]	**15.57**	**331.9**	***227*, 274**						
Salicylic acid	16.45	366.7	195, 251, *309*	8.1	96.8 (5.3)	1.6	2.1	85.2 (5.8)	2.7
OP	17.66	320.6	*263*, 320	2.6	85.1 (3.5)	1.1	3.8	62.8 (4.9)	1.5
NP	19.09	334.6	165, *277*, 334	4.9	74.4 (5.7)	1.8	9.5	55.5 (5.5)	3.3
Gemfibrozil	20.01	364.6	*243*, 307, 364	4.2	83.1 (9.3)	2.4	4.7	55.2 (3.9)	0.9
NP1EO	20.70-21.00	378.7	*321*	10.3	60.3 (12.9)	7.8	5.4	56.8 (10.5)	73.7
BPFBB[2]	**21.3**		***299*, 466**						
NP1EC	22.00-22.80	392.7	*307*	8.9	146 (26.4)	16.2	7.8	63.6 (22.5)	136.3
Naproxen	22.31	344.5	185, *287*	4.9	101.7 (16.3)	2.1	6.2	116 (17.0)	3.6
Triclosan	22.49	403.8	200, *347*	9.0	80.3 (12.6)	2.4	3.6	47.1 (3.5)	7.0
Propranolol	23.16	410.1	*72*	6.2	70.7 (15.8)	1.9	8.3	64.5 (7.9)	4.6
DCH[1]	**25.90**	**352.6**	***195*, 295**						
Diclofenac	26.32	410.4	214, *352*, 409	3.9	65.9 (5.7)	1.2	6.2	76.2 (10.2)	2.3
Carbamazepine	26.91	350.6	*193*, 293	9.6	64.4 (12.3)	0.7	3.6	75.4 (3.3)	1.5
Meclofenamic acid[1]	**27.52**	**432.4**	**243, *352*, 409**						
Nifedipine	32.94	460.6	*284*, 329	25.5	108.7 (50.5)	15.5	na	129.7 (39.6)	na
E1-d4[1]	**33.50**	**388.6**	***331*, 388**						
E1	33.59	384.6	*327*, 384	6.7	89.1 (8.9)	0.6	7.3	90.7 (31.8)	4.0
EE2	34.31	410.7	327, *353*, 410	17.1	85.1 (27.3)	4.8	9.1	83.4 (12.8)	7.3
Diltiazem	36.20	414.5	*58*, 71	27.6	99.7 (26.4)	13.0	15.3	93.3 (23.3)	40.4

1. *surrogates used for quantification of compounds in their respective block, DCH used only for carbamazepine quantification*
2. *internal standard*
3. *m/z in italic are quantification ions*
4. *RSD of 5 replicate GC injections in %*

na not available

Since each target compound had a specific response in one experimental run, a multiple-response case was formed in this study. Although ideally all the responses should be maximized simultaneously, it is very difficult and often impossible to achieve this goal. Alternatively, a tradeoff is often employed to find a set of optimal conditions, which achieves overall satisfaction for the majority of the analytes (US NIST, 2006). Therefore, a desirability approach was applied to analyze the data in this study. Specifically, the response for each target compound in each run was transformed into a dimensionless single desirability scale (d_i), which ranged from 0 and 1, with the fully desired response as 1. More concretely, for a target compound with only one derivative, the d_i value corresponding to the highest response out of 40 experimental runs for that derivative was 1. Accordingly, the d_i value corresponding to the lowest response was 0. For a given compound, the single desirability, d_i, for each experimental run can be calculated as:

$$d_i = \frac{X_i - X_{low}}{X_{high} - X_{low}} \qquad \textbf{4.1}$$

X_i: the i^{th} response (i = 1~ n) for the compound in 40 runs

X_{low}: the lowest response for the compound in all 40 runs

X_{high}: the highest response for the compound in all 40 runs

n: total number of experimental runs (40)

For compounds with two derivatized products or incomplete derivatization, such as EE2 derivatized by BSTFA or codeine derivatized by MTBSTFA, equation 4.1 and 4.2 were applied. The relative responses of the desired peaks (mono-TMS-EE2 or underivatized codeine) were transformed using equation 1, thus maximizing them, while equation 2 was used for the response transformation of the undesired peaks (di-TMS-EE2 or TBS-codeine). When using equation 2, responses for conditions leading to the formation of the undesirable derivatives were minimized because the d_i value corresponding to the highest response of the undesirable peak was 0. It should be noted that equation 2 produced lower d_i values the higher the response of the undesirable peak. Thus two d_i values were obtained for each EE2 or codeine test, one for the desired derivative and one for the undesirable one.

$$d_i = \frac{X_{high} - X_i}{X_{high} - X_{low}} \qquad \textbf{4.2}$$

After this step, it was feasible to determine statistically which factors (reagent, reagent dose, temperature and time) or their interactions were significant for the derivatization of the individual target compounds. The results are presented in the next section.

Then, the total desirability function, which is a measure of the overall quality of all responses for one run, was used to evaluate and seek for the optimal derivatization conditions. The total desirability (D_i, Equation 4.3) for each run was calculated as the geometric mean of all its single desirabilities and hence, each test was assigned a total desirability. Note that single desirabilities of both, the desired and undesired peaks were included for EE2 and codeine.

$$D_i = \left(d_1 d_2 ... d_m\right)^{1/m} \qquad \textbf{4.3}$$

m: the total number of single desirabilities under the same derivatization condition, i.e. in one run

4.4.3 Results and Discussion

The evaluations of the experimental data were based on the regression analysis, which is commonly used as a statistical tool for examining the relationship between variables. Generally an empirical polynomial model was applied for simulating the relationships between desirabilities and factors considered in this study.

The effects of factors (reagent, reagent dose, temperature and time) and their interactions on the derivatization of the individual target compounds were analyzed based on the single desirabilities for each target compound. The main effects, two-effect interactions, and quadratic main effects were considered when doing a step-wise regression analysis. Statistical analysis of the significance of the effects at the 5 % significance level for the first two items is shown in Table 4-3. Obviously, the derivatization reagent was a significant factor for all the target compounds. Among the other three factors, the reaction temperature significantly affected the derivatization yield for eight target compounds, while reaction time and dosage were only significant for four and five target compounds, respectively. However, every two factor-interaction in Table 4-3 was statistically significant for the derivatization reaction of certain target compounds. Therefore, the statistical relations between factors were not negligible, and all factors had to be considered in subsequent evaluations.

Table 4-3 Statistical analysis of main effects and two factor interactions of target compounds

Compound	Main effects				Two factors interaction					
	A	B	C	D	AB	AC	AD	BC	BD	CD
Ibuprofen	+	-	-	+	+	-	-	+	-	-
Salicylic acid	-	-	+	+	-	-	-	+	+	-
OP	-	+	-	+	-	+	-	-	+	-
NP	-	+	-	+	+	+	-	-	+	-
Acetaminophen	-	+	+	+	-	-	+	-	+	+
Gemfibrozil	-	+	-	+	-	-	-	-	+	-
NP1EO	-	+	+	+	-	-	-	+	+	+
NP1EC	-	-	-	+	-	+	-	-	-	-
Naproxen	-	+	-	+	-	-	-	-	-	-
Triclosan	-	-	-	+	-	+	-	-	-	-
Propranolol	+	-	+	+	-	+	-	-	-	+
Diclofenac	+	+	-	+	+	-	+	-	-	-
Carbamazepine	-	-	-	+	-	+	-	-	-	-
Codeine	-	-	-	+	-	-	-	+	+	+
E1	-	+	-	+	-	-	-	-	-	-
EE2	-	-	-	+	-	+	-	-	-	+
Diltiazem	+	-	+	+	-	+	-	-	-	+

A: time; B: temperature; C: derivatization reagent dosage; D: derivatization reagent
+: significant effect; -: insignificant effect
Nifidipine was not derivatized by both MTBSTFA and BSTFA, hence it was not considered in regression analysis

The regression analysis of the total desirabilities for all BSTFA and MTBSTFA derivatization runs was done by using a statistical software package (Design-Expert v6.0 trial). The regression analysis of the total desirabilities of MTBSTFA reactions indicated that the dosage term and interaction between dosage and time were significant. Contour plots of the total desirability at the highest yield experimental point projection shown in Figure 4-3 were examined to search for the optimal reaction conditions. The total desirability increased when experimental conditions were approaching a temperature of 60 ^{o}C, a reaction time of 90 min and a reagent dose of 200 µL. In the boundary of the experimental domains, these were therefore the optimal conditions to achieve maximum yields of derivatized products for all target compounds. The contour plots (Figure 4-3) predicted a maximum total desirability of 0.44 for these conditions while the total desirability for the corresponding experimental test was 0.45. With respect to BSTFA reactions, the main effects of time and temperature and their interaction were significant, while the result was not sensitive to the BSTFA dosage at optimal time and temperature over the range of 60 to 150µL. By observing the contour plots as shown in Figure 4-4, the optimal conditions for the BSTFA derivatization were found to be around 130 µL of BSTFA in 70 µL of acetone at 100 ^{o}C for 90 min with a total desirability of

0.41. Therefore, due to its higher total desirability, further experiments were conducted using the optimal MTBSTFA derivatization conditions. It should be noted that the contour plot for MTBSTFA seems to indicate an upward trend continuing outside the chosen experimental domains. Hence, MTBSTFA reaction could be optimized further by increasing reaction time and dosage, thus exceeding the chosen experimental domains. However, no further investigations outside the chosen experimental domains were carried out, because longer reaction time and more dosage might not be economical for further research.

4.5 Optimization of Solid Phase Extraction

In order to achieve an overall satisfactory extraction efficiency of all the target compounds, the sample enrichment conditions, such as extraction pH, loss of pre-filtration, and types and ratio of elution reagents, should be determined or further optimized. In particular, the optimal elution conditions were investigated using a full factorial design and a similar regression approach as discussed in previous section.

4.5.1 Extraction pH, Cartridge Capacity and Pre-filtration

To extract acidic drugs, water samples are usually acidified (Rodríguez *et al.*, 2003; Öllers *et al.*, 2001; Hilton and Thomas 2003) in order to suppress dissociation, thus making the analytes more adsorbable on SPE resins. The extraction of neutral compounds is commonly carried out at neutral pH which provides the added advantage of reducing the retention of humic acids on the SPE cartridge (Quintana *et al.*, 2004). Here, due to the different acid-base properties of the selected target compounds, the overall best extraction pH was determined experimentally. Briefly, 2 L of Milli-Q water were spiked with 100 ng/L of each target compound and extracted at pH 2 and 7 using Oasis HLB cartridges (3 mL, 60 mg), which was followed by MTBSTFA derivatization. The amounts were calculated using calibration curves where target compounds in solvent had been derivatized and the peak ratios of target compounds to I.S. (BPFBB) had been plotted. As shown in Figure 4-5, except for propranolol, codeine, and diltiazem, the extraction recoveries under acidic extraction conditions were better or similar for most of the target compounds than under neutral conditions. The recovery of salicylic acid was close to zero under neutral condition. Surprisingly, acetaminophen was not detected at either pH. The reason is still unclear. Overall results lead to the conclusion that extractions should be performed under acidic conditions – namely pH 2. It should be noted that the extraction recovery of codeine was very low at pH 2.

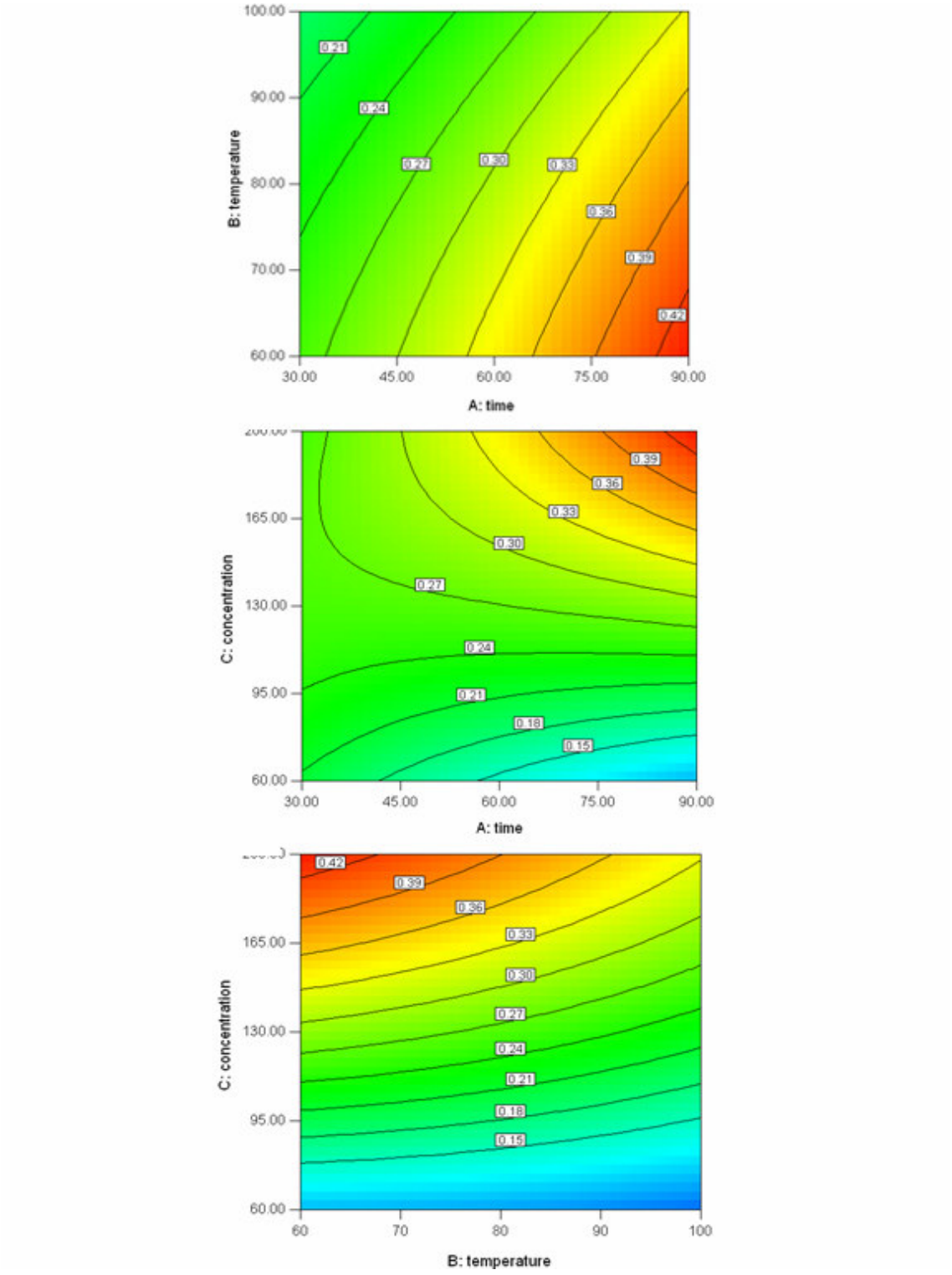

Figure 4-3 Contour plots of total desirability of MTBSTFA at optimal point projection

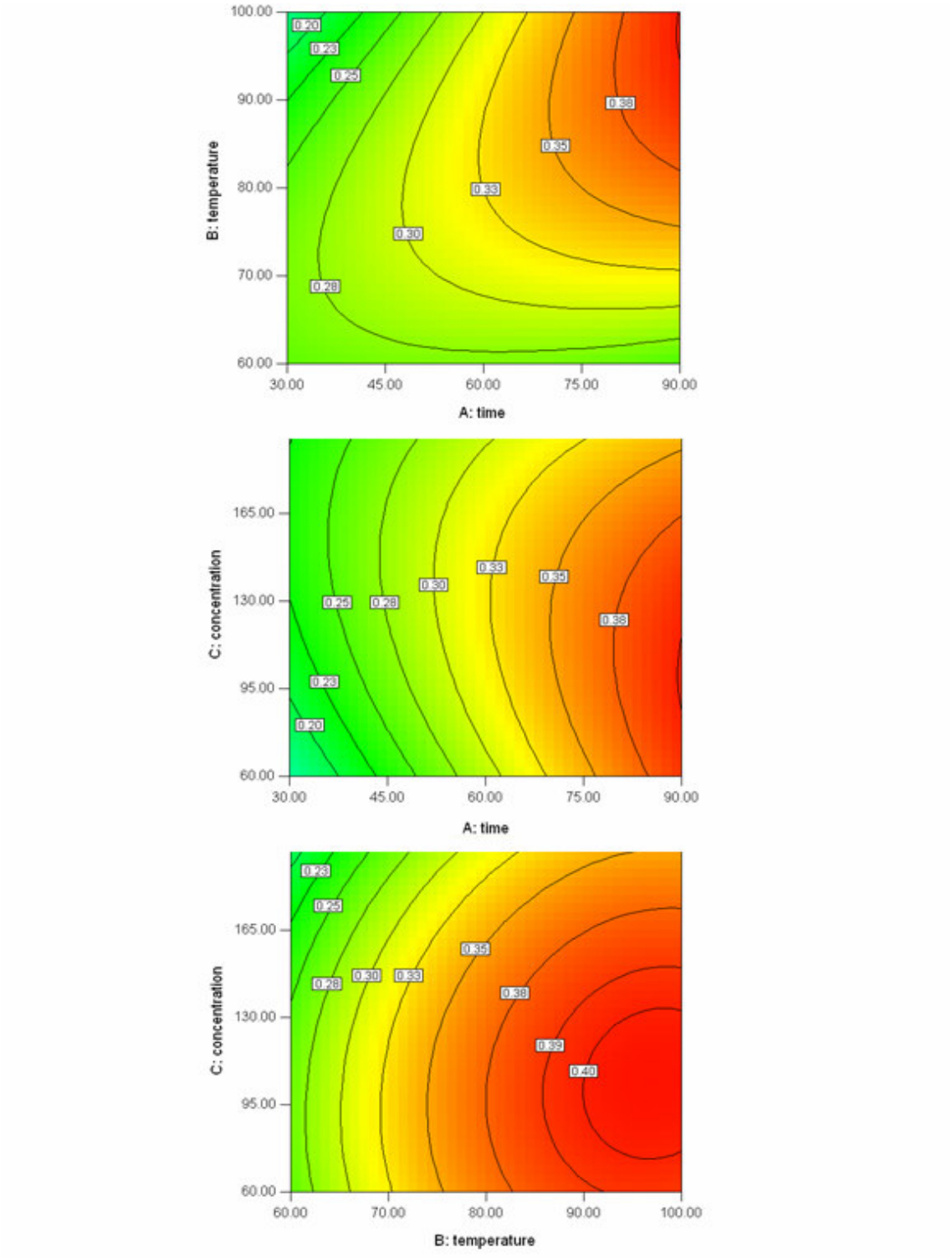

Figure 4-4 Contour plots of total desirability of BSTFA at optimal point projection

The capacity of the Oasis HLB cartridges in terms of retaining target compounds quantitatively was investigated using 2 L of spiked river water (100 ng/L). Acidified water samples were pumped through two sequentially connected cartridges, but the first cartridge was totally blocked after passing through of only 1 L of river water. Nevertheless, both cartridges were processed individually and it was found that several compounds had broken through since they were present in the eluate of the second cartridge. The amount of salicylic acid and NP accumulated in the second cartridge was less than 10% of the amount of the first cartridge whereas the other three breakthrough compounds namely nifidipine, propranolol, and codeine lost more than 50% compared to the first cartridge thus indicating incomplete extraction. Breakthrough might be caused by competition of natural organic matter and other compounds present in the river water matrix. Therefore, in other matrices e.g. drinking water, the competition may not be as pronounced, and less breakthrough may be observed. Another possible reason of the breakthrough of propranolol and codeine might be the acid condition applied for extraction. Nevertheless, propranolol and nifidipine were still included in further investigations - mainly to determine the influence of low extraction rates on overall analytical results. Note though that at this point it was unlikely that these 2 compounds would have been chosen for our drinking water treatment studies. Since codeine could not be extracted satisfactorily under acidified conditions and other difficulties had been experienced during derivatization, it was excluded from the list.

When extracting the surface water, it was observed that the particles in the water matrix quickly slowed down the flow, and finally blocked the cartridges. So, a prefiltration with 0.45µm pore size cellulose filter pre-washed with Milli-Q water was carried out before extraction. The system loss due to pre-filtration was tested using 1 L of spiked river water (50 ng/L). As shown in Figure 4-6, no significant differences were found between responses for unfiltered and filtered samples, as had been reported previously for some of these compounds (Rodríguez *et al.*, 2003).

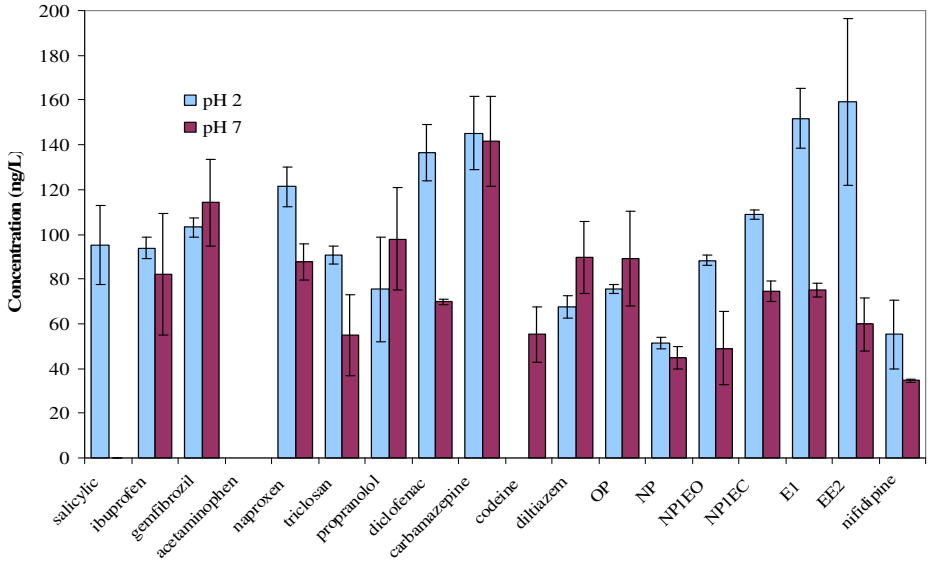

Figure 4-5 Effect of pH on extraction yield (n=3)

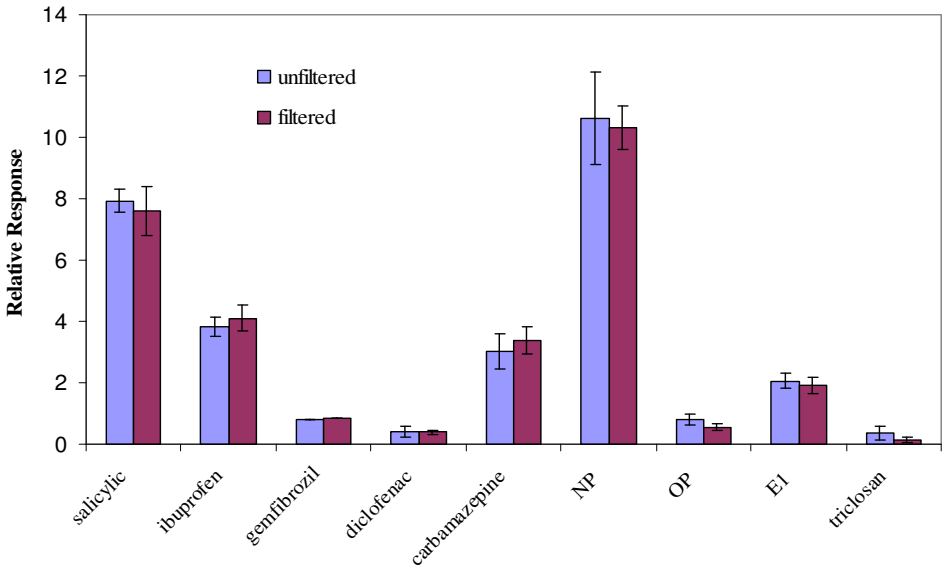

Figure 4-6 Sample pre-treatment by membrane filtration (n=3)

4.5.2 Investigation of Optimal Elution Conditions using Factorial Design

Solvents are used to desorb the target compounds from SPE cartridges. The type and volume of the elution solvent are important factors affecting the recoveries of the target compounds. The choice of elution solvent is dependent on the target compounds to be eluted from the cartridges and the

elution strength of the solvent. Ethylacetate, acetone and methanol, which have different elution strength and polarity, are most commonly used (Souali *et al.*, 2003; Kelly 2000; Bolz *et al.*, 2000; Quintana *et al.*, 2004). Since the target compounds spanned a large polarity range, the combination of two solvents, namely ethylacetate and acetone, was examined systematically by employing a factorial experimental design.

Here a full 2^2 factorial experiment with triplicates at the central point was used to determine the optimal solvent mixing ratio and elution volume. The designed experiment required 7 runs in total (as shown in Table 4-4). Volumes of 2 and 6 mL and, ethylacetate alone vs. ethylacetate and acetone in a ratio of 50/50 were chosen as high and low levels. Additional tests at the central point (runs 5-7) were added to substantiate trends gained from the high and low level tests.

Table 4-4 Factorial design scheme for optimizing solid phase extraction

Run	Solvent (v:v)	Volume (mL)
1	100% ethyl acetate	2
2	100% ethyl acetate	6
3	50% ethyl acetate+50% acetone	2
4	50% ethyl acetate+50% acetone	6
5,6,7	75% ethyl acetate+25% acetone	4

The target compounds were loaded on the sorbents by extracting 1 L of spiked ultrapure water (50 ng/L) with the Oasis HLB cartridges. After elution, BPFBB was added as an I.S., samples were derivatized, measured by GC/MS and the relative response of each compound to BPFBB was quantified for each test. The relative response of each compound in each run was then transformed into a single desirability, which were then used to calculate the total desirability of each run (as explained in 4.4.2). Total desirabilities, which are a measure of the overall quality of the responses of all compounds for one run, were then statistically evaluated in order to determine the effects of the solvent ratio and the elution volume. The two main effects and their interaction were analyzed by analysis of variance (ANOVA) table. The null hypothesis in this case was that the two main effects and their interaction had no effect on the elution efficiency. As shown in Table 4-5, only the F_{obs} of the ratio of acetone to ethylacetate is larger than $F_{critical}$ at the 5 % significance level. This means that only this main factor significantly influenced the total desirabilities, thus rejecting the null hypothesis. The optimum ratio was found to be 50:50 (v:v) with the overall maximum total desirability at 0.96.

Although the solvent volume was not a significant factor, from a conservative point of view, 6 mL was chosen for further work.

Table 4-5 ANOVA table for elution test

main effect	Sum of square	Degree of freedom	Mean square	F_{obs}	$F_{critical}$
Ratio of the solvents	686.17	1	686.17	59.512	18.51
Solvent volume	155.63	1	155.63	13.498	
Interaction	92.64	1	92.64	8.0348	
Error		2	11.53		

4.6 Performance of the Analytical Method

Note that codeine had been excluded from this optimal method - in part due to its breakthrough on the SPE cartridge and in part due to the formation of two products when using MTBSTFA. EE2 remained in the method since it only forms one derivatization product (TBS-EE2) with MTBSTFA. However, TBS-EE2 partially degrades to TBS-E1 and, although the percentage conversion should remain constant when applying the same experimental conditions it is recommended to use additional confirmation with another method, such as Shareef *et al.*, (2004; 2006) for E1 and EE2 quantification.

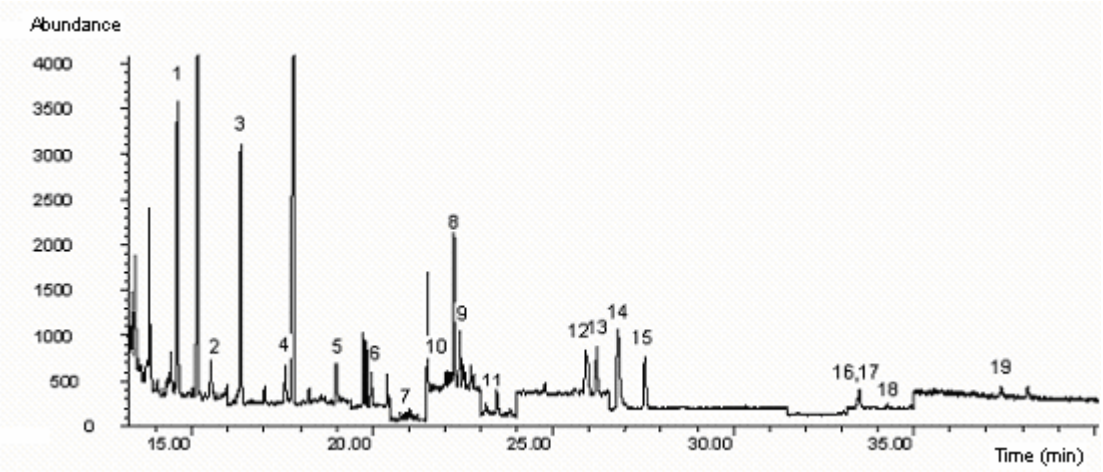

Figure 4-7 Chromatogram in SIM of 50ng/L of analytes

(1. ibuprofen, 2. mecopop-d_3, 3. salicylic acid, 4. OP, 5. NP, 6. gemfibrozil, 7. NP1EO, 8. naproxen, 9. triclosan, 10. NP1EC, 11. propranolol, 12. DHC, 13. diclofenac, 14. carbamazepine, 15. meclofenamic acid, 16. E1-d_4, 17. E1, 18. EE2, 19. diltiazem)

4.6.1 Identification and Quantification

As shown in Table 4-2, the target compounds were divided into three groups and quantified using three different surrogate standards. DCH was chosen as surrogate for carbamazepine only.

A typical chromatogram containing the target compounds and surrogates is shown as Figure 4-7. Normally, two or three ions of each compound were selected as qualification ions. However, it should be noted that only one ion each was used for NP1EO and NP1EC (Table 4-2) because this was the only common ion for the different isomers of each compound. Both propranolol and diltiazem displayed mass spectra which only had abundant mass peaks at low masses, and hence m/z = 72 was used for propranolol and m/z = 71 for diltiazem as quantification ions. In these cases, some coextracted matrix impurities may have potential to interfere with compound identification, and decrease the analytical accuracy when water samples with complex matrices are analyzed. Therefore, caution needs to be exercised when interpreting field analysis results. Additional confirmation using an independent analytical method would be necessary for the compounds which only use one ion for identification and quantification. It was reported that diltiazem and propranolol were successfully determined using high-performance liquid chromatography (HPLC) coupled with MS (e.g. Kolpin *et al.*, 2002; Hilton and Thomas, 2003).

Calibration curves were established by using spiked ultrapure water at different concentration levels ranging from 5 to 200 ng/L through the entire analysis process. The curves were linear over this concentration range since, in most cases, regression coefficients were larger than 0.99.

4.6.2 Recoveries, Detection Limits and Instrument Precision

Relative recoveries were determined by processing spiked water (50 to 200 ng/L depending on target compound, n = 5) through the entire procedure (Table 4-2). The typical recoveries in drinking water ranged from 60 % for NP1EO to 109 % for nifidipine, with the exception of NP1EC (147 %) (Table 4-2). For surface water, recoveries ranged from 47 % for triclosan to 130 % for nifidipine (Table 4-2). Considering the low concentration range, recoveries were satisfactory. As expected, recoveries in drinking water were generally better than those in surface water.

The limit of detection (LOD) of individual compounds in drinking and surface water was determined by calculating the standard deviation of seven replicates (spiked at a concentration close to the expected LOD i.e. 5 to10 ng/L in drinking water, and 10 to 20 ng/L in surface water) at the 99 % confidence level. With the exception of nifidipine, diltiazem, NP1EO and NP1EC, the LODs of the other target compounds were all below 5 ng/L, which is satisfactory for analyzing the target

compounds in drinking water. Similar behaviour was also observed in surface water where the LODs of the majority of target compounds were less than 10 ng/L. A LOD for nifidipine in surface water could not be determined since the 20 ng/L spike surface water did not give a clear signal above the baseline noise. As mentioned in 4.5.1, this low response may be due to low extraction yields which may also explain the high standard deviation for the recoveries both in surface and in drinking water. A possible reason for the relatively high LOD but also for the high precision and the high standard deviation of the recoveries for diltiazem might be its potential degradation in the GC injector or the column. However, MTBSTFA obscures early parts of the chromatograms thus hiding any potential break down products. High LODs of NP1EO and NP1EC might be caused by other isomers from unidentified sources present in this more complex matrix. The limit of quantification (LOQ) of each compound was set to three times of the LODs.

The instrument precision of the GC/MS (Table 4-2) was determined by five consecutive injections of one of the low concentration extracts used for LOD determination. It seemed acceptable (ranging from 2.6 – 10.3 % in drinking water and from 2.1 – 15.3 % in surface water) for most of the target compounds.

4.6.3 Application of the Analytical Method

The developed method was applied to a local river and tap water. The first sampling site was located about 20 meters downstream from a STP discharge pipe, where, based on visual observation, the effluent was considered to be completely mixed with the river water. The next sampling location was approximately 20 km downstream of the STP discharge close to a drinking water treatment plant (WTP) intake. The tap water samples were taken in the laboratory which is a mixture of water from the previously mentioned WTP and groundwater. The findings of the study are presented in Table 4-6.

Eleven target compounds exceeded measurable levels in the river water close to the STP discharge. The concentrations ranged from > LOD to 143 ng/L of ibuprofen. In general, the concentrations decreased at the second site, though ten compounds were still identified indicating that this site may still have been influenced by the STP effluent. Surprisingly, the acidic drugs salicylic acid, and gemfibrozil, and also the EDC OP were found in higher concentrations at the second location, possibly due to other contaminating sources than the STP effluent. As expected much lower concentrations, if a substance was detected at all, were observed in tap water suggesting that the applied treatment technologies or dilution provided by the groundwater were to a large extent effective in substantially reducing the concentrations of these target compounds. It should be noted

that the concentrations of E1 should be confirmed by a different method since EE2 partially degrades into E1 when derivatized with MTBSTFA (4.4.1). In all cases, the pharmaceuticals salicylic acid, ibuprofen, gemfibrozil and carbamazepine, and the EDCs E1 and NP1EC were the most commonly detected contaminants at each site.

Table 4-6 Concentrations of selected PhACs and EDCs in river and tap water

Compound	Mean concentration (ng/L) ± S.D. (n = 3)		
	Downstream of STP	Upstream of DWT	tap water
salicylic acid	8.0 ± 2.8	19.3 ± 6.3	4.2 ± 0.3
ibuprofen	142.6 ± 2.3	11.3 ± 1.5	3.4 ± 0.4
gemfibrozil	2.5 ± 0.6	11.9 ± 0.5	> LOD
naproxen	83.1 ± 24.1	35.1 ± 3.8	ND
triclosan	> LOD	> LOD	> LOD
propranolol	ND	ND	ND
diclofenac	13.2 ± 6.9	ND	ND
carbamazepine	98.9 ± 36.5	> LOD	> LOD
nifidipine	ND	ND	ND
diltiazem	ND	ND	ND
E1	88.0 ± 35.6	> LOD	1.7 ± 1.2
EE2	ND	ND	ND
OP	> LOD	6.2 ± 1.8	ND
NP	> LOD	>LOD	ND
NP1EO	ND	ND	> LOD
NP1EC	> LOD	>LOD	> LOD

ND: calculated concentrations less than LOD or non detected
> LOD: calculated concentrations larger than LOD but less than LOQ

4.7 Summary of Analytical Method

Selected acidic and neutral pharmaceuticals and EDCs were simultaneously determined using GC/MS after solid phase extraction under acidic conditions and subsequent derivatization. The optimal derivatization conditions were determined systematically using a factorial design more specifically, a central composite design. The extraction was optimized in terms of extraction pH, cartridge capacity, and elution solvent type and volume. Overall, the acidic extraction had a better performance than the neutral extraction. The optimum elution could be accomplished by using 50:50 (v:v) ethylacetate and acetone. The developed method had satisfactory recoveries and LODs to

analyze for most of the target compounds in surface and tap water. However, restrictions apply to some compounds (e.g. E1, EE2, nifidipine and diltiazem) and hence, results for these compounds should be confirmed with an independent method. The developed analytical method was successfully applied to river water and tap water, where pharmaceuticals such as salicylic acid, ibuprofen, gemfibrozil, naproxen and carbamazepine, and EDCs such as E1 and NP1EC were identified as the most common contaminants. This method is used to further study the adsorption of three target compounds on GAC. Accordingly, a brief flowchart describing the whole analysis procedure with GC/MS is shown as Figure 4-8.

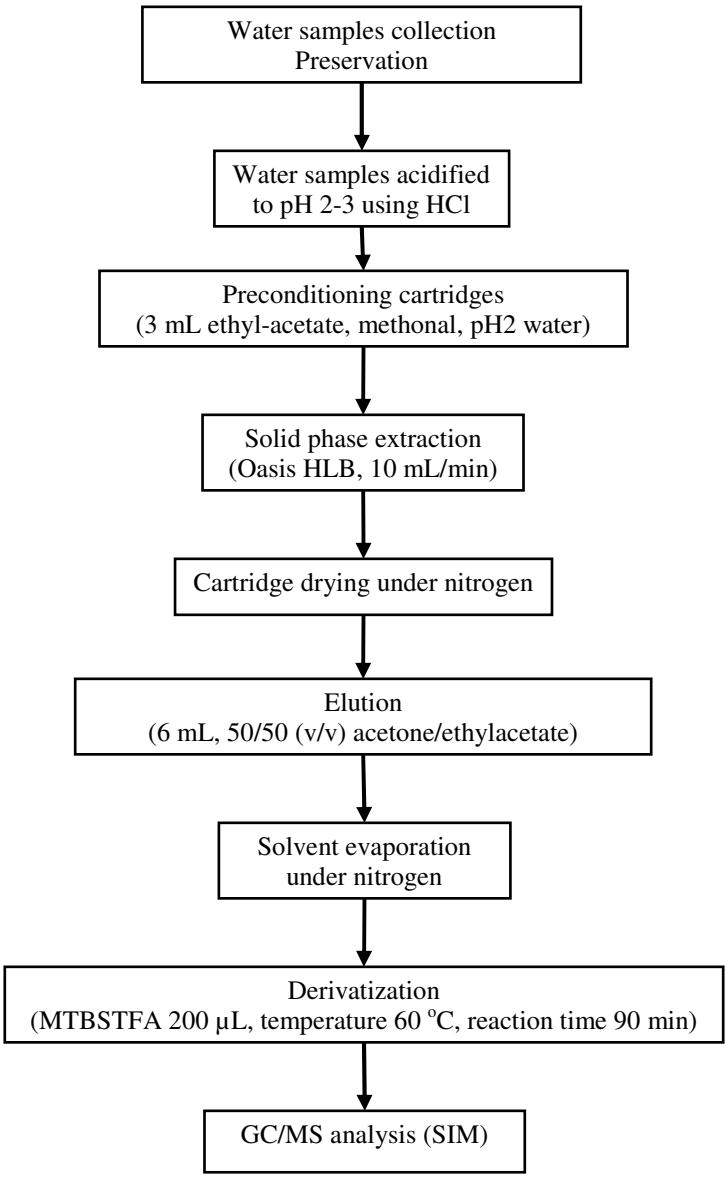

Figure 4-8 Flowchart of the optimal GC/MS analysis procedure

CHAPTER 5
MATERIALS AND EXPERIMENTAL APPROACHES FOR ADSORPTION STUDY

5.1 Target Compounds

As discussed in Chapter 3, three target compounds, including naproxen, carbamazepine, and NP, were finally selected for adsorption studies. Naproxen is an anti-inflammatory drug; and carbamazepine is an anti-epileptic agent. As shown in Table 3-4, both of them are among the top 50 prescribed drugs in Canada. According to Table 2-1 and Table 4-6, they have all frequently been found in the environment. NP, one of the degradation products of NPEOs, also occurred widely in the environment because of high consumed amounts of NPEOs consumed throughout the world. In this study, only one NP isomer is considered in order to facilitate the research. Some important properties are presented in Table 5-1. As shown in this table, although the three compounds selected for this study have similar molecular weights, they are markedly different in their physicochemical properties. Naproxen displays acidic properties in waters at typical drinking water treatment conditions (Table 5-6). In contrast, carbamazepine and NP are uncharged in the same pH (~7) range. According to their $\log K_{ow}$, both carbamazepine and naproxen are hydrophilic, while NP is a hydrophobic compound. However, it was found that all three compounds were not easily dissolved in ultrapure water at room temperature, though naproxen and carbamazepine have relatively higher water solubilities than NP. Consequently, in this study, the stock solutions in ultrapure water for all the compounds were approximately 1 mg/L (the actual concentrations were measured at the beginning of each experiment). In addition to the physicochemical properties, molecular dimensions of solutes are also important factors for adsorption processes (Karanfil *et al.*, 2006). Therefore, the dimensions of the three target compounds are listed in Table 5-2. It should be noted that the dimensional data was only estimated based on the original atom size and bond length given in the software.

As reviewed in Chapter 2, the free diffusivity (D_L) of a solute is an important physicochemical factor influencing the estimation of film diffusion by empirical correlations and pore diffusion coefficients for adsorption processes. The calculation of D_L was based on Equation 2.44; and the results are listed in Table 5-3. The detailed methodology is presented in Appendix D.

Table 5-1 Physicochemical properties of the three target compounds

Compound	CAS no.	Molecular formula	MW	Log K_{ow}	pK_a	Water Solubility (mg/L at 25°C)
Naproxen	22204-53-1	$C_{14}H_{14}O_3$	230.3	3.18[a]	4.15[a]	15.9[a]
Carbamazepine	298-46-4	$C_{15}H_{12}N_2O$	236.3	2.45[a]	2.3[c], 13.9[a]	17.7[a]
4-n-NP	104-40-5	$C_{15}H_{24}O$	220.4	5.92[b]	10.25[d]	1.6[e]

a: data from Trenholm et al. (2006);
b: data from Yoon et al. (2002)
c: data from Nghiem et al. (2005);
d: data obtained from the US EPA EPI suite program V2.0
e: data estimated from http://www.pbtprofiler.net

Table 5-2 Estimated molecular sizes of the three target compounds†

Dimensions (Å)	Naproxen	Carbamazepine	NP
Width	12.41	10.06	15.78
Depth	6.06	7.26	4.99
Thickness	~ 3	~ 3	~ 3

†: molecular dimension data were obtained using ChemSketch 10.0 (Advanced Chemistry Development Inc., Toronto, Canada) based on the molecular structures shown in Figure 5-1.

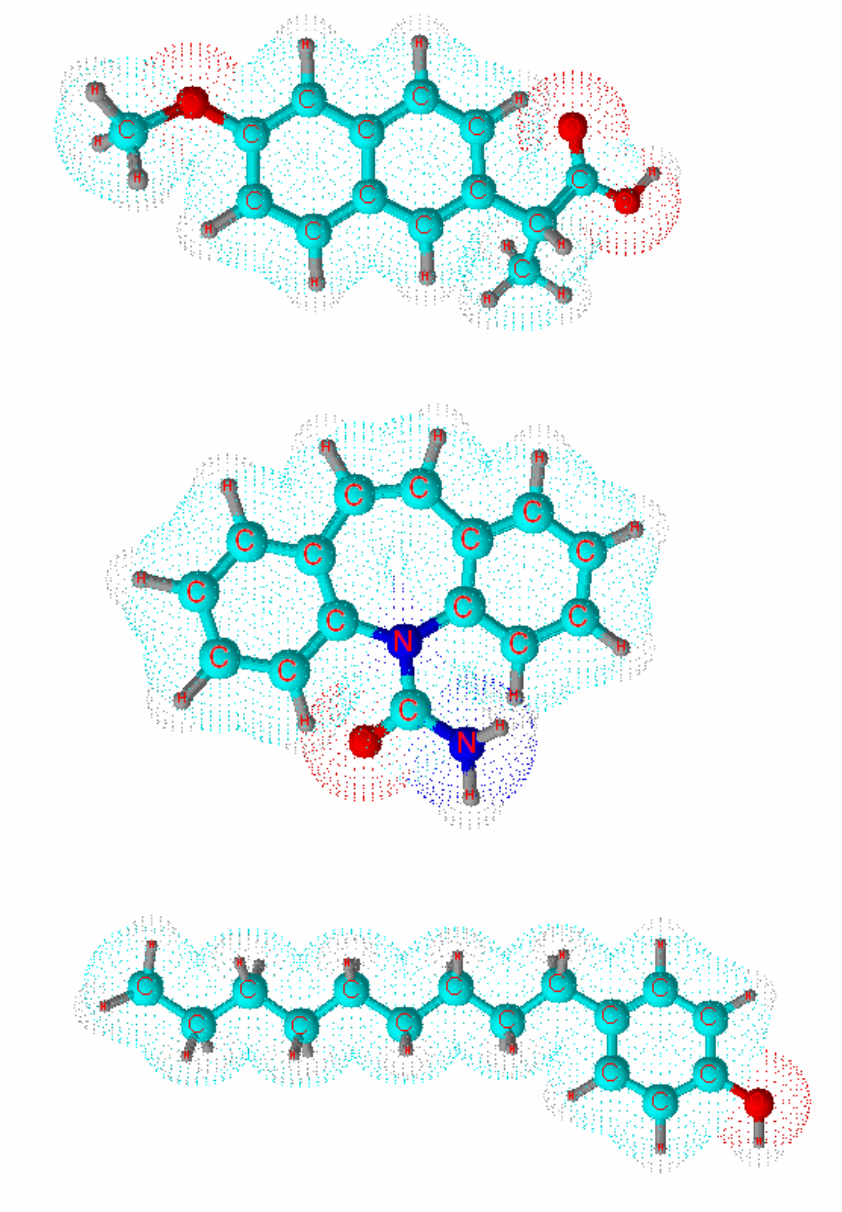

Figure 5-1 Structural formulas of naproxen (top), carbamazepine (mid), and NP (bottom)

Table 5-3 Estimated free diffusivities of the three target compounds

	Naproxen	Carbamazepine	NP
D_L (x 10^{-6} cm^2/s)	5.005	5.269	4.618

5.2 Activated Carbon Characterization

In this study, two types of GAC – coal-based Calgon Filtrasorb® 400 (F400) (Pittsburgh, PA, USA) and coconut-based PICATIF TE (PICA) (Columbus, OH, USA) – were selected for evaluation. They were both used in preloading and pilot-scale experiments as received. For isotherm tests, only the 30x40 US mesh fractions, which came from the sieve analysis, were employed. Original size virgin and preloaded carbons were used for the kinetic tests.

Density and Porosity

Particle density and porosity are important for both the experimental design and modelling in this study. These parameters were determined using the method provided by Sontheimer *et al.* (1988). In total, four tests were carried out, and the average values as well as their standard deviations are reported in Table 5-4. The detailed methodology is presented in Appendix E.1.

Table 5-4 Characteristics of F400 and PICA carbon

	F400	PICA
Particle mean diameter (mm)	1.13 ± 0.03	1.12 ± 0.04
Particle density (g/mL)	0.85 ± 0.02	0.86 ± 0.03
Material density (g/mL)	1.69 ± 0.02	1.67 ± 0.04
Particle porosity	0.50 ± 0.01	0.48 ± 0.03

Sieve Analysis

Sieve analyses were conducted on F400 and PICA carbon as received. The purpose of these analyses was to determine the effective mean diameters of the GAC particles. The methodology of sieve analysis generally followed the standard of ASTM D2862-97. Sieve analyses on virgin F400 and PICA carbon were repeated four times. The results of the particle mean diameter calculations are presented in Table 5-4. The detailed procedures for the sieve analysis are provided in Appendix E.2.

SEM Images

The scanning electron microscope (SEM) images of virgin and preloaded F400 and PICA carbon were taken using JEOL® JSM-6460 available from the Department of Mechanical Engineering at the University of Waterloo. The SEM images of virgin F400 and PICA carbon are shown in Figure 5-2. It turns out that both carbons have particles which are not spherical in shape. They both have pretty

rough surfaces, but rather different topographic characteristics. Large caves and some cracks in the scale of tens of micrometers are apparent on the F400 carbon. In contrast, the surface of the PICA carbon seems to be smoother with large pores distributed throughout. More images with higher resolution on both virgin and preloaded carbons are available for comparison in Chapter 7.

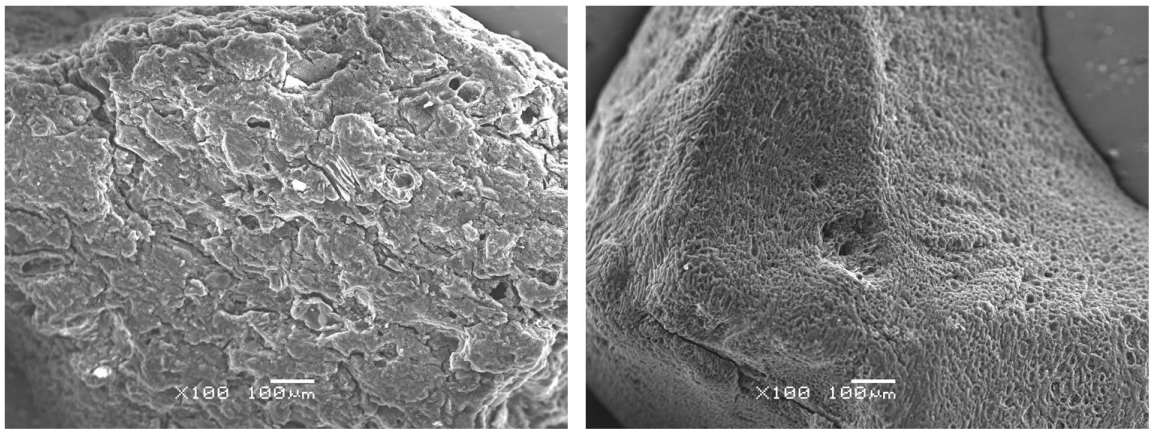

Figure 5-2 SEM images for virgin F400 (left) and PICA (right) carbon

BET Surface Area and Pore Volume Distribution

In order to determine Brunauer-Emmett-Teller (BET) surface area and pore volume distributions of both carbons, nitrogen isotherms were conducted on a Micromeritics Surface Area and Porosimetry Analyzer (ASAP 2020) at the National Engineering and Technology Research Center of Forest Chemical Industry (China). The tests were carried out on approximately 0.2 g carbon samples at a temperature of 77.5 K. Nitrogen isotherms were determined at partial pressures ranging from 0 to 1. From the nitrogen isotherm data, the BET surface area can be calculated. The two partial pressure ranges used for calculations were 0.001 – 0.15 and 0.05 – 0.35. It was found that the BET surface areas calculated at the low partial pressure range were generally larger than, and had better regression coefficients than, the values obtained at high partial pressure range. Pore volumes were determined using single point adsorption at a partial pressure of 0.99. Pore volume distributions were analyzed in the range of 5 – 55 Å using the Horvath-Kavazoe method available in the ASAP 2020 V3.0 software. The results of the analyses are shown in Table 5-5 for virgin F400 and PICA carbon.

Table 5-5 BET surface area and Pore volume

Carbon	SA BET (m^2/g)[§]	Total pore volume (cm^3/g)[†]	Pore volume distribution (cm^3/g)		
			< 8 Å	< 20 Å	< 50 Å
F400	1030	0.549	0.273	0.422	0.468
PICA	1156	0.527	0.340	0.480	0.505

§: determined in P/P_o range of 0.001-0.15

†: determined at P/P_o around 0.99

As shown in Table 5-5, both F400 and PICA carbons have majority pore volume distributed at less than are 20 Å range, thus are regarded as microporous carbons. Nevertheless, PICA carbon has a greater percentage of primary and secondary micropores and larger BET surface area than F400 carbon.

5.3 Waters

Three types of "organic free" waters were used in isotherm and kinetic tests.

Milli-Q water was obtained from an ultrapure water system (Milli-Q UV Plus) which used deionized (DI) water as a source. The pH value of the Milli-Q water was 6.44 (± 0.24). The DOC concentration of the Milli-Q water ranged from 0.08 – 0.37 mg C/L with a mean value at 0.18 mg C/L. It was initially used for all the isotherm tests on virgin and preloaded GAC. However, it was suspected that direct competition from background DOC led to different isotherms for the same target compound when using different initial concentrations. Therefore, higher quality water was purchased from VWR International (West Chester, PA, USA). This water met the ASTM type II criteria (TOC/USP ≤ 0.05 ppm), and was used for repeating the isotherm tests under the same experimental conditions. The DOC analysis showed that the ASTM type II water had an average DOC value of 0.05 mg C/L, which was substantially lower than in the Milli-Q water. Nevertheless, the isotherm tests on preloaded carbons were still carried out in Milli-Q water, because it is expected that the direct competitive effect from background NOM in Milli-Q water would be insignificant on preloaded carbon. The reasoning is that this effect can be negligible on preloaded carbon in natural water, which has much higher concentration of background NOM than Milli-Q water. The conclusion can be supported by the facts that no direct competitive effect was observed for both atrazine (Knappe *et al.*, 1999) and MIB (Gillogly, 1998) on preloaded carbon in natural water.

DI water was used for the kinetic tests. This water was supplied by the Department of Chemical Engineering (University of Waterloo) and produced by passing tap water through cation and anion ion exchange resins. The water had a conductivity value of less than 0.2 μS/cm. The DOC for the DI water in all kinetic tests ranged from 0.09 to 0.47 mg C/L with a mean value at 0.27 mg C/L.

Natural water used for investigating direct competitive effects on adsorption was post-sedimentation (PS) water obtained from the Mannheim Water Treatment Plant (Region of Waterloo, ON, Canada). The PS water went through two sand filtration columns prior to preloading columns (Figure 5-3) in order to remove suspended particles. The water characteristics are summarized in Table 5-6. The specific DOC values for the tests are presented in Section 6.2.

In addition, all the "organic free" water and natural water used for determining isotherm parameters were sterilized before the experiments.

Figure 5-3 GAC preloading facilities

Table 5-6 Water parameters for post-sedimentation water from the Mannheim WTP

Parameters	Values
Water temperature (^{o}C)	0.9 – 21
DOC before sand filters (mg C/L)	3.4 – 5.4
DOC after sand filters (mg C/L)	3.3 – 5.3
Turbidity before sand filters (NTU)	0.6 – 5.5
Turbidity after sand filters (NTU)	0.1 – 0.8
pH in the influent to preloading column	7.5 – 7.9
Hardness in the influent to preloading column (mg $CaCO_3$/L)	72 – 80
Alkalinity in the influent to preloading column (mg $CaCO_3$/L)	127 – 200
Conductivity in the influent to preloading column (μS/cm)	551 – 599

5.4 Preloading GAC Column Design and Operation

A set of preloading columns was designed to obtain preloaded carbon for evaluating the reduction in adsorptive capacity and the change in kinetics attributable to fouling of the GACs with background NOM from natural water. In order to use typical water from the local region, the preloading facilities (Figure 5-3) were set up at the Mannheim WTP (Kitchener, ON, Canada). The water from the full-scale sedimentation tanks (following flocculation) was directed to two sand filtration columns (column I.D.: 5.08 cm; filtration media: 10 cm anthracite + 10 cm sand + 5 cm gravel), which were designed to remove particulates, thus reducing the clogging of downstream GAC preloading columns. The columns used for preloading had an I.D. of 2.54 cm (1 inch). Both types of GAC were preloaded simultaneously using six preloading columns (bed depth ~25 cm, three for F400 carbon, another three for PICA carbon), which were installed in parallel on the backplate. The up-flow rate was set to 50 mL/min (hydraulic loading ~6 m/h). However, it was determined that the approximately average flow rate could only achieve 41 mL/min, because the headloss build-up in the sand filters led to declining flow rates over time in the preloading columns. The carbons were preloaded for varying amounts of time, then removed from the columns, and immediately stored in a freezer. The carbon was preloaded for up to 16 weeks, during which time several water quality parameters were monitored. These are shown in Table 5-6. The sand filters were backwashed three times per week. The backwash was controlled manually with an approximately bed expansion of 50%. Backwashing of GAC filters was not carried out unless the head loss in the filter was found to be too

high to achieve the designed flowrate, even right after backwashing the sand filters. The preloading period lasted from Fall 2005 to Spring 2006. The monitored PS water temperature range is available in Table 5-6. A detailed figure (Figure I-1) for the temperature trend and preloading time intervals is shown in Appendix I.

In order to minimize loss of adsorbed organics, freeze-drying rather than oven-drying was employed as recommended by Andrews (1990). Therefore, the frozen preloaded GAC were directly dried for at least 48 hours using a freeze-drier available in the Department of Biology (University of Waterloo). To facilitate the determination of isotherm parameters of preloaded carbons and also to avoid crushing the preloaded carbon, a portion of the 30x40 US mesh preloaded carbon was obtained immediately after drying, using a sieving process. According to the results from the sieve analysis (See Appendix E.2, Figure E-1), removal of a small amount of the 30x40 portion seemed not to significantly influence the overall particle size distributions of both types of carbons. All preloaded carbons were stored in desiccators until they were used in isotherm and kinetic tests.

5.5 Pilot-scale GAC Design and Operation

In order to conduct treatability tests under real water treatment conditions and validate model predictions, a pilot-scale column system (as shown in Figure 5-4) was designed and also operated at the same location. The pilot-scale columns consisted of two 5.08 cm (2 inch) diameter columns with approximately 25 cm of F400 carbon and PICA carbon separately loaded in each column. Since the mean diameters of both carbons are around 1 mm, the ratio of column diameter to particle size is much larger than 25, which is considered to essentially eliminate 'wall effects' (Chu and Ng, 1989; Lang *et al.*, 1993; Kwapinski *et al.*, 2004). Each column was equipped with a three way valve, which enabled regular backwashing three times every two weeks. The two pilot columns were operated in down-flow mode at a flow rate of 200 mL/min (~6 m/h). The main flow was provided by pumping the filtered PS water from an approximately 80 L reservoir. The addition of a reservoir and a pump between the sand filters and the GAC columns was necessary in order to provide a stable flow rate through the GAC pilot columns. In this experiment, six sand filters, which were regularly backwashed three times per week, were used to supply enough water to the pilot columns. Another pump equipped with a micro-injection pump head was used to inject the stock solution of target compounds into the influent of the GAC pilot columns at a constant rate. The stock solution was made by dissolving the three target compounds simultaneously directly into Milli-Q water without any organic solvent, in order to avoid enhanced biological activity in the GAC columns. The influent

concentrations for the three target compounds were set at 500 ng/L. Several surveys performed before and during the pilot experiments indicated that the background concentrations of three target compounds in unspiked PS water were generally below 50 ng/L (in a few cases, the concentration of naproxen exceeded 100 ng/L). The spiked concentration of 500 ng/L was well above the background concentration and provided therefore a relatively constant influent concentration. This concentration was also at an acceptable low range, close to environmentally relevant concentrations (e.g. locations close to a wastewater treatment discharge). The influent flow passing through an inline mixer was equally distributed to the pilot columns by adjusting the inlet valve over each column. The feed to each column was set a little higher than the effluent flow rate in order to keep a constant head pressure.

In order to handle the effluent from the pilot columns in a safe manner, it was first treated by GAC adsorbers which contained far more GAC than the pilot columns, before it was collected in the tanks and then delivered to the local wastewater treatment plant.

Sampling ports located both before and after the columns were used to monitor the influent and effluent concentrations of the three target compounds. DOC in both the influent and effluent were also monitored at the same time. The pilot experiment was run for 79 days from Jan to Mar., 2007. The average temperature monitored for PS water was 1.2 ^{o}C (detailed temperature record during the pilot test is shown as Figure I-2, Appendix I). Figure 5-4 provides more details of this design.

Although the PS water going through the pilot GAC columns was pre-treated by sand filters, it was still found that headloss slowly increased overtime. As a result, the effluent flow rate could not satisfy the designed value after the GAC columns ran for approximately one week. In order to maintain a constant flow, periodic backwashing was carried out, though it was reported that this operation may reduce the removal efficiencies and thus change the breakthrough profiles (Sontheimer *et al.*, 1988). Note though that frequent backwashing is standard practice in full-scale operations.

5.6 Investigation of Isotherm Performance

5.6.1 Isotherm Tests

Adsorption isotherm experiments for each target compound were conducted using the bottle point method. Prior to the isotherm tests, a series of preliminary tests were carried out to determine the appropriate equilibrium time for the bottle point method. In these tests, 5 mg of virgin GAC was added to individual solutions each containing 1000 ng of the target compounds in 1 L of ultrapure

water. At different time intervals (up to 15 days on virgin GACs), the samples were analyzed and target compound concentrations were compared to the initial concentrations (detailed results in Section 6.1). The results from these experiments showed that original size virgin PICA carbon (12x30 US mesh) could not achieve equilibration even after 15 days. On the other hand, adsorption equilibrium (for all practical purposes) was achieved on both 30x40 US mesh carbons in 12 days. As a result, 30x40 US mesh fractions of both F400 and PICA carbons were selected for further isotherm tests (see Section 6.1). Furthermore, a twelve-day period was used in the isotherm tests on virgin GAC in ultrapure water and PS water. For the isotherm tests involving preloaded carbons, a similar approach was applied to select an appropriate equilibrium time. As a result, a 21 day equilibrium period was used for all isotherm tests on preloaded carbon. A more detailed discussion is presented in Section 7.1.

The 30x40 US mesh fractions were obtained by sieving the "as received" carbons. Both this fraction and the remaining fractions were washed in a 2 L beaker with ultrapure water, then placed in alum dishes and dried in the oven at 105 ^{o}C for 24 hours. After drying, the GACs were stored in a dessicator. Preloaded GAC were first freeze-dried and then sieved to obtain 30×40 US mesh fractions.

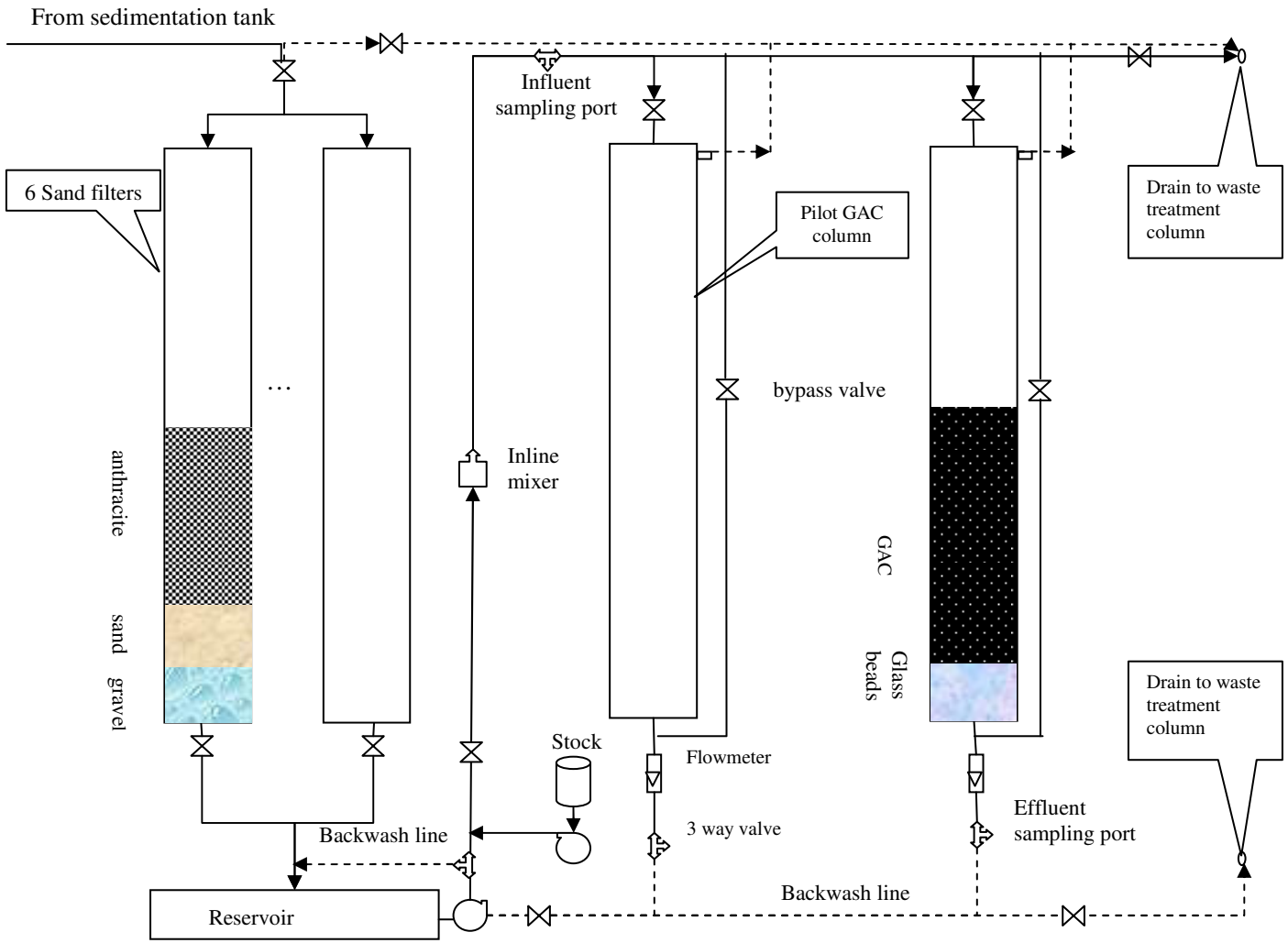

Figure 5-4 Pilot-scale columns system

Isotherm tests were conducted according to the following protocol:

1) Two initial concentration levels (500 and 1000 ng/L) were tested on each virgin GAC for each target compound. An initial concentration of 1000 ng/L of each target compound was applied for each preloaded carbon.

2) The carbon dosage ranged from 0.5 – 10 mg in 1 L of water.

3) Ultrapure or PS water in 1 L amber bottles were used; they were autoclaved prior to the tests.

4) All bottles (containing different carbon dosages) were tightly sealed and placed on a shaker with the rotation speed set at 120 rpm (150 rpm was used for isotherm tests on preloaded GACs) in darkness at 23±1^{o}C (room temperature). The pH of the water matrices was not adjusted (6.4 for ultrapure water; 7.5 – 7.9 for PS water).

5) Two process control samples and two end-point control samples were included in each batch in order to monitor for system losses during the bottle tests. A final concentration in the control samples of greater than 90% of the initial concentrations was considered acceptable.

6) Equilibrium times were 12 days and 21 days for virgin GAC and preloaded GAC, respectively.

7) After equilibrium, the supernatants were filtered using a 100 mesh stainless steel support screen funnel (VWR International, ON, Canada) to remove the GAC particles prior to analysis by GC/MS, as outline in Figure 4-8.

5.6.2 Calculation of the Likelihood Joint Confidence Region and Approximate Confidence Intervals for Estimated Freundlich Parameters

The calculation of confidence intervals for the least squares estimates can be classified into one-at-a-time confidence intervals and joint confidence regions (JCRs). Although the method of constructing one-at-a-time confidence intervals at a selected probability level of (1-α) are most widely used because of its simple implementation, in cases where more than one parameter is estimated, this approach is not as representative of the statistical significance of the results as the JCRs. The JCRs of the parameters give more information about the interaction between parameters and their accuracy. In this study, the evaluation of the statistical uncertainties of the estimated Freundlich parameters can be

made by drawing the likelihood joint confidence region (LJCR) using Equation 5.1 (Duever, 2002; Rotkowsky, 1990, Motulsky and Chrostopoulos, 2004), which is based on finding values of θ^*, where the residual sum of squares (RSS) is less than or equal to a constant value determined by the level of confidence required.

$$\frac{[RSS(\theta^*) - RSS(\hat{\theta})]/p}{RSS(\hat{\theta})/(n-p)} = F(p, n-p, \alpha) \qquad \textbf{5.1}$$

where $RSS(\hat{\theta})$ is the residual sum of squares corresponding to estimated parameter vector $\hat{\theta}$;, $RSS(\theta^*)$ is the residual sum of squares corresponding to vector θ^*; n is the number of data points; p is the number of parameters; and F is the tabulated value of an F-distribution with numerator p; denominator n-p, and a specified significance level α.

In this way, one would be able to determine the interaction between the parameters. Generally, for a linear model with more than one parameter, an elliptically JCR can be relatively easily obtained based on the covariance matrix from the linear least square estimation. For a nonlinear system, the shape of JCR would be bent like a "banana" due to the nonlinearity (Figure 5-5). Since the use of a linearized JCR for a nonlinear model might be misleading (Duever, 2002), while determination of exact JCR is computationally tedious, the relatively easier method of plotting LJCR (based on Equation 5.1) was applied, in particular for the estimated Freundlich parameters on virgin carbons in this study. Specifically, in terms of calculating a LJCR for the estimated Freundlich parameters, the following procedures were adopted:

1) perform nonlinear regression analysis on isotherm data using the Freundlich model in Matlab® Curve Fitting toolbox;
2) then calculate the Jacobian matrix and the vector of residues corresponding to nonlinear regression using an automatically produced m-file from the Matlab® toolbox;
3) finally input experimental data, estimated parameters, Jacobian matrix, and vector of residues into the m-file program "JCRplot" (Appendix C) to compute and plot the LJCR for a specific regression analysis.

For ease of summarization and discussion, the approximate confidence intervals (CI) for individual parameters were also determined based on the plots of the LJCRs. This method was provided by Olmstead and Weber (1990), and rationalized by assuming the $RSS(\hat{\theta})$ obtained in

nonlinear regression had some meaning, and that the extreme value of one parameter in the LJCR was unlikely to yield a true parameter value if the other parameter must deviate far from the best value. However, the resulting approximate CIs are in general smaller than the absolute CIs corresponding to the entire LJCR. Nevertheless, from a practical perspective, the author of this thesis agrees with Olmstead and Weber that more widely absolute CIs for individual parameters are less meaningful, provided that the best fit parameters are close to true values and thus unlikely to change too much when the experiments are repeated or further optimized. As shown in detail in Figure 5-5, the CI for K_F can be directly calculated by varying K_F to the edge of the LJCR when fixing 1/n, and vice versa, the CI of 1/n can be approximated. The computation can be implemented using relevant commands in Matlab®. The more direct way is to read CIs from the LJCR plot.

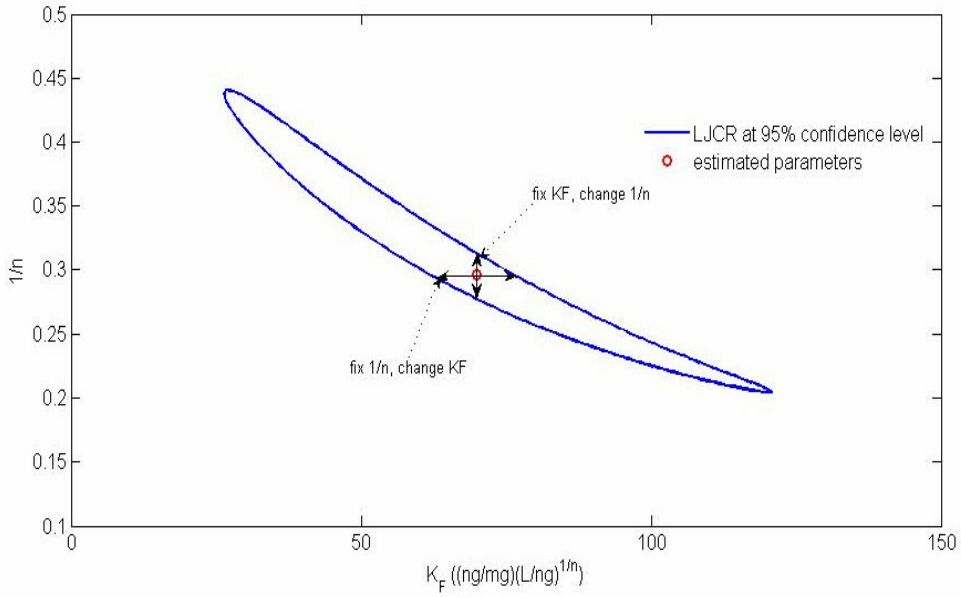

Figure 5-5 Likelihood joint confidence region and search for approximate confidence intervals

5.6.3 Equivalent Background Compound (EBC) Method

As mentioned in Chapter 2, the direct competitive adsorption equilibrium is usually described by the ideal adsorbed solution theory (IAST); however, it is difficult to apply IAST directly to the adsorption in natural water because the NOM in natural water is varied and thus hard to define. A single equivalent background component (EBC), a concept introduced by Najm *et al.* (1991), was defined to represent the portion of the background NOM that competes for adsorption sites simultaneously with the target compound in natural water, thus forming a pseudo-bisolute system. Based on the IAST model coupled with the Freundlich equation (equation 5.2) and the mass balance

equation (equation 5.3), equations 5.4 and 5.5 could be derived and were subsequently used to determine the equilibrium solid phase concentrations of the target compound and EBC. The EBC approach is easily applied, however, once an EBC is determined it is highly specific to the target compound as well as the raw water and the activated carbon characteristics (Ebie *et al.,* 2001; Graham *et al.*, 2000).

$$q_e = K_F C_e^{1/n} \qquad \textbf{5.2}$$

q_e: equilibrium solid phase concentration

C_e: equilibrium liquid phase concentration

K_F, 1/n: Freundlich parameters

$$q_e = \frac{C_0 - C_e}{D} \qquad \textbf{5.3}$$

C_0: initial concentration

D: carbon dosage

$$C_{1,0} - q_{1,eq}D - \frac{q_{1,eq}}{q_{1,eq} + q_{2,eq}}\left(\frac{n_1 q_{1,eq} + n_2 q_{2,eq}}{n_1 K_{F1}}\right)^{n_1} = 0 \qquad \textbf{5.4}$$

$$C_{2,0} - q_{2,eq}D - \frac{q_{2,eq}}{q_{1,eq} + q_{2,eq}}\left(\frac{n_1 q_{1,eq} + n_2 q_{2,eq}}{n_2 K_{F2}}\right)^{n_2} = 0 \qquad \textbf{5.5}$$

$C_{1,0}$, $C_{2,0}$: initial concentration of component 1 (target compound) and 2 (EBC)

$q_{1,eq}$, $q_{2,eq}$: equilibrium solid phase concentrations of component 1 and 2 in a bi-solute system

K_{F1}, K_{F2}, n_1, n_2: Freundlich parameters of component 1 and 2 obtained from single solute system

Search for EBC Parameters – IAST-EBC Program

The IAST-EBC search program (Appendix D) was obtained from Gillogly (1998) and applied with minor modifications to satisfy the specific requirements of this study. To estimate the EBC parameters in PS water, the isotherm test on virgin F400 and PICA carbon on each target compounds were carried out following the isotherm testing protocols described in the previous section. The input data file was composed of Freundlich K_F, 1/n in ultrapure water, the initial concentrations, applied dosages, and corresponding equilibrium liquid phase concentrations in PS water. The detailed program is listed in Appendix C.

The optimization routine available by IMSL® (Visual Numerics, 2006) to estimate the EBC parameters was based on the method of Leverberg-Marquardt to minimize the value of the objective function. It was found that several objective functions were included in the program. Applying a suitable objective function would be important for estimating the parameters in the implementation of the nonlinear least squares optimization routine (Knappe *et al.*, 1993). Knappe (1996) provides a detailed discussion on selection of the objective functions. It was recommended to use the objective function described in equation 5.6, since it considered inaccuracies in both low liquid concentrations at high dosages and low dosages at a high liquid concentration range.

$$f_{obj} = \sum_{i=1}^{n} \left(\left| \frac{C_{cal,i} - C_{\exp,i}}{C_{\exp,i}} \right| + \left| \frac{C_{cal,i} - C_{\exp,i}}{C_M} \right| \right) \qquad \textbf{5.6}$$

where, $C_M = \dfrac{\sum_{i=1}^{n} C_{\exp,i}}{n}$*, and n = the number of data points*

$C_{exp,i}$*: experimentally determined equilibrium liquid phase concentration for point i*

$C_{cal,i}$*: calculated equilibrium liquid phase concentration for point i*

Although the method of EBC has been applied widely, there is no protocol for estimating the EBC parameters. Najm *et al.* (1991) solved the initial concentration, $C_{2,0}$, Freundlich K_{F2}, and $1/n_2$ simultaneously for TCP adsorption in natural water. The fixed value of $1/n_2$ was applied in estimating the other two parameters in studies by Newcombe *et al.* (2002) and Knappe *et al.* (1998). In addition, Graham *et al.* (2000) used constant Freundlich K_{F2} and $1/n_2$ (assuming same adsorbability of EBCs) in order to compare the estimated initial concentrations of EBC in different water matrices. It is obvious that the more the parameters are varied during regression, the more possible it becomes to obtain a better fit. Therefore, in this study, all three parameters were allowed to change during regression. It was later found that for this application, different optimal parameters were often obtained with different initial values, possibly due to different local minima achieved using a certain set of initial guesses. Najm *et al.* (1991) stated that different EBC characteristics determined by applying different initial guesses had no effect in predicting the adsorption of target compounds in the same water matrix. However, the validity of this statement should be based on the fact that the different initial guesses could achieve same sum of squared error (SSE) in optimization. As shown in Figure 5-6, the optimization produced significantly different results when applying different initial guesses of K. This is due to the fact that two sets of initial guesses substantially influenced

optimization quality, leading to different SSE. Therefore, in this study, wide initial guesses of initial concentration, $C_{2,0}$ and Freundlich K_{F2} were tried. The results with minimum SSE was chosen as the best estimates for EBC parameters.

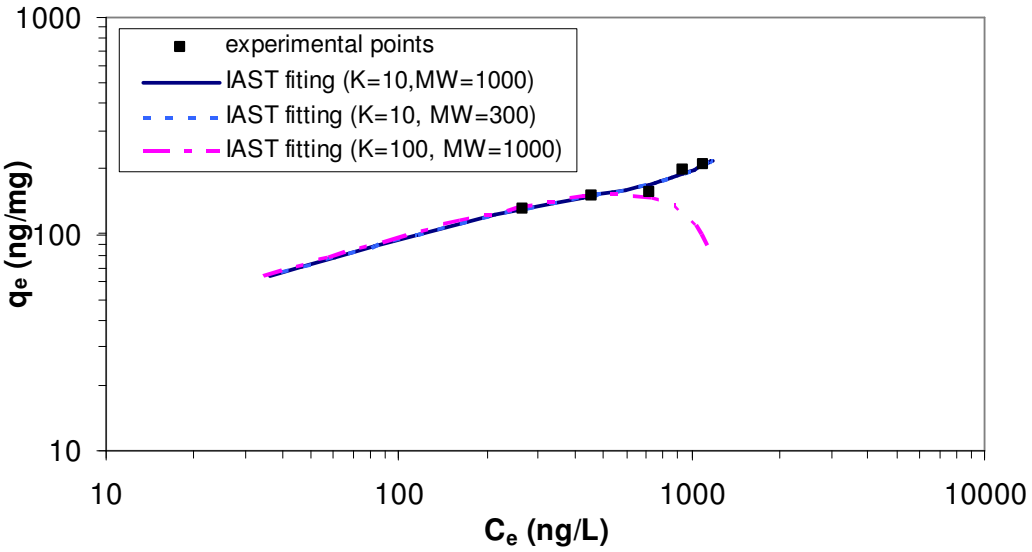

Figure 5-6 Fitting experimental data from carbamazepine adsorption on F400 carbon in PS water by different sets of initial guesses

The following procedures were implemented when fitting the experimental data using the IAST-EBC program.

1) Molecular weight (MW) of EBC was fixed as 1000 g/mol in nonlinear regressions (the change of MW had no effect (Figure 5-6) because all calculations in the IAST model are based on molarities); however parameters ,$C_{2,0}$, Freundlich ,K_{F2}, and $1/n_2$ were allowed to vary during optimization.

2) The initial guesses for K_{F2} were set to 10, 50, and 100 $(mg/g)(L/\mu g)^{1/n}$. The initial guess of $1/n_2$ was always set the same as the $1/n_1$ of the target compound in ultrapure water. The initial guesses of $C_{2,0}$ were 10, 100, and 500 (μg/L).

3) Sum of Squared Errors (SSE) among different sets of initial guesses were compared. The one with the smallest SSE was finally chosen and used to further estimate the parameters.

Once the EBC parameters were determined for a pair of target compounds and GAC in PS water, the IAST program (Appendix E) written by Qi (1992) computed the predicted isotherm of a target compound at initial concentrations of 500 ng/L or other lower initial concentrations of interest in the PS water.

Since the adsorption characteristics of pulverized GAC (PGAC) is the same as the original virgin GAC (Weber and Wang, 1987; Sontheimer *et al.*, 1988, Najm *et al.*, 1990), if adsorption kinetics are not taken into consideration, then the predicted isotherms on virgin GAC can be used to estimate the ultimate adsorption efficiency of PGAC at a specific initial concentration in PS water. A detailed discussion is given in Section 6.2 for the scenario of achieving a 1-log removal of the target compounds. For example, a prediction was made for the minimum dose required to reduce 50 ng/L to 5 ng/L. This is equivalent to reducing probable surface water concentrations of the target compounds to levels at or below their limits of quantification, which is considered satisfactory at this time since there are no regulated concentrations for these three target compounds in drinking water.

5.7 Determination of Kinetic Parameters

5.7.1 Short Fixed-bed Reactor (SFB)

To determine the kinetic parameters that describe the rates of adsorption for the three target compounds by virgin and preloaded GAC, the SFB approach, introduced by Weber and Liu (1980), was applied. As shown in Figure 5-7, the SFB reactor is a small glass column filled with a short bed of the GAC of interest. To avoid the errors induced by crushing preloaded carbon, the original size freeze-dried preloaded GAC was directly packed into the glass column. In order to wet all pores and preloaded material, the GAC sample was soaked for 24 hours in DI water before packing. The packing was performed in water to avoid introducing air bubbles. The I.D. of the glass column was 2.54 cm (1 inch), which ensured that the ratio of the column I.D. to the GAC particle size was approximately 25. Therefore, "wall effects" were considered to be eliminated in SFB experiments. The GAC bed was located between two layers of glass beads similar in size to the GAC particles. The bed depth was short enough to achieve an immediate breakthrough of the adsorbate. The ideal initial breakthrough ratio should be between 0.2 and 0.6. Therefore, the bed depth should increase with increased preloading time of the tested GAC.

The GAC bed was continuously fed with a solution containing the three target compounds at constant concentration (approximately 500 ng/L for each target compound) with a hydraulic loading rate of 6 m/h which corresponds to flows of 50 mL/min. This was the same hydraulic loading rate as

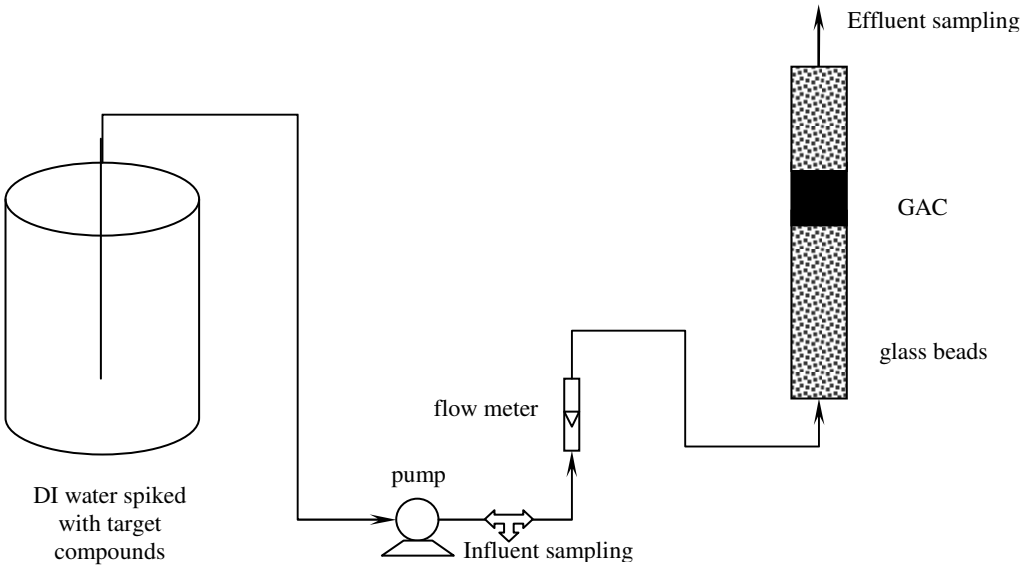

Figure 5-7 SFB reactor setup

in the pilot columns. Long-time (380 hours) and short-time (27 – 30 hours) SFB tests were conducted for virgin and preloaded carbons, respectively. Influent and effluent concentrations were measured regularly to construct the breakthrough curves which were then used to determine external and internal diffusion coefficients based on the nonlinear regression of the PSDM. As discussed in Chapter 2, the advantage of this method is its ability to accurately estimate kinetic parameters at similar hydrodynamic conditions as in real GAC filters.

5.7.2 Calculation of Film Diffusion Coefficients by Gnielinski Correlation

Film diffusion coefficients (β_L) for the three target compounds on a specific GAC were first estimated using the Gnielinski correlation, and these were later used as an initial value for nonlinear regression analysis using the PSDM program. As presented in Chapter 2, the calculation of β_L is based on applying the empirical Gnielinski correlation (Equation 2.41 to Equation 2.44) and the calculated free diffusivities (D_L) of the three target compounds presented in Table 5-3. In the calculation of the Gnielinski correlation β_L, the Schmidt number (Sc) was constant for each compound, while the Reynolds number (Re) would vary slightly (approximately 4.5 under the typical

conditions applied in this study) according to different experimental conditions (e.g. actually determined flow rate and GAC packing). The typical film diffusion coefficients estimated on F400 and PICA carbons are shown in Table 5-7. It is not surprising that the estimated film diffusion coefficients on F400 and PICA carbons are similar because of their similar particle size distributions.

Table 5-7 Film diffusion coefficients estimated using the Gnielinski correlation

β_L (x10^{-3} cm/s)	Naproxen	Carbamazepine	NP
F400	1.56	1.62	1.48
PICA	1.50	1.56	1.42

5.7.3 Determination of Kinetic Parameters using the PSDM Program

Experimental data from SFB tests were used to determine actual film diffusion coefficients and internal diffusion coefficients (either D_s or D_p). Generally speaking, kinetic parameters can be determined by a nonlinear least-squares optimization technique that minimizes the error between the experimental data and the model prediction. The PSDM program was obtained from Carter (1993). This program essentially follows the methodology provided by Crittenden *et al.* (1986). The program was modified to fit the requirements of this study. Figure 5-8 gives an overview of the fitting and prediction procedures performed in the PSDM program. More specifically, a set of PDEs, which describe radial and axial mass transports in GAC adsorbers (refer to Section 2.6 and Appendix A) are transformed into a set of ODEs, which is solved using an external subroutine package – LSODE (Lawrence Livermore National Laboratory, CA, USA). In the model calibration process, the optimization routine – UNLSF available by IMSL® (Visual Numerics, 2006) – was used to estimate the kinetic parameters. This program is based on the method of Leverberg-Marquardt to minimize the sum of squared errors (SSE). The detail program code is included in Appendix F.

The program was equipped with a switch that enabled estimation of one parameter at one time or two or three parameters simultaneously. Generally, the following protocol was implemented in fitting the experimental data from the SFB test:

1) Either pore diffusion or surface diffusion was considered at one time. Accordingly, model calibration was performed in both film-pore diffusion and film-surface diffusion modes.

2) For virgin GAC, the initial value for β_L was set as the estimated value from the Gnielinski correlation. The initial valve for D_p was the free diffusivity of the corresponding compound (impedance is 1). The initial value for D_s was 1.0×10^{-11} cm^2/s, which is the typical magnitude for MIB (Gillogly, 1998). For preloaded GAC, initial values were set using an iterative approach meaning that virgin GAC values were used as initial guesses for 1-week preloaded GAC, and estimated values for 1-week preloaded GAC were used for 3-week preloaded GAC, and so on. This seemed reasonable because it was expected that the kinetic parameters decreased with increasing preloading time.

3) Initially, β_L was fitted on the basis of only early breakthrough data. Once β_L was obtained, D_s or D_p could be determined with fixed β_L using late breakthrough data. However, it was found that film diffusion significantly influenced the entire breakthrough duration on both virgin and preloaded carbon in this study. Therefore, β_L and D_s or D_p were optimized simultaneously. This point will be discussed in detail in Chapter 6 and 7.

4) The confidence intervals of the determined parameters were calculated using the approach of LJCR, which is discussed in Section 5.6.2. The PSDM program automatically searches the CIs in the range between 0 and 4 times of the determined parameters.

Although it has been pointed out that the dispersion effect can be negligible in most cases (see Section 2.6.2), to maintain a conservative approach, it was still considered when fitting experimental data from the SFB tests. Carter (1993) described an approach for estimating dispersion coefficients (Equation 5.7).

$$\frac{D_z}{v \cdot d} = P_{e\ particle} \qquad \textbf{5.7}$$

where $P_{e\ particle}$ is the particle Peclet number; other parameters have been defined in Chapter 2.

It was reported that, in the typical flow range (4.8-24 m/h) encountered in drinking water treatment applications, $P_{e\ particle}$ stays approximately constant at 2 (Liu and Weber, 1981, cited by Carter, 1993). Therefore, the typical dispersion coefficient in SFB tests was approximately 8.0×10^{-2} cm^2/s at a hydraulic loading of 6 m/h. This value may change slightly among different SFB tests because of slightly different packing. Nevertheless, it was later found in this study that dispersion effects did not significantly influence breakthrough profiles under the experimental conditions of this study.

5.7.4 Simulation of Pilot-scale GAC Adsorber Performance

After isotherm and kinetic parameters were determined, the relationships between these parameters and the preloading time were simulated by searching for an appropriate mathematical function in the function library available from a statistics software package – Labfit®. As a result, each of the isotherm and kinetic parameters were expressed as a function of preloading time. Once the empirical functions for the time-variable parameters were determined, the PSDM program in combination with these empirical functions was used to simulate the performances of the pilot-scale columns. Furthermore, the validity and accuracy of the mathematical predictions of the adsorption of the three target compounds in the two types of GAC pilot columns are evaluated and discussed in Chapter 8.

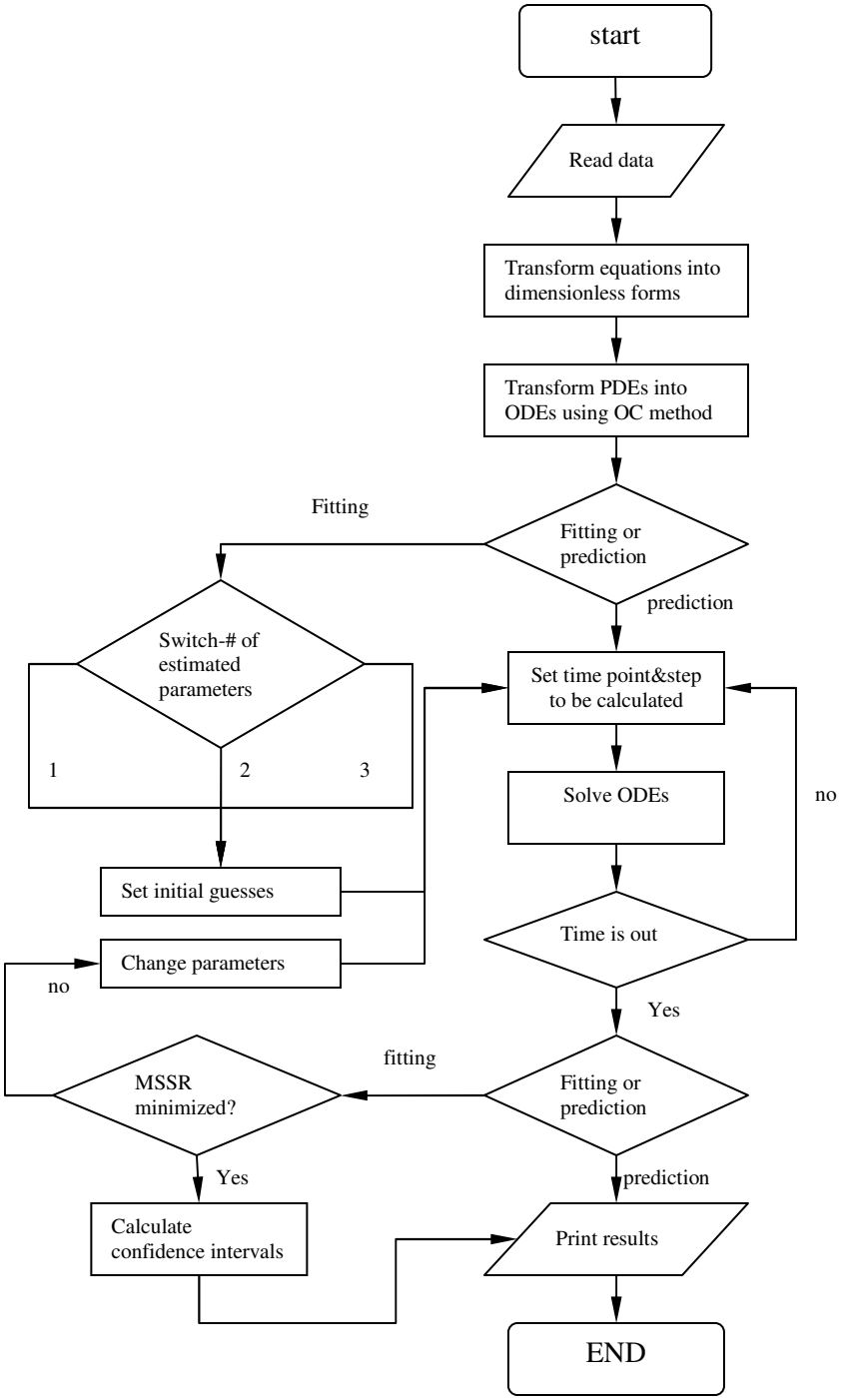

Figure 5-8 Flow chart of PSDM program

CHAPTER 6
ADSORPTION PERFORMANCE ON VIRGIN GAC

6.1 Single Solute Isotherms in Ultra-pure Water

6.1.1 Equilibrium Time on Virgin Carbons

To determine the equilibrium times for all target compounds on the different GACs in ultrapure water, a series of static kinetic tests were performed. This was done by adding 5 mg/L GAC to individual solutions of the target compounds (C_0 = 500 - 1000 ng/L) in 1 L amber bottles and then determining the remaining concentrations of the solution in the individual bottle at different time intervals (more detailed procedures described in Chapter 5). The first trial was performed on the original size carbons (12×30 PICA and 12×40 F400 carbons). Plots of normalized concentrations versus time are shown in Figure 6-1 (the actual determined concentrations are shown in Appendix F). The concentrations of NP after 6 days were very low (~ 9 ng/L), but they were still higher than the limit of quantification (LOQ) of the analytical method.

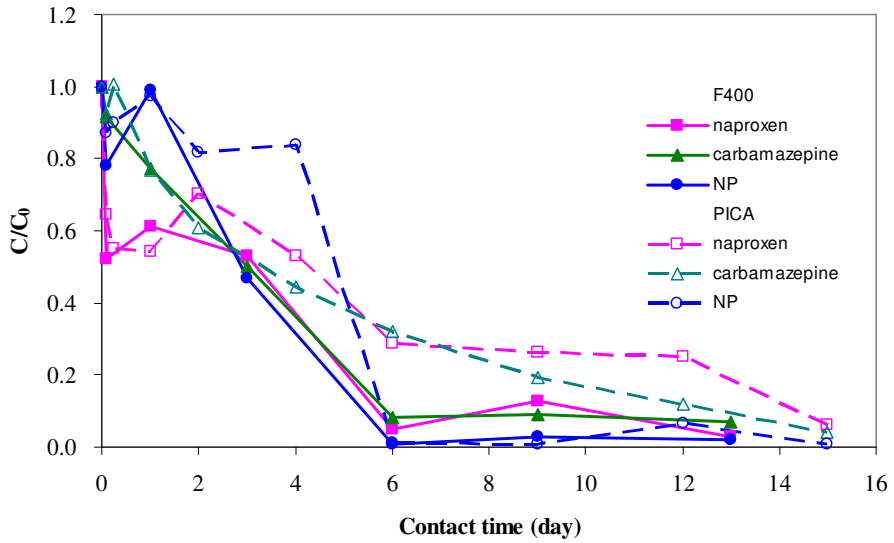

Figure 6-1 Concentration profiles of target compounds on original size PICA and F400 carbons in ultrapure water

It was observed in Figure 6-1 that all three target compounds were more quickly adsorbed onto F400 carbon, with apparent equilibrium being reached after 6 days. However, for PICA carbon, with the exception of NP, none of the other two PhACs could achieve apparent equilibrium, even after 15 days of adsorption. This suggested that the mass transfer rates of the target compounds onto the PICA carbon under this experimental condition were slower than those onto the F400 carbon. In an attempt to shorten the time required for reaching apparent equilibrium, a second trial was conducted in which the original size PICA carbon was sieved through 30x40 US mesh. Results for equilibrium tests conducted on the smaller size PICA carbon are shown in Figure 6-2.

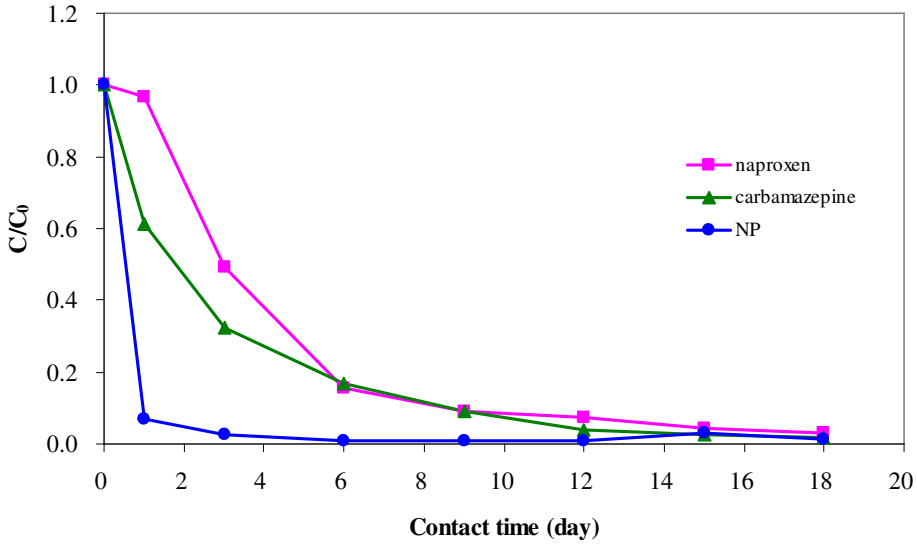

Figure 6-2 Concentration profiles of target compounds on 30x40 US mesh PICA in ultrapure water

As expected, adsorption was more rapid for all target compounds; apparent equilibria for all target compounds were essentially achieved after 12 days. As a result, a cutoff time of 12 days was selected for the equilibrium isotherm tests on 30x40 US mesh PICA and F400 carbons. Although the equilibria on 30x40 F400 carbon should be less than 6 days, it was decided that using the same equilibrium time would allow for improved direct comparisons between the two carbons. In addition, it has been proven that the capacity of virgin GAC is independent of particle size (Sontheimer *et al.*, 1988; Gillogly, 1998), hence, the adsorption parameters determined using a small particle size should be considered to be representative of those for original-sized GAC. Nevertheless, ground GAC was not used in this study, in order to facilitate direct comparisons between virgin and preloaded carbons later in the study.

The two figures show that of all the compounds, NP was adsorbed the fastest, while naproxen and carbamazepine had similar adsorption rates late in the time interval on both carbons.

6.1.2 Statistical Analysis of Isotherms

Adsorption isotherms describe how adsorbates interact with adsorbents, thus they are of critical importance in choosing and optimizing the use of adsorbents. It is important to establish the most appropriate methods to analyze the experimental equilibrium data. In this study, three isotherm equations, Langmuir (Equation 6.1) (Langmuir, 1918), Freundlich (Equation 6.2) (Freundlich, 1906), and Langmuir-Freundlich (LF, Equation 6.3) (Derylo-Marczewska *et al.*, 1984) equations were applied to analyze the isotherm data because they have been widely used for describing the activated carbon adsorption characteristics in water treatment applications (e.g. Sontheimer *et al.*, 1988; Kilduff and Wigton, 1999; Kumar and Sivanesan, 2005a, b).

$$q_e = \frac{q_m K_a C_e}{1 + K_a C_e} \qquad \textbf{6.1}$$

$$q_e = K_F C_e^{\,1/n} \qquad \textbf{6.2}$$

$$q_e = \frac{Q_o (bC_e)^{n_2}}{1 + (bC_e)^{n_2}} \qquad \textbf{6.3}$$

in which q_e is solid phase concentration at equilibrium, C_e is liquid phase concentration at equilibrium; K_F and n are Freundlich constants; K_a is Langmuir constant; q_m indicates maximum saturation capacity of the compound on the carbon at the isotherm temperature; Q_o represents the adsorption capacity, b and n_2 are LF isotherm constants, representing the average site energy, and the heterogeneity of site energies, respectively (Kilduff and Wigton, 1999).

The three selected isotherm equations are closely related. The Langmuir equation is based on the assumption of a structurally homogenous adsorbent where all sorption sites are identical and energetically equivalent. The Freundlich equation is an empirical equation employed to describe a heterogeneous system. The LF equation combines elements from both the Langmuir and Freundlich equations, and thus can be reduced to either form under different conditions. When the heterogeneity index (n_2) is close to 1, the LF equation simplifies to the Langmuir equation. The LF equation simplifies to the Freundlich equation when $bC_e << 1$, i.e. at very low equilibrium concentrations, or a small constant b.

Initially, it was expected that the LF equation would have the best fit for isotherm data because it includes the hybrid mechanisms of adsorption. However, in order to confirm the most appropriate model for use in this research, all three equations were compared.

Decision to Use Non-linear Regression

The parameters of the Langmuir and Freundlich equations can be determined using their linear forms. The linear least-squares method has been widely applied to determine isotherms using the coefficient of determination (R^2) (Ho, 2004). On the other hand, the parameters of the LF equation cannot be estimated by the linear least-squares method because this three parameter model equation can not be easily solved from the linear equation. Linear regression analysis of isotherm data using the linearized forms of Langmuir and Freundlich equations were carried out as the first step.

Two linear forms (Equation 6.4 and 6.5) of the Langmuir formula have been commonly used (Sontheimer *et al.*, 1988; Ho, 2004; Kumar and Sivanesan, 2005a) to describe the adsorption of organics in water. Equation 6.6 is the linear form of Freundlich equation.

$$\frac{C_e}{q_e} = \frac{1}{q_m} C_e + \frac{1}{K_a q_m} \qquad \textbf{6.4}$$

$$\frac{1}{q_e} = \left(\frac{1}{K_a q_m} \right) \frac{1}{C_e} + \frac{1}{q_m} \qquad \textbf{6.5}$$

$$\log q_e = 1/n \log C_e + \log K_F \qquad \textbf{6.6}$$

The results of the linear regression of the isotherm data for naproxen on PICA and F400 carbons in ASTM type II water are shown as Figure 6-3, Figure 6-4, and Figure 6-5 (linear adsorption isotherms for carbamazepine and NP are shown in Appendix G). The corresponding isotherm parameters obtained using linear regression are summarized in Table 6-1. Overall, based on R^2 values, it seems that regressions using the linear Freundlich equation were better than those carried out using the two linear Langmuir forms. Comparison between results from the two linear forms of Langmuir equation indicated that equation 6.4 generally performed better than equation 6.5 in regressing the isotherm data of naproxen and carbamazepine, but was worse for the analysis of NP data. The difference between the two linearized forms of Langmuir equation results from the change in error structure of the data when transforming the nonlinear equation to its linear forms, which may impact the normality assumptions of standard least squares in linear regression (Rotkowsky, 1990).

Regression is based on the assumption that the error distribution is the same at every value, following a Gaussian distribution (Kumar and Sivanesan, 2005b). If the original error structure follows this distribution, the transformed data may not have the same distribution structure. As shown in Figure 6-3, Figure 6-4, and Figure 6-5, three linear equations led to different axial settings(different units for x- and y-axes in the different linearized plots), hence probably leading to different error structures of variables and consequently altering the result of a linear regression and influencing the determination process. Therefore, direct comparisons of R^2 shown in Table 6-1 are misleading because they were highly specific to each linearization method and might not provide the best isotherm constants to correlate the original isotherm equation with experimental data (Wong *et al.*, 2004).

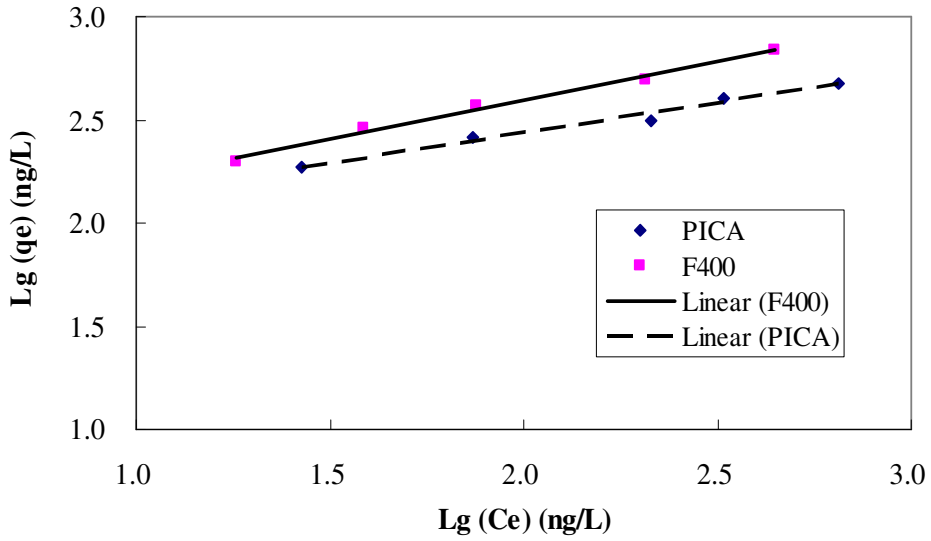

Figure 6-3 Linear Freundlich isotherms of naproxen in ASTM type II water

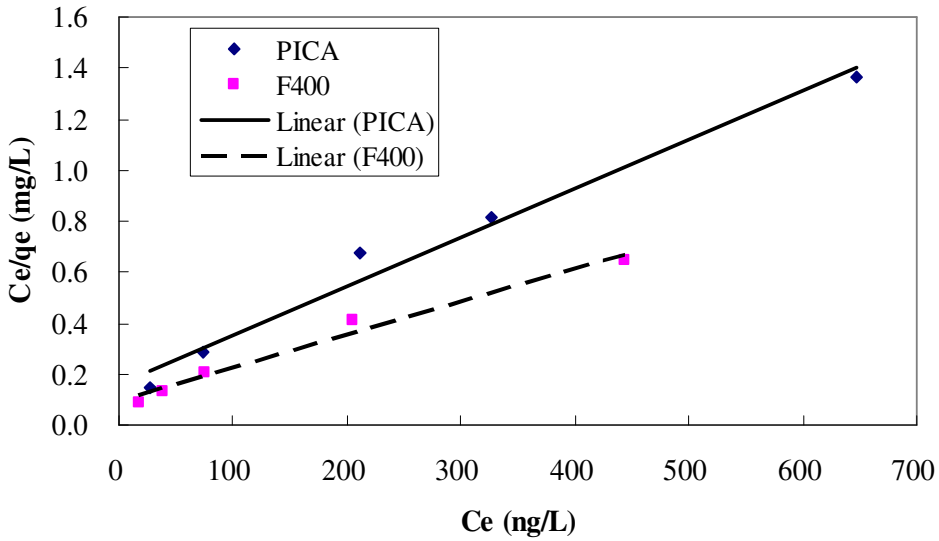

Figure 6-4 Linear Langmuir isotherms (Equation 6.4) of naproxen in ASTM type II water

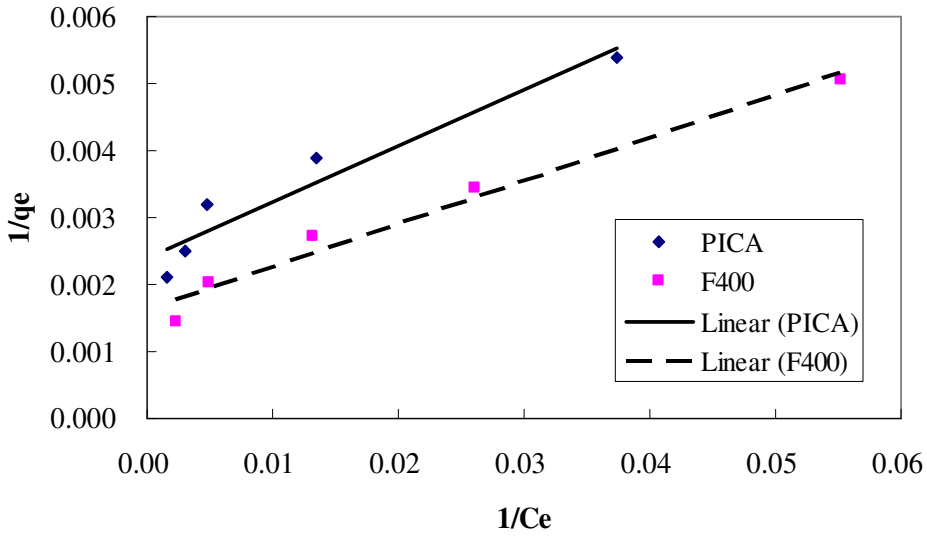

Figure 6-5 Linear Langmuir isotherms (Equation 6.5) of naproxen in ASTM type II water

Table 6-1 Isotherm parameters obtained using linear regression (ASTM type II water)

		Compounds					
		naproxen		carbamazepine		NP	
Model	Carbon	PICA	F400	PICA	F400	PICA	F400
Linear	K_F (ng/mg)(L/ng)$^{1/n}$	71.3	70.6	61.4	74.7	3.06	3.01
Freundlich	1/n	0.29	0.37	0.42	0.42	0.83	0.85
Eq. 6.6	R^2	0.980	0.991	0.980	0.999	0.992	0.976
Linear	q_m (ng/mg)	526	769	1111	1111	2500	2500
Langmuir	K_a (L/ng)	0.0116	0.0136	0.0068	0.0108	0.0006	0.0006
Eq. 6.4	R^2	0.979	0.980	0.964	0.980	0.737	0.723
Linear	q_m (ng/mg)	417	6257	714	8337	2000	5000
Langmuir	K_a (L/ng)	0.0287	0.0250	0.0203	0.0219	0.0007	0.0003
Eq. 6.5	R^2	0.925	0.975	0.891	0.975	0.991	0.967

Unlike the linear analysis, nonlinear methods avoid the downsides of linearization, and they are therefore more appropriate to obtain the isotherm parameters.

Selection of Isotherm Models

Nonlinear regression analyses were performed on all isotherm data using three isotherm equations in the Matlab® toolbox titled Curve Fitting. Nonlinear least squares based on the calculation of weighted sum of square was chosen as the method for regression. As indicated in the manual of Curve Fitting (MathWorks, 2004), standardized adjusted residuals, which can downweight high influential data points, are used for calculating a weight for each residue. As a result, the outliers are automatically excluded. More details are presented in the manual (MathWorks, 2004).

It has been recommended that replicated datasets should be used in order to adequately judge the preference of one model over another (Rotkowsky, 1990); however, due to the considerable time requirements of the isotherm tests in this study, the selection of a preferable model was carried out by simply examining the minimum sum of squared errors (SSE) for each adsorbent–adsorbate pair. In addition, the residual plots were tried to examine the goodness of fit. However, due to the limited experimental data were available for each adsorbent-adsorbate pair, this exercise seemed not applicable in this study. As shown in Table 6-2, the two parameter Freundlich model and the three

parameter LF model demonstrated a similar quality of regression for the naproxen and carbamazepine isotherm data for both carbons. The determined Freundlich 1/n values or LF n_2 values for these two compounds on both carbons were substantially less than unity, suggesting that the adsorption processes were heterogeneous. The Langmuir model only showed good fitting performance for NP adsorption. It was observed that, in this case, the adsorption of NP on carbon tended to be homogenous (Freundlich 1/n and LF n_2 close to unity).

Table 6-2 Isotherm parameters obtained using nonlinear regression (ASTM type II water)

		Compounds					
		naproxen		carbamazepine		NP	
Model	Carbon	PICA	F400	PICA	F400	PICA	F400
Freundlich Eq. 6.2	K_F (ng/mg)(L/ng)$^{1/n}$	69.96	73.15	57.56	73.79	2.49	4.44
	1/n	0.296	0.366	0.431	0.417	0.866	0.784
	SSE	1049	943	5137	163	1154	1963
Langmuir Eq. 6.1	q_m (ng/mg)	475.4	730.9	1111	1077	3558	1869
	K_a (L/ng)	0.0168	0.0153	0.0061	0.0108	0.0004	0.0009
	SSE	6945	9487	15860	13970	1471	432
Langmuir - Freundlich Eq. 6.3	Q_0 (ng/mg)	1715	3212	4524	4952	8783	2101
	n_2	0.369	0.424	0.495	0.469	0.908	0.999
	b (L/ng)	0.0001	0.0001	0.0001	0.0001	0.0001	0.0008
	SSE	1261	1001	4895	400	1497	1061

In most cases, the LF equation did not provide a better fit than the Freundlich equation (Table 6-2). It was found that, with the exception of NP on F400, Q_0 and b could not be accurately estimated (estimated b values were extremely low, and the standard deviations (not shown) were larger than the estimated values). The inaccuracy of estimating Q_0 and b was possibly due to the fact that the measured concentration range did not cover the saturation part of the isotherm, thus leading to large standard deviations of the estimated values (Kim, 2004). In other words, the LF model is only advantageous in describing a wide concentration range covering both sub-saturation and saturation situations. Since only the low concentration range is of interest in this study, the Freundlich model is superior for describing this 'sub-saturation' behaviour of the isotherm.

6.1.3 Isotherms on Virgin Carbon

Single solute adsorption isotherms were conducted using initial concentration of both 500 and 1000 ng/L for naproxen, carbamazepine, and NP in "organic free" water. Surprisingly, small differences between isotherms starting from different initial concentrations were observed in both Milli-Q water and ASTM type II water, possibly indicating adsorption competition due to the existing background organics. These observations are discussed in detail later in this section. Nevertheless, as a compromise (as discussed in the later section), it was finally decided that the isotherms at high initial concentration (1000 ng/L) in ASTM type II water would be used for further applications in this study.

Since the Freundlich isotherm model is dependant on the concentration range (Sontheimer *et al.*, 1988), GAC adsorption capacity evaluations for drinking water treatment purposes should be carried out in a relevant equilibrium concentration range. Therefore, appropriate initial concentrations and dosages were applied in order to achieve the equilibrium ranges covering the actual observed concentrations in surface water and drinking water. Table 6-3 lists the single solute Freundlich isotherm parameters obtained from nonlinear regression (Figure 6-6 and Figure 6-7), and their approximate individual CIs at 95% level computed using LJCR plots (Figure 6-9, Figure 6-10, and Figure 6-11) (The approach of calculating LJCRs was discussed in Section 5.6).

Table 6-3 Freundlich parameters obtained in ASTM type II water

Compound	Parameters	Carbon	
		PICA	F400
Naproxen	K_F (ng/mg)(L/ng)$^{1/n}$	69.96 (62.01, 76.84)	73.15 (67.50, 77.30)
	1/n	0.296 (0.277, 0.314)	0.366 (0.351, 0.378)
Carbamazepine	K_F (ng/mg)(L/ng)$^{1/n}$	57.56 (49.30, 69.02)	73.79 (71.84, 76.05)
	1/n	0.431 (0.407, 0.454)	0.417 (0.413, 0.424)
NP	K_F (ng/mg)(L/ng)$^{1/n}$	2.49 (2.27, 2.70)	4.44 (3.91, 4.93)
	1/n	0.866 (0.853, 0.881)	0.784 (0.765, 0.803)

Numbers in the parentheses are 95% confidence intervals

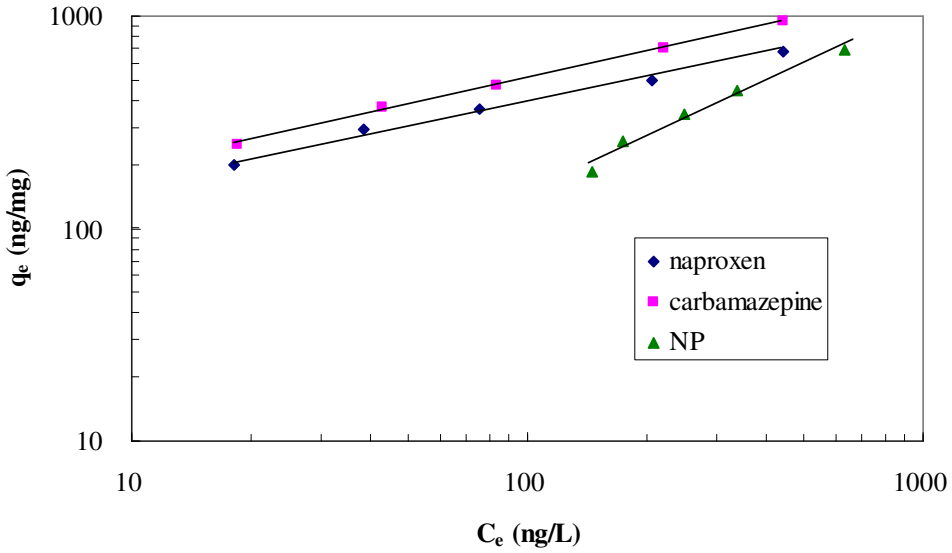

Figure 6-6 Isotherms on virgin F400 carbon in ASTM type II water

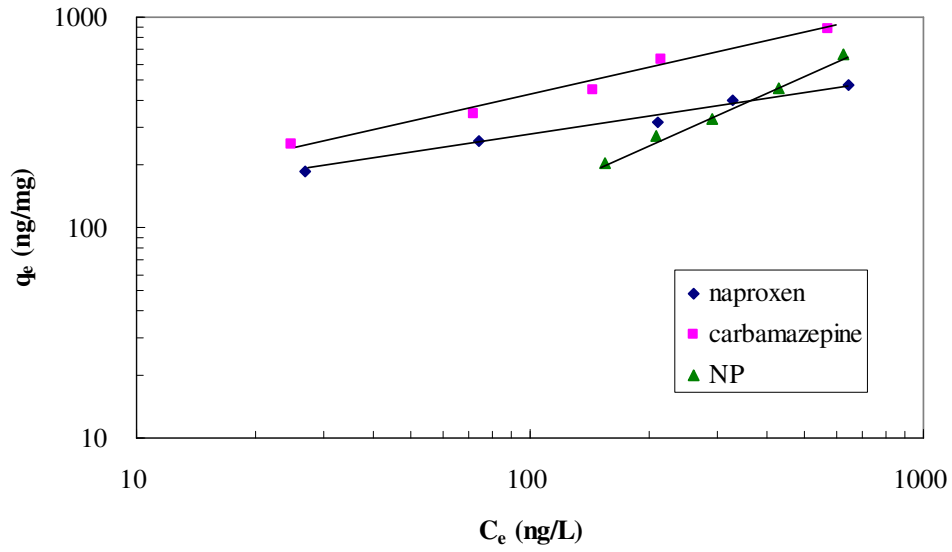

Figure 6-7 Isotherms on virgin PICA carbon in ASTM type II water

Although the Freundlich K_F values are somewhat indicative of the adsorptive capacity, it would be improper to carry out direct comparisons because K_F is correlated to 1/n (as discussed in Section 5.6 and shown in Figure 5-5) and unit specific (Andrews, 1990). Therefore, comparisons were made directly using isotherms within the same investigated concentration range. As shown in Figure 6-6, the absorbabilities of the three target compounds varied substantially as follows: carbamazepine >

naproxen > NP on virgin F400 carbon. The adsorptive capacities of the three target compounds on virgin PICA carbon also followed the same trend (Figure 6-7).

It is interesting to note that in the investigated concentration range for both F400 and PICA carbons, the absorbabilities of the three target compounds are not in agreement with the magnitude of their hydrophobicity, which can be expressed as their octanol-water partition coefficients (log K_{ow}) (5.92, (Yoon *et al., 2002*), 3.18, and 2.45 (Trenholm *et al.*, 2006) for NP, naproxen, and carbamazepine, respectively). Log K_{ow} is the important factor in the evaluation of adsorption. A general sense is that compounds with a higher log K_{ow} value should have higher sorption affinity on activated carbon. This was confirmed by some studies in evaluating adsorptions of other EDCs (Choi *et al.*, 2005), PPCPs (Westerhoff *et al.*, 2005) and neutral pesticides (Hu *et al.*, 1997) in water. However, the results obtained in the present investigation at ng/L concentrations indicated that this may not be the case in very dilute solutions. The relatively lower adsorption affinity of naproxen compared to carbamazepine found in the present study was in accordance with the observations reported by Westerhoff *et al.* (2005) and Snyder *et al.* (2007), who applied one dosage of PAC to a water matrix spiked with several PPCPs. This could be mainly attributed to the dissociation of the acidic naproxen (pK_a = 4.15) at pH typically observed in surface and drinking water. Hu *et al.*, (1998) recommended using a modified log K_{ow} value to predict the adsorbability of an acidic or basic pesticide.

$$K_{ow}^{'} = K_{ow} / (1 + 10^{(pH - pK_a)}) \qquad \textbf{6.7}$$

where $K_{ow}^{'}$ *represents the pH corrected octanol-water partition coefficient for neutral species.*

Accordingly, the modified log K_{ow} value of 0.89 at a pH of 6.4 was calculated for naproxen based on equation 6.7 (Hu *et al.*, 1998) and the log K_{ow} and pK_a values given in Table 5-1. The modified log K_{ow} value is substantially lower than that of carbamazepine, thus explaining the aforementioned difference between the two PhACs. Nonetheless, the mechanism of deprotonation could not be successfully applied to the case of the lowest adsorption affinity of nonylphenol on both carbons, since nonylphenol should be neutral at typical pH in water. The exact reasons are not clear but, in addition to log K_{ow}, the adsorption might be influenced by other properties of either the adsorbate or adsorbent, such as functional groups and surface charges on adsorbents (Newcombe *et al.*, 2002a, b; Fairey *et al.*, 2006), and the relationship between the molecular size of adsorbates and the pore size distribution of the adsorbent (Karanfil *et al.*, 2006), etc. Further studies are required to elucidate the underlying mechanisms for the NP adsorption results.

As mentioned above, the adsorptive capacity of NP on both PICA and F400 carbons, was not as would have been anticipated based on its high hydrophobicity, but was much lower than for naproxen and carbamazepine in the very low equilibrium concentration range. Nevertheless, the adsorption affinity of NP would approach and subsequently exceed those of naproxen and carbamazepine when the equilibrium concentrations increase (Figure 6-8). Furthermore, it was found that the reported Freundlich parameters on F400 carbon in this study are different from those reported in other studies. For the purpose of practical use, the special adsorption feature of NP at low concentration levels is of great concern. It has been reported that F300 and F400 carbons had very high capacities of approximately 100 μg/mg for NP at a liquid equilibrium concentration of 1 μg/L, based on extrapolation of adsorption isotherms for high initial concentrations (1000 to 10000 μg/L) (Choi *et al.*, 2005; Tanghe and Verstraete, 2000). In the present study, the capacity of F400 was 1 μg/mg at an equilibrium liquid concentration of 1 μg/L. This result is close to that reported by Perrich (1981). The Freundlich 1/n value on F400 carbon was 0.784 in the present study, compared to a value of 0.145 given by Choi *et al.* (2005). This is in agreement with the change of Freundlich 1/n for MIB as summarized by Chen *et al.* (1997) that the Freundlich 1/n of MIB on F400 carbon in very diluted solutions was substantially higher than those obtained in high concentration solutions. The curvatures of Freundlich isotherms for MIB and geosmin adsorption on F400 carbon over a wide liquid concentration range were confirmed by Pirbazari *et al.* (1993). A similar decreasing trend for the Freundlich 1/n of atrazine was also evidenced when its equilibrium liquid phase concentration increased from 0.1 to 10,000 μg/L (Pelekani and Snoeyink, 2000). Therefore, it is possible that, as other conventional micropollutants mentioned above, the isotherm of NP on a logarithmic plot possesses high deviation from linearity (as shown in Figure 6-8), and thus can not be expressed as a single Freundlich equation in the wide concentration range. The difference of the Freundlich 1/n in two different concentration ranges might be interpreted by the fact that the Freundlich exponent on a heterogeneous adsorbent may approach unity in extremely dilute solution (Suffet, 1980; Sontheimer *et al.*, 1988). This trend was also confirmed by Chang *et al.* (2004), who found that the Freundlich 1/n of another EDC (estrone) determined for a PAC in very dilute solution (1 – 20 ng/L) was 1.

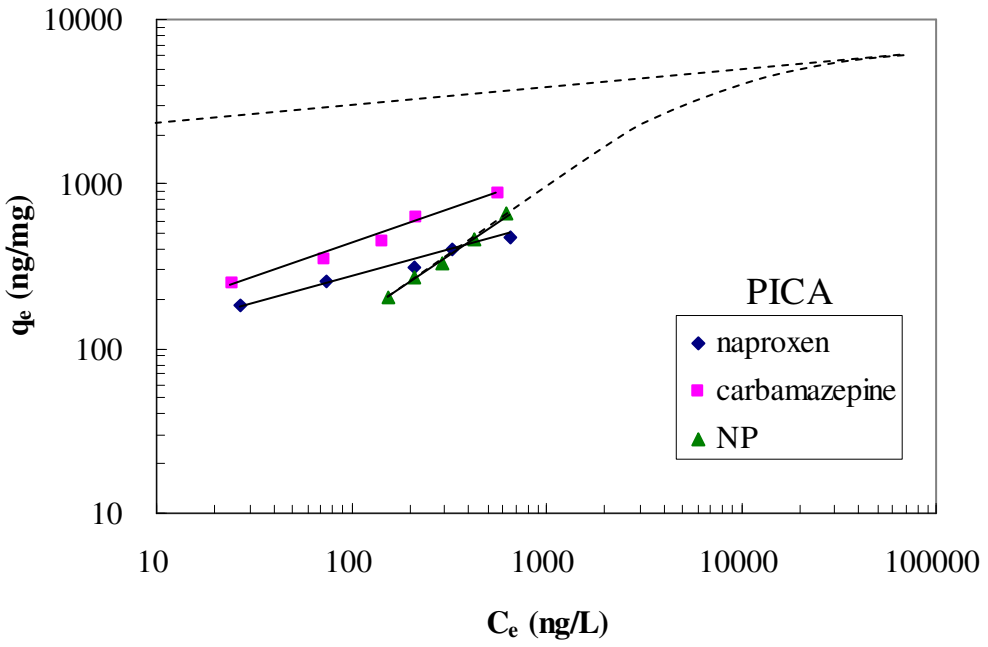

Figure 6-8 Hypothetical extrapolation of isotherm trend to higher concentrations (on PICA carbon)

Based on above discussion, it could be concluded that, if an inappropriate extrapolation from the high concentration range is applied for predicting the removal of NP in the very low concentration range (as shown in Figure 6-8), the removal efficiency may be overestimated and misleading in the design of PAC processes and GAC filters for drinking water treatment purposes. Furthermore, the observed isotherm performance for NP adsorption at the low concentration range may also provide a reasonable explanation for the low removal efficiencies for NP in a bench-scale PAC study and in a full-scale GAC adsorber as reported by Snyder *et al.* (2007) and Stackelberg *et al.* (2007), respectively.

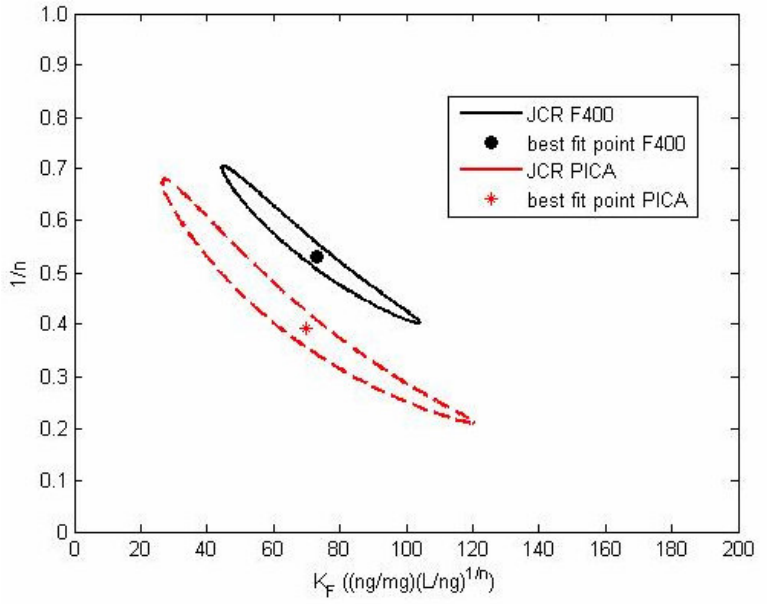

Figure 6-9 Comparison of JCRs for naproxen adsorption parameters on PICA and F400 carbons

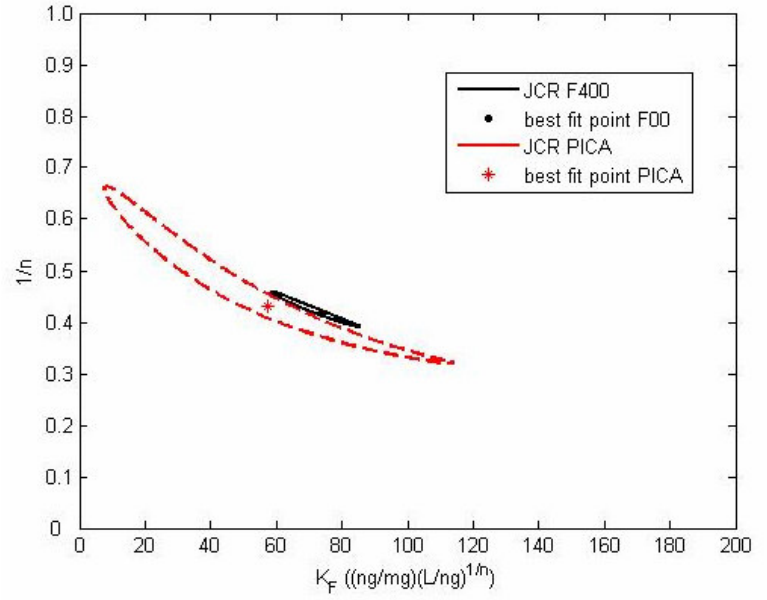

Figure 6-10 Comparison of JCRs for carbamazepine adsorption parameters on PICA and F400 carbons

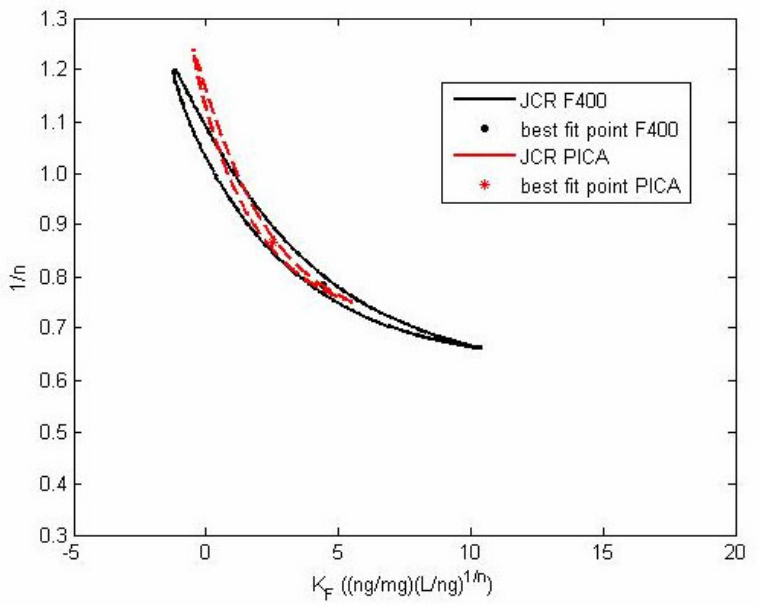

Figure 6-11 Comparison of JCRs for NP adsorption parameters on PICA and F400 carbons

Since the structure of the Freundlich model leads to a high correlation between the estimates of K_F and 1/n, it would be more appropriate to compare the Freundlich parameters directly using LJCR, rather than using the individual parameter estimates. Figure 6-9 to Figure 6-11 can be used to compare the adsorption characteristics between F400 and PICA carbons. In Figure 6-9, with respect to naproxen, F400 carbon showed higher adsorptive capacity but more homogeneous adsorption (lower range of 1/n) than PICA carbon. The difference in the adsorption of carbamazepine was less as shown in Figure 6-10, but was still significant. However, the LJCR of the two carbons in terms of adsorbing NP nearly overlapped (Figure 6-11), indicating that the adsorption characteristics for NP were similar on F400 and PICA carbon. However, it should be noted that, in all cases the above discussion is valid only for the experimental conditions actually tested.

F400 carbon has been widely used in many studies for removal of other conventional micropollutants, e.g. TCE (Carter *et al.*, 1992; Carter and Weber, 1994), atrazine (Schideman *et al.*, 2006), MIB and geosmin (Pirbazari *et al.*, 1993), whereas no adsorption isotherm data have been published for the three target compounds used in this research on F400 carbon. Nonetheless, the published single solute isotherm data obtained for other compounds on F400 carbon (as shown in Table 6-4) provide an opportunity to compare the adsorbabilities between extensively studied micropollutants and the target compounds in this study, and consequently, a rough impression could be obtained about the appropriateness of a judgement of the removals of PhACs and EDCs inferred from the results for other conventional micropollutants. Generally, as shown in Figure 6-12 (plotted

according to Freundlich parameters given in Table 6-3 and Table 6-4), the three target compounds in this research show lower adsorbability than the other four compounds, especially in the concentration range from 100 – 1000 ng/L. Atrazine demonstrates a much higher adsorption affinity than all of the other compounds. The isotherms of the other examined compounds are close but cross each other in the equilibrium liquid phase concentration of approximately 100 ng/L. With respect to the Freundlich 1/n, the performances of MIB and geosmin are very similar to that of NP, though both of them show higher adsorption capacity than NP in the same concentration range. As a result, the removals of both MIB and geosmin are expected to be finally lower than of naproxen and carbamazepine at liquid concentrations below approximately 30 - 50 ng/L. This point is of practical significance because, like PhACs and EDCs, MIB and geosmin occur in the aquatic environment at same or even lower concentration ranges. Therefore, it can be preliminarily concluded that the PAC dosage applied for mitigating these taste and odorous compounds could effectively remove carbamazepine and naproxen at same low concentration levels. TCE may be the most studied compound. Unfortunately, the reported isotherm concentration range was mostly from 10 to 1,000 μg/L, which was much higher than for the other compounds. The isotherm of TCE shown in Figure 6-12 is extended based on its isotherm at the range of 10 to 1,000 μg/L down to the concentration of interest in this study. In this case, if the possible curvature when extending isotherm in a large concentration range is not considered, TCE exhibits a slightly higher sorption affinity than carbamazepine in particular at low concentrations. Finally, it seems from Figure 6-12 that none of the selected conventional micropollutants could serve as a reference for removing NP at the low concentration levels of interest.

Table 6-4 Published Freundlich parameters for other conventional micropollutants on F400 carbon

compound	K_F (μg/mg)(L/μg)$^{1/n}$	1/n	liquid phase concentration range (μg/L)	reference
TCE	1.94	0.52	10 – 1000	Carter *et al.*, 1992
atrazine	18.6	0.39	0.03 – 3.0	Schideman *et al.*, 2006
MIB	7.25	0.99	0.02 – 0.8	Pirbazari *et al.*, 1993
geosmin	3.96	0.74	0.02 – 5.0	Pirbazari *et al.*, 1993

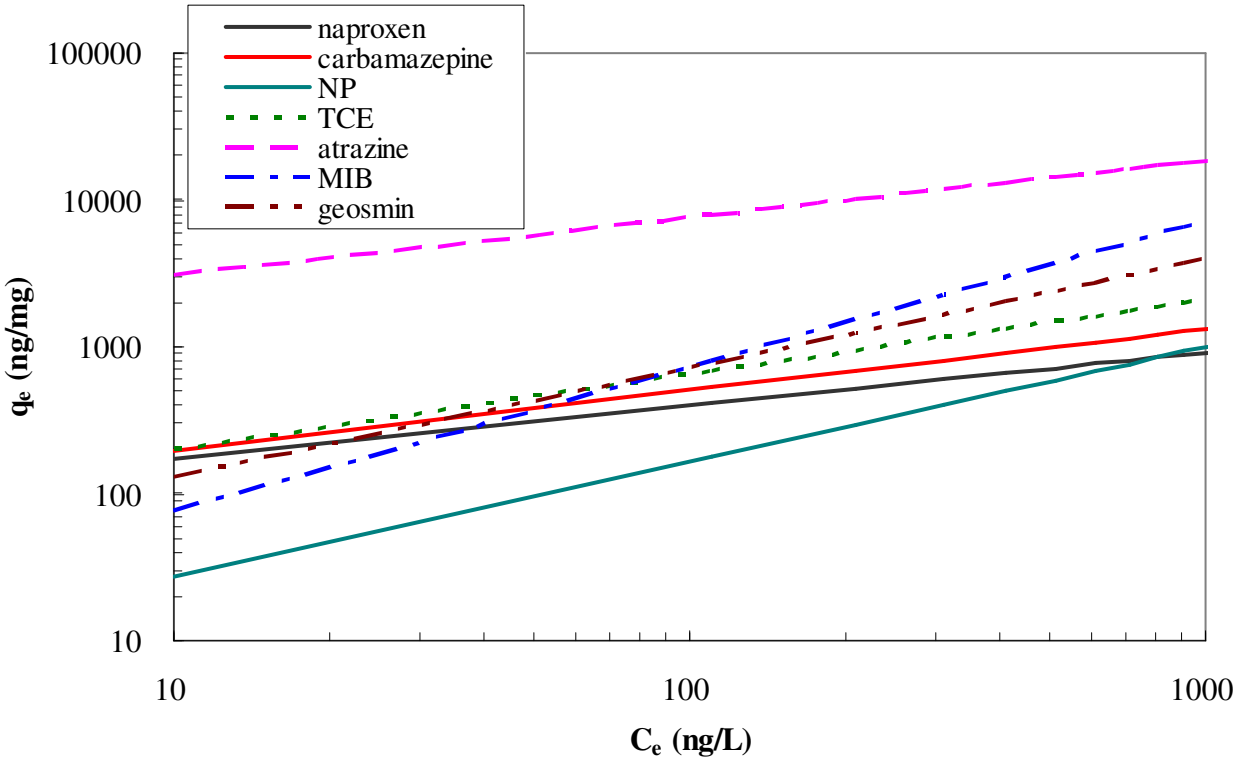

Figure 6-12 Comparison of adsorbabilities of three target compounds with other micropollutants on F400 carbon in ultrapure water

6.1.4 Possible Minor Competitive Effect from Ultrapure Water Background

Since the isotherm tests on the target compounds were designed to be conducted at trace concentration levels, it is possible that even the minor organic background matter in 'ultrapure' water could induce a competitive effect, thus leading to inaccurate estimations of adsorption parameters. The available ultrapure water system (Milli-Q UV Plus) in the lab was not designed to remove DOC (information provided by the manufacture). To investigate the possibility of competition, two isotherms on virgin F400 starting from different initial concentrations (500 and 1000 ng/L) were obtained in Milli-Q water for each compound and compared. If adsorption competition was significant in these isotherm tests, the two isotherms would be different, and nearly parallel (Najm *et al.*, 1990), which is exactly what can be observed in Figure 6-13 and Figure 6-14. The isotherm with the lower initial concentration is lower than and parallel to the one starting from the higher initial concentration. The DOC in those experiments ranged from 0.08 – 0.37 mg C/L with a mean value at

0.18 mg C/L, which is orders of magnitude higher than the spiked target compound concentrations of 1000 and 500 ng/L. Wang and Alben (1998) also observed a similar trend in the adsorption of atrazine on pulverized F300 at a low equilibrium concentration range in "organic free" water. In order to estimate the isotherm parameters more accurately, purchased ultrapure water (VWR International, West Chester, PA, USA), which met the ASTM type II criteria, was used for repeating the isotherm tests under the same experimental conditions. The ASTM type II water had an average DOC value of 0.05 mg C/L, which was substantially lower than in Milli-Q water. The isotherms obtained for naproxen and carbamazepine on virgin F400 carbon are also shown in Figure 6-13 and Figure 6-14, respectively, for comparison. The difference between the two initial concentrations is still visible, though less substantial, possibly due to the lower DOC in ASTM water. It was also observed that the capacities of virgin F400 carbon for two selected PhACs in ASTM type II water were higher than in Milli-Q water. This may be further evidence that the differences between isotherms were possibly caused by competition. A similar trend was also observed on virgin PICA carbon in adsorbing carbamazepine (Figure G-10 in Appendix G). A competitive effect from background organic matter in ultrapure water as discussed above is a possible reason explaining the discrepant isotherms starting at different initial concentrations. However, this judgement should be further confirmed experimentally and theoretically.

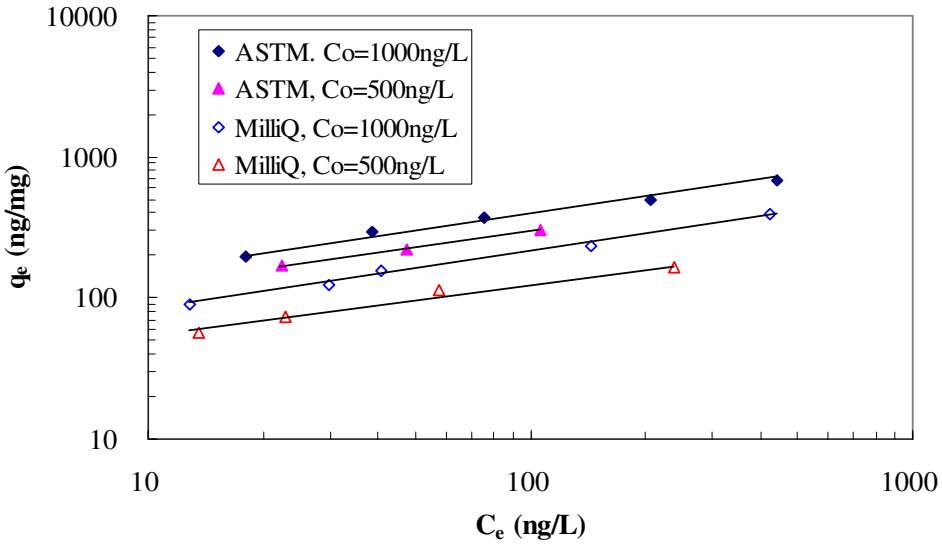

Figure 6-13 Naproxen adsorption on virgin F400 carbon

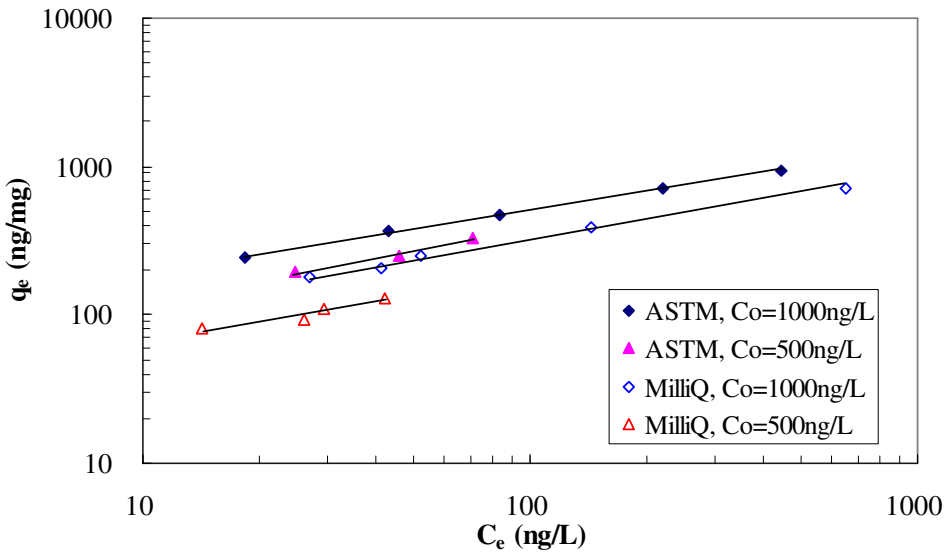

Figure 6-14 Carbamazepine adsorption on virgin F400 carbon

Figure 6-15 depicts the isotherms for NP on virgin F400 carbon starting from different initial concentrations in both Milli-Q and ASTM type II water. It illustrates the different performance for naproxen and carbamazepine. All of the isotherms obtained in either Milli-Q water or ASTM type II water appear to have negligible differences. A similar observation was also made on virgin PICA carbon in two types of ultrapure water (Figure G-11 in Appendix G). One possible explanation may be that fewer background organics in water can compete with NP, though NP showed less absorbability than the other two compounds at lower equilibrium liquid phase concentration ranges in ultrapure water, as discussed in the previous section.

Chen *et al.* (1997) used ultrapure water that was further purified by a second glass-distilling of the Milli-Q water to conduct isotherm studies for MIB at approximately the same concentration range as in this study, and did not find any discrepancy among the isotherms with different initial concentrations. This type of water could be used in the future in order to obtain the "true" isotherms in "organic free" water. However, due to technical and time limitations during this study, isotherms in ASTM type II water were used for determining single solute isotherms, which are considered to be the best representations of the "true" isotherms for the tested carbons under the current experimental conditions.

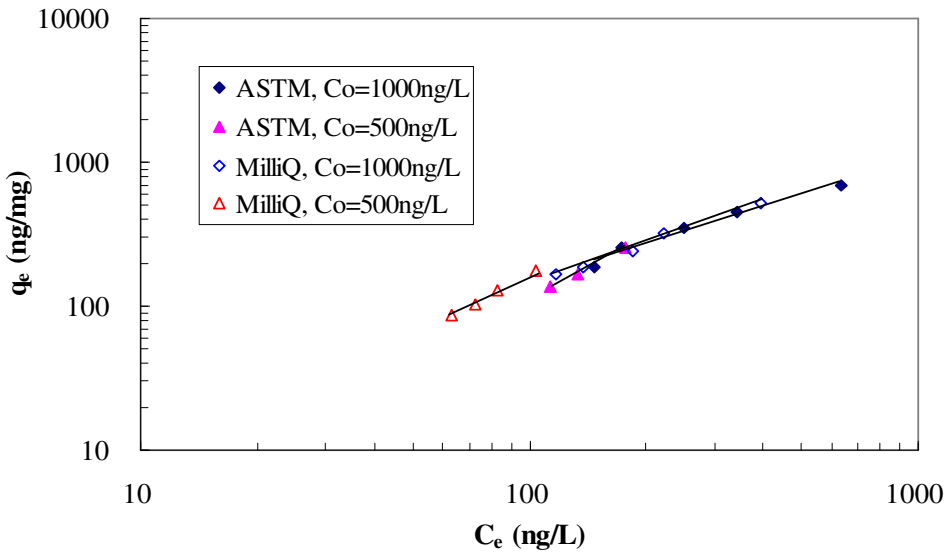

Figure 6-15 NP adsorption on virgin F400 carbon

6.2 Competitive Adsorption in Post-sedimentation Water

6.2.1 Observations

The effects of direct competition due to the presence of background NOM in the post sedimentation (PS) water at the Mannheim Water Treatment Plant were assessed by performing isotherm tests on each of the three target compounds separately at a spiked concentration of 1000 ng/L. Figure 6-16 to Figure 6-21 depict the resulting isotherms. It should be noted that, possibly by chance, the PS water had unexpectedly high background concentration of naproxen. Nonetheless, it would not have influenced the calibration of EBC parameters, because a specific set of EBC parameters represents the characteristics of natural water and should not change with the initial concentration of a target compound.

To a specific micropollutant – natural water system, the capacity of carbon for adsorbing the micropollutant in the presence of background NOM is a function of the initial concentrations of the micropollutant; the lower the initial concentration of micropollutant in natural water, the lower the observed adsorptive capacity (Najm *et al.*, 1991; Knappe *et al.*, 1998). Although the initial concentration of naproxen in PS water was three times the spiked concentration used in its single-

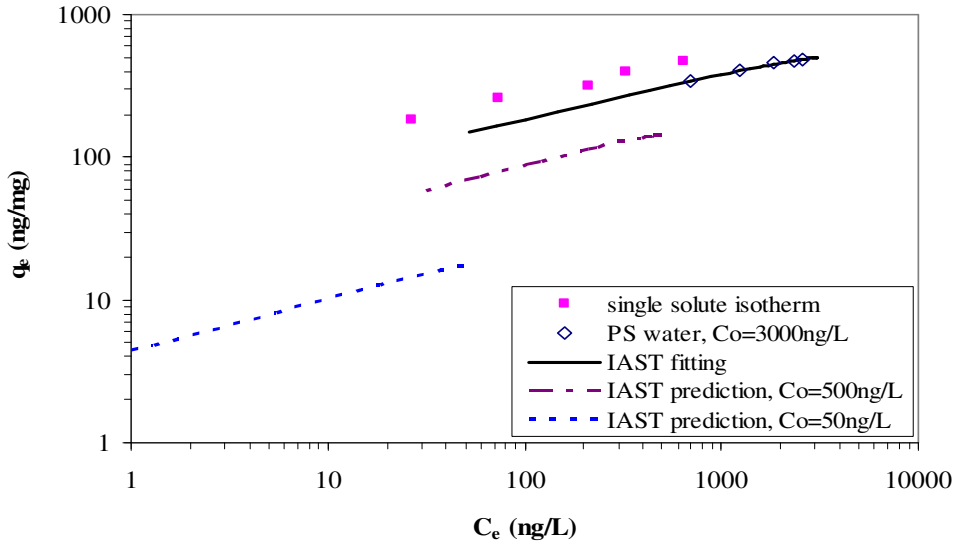

Figure 6-16 Competitive adsorption and EBC model results for different initial naproxen concentrations on PICA carbon

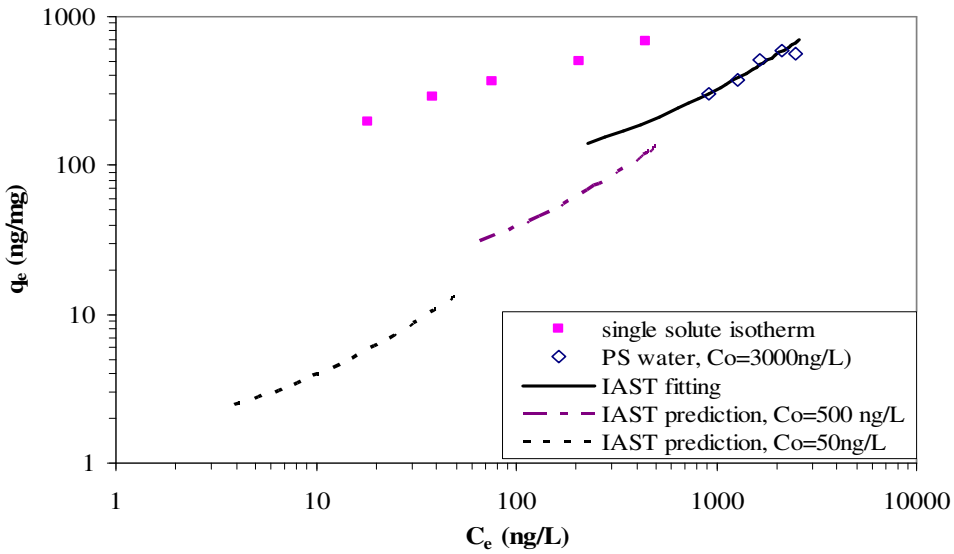

Figure 6-17 Competitive adsorption and EBC model results for different initial naproxen concentrations on F400 carbon

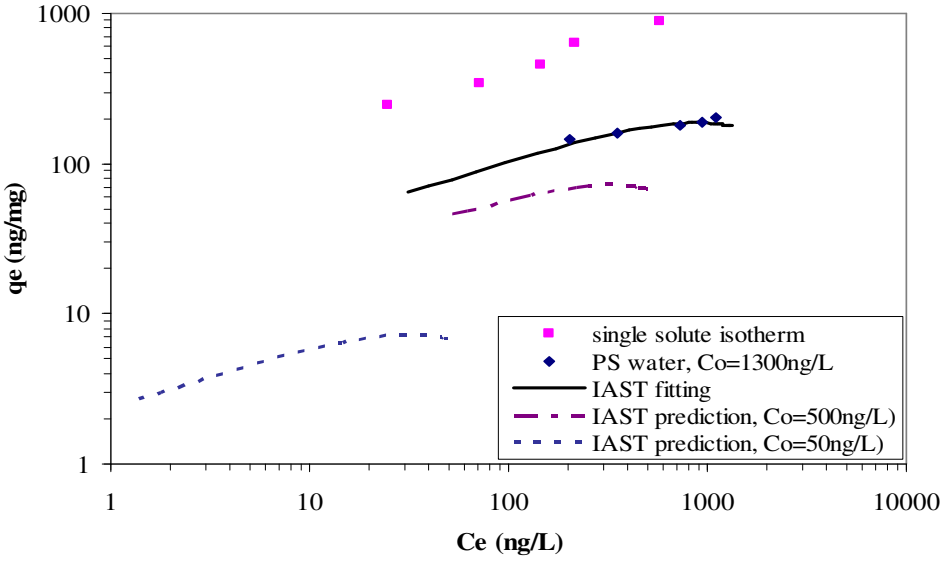

Figure 6-18 Competitive adsorption and EBC model results for different initial carbamazepine concentrations on PICA carbon

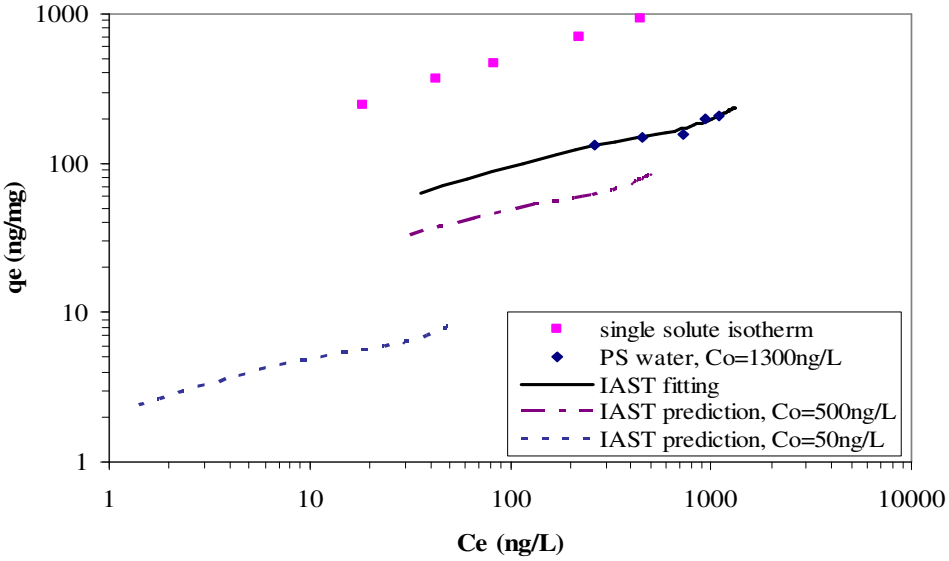

Figure 6-19 Competitive adsorption and EBC model results for different initial carbamazepine concentrations on F400 carbon

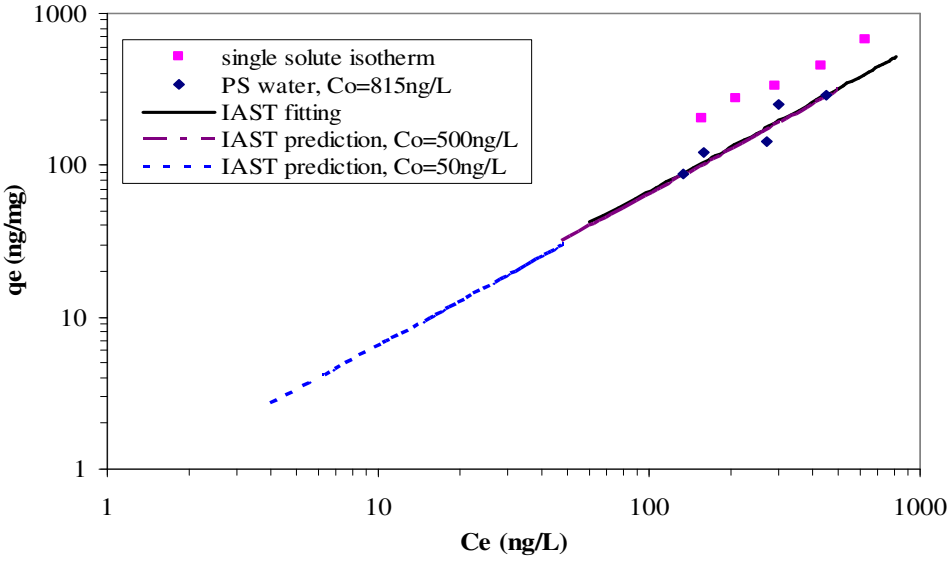

Figure 6-20 Competitive adsorption and EBC model results for different initial NP concentrations on PICA carbon

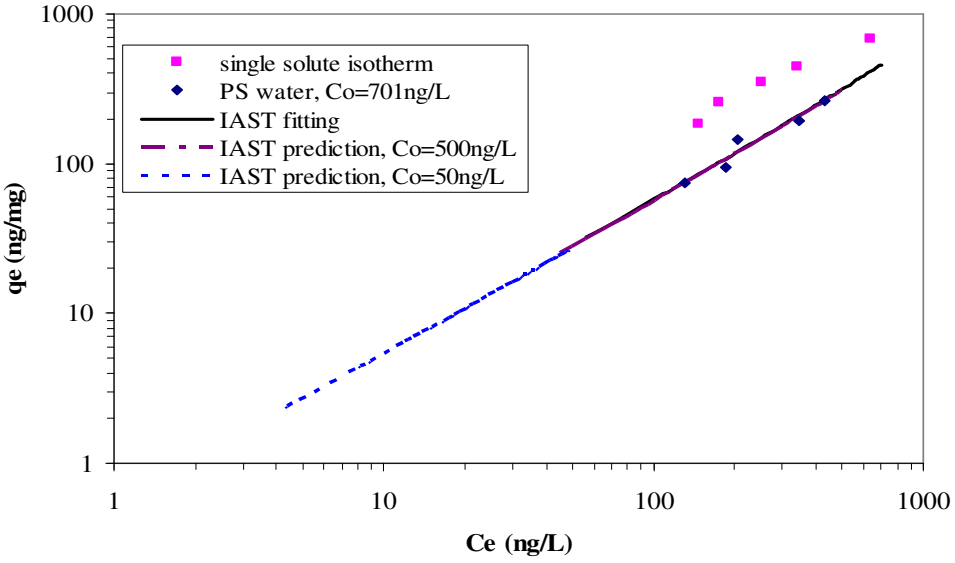

Figure 6-21 Competitive adsorption and EBC model results for different initial NP concentrations on F400 carbon

solute isotherm test, the lower levels of the isotherms obtained in PS water in Figure 6-16 and Figure 6-17 indicated the lower adsorptive capacities of both PICA and F400 carbons in PS water than in

ultrapure water, thus giving evidence of a strong competitive effect in the tested water. When comparing the two carbons it was found that, with respect to adsorbing naproxen, the direct competitive effect of background NOM had a greater impact on F400 carbon, with a larger difference between the isotherms in ultrapure water and in PS water. As discussed in Section 6.1.3, F400 carbon was superior to PICA carbon in adsorbing naproxen; however, the advantage may be lost in real water due to a stronger competitive effect.

Similarly, lower isotherms for carbamazepine and NP onto two carbons were observed in Figure 6-18 to Figure 6-21, respectively, confirming the competitive effects from the PS water. Visually, unlike different capacity reduction on the two carbons for adsorbing naproxen, the two carbons were subject to comparable adsorptive capacity reductions for carbamazepine (Figure 6-18 and Figure 6-19) and for NP (Figure 6-20 and Figure 6-21). Compared to naproxen and carbamazepine, NP seems to be subject to the least competition.

It was found that, in most figures, the isotherms in PS water do not show a curvature at high equilibrium liquid phase concentration, as is commonly presented by other researchers for the adsorption of micropollutants in natural water (Ebie *et al.*, 2001; Newcombe *et al.*, 2002). This is possibly because the concentration range applied in this study was very low, and did not extend to the curved part of the isotherm (Najm *et al.*, 1991).

6.2.2 Estimated EBC Parameters and Prediction in Post-sedimentation Water

Typically, more than one experiment is needed to calibrate the competitive adsorption model; however, this process increases not only model computation time but also considerably increases lab requirements due to the complexity of the analysis and the isotherm tests. Since the concepts of the IAST and EBC have been previously well established and widely demonstrated to be valid in the application for adsorption of micropollutants in natural water, in this study, only one isotherm for each target compound–carbon combination was used to calibrate the IAST-EBC model in order to obtain the EBC parameters. Using the isotherm data shown in Figure 6-16 to Figure 6-21 as inputs for the EBC search routine, the EBC parameters specific to each adsorbent-adsorbate pair were estimated; these are summarized in Table 6-5. The results of regression fitting are also illustrated in the related figures.

Table 6-5 Estimated EBC parameters

	Carbamazepine		Naproxen		NP	
	F400	PICA	F400	PICA	F400	PICA
C_o^* (μg/L)	16.0	32.1	37.6	30.1	270.6	1004
K_F (mg/g)(L/μg)$^{1/n}$	2.82	4.53	1.48	1.04	0.230	0.180
1/n	0.150	0.314	0.206	0.557	0.430	0.807
background DOC (mg C/L)	3.71		3.71		5.37	

** calculated based on assumed molecular weight of 1000 g/mol*

As mentioned previously, the actual initial concentrations of the target compounds for the isotherm tests were influenced by their background concentrations, and thus substantially different. This made it difficult to directly compare the direct competitive impacts on adsorption capacity for different target compounds because the carbon capacity for micropollutants' removal in natural water is influenced by the initial micropollutant concentration (Najm *et al.*, 1991; Knappe *et al.*, 1998; Graham *et al.*, 2000; Qi *et al.*, 2007). This point has very important implications for the estimation of activated carbon usage rates for drinking water treatment, because if an adsorption isotherm obtained at high initial micropollutant concentration in natural water was directly used to estimate the carbon dosage for achieving a certain desired effluent concentration, the dosage would be significantly underestimated (Najm *et al.*, 1991). Therefore, in order to estimate the applied carbon dosages for scenarios with influent target compound concentrations of 500 and 50 ng/L in PS water, the IAST program was run for predicting isotherms at the two different initial concentrations using compound-specific EBC parameters (Table 6-5). The predicted results are also included in Figure 6-16 to Figure 6-21.

It is easy to observe that, for naproxen and carbamazepine (Figure 6-16 to Figure 6-19), the carbon capacity significantly decreased with decreasing initial target compound concentrations on both PICA and F400 carbons. In contrast, for NP (Figure 6-20 and Figure 6-21) the isotherms for the different initial concentrations in PS water nearly overlapped. This trend is similar to that observed for NP adsorption isotherms in two types of ultrapure water (Figure 6-15). In Figure 6-20 and Figure 6-21, the shift-down distance from single-solute isotherms to the isotherms of NP in PS water are much less than those for the other two target compounds, also suggesting that NP adsorption was less subject to competition from background NOM. However, in Table 6-5, the estimated EBC initial concentrations for NP on the two carbons are substantially higher than those for naproxen and carbamazepine. Therefore, the EBC initial concentrations obtained from regression analyses may not

suitable for comparison of competitive strength of background NOM between different compounds or carbons. It is difficult to explicitly explain why NP was subject to less competition in PS water in this study. One possible reason is that NP has stronger adsorption affinity due to its hydrophobicity. This was confirmed by Choi *et al.* (2005) and Tanghe and Verstraete (2000) at a higher concentration range (μg/L), though NP was adsorbed much less at the low concentration range. Therefore, it could be expected that the "strongly adsorbable" NP may have a strong competitive capability with background NOM. Another tentative explanation is that NP's small molecular depth (< 5 Å, see Table 5-2) allows it to access small micropores similar in size (Pelekani and Snoeyink, 2000). In contrast, the shapes of naproxen and carbamazepine molecules are comparable to atrazine (9.6 x 8.4 x 3 Å, Pelekani and Snoeyink, 2000), whose adsorption pore size region is 8 – 20 Å (Karanfil *et al.*, 2006). According to the study by Karanfil *et al.* (2006), typical aquatic NOM molecules can only compete with target compounds in the pores larger than 10 Å. Therefore, naproxen and carbamazepine may undergo more competition from background NOM. However, the above inferences require further research to confirm. In this case, the premier adsorption pore size regions for the target compounds should be determined first.

It has been reported that, for both single-solute and multicomponent system, the adsorptive capacity of pulverized GAC (PGAC), which was ground from the same virgin GAC, was not different from that of the original carbon (Weber and Wang, 1987; Sontheimer *et al.*, 1988, Najm *et al.*, 1990). Hence, without considering adsorption kinetics, the predicted isotherms on virgin GAC can be extended to estimate the ultimate adsorption efficiency of PGAC at a specific initial contaminant concentration in PS water. Accordingly, the dosage can be predicted when the desired removal target is set. Table 6-6 shows the predicted PGAC dosages for achieving 90% removal of the target compounds at influent concentrations of 500 and 50 ng/L in PS water using the isotherms in Figure 6-16 to Figure 6-21 in combination with the mass balance principle. The results are somewhat comparable to those for MIB removal at approximately the same concentration range reported by Gillogly *et al.* (1999). Note that the adsorption kinetics cannot be considered because they are closely related to the particle size and operating conditions, so the dosage data in the table represent only a minimum bound on the amount of carbon necessary to accomplish the task. However, it can be inferred from the discussion in Section 6.1.1 that the virgin powdered F400 carbon may have superior kinetic performance to the powdered PICA carbon. As shown in Table 6-6, in general the PICA carbon is more effective than F400 carbon in PS water with respect to adsorptive capacity. This is not in agreement with the trend determined without consideration of competitive effects (F400 carbon has higher capacity the PICA carbon in ultrapure water), and suggests that, in this investigation, PICA

carbon has an advantage over F400 carbon with respect to minimizing direct competition from background NOM in natural water. The comparisons among the removal of the three target compounds on the same carbon indicate that naproxen is the most easily mitigated compound if PICA carbon is applied, as is the case for carbamazepine with F400 carbon. On the other hand, the removal of NP at a few ng/L concentration levels is not likely to be substantial with either carbon.

Table 6-6 Predicting PGAC dosage for 90% removal of target compound in PS water

compound	C_o (ng/L)	PICA				F400			
		dosage (mg/L)	$f^{\dagger}$	q_e EBC (mg/g)	approximate f_{min}^{*}	dosage (mg/L)	$f^{\dagger}$	q_e EBC (mg/g)	approximate f_{min}^{*}
naproxen	500	6.5	10.6	3.2	47	16	23.3	2.0	4
	50	6.0	106	3.5		16	233	2.0	
carbamazepine	500	10	16.7	3.2	6	11	8.5	1.5	3
	50	10	166	3.2		11	85	1.5	
NP	500	13	203	32	1	16	18.9	2.4	2
	50	13	2031	32		16	190	2.4	

$\dagger$: calculated molar ratio of EBC and target compound surface loading

**: approximate readings from Figure 6-22*

It has been reported that for trace micropollutants in natural water, the IAST-EBC model can be further simplified (Knappe *et al.*, 1998; Gillogly *et al.*, 1999; Graham *et al.*, 2000; Matsui *et al.*, 2003). Knappe *et al.* (1998) proved that, at any given dosage, the PAC capacity for a micropollutant was directly proportional to its initial concentration. In other words, the percent removal of the target compound at a given PAC dosage is independent of the initial target compound concentration (equation 6.8). This is also illustrated in Table 6-6, as the calculated dosages required to achieve 1-log removal are similar at two different initial concentrations. However, the simplified the IAST-EBC model was developed based on the following assumptions: 1) solid phase concentration ($q_{2,eq}$) of the EBC is much greater than that of the target compound; 2) the Freundlich exponents of both EBC and target compound are comparable (both between 0.1 and 1); and 3) the solid phase concentration ($q_{2,eq}$) of EBC at a given carbon dosage is not affected by trace levels of the target compound (Knappe *et al.*, 1998). The assumptions were further theoretically justified and experimentally proven by Qi *et al.*

(2007), who summarized the minimum molar ratio of EBC and trace compound surface loading that allows the simplified IAST to satisfy a 10% deviation from the original IAST (Figure 6-22).

$$\frac{C_{1,eq}}{C_{1,0}} = \frac{\frac{1}{C_{2,0}}\left(\frac{n_2 C_{2,0}}{n_1 K_1}\right)^{n_1}}{D^{n_1}} \qquad \textbf{6.8}$$

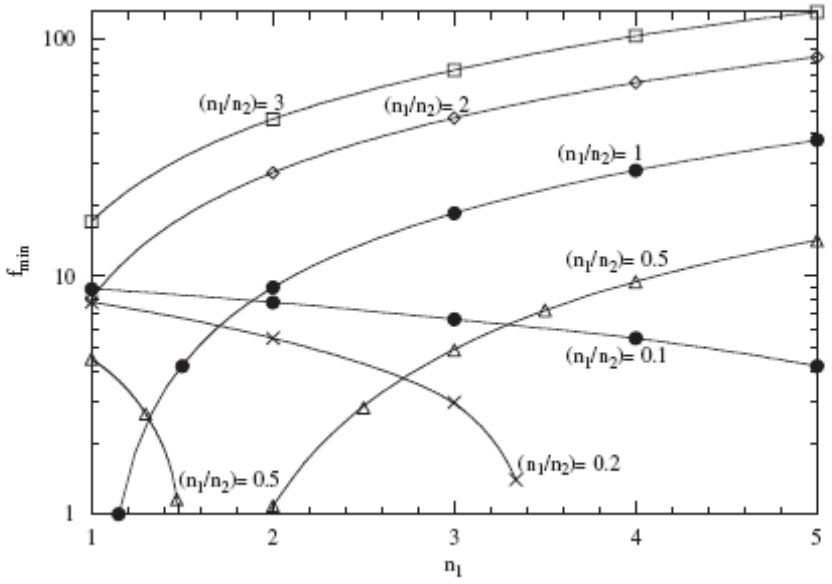

Figure 6-22 Minimum molar ratio of EBC and trace compound surface loading that allows the simplified IAST to satisfy a 10% deviation from the original IAST (Qi *et al.*, 2007)

In Figure 6-22, a specific f_{min} value can be read for a target compound-carbon-natural water system when the values of $1/n_1$ and n_1/n_2 are known. For example, in the case for adsorption of naproxen on F400 carbon, an approximate value of 4 is obtained for f_{min} with n_1 of 2.7 ($1/n_1$ as shown in Table 6-3) and n_1/n_2 of approximately 0.5 ($1/n_2$ as shown in Table 6-5).

If the adsorption of the target compounds in this study can satisfy the above three conditions, it would instil more confidence in applying the same estimated dosage to any other reasonable initial concentration in the same natural water to achieve the same removal percentage. It is obvious that the Freundlich 1/n of both the target compound and EBC meet the requirement of the second condition when comparing them in Table 6-3 and Table 6-5. Table 6-6 also illustrates the calculated molar ratio of EBC and target compound surface loading (*f*), which can be directly compared to the f_{min} obtained

from Figure 6-22. It can be seen that, with the exception of naproxen adsorption on PICA carbon at 500 ng/L, other *f* values are all well above the approximate f_{min}, thus suggesting that the first condition is satisfied. Similarly, Table 6-6 illustrates that the EBC surface loadings remain constant at two different initial target compound concentrations. Therefore, with the exception for predicting PICA carbon dosage to remove naproxen, the simplified IAST can be successfully applied for predicting the PGAC usage for removing the target compounds in PS water. In other words, to achieve the same removal percentage of naproxen, the applied dosage of PICA carbon would be different for different naproxen influent concentrations, as illustrated in Table 6-6. In contrast, other estimated dosage data shown in Table 6-6 can be applied to any influent concentrations lower than 500 ng/L to achieve the same removal goal.

6.3 Kinetic Performance on Virgin GACs

6.3.1 Short-term Kinetic Tests

To preliminarily investigate actual ranges of the kinetic parameters β_L and D_p (in the form of the impedance factor τ) or D_s, two short fixed bed (SFB) tests were performed for the uncrushed virgin F400 and PICA carbon, respectively. Initially, the experimental time for the SFB tests was set as approximately 30 hours, which has been used in many kinetic studies (e.g. Weber and Wang, 1987; Smith and Weber, 1989; Carter and Weber, 1994). Figure 6-23 and Figure 6-24 present the experimental data and calibration results for the two carbons, respectively. Based on the pore diffusion model (PDM), all the breakthrough data were used to estimate β_L and τ, which were shown in Table 6-7.

Table 6-7 Kinetic parameters determined on virgin GACs from short-time SFB tests

	Naproxen		Carbamazepine		NP	
	β_L (x 10^{-3}cm/s)	τ	β_L (x 10^{-3}cm/s)	τ	β_L (x 10^{-3}cm/s)	τ
F400	3.39	1	3.37	1	5.04	1
	(3.32-3.53)†	nd	(3.30-3.51)	nd	(4.78-5.19)	nd
PICA	3.28	0.99	3.60	1.2	5.23	1
	(3.22-3.35)	nd	(3.53-3.67)	nd	(5.10-5.36)	nd

†: confidence intervals at 5 % significant level
nd: could not be determined

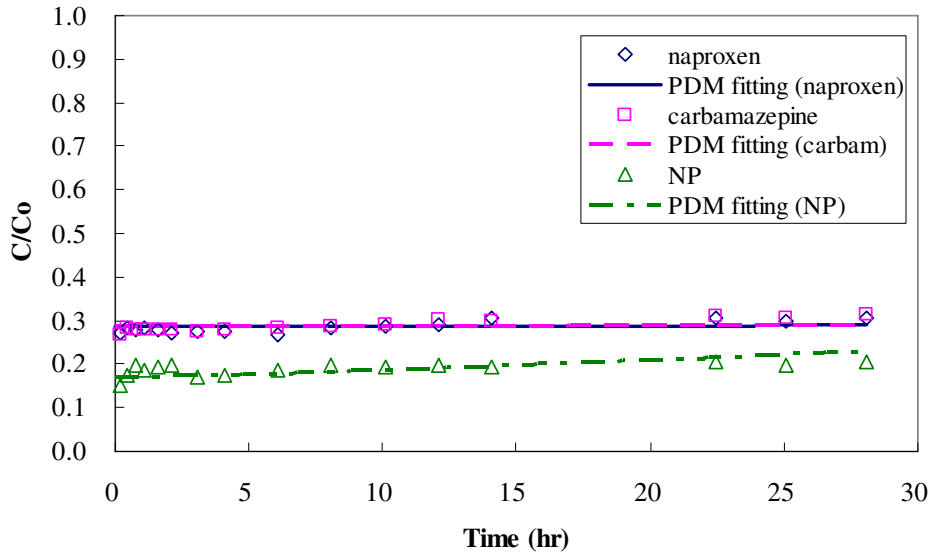

Figure 6-23 Short-time SBF test data and model calibration on F400 carbon (bed depth 2.53 cm, flowrate 50.5 mL/min)

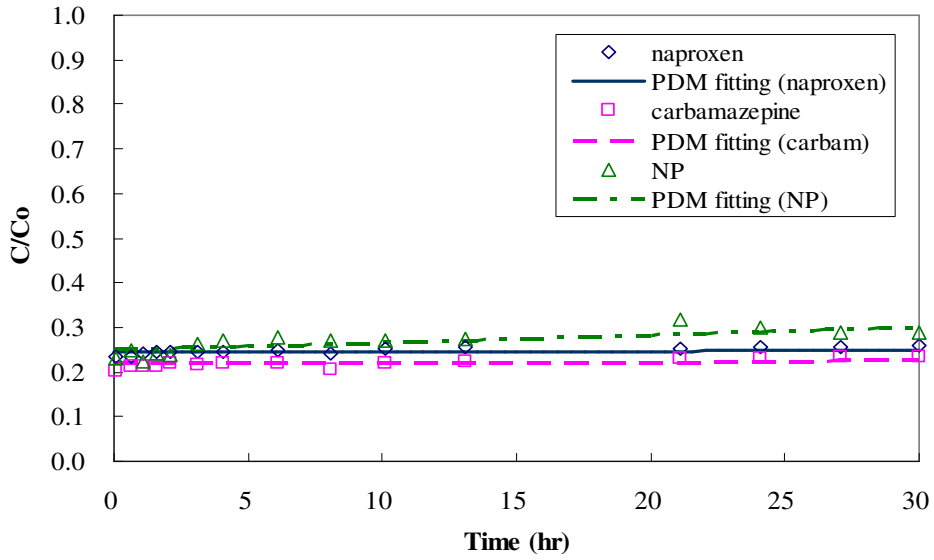

Figure 6-24 Short-time SBF test data and model calibration on PICA carbon (bed depth 2.50 cm, flowrate 49.02 mL/min)

It was observed that the β_L values calculated from these SFB tests were generally at the same magnitude as the values calculated based on the Gnielinski correlation. The tight 95 % confidence intervals of β_L suggest that the experimental data was sufficient to provide precise estimates. However,

the calibrations could not give appropriate confidence intervals for the estimated τ values. More specifically, in determining the estimate, the calibration program automatically searches for the LJCR in the range between 0 and 4 times the determined parameters. Therefore, no output of a confidence interval for τ equal to 1 from the program means that its confidence interval ranges from less than 0 to larger than 4, which is considered not to be physically realistic. As described in Section 5.7.3, the calibration was also performed using the SDM. The results were similar to those obtained from the PDM calibration. While the β_L in all cases could be precisely determined, estimates of D_s, except for NP, were even negative. Therefore, sensitivity analyses were carried out in order to investigate the impact of different parameters on the PSDM applied under the specific experimental conditions in this study.

The reasons for not being able to determine D_s for naproxen and carbamazepine are not clear. It may suggest that pore diffusion is a more prominent mechanism for these two compounds. A possible explanation is that the polarity of naproxen and carbamazepine leads to a lower affinity between the adsorbates and adsorbents. In particular, dissociation of naproxen in water in the typical pH range of these experiments may make a main contribution because the ionized adsorbate tends more to follow the pore diffusion mechanism (Sontheimer *et al.*, 1988). However, for NP, which has strong adsorbent-affinity, it is reasonable that the mass transfer process is mainly attributable to surface diffusion, perhaps with pore diffusion simultaneously.

6.3.2 Sensitivity Analysis of PSDM on SFB Reactor

According to the results from the short-term kinetic tests, it was necessary to investigate the sensitivity of the PSDM in combination with the SFB reactor to changes in isotherm and kinetic parameters. Operational, isotherm and kinetic parameters for the baseline predictions are presented in Table 6-8. Operational parameters were similar to what was used in the short-time SFB tests, except for influent concentrations, which were fixed at 500 ng/L in this analysis, whereas influent concentrations fluctuated from 350 to 700 ng/L in the various SFB tests, depending on the stock solutions and spiking conditions. The isotherm parameters for the baseline case were those determined in ASTM type II water. Kinetic parameters from the short-term SFB tests were also used as input for baseline calculations. As described previously, surface diffusion coefficients could not be determined for naproxen and carbamazepine in the short-term SFB tests on virgin GACs. Therefore, the sensitivity analyses for these two compounds could only be based on the determined τ values. In contrast, the analyses for NP included both pore and surface diffusion coefficients determined previously. In order to compare the impact of each parameter, they were all varied by 50%, if possible.

The Freundlich 1/n values for NP on F400 and PICA carbons were only changed +25% and +15%, respectively, because they approached unity. The changes in τ value were set as an increase of 100% and infinity in order to highlight the impact of this parameter. Sensitivity analyses involving a 50% decrease of the other parameters were carried out. In this way, it is also possible to preliminarily investigate possible effects from preloading of background NOM.

Table 6-8 Parameters for baseline prediction for sensitivity analysis

carbon	Operation parameters	compound	K_F $(ng/mg)(L/ng)^{1/n}$	1/n	β_L $(x\ 10^{-3}cm/s)$	τ	D_s $(x10^{-11}cm^2/s)$
F400	Co = 500 ng/L Carbon dose = 5.45 g Bed depth = 2.35 cm Flowrate = 50 mL/min	naproxen	73.15	0.37	3.40	1	na
		carbamazepine	74.60	0.42	3.37	1	na
		NP	4.44	0.78	5.04	1	2.43
PICA	Co = 500 ng/L Carbon dose = 6.22 g Bed depth = 2.50 cm Flowrate = 50 mL/min	naproxen	69.96	0.30	3.28	1	na
		carbamazepine	57.56	0.43	3.60	1	na
		NP	2.49	0.87	5.23	1	3.74

Figure 6-25 and Figure 6-26 depict the sensitivity to isotherm and kinetic parameters of the PDM breakthrough profiles for naproxen in the SFB reactor. As evidenced in these plots, the predicted profiles are more sensitive to the isotherm parameters (K_F and 1/n) than to the pore diffusion coefficient in form of the impedance factor (τ). The Freundlich K_F, as an index of adsorptive capacity, has the greatest impact on the breakthrough profile no matter which carbon is used. Both figures show that, as the Freundlich K_F decreases, the profiles break more sharply upward, suggesting that a small reduction of adsorptive capacity due to preloading could have a great impact on breakthrough. At the same time, the increase of Freundlich 1/n, though not as strong as Freundlich K_F, still significantly sped up the breakthrough. The significant effect of Freundlich K_F and 1/n can also be observed for the breakthrough profiles of carbamazepine (Figure 6-27 and Figure 6-28) and of NP (Figure 6-29 and Figure 6-30) on both carbons.

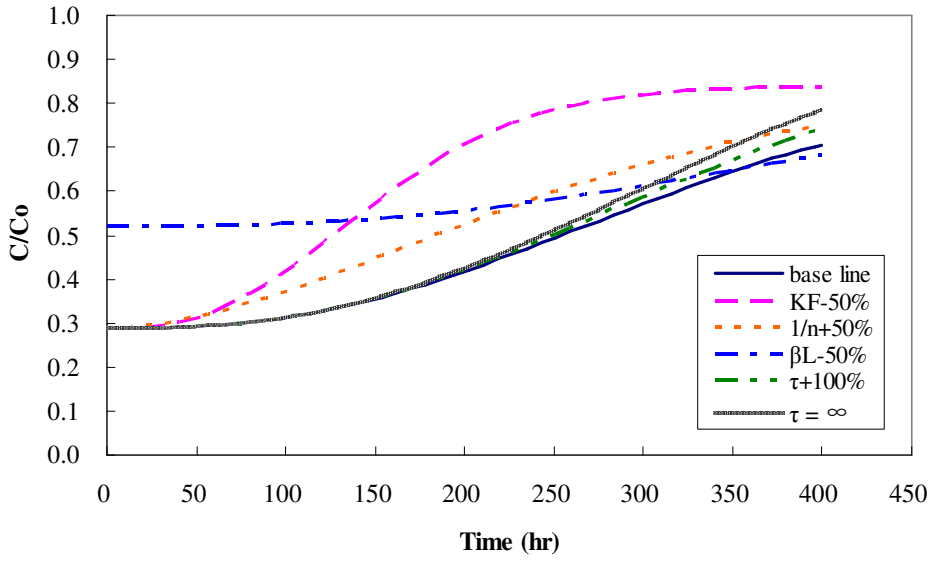

Figure 6-25 PDM sensitivity analysis based on SFB test of naproxen adsorption on F400 carbon

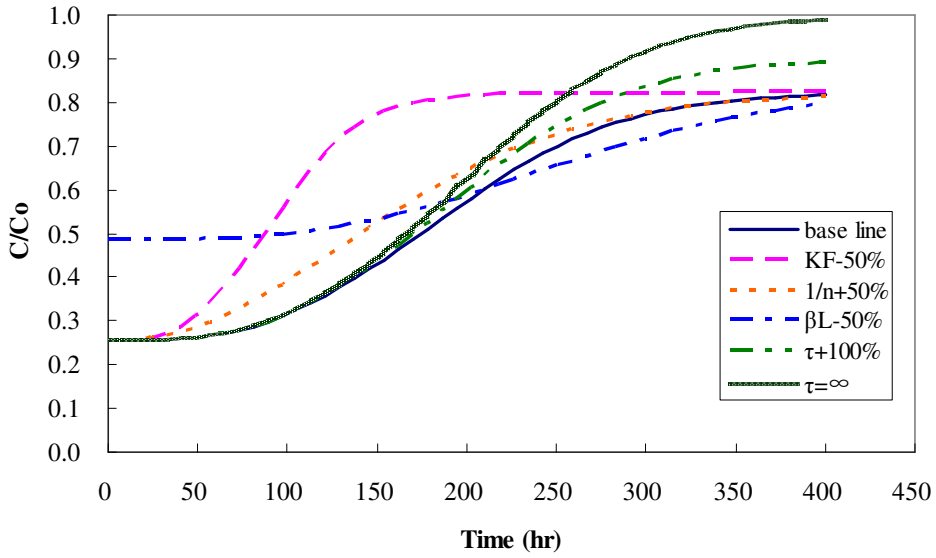

Figure 6-26 PDM sensitivity analysis based on SFB test of naproxen adsorption on PICA carbon

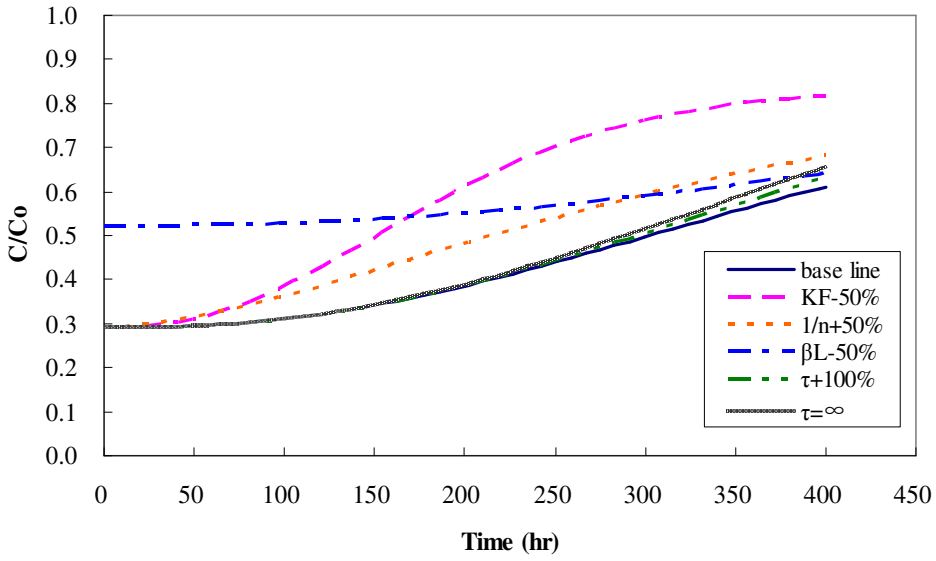

Figure 6-27 PDM sensitivity analysis based on SFB test of carbamazepine adsorption on F400 carbon

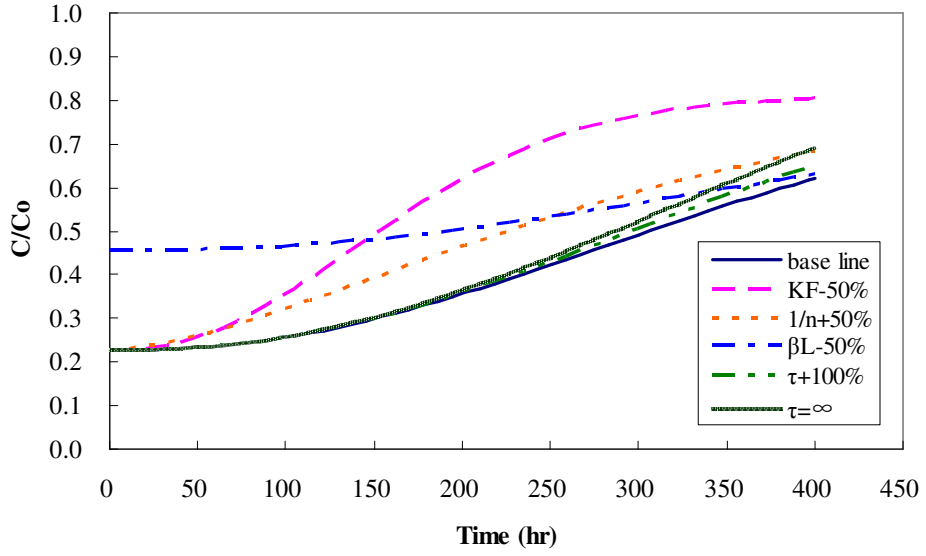

Figure 6-28 PDM sensitivity analysis based on SFB test of carbamazepine adsorption on PICA carbon

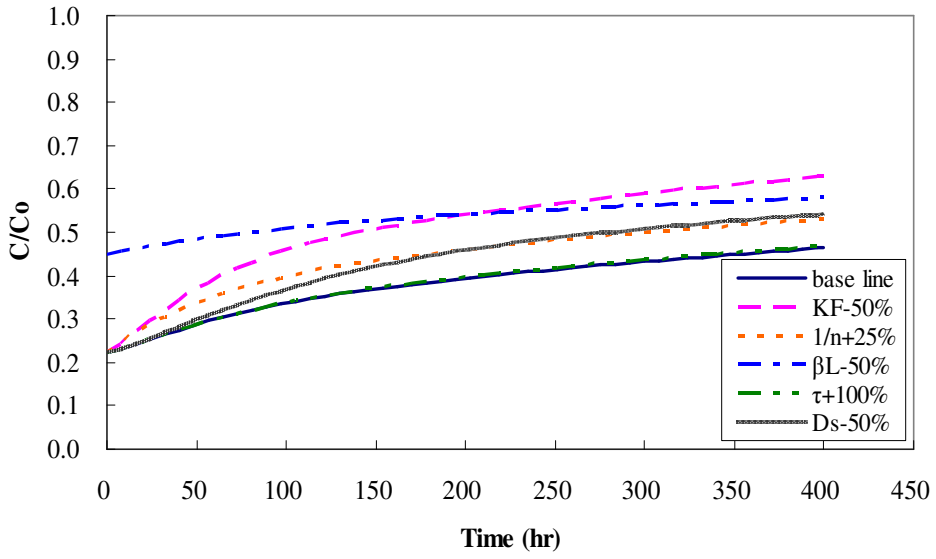

Figure 6-29 PSDM sensitivity analysis based on SFB test of NP adsorption on F400 carbon

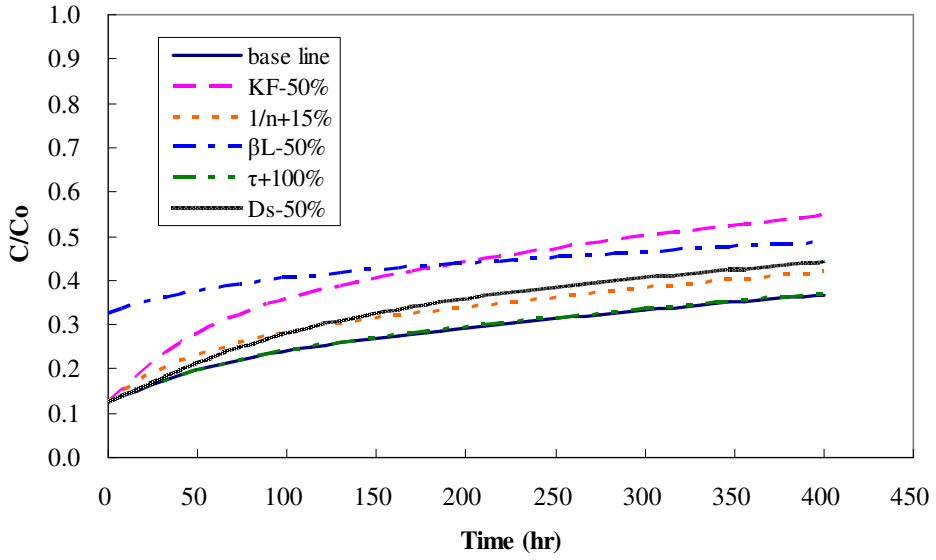

Figure 6-30 PSDM sensitivity analysis based on SFB test of NP adsorption on PICA carbon

Larger changes in the model simulations were observed for β_L on both carbons than for the impedance τ, even though the latter was changed by 100% in the analyses (Figure 6-25 to Figure 6-28). As expected, the simulations show that film diffusion controls the early stage of the breakthrough profiles. The impact of β_L decreased when run time increased. Surprisingly, it is found that the 100% changes in the impedance (τ) have a small bearing throughout the whole breakthrough

process compared with the changes of β_L. In the cases of naproxen, the impacts of τ seem to only slightly exceed those of β_L for simulations of SFB tests lasting more than 300 and 200 hours on F400 and PICA carbon, respectively (Figure 6-25 and Figure 6-26), For carbamazepine, the significance of film diffusions seems predominant until 400 and 350 hours on F400 and PICA carbon, respectively (Figure 6-27 and Figure 6-28). In contrast, film diffusion was reported to only control the mass transport during the first 2 – 4 hours in most studies (Knappe *et al.*, 1999; Carter and Weber, 1994; Smith and Weber, 1989, Sontheimer *et al.*, 1988). If the same degree of reduction (50%) on τ was considered, the insensitivity of the model to this parameter would further increase. An analysis of extreme conditions – setting τ at infinity was also performed, and indicated that the predicted performance of the SFB reactor was not sensitive to the impedance (τ) parameter before 300 and 200 operation hours at all, though τ seems to have a visibly higher impact on PICA carbon breakthrough profiles at later stages. Therefore, it suggests that the mass transports for naproxen and carbamazepine under the current experimental conditions were predominantly controlled by film diffusion. This situation is expected to contribute to the difficulties in accurately determining the pore diffusion coefficient and calculating confidence intervals. In the case of NP breakthrough in SFB reactor, Figure 6-29 and Figure 6-30 illustrate that a 50% increase of the film diffusion resistance raises the baseline breakthrough profiles in an almost parallel way, with two the profiles slightly approaching each other at the end. Compared to naproxen and carbamazepine, the influence of pore diffusion on NP breakthrough profiles was shown to be much less significant. This was demonstrated in Figure 6-29 and Figure 6-30, where a 100% increase in impedance produced breakthrough profiles that almost overlapped with the baseline curves. In contrast, surface diffusion, though showing less effect compared to film diffusion, seems to evidently influence the NP breakthrough profiles. Therefore, it can be judged at this point that the mass transport of NP for both F400 and PICA carbon are simultaneously controlled by film and surface diffusion. Nevertheless, according to the sensitivity analyses in Figure 6-29 and Figure 6-30, the determination of β_L is much easier and more accurate than that of D_s even if SFB tests were run for 400 hours.

This situation, in which film diffusion exerts much greater effect on breakthrough profiles than internal diffusion, was also reported by Gillogly (1998) in applying the homogenous surface diffusion model (HSDM) in combination with an SFB reactor for determining the surface diffusion coefficients for MIB at low concentration ranges (ng/L level) on virgin GAC. In that study, the sensitivity analysis demonstrated that the HSDM became sensitive to the surface diffusion coefficient only after the film diffusion increased approximately 250 times, which seems extremely unlikely in a real situation. Gillogly (1998) attributed the observation to a low flow rate used for the SFB system. However, in

the present study, the velocity was approximately 6 m/h, which is close to the lower practical limit of surface loading in full-scale systems. The film diffusion still showed significant effect on the breakthrough profile. Therefore, it is suspected that the control by film diffusion can be attributed to the low concentrations applied in the kinetic tests. Since the internal diffusion limitations do not show significant effect on mass transport before the adsorbent surface is appreciably saturated (Roberts *et al.*, 1986), it is not unreasonable to assume that low concentrations applied in the SFB tests led to a considerably long time being necessary to saturate the adsorbent surface. Hence, the film diffusion was the rate limiting process throughout most of the breakthrough duration.

Smith and Weber (1989) found that a negative feature of the SFB reactor was its lower sensitivity to internal diffusion, such as D_s in their study, than film diffusion. In contrast, a deep fixed bed (DFB) reactor seemed to exhibit a greater sensitivity to internal diffusion (Smith and Weber, 1989). Therefore, a DFB reactor could be designed to determine internal diffusion coefficients. However, it is expected that this would greatly extend the operation time. Another potential way also recommended by Smith and Weber (1989) to accurately determine internal diffusion coefficients is to keep the SFB running close to complete breakthrough. This finding is confirmed by observing that the PDM breakthrough profiles were more sensitive to internal diffusion after at least 70% breakthrough in Figure 6-25 to Figure 6-28. This point, on the other hand, proves that isotherm parameters and the influent concentrations of target compounds have a strong influence on determining the internal diffusion coefficients, because the less the adsorptive capacity and the higher the influent concentration, the faster the SFB reactor breakthrough. However, since the parameters of adsorptive capacity are constant in kinetic tests and internal diffusion are closely related to the liquid phase concentrations, it seems that the only possible way to determine the internal diffusion parameters is to extend the SFB tests to longer times (e.g. 350 hours). In addition, it is reasonable to expect that the decrease in adsorptive capacity due to preloading would enhance the rate limiting effect due to internal diffusion. However, this inference should be based on no or only slight reduction of film diffusion flux due to preloading. These features will be investigated in Chapter 7.

6.3.3 Long-term Kinetic Tests

It was necessary to define reference maximum adsorption rates on virgin GAC in order to further investigate the impact of preloading on adsorption. Therefore, based on the sensitivity analyses described in the last section, long-term kinetic tests on F400 and PICA carbons were performed using the SFB reactor. The experimental data were used to calibrate the PDM for naproxen and carbamazepine, while the SDM was applied for simulating the breakthrough of NP. The calibration

results are shown in Figure 6-31 and Figure 6-32 for F400 and PICA carbon, respectively, with numerical data presented in Table 6-10. By applying long-term kinetic tests, D_s for NP could be accurately determined and was found to be of the typical magnitude expected. The calibration of impedance (τ) in these tests was somewhat more precise than those in the short-term SFB tests.

The experimentally determined film diffusion coefficients shown in Table 6-10 were compared with the values estimated using the Gnielinski correlation (Table 6-9). The comparison indicates that the Gnielinski correlation underestimated β_L by a factor of 2 – 4 depending on the specific compound. Therefore, the application of the Gnielinski β_L may introduce errors in predicting the stage of the breakthrough profile that is mainly controlled by film diffusion. The discrepancies are likely attributable to the deviations of real GAC particles from the spherical shape assumed in the correlation method (Roberts *et al.*, 1986; Sontheimer *et al.*, 1988, also see Figure 5-2 for SEM images for the real shapes of the two carbons). Roberts *et al.* (1986) recommended a factor of 2 to account for irregular topography of adsorbent particles, such as F400 carbon. However, if the discrepancy was only due to the hydrodynamic factor, it should have a similar impact on film diffusions for all compounds. This is in disagreement with the observations from the current study. According to the Gnielinski correlation, NP should have the smallest film diffusion coefficient among the three target compounds (Table 6-9). In contrast, it shows a 1.5 – 2 times faster film diffusion rate than naproxen and carbamazepine in this study (Table 6-10). This difference may be due to the the different electrostatic interaction between adsorbates and adsorbents. It could also be attributable to the much higher hydrophobicity of NP than those of the other two compounds. Future study should be carried out to clarify the exact mechanisms.

Table 6-9 Film diffusion coefficients estimated using the Gnielinski correlation

β_L (x10^{-3} cm/s)	Naproxen	Carbamazepine	NP
F400	1.56	1.62	1.48
PICA	1.50	1.56	1.42

Table 6-10 Kinetic parameters determined on virgin GACs from long-time SFB tests

	Naproxen		Carbamazepine		NP	
	β_L (x 10^{-3}cm/s)	τ	β_L (x 10^{-3}cm/s)	τ	β_L (x 10^{-3}cm/s)	D_s (x10^{-11} cm^2/s)
F400	3.12	1	3.04	0.99	5.99	3.24
	(2.50 - 3.53)†	(0.77 ->4)	(2.13 - 3.34)	(0.52 ->4)	(4.80 - 6.84)	(1.94 - 4.40)
PICA	3.06	1	3.79	1.50	5.47	3.74
	(2.21 - 4.64)	(0.53 ->4)	(3.43 - 4.27)	(1.05 -4.51)	(5.03 - 6.01)	(3.18 - 7.18)

†: 95% confidence intervals

Comparisons of kinetic parameters determined on F400 and PICA carbon indicate that, except for β_L for carbamazepine, no statistically significant difference between the two carbons can be distinguished for β_L values of naproxen and NP, respectively, based on their corresponding CIs shown in Table 6-10. Therefore, the breakthrough profiles of the SFB systems consisting of virgin GAC are largely influenced by isotherm parameters under extremely low concentration conditions.

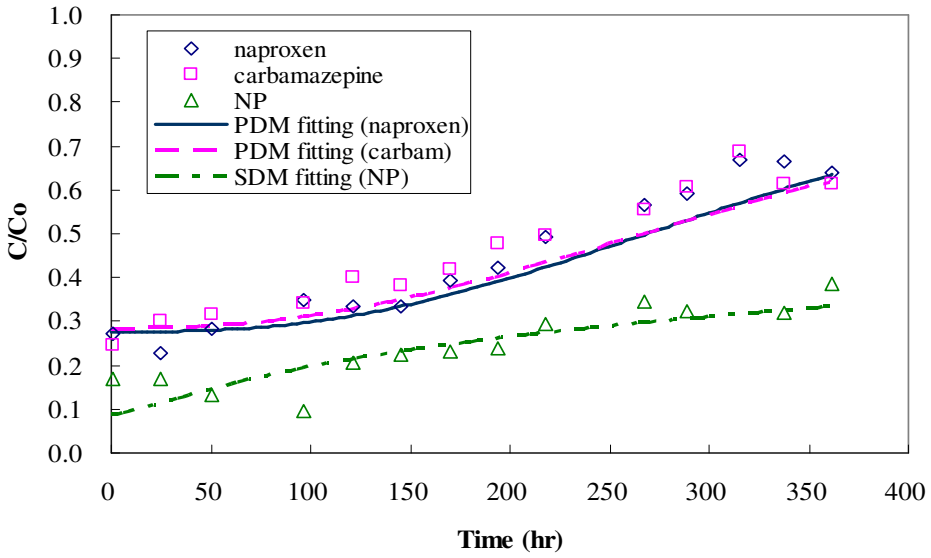

Figure 6-31 Long-term SFB test data and model calibration on F400 carbon (bed depth 2.55 cm, flowrate 49.4 mL/min)

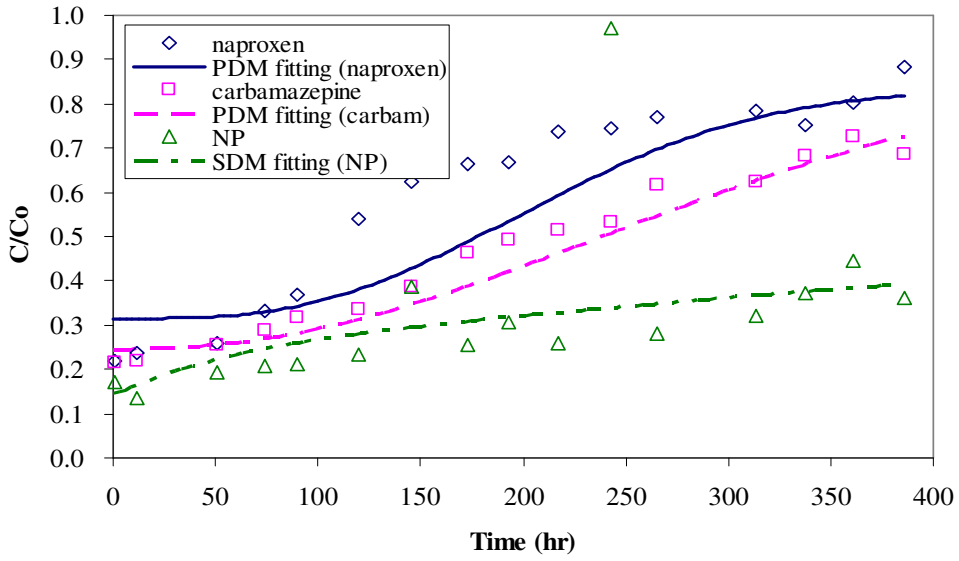

Figure 6-32 Long-term SFB test data and model calibration on PICA carbon (bed depth 2.40 cm, flowrate 49.5 mL/min)

From Figure 6-31 and Figure 6-32, it can be observed that there are some biased deviations between the experimental data and simulated profiles of naproxen and carbamazepine. The bias is more pronounced for naproxen on PICA carbon. Therefore, two possible reasons were investigated. In the experiments, it was inevitable that air bubbles emerged in the SFB system after two or three days running. This factor was accounted for by only assuming that bed porosity decreased either 20% or 80%. As shown in Figure 6-33, the change of bed porosity only influences the early breakthrough profiles. Although this factor could contribute to the error in early breakthrough phase, it cannot explain the bias in intermediate breakthrough phase. Nevertheless, it should be noted that the entrapment of air bubbles would not only decrease the bed porosity but also change the hydrodynamics in SFB reactors, leading to a possible change on film diffusion rates. Unfortunately, this effect could not be easily quantified in above calculations. On the other hand, the competition from the background organics in DI water was not considered in the calibration. This factor was taken into consideration assuming that compositions of background organics were the same in DI water as in PS water. In this case, the EBC Freundlich parameters of background organics in DI water are the same as the ones of background NOM in PS water (see Table 6-5). The initial EBC concentration of background organics in DI water can be calculated based on the ratio of DOC values in DI water and PS water. The mean DOC value for the long-term SFB test was 0.406 mg C/L. Figure 6-33 illustrates that this factor possibly contributes to the bias in calibration. Nonetheless, the influence from direct

competition should be insignificant in SFB tests for preloaded carbon (in the next chapter) because even the direct competition in natural water with its higher DOC values is negligible on preloaded carbon (Knappe *et al.*, 1999).

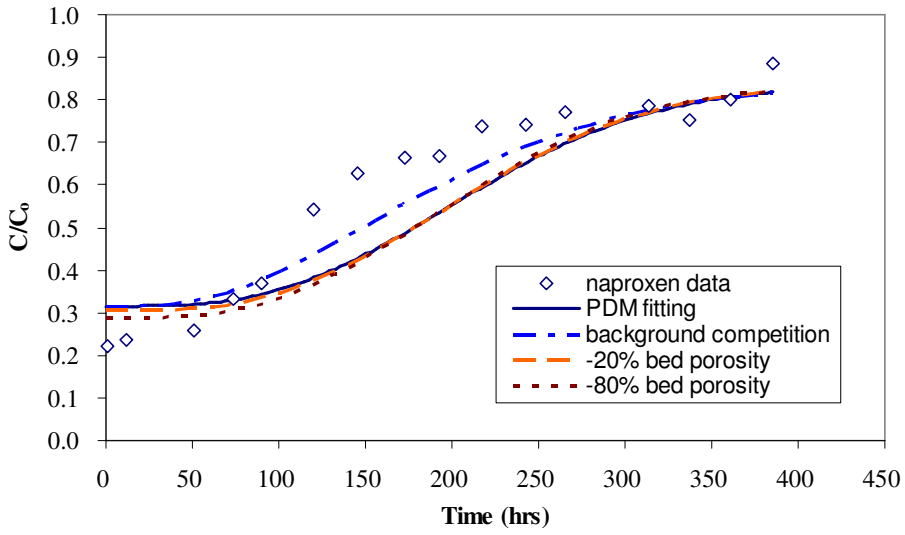

Figure 6-33 Analysis of discrepancy in regressing naproxen breakthrough on PICA in long-term SFB test

6.4 Summary

This was the first time detailed investigations have been carried out into the adsorption of selected PhACs and EDCs on activated carbon at environmentally relevant concentrations. The establishment of baselines for either isotherms or kinetics provides a chance to look at the adsorption mechanisms of this group of emerging contaminants, and hence to compare them with other micropollutants. In addition, the results obtained on virgin GAC will serve as a baseline for the subsequent investigations on preloaded GAC described in the next chapter.

6.4.1 Isotherm Performance on Virgin GAC

The isotherm experiments conducted on virgin GAC for three target compounds led to the following conclusions:

1) The Freundlich model was found to be capable of expressing well the isotherms at the investigated "sub-saturation" concentration range, based on comparing the nonlinear

regression SSE among the candidate models, which include the Langmuir model and the three parameter Langmuir-Freundlich (LF) model. In addition, the choice of the Freundlich model makes the parameters describing adsorption characteristics of target compounds more representative and comparable, because it is widely applied in engineering design, and thus more data on other micropollutants could be easily accessed in the literature.

2) The isotherm data determined for both carbons in ultrapure water at ng/L concentrations showed that the adsorbabilties of the three target compounds were not in agreement with expectations based on their log K_{ow} values. Overall, in the investigated concentration range, carbamazepine was the most easily removed, and NP was shown to be the least adsorbable, with removal of naproxen in between. Dissociation of naproxen led to its lower adsorption affinity than carbamazepine.

3) The adsorption affinity of NP approached and subsequently exceeded those of naproxen and carbamazepine when the equilibrium concentrations increased. This observation is in agreement with a statement that the Freundlich exponent on a heterogeneous adsorbent may approach unity in extremely dilute solution (Suffet, 1980; Sontheimer *et al.*, 1988). Therefore, if an inappropriate extrapolation from the high concentration range is applied for predicting the removal of NP in the very low concentration range, the results may be overestimated and misleading in the design of GAC filters or selection of PAC doses for drinking water treatment purposes.

4) Based on the experimental accuracy and related likelihood joint confidence regions, virgin F400 carbon generally has higher adsorptive capacity than virgin PICA carbon for the compounds studied, without considering direct competition from background NOM.

5) However, isotherm tests in post-sedimentation water proved that F400 carbon is subject to more competition from background NOM than PICA carbon, thus leading to a greater required dosage to achieve the same removal in post-sedimentation water.

6) Comparisons of isotherms on F400 carbon between the target compounds and other conventional micropollutants show that the three target compounds in this research have generally comparable isotherm performance to TCE, MIB and geosmin, whereas atrazine presents much higher adsorptive affinity than all other compounds. The performance of MIB and geosmin are very similar to that of NP with respect to the

Freundlich 1/n. The removals of both MIB and geosmin are expected to be lower than those of naproxen and carbamazepine at liquid concentrations of approximately 30 ng/L.

7) Isotherm tests in PS water demonstrated that the removals of all target compounds decreased substantially due to the presence of background NOM. However, the degree of reduction depends on the specific target compound.

8) Equivalent background compound (EBC) parameters estimated using isotherm data from both ultrapure and post-sedimentation water are specific for each pair of target compounds and activated carbon. The adsorptive capacity of NP reduces least compared to the other two compounds. It may be due to its strong hydrophobicity and smallest molecular depth.

9) Based on the principle that the percent removal of the target compound at a given PAC dosage is independent of the initial target compound concentration under certain conditions, the minimum carbon dosages for removing 90% of three target compounds were calculated at two low initial concentrations (50 and 500 ng/L). It was theoretically confirmed that the calculated dosages could provide 90% removal of the target compounds occurring in the raw water at the concentration less than 500 ng/L.

10) In addition, a suspected minor competitive effect was found in two types of ultrapure water. Although it was assumed that the isotherms obtained in ASTM type II water were closer to the "true" isotherms, this problem requires further study.

6.4.2 Kinetic Performance on Virgin GAC

The SFB tests and related sensitivity analysis led to the following conclusions with respect to kinetic performances on virgin GAC:

1) Short-term SFB tests on virgin GAC are sufficient to accurately determine film diffusion coefficients for all cases. This is because film diffusion controls the mass transfer process at the early breakthrough stage.

2) Sensitivity analyses demonstrated that both PDM and SDM breakthrough profiles for the three target compounds under the experimental conditions used in this research are more sensitive to isotherm parameters than internal kinetic parameters throughout all phases of the breakthrough curve.

3) Under the low influent concentration conditions applied in the present study (500 ng/L), film diffusion exerts a much greater effect on breakthrough profiles than internal diffusion. This could be explained by the slow accumulation of adsorbates on the surface of adsorbents. This situation increases the difficulty in accurately calibrating the internal diffusion coefficients. In the case of naproxen and carbamazepine breakthrough, pore diffusion only significantly influences the breakthrough profiles after an extremely long running time.

4) Surface diffusion accounts for the main internal diffusion mechanism for NP mass transport, though it exhibits less impact on the breakthrough profile than does film diffusion.

5) Long-term SFB tests increased the accuracy and precision in determining the internal diffusion coefficients. Except for β_L for carbamazepine, no statistically significant difference in the determined β_L values could be distinguished on the two carbons. Therefore, the breakthrough profiles of the SFB systems using virgin GAC are largely influenced by isotherm parameters under very low concentration conditions.

6) The film diffusion coefficients determined for virgin GAC are in disagreement with the values estimated by the Gnielinski correlation, which underestimates β_L by a factor of 2 – 4 depending on the specific compound. The different discrepancy factor may be attributable to different electrostatic interaction between adsorbates and adsorbents and much higher hydrophobicity of NP than those of the other two compounds.

7) Direct competition from background organics in DI water used for SFB tests may lead to the errors in determining kinetic parameters under low concentration conditions. This factor was not overcome in this study and requires further work.

CHAPTER 7
ADSORPTION PERFORMANCE ON PRELOADED GAC

7.1 Adsorption Isotherms on Preloaded Carbons

7.1.1 DOC Breakthrough on Preloaded Carbons

As discussed in the Literature Review (Chapter 2), background NOM profoundly affects the adsorption of micropollutants in terms of both equilibrium capacity and mass transport. Since the concentration of background NOM (expressed as DOC) is present at much higher levels than the target compounds investigated in the current study, and background NOM generally has a much longer mass transfer zone (MTZ) than the micropollutants (Sontheimer *et al.*, 1988; Hand *et al.*, 1989; Carter and Weber, 1994), it is reasonable to imagine that most adsorption of target compounds occurs on GAC already preloaded with background NOM. Therefore, in this study, the F400 and PICA carbons, which were preloaded with background NOM at the Mannheim WTP, were subsequently used to determine the reduction of adsorptive capacity and kinetics due to preloading.

The design and operation of preloading facilities were described in Section 5.4. Figure 7-1 presents the DOC values for influent into and effluents from the F400 and PICA preloading columns.

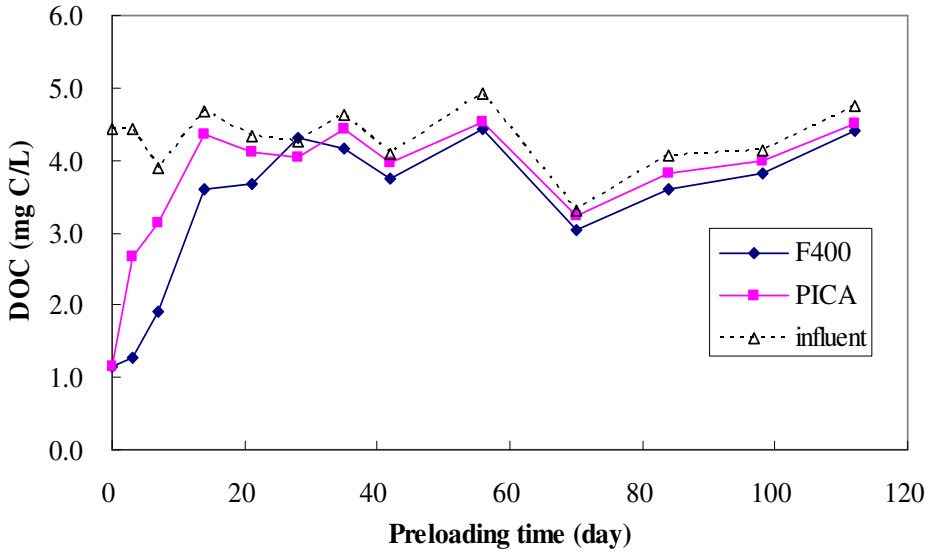

Figure 7-1 DOC breakthrough on preloading columns

The first batch of samples was taken approximately one hour after the columns began preloading. It was observed that approximately 25% DOC had already broken through both columns. This is reasonable because it accounts for the presence of non-adsorbable and poorly adsorbable NOM fractions in natural water (Roberts and Summers, 1982).

As shown in Figure 7-1, except for a few points, the influent DOC fluctuated at around 4 mg C/L (average 4.3 ± 0.42 mg C/L). It is evident that the PICA carbon columns broke through faster than the F400 carbon columns. However, both F400 and PICA columns approached almost 90% breakthrough in three to five weeks. Nevertheless, the preloading columns were kept running till the sixteenth week, because it was expected that the pore blockage effect, the displacement of poorly adsorbable NOM by strongly adsorbable NOM (Roberts and Summers, 1982) and reorientation of adsorbed NOM (Summers *et al.*, 1989; Knappe *et al.*, 1999) might influence the adsorptive capacity and kinetics of trace compounds in the long run.

7.1.2 Adsorption Equilibria on Preloaded Carbons

Adsorption Equilibrium Time on Preloaded Carbons

To establish the appropriate equilibrium time for determining isotherms on preloaded carbons, static kinetic tests were performed for 30x40 US mesh uncrushed five-week preloaded F400 and PICA carbons. As discussed in Section 2.6, the use of smaller size of uncrushed carbon is a trade-off between inaccuracy in determining adsorption capacity due to crushing process and equilibrium time on preloaded carbon. The use of finer preloaded carbon obtained from sieving original size preloaded carbon was based on a statement made by Summers *et al.* (1989) that the preloading effect is independent of particle size. In their study for TCE, it was found that GAC fouling by NOM was independent of particle size. Another study by Gillogly (1998) showed that different size GAC preloaded for the same period of time exhibited similar isotherms for adsorbing MIB. Therefore, these two cases suggested that it would be reasonable to use small size preloaded GAC to determine the remaining capacities for the target compounds.

Figure 7-2 and Figure 7-3 show the static kinetic results for preloaded F400 and PICA carbon, respectively. A comparison between the latter two figures and Figure 6-1 and Figure 6-2, respectively, indicates that the adsorptive capacity and kinetics on preloaded carbon significantly decreased for all target compounds as expected. Although it was found that the liquid concentrations of all target

compounds continuously decreased slightly even after 21 days, for practical purposes, apparent equilibria for all target compounds was considered to have essentially been achieved on the 21st day.

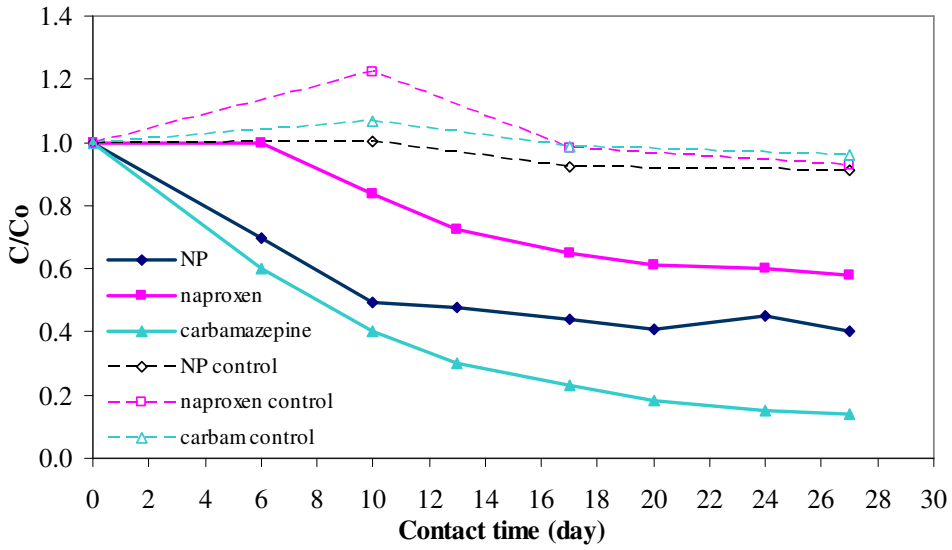

Figure 7-2 Target concentration profiles on 5-week preloaded 30x40 F400 carbon in ultrapure water

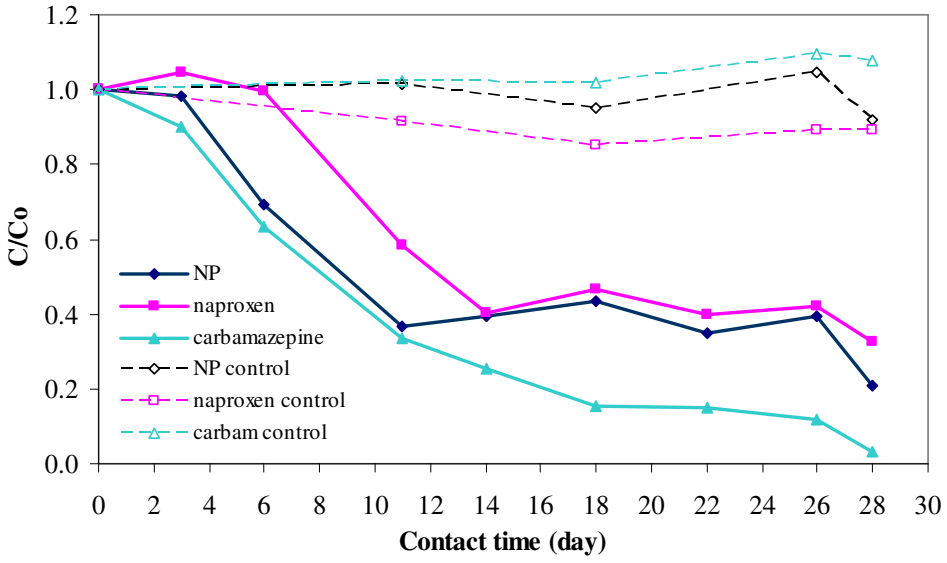

Figure 7-3 Target concentration profiles on 5-week preloaded 30x40 PICA carbon in ultrapure water

As a result, a cutoff time of 21 days was applied for the later isotherm tests on all preloaded F400 and PICA carbon. It is also interesting to note that, on both carbons, naproxen seemed to exhibit little adsorption before 6 days of contact time. This suggests that the mass transport of naproxen was severely slowed down due to preloading by background NOM. Therefore, it can be expected that naproxen could break through much faster than the other two compounds. This inference was confirmed in the subsequent SFB kinetic study and pilot-scale experiments.

Adsorption Isotherms on Preloaded F400 Carbon

To investigate the capacity reductions, the isotherms for naproxen and carbamazepine were run using the GAC samples taken from the preloading columns preloaded for one, three, five, eight and sixteen weeks. According to the results on naproxen and carbamazepine (relatively smaller differences of adsorption isotherms between virgin and one-week carbon and between five- and eight-week carbon) and for saving experimental time, the isotherms for NP were only determined for three, five and sixteen-week preloaded carbons. Same as the isotherm analyses for adsorption on virgin carbon in the previous chapter, nonlinear analyses based on the Freundlich equation were performed for all isotherm data obtained for preloaded carbon. The Freundlich parameters were estimated coupling with their 95% confidence intervals, which were obtained from the corresponding likelihood joint confidence region (LJCR) (the approach refers to section 5.6). The subsequent comparisons of difference among isotherm parameters were based on the overlap between the examined confidence intervals.

Figure 7-4, Figure 7-5, and Figure 7-6 show the isotherms for the adsorption of naproxen, carbamazepine, and NP, respectively, on 30x40 virgin and preloaded F400 carbon. The corresponding isotherm parameters and the confidence intervals are presented in Table 7-1. It should be noted that, for the illustrative purpose, three figures are shown in different x-axis range. The corresponding figures are also demonstrated in Appendix H with same x- and y- axis range for the convenience of visiual comparison. The same practice has also been done for the PICA carbon isotherm figures in the next section.

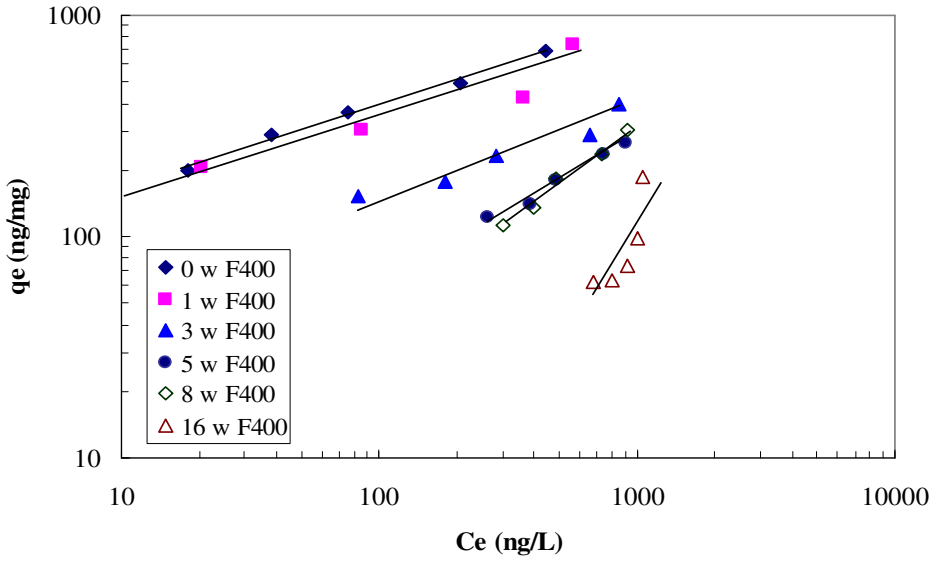

Figure 7-4 Naproxen adsorption isotherms on preloaded F400 carbon

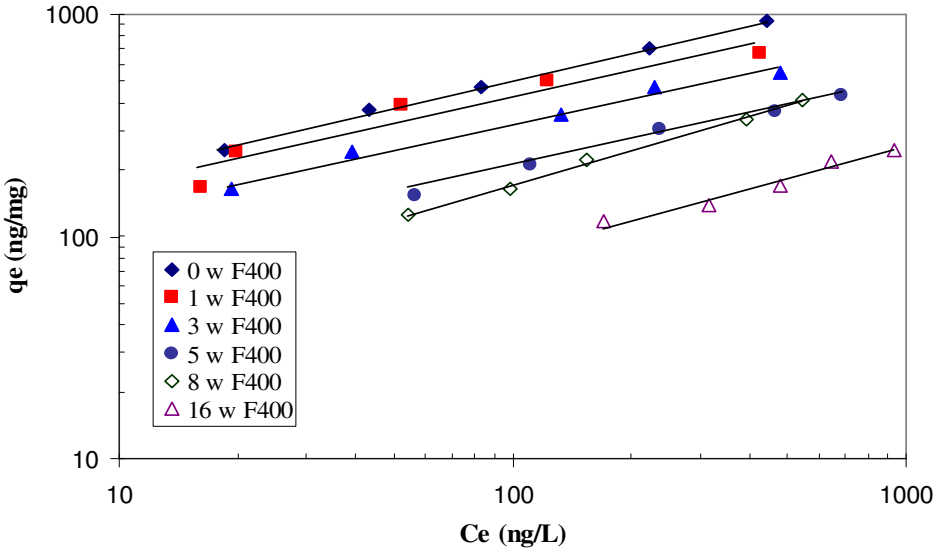

Figure 7-5 Carbamazepine adsorption isotherms on preloaded F400 carbon

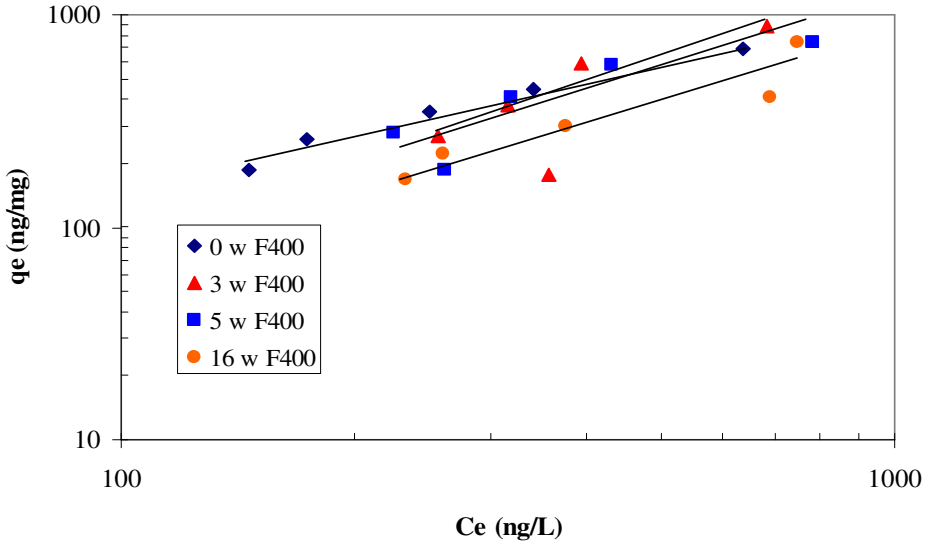

Figure 7-6 NP adsorption isotherms on preloaded F400

Comparison of the isotherms obtained for naproxen on virgin and preloaded F400 carbon (Figure 7-4 and Table 7-1) clearly reveals a significant loss of adsorptive capacity with increasing preloading time. The Freundlich K_F decreased from 73.2 to 0.09 (ng/mg)(L/ng)$^{1/n}$ on F400 carbon. Therefore, the remaining capacity expressed as the Freundlich K_F for naproxen is less than 1% of original value after sixteen weeks. The decreasing trend is also shown in Figure 7-10. It is interesting to note that in Figure 7-10 the adsorptive capacities between virgin and one-week preloaded F400 carbon, though having some difference, were not statistically significantly different. This observation is in disagreement with the findings in many studies (Carter and Weber, 1994; Knappe *et al.*, 1999) that the Freundlich K_F for SOCs such as TCE and atrazine rapidly decreased at the initial preloading time. Nonetheless, it is also observed that the adsorptive capacities of both carbons decreased dramatically from the one-week to the five-week preloading times, then slowly decreased continuously until the sixteenth week. With respect to the Freundlich 1/n values, they greatly increased due to preloading from 0.34 on virgin F400 carbon to unity on sixteen-week preloaded F400 carbon, suggesting that preloading of background NOM dramatically changed the heterogeneity of F400 carbon. Similar to the observation of the Freundlich K_F, the reduction of the Freundlich 1/n was not statistically significant (α = 0.05) before three-week preloading, after which it increased quickly to unity.

Table 7-1 Isotherm parameters obtained on virgin and preloaded F400 carbon

Compound	Naproxen		Carbamazepine		NP	
Preloading time (week)	K_F $(ng/mg)(L/ng)^{1/n}$	1/n	K_F $(ng/mg)(L/ng)^{1/n}$	1/n	K_F $(ng/mg)(L/ng)^{1/n}$	1/n
0	73.2 (67.5 - 77.3) [§]	0.37 (0.35 - 0.38)	73.8 (71.8 - 76.1)	0.42 (0.41 - 0.42)	4.44 (3.91 - 4.93)	0.78 (0.77 - 0.80)
1	63.9 (27.6 - 88.0)	0.36 (0.28 - 0.45)	92.9 (67.8 - 119)	0.33 (0.28 - 0.39)	ND ND	ND ND
3	19.7 (14.5 - 23.8)	0.43 (0.41 - 0.48)	64.6 (54.5 - 72.4)	0.35 (0.33 - 0.38)	1.29 (0.58 - 1.75)	1.00[†] (0.93 - 1.07)
5	3.81 (1.46 - 6.16)	0.62 (0.53 - 0.72)	32.8 (29.6 - 35.7)	0.40 (0.38 - 0.41)	1.21 (-0.17 - 1.61)	1.00[†] (0.900 - 1.06)
8	0.77 (0.69 - 0.85)	0.87 (0.86 - 0.87)	15.8 (14.7 - 17.0)	0.51 (0.50 - 0.54)	ND ND	ND ND
16	0.09 (0.07 - 0.11)	1.00[†] (0.95 - 1.06)	9.16 (8.12 - 10.9)	0.48 (0.47 - 0.50)	0.80 (0.31 - 1.32)	1.00[†] (0.914 - 1.09)

ND: not determined

†: the regression analysis achieved the upper bound of 1.0

§: numbers in parentheses are 95% confidence intervals for determined parameters

With respect to carbamazepine, the data shown in Figure 7-5 and Table 7-1 indicate a significant loss of adsorptive capacity on preloaded F400 carbon. The Freundlich K_F of carbamazepine dropped from 73.8 on virgin F400 to 9.16 $(ng/mg)(L/ng)^{1/n}$ on sixteen-week preloaded F400 carbon. The decreasing trend vs. preloading time is also shown in Figure 7-11. Similar to the deceasing pattern of Freundlich K_F for naproxen, the reduction of K_F for carbamazepine was not statistically significant (see Table 7-1) before three weeks of preloading. Subsequently, a rapid loss of capacity was found from three to eight weeks, followed by relatively slower capacity reduction from eight to sixteen weeks. As seen in Figure 7-5, the isotherms determined for carbamazepine on different preloaded F400 carbon were virtually parallel, with the only visible departure from this happening for the eight-week preloaded carbon. Further examination of the data in Table 7-1 indicates that, unlike the rapidly increasing trend of naproxen Freundlich 1/n, the Freundlich 1/n of carbamazepine remained statistically constant for five weeks of preloading and then slightly increased after preloading for eight weeks. This difference implies that the same preloading of background NOM exerts different impacts on different adsorbent-adsorbate systems.

Figure 7-6 shows NP isotherms data obtained on preloaded as well as virgin F400 carbons. Isotherm parameters are tabulated in Table 7-1 and corresponding preloading trends are presented in Figure 7-12. Compared to naproxen and carbamazepine, the determination of NP was lacking in precision, leading to more scatter of the data points. This might be due to disturbances from other isomers of NP or from the same NP isomer leaking from containers or detergents into the water matrix. Nevertheless, the general trends can still be distinguished in Figure 7-12. It is very interesting to find that, unlike naproxen and carbamazepine, except for the fact that the Freundlich K_F of NP after the first week of preloading significantly decreased from 4.44 on virgin F400 carbon to 1.29 $(ng/mg)(L/ng)^{1/n}$, there was no statistically significant change in the Freundlich K_F even for sixteen-week preloading. Similarly, examination of Table 7-1 and Figure 7-12 indicates that the Freundlich 1/n of NP quickly approached unity after the first week of preloading, then remained constant at this level.

Adsorption Isotherms on Preloaded PICA Carbon

The isotherm experiments to investigate the capacity reductions on preloaded PICA carbon were carried out under the same conditions as for preloaded F400 carbon. Figure 7-7 shows the comparison of naproxen isotherms obtained on virgin and different preloaded PICA carbon. The estimated isotherm parameters are tabulated in Table 7-2. In general, the figure and table both show that naproxen capacity on PICA carbon deceased with increasing preloading time, as expected. Similar to

the performance of naproxen on F400 carbon, its Freundlich K_F severely decreased from 70 on virgin PICA carbon to 0.26 $(ng/mg)(L/ng)^{1/n}$ on sixteen-week preloaded carbon. Correspondingly, the remaining capacity expressed as Freundlich K_F for naproxen is less than 1% of its original value. However, the decreasing trend shown in Figure 7-10 indicates a rapid initial capacity reduction after the first week of preloading, unlike the F400 carbon. As can be seen in Figure 7-10, the adsorptive capacities markedly decreased within the first eight weeks of preloading, and then continued to slowly approach essentially zero by sixteen weeks. With respect to the Freundlich 1/n values, a significant change could not be identified from zero to three-week preloading, whereas a great increase can be observed from five to sixteen-week preloading. Similar to F400 carbon, the Freundlich 1/n for sixteen-week preloaded PICA carbon approached unity, again suggesting that preloaded carbon in terms of adsorbing naproxen tends to be more homogeneous.

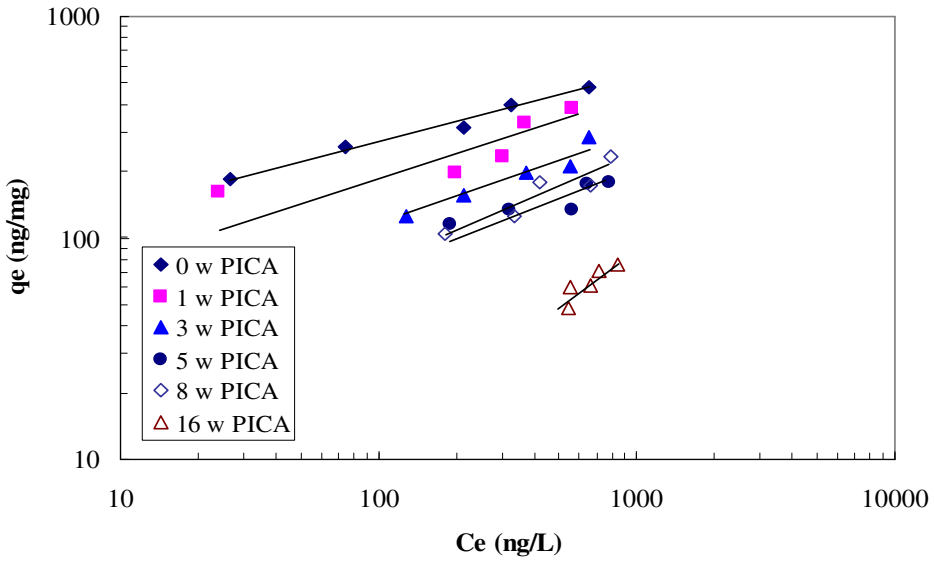

Figure 7-7 Naproxen adsorption isotherms on preloaded PICA carbon

Figure 7-8 compares carbamazepine isotherms on virgin and preloaded PICA carbon. Corresponding isotherm parameters are listed in Table 7-2. It is worth noting that all isotherms are parallel, and more detailed Freundlich 1/n data in Table 7-2 further demonstrate no significant difference among them. This is interesting because the carbamazepine Freundlich 1/n on preloaded F400 carbon also did not substantially change. This trend is similar to the observation by Knappe *et al.* (1999) for atrazine adsorption and to the summary made by Sontheimer *et al.* (1988) for other SOCs.

The reduction of K_F for carbamazepine was found to be not significant (see Table 7-2 and Figure 7-11) prior to three weeks of preloading. Subsequently, the capacity was found to continuously decline from the third to sixteenth weeks. This trend was somewhat similar to the observations for adsorption of carbamazepine on F400 carbon (Figure 7-11), although on PICA carbon carbamazepine was less extent affected by preloading.

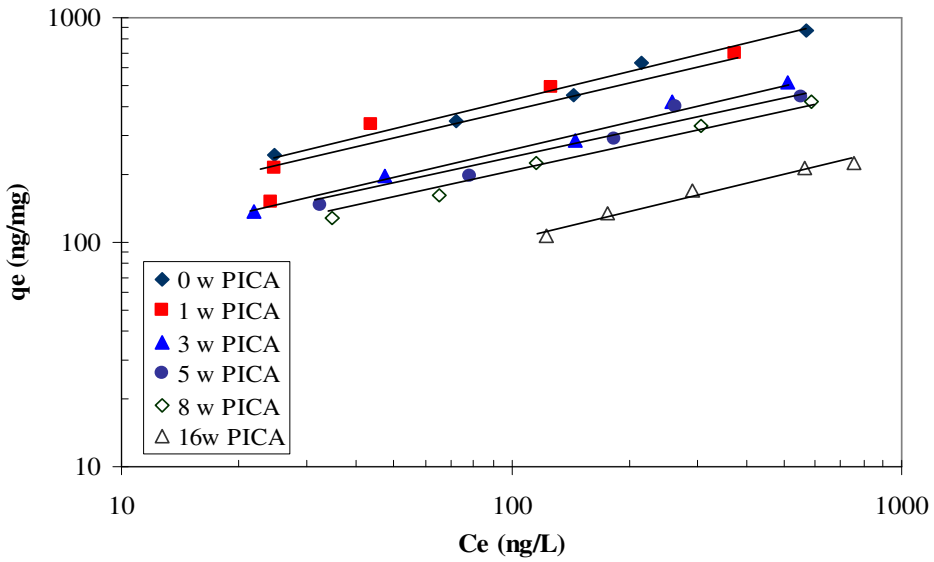

Figure 7-8 Carbamazepine adsorption isotherms on preloaded PICA carbon

The isotherms in Figure 7-9 and the corresponding isotherm data in Table 7-2 demonstrate the changes of Freundlich K_F and 1/n for NP on preloaded PICA carbon. Similar to the NP performance on F400 carbon, the impact of preloading is virtually absent in Figure 7-9. Nonetheless, the isotherm data in Table 7-2 did show some significant difference between virgin and preloaded PICA carbons. However, both the Freundlich K_F and 1/n rapidly level off after preloading for five weeks. These trends were unexpected and it seemed that the mechanisms for adsorptive capacity reduction based on both pore filling and pore blockage were not able to explain the NP phenomenon.

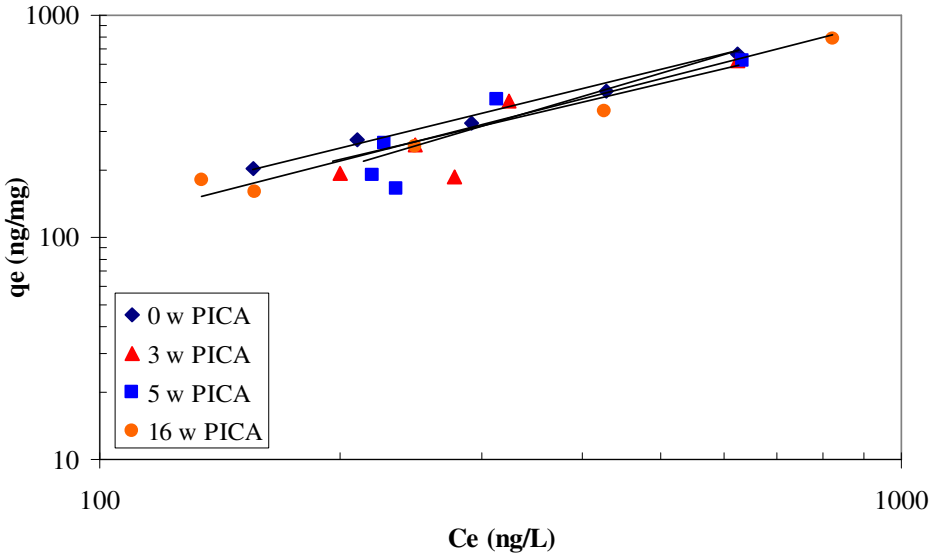

Figure 7-9 NP adsorption isotherms on preloaded PICA carbon

In summary, the adsorptive performances of the three target compounds on preloaded carbon were markedly different. Although they show somewhat different results, the two carbons seem to follow a similar reducing trend for the same compound due to preloading. More discussion will be included in the next section.

Table 7-2 Isotherm parameters obtained on virgin and preloaded PICA carbon

Compound	Naproxen		Carbamazepine		NP	
Preloading time (week)	K_F $(ng/mg)(L/ng)^{1/n}$	1/n	K_F $(ng/mg)(L/ng)^{1/n}$	1/n	K_F $(ng/mg)(L/ng)^{1/n}$	1/n
0	70.0 (62.0 - 76.8) [§]	0.30 (0.28 - 0.31)	57.6 (49.3 - 69.0)	0.43 (0.41 - 0.45)	2.49 (2.27 - 2.70)	0.87 (0.85 - 0.88)
1	35.7 (19.0 - 46.9)	0.36 (0.30 - 0.43)	57.8 (40.3 - 71.5)	0.42 (0.37 - 0.47)	ND ND	ND ND
3	24.2 (15.2 - 29.5)	0.35 (0.28 - 0.39)	38.0 (32.3 - 41.4)	0.42 (0.40 - 0.44)	1.94 (1.02 - 2.58)	0.90 (0.84 - 0.96)
5	13.9 (11.1 - 16.9)	0.40 (0.37 - 0.45)	35.9 (26.6 - 46.2)	0.40 (0.36 - 0.46)	1.28 (0.62 - 1.73)	0.96 (0.89 - 1.06)
8	5.69 (3.43 - 8.85)	0.56 (0.50 - 0.62)	30.3 (28.6 - 32.0)	0.41 (0.40 - 0.43)	ND ND	ND ND
16	0.26 (0.21 - 0.30)	0.85 (0.82 - 0.87)	18.7 (16.7 - 20.6)	0.38 (0.36 - 0.40)	1.46 (1.20 - 1.68)	0.93 (0.91 - 0.96)

ND: not determined

†: the regression analysis achieved the upper bound of 1.0

§: numbers in parentheses are 95% confidence intervals for determined parameters

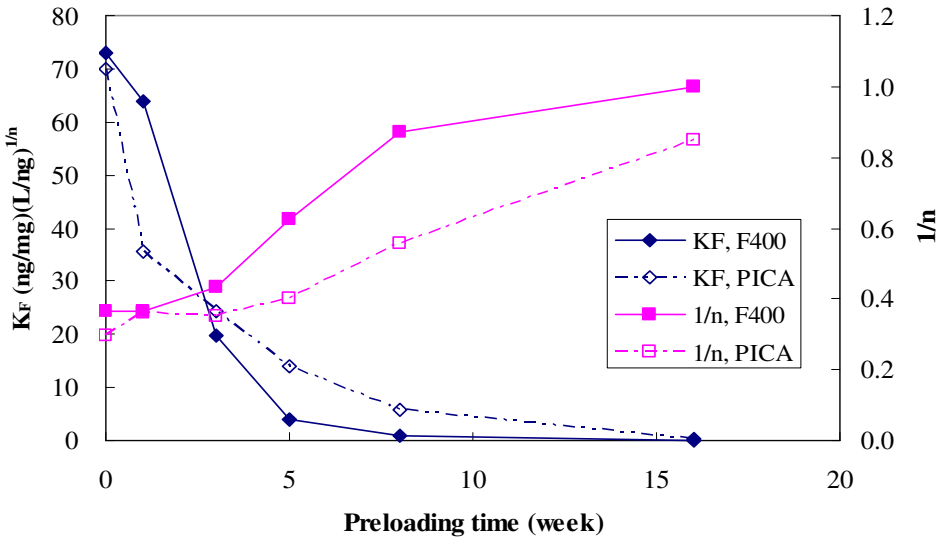

Figure 7-10 Effect of preloading time on naproxen Freundlich parameters

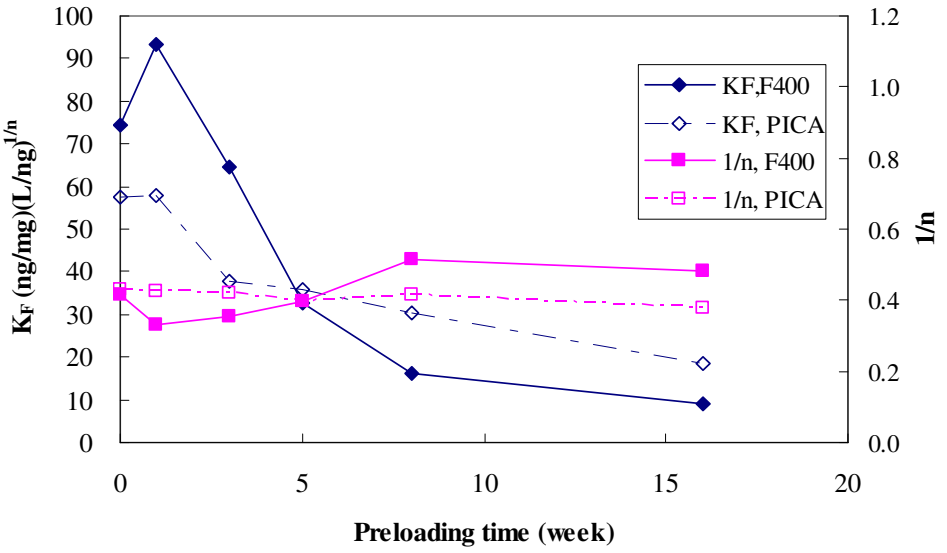

Figure 7-11 Effect of preloading time on carbamazepine Freundlich parameters

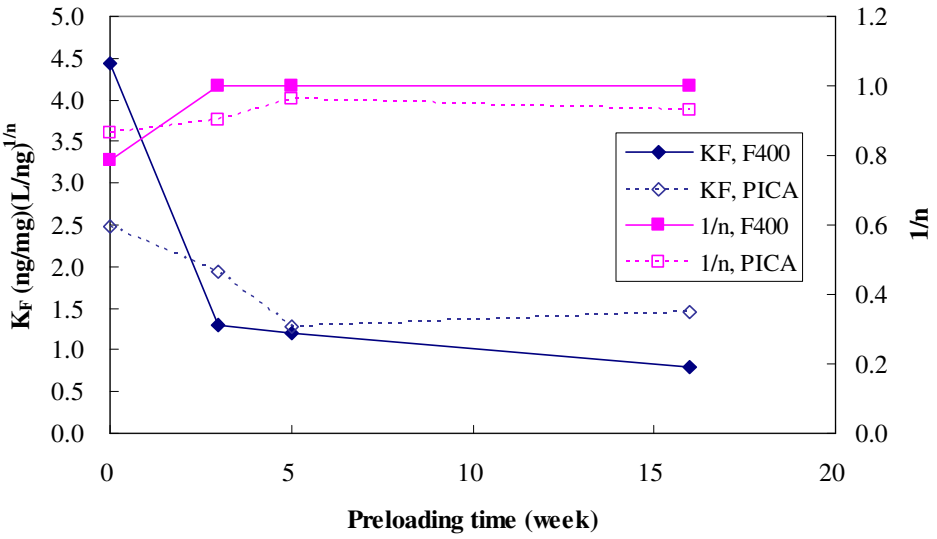

Figure 7-12 Effect of preloading time on NP Freundlich parameters

7.1.3 Preloading Effect on Adsorptive Capacity

Impact of Preloading on Adsorptive Capacity

As shown in Figure 7-10 for naproxen and Figure 7-11 for carbamazepine, the Freundlich K_F for both compounds were subject to severe impacts from the preloading of background NOM. In particular, the remaining Freundlich K_F values for naproxen on both F400 and PICA carbon were less than 0.5% of the values on the virgin carbons within only sixteen weeks of preloading. With respect to carbamazepine, the remaining Freundlich K_F on F400 was only 1.2% of the initial value on the virgin carbon, whereas the Freundlich K_F remained approximately 30% of its initial value on PICA carbon preloaded for sixteen weeks. Compared to other conventional SOCs, such as atrazine and TCE, the extent of Freundlich K_F reductions for naproxen and carbamazepine obtained in this study are substantially larger. For instance, Knappe *et al.* (1999) reported that the remaining atrazine capacity on a wood-based GAC decreased to approximately 50% of the virgin GAC after five months of preloading by a type of rive water. In addition, 40 – 60% capacity reduction (Freundlich K_F at C_e = 0.31 mg/L) was observed for TCE on the GAC, which was preloaded by a river water for 25 weeks and extracted from different bed depths (Summers *et al.*, 1989). The markedly different capacity reductions between the data reported in the literature and in this study could be due to the different water and carbon used. Nevertheless, the low concentrations applied in this study may also contribute

to this discrepancy. The applied concentration for the isotherm tests in the above two references were all several orders of magnitude higher than the concentration levels used in this study. Hence, it is not unreasonable to suspect that the low concentration of the target compounds led to a reduced ability to compete with the partially preloaded NOM or to access the effective adsorption sites. However, further confirmation should be made possibly using higher concentrations of the target compounds for isotherm tests.

Based on the isotherm results for the three target compounds on preloaded carbons, it can be visually judged that impacts of preloading on Freundlich parameters for different compounds followed different trends, hence leading to diverse reduction patterns of adsorptive capacities. Since Freundlich 1/n values more or less varied in all cases and correlated to Freundlich K_F, it is difficult to compare the reduction of adsorptive capacity directly through Freundlich K_F values. Therefore, for illustrative purposes, the adsorptive capacity for each compound on each preloaded carbon was calculated for liquid phase concentrations of 500 and 50 ng/L (Table 7-3). The high concentration corresponds to the influent concentration used in SFB and pilot-scale experiments. The low concentration is considered as a likely environmentally relevant concentration, respectively.

Table 7-3 Comparison of adsorptive capacities (ng/mg) at two liquid phase concentration levels on virgin and preloaded carbons (based on isotherm results)

compound	naproxen				carbamazepine				NP			
carbon	F400		PICA		F400		PICA		F400		PICA	
concentration (ng/L) / time (wks)	50	500	50	500	50	500	50	500	50	500	50	500
0	306	711	223	440	377	985	311	838	95.4	580	73.7	541
1	261	610	147	339	327	731	304	806	n/a	n/a	n/a	n/a
3	108	293	95.9	216	257	579	197	520	64.5	645	65.9	524
5	43.6	183	66.7	168	154	382	171	428	60.5	605	55.2	505
8	23.7	175	49.9	179	118	385	153	397	n/a	n/a	n/a	n/a
16	4.50	45.0	7.20	50.5	60.1	182	82.6	198	40.0	400	55.9	478
Capacity reduction at week 16 (%)	98.5	93.7	96.8	88.5	84.1	81.5	73.4	76.3	58.1	31.0	25.1	11.6

n/a: not applicable

As shown in Table 7-3, on both F400 and PICA carbon, preloading of background NOM had the greatest impact on the removal of naproxen. The GACs preloaded for sixteen weeks only had

approximately 2 – 10% of its capacity remaining for naproxen at the two equilibrium concentration levels. In contrast, 15 – 25% of the original adsorptive capacity remained for the removal of carbamazepine. Among the three target compounds, NP experienced the least impact from preloading, and its capacity was only reduced by approximately 11 – 58% after sixteen weeks. It is interesting to note that the capacity reduction order for the three target compounds interestingly coincides with the reduction order caused by direct competition. Although the long time preloading of NOM can not be simply considered as direct competition, it may be not unreasonable to hypothesize that the compounds with stronger competitive potential with NOM molecules would be subject to less capacity loss even on extensively preloaded GAC. It is possible that the micropollutant molecules could partially replace the NOM molecules, which are pre-adsorbed on adsorption sites, if they are not prevented by large-molecular-size NOM molecules from accessing adsorption sites. This hypothesis is also supported by the observation that the capacity reduction at high concentration (500 ng/L) is generally less than that at low concentration (50 ng/L) (see Table 7-3). It is inferred that the target compounds at higher concentrations are better able to compete for adsorption sites. If the impact of preloading on kinetics is not considered, the data shown in Table 7-3 suggests that NP would be the last of the three target compounds which would break through GAC adsorbers in the long run.

Based on data in Table 7-3, a comparison can also be made between F400 and PICA carbons. In general, PICA carbon retained more adsorptive capacity for all three target compounds than F400 carbon after sixteen-week preloading. Since virgin F400 carbon exhibited higher capacity, it can be concluded that, with respect to adsorptive capacity, F400 carbon is more vulnerable to preloading than PICA carbon. Coincidently, F400 carbon was found to be more severely impacted than PICA carbon in terms of direct competition, as discussed in Chapter 6. More vulnerability of F400 carbon under the impact of background NOM is in accord with the fact that F400 carbon had higher DOC surface loading than PICA, as shown in Figure 7-1. Thus, it could be reasoned that more adsorption sites were taken over by NOM molecules in F400 carbon. In relating these observations to the pore distribution data in Table 5-5, it is seen that F400 carbon has more pore volume distributed in the range larger than 8 Å (50% and 36% for F400 and PICA carbon, respectively), which is also accessible to typical NOM molecules. This may support the observation that more NOM could be adsorbed by F400 carbon than PICA carbon (see Figure 7-1), assumed that biodegradation of adsorbed NOM is negligible or at the same extent on both carbons. Therefore, it seems that a positive correlation exists between the severity of impact from preloading effect and a higher percentage of secondary micro- to macro-pores in a carbon since more NOM tends to be taken up on this carbon.

Influence of Preloading on BET Surface Area and Pore Structure

Having established the effect of background NOM preloading on the reduction of adsorptive capacities for both carbons, it is of interest to examine the impact of preloading on the BET surface area of GAC. The BET surface areas of virgin and three-, five-, sixteen-week preloaded F400 and PICA carbons were determined using N_2 adsorption isotherms at 77 K. The results are plotted in Figure 7-13. Correspondingly, the percentage DOC remained (reversed DOC breakthrough profiles from Figure 7-1) in the preloading columns were determined at the same time points, and are also shown in Figure 7-13.

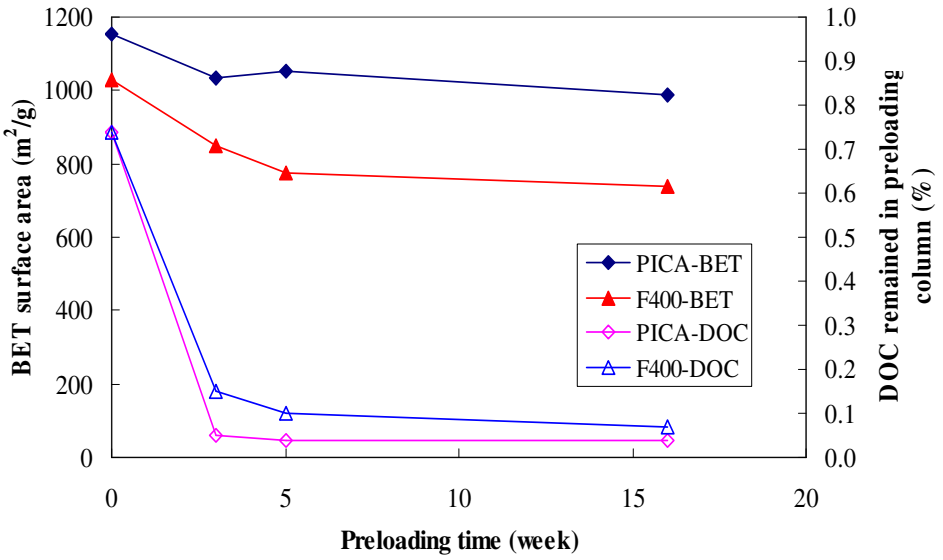

Figure 7-13 Relationship between DOC adsorption and reduction of BET surface area

As shown in Figure 7-13, the BET surface area of PICA carbon decreased within the first three weeks of preloading, and thereafter essentially leveled off throughout the remaining preloading time. In contrast, the BET surface area of F400 carbon experienced a greater reduction during the initial preloading time up to five weeks, and then continued to decrease slowly for longer preloading times. A comparison between DOC breakthrough trends in the F400 and PICA carbon preloading columns (expressed as %DOC retained in columns in Figure 7-13) and the corresponding BET surface area reduction trends indicates that they are somewhat in agreement with each other. In the early stage of preloading, large amounts of NOM were adsorbed on both F400 and PICA carbon, hence leading to the significant reduction of the BET surface areas. Furthermore, the later slight or no decrease in the

BET surface areas corresponded to a low DOC adsorption efficiency phase for the preloading columns.

Kilduff *et al.* (1998b) used humic acid to preload F400 carbon and found that 20% reduction in BET surface area was caused by preloading 87 mg/g humic acid, among which the first 13 mg/g preloading accounted for approximately 50% of the total reduction. Those authors attributed the reduction of the BET surface area to pore blockage by preloaded humic acid. However, the conflicting evidence in this study is that, while the pore blockage effect expressed as the reduction of the BET surface area slowed down or totally stopped after three weeks of preloading, the adsorptive capacities of naproxen and carbamazepine (see Figure 7-10 and Figure 7-11) continued to decrease. In addition, the total reductions of the BET surface areas were 15% and 28% for PICA and F400 carbon, respectively, after preloading for sixteen weeks. These trends were not in accord with the capacity reduction of the three target compounds on preloaded carbons. Therefore, it can be suggested that the BET surface area can not solely explain the effective adsorption area for micropollutants. Since the BET surface area is measured by monolayer coverage of nitrogen molecules on the total carbon surface (Brunauer *et al.*, 1938), it accounts for the adsorption sites which can be accessed by nitrogen molecules. Therefore, if the adsorption sites are filled with micropollutant or low-molecular-weight NOM molecules, or the access to adsorption sites is totally blocked by high-molecular-weight NOM molecules, the determined BET surface area should decrease. It is quite possible that the high-molecular-weight NOM, which cannot diffuse throughout the carbon structure, only partially blocks pores, closing accesses for micropollutant molecules to some adsorption sites. However, this type of blockage would not be able to completely shut down mass transport routes for much smaller nitrogen molecules. Therefore, although this type of partial pore blockage contributes to the reduction of effective adsorption area for micropollutants, it can not be effectively distinguished by the N_2 BET method. Since the diffusion rates of high-molecular-weight NOM molecules are much lower than micropollutant molecules, this type of pore blockage effect may be predominant at a later preloading stage. This hypothesis can successfully explain the phenomenon of continuous capacity reduction of naproxen and carbamazepine without significantly decreasing BET surface area. In addition, it can be concluded that the BET surface area cannot be regarded as an index of effective adsorption area for adsorbing micropollutants, especially at a long preloading time.

In addition, the pore structures of virgin and five-, sixteen-week preloaded F400 and PICA carbons were also measured using N_2 adsorption isotherms, and are shown in Table 7-4.

Table 7-4 Carbon structure change due to preloading

Carbon	Preloading time (wks)	SA BET (m^2/g)	Total pore volume (cm^3/g)	Pore volume distribution (cm^3/g)		
				< 8 Å	8-20 Å	20-50 Å
F400	0	1030	0.549	0.273	0.149	0.046
	5	774	0.448	0.210	0.108	0.043
	16	739	0.417	0.199	0.107	0.034
PICA	0	1156	0.527	0.340	0.140	0.025
	5	1051	0.483	0.308	0.121	0.026
	16	987	0.457	0.290	0.115	0.023

It can be seen from Table 7-4 that total pore volumes for both carbons were reduced, generally following the similar trend of reduction as BET surface areas. This suggests that the total pore volume can not fully account for the great adsorptive capacity reductions for naproxen and carbamazepine. The changes of pore volume distributions on both preloaded F400 and PICA carbon further indicated that the reduction of total pore volume was mainly caused by the loss of primary and secondary micropore volumes. In general, mesopore volumes were not substantially changed throughout the preloading. This is reasonable because most NOM would be adsorbed in secondary micropores (Karanfil *et al.*, 2006). The reduction in primary micropore volumes may be due to the adsorption of some unknown small-molecular-weight organics in the PS water or pore blockage by adsorption of NOM in secondary micropores. Comparison of F400 carbon to PICA carbon suggested that wider pore distribution of F400 carbon could lead to more reduction in the micropore volume probably because the structure of F400 carbon made NOM molecules more easily access to micropores.

Possible Explanations for Different Impact of Preloading on Target Compounds

Based on the observations of isotherm results for the three target compounds on preloaded carbons, it could be seen that the impacts of preloading on different compounds were surprisingly inconsistent. They generally followed three different patterns:

1) For naproxen (Figure 7-10), the Freundlich K_F greatly decreased before the fifth week of preloading and continued to slowly decrease until the sixteenth week, while the Freundlich 1/n remained relatively constant for less than three-week preloaded carbon and then increased with increasing preloading time, finally approaching unity.

2) As shown in Figure 7-11 for carbamazepine, the Freundlich K_F did not exhibit a substantial reduction during the first week of preloading, and then continuously decreased thereafter; the Freundlich 1/n increased only slightly or essentially remained constant throughout the entire preloading period.

3) As illustrated in Figure 7-12 for NP, the Freundlich K_F only experienced a slight initial decrease and remained constant thereafter; correspondingly, the Freundlich 1/n slightly increased, approaching unity with increasing preloading time. Overall, the isotherms for NP clearly did not more downwards in Figure 7-6 and Figure 7-9 in the investigated concentration range throughout the whole preloading time.

Interestingly, the changing Freundlich 1/n trends for naproxen and carbamazepine on preloaded carbons, to some extent, reflect two contradictory patterns reported in the literature. Like the isotherms for carbamazepine, a group of almost parallel isotherms for TCE on GAC preloaded for various times was observed by Sontheimer *et al.* (1988) and Summers *et al.* (1989). Similarly, the Freundlich 1/n for atrazine determined on preloaded carbon did not show a significant increase even on GAC preloaded for twenty-five months (Knappe *et al.,* 1999). In addition, the Freundlich 1/n for MIB only reduced 0.1 after one year of preloading (Gillogly, 1998). On the other hand, as evidence for an increasing Freundlich 1/n with time or adsorbed amount of NOM, Carter and Weber (1994) and Kiduff *et al.* (1998a, b) observed an increasing trend for TCE Freundlich 1/n on preloaded carbon. Conflicting results in the present study and the literature regarding the impact of preloading on the heterogeneity of GAC suggest that it is very difficult to come up with a generalization about competitive effects, which include direct competition and pore blockage, and probably other mechanisms for a particular adsorbate–adsorbent pair. The complex competitive effect can be attributed to diverse interactions among many factors, such as the composition of the background NOM, the properties of the target micropollutants, and the characteristics of the activated carbons. As far as this study is concerned, generally similar adsorptive capacity reduction trends were observed for a specific compound on both F400 and PICA carbon. Therefore, it was felt that the different adsorption performance of target compounds is mainly attributable to the interactions between the target compound and the background NOM, which were similar on the two types of carbons.

With respect to adsorption of naproxen on the two carbons, its Freundlich 1/n did not substantially change within a three-week period of preloading, while the Freundlich K_F deceased sharply during this same time. Two possible mechanisms might contribute to this phenomenon. Firstly, at the early stage of preloading, only NOM molecules with similar sizes to the target

compound, i.e. so-called very-low-molecular-weight NOM, can diffuse to the adsorption sites. This fraction of NOM may not be permanently sterically filled into the adsorption sites, and therefore could be replaced by target compound molecules. Since naproxen molecules can access the adsorption site equally with this type of NOM molecules, this could be regarded as similar to direct competition, which leads to reduction of only the Freundlich K_F, thus producing a group of nearly parallel isotherms (Najm *et al.*, 1991). However, evidence of irreversible adsorption of humic substances inside activated carbon pores (Summers *et al.*, 1988) is usually used for rejecting the likely mechanism of direct competition occurring on preloaded carbon. It should be noted that the previous desorption studies (Summers *et al.*, 1988) were carried out in buffered ultrapure water without introducing any other solute. However, it could be expected that some pre-adsorbed NOM could be forced to release from adsorption sites if competition from micropollutants is introduced. This fraction of desorbable NOM could vary depending on different competing micropollutants. Nevertheless, according to the direct competition results in Chapter 6, this fraction of NOM should be only a small percentage of the overall NOM. This is inconsistent with the fact that large amounts of NOM were adsorbed in the preloading columns during the early stages. Therefore, another factor accounting for the observed pattern for naproxen is complete pore blockage caused by low-molecular-weight NOM, which is slightly larger than target compound molecules (Newcombe *et al.*, 2002b). This mechanism leads to a loss of adsorptive capacity without changing the overall adsorption site energy distribution (Carter *et al.*, 1992). In addition, it also brings about a reduction of the overall BET surface area (Kilduff *et al.*, 1998b), as evidenced in Figure 7-13. Unfortunately, the two mechanisms are simultaneously occurring inside the carbon, and thus are indistinguishable. When preloading time increases, the simultaneous decrease in Freundlich K_F and increase in Freundlich 1/n could be interpreted as that more strongly adsorbable low-molecular-weight NOM molecules replace weakly adsorbable NOM molecules, and then tightly bond to high energy adsorption sites. These molecules cannot be desorbed, leading to the change of heterogeneity of the carbon (Carter *et al.*, 1995). Meanwhile, slow-diffusing large-molecular-weight NOM deposits on the diffusion pathway of the target compound molecules, blocking or slowing down access to adsorption sites. This type of adsorption of NOM becomes predominant in the late preloading phase (Carter *et al.*, 1992), and may not lead to a significant loss of BET surface area as shown in Figure 7-13.

For carbamazepine, only minor change of or even constant Freundlich 1/n on preloaded F400 and PICA carbons, respectively, demonstrate that the heterogeneity of the carbon was not substantially impacted by preloading of NOM, in terms of its ability to adsorb this target compound. This is quite different from the adsorption trends of naproxen. Since isotherms of carbamazepine were

determined on the same preloaded carbon, and these two compounds are approximately the same size, the reduction in adsorptive capacity due to complete pore blockage in the early preloading stages should be comparable for the two compounds, thus does not help to explain the difference. Based on the comparison of isotherm performance in ultrapure and PS water, it can be judged that carbamazepine is more strongly adsorbable than naproxen. Hence, it is expected that carbamazepine could compete for more adsorption sites already occupied by NOM molecules, resulting in a higher fraction of desorbed NOM on the same preloaded carbon. This would lead to more parallel isotherms on GAC preloaded for a longer time. Overall, the mechanisms responsible for the decreasing adsorption capacity for carbamazepine of preloaded carbon are comprised of direct competition with desorbable NOM and pore blockage.

The adsorption of NP likely follows very different mechanisms from those for naproxen and carbamazepine. NP is as a more hydrophobic long straight chain molecule (see Figure 5-1). A small cross section area makes it more accessible to primary micropores. It has been summarized by Karanfil *et al.* (2006) that the majority of NOM cannot access to primary micropores. Therefore, the overall capacity reduction of NP due to direct competition should be limited. Another possible mechanism may be the fact that NP has a high $\log K_{ow}$, thus giving it a greater tendency to absorb or partition to the surface of GAC. As was the case in work reported by Carter (1993), this hypothesis is based on the observation that the Freundlich 1/n values of NP in this study are close to unity. Therefore, as preloading increases, the organic matrix formed by adsorbing NOM on the GAC particles would not influence its partitioning tendency.

In summary, although the preloading mechanisms raised by other researchers and the author of this thesis can presumably interpret the different performances of the three target compounds on the preloaded carbons, it is obvious that complex sorption process can not be simply attributed to one mechanism, thus not allowing for generalization. Furthermore, the conflicting observations and their possible explanations require further study with additional adsorbates and adsorbents.

7.2 Adsorption Kinetics on Preloaded Carbons

7.2.1 Sensitivity Analysis of PSDM on SFB Reactor for Preloaded Carbons

In order to obtain an initial indication of breakthrough on preloaded carbon, two short-term SFB tests (27 – 30 hours) were carried out separately on five-week preloaded F400 and PICA carbons (as demonstrated in Figure 7-18 and Figure 7-23, data also shown in Appendix H). Because the two

carbons were considered to be apparently exhausted with respect to DOC removal after running for five weeks, it was originally thought that the effluent concentrations from the SFB reactor would increase much more than for virgin carbons. Surprisingly, similar to the results from short-time SFB tests on virgin carbons, the effluent concentrations increased very slowly, which seemed to suggest that the mass transport processes were still controlled by film diffusion. Therefore, sensitivity analyses were performed based on five-week preloaded carbon to investigate diffusion mechanisms.

Table 7-5 Parameters for baseline prediction for sensitivity analysis on five-week preloaded GAC

carbon	Operational parameters	compound	K_F $(ng/mg)(L/ng)^{1/n}$	1/n	β_L $(x\ 10^{-3}cm/s)$	τ	D_s $(x10^{-11}cm^2/s)$
F400	Co = 500 ng/L Carbon mass = 7.2 g Bed depth = 3.0 cm Flowrate = 50 mL/min	naproxen	3.81	0.62	0.50	8	na
		carbamazepine	32.8	0.40	1.12	8	na
		NP	1.21	1.0	2.91	na	2.03
PICA	Co = 500 ng/L Carbon mass = 7.5 g Bed depth = 3.2 cm Flowrate = 50 mL/min	naproxen	13.9	0.40	0.46	8	na
		carbamazepine	35.9	0.40	1.43	8	na
		NP	1.28	0.96	2.71	na	1.01

na: not applicable

The operational, isotherm and kinetic parameters for the baseline calculations in these sensitivity analyses are presented in Table 7-5. The influent concentrations and flowrate were set as 500 ng/L and 50 mL/min, respectively, values which were later used for all kinetic tests. Compared to the SFB tests on virgin GAC, a greater bed depth and therefore carbon mass were used for preloaded carbons, in order to keep initial breakthrough to relatively low concentrations. The baseline isotherm parameters were those determined on five-week preloaded carbons (from Table 7-1 and Table 7-2). Kinetic parameters were those estimated, if possible, from the short-term SFB tests on five-week preloaded carbons. The impedance τ, which could not be accurately determined, was fixed at 8. This value represented the upper end of the range reported by Carter and Weber (1994) for TCE on extensively preloaded F400 carbon. Therefore, it was assumed that the slow pore diffusion rate corresponding to the τ value of 8 would lead to a mass transport process largely controlled by pore diffusion. In these sensitivity analyses, film diffusion coefficients were varied by -50%. The surface diffusion coefficient for NP also was changed by -50%. The variation in impedance was set at four times the baseline value (equals $\tau = 32$). This variation also corresponded to the CIs search strategy used in the PSDM program (see Section 5.7 for more details).

As results, Figure 7-14 and Figure 7-15 present the results of the sensitivity analyses for the three target compounds on F400 and PICA carbon, respectively. It is surprising to find that, contrary to what had originally been thought, the PDMs for adsorbing naproxen and carbamazepine were not sensitive to pore diffusion even after 400 hours for both SFB reactors. Visual comparisons between these two figures (Figure 7-14a and Figure 7-15a) and the sensitivity analyses figures (Figure 6-25 and Figure 6-26) in the previous chapter reveal that the sensitivity of the breakthrough profiles to the pore diffusion on preloaded carbons was even lower than for virgin carbons. The variations in profiles caused by varying the impedance may be even smaller than the experimental error. In contrast, the film diffusion (Figure 7-14b and Figure 7-15b) exerted a large influence on the shape of the breakthrough profiles. These observations suggest that film diffusion was still a predominant mechanism influencing the SFB breakthrough profiles of naproxen and carbamazepine on five-week preloaded carbons at extremely low influent concentrations. With respect to the breakthrough profiles for NP, the influence of surface diffusion was easily visible in the later stages of the SFB test. This trend is similar to what was observed for virgin carbons. In addition, the comparisons between Figure 7-14 and Figure 7-15 and their corresponding figures (Figure 6-29 and Figure 6-30) in the previous chapter show that the influence of surface diffusion on NP breakthrough profiles was not enhanced on the preloaded carbons as expected. The influence of film diffusion on the breakthrough profiles of NP was still stronger than that of surface diffusion.

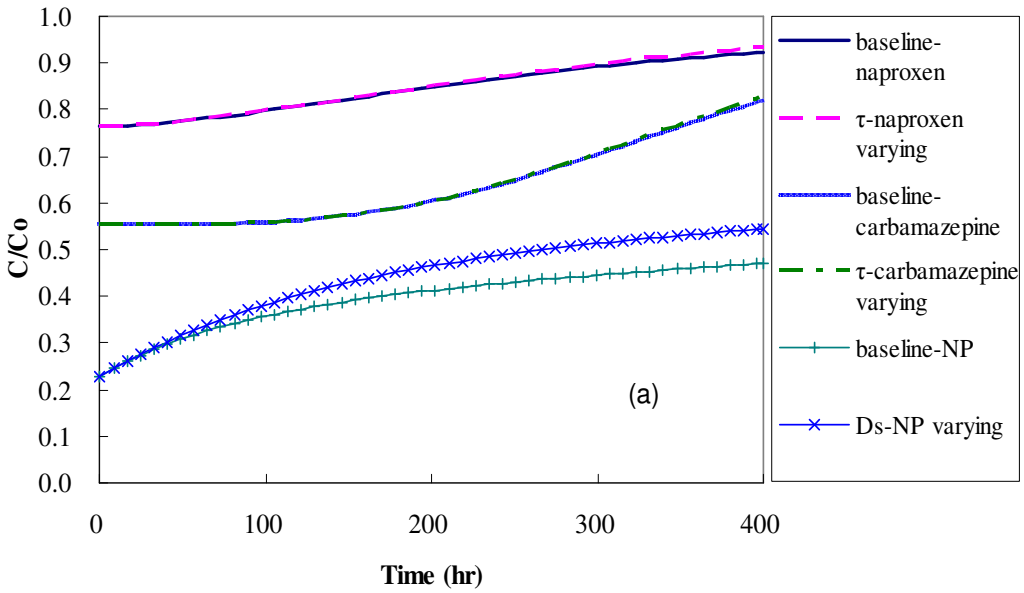

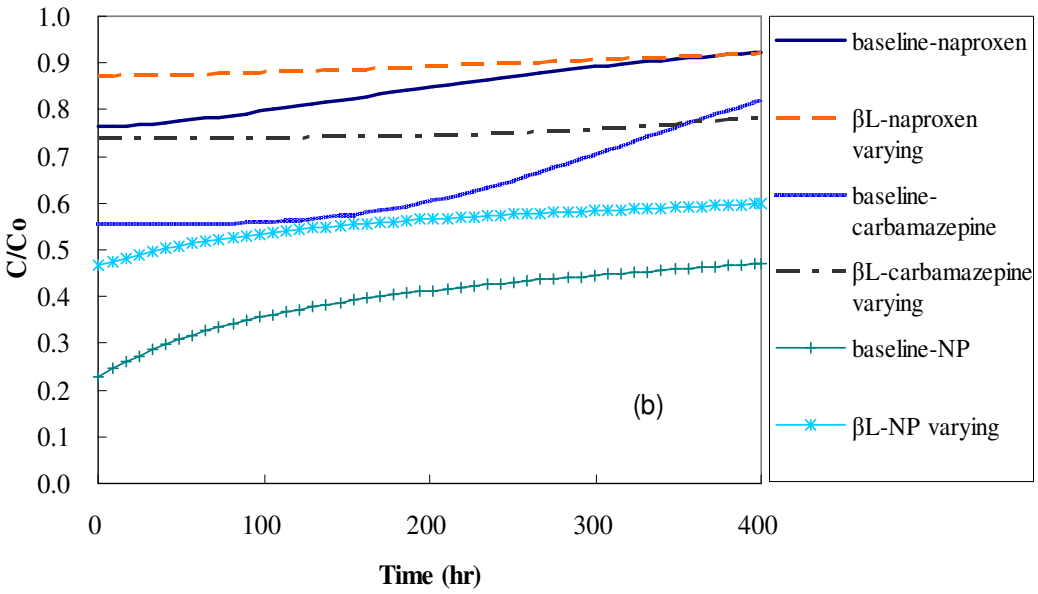

Figure 7-14 Sensitivity of PSDM to kinetic parameters on five-week preloaded F400 carbon in SFB reactor

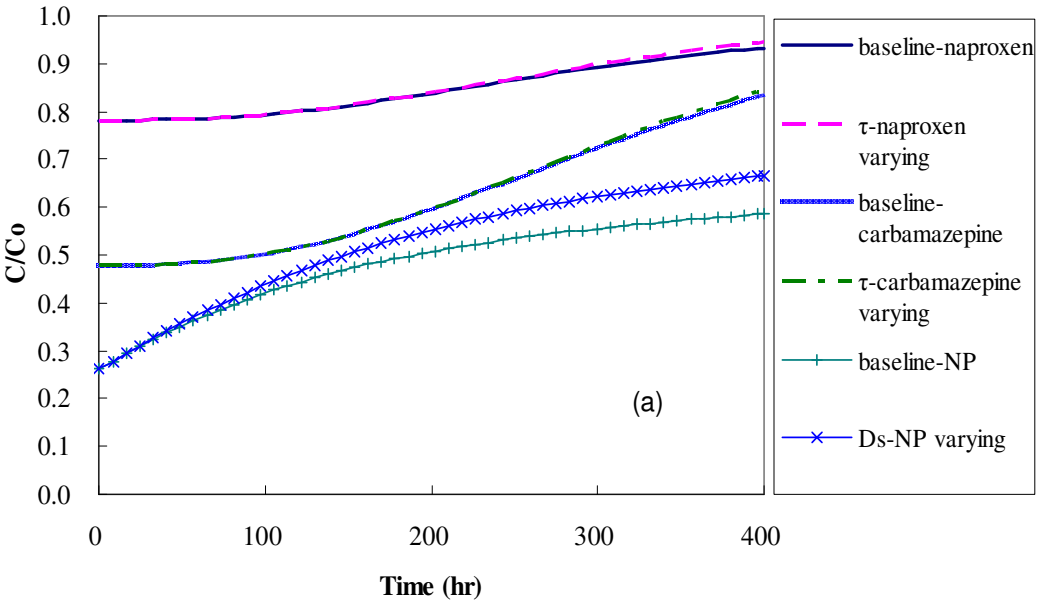

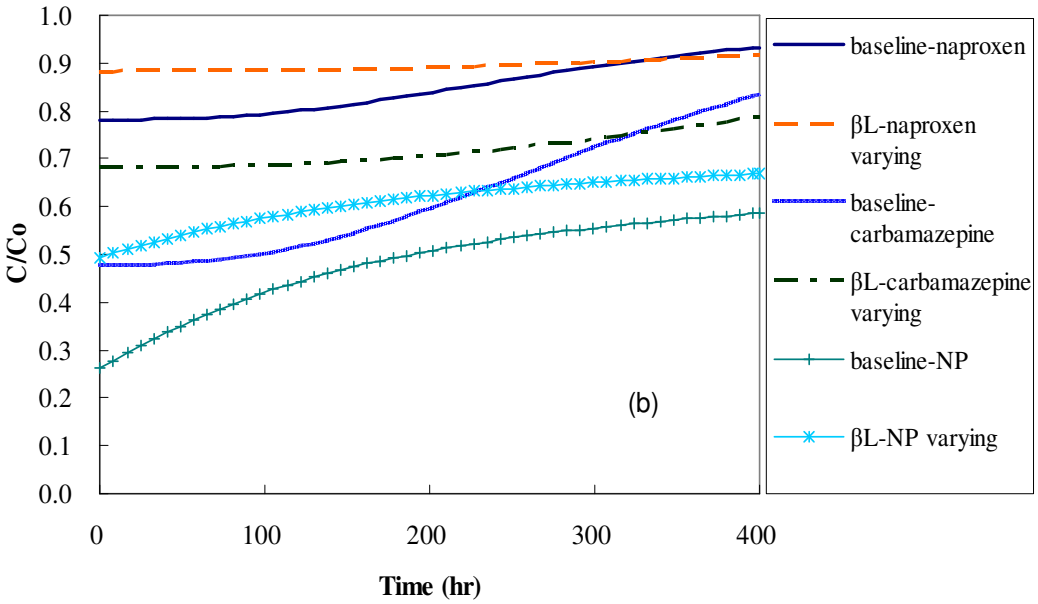

Figure 7-15 Sensitivity of PSDM to kinetic parameters on five-week preloaded PICA carbon in SFB reactor

It was surprising that film diffusion remained responsible for mass transport processes for all cases analyzed on five-week preloaded carbons, because in general the internal diffusion limitations were expected to become more predominant and thus exert more influence on breakthrough profiles for preloaded carbons. The lack of influence for internal diffusion found in the sensitivity analyses could be attributable to the more rapid reduction of film diffusion than of internal diffusion. This matter will be further investigated in a later section of this chapter. In addition, the ng/L level concentrations of the target compounds applied in this study led to smaller driving forces, further resulting in smaller solute fluxes across the film layer. In the present research, the pore diffusion coefficients could not be accurately determined even after simulating the SFB tests of 400 hours. For example, the difference between the baseline and the varied breakthrough curve (τ = 32) of naproxen in Figure 7-14a would be smaller than the experimental errors. Therefore, it was finally decided that the SFB tests for all preloaded carbons would only be carried out for short times (27 – 30 hours). In these cases, only film diffusion coefficients could be accurately estimated with tight confidence intervals, whereas the coefficients for pore diffusion were obtained as results of regression with confidence intervals unavailable.

7.2.2 Adsorption Kinetics on Preloaded Carbons

Kinetic Tests on F400 Carbon

The SFB tests were carried out for the three target compounds on one-, three-, five-, eight- and sixteen-week preloaded F400 carbon. The kinetic parameters for NP were not determined on the F400 carbon preloaded for one and eight weeks, because isotherm parameters were not determined on the corresponding carbon (as mentioned early in this chapter, it was expected that small differences were between virgin and one-week carbon and between five- and eight-week carbon). The experimental data as well as model calibrations are presented in Figure 7-16 to Figure 7-20. The model calibration results are listed in Table 7-6 and Table 7-7 for estimated film diffusion coefficients and internal diffusion coefficients, respectively. The data in both tables show that the preloading of background NOM resulted in the reduction of both film diffusion and internal diffusion. For example, for naproxen adsorbed on F400 carbon, β_L ($x10^{-3}$ cm/s) decreased from 3.12 at zero week to 0.28 at 16 weeks, and τ increased from 1.00 at zero week to 2.94 at 16 weeks. However, it should be noted that some impedance values shown in Table 7-7 on preloaded carbon are extraordinary large. Since the PDM became more insensitive to τ on preloaded carbon and only short-term SFB test data were available for analysis, the τ data in Table 7-7 were only output from calibrations, and no confidence intervals could be determined by the PSDM program. Therefore, it was felt that the τ values in Table 7-7 were too inaccurate to describe the preloading effect on pore diffusion. The calibration processes for surface diffusion coefficients of NP on preloaded F400 carbon were much better than for pore diffusion coefficients of naproxen and carbamazepine. Nevertheless, the PSDM program still could not find full confidence intervals for the determined parameters in the range of zero to four times the estimated values.

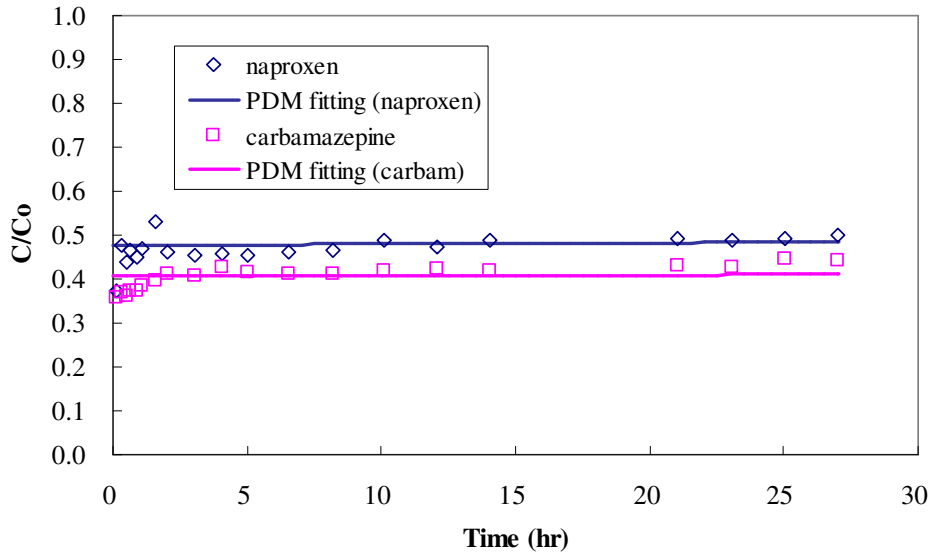

Figure 7-16 SBF test data and model calibration on one-week preloaded F400 carbon (bed depth 2.9 cm, flowrate 49.7 mL/min)

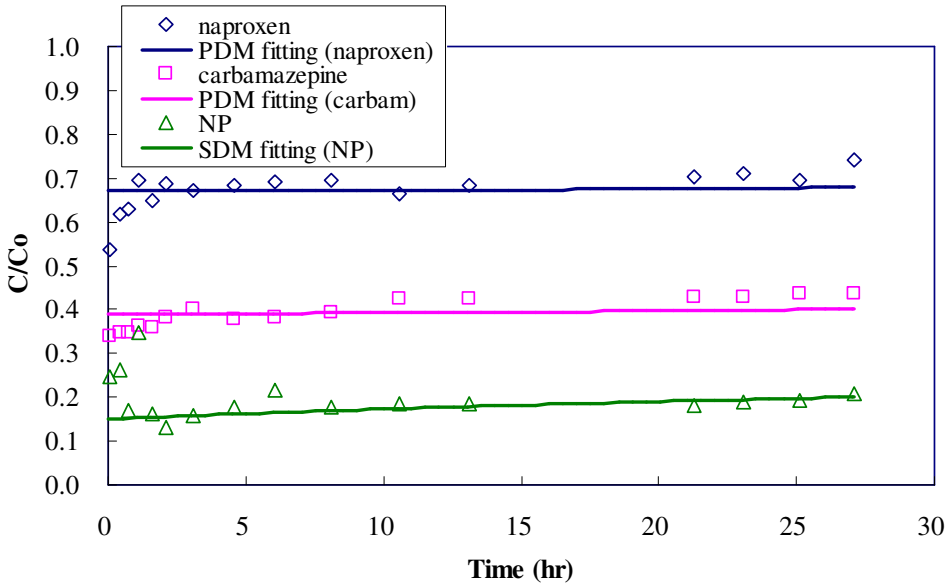

Figure 7-17 SBF test data and model calibration on three-week preloaded F400 carbon (bed depth 3.1 cm, flowrate 49.6 mL/min)

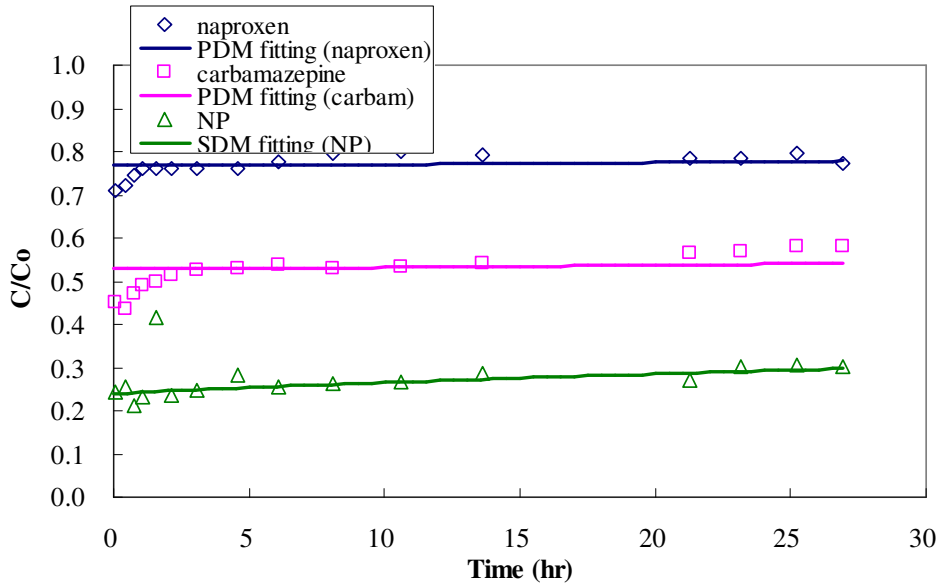

Figure 7-18 SBF test data and model calibration on five-week preloaded F400 carbon (bed depth 3.0 cm, flowrate 50.3 mL/min)

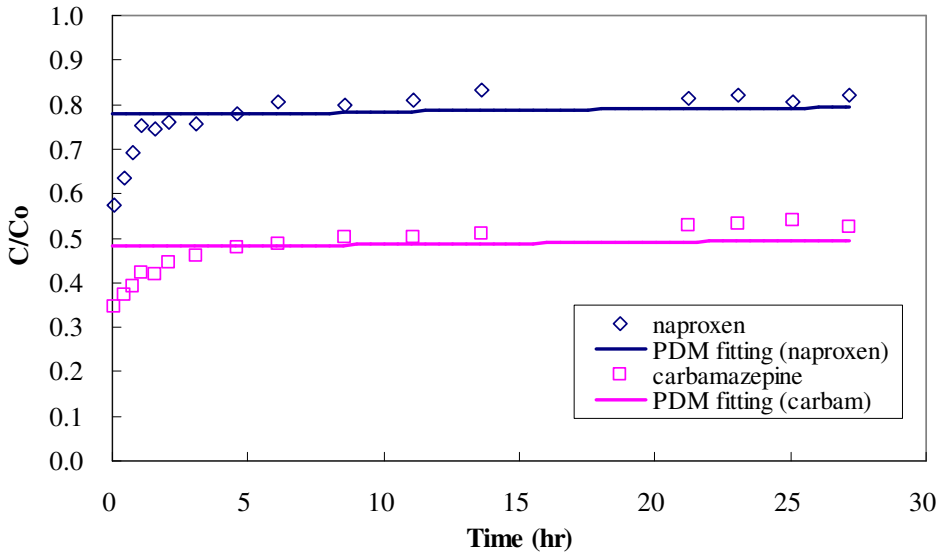

Figure 7-19 SBF test data and model calibration on eight-week preloaded F400 carbon (bed depth 3.7 cm, flowrate 50.3 mL/min)

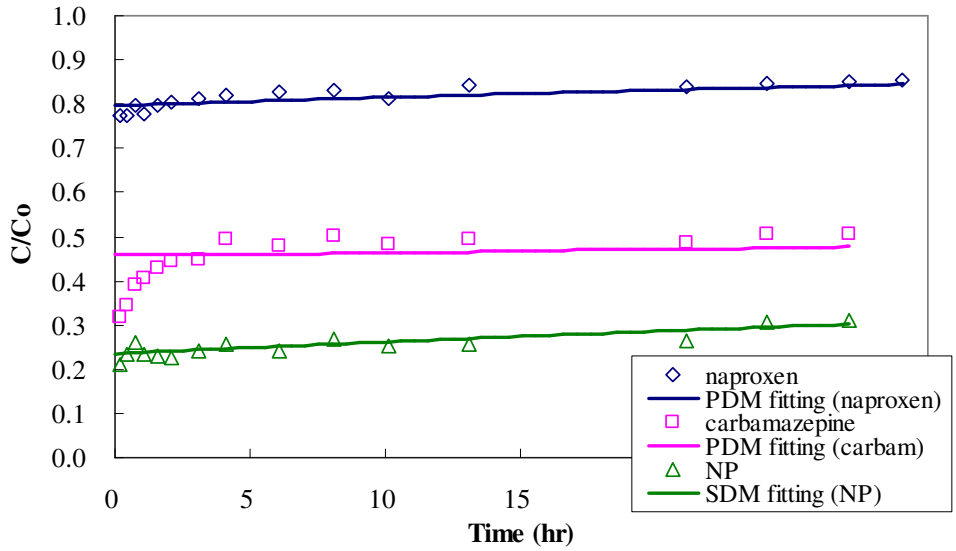

Figure 7-20 SBF test data and model calibration on sixteen-week preloaded F400 carbon (bed depth 4.4 cm, flowrate 49.9 mL/min)

It is interesting to observe that the distance between the breakthrough curves for different target compounds (comparing Figure 7-16 to Figure 7-17) rapidly increased, as shown for the carbon preloaded for three weeks (Figure 7-17). More specifically, although the breakthrough curves of naproxen and carbamazepine on virgin F400 carbon almost overlapped (see Figure 6-23), the removal of naproxen exhibited much more reductiondue to preloading than was the case for carbamazepine for the same SFB reactor, leading to the breakthrough curve of naproxen pulling away from that of carbamazepine. Compared to naproxen and carbamazepine, the elevation of breakthrough curves for NP on carbon preloaded for a long time was not so pronounced. This finding may be attributable to the different rates of reduction of both capacity and kinetics for different compounds. Different patterns of capacity reduction as evidenced by isotherm parameters among target compounds have been presented and discussed in previous sections. Different reduction rates of both film and internal diffusion coefficients can be observed by comparing data shown in Table 7-6 and Table 7-7, respectively. Similar to the impact of preloading on capacity reduction, naproxen once again was subject to the most severe impact from preloading, with its film diffusion coefficient dramatically decreasing by more than an order of magnitude from 3.12×10^{-3} cm/s on virgin F400 carbon to 0.28×10^{-3} cm/s on sixteen-week preloaded carbon. In contrast, the film diffusion coefficients for both carbamazepine and NP on sixteen-week preloaded F400 carbon decreased approximately 70%.

By observing Figure 7-16 through to Figure 7-20, the early breakthrough data for naproxen and carbamazepine all had a sharp increase before approximately three hours, and then turned into a relatively steady and slow increase. However, a similar trend was not observed on virgin F400 (Figure 6-23). Furthermore, this type of early sharp increase became more pronounced on F400 carbon preloaded for increasing times. Therefore, this suggests that the phenomenon might be caused by loading of background NOM on the carbon. This pattern is similar to the results for atrazine adsorption in a F400 SFB reactor reported by Schideman *et al.* (2006a, b). Those authors attributed these observations to the rapidly declining film diffusion coefficients at the beginning of SFB tests, because more NOM was adsorbed from a natural water, which was used for their SFB tests, during this initial time (Schideman *et al.*, 2006a). However, this mechanism can not successfully explain the similar trend in this study, because the SFB tests were performed in DI water. Therefore, it is suspected that naproxen and carbamazepine could quickly be adsorbed on the external NOM "film" formed on the surface of the carbon, and saturate it in short time. Nevertheless, the exact reason is not clear. As a result, some initial points were considered as outliers and removed in subsequent calibrations (the excluded points are identified in Appendix H).

Table 7-6 Determined film diffusion coefficients β_L (x 10^{-3}cm/s) for three target compounds on virgin and preloaded GACs

compound	Naproxen		Carbamazepine		NP	
Preloading time (week)	F400	PICA	F400	PICA	F400	PICA
0	3.12 *(2.50-3.53)*†	3.06 *(2.21-4.64)*	3.04 *(2.13-3.34)*	3.79 *(3.43-4.27)*	5.99 *(4.80-6.84)*	5.47 *(5.03-6.01)*
1	1.48 *(1.44-1.57)*	1.68 *(1.54-1.74)*	1.84 *(1.75-1.90)*	2.80 *(2.69-2.89)*	ND	ND
3	0.71 *(0.64-0.75)*	0.80 *(0.71-0.89)*	1.58 *(1.47-1.66)*	1.85 *(1.78-1.90)*	3.71 *(3.56-3.79)*	3.92 *(3.88-4.00)*
5	0.50 *(0.47-0.53)*	0.46 *(0.42-0.52)*	1.12 *(0.96-1.28)*	1.43 *(1.36-1.48)*	2.91 *(2.82-3.00)*	2.71 *(2.65-2.79)*
8	0.42 *(0.34-0.46)*	0.81 *(0.71-0.88)*	1.01 *(0.88-1.14)*	1.44 *(1.42-1.51)*	ND	ND
16	0.28 *(0.26-0.30)*	0.35 *(0.27-0.43)*	0.95 *(0.87-1.01)*	0.72 *(0.68-0.74)*	1.91 *(1.85-1.97)*	2.61 *(2.53-2.74)*

ND: not determined
†: data in parenthesis are 95% confidence intervals

Table 7-7 Determined internal diffusion coefficients for three target compounds on virgin and preloaded GACs

Compound Parameter	Naproxen impedance τ		Carbamazepine Impedance τ		NP D_s ($x10^{-11}$ cm^2/s)	
Preloading time (week)	F400	PICA	F400	PICA	F400	PICA
0	1.0 *(0.77 ->4.0)*	1.0 *(0.50 ->4.0)*	1.0 *(0.52 ->4.0)*	1.5 *(1.1 -4.5)*	3.2 *(1.9 - 4.4)*	3.7 *(3.2 - 7.2)*
1	3.0 *(ND)*	1.0 *(ND)*	3.2 *(ND)*	1.5 *(ND)*	ND	ND
3	3.0 *(ND)*	1.0 *(ND)*	9.3 *(ND)*	2.4 *(ND)*	3.1 *(<0 - 12)*	1.0 *(<0 – 3.4)*
5	3.0 *(ND)*	48 *(ND)*	9.3 *(ND)*	1.9 *(ND)*	2.0 *(<0 - 8.0)*	1.0 *(<0 – 2.5)*
8	3.0 *(ND)*	48 *(ND)*	69 *(ND)*	3.3 *(ND)*	ND	ND
16	2.9 *(ND)*	48 *(ND)*	69 *(ND)*	3.3 *(ND)*	0.42 *(ND)*	1.0 *(ND)*

Numbers in parentheses are confidence intervals at 5 % significant level
ND: not determined

Kinetic Tests on PICA Carbon

The SFB tests were carried out on preloaded PICA carbon under conditions similar to those on the preloaded F400 carbon. The experimental results and model calibrations are shown in Figure 7-21 to Figure 7-25 for PICA carbon preloaded for various times. Correspondingly, the numerical results from model calibrations were summarized in Table 7-6 and Table 7-7 for film diffusion and internal diffusion coefficients, respectively.

As can be seen in Table 7-6 and Table 7-7, both film diffusion and internal diffusion coefficients experienced negative impacts (i.e. β_L values decreased and τ values increased) due to preloading. The β_L of naproxen severely dropped almost an order of magnitude from $3.06x10^{-3}$ cm/s for virgin PICA carbon to $0.35x10^{-3}$ cm/s for sixteen-week preloaded PICA carbon. In contrast, the β_L values for carbamazepine and NP after sixteen weeks of preloading remained at 19% and 48%, respectively, of the values determined on virgin PICA carbon. The decrease in the film diffusion coefficients for all three target compounds is to some extent the same as observed on preloaded F400 carbon. Possible explanations for having varying decreases for film diffusion coefficients for different target compounds will be discussed in the next section.

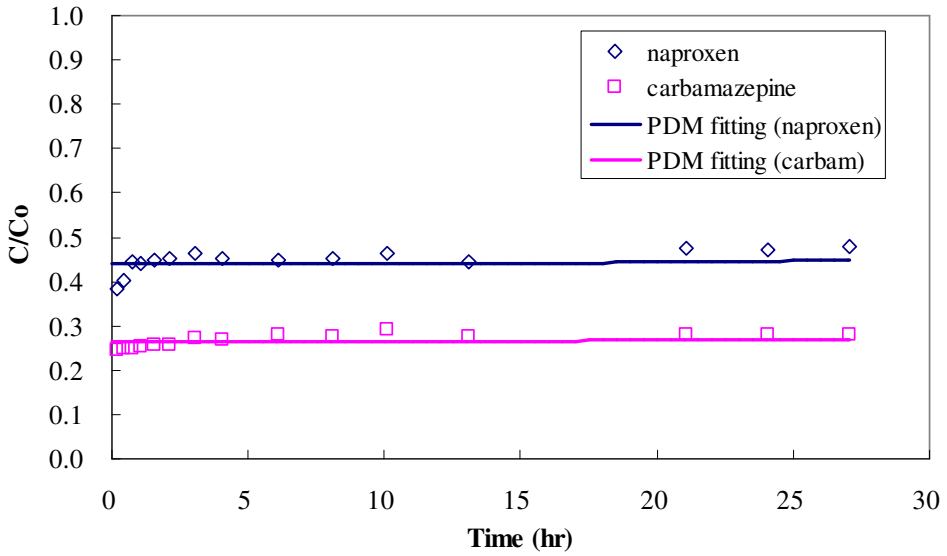

Figure 7-21 SBF test data and model calibration on one-week preloaded PICA carbon (bed depth 3.0 cm, flowrate 50.3 mL/min)

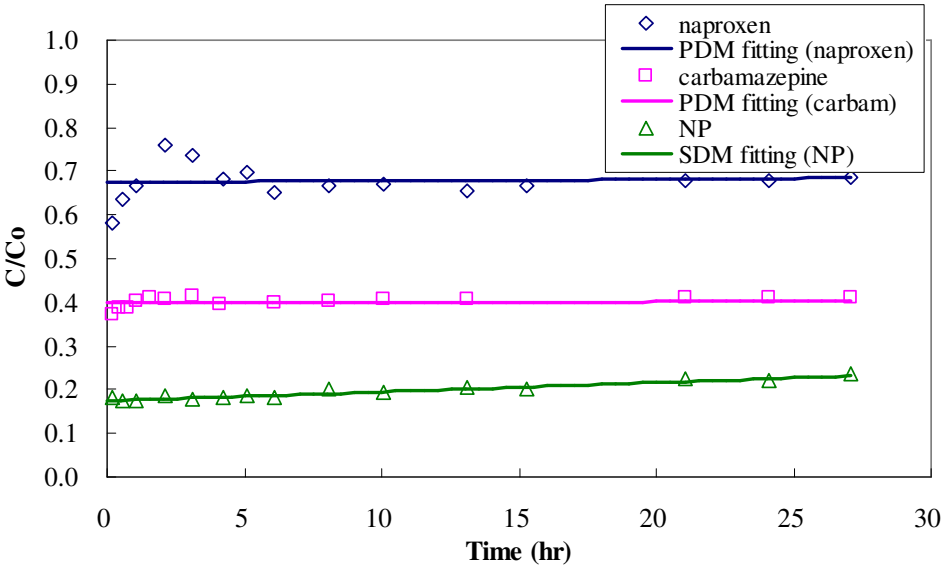

Figure 7-22 SBF test data and model calibration on three-week preloaded PICA carbon (bed depth 2.9 cm, flowrate 49.8 mL/min)

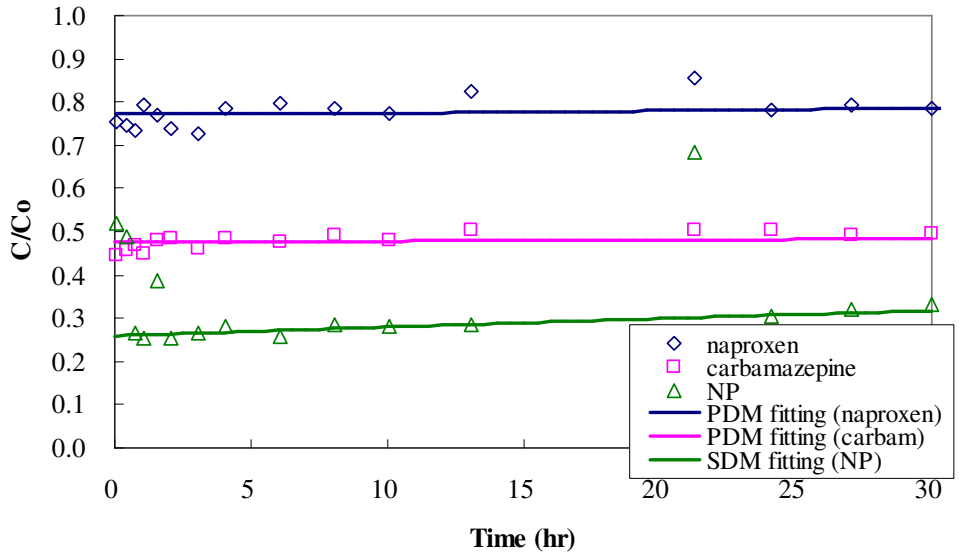

Figure 7-23 SBF test data and model calibration on five-week preloaded PICA carbon (bed depth 3.2 cm, flowrate 50.5 mL/min)

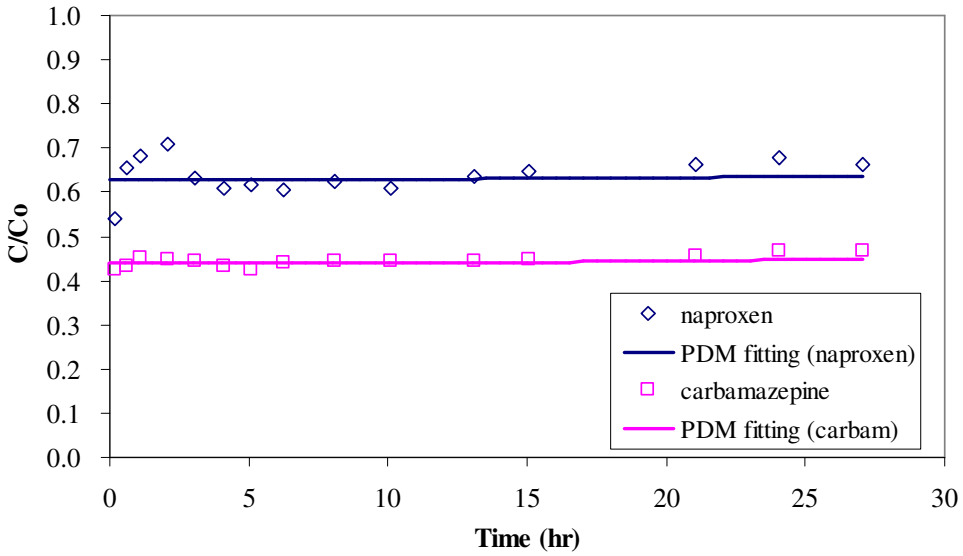

Figure 7-24 SBF test data and model calibration on eight-week preloaded PICA carbon (bed depth 3.4 cm, flowrate 49.7 mL/min)

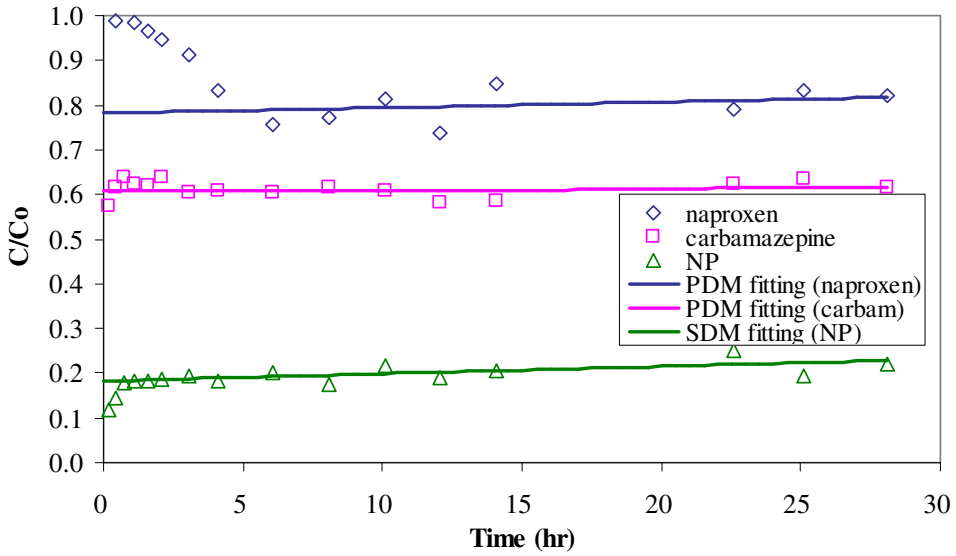

Figure 7-25 SBF test data and model calibration on sixteen-week preloaded PICA carbon (bed depth 4.2 cm, flowrate 50.3 mL/min)

A comparison between the surface diffusion coefficients obtained on preloaded PICA and F400 carbons reveals that they decreased following different patterns. On preloaded F400 carbon, surface diffusion coefficients kept relatively steady for the first three weeks and then decreased from 3.24×10^{-11} cm^2/s on virgin carbon to 0.42×10^{-11} cm^2/s on sixteen-week preloaded carbon. In contrast, on PICA carbon, the surface diffusion coefficients decreased sharply from 3.74×10^{-11} cm^2/s to 0.96×10^{-11} cm^2/s within the first three weeks of preloading, and then reached a steady state. The decreasing trend on F400 carbon is in accordance with the observations for atrazine adsorption on the same GAC by Schideman *et al.* (2006a,b) and on PAC by Li *et al.* (2003b). Therefore, it seems that the decreasing pattern for D_s is adsorbent- and adsorbate-specific.

Some "weird" breakthrough profiles were noted for naproxen adsorption on three-, eight-, and sixteen-week preloaded PICA carbon. As shown in Figure 7-22 and Figure 7-24, the naproxen effluent concentration sharply increased at the beginning and then decreased, being at a maximum in the first three hours of the SFB test. In Figure 7-25, the effluent concentration of naproxen was detected at 100% of the influent concentration at time zero, and then decreased steadily to 80% breakthrough within the first five hours of operation. These strange breakthroughs were originally suspected to be caused by desorption of pre-adsorbed naproxen during the preloading process of the PICA carbon because of competition from a highly adsorbable fraction of the backgrounds DOC in

DI water. The suspicion was based on two facts. One is that the occurrence of naproxen in PS water was occasionally detected, though mostly at tens of ng/L levels, which was one order of magnitude less than the concentration applied in the SFB tests. The other is that the mean value of the DOC for DI water in all kinetic tests was 0.27 mg C/L, which might introduce a competition with pre-adsorbed naproxen. Therefore, two supplementary desorption tests in DI water (shaken for 24 hours) and acetone (Soxhlet extraction for ten hours) were performed. However, no naproxen could be detected in the extracts from either desorption tests (detection limit less than 2.1 ng/L). Unfortunately, the reasons for the phenomena could not be determined in this study. As a result, some "weird" points in Figure 7-25 were excluded in the calibration processes (as identified in Appendix H).

7.2.3 Preloading Effect on Adsorption Kinetics

Impact of Preloading on External Mass Transport

Having determined the film diffusion coefficients from SFB tests on virgin and preloaded carbons, it is now of interest to investigate the decreasing trends, and compare the differences between carbons and among compounds, thus further understanding the mechanism of preloading impacts from background NOM. Figure 7-26 depicts the decreasing trends of the three target compounds on the two carbons preloaded for various times.

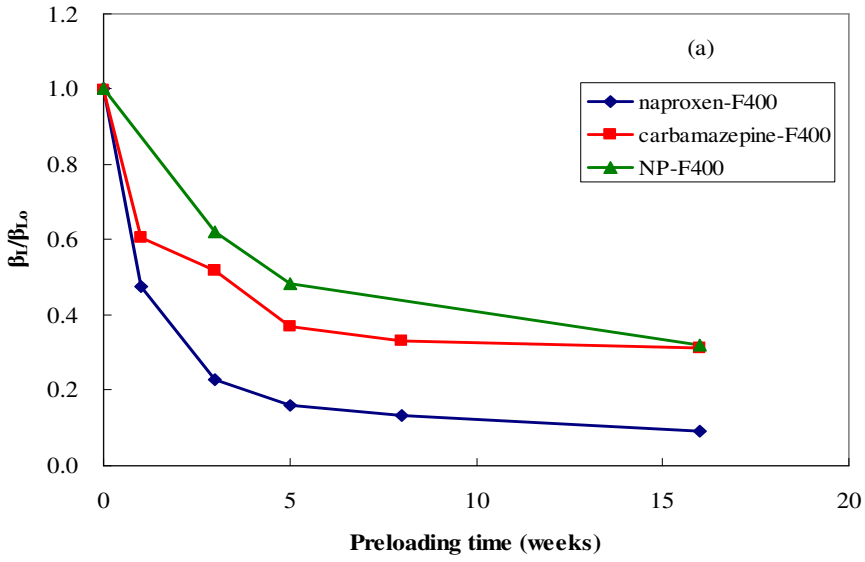

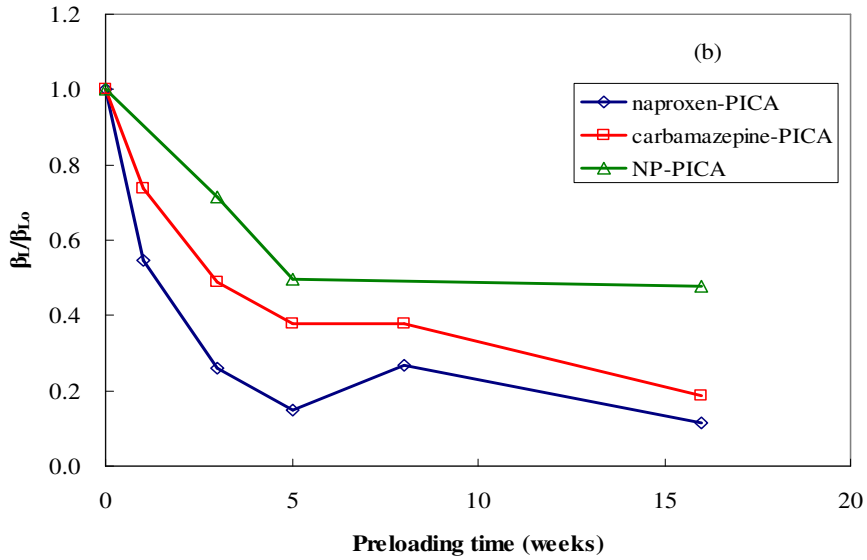

Figure 7-26 Decreasing film diffusion coefficients on F400 (a) and PICA (b) due to preloading

A comparison between F400 and PICA carbons in Figure 7-26 indicates that the differences between the two carbons were not very pronounced, though naproxen and NP generally showed slightly larger reductions in the β_L values on F400 carbon than on PICA carbon. As can be seen from Figure 7-26, the β_L values for all three target compounds generally followed a similar decreasing trend. They reduced rapidly during the first five weeks of preloading and then continued to slowly decrease during the following eleven weeks. This is in agreement with the DOC breakthrough profiles for both carbons in that they were almost exhausted within five weeks of preloading. Accordingly, slow adsorption of NOM after five weeks could partially contribute to the slow decreasing trend of the β_L values after sharp reduction at the early time. Meanwhile, the possible growth of biofilm at the long operation time would also cause the reduction of film transport (this point will be discussed later this section). The observed decreasing trend of the β_L values in the current study is in accordance with several previous studies on different micropollutants, such as TCE (Carter and Weber, 1994), and atrazine (Knappe *et al.*, 1999; Schideman *et al.*, 2006b). The similarity among these studies supports the conclusion that the adsorption of background NOM severely changes the surface characteristics of activated carbon, thus resulting in major reductions of film mass transfer, in the early stages of preloading. This result is also theoretically expected because a large fraction of the adsorbed NOM can not go fast and deeply into the carbon, and thus it accumulates on the external surface of the carbon. Since intensive adsorption of NOM was within the first five weeks (Figure 7-1), and the mass transport of NOM is expected much slower than micropollutants because of its larger molecular

weight, the accumulation would happen intensively during the early stages of preloading. In addition, the agreement between DOC breakthrough and decreasing trends of β_L values suggests that the latter could be directly related to the overall DOC loading on the GAC.

Figure 7-26 also compares the percentage decrease in the determined film diffusion coefficients for different target compounds. It is noted that the impact of a given preloading time on the film diffusion coefficient depends on the specific compound. For virgin carbons, naproxen has similar β_L values to carbamazepine. However, according to Figure 7-26, naproxen was subject to the much more severe impacts from preloading than carbamazepine. The β_L values of both naproxen and carbamazepine for the 16-week preloaded carbons are substantially less than their corresponding experimentally and even Gnielinski estimated values for the virgin carbons (Table 7-6 and Table 6-9). In contrast, NP was least impacted with respect to the percentage decrease shown in Figure 7-26. Although the absolute decrease in the β_L values for NP were larger than those for the other two compounds, it is found that the 16-week β_L values for NP were still substantially larger than the Gnielinski estimated values. The above phenomena make the explanation for the decrease in film diffusions on preloaded carbon very complicated. If the larger β_L values experimentally determined for NP on preloaded carbons can be explained by having the real carbon surface deviate from a spherical and smooth surface (Roberts *et al.*, 1986; Sontheimer *et al.*, 1988), one can not simply attribute lesser β_L values for carbamazepine and naproxen to topographic factors. It is expected that the change of hydrodynamic conditions around a preloaded carbon particle should affect all the compounds similarly. Therefore, other factors from preloading would have different effects on the different compounds.

Even though the effect of background NOM preloading on the film diffusion has been observed in current and other studies, the mechanisms are not well understood. Carter (1993) proposed two main mechanisms based on the observation of reductions in the experimentally determined film diffusion coefficient for TCE adsorption. Firstly, the accumulation of NOM on the outer surface of the carbon increases the viscosity and thickness of the mass transfer film, thus decreasing the diffusive rates and fluxes of solutes. Secondly, the adsorbed NOM forms a film to cover the outer surface of the carbon, resulting in a reduced effective external surface area (or surface area not covered by NOM film) for film diffusion. However, it could be better to interpret that the accumulation of NOM only introduces another mass transfer resistance layer in addition to the hydrodynamic boundary layer on the NOM covered carbon surface. The kinetic test could not explicitly distinguish the mass transports through the hydrodynamic boundary layer and new-formed

NOM layer, separately. Instead, the reduced film diffusion flux due to NOM film formation on preloaded carbon can be automatically compensated into the experimentally determined β_L value in a calibration process. Therefore, it may be more accurate to describe the β_L values experimentally determined on preloaded carbon as "apparent film diffusion coefficients". Nevertheless, the term "film diffusion coefficient" or "β_L value" was still used for preloaded carbon in this study to provide consistent terminology but with understanding that an appropriate term should be "apparent film diffusion coefficients".

SEM images were taken for virgin and sixteen-week preloaded F400 (Figure 7-27) and PICA carbon (Figure 7-28) in order to observe the surface characteristic change on preloaded carbon. As can be seen in the two figures, the two virgin carbons show more visual roughness than their corresponding preloaded carbons. The reduced roughness may decrease hydrodynamic perturbations, leading to lower film diffusion coefficients, if the scale of the carbon surface roughness is larger than the hydrodynamic boundary layer thickness. However, both parameters could not be further measured in this study.

According to the comparisons in Figure 7-27 and Figure 7-28, it seems that some flocculent films were formed on the preloaded carbon surfaces, making the images of preloaded carbons blurred. In general, compared to the surfaces of virgin carbons, the surface pore structures on preloaded carbons shrank, and some of them were visibly partially or totally covered by the film formed by the NOM fouling or biological growth (the evidence of biological growth will be discussed later). This is more evident on the preloaded PICA carbon. As shown in Figure 7-28, large pores of approximately 1 – 3 μm diameter are distributed all over the surface of the virgin PICA carbon. In contrast, on the sixteen-week preloaded PICA carbon, those pores were covered or partially blocked by the NOM/bio film. Furthermore, Sontheimer *et al.* (1988) reported that the macropore (> 50 Å) surface area could also contribute to the external diffusion surface area of the adsorbent. Therefore, it is quite possible that the macropores, which are not visible in the SEM figures, were also partially blocked by the NOM foulant, thus reducing the effective external surface area. Nevertheless, it was found that the coverage of NOM/bio film on the carbon surface was not uniform, possibly due to the irregular shape of carbon particle.

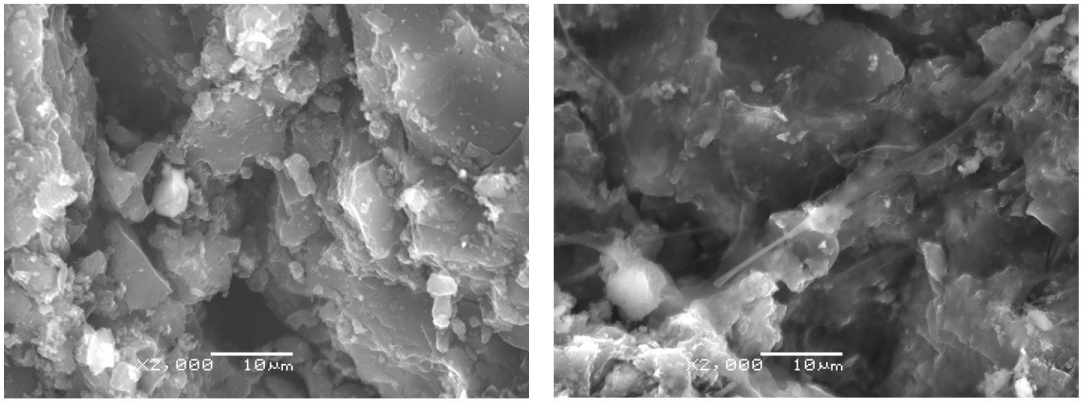

Figure 7-27 Comparison of SEM images between virgin (left) and sixteen-week (right) preloaded F400 carbon

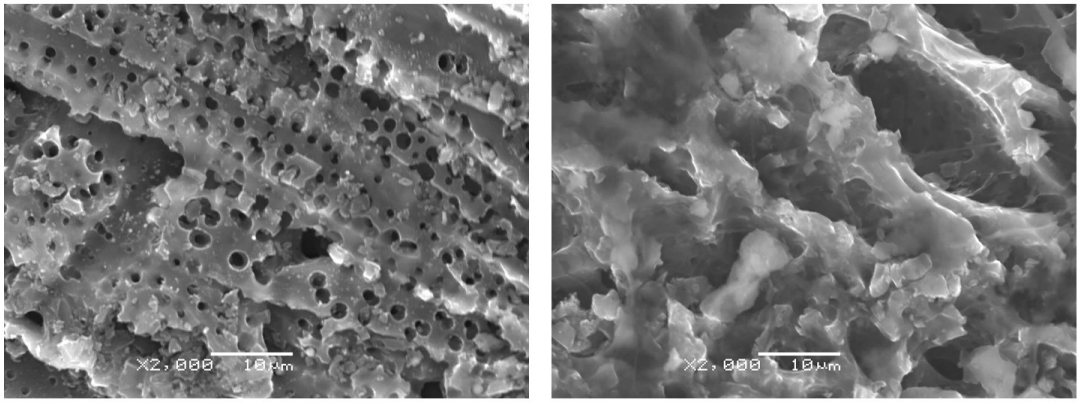

Figure 7-28 Comparison of SEM images between virgin (left) and sixteen-week (right) preloaded PICA carbon

Nonetheless, the above two mechanisms could not fully explain the different reduction rates for different target compounds, because they are considered to contribute equally to the slowing of film diffusion. Examination of the electrostatic properties of both adsorbents and adsorbates may provide some insight into other possible reasons. Virgin F400 carbon at the typical pH of practical drinking water treatment is nearly neutrally charged, because its pH_{zpc} (the pH at the zero point of charge) has been reported to be 6.7 – 7.0 (Fairey *et al.*, 2006). However, the preloading of NOM on carbons can

shift the pH_{zpc} of carbon down to lower values, thus making it become negatively charged. This is because the NOM typically present in surface water has carboxylic acid functional groups and is therefore negatively charged at the typical pH of practical drinking water treatment (Newcombe *et al.*, 1997a; Summers and Roberts, 1988b). The change of F400 carbon surface charge was substantiated by Fairey *et al.* (2006). In that study, pH_{zpc} dropped from 6.7 – 7.0 on virgin F400 carbon to 1.9 – 2.2 on preloaded carbon with a lake water. A similar decrease in pH_{zpc} (from ~7.5 to ~4.5) was also observed on F300 carbon by Newcombe (1994). Therefore, it is not unreasonable to think that naproxen, which is dissociated and thus negatively charged in typical natural water pH ranges, would be subject to the most severe impact due to the repulsive force from the negatively charged surface of the carbon. This repulsive effect is expected to be enhanced when extremely low bulk liquid concentrations are applied, as in the present study. In addition, it was found that even a small amount of NOM loading on carbon would lead to a dramatic change on surface charge (Morris and Newcombe, 1993; Fairey *et al.*, 2006). Therefore, it could be expected that the repulsive effect from electrostatic interactions would be a dominant mechanism accounting for the more rapid decay of film diffusion for a negatively charged solute such as naproxen in the early stages of preloading. In contrast, the impact from electrostatic interactions would be weaker for carbamazepine and NP. The larger experimentally determined β_L values for NP than its Gnielinski estimated values for the 16-week preloaded carbons may also be attributable to its tendency to partition into the "organic phase" formed by preloaded NOM on the surface of the carbon because of the high hydrophobicity of NP.

Another possible factor that might contribute to the different rates of decrease rates of film diffusion coefficients at long operation times is the adsorption or growth of bacteria on the surface of carbon. The formation of bacterial colonies on carbon modifies its surface characteristics by decreasing the volume of the largest macropores as well as lowering the pH_{zpc}, thus possibly slowing down the film mass transport of solutes by partially blocking the diffusion routes and by increasing electrostatic repulsions. This mechanism was confirmed by Rivera-Utrilla *et al.* (2003) using *E. coli* as model bacteria. As shown in Figure 7-27 and Figure 7-28, some threadlike substances, though not easily visible, were noticed to bridge cross the big openings on the surfaces of the sixteen-week preloaded carbons. This was a possible evidence of the growth of bacteria. However, no bacterium was evidently found during the examination of all SEM images. A heterotrophic plate count (HPC) test on sixteen-week preloaded PICA carbon showed a small value of 920 CFU/g carbon. The limited presence of bacteria on the freeze-dried carbon suggested the previous biological growth on this carbon, although the HPC number on the freeze-dried carbon was much less than those reported on biological activated carbon (10^8 – 10^9/g wet carbon as summarized by Sontheimer *et al.*, 1988). It

would be expected that the freeze-drying process would destroy the bacteria on the surface of carbon and dessicate extracellular materials, thus severely decreasing the number of bacteria and making it impossible to see exactly what the biological growth would have looked like '*in situ*'. It is recommended that the fresh wet carbon would be examined using the environmental SEM for possible existence of bacteria. However, this instrument was not available at the time of this research. At this point, the contribution of bacteria on the carbon surface to the effect of decrease in film diffusion coefficient is very uncertain and needs to be further investigated.

Controlling Mass Transport Mechanism at Low Concentration

As shown in Table 7-7, some of the estimated impedance values for naproxen and carbamazepine on preloaded carbons seem quite absurd, since the largest reported impedance value in the literature was 8 (Carter and Weber, 1994), and other operational results showed that the maximum impedance value for GAC preloaded for fifty-five weeks was 4 (Sontheimer *et al.*, 1988). This suggests that the model used in the present research lost virtually all sensitivity to pore diffusion. This was unexpected and requires special attention. Originally, it was assumed that pore diffusion would control the mass transport of solutes once preloaded NOM had significantly obstructed the pores inside the carbon. Furthermore, the model should become sensitive to internal diffusion once the equilibrium capacity of the carbon significantly decreases upon preloading (Sontheimer *et al.*, 1988; Carter, 1993). However, both sensitivity analyses on five-week preloaded carbons (Figure 7-14 and Figure 7-15) and experimental results indicated that the insensitivity condition was severe on preloaded carbons used in the SFB experiments. To interpret this observation, it is necessary to investigate which mechanism is controlling the mass transport under the experimental conditions applied in this study. Thus, the Biot numbers for the PSDM, which can be used to determine the relative importance of internal or external mass transfer resistance, were employed as Equation 7.1 for film-pore diffusion and Equation 7.2 for film-surface diffusion, respectively.

$$Bi_p = \frac{\beta_L d_p}{2D_p} \qquad \textbf{7.1}$$

$$Bi_s = \frac{\beta_L d_p C_0}{2D_s \rho_p q_0} \qquad \textbf{7.2}$$

In the above equations, Bi_p is pore diffusion Biot number representing the ratio of the external liquid phase mass transfer rate to the pore diffusion rate; Bi_s is surface diffusion Biot number representing the ratio of the external liquid phase mass transfer rate to the surface diffusion rate; C_0 is the initial liquid phase concentration; q_0 is the solid phase concentration in equilibrium with C_0. Other parameters are as defined in Chapter 2.

Sontheimer *et al.* (1988) indicated that both Biot numbers must be greater than 50 – 100 in order for either of the two internal diffusion mechanisms to significantly control mass transport. Therefore, according to Equation 7.1 and Equation 2.47, it is possible to calculate the impedance values required to trigger the pronounced control by pore diffusion of the mass transfer processes for naproxen and carbamazepine. Similarly, the D_s values required for surface diffusion to predominantly control NP mass transfer process can be determined by using Equation 7.2. Accordingly, the required τ and D_s values calculated based on F400 carbon are shown in Table 7-8. For naproxen and carbamazepine, the actual τ larger than the required τ value will lead to significant pore diffusion controlled mass transport. For NP, significant surface diffusion controlled mass transport will be triggered when actual D_s is less than required D_s value in Table 7-8.

Table 7-8 Required impedance and surface diffusion coefficients to trigger the mass transport predominantly controlled by internal diffusion on F400 carbon

compound	Naproxen	Carbamazepine	NP
Preloading time (weeks)	$\tau^{\dagger}$	$\tau^{\dagger}$	$D_s^{\dagger}$ ($x10^{-11}cm^2/s$)
0	1.5 – 3.0	1.5 – 3.0	0.30 – 0.60
1	3.5 – 7.0	3.0 – 6.0	n/a
3	7.0 - 14	3.5 – 7.0	0.17 – 0.34
5	10 - 20	4.5 – 9.0	0.14 – 0.28
8	12 - 24	5.0 - 10	n/a
16	18 - 36	6.0 - 12	0.14 – 0.28

n/a: not applicable

†: the ranges for required τ and D_s were calculated from the minimum Biot number range to trigger the significant internal diffusion controlled mass transport.

It can be clearly seen from Table 7-8 that the required τ values on virgin F400 carbon were 1.5 – 3 for both naproxen and carbamazepine. However, in general, the pore diffusion coefficient of a compound adsorbing on virgin carbon should be close to its free diffusivity, leading to a τ value of

nearly unity, because the pores in virgin carbon should be clear before preloading. Therefore, the results in Table 7-8 suggest that the mass transfer limitations for naproxen and carbamazepine would be attributable to strong film and minor pore diffusion controlling mechanisms on virgin F400 carbon. This judgement is consistent with the observations in the SFB test for virgin F400 carbon presented in Chapter 6. Furthermore, as shown in Table 7-8, the required τ value for naproxen greatly increases between zero and sixteen weeks, at the same time as a significant decrease of the film diffusion coefficient on preloaded F400 carbon occurs. It should be noted that an extremely large required τ value of 18 – 36 was obtained for naproxen on sixteen-week preloaded F400 carbon, suggesting that it is not possible for pore diffusion alone to significantly control the mass transport. In the case of carbamazepine, as shown in Table 7-8, the expected τ value increases from 1.5 – 3 on virgin carbon to 6 – 12 on sixteen-week preloaded carbon, implying the possibility of pore diffusion to significantly control the mass transfer if the carbon is extensively preloaded, based on a maximum τ value of 8 found in a reference for TCE adsorption (Carter and Weber, 1994). Unfortunately, the application of short-term SFB tests on preloaded carbon made it difficult to properly investigate this possibility.

With respect to NP adsorption, comparison between the values in Table 7-8 and Table 7-7 reveals that, except for sixteen-week preloaded F400 carbon, the required values are substantially lower than the correspondingly estimated values, suggesting that surface diffusion would not mainly control the mass transport of NP for at least up to sixteen weeks. This reasonably explains the fact that the tight confidence intervals of estimated D_s values could not be determined using the PSDM program.

7.3 Summary

Isotherm and kinetic experiments were conducted for naproxen, carbamazepine, and NP on F400 and PICA carbon preloaded for various time. The analyses of the data bring out the following conclusions and hypotheses:

7.3.1 Isotherm Performance on Preloaded GAC

The isotherm experiments conducted on preloaded GAC for the three target compounds led to the following conclusions:

1) Compared to their adsorption capacity on virgin GACs, the isotherm tests demonstrated that all the target compounds were subject to significant negative impacts from preloading of NOM, albeit to different extents. Among the three target compounds,

naproxen experienced the most severe loss of adsorption capacity, followed by carbamazepine. After an initial reduction within three weeks, the adsorption capacity of NP did not substantially decrease for longer preloading times.

2) Compared to other conventional SOCs, which have relatively higher concentrations in raw water, the reductions of the Freundlich K_F on preloaded carbons for naproxen and carbamazepine were substantially larger. The low concentrations applied in this study may contribute to the large discrepancy with the results for these other compounds. However, this inference needs to be further confirmed due to the absence of data for the other compounds on the same carbon and in the same water matrix.

3) The three target compounds followed quite different patterns of decreasing adsorption capacity with time, thus revealing different competitive mechanisms at work for the different compounds. For naproxen, the change in heterogeneity of the carbons due to preloading suggests that some pre-adsorbed NOM could not be replaced by naproxen. However, both direct competitive and pore blockage mechanisms could successfully explain the adsorption performance of naproxen and carbamazepine. The removal of NP in the late preloading phase could be explained by absorption or partitioning in the NOM matrix on the surface of or inside the carbons.

4) The reductions of the BET surface areas for the two carbons were in agreement with their corresponding DOC breakthrough profiles. However, inconsistency between reductions of the BET surface areas and of adsorption capacities for the target compounds suggests that the former could not fully account for the effective surface area for adsorption of micropollutants. A partial pore blockage mechanism was proposed to explain this inconsistency.

5) Comparison of adsorptive capacity between the two carbons indicated that PICA carbon was subject to a lesser preloading effect than F400 carbon. This is in agreement with the fact that the NOM surface loading on F400 carbon was higher than on PICA carbon, especially in the early preloading stages. It seems that the preloading effect would be more severe on the carbon with a higher percentage of pores larger than 10 Å.

7.3.2 Kinetic Performance on Preloaded GAC

The SFB tests and related sensitivity analyses led to the following conclusions and hypotheses with respect to kinetic performance on preloaded GACs:

1) Mass transport of all the target compounds decreased with time due to preloading of NOM. Similar to the impact of preloading on adsorption capacity, naproxen suffered the most deteriorative effect, followed by carbamazepine.

2) Film diffusion for all three target compounds reduced rapidly in the first five weeks of preloading and then continued to slowly decrease during the following weeks. Up to five weeks, F400 and PICA carbon did not demonstrate much difference in the reduction of film diffusion due to preloading.

3) Through inspecting SEM images of virgin and preloaded carbons, a type of film formed due to NOM fouling or biological growth was observed on the surfaces of preloaded carbons. The NOM/bio film introduced an additional mass transfer resistance layer, leading to decrease in film diffusion flux. Kinetic tests could only determine the "apparent film diffusion coefficients" for preloaded carbons.

4) Different extents of film diffusion reductions for naproxen and carbamazepine point to a mechanism where electrostatic interactions between preloaded carbon and specific compounds may contribute to the reduction of film mass transport. The carbon may become negatively charged due to both the loading of NOM as well as the growth of bacteria.

5) Sensitivity analyses and subsequent calculations of the Biot numbers indicated that film diffusion was the predominant mechanism controlling the mass transport processes in all cases, in particular for naproxen. In contrast, internal diffusion, including both pore and surface diffusion, did not significantly control the mass transport even after the carbon was preloaded for sixteen weeks. This may be due to the extremely low concentration applied in this study.

CHAPTER 8
PREDICTING TARGET COMPOUNDS REMOVAL IN GAC ADSORBERS

8.1 Simulations for Time-variable Parameters due to Preloading Effect

In order to incorporate the variation in isotherm and kinetic parameters as a function of preloading time into the model predictions for GAC adsorbers, the time-variable functions should be defined for each target compound–GAC pair. As described in Section 5.7, the most appropriate empirical expressions for the varying parameters were obtained by searching the function library in Labfit®. In addition, the regression analyses for the varying parameters were also carried out using user-defined functions, which were collected from the literature. Subsequently, the best fit functions were applied in conjunction with the PSDM for predicting pilot-scale GAC adsorber breakthroughs.

The fitting results and corresponding empirical functions for each target compound–carbon pair are shown in Figure 8-1 to Figure 8-6.

For the Freundlich K_F, it was found that an exponential model (Equation 8.1) successfully described the decreasing trends for all the target compounds on both carbons. This function is in the same form as the one which was used by Carter and Weber (1994) for simulating a time-variable Freundlich K_F of TCE adsorption (Equation 2.46). In contrast, the function (Equation 2.45) proposed by Sontheimer *et al.* (1988), although generally fitting the experimental data well, was not as good as Equation 8.1. Equation 8.1 implies an initial rapidly and later slowly decreasing trend for the Freundlich K_F.

$$y = A \cdot \exp(-B \cdot x) + C \qquad \textbf{8.1}$$

Where A, B, C are fitted parameters; y is the time-variable parameter of interest; x is preloading time in days

The initial values of parameter *A* were always set as the Freundlich K_F values determined on virgin GAC. The regression results indicated that the calibrated *A* values were similar to the initial values, thus suggesting that the parameter *A* could be interpreted as the maximum Freundlich K_F without preloading. The parameter *B* in equation 8.1 was considered as a decay factor, which accounted for the decreasing rate for the Freundlich K_F and was possibly influenced by the properties

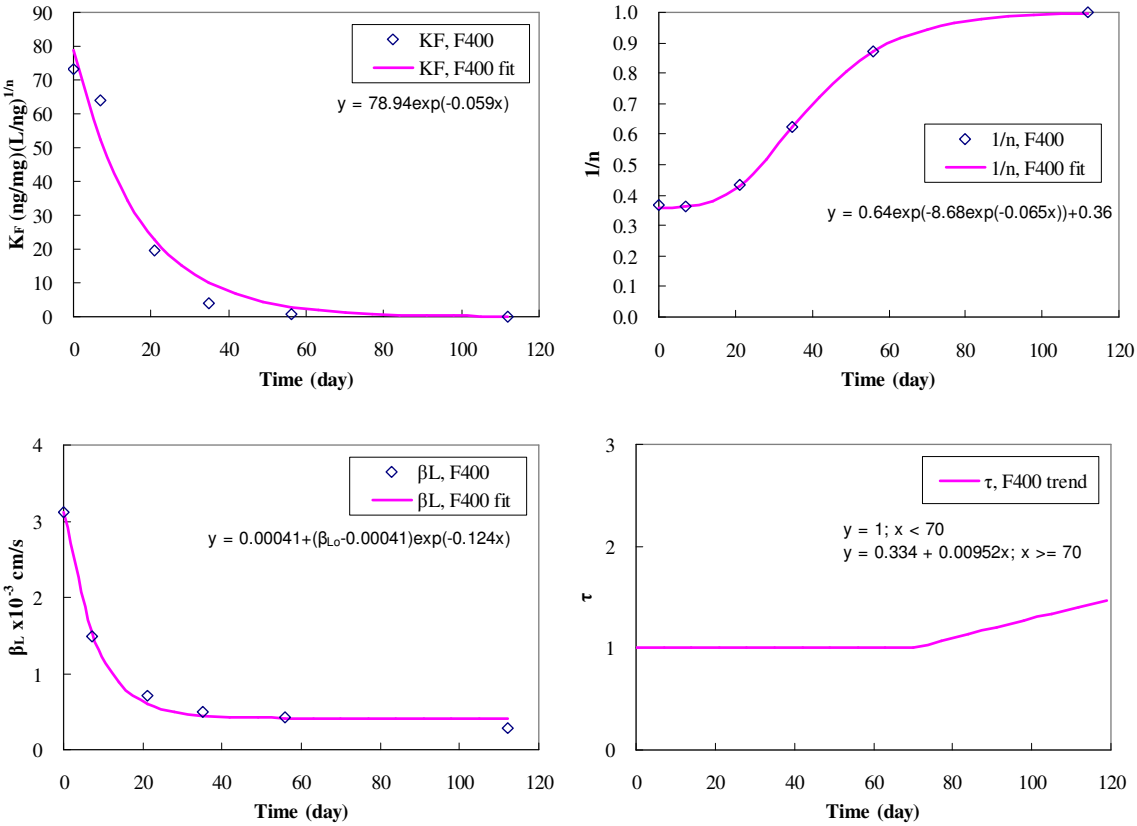

Figure 8-1 Time variable functions for naproxen adsorption on F400 carbon

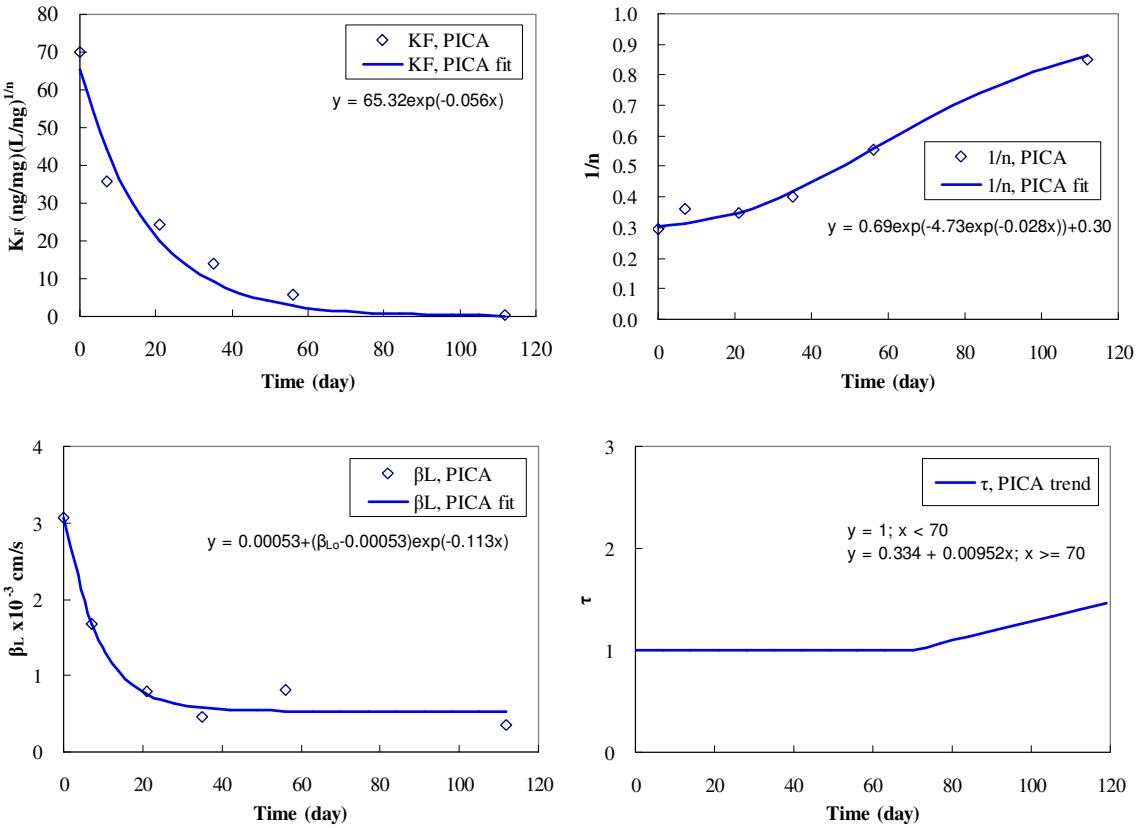

Figure 8-2 Time variable functions for naproxen adsorption on PICA carbon

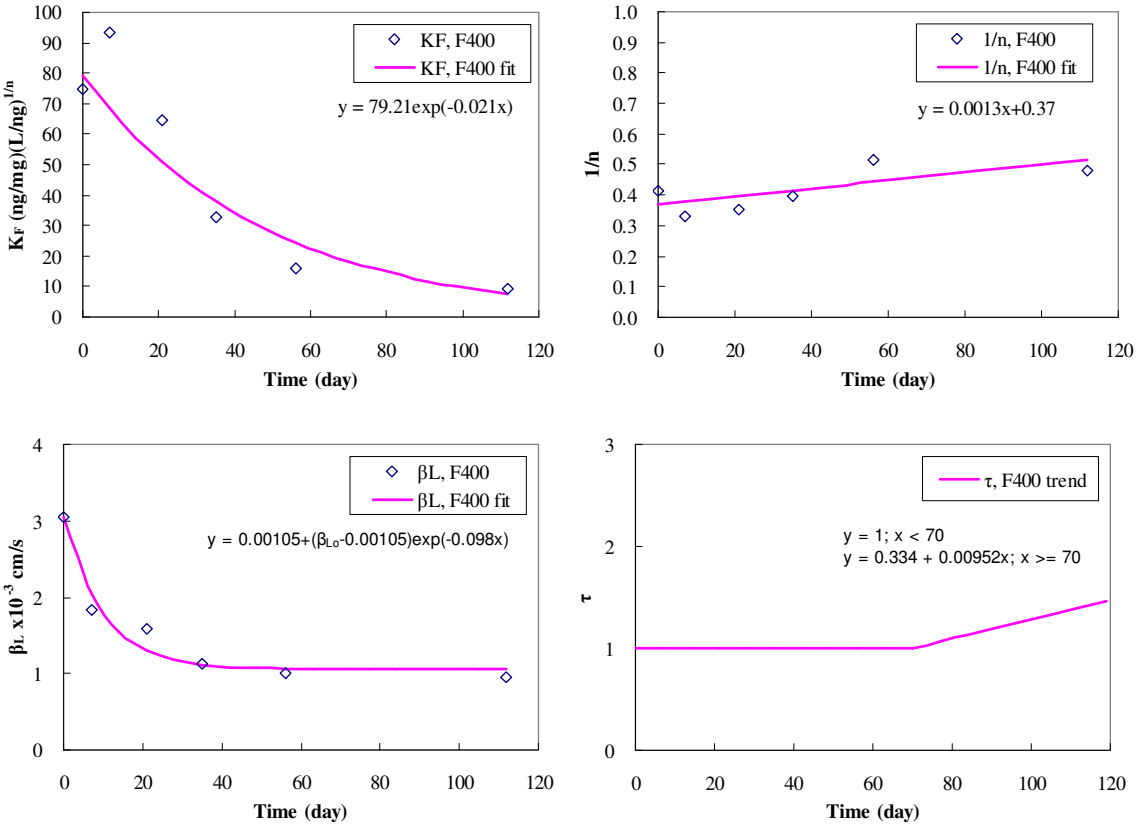

Figure 8-3 Time variable functions for carbamazepine adsorption on F400 carbon

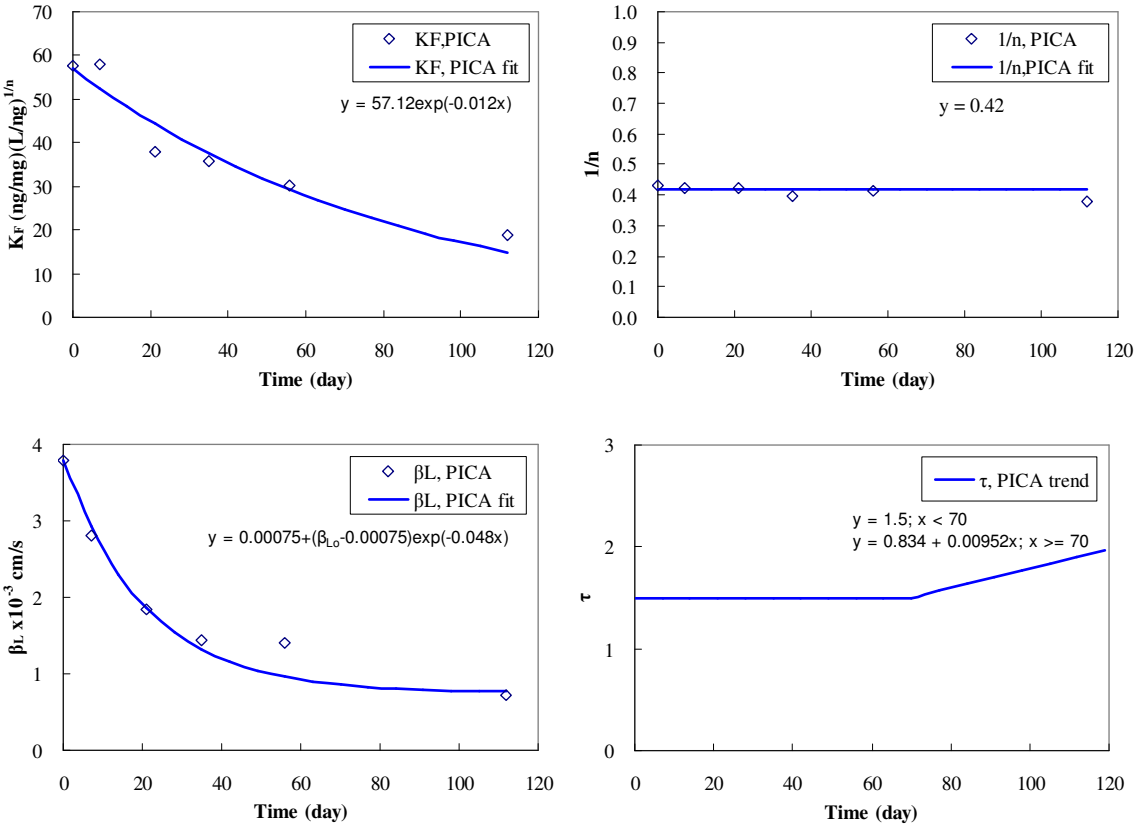

Figure 8-4 Time variable functions for carbamazepine adsorption on PICA carbon

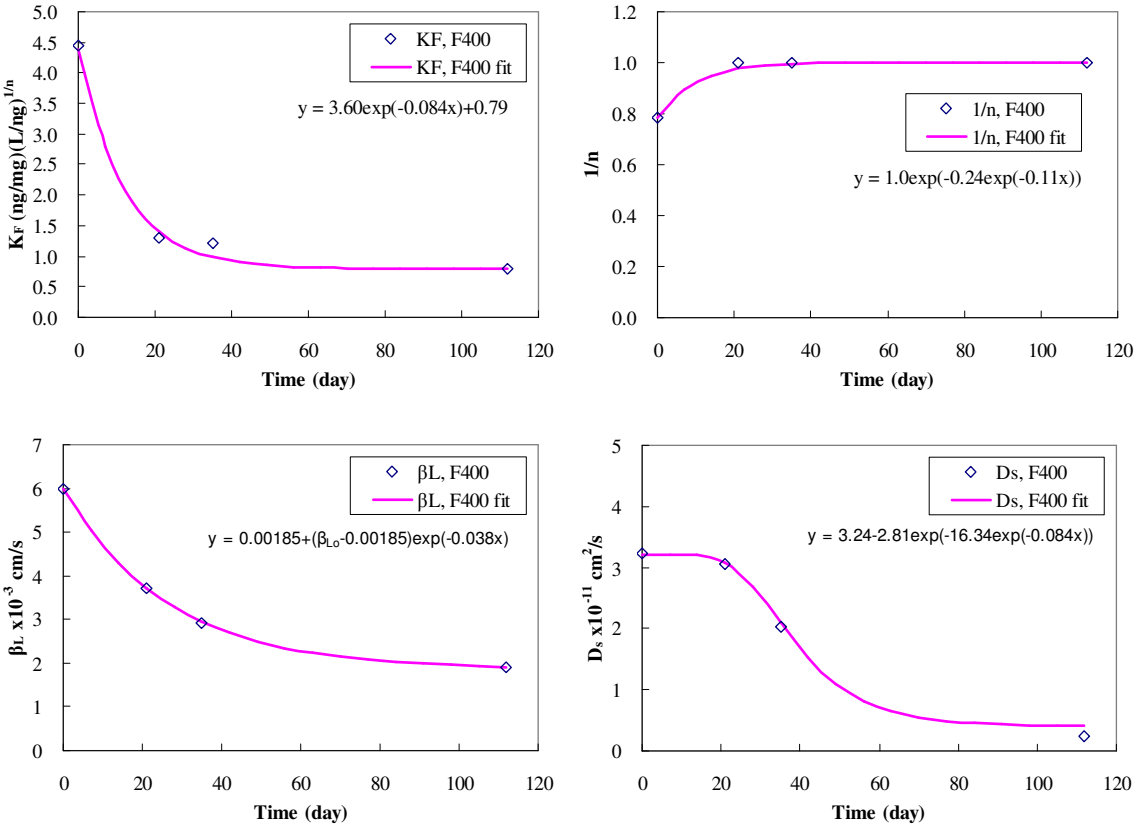

Figure 8-5 Time variable functions for NP adsorption on F400 carbon

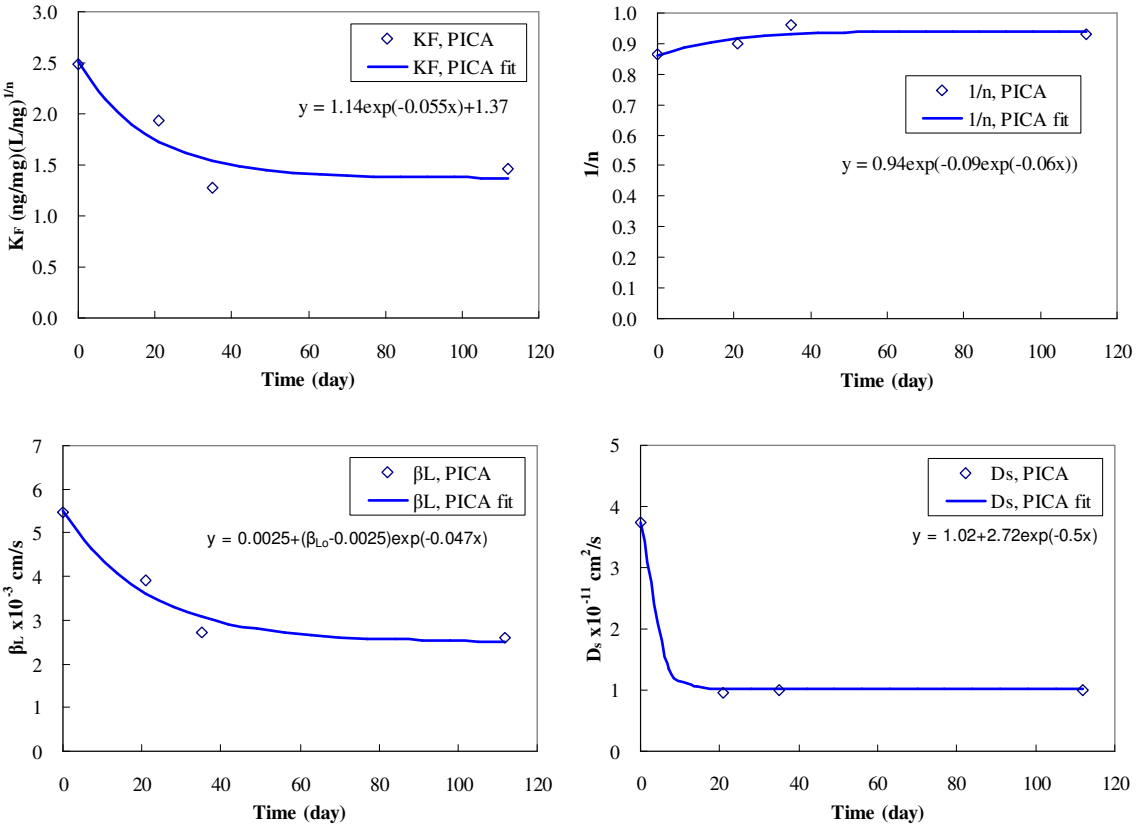

Figure 8-6 Time variable functions for NP adsorption on PICA carbon

of the adsorbent, the adsorbate, and the background NOM in natural water. The parameter *C* was interpreted to be the minimum Freundlich K_F, or a non-competition factor. The existence of this parameter can be attributed to two hypotheses: 1) if the adsorbate is small enough to access the primary micropores, a fraction of the adsorption capacity for the target compound can not be competed by NOM (Kiduff and Wigton, 1999; Karanfil *et al.*, 2006), thus leading to a minimum value even after extensive preloading; and 2) a hydrophobic compound could partition to the "organic solution" formed at long preloading time (Carter, 1993). In the applications for this study, the parameter *C* for naproxen and carbamazepine was zero considering that these two compounds could only access secondary micropores, thus being subject to strong competition from background NOM. In contrast, the initial *C* values for NP adsorption were set as the minimum values obtained on sixteen-week preloaded carbons. It should be mentioned that the above interpretations of the physical meaning of the parameters were only based on the observations in this study, and should be further confirmed.

With respect to the Freundlich 1/n, no general function could be found because, as discussed in Chapter 7, different trends were observed for different compounds. Nevertheless, it was found that a modified Gompertz model (Equation 8.2) provided the flexibility for a time-variable Freundlich 1/n

$$y = A \cdot \exp(-B \cdot \exp(-C \cdot x)) + D \qquad \textbf{8.2}$$

in the cases of naproxen and NP adsorption. However, no tentative interpretation for the fitted parameters can be made at this point. Correspondingly, Figure 8-1, Figure 8-2 and Figure 8-5, Figure 8-6 present the best fit Gompertz model for naproxen and NP adsorption, respectively. For the Freundlich 1/n for carbamazepine adsorption, a simple linear expression was used for F400 carbon (Figure 8-3), expressing a slow but significantly increasing trend of Freundlich 1/n with preloading time. A horizontal line expressing an average Freundlich 1/n value for carbamazepine adsorption on PICA carbon preloaded for various time was used as shown in Figure 8-4.

As discussed in Chapter 6, a similar decreasing trend that follows a rapid reduction at early stage, then slowly deceasing and finally levelling off (Carter and Weber, 1994; Knappe *et al.*, 1999; Schideman *et al.*, 2006b), was observed for film diffusion coefficients for all target compound–carbon pairs. To describe the general trend, Carter and Weber (1994) used an exponential function as in Equation 8.3, while Equation 8.4 was proposed in this study. The latter has a similar form to the function used by Schideman *et al.* (2006). Both Equation 8.3 and Equation 8.4 were applied for fitting

the experimentally determined film diffusion coefficient data. It was found that the second model (Equation 8.4) demonstrated superior performance in most cases, and thus was chosen for further use.

$$y = A \cdot \exp(-B \cdot x) \qquad \textbf{8.3}$$

$$y = A + (\beta_{L,o} - A) \cdot \exp(-B \cdot x) \qquad \textbf{8.4}$$

In which $\beta_{L,o}$ *is the film diffusion coefficient on virgin GAC.*

Furthermore, it should be noted that Equation 8.4 actually has the same mathematical form as Equation 8.1. In Equation 8.3, the parameter *A* is the initial film diffusion coefficient before preloading, while B accounts for a decay factor. Equation 8.3 assumes that the film diffusion would keep decreasing and approach zero for a long preloading time. This does not agree with most observations reported in this study and other references (Knappe *et al.*, 1999; Schideman *et al.*, 2006a, b). In Equation 8.4, the parameter *A* is close to the minimum value of the film diffusion coefficient, representing a steady NOM film formed on the surface of carbon for a long preloading time. The parameter *B* in Equation 8.4 quantifies the rate of exponential decay, which may depend on the specific preloading conditions. In the regression analyses of the current study, the initial values of parameter *A* in Equation 8.4 were always set as the β_L experimentally determined on the carbons preloaded for sixteen weeks. The resulting fitted curves for all cases are shown in Figure 8-1 to Figure 8-6.

Although some fitted τ values from the SFB tests were shown in Table 7-6, no reasonable model for increasing impedance could be obtained because the "true" τ values on preloaded carbons could not be accurately estimated due to lack of sensitivity of the PDM to this parameter in the SFB reactor. Instead, an empirical model depicting the decay of pore diffusion recommended by Sontheimer *et al.* (1988) and Jarvie *et al.* (2005) was used for the time-variable modeling. The application of this model will be validated by subsequent experimental data from pilot-scale columns, presented later in this chapter. Equation 8.5 came from a slight modification of the originally recommended model. It shows that the τ value remains constant and is equal to the initial τ value determined on virgin GAC for the first ten weeks (70 days) of operation, and then linearly increases to a maximum value of four. This expression also suggests that pore diffusion would not be retarded in the early stages of preloading because high-molecular-weight NOM diffuses into the GAC grain slowly.

$$y(\leq 4) = \begin{cases} \tau_o & (x < 70) \\ \tau_o + 0.00952 \times (x - 70) & (x \geq 70) \end{cases} \qquad \textbf{8.5}$$

where τ_o is the impedance estimated on virgin carbon; y is the τ value corresponding to preloading time x.

As shown in Figure 8-1 to Figure 8-4, Equation 8.5 describes a linear increase of pore diffusion impedance after preloading for ten weeks. In contrast to a maximum τ value of four used in Equation 8.5, a higher τ value of 8 was reported for an extensively preloaded crushed GAC by Carter and Weber (1994). However, the higher τ value might be attributable to a higher extent of preloading caused by faster diffusion of NOM molecules into the much smaller GAC particles used in their experiments. Therefore, it was decided that the maximum τ value of four would be implemented for further predictions in this study.

As discussed in Chapter 6 and 7, the internal diffusion for NP on both carbons was quantified using surface diffusion coefficients. Although it has been generally thought that pore diffusion might be a predominant mechanism of mass transport at very dilute solute concentration (Sontheimer *et al.*, 1988; Hand *et al.*, 1989; Matsui *et al.*, 2003), it was demonstrated in this study that the surface diffusion mechanism could more accurately interpret the breakthrough performance for preloaded GAC in the SFB reactor. Schideman *et al.* (2006a, b) proposed a model with decreasing D_s to describe the relationship between D_s and NOM surface loading for atrazine adsorption on F400 carbon. The early constant and later decreasing value of D_s was modeled by introducing a critical NOM surface loading point. The reported lagged decreasing trend of D_s on F400 carbon is consistent with the observation of NP adsorption on the same carbon in this study. However, in the present study, a Gompertz model was directly used to depict the inverse "S" shape (Figure 8-5) in order to facilitate the nonlinear regression process, avoiding additional determination of the critical point. An simple exponential model similar to Equation 8.1 was used to quantify the decreasing trend for NP adsorption on PICA carbon (Figure 8-6). It should be noted that the parameter *B* accounting for the decay factor could not be well estimated because no additional D_s values were available during the time period of zero to three weeks.

8.2 Pilot Experimental Results and Time-variable Model Predictions

8.2.1 Time Variable Parameter Modelling

To validate the experimentally determined isotherm and kinetic parameters and time-variable modeling approach, two pilot columns were operated at the Mannheim Water Treatment Plant. The design of the pilot columns was presented in Section 5.5. The operating parameters are given in Table 8-1. The results for each of the compounds are discussed separately.

Table 8-1 Operating conditions for pilot columns

Operating parameters		F400	PICA
Average influent target compound concentration (ng/L)	Naproxen	516	516
	Carbamazepine	558	558
	Nonylphenol	445	445
Average influent DOC concentration (mg C/L)		4.77	4.77
Approximate amount of carbon used (g)		190	170
Bed depth (cm)		26	25
Approximate surface loading (m/h)		6	6
Total operating time (days)		79	79

Naproxen

The measured influent and breakthrough concentrations for naproxen on F400 and PICA carbon pilot columns are shown in Figure 8-7 and Figure 8-8, respectively. The pilot experiments indicated that naproxen achieved approximately 70% and 80% breakthrough on F400 and PICA columns, respectively, suggesting that both carbons were relatively exhausted for naproxen after 79 days' operation.

In addition, the time-variable model predictions using the functions shown in Figure 8-1 and Figure 8-2 are also presented in Figure 8-7 and Figure 8-8, respectively, for comparison. Both figures show that the model predictions agreed well with the experimental data. This demonstrates that the fitted time-variable functions based on experimentally determined isotherm and kinetic parameters were sufficient to describe naproxen removals on the two types of carbons under preloading conditions. Nevertheless, when taking a close look at the two figures, it was found that the model predictions best captured the experimental data at the mid breakthrough phase (20 – 60 days), whereas at the early stage before 20 days, the removals on both F400 and PICA carbon pilot columns

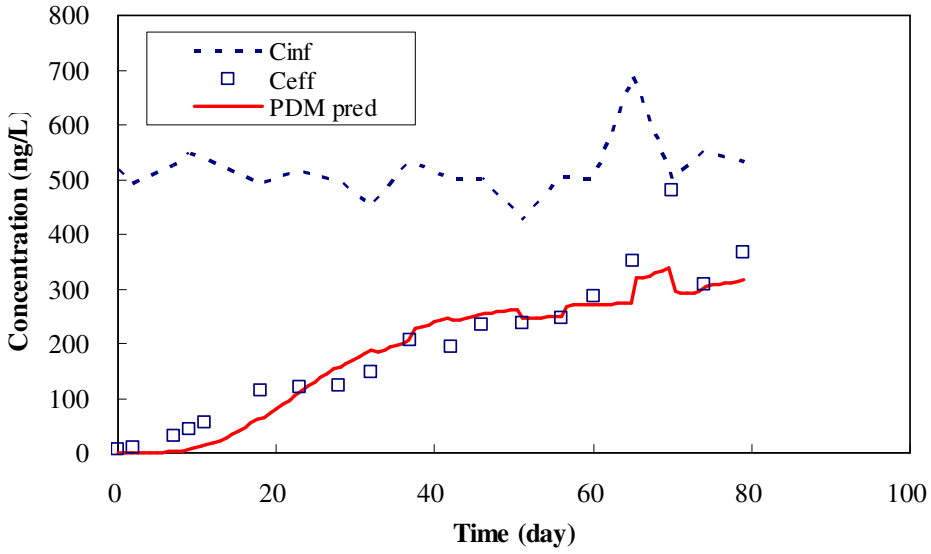

Figure 8-7 Time variable simulation of naproxen breakthrough on pilot F400 column

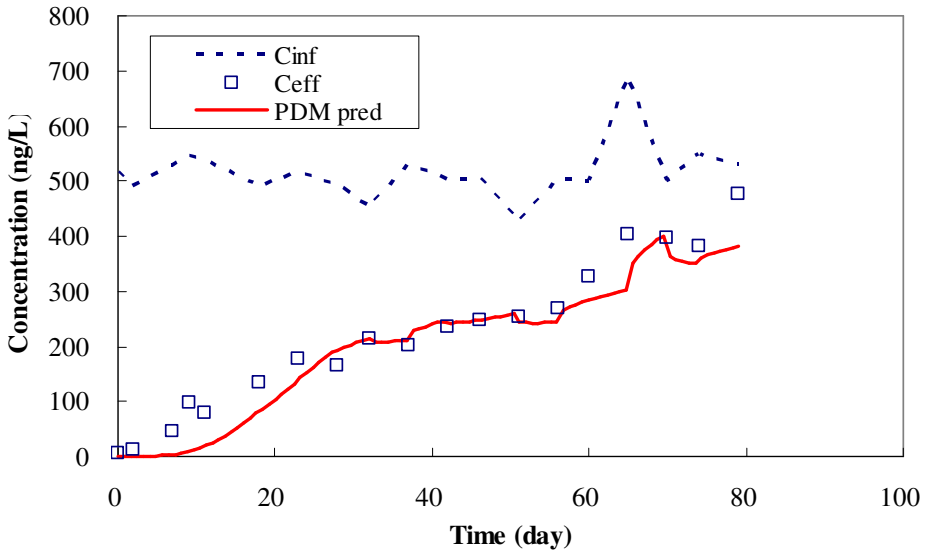

Figure 8-8 Time variable simulation of naproxen breakthrough on pilot PICA column

were overestimated by the time-variable model. These discrepancies may lead to an overestimation of GAC adsorber capacities when 80 – 90 % removal is set as the operational goal. Furthermore, slight overestimations of removals were observed on pilot F400 and PICA columns after running for 60 days. The possible reasons for these overestimations may be that the model did not consider some operational factors, e.g. backwashing, or other potential differences, such as actual NOM surface loading. The potential reasons for the differences will be analyzed in later sections.

Carbamazepine

Breakthrough data obtained from F400 and PICA carbon pilot columns for carbamazepine are shown in Figure 8-9 and Figure 8-10, respectively. The breakthroughs of carbamazepine on the two pilot columns after running for 79 days were approximately 45% and 60% respectively.

The higher removal efficiencies (or slower breakthrough) for carbamazepine than for naproxen were expected because both adsorption capacity and mass transfer rates for carbamazepine were reduced at a lesser extent than for naproxen due to background NOM preloading.

The time-variable model predictions using fitted functions in Figure 8-3 and Figure 8-4 for F400 and PICA carbon respectively were also plotted in Figure 8-9 and Figure 8-10. The comparisons between experimental data and predicted profiles indicate that the time-variable modeling approach could generally match the measured breakthrough data in the pilot columns. However, strictly speaking, the time-variable model slightly overpredicted the removals throughout the entire breakthrough durations. A relatively larger difference between model predictions and measured data was noticed at the early run times. These observations were consistent with those for naproxen, suggesting that possibly the same factors contributed to the prediction errors. Nevertheless, the prediction agreed well with the experimental data in the later stage, in particular for the PICA column.

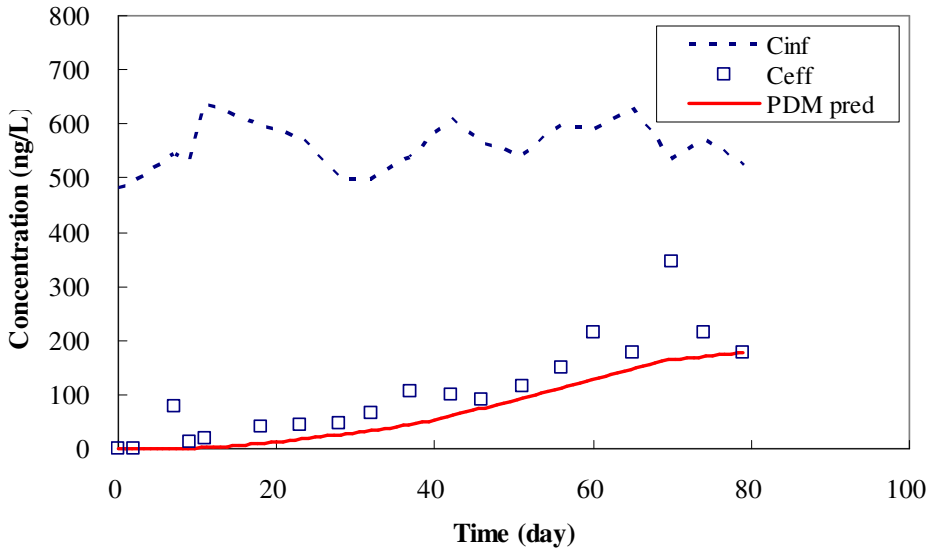

Figure 8-9 Time variable simulation of carbamazepine breakthrough on pilot F400 column

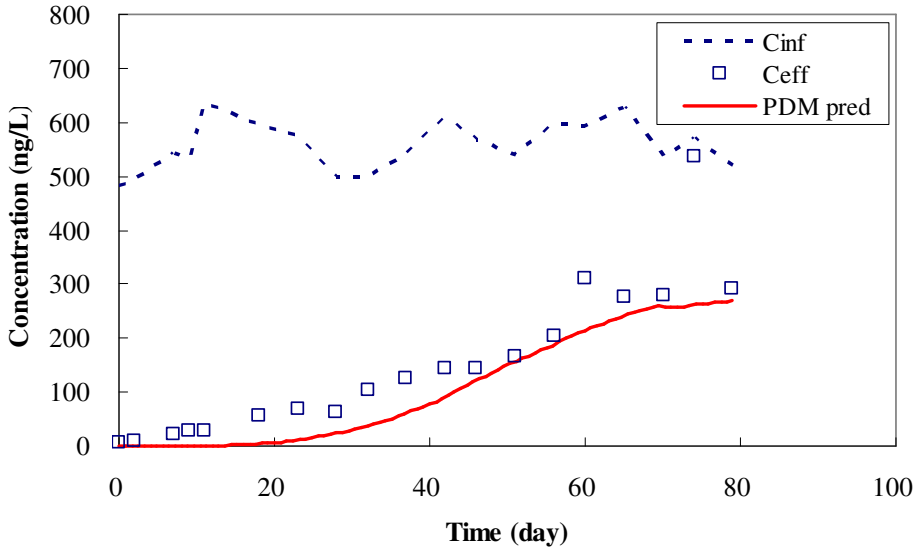

Figure 8-10 Time variable simulation of carbamazepine breakthrough on pilot PICA column

Nonylphenol

With respect to removals of NP, pilot column breakthrough data over a period of 79 days are presented in Figure 8-11 and Figure 8-12 for F400 and PICA carbons, respectively. The detected breakthrough at the end of the experiment was 20% and 15%, respectively, for the F400 and PICA pilot columns. Therefore, the removal efficiencies of NP were much higher than of naproxen and carbamazepine on both carbons. The high removal efficiencies of NP were attributable to both adsorption capacity and mass transport factors. As shown in Figure 7-12 and Table 7-3, NP was subject to the least impact on adsorptive capacity from preloading, leading to higher adsorptive capacity especially at longer preloading times, though NP is the least adsorbable among the three target compounds at extremely low concentration levels in ultrapure water. As discussed in Chapter 7, the external mass transfer rates of NP, though decreasing 50 – 60%, were still substantially higher than the corresponding values from the Gnielinski correlation. Therefore, it can be considered that rapid mass transport allows better use of the adsorptive capacity, resulting in on a slower breakthrough, especially in the early stages. In addition, it was noted that the F400 carbon adsorber showed a relatively lower removal efficiency than the PICA carbon adsorber even though the amount of carbon applied dose was approximately 10% higher for F400 carbon in the pilot-scale experiments. The slightly higher adsorptive capacity and mass transfer rates on PICA carbon (see Figure 8-5 and Figure 8-6) at long preloading times may contribute to this observation.

The time-variable model predictions using the fitted functions in Figure 8-5 and Figure 8-6 for F400 and PICA carbon respectively were also plotted in Figure 8-11 and Figure 8-12. As shown in these two figures, the predicted breakthrough curves described the experimental data well. The observations in both figures confirmed that a slight overestimation of removals by the time-variable model happened at the early run times.

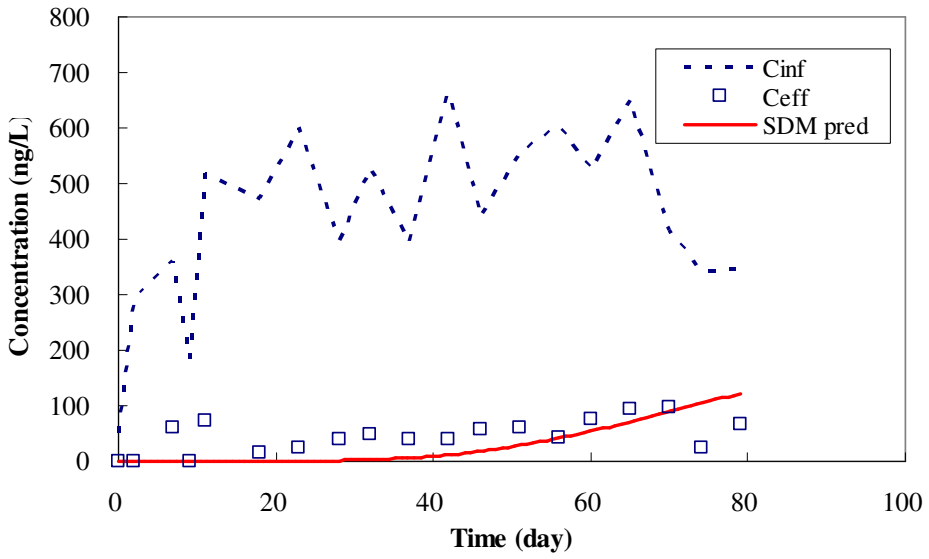

Figure 8-11 Time variable simulation of NP breakthrough on pilot F400 column

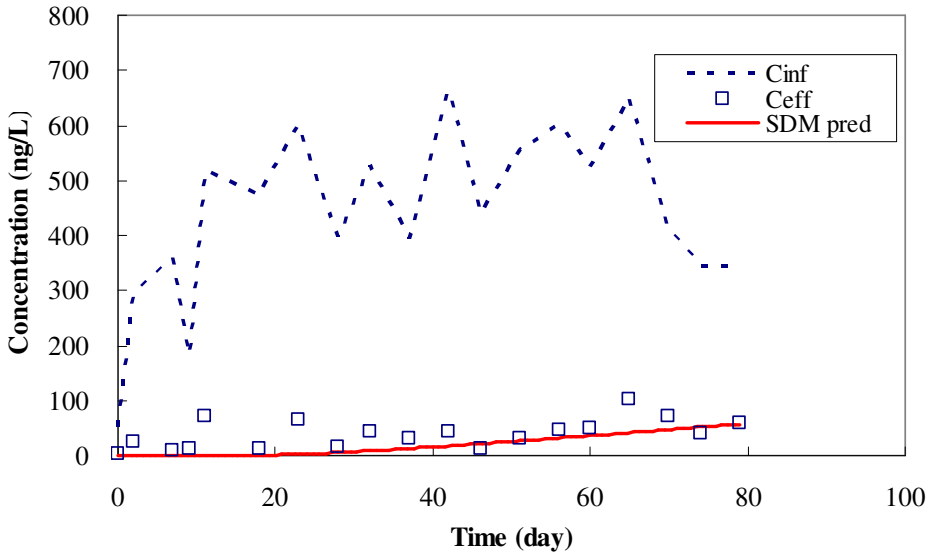

Figure 8-12 Time variable simulation of NP breakthrough on pilot PICA column

Summary

As observed above, for all cases, the agreements between experimental data and time-variable model predictions were generally satisfactory. These findings suggest that the time-variable functions including the empirical impedance functions, which were not obtained by fitting experimental data in this research, provided good descriptions of preloading characteristics for both carbons. This modeling approach was shown to be effective in predicting the breakthrough at very low concentrations. The observed behaviour could be explained by considering that a more pronounced preloading effect would be expected for extremely large concentration differences between target compounds and background NOM, and thus isotherm and kinetic parameters were more related to operating time. Since the target compounds and carbons used in this study were different in materials and physicochemical properties, the successful application of time-variable modeling approach indicates that it should be robust for future predictions for other EDCs and PhACs.

From observing Figure 8-7 to Figure 8-12, a general difference between model predictions and experimental data was found in the early breakthrough phase. Moreover, slight overestimations of removals took place late in the run time for some cases, such as in Figure 8-7 for naproxen and Figure 8-9 for carbamazepine in the F400 adsorber.

To investigate the possible reasons for modeling errors and to further improve the accuracy of predictions, "backward" sensitivity analyses were performed for the breakthroughs of the three target compounds in the F400 pilot column. These are discussed in the next section.

8.2.2 Impact of Variable Parameters on Breakthrough Profiles

The "backward" sensitivity analyses may provide insight into the adsorption mechanisms in the pilot GAC adsorbers. The exercises were performed by keeping one parameter constant at the value obtained with virgin GAC while changing other parameters using time-variable functions. Therefore, in these analyses, the baselines were the "true" breakthrough profiles accounting for the preloading impact on all parameters. The comparisons were made between the baselines and the changed breakthrough profiles. The choice of "backward" sensitivity analysis instead of the usually performed "forward" sensitivity analysis was based on the understanding that the actual breakthrough profiles resulted from the combined effect of both the changing adsorptive capacity and mass transfer rates. Thus, it was felt that the "backward" sensitivity analysis would be at larger extent than the "forward" sensitivity analysis to consider the interactions between capacity and mass transfer parameters.

The pilot-scale tests and the previous modeling results showed that the breakthrough trends on F400 and PICA carbon were similar. Therefore, to ease the task, the analyses were only carried out on the F400 carbon adsorber. In the analyses, the baselines were produced by simulating breakthroughs in a pilot F400 column (26 cm bed depth with 200 g carbon, i.e. the same operational conditions as used for the pilot-scale experiments) using the corresponding time-variable functions. One by one, each parameter was then changed back to the corresponding value obtained on virgin F400 carbon, creating a new breakthrough profile. The Freundlich K_F and 1/n were varied together considering that they are highly correlated and together express the adsorptive capacity. The time duration for simulation was extended to 100 days compared to 79 days for the pilot-scale experiments. In addition, for the adsorption of naproxen and carbamazepine, an extreme impedance value of four (as suggested by Sontheimer *et al.*, 1988) was applied for simulations in order to simulate the effect of an extremely high pore diffusion resistance on breakthrough profiles.

Figure 8-13 depicts the time-variable modeling result together with the correspondingly varied breakthrough profiles for removing naproxen in the F400 carbon adsorber.

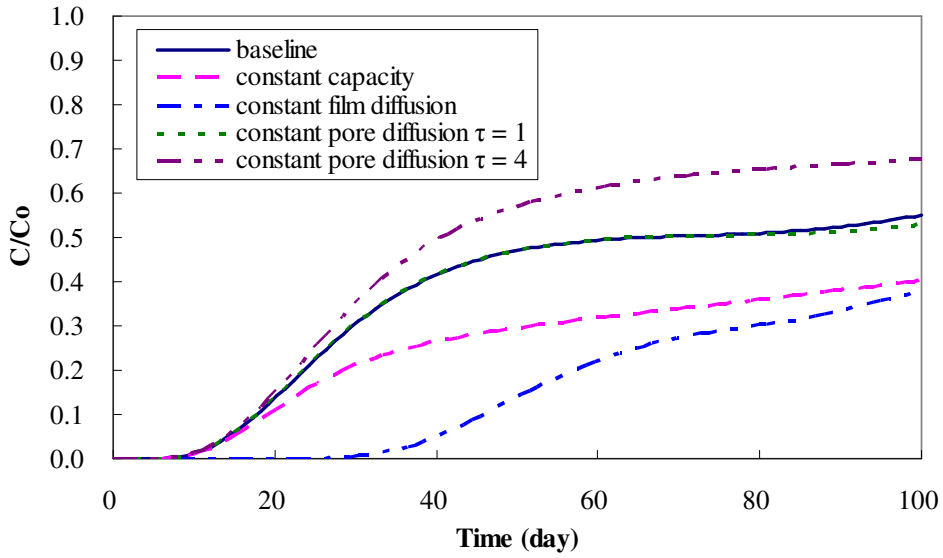

Figure 8-13 Impact of time variable parameters on model simulation (naproxen on F400 carbon)

Examination of the curves in Figure 8-13 reveals that the greatest impact on the breakthrough profile was caused by the change in film diffusion coefficient. In this case, by maintaining β_L at the initial value, breakthrough was severely delayed from approximately 10 days to 30 days. It can be observed that film diffusion had an extremely important influence on the early and intermediate

stages of the breakthrough profile. This influence, though gradually lessening at longer operating times, still exerted the most substantial impact on the entire breakthrough profile. This observation is different from other adsorption studies on some conventional SOCs, such as TCE (Carter and Weber, 1994) and atrazine (Knappe *et al.*, 1999). In those studies, film diffusion was found to have the least impact on the breakthrough profiles, although its influences were evident throughtout the entire breakthrough profiles. The severe impact from film diffusion in the present study was ascribed to the extraordinarily large decrease in the film diffusion coefficient for naproxen (see Table 7-5). This finding suggests that the accuracy of the determined film diffusion coefficient is critical to predicting the removal of naproxen in GAC adsorbers, particularly if high removals are desired. In contrast, the change in adsorptive capacity had less effect on the predicted naproxen breakthrough profile. The initial breakthrough up to 20 days was not substantially influenced by increasing the adsorptive capacity if the preloading effect on the other parameters was taken into account. Nonetheless, the impact from the increased adsorptive capacity became pronounced after intermediate operating times, and then remained steady throughout the remaining time. A small impact was noted for the variation in the impedance value after 90 days. The analysis employing a constant impedance at a value of four demonstrated a significant influence at the late breakthrough stage, though this influence was not as strong as those exerted by an increased film diffusion coefficient and increased adsorptive capacity. This observation is reasonable because, as shown in Table 7-7, a very small film diffusion coefficient restricts the controlling effect by pore diffusion. Nevertheless, a deeper bed adsorber would become sensitive to the less-controlling pore diffusion mechanism at a later time. Therefore, it could be expected that, for longer operating times, pore diffusion would gradually influence the breakthrough profile of naproxen to a larger extent if the impedance increased to a high enough value.

The impact of time-variable modeling on the carbamazepine breakthrough profile in the F400 carbon adsorber is shown in Figure 8-14. As illustrated in Figure 8-14, the change in β_L profoundly altered the early breakthrough profile, leading to the lagged occurrence of the initial breakthrough at 45 days and a severe change of the entire breakthrough profile shape. However, compared to the impact on naproxen breakthrough profile, the influence from changing β_L for carbamazepine seems to attenuate quickly at longer operating times. Instead, the increase in adsorptive capacity displayed the most important influence on the profile at longer times. This observation is understandable because, as shown in Figure 8-3, the decreasing trend of film diffusion diminished after eight-weeks of preloading, while the Freundlich K_F kept significantly decreasing until the sixteenth week. The comparison between the different effects from film diffusion and adsorptive capacity changes on naproxen and carbamazepine breakthrough profiles reveals that the decay rate of external mass

transport actually significantly influences the efficiency of making use of the adsorptive capacity of activated carbon at very low concentrations of the target compound(s). Similar to naproxen, a small impact was found for the change of impedance after 80 days. However, application of the constant maximum impedance led to a greater change in the breakthrough profile of carbamazepine than of naproxen, suggesting that pore diffusion would possibly predominantly control the mass transport of carbamazepine after the influence of the rapidly decreasing film diffusion diminishes. It also confirmed the judgment made based on Table 7-7. In this case, it seems necessary to accurately determine the pore diffusion coefficient in order to adequately predict the late breakthrough profile of carbamazepine. Nevertheless, as illustrated in Figure 8-9 and Figure 8-10, the application of the impedance-increasing scheme proposed by Sontheimer *et al.* (1988) generally satisfied the requirements for making successful predictions in this study.

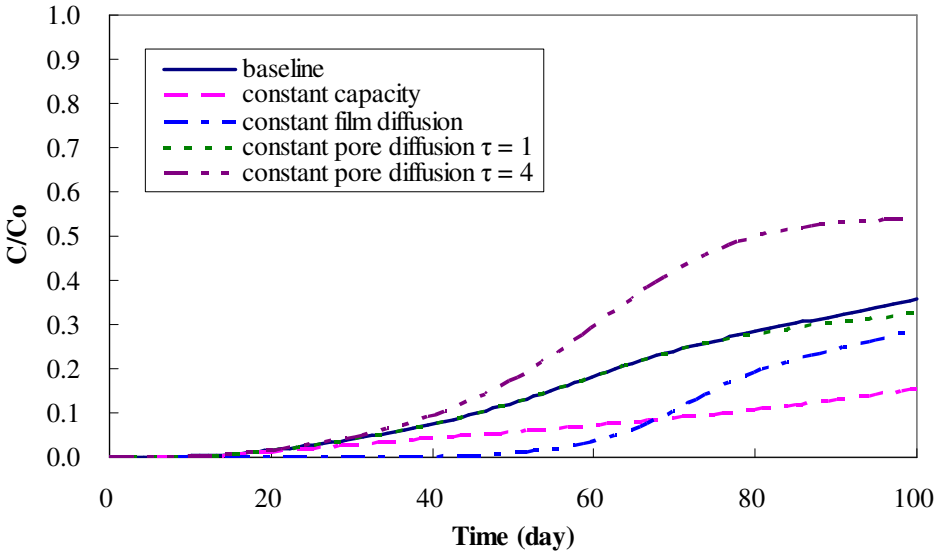

Figure 8-14 Impact of time variable parameters on model simulation (carbamazepine on F400 carbon)

The simulations of different scenarios for NP adsorption on F400 carbon adsorber were plotted in Figure 8-15. The greatest impact was noted for variation in the adsorptive capacity for NP, suggesting that the rise in profile was mainly caused by the decay of adsorptive capacity. Another notable feature in Figure 8-15 is that the decay of the film diffusion coefficient exerted the least impact on the breakthrough profile. This was on account of a smaller decrease in the film diffusion coefficient compared to the other two compounds. In contrast, change in the surface diffusion

coefficient led to a greater impact on breakthrough profile than film diffusion after 60-day operation. Such behaviour reveals that the mass transfer process for NP would be influenced by both film and surface diffusions.

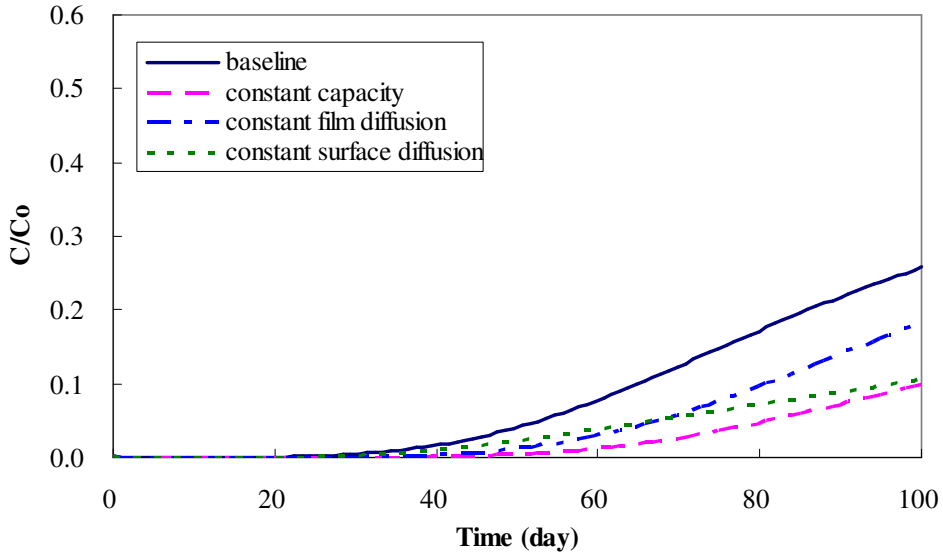

Figure 8-15 Impact of time variable parameters on model simulation (NP on F400 carbon)

Overall, compared to the other studies on conventional SOCs, the film diffusion-controlling mechanism for adsorbing two PhACs at very low concentrations was found to be strengthened, albeit to different extents depending on the interaction between target compounds and adsorbent. According to the analyses, overestimations of removals using the time-variable modeling approach, in the early stages in particular, for two PhACs was possibly due to inaccurate description of the film diffusion decay for the pilot-scale adsorber. Since the reductions in both adsorptive capacity and mass transfer rates are attributable to the loading of background NOM, to possibly improve the model prediction, it is of interest to examine the effect of NOM surface loading on predictions.

8.3 Improving Time-variable Modeling in Consideration of NOM Surface Loading

It is commonly accepted that the adsorption of background NOM directly leads to reductions of adsorptive capacity and mass transfer rates, thus resulting in severe deterioration of removal efficiency of SOCs in a GAC adsorber. Some attempts to simulate fouling situations have been made by using time-variable parameters (Sontheimer *et al.*, 1988; Carter and Weber, 1994; Jarvie *et al.*,

2005). Another approach in which isotherm parameters were based on the IAST in combination with kinetic parameters variable as a function of NOM surface loading was studied for PAC systems (Li *et al.*, 2003c; Ding *et al.*, 2006) and for a GAC system (Schideman *et al.*, 2006a, b). The latter approach mechanistically improved the predictions of removing SOCs. However, the complexity of the model and workloads for determining parameters substantially increased. Therefore, the following attempts were made to improve the predictions in consideration of the NOM surface loading factor based on the previous time-variable approach without substantially increasing the workload. In addition, the NOM surface loading approaches were based on the assumption that the composition of a specific type of natural water was constant and did not vary too much seasonally. Therefore, it would be reasonable to expect that the different fractions causing decay in different parameters were also an invariable part of the total background NOM. Accordingly, NOM surface loading (indexed as DOC surface loading) could be used as a general measure for the decay of all parameters.

8.3.1 NOM surface loading for GAC

The calculations of NOM adsorbed in GAC adsorbers can be carried out by integrating the area over a DOC breakthrough curve. To do this, accurate mathematical descriptions of DOC breakthrough curves are important. In general, two approaches can be applied for obtaining DOC breakthrough curves. The first one creates predicted breakthrough profiles using the PSDM based on DOC component analysis (Crittenden *et al.*, 1993; Sontheimer *et al.*, 1988), and the second approach directly utilizes the measured DOC influent and effluent concentrations, based on which an appropriate empirical function can be obtained to describe the DOC breakthrough profile for further integration calculations. Since the measurement of DOC values and monitoring of other operating conditions, such as flow rate, were routinely performed in this study, the available data facilitated the calculation of NOM surface loading using the latter method.

The most appropriate function (Equation 8.6) was obtained by searching the function library in Labfit®. It was found that this function could successfully fit all DOC breakthrough profiles for both preloading columns (Figure 8-16) and pilot columns (Figure 8-17) in this study. The regression results indicated that parameter A in equation 8.6 was probably a value for steady state DOC breakthrough. In the regressions, the initial guesses for parameter B were always set as the initial adsorbed DOC ratio. Meanwhile, parameter C was considered as a decay factor.

$$y = A - B \cdot \exp(-C \cdot x) \qquad \textbf{8.6}$$

where A, B, and C are fitted parameters, x is GAC adsorber operation time in days.

Subsequently, the normalized adsorbed NOM amount ($\overline{Y}$) in the adsorber could be calculated by integrating equation 8.6 over the duration of the operating time (Equation 8.7).

$$\overline{Y} = \int_0^T \left[1 - \left(A - Be^{-cx}\right)\right] dx = T - A \cdot T - \frac{B}{C} e^{-cT} + \frac{B}{C} \qquad \textbf{8.7}$$

where T is the total operation time for GAC adsorber.

As a result, NOM surface loading per unit weight of GAC (q_{NOM}) was calculated using equation 8.8.

$$q_{NOM} = DOC_{avg-in} \cdot V \cdot \overline{Y} / M_{GAC} \qquad \textbf{8.8}$$

where DOC_{avg-in} is average influent DOC, V is volumetric flow rate per day, and M_{GAC} is total GAC mass in the adsorber.

The measured average influent DOC during the pilot experiments was 4.77 ± 0.48 mg C/L. The resulting NOM surface loadings for F400 and PICA carbons in preloading and pilot columns are shown in Figure 8-18.

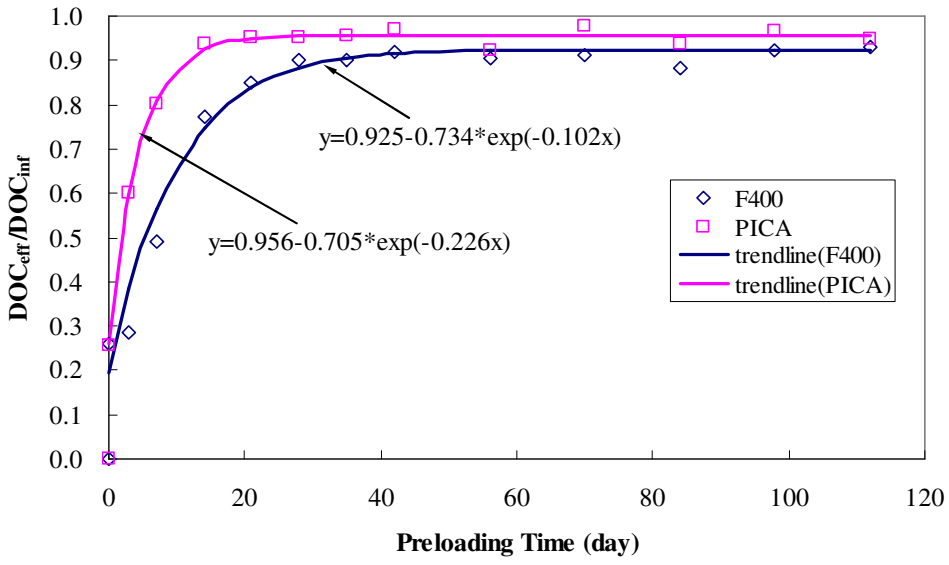

Figure 8-16 Simulating DOC breakthrough curves on preloading columns

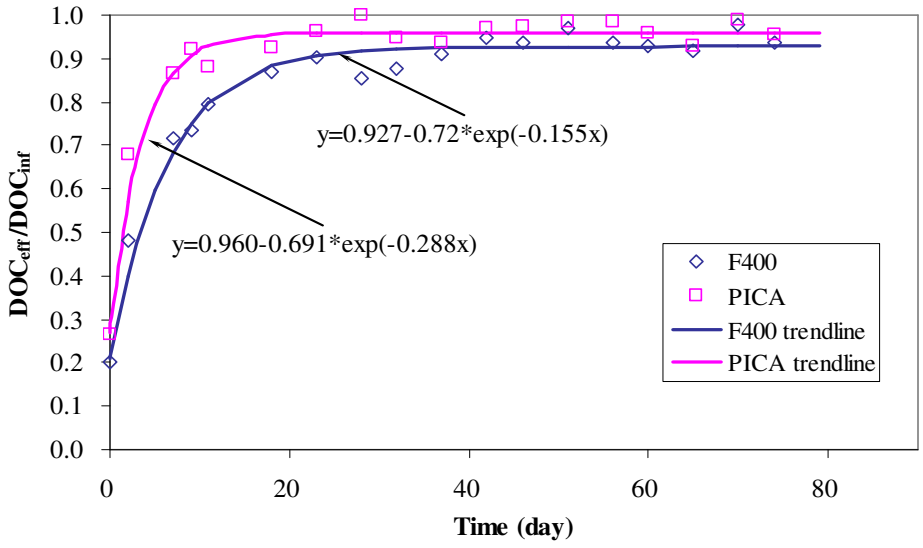

Figure 8-17 Simulating DOC breakthrough curves on pilot columns

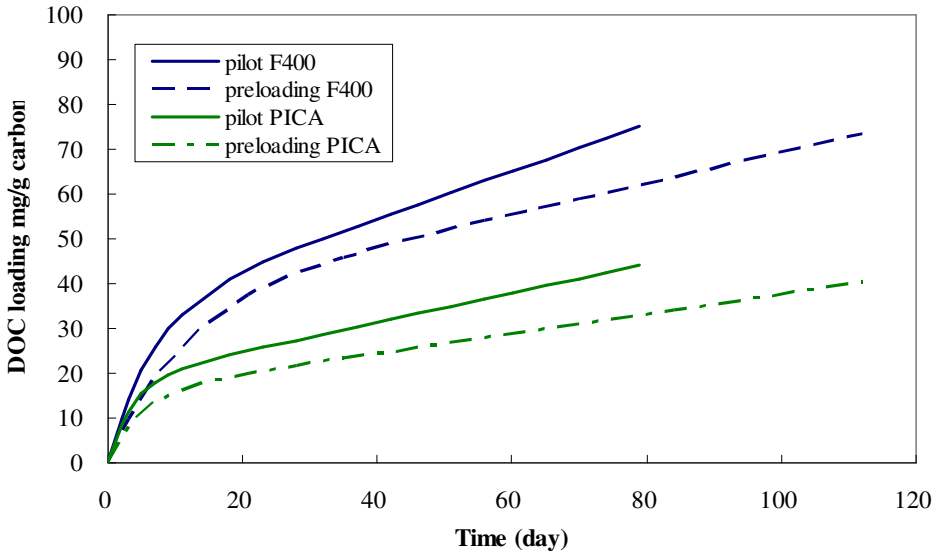

Figure 8-18 Comparison of estimated DOC surface loadings between pilot and preloading GAC

As shown in Figure 8-18, the estimated cumulative NOM surface loadings for F400 and PICA carbon in the pilot columns at a given time were higher than in the preloading columns. This was caused by higher average DOC in the influent and a higher influent flow rate for the pilot experiments than for preloading operations. Therefore, simple application of the time-variable functions obtained on carbons from the preloading experiments for simulating breakthroughs in the pilot columns may

have overestimated the removal efficiencies, because it was believed that the preloading of background NOM would be closely related to the decreasing trends of both isotherm and kinetic parameters. Therefore, it was of great interest to see how different NOM surface loadings between pilot and preloading carbon would influence the breakthrough profiles.

However, it should be noted that, for the calculations of NOM surface loading, a hypothetical 100% breakthrough for DOC was applied based on the assumption that no significant biological activity occurred in the preloading and pilot GAC columns. This assumption is supported by the fact that the PS water which served as the influent to the experimental facilities, was obtained from the full-scale plant before the addition of ozone. In addition, the preloading experiment, and especially the pilot test, were carried out mostly at relatively low temperatures (when the influent PS water was at a low temperature, see Chapter 5). With the assumption that significant biological activity was not occurring, the low breakthrough rate that occurred when approaching a "steady-state" at late breakthrough time could be mainly attributable to the slow diffusion of NOM into the depths of the GAC grains and the possible displacement of weakly-adsorbed NOM by more strongly-adsorbed NOM (Sontheimer *et al.*, 1988). This judgment is supported by the observation that adsorptive capacities for the three target compounds kept decreasing until the end of preloading. Nevertheless, it should be kept in mind that, over a longer time, biological activity would eventually be intensive enough to account for the entire "steady-state" removal (Sontheimer *et al.*, 1988; Robert and Summers, 1982). Accordingly, the cumulative NOM surface loading curves shown in Figure 8-18 would gradually level off. However, in this study, it was very difficult to determine when and how much the biological activity was present. A low HPC value was measured on the sixteen-week preloaded carbon in this study, suggesting that there was biological activity, but it could not be quantified due to the sample preparation procedures used. The use of 100% breakthrough for calculations was a compromise for accurately determining NOM surface loading in the early phases and possibly introducing errors for longer times. Therefore, it was realized that possible errors might be associated with predictions for longer times if NOM surface loadings, as shown in Figure 8-18, were used without consideration of biological effects.

8.3.2 NOM Surface Loading Associated Time-Variable Modeling

Approach for Adjusting Time-variables with NOM Surface Loading

NOM surface loading was the fundamental reason for the decays of adsorption capacity and kinetics, this assumption serves therefore as the basis for improving the modeling predictions. One

approach to improve the model was to find direct relationships (functions) between varying parameters and increasing NOM surface loading. Similar exercises were performed by Schideman *et al.* (2006a, b) to model the NOM surface loading variable film and surface diffusion coefficients for an atrazine adsorption system. Since the time-variable functions have previously been defined in this study, a more convenient approach applied here was to adjust the various isotherm and kinetic parameters based on the same amount of NOM surface loading on preloaded carbon and on carbon in the pilot columns. More specifically, NOM surface loading for a carbon in the pilot column at a specific time was calculated based on the solid curve in Figure 8-18; then the broken curves in Figure 8-18 was used to obtain a "transformed" time to achieve the same amount of NOM surface loading on the preloaded carbon; and finally the isotherm and kinetic parameters were calculated using the "transformed" time. The approach applied in this study was essentially the same as the first method, but saved some time to regenerate new models for varying parameters and corresponding programs.

Using the above approach, all time-varying parameters were adjusted simultaneously based on the same NOM surface loading at a specific time. In addition, a simulation was run where only the time-variable film diffusion coefficient was adjusted so that it was possible to investigate the extent by which it would influence the breakthrough profiles. The simulation results for the three target compounds are shown in Figure 8-19 to Figure 8-24.

Naproxen

Figure 8-19 and Figure 8-20 show the NOM surface loading associated time-variable modeling profiles and the original time-variable predictions for naproxen in F400 and PICA pilot columns, respectively. A comparison between adjusted and original breakthrough profiles in the two figures demonstrates that simultaneously adjusting all time-variable parameters improved the agreement between predictions and experimental data at the early run times but overestimates the intermediate breakthrough phase on F400 and PICA columns. In contrast, only adjusting film diffusion coefficients mainly improved predictions at the early phase without changing the predictions after 40 days. A comparison between the two NOM adjusted breakthrough profiles at early run times indicates that an improvement in model predictions is mainly attributable to the changes in the adjusted film diffusion coefficients. The increase in the intermediate part of the profile was mainly due to an increased capacity decay rate. For F400 carbon, all predicted breakthrough profiles tended to converge at long operating times, suggesting that slight differences in surface loading and therefore the use of the NOM adjusted time-variable parameters was only relevant for early and intermediate predictions for naproxen.

Examining the time variable functions of all parameters (Figure 8-1 and Figure 8-2) aids in the interpretation of the predicted NOM adjusted breakthrough profiles. The dramatic decrease in β_L over the initial 40 days makes this parameter very sensitive to any deviation in NOM surface loading between the pilot and preloading columns. Thereafter, film diffusion coefficients decrease more slowly, resulting in a lower sensitivity to NOM surface loading differences. It is not unreasonable to suspect that the decay of film diffusion may be more closely related to the overall NOM surface loading because large fractions of adsorbed NOM may only deposit at the external surface of carbon, thus influencing the film diffusion at the early phase. Hence, only adjusting film diffusion was adequate to lead to a better fit of the measured data at the early phase. Both, these simulations and previous sensitivity analyses support the finding that the accurate application of film diffusion coefficients are very important for predicting early and intermediate breakthroughs for dissociated compounds, such as naproxen at low-concentrations.

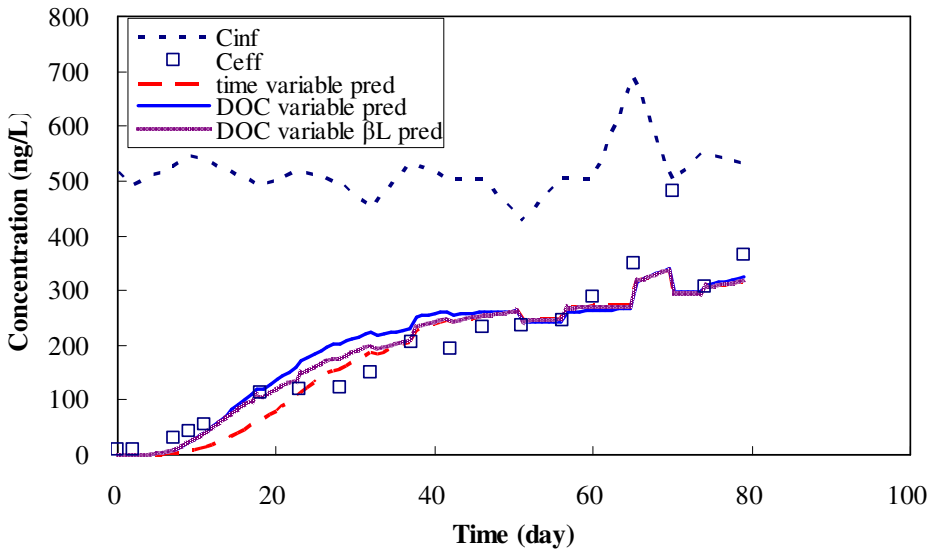

Figure 8-19 NOM surface loading associated time-variable simulation for naproxen breakthrough on pilot F400 column

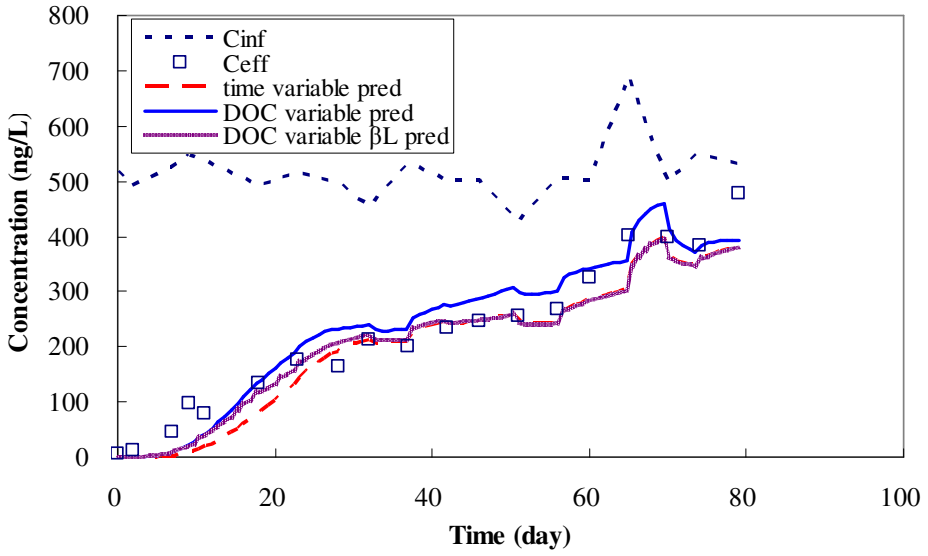

Figure 8-20 NOM surface loading associated time-variable simulation for naproxen breakthrough on pilot PICA column

In the intermediate breakthrough phase, overpredictions of breakthroughs using the all parameter NOM adjusted curve were observed, and could be attributable to an overestimation of the decay in adsorptive capacity, since only adjusing film diffusion led to a better agreement between experimental and prediction data. Furthermore, it was observed from the sensitivity analysis (Figure 8-13) that the impact of adsorptive capacity became more influential in the intermediate and late breakthrough phase. Hence, it could be postulated that a link between decreasing adsorptive capacity and overall NOM surface loading might lead to an overestimation of the capacity decay, where several mechanisms (e.g. direct site competition and pore blockage) attributable to different NOM fractions may have contributed to the reduction of adsorptive capacity. In particular, as discussed in the previous chapter, the mechanisms causing a decrease in adsorptive capacity for naproxen were quite complex because the heterogeneity (indexed as Freundlich 1/n) was shown to change dramatically due to the non-desorbable adsorption of low-molecular-weight NOM at longer operation times. Therefore, in the cases for naproxen, the simulation results from only adjusting film diffusion coefficients seemed more realistic.

For F 400 carbon, the convergent trends of three predicted breakthrough profiles at the late phase could be explained by the fact that both, the adsorptive capacities and film diffusions only experienced small decreases or levelled off for long run times, as shown in Figure 8-1 and Figure 8-2,.

Overall, the impedance did not make any significant contributions to the predictions even at the late phase because the adsorption of naproxen was not very sensitive to pore diffusion, as demonstrated in Figure 8-13. Nevertheless, it could be imagined that, if the slope in equation 8.5 was large enough to make the impedance rapidly approach four, a closer agreement between modeling result and measured data were expected. Thus, it may desirable to improve equation 8.5 to better describe the pore diffusion for naproxen especially for longer operating times, though it was obviously appropriate for early phase predictions. Unfortunately, the pore diffusion could not be well defined in this study. It seems that efforts should be made in the future to improve or change the experimental approach for determining the internal diffusion coefficients at extremely low concentrations.

Carbamazepine

The comparisons between the NOM surface loading associated time-variable model predictions and time-variable predictions of carbamazepine breakthrough profiles in F400 and PICA pilot columns are shown in Figure 8-21and Figure 8-22 Figure 8-21 and Figure 8-22, respectively. Compared to the simulations for naproxen, simultaneously adjusting all parameters improved overall agreements of the predictions with the experimental data from the early to the late phases. However, the very early predictions were unchanged and still below the measured data. This was probably caused by some operational factors, e.g. backwashing, which were not taken into consideration in the modeling.

Figure 8-21 illustrates that adjusting film diffusion coefficient alone only slightly improved the predictions from 10 to 30 days run time. Thereafter, the more pronounced improvements were ascribed to the adjustments of capacity parameters, and possibly pore diffusion coefficients. More insight into the reasons for this performance can be gained through the previous sensitivity analysis. As manifested in Figure 8-14, the major influence on the breakthrough profile shifted from film diffusion at early run times to adsorptive capacity at the late phase. A higher sensitivity of the breakthrough to pore diffusion, compared to naproxen, might also contribute to the improvements in the late phase. PICA carbon (Figure 8-22) showed an overall similarly improved performance to the illustration in Figure 8-21. However, in this case, it seemed that only adjusting film diffusion could adequately match the predictions to the measured data at the intermediate run time whereas the addition of adjustments of the other parameters slightly overpredicted the late breakthrough.

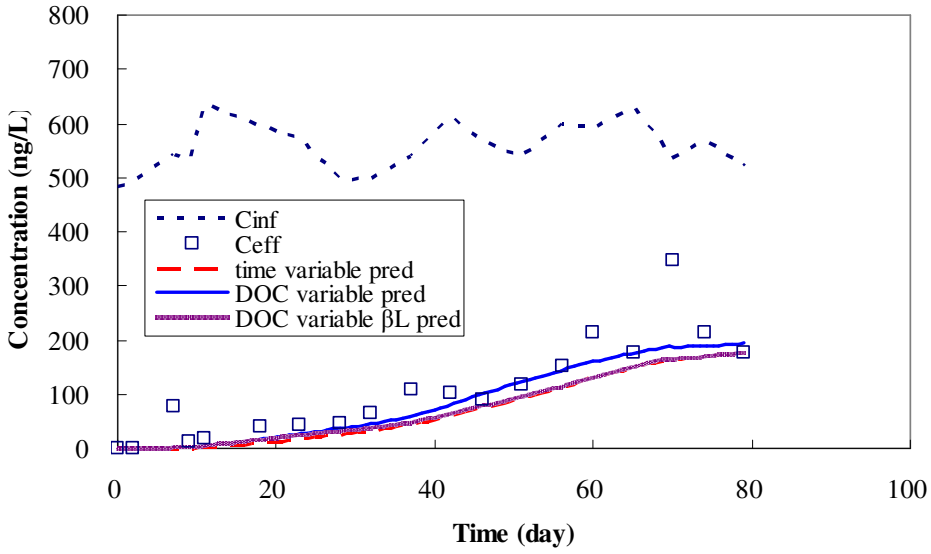

Figure 8-21 NOM surface loading associated time-variable simulation for carbamazepine breakthrough on pilot F400 column

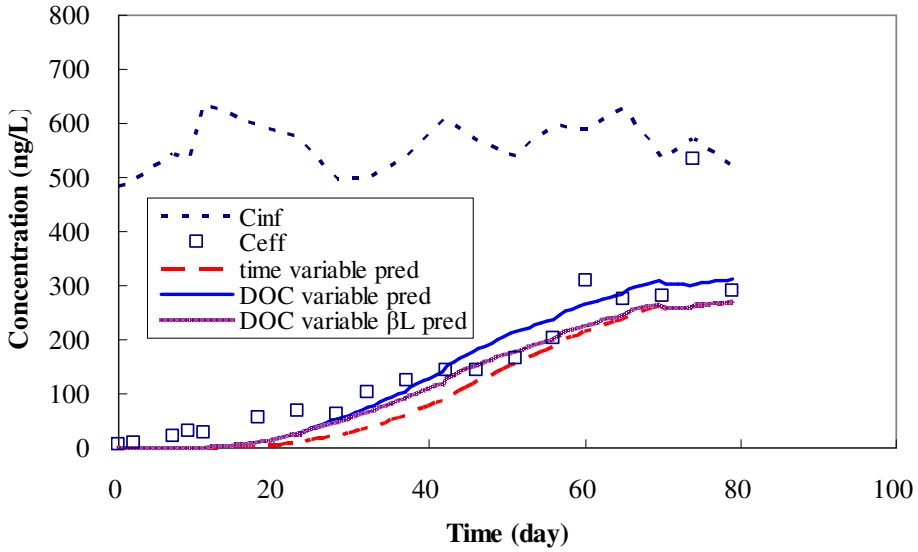

Figure 8-22 NOM surface loading associated time-variable simulation for carbamazepine breakthrough on pilot PICA column

Nonylphenol

The simulations associated with NOM surface loading on NP breakthrough profiles in F400 and PICA pilot columns are shown in Figure 8-23 and Figure 8-24, respectively. The single adjustments of film diffusions did not significantly improve the breakthrough profiles for both columns. This confirmed the finding of a relatively smaller impact of film diffusion on NP adsorption compared to the other two compounds. It is of interest to note that, in Figure 8-23, simultaneously adjusting all time-variable parameters significantly increased the predicted breakthrough for NP in F400 column. From time-variable functions (Figure 8-5) and sensitivity analysis (Figure 8-15), it can be concluded that the rise in profile was attributable to the adjustments of adsorptive capacity and the surface diffusion coefficient. No obvious changes due to adjusting the parameters were observed in Figure 8-24, indicating that the time-variables had already given a good description of experimental data.

It should be noted that only 20% breakthrough was achieved for NP in both pilot columns. Good agreement of the predictions with the experimental data was achieved by the above approaches but the validity of these models needs to be accessed for longer run times. Therefore, it is recommended to run pilot columns for NP for longer periods of times and examine the fit of these models in future research.

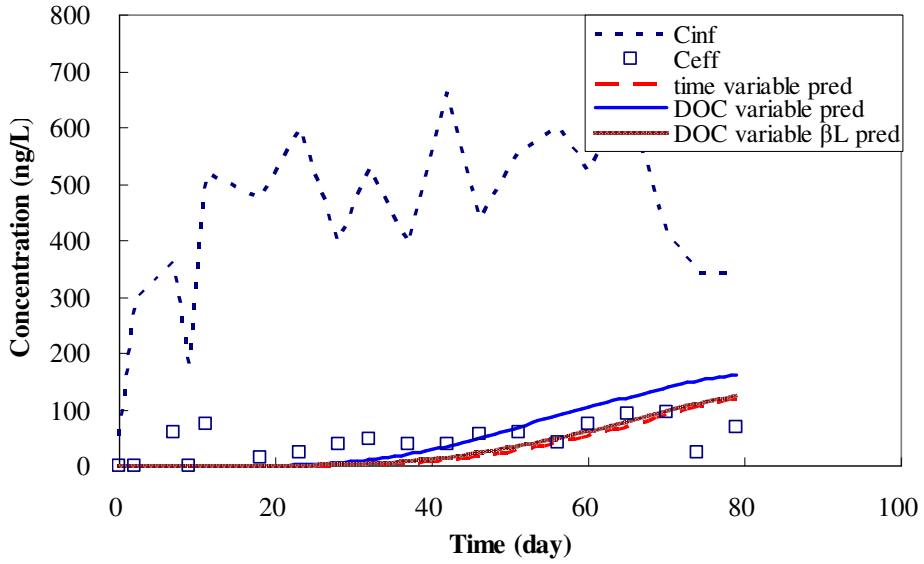

Figure 8-23 NOM surface loading associated time-variable simulation for NP breakthrough on pilot F400 column

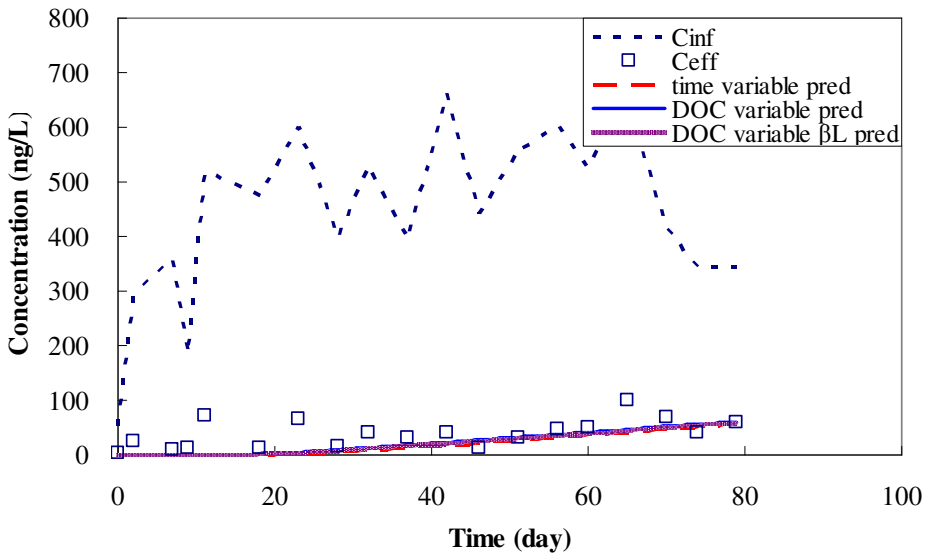

Figure 8-24 NOM surface loading associated time-variable simulation for NP breakthrough on pilot PICA column

Summary

Overall, it has been demonstrated that the use of NOM surface loading associated time-variable parameters improved the accuracy of predictions, albeit to different extents depending on the different adsorbate/adsorbent pairs. With the improved approach, the variance of breakthrough profiles due to different NOM surface loadings in preloading and pilot adsorbers can be compensated for. Since film diffusion seemed to be impacted most by overall NOM surface loading, it was more suitable to only adjust film diffusion coefficients instead of all parameters. This improved early predictions, which is particularly important for stringent removal objectives. This point is of special importance for predicting removals of dissociated compounds, such as naproxen, at low concentrations.

Since it was very difficult to find a general interpretation of the relationships between overall NOM surface loading and adsorptive capacity for all adsorbent/adsorbate pairs, it was felt that the prediction in association with adjusted adsorptive capacity parameters according to NOM surface may lead to possible errors, e.g. under-predicting the removel of naproxen in the intermediate phase . Thus, in actual applications, from a conservative perspective, it may be better to interpret breakthroughs first by using the original time-variable approach and then applying the NOM adjusted time-variable approach.

8.4 Predicting Service Life for Full-scale GAC Adsorbers

Having demonstrated the correctness of the estimated isotherm and kinetic parameters and validated the variable parameters modeling approach, it was now possible to make predictions for the service lives of full-scale GAC adsorbers. The predictions considering fouling effects were made using the time-variable PSDM with only adjusting film diffusion coefficients associated for NOM surface loading. In addition, the predictions without considering fouling effects were also calculated for comparisons. In the assumed scenario, the designed EBCT was 10 min, with a hydraulic loading of 6 m/h. The bed depth for the assumed GAC adsorbers was 100 cm. The bed densities for F400 and PICA adsorbers were the same as the values obtained for the corresponding pilot columns. The removal objectives were set as 90% and 20% removals of 500 ng/L target compounds in the influent. Maximum prediction time was three years for the cases considering fouling effects. Table 8-2 presents the predicted service lives of assumed full-scale F400 and PICA carbon adsorbers.

Table 8-2 Predicted service lives (days) of assumed full-scale GAC adsorbers

		F400		PICA	
Expected Removals		90%	20%	90%	20%
naproxen	fouling	109	399	80	160
	no fouling	1605	nc	942	nc
carbamazepine	fouling	179	326	167	352
	no fouling	2180	nc	1208	nc
nonylphenol	fouling	329	> 1095	963	> 1095
	no fouling	2274	nc	1827	nc

nc: not calculated

As shown in Table 8-2, for the cases not considering fouling effects, naproxen had the fastest breakthrough, followed by carbamazepine. Both carbon adsorbers demonstrated highest effectiveness for removing NP. Since NP has lowest adsorption affinity at very low concentration levels, the higher removal efficiencies for NP in both carbon adsorbers may be attributed to the faster mass transfer rates of NP compared to the other two compounds. The F400 carbon adsorber was more efficient than the PICA carbon adsorber for removing 90% of all the target compounds if fouling effects were not taken into consideration. The comparison between the scenarios with and without considering fouling effects points to that the adsorbers service lives (to achieve > 90% removals) were reduced by 50% to

more than 90% due to the fouling of background NOM in natural water, depending on target compound and carbon combination. In general, NP was least impacted by fouling among the three compounds. The PICA carbon adsorber was subject to a lower reduction in effectiveness than the F400 carbon adsorber due to fouling. The order of achieving 90% removals for different compounds was as expected with naproxen breaking through the adsorbers first, followed by carbamazepine and then NP. The modeling results showed that F400 and PICA adsorbers would be very effective in removing NP because the predicted operation times to exceed 10% breakthrough were almost 1 and 2.5 years for F400 and PICA adsorbers, respectively. If the worst case scenario is used for triggering the regeneration of GAC, the service lives for F400 and PICA adsorbers are approximately 3.5 and 2.5 months, respectively, based on the breakthroughs of naproxen. However, considering that the environmentally relevant concentration of naproxen is generally less than 500 ng/L, both adsorbers should be effective for longer periods of time. A comparison between the two carbons at 10% breakthrough level indicates that the F400 adsorber was slightly more efficient than the PICA adsorber for removing the two PhACs, but it showed a lower efficiency than the PICA adsorber for removing NP.

If 80% breakthrough was set as a removal target, it was surprising to find that the PICA adsorber would be almost exhausted after only five months of operation. However, for other cases of removing naproxen and carbamazepine, the 80% exhaustion of GAC adsorbers would take place after run for approximately one year. This may be regarded as a satisfactory performance. It seems that NP would not be of any concern because both adsorbers would provide an effective barrier probably until the GAC in adsorbers is replaced or regenerated.

Table 8-3 Comparison between GAC and PAC for removing the target compounds

Carbon usage rate (mg/L)†	F400		PICA	
	GAC	PAC	GAC	PAC
naproxen	23	16	29	7
carbamazepine	14	11	14	10
nonylphenol	8	16	3	13

†: calculated at 1 log removals for 500 ng/L target compounds

In order to roughly compare the two options for applying activated carbon, the CUR values were calculated for both GAC adsorbers based on achieving 1 log removal of the individual target

compounds. The CUR value for a GAC adsorber was calculated based on the total volume of treated water before achieving 10% breakthrough and carbon amount in the adsorber. The data as well as the minimum required dose for PAC (from Table 6-5) are shown in Table 8-3 Comparison between GAC and PAC for removing the target compounds. When looking at this table, it should be kept in mind that the applied PAC dose in practise may be substantially higher than the corresponding minimum PAC dose, since kinetics and reactor configuration were not considered in the calculation of the minimum values. If the PAC adsorption process is optimized, 80% of the possible equilibrium loading is usually expected (Huber *et al.*, 1989). For GAC adsorber, it is possible to further minimize the CUR by optimizing the EBCT and other design factors. The choice of 10 min for the EBCT in this scenario was roughly based on an optimal value for removing atrazine as summarized by Knappe (1996) and on the optimal range for TCE removal as reported by Zimmer (1988, cited by Sontheimer *et al.*, 1988). It can be seen that, for removing naproxen in PS water, PICA PAC may be the most effective if an appropriate reactor and contact time were to be chosen. Interestingly, it was found that if PICA carbon was used for a fixed bed adsorber, it conversely had the least efficiency. Although it is difficult to interpret these differences mechanistically, it may be inferred that, at low concentrations the application of PAC for dissociated compounds, such as naproxen, which is very sensitive to the fouling effect, may take advantage of its adsorption capacity which is typically not impacted by NOM fouling due to the short contact times. In contrast, a PICA GAC adsorber would offer the highest removal efficiency in eliminating NP. This can be explained by the finding that NP is very resistant to fouling effects compared to the other two target compounds, and thus capacity of the GAC adsorber could be better used. With respect to removing carbamazepine, at this point, it is difficult to determine which option would the best. Both carbon show virtually identical performance and PAC application seem to be slightly more favourable. More detailed kinetic data for PAC adsorption would be desirable to make a final decision. It should be emphasized that above comparisons were only made based on theoretically calculated CUR values, without considerations of any other cost associated with construction, operation, maintenance, and disposal of waste. Therefore, other factors should be considered before a final recommendation can be made.

When applying the laboratory and pilot data for predicting full-scale adsorber performance, some limitations should be kept in mind. One consideration may be the dependence of preloading on bed depth. The reports on bed depth effect were conflicting. Speth (1991) observed significant difference of determined film diffusion coefficients for GAC from the inlet and from the outlet of a GAC adsorber. In contrast, Knappe (1996) found that GAC from different depths of a full-scale adsorber operated for five months showed similar isotherm and kinetic parameters for atrazine,

suggesting that the preloading was homogeneous at least for run times longer than five months. The similar observation was also reported by Summers *et al.* (1989) based on TCE isotherms on a 25-week preloading GAC. Therefore, it may be postulated that the bed depth difference due to preloading may be evident at the early stage and then eliminated at longer run times. Note that the bed depth effect was not investigated in this research. However, it is expected that this effect would not be very pronounced because much higher concentration of NOM than those of the target compounds led to a saturation of GAC by NOM well in advance before the wave fronts of the target compounds arrived. If the dependence of preloading on bed depth were significant, then the predicted performance in this study would represent the worst scenario, since the GAC used for estimating parameters were most extensively preloaded.

Another possible significant limitation of simulating full-scale adsorber performance is that biological activity would have a great impact, especially at longer operating times. The *US EPA EPI suite program V2.0* estimates that naproxen and NP are biodegradable whereas carbamazepine is resistant to biodegradation. However, these estimations are empirically based on the quantitative structure activity relationship (QSAR) and some wastewater treatment experience. A study performed by Boyd *et al.* (2005) indicated that naproxen at 5 mg/L was not biodegraded in a biofilm reactor. This observation could be confirmed by survey data for STPs reported by Metcalfe *et al.* (2003a). Therefore, although to date no detailed report has been released on the biodegradation of the target compounds at extremely low concentration levels, it is expected that low biodegradation efficiency would be encountered for the target compounds during a GAC adsorption process in a WTP. Nonetheless, biological activity is expected to reduce the fouling effect of GAC in adsorbers by reopening some adsorption sites and accesses (Huck *et al.*, 1993). The capacities for removing the target compounds are thus probably larger than the predicted values. In this case, the modeling results in this study still provide a most conservative prediction.

8.5 Summary

The modeling predictions using the time-variable approach and the NOM surface loading associated time-variable approach in the preceding sections lead to the following summaries:

1) General functions were established to describe the varying trends of isotherm and kinetic parameters for different target compounds with increasing preloading time. It was found that the varying trends for Freundlich K_F, 1/n, and film diffusion coefficient β_L could be

generally depicted by a corresponding empirical model. Some interpretations were provided based on observations of the fitted parameters.

2) Although impedance for naproxen and carbamazepine could not accurately be estimated with SFB tests, the time-variable modeling results demonstrated that proposed general functions could satisfy the modeling requirements in this study. However, a sensitivity analysis of carbamazepine adsorption suggested that further efforts should be made in the future to accurately determine its pore diffusion.

3) Satisfactory agreement between the predictions made by the time-variable modeling approach and the measured data from pilot-scale experiments proved the effectiveness and robustness of employing this approach for predicting PhACs and EDCs adsorption performance at low concentration levels. This overall approach is therefore suitable for prediction the behaviour of other PhACs and EDCs not covered in this study.

4) However, consistent overestimations of removals at early run times were observed in all cases when using the model with the time-variable approach. Subsequent sensitivity analyses suggested the possibility of underestimating the decay in capacity and kinetic parameters due to fouling which may have contributed to the observed differences.

5) The sensitivity analyses confirmed that film diffusion contributed most to the breakthrough profiles for carbamazepine and in particular for naproxen under the experimental conditions investigated in this study. The very low concentrations were thought to be the most likely reason.

6) The time-variable approach was expanded to include adjustments for differences in NOM surface loading for preloaded and pilot GAC. The NOM surface loading associated time-variable approach successfully compensated for differences at the early phase. Improved predictions were mostly attributable to the adjusted film diffusion coefficients.

7) Adjusting adsorptive capacity according to overall NOM surface loading led to overpredictions in some cases. Thus, in actual applications, from a conservative perspective, it was recommended to only adjust film diffusion coefficients if early breakthrough prediction is required. Alternatively, breakthroughs could be predicted using all possibilities from original over time-variable to adjusted time-variable approaches.

8) The performances on F400 and PICA full-scale adsorbers were predicted using NOM surface loading associated time variable approach. Both adsorbers were expected to provide satisfactory performance in achieving 90% removals for carbamazepine and NP. Naproxen was predicted to have a fast breakthrough in both adsorbers.

9) Comparisons between the CUR values for GAC and the minimum required doses for PAC suggested that PICA PAC and GAC would be most appropriate for achieving 1 log removal of naproxen and NP, respectively. PICA and F400 showed the same performance for carbamazepine with PAC being a slightly better option over GAC. However, final recommendations for carbamazepine require additional kinetic data.

CHAPTER 9
CONCLUSIONS AND RECOMMENDATIONS

9.1 Summaries and Conclusions

This study provided detailed investigations on adsorption performances of naproxen, carbamazepine and nonylphenol on F400 and PICA carbon at environmentally relevant concentrations. As a starting point, isotherm and kinetic parameters were determined on virgin granular activated carbons (GACs) in ultrapure water. In addition, the direct competitive effect was examined in post-sedimentation (PS) water from a full-scale water treatment plant using the ideal adsorbed solution theory (IAST) model in combination with the equivalent background compound (EBC) concept. Furthermore, long term preloading effects were studied using preloaded GAC from a preloading system using the same PS water. The isotherm and kinetic parameters for GAC preloaded for different time intervals were interpreted using a time-variable approach. Subsequently, pilot column breakthrough data obtained in PS water was used to validate the pore and surface diffusion model (PSDM) incorporating either the time-variable approach or the natural organic matter (NOM) surface loading associated time-variable approach. Finally, the validated PSDM coupled with an improved time-variable approach was applied for predicting removal of the target compounds in full-scale F400 and PICA carbon adsorbers. More concretely, the following major conclusions may be drawn from this study:

Adsorption of Target Compounds

1) As a basis for studying adsorption of a group of emerging contaminants at low concentration levels, comparisons between three isotherm models including the Langmuir, the Freundlich and the Langmuir-Freundlich model, were carried out. It was demonstrated that the two parameter Freundlich model was capable of well expressing the isotherms at the investigated "sub-saturation" concentration range for the target compounds.

2) The isotherm tests in ultrapure water on both virgin carbons indicated that carbamazepine was most adsorbable, and nonylphenol (NP) was adsorbed most weakly, with intermediate removal of naproxen, at the equilibrium liquid concentration range of 10 – 1000 ng/L. The adsorbabilties of the three target compounds were not in agreement

with expectations based on their log K_{ow} values. Interestingly, NP demonstrated the most homogeneous adsorption on both carbons. It had lesser adsorption affinity than carbamazepine and naproxen at very low concentration range (e.g. < 300 ng/L); however, the adsorption affinity of NP approached and subsequently exceeded those of naproxen and carbamazepine at higher equilibrium concentrations. The smaller Freundlich exponent for NP in the references than the one in this study suggests that the isotherm of NP on a logarithmic plot has a severe curvature over a wide liquid phase concentration range. This finding suggests that if an inappropriate extrapolation from high concentration range is applied for predicting the removal of NP in the very low concentration range, the predicted removal may be overestimated and misleading in designing adsorption processes for drinking water treatment.

3) Comparisons of isotherms on F400 carbon between the target compounds and other frequently reported micropollutants showed that the three target compounds had generally comparable isotherm performance to TCE, MIB and geosmin, whereas atrazine demonstrated a much higher adsorptive affinity than all others. The performance of NP was similar to that of MIB and geosmin with respect to the Freundlich 1/n. The comparable adsorption affinities between MIB and geosmin and naproxen and carbamazepine in equilibrium liquid concentration range of 10 – 100 ng/L suggest that PAC dosage applied for controlling taste and odour events may be adequate for removing these two PhACs.

4) EBC parameters estimated using the IAST-EBC program were specific for each target compound and carbon pair. The isotherm tests in PS water demonstrated that for both carbons, the adsorptive capacity of NP was reduced the least compared to the other two compounds. This finding may be due to the compound's strong hydrophobicity and smallest molecular depth of the three compounds. Nevertheless, to achieve equivalent removals (e.g. 90%) of their environmentally relevant concentrations, by PAC, the calculation results, based on the principle that the percent removal of the micropollutants at a given PAC dosage is independent of the initial target compound concentration under certain conditions, indicated that, in general, a higher minimum dosage might be required for NP using either F400 or PICA carbon compared to naproxen and carbamazepine. To remove naproxen, F400 carbon, if being used as PAC, was

recommended over PICA carbon. While for removing carbamazepine, F400 and PICA carbon had similar performance in PS water.

5) Compared to their adsorption capacity on virgin GACs, the isotherm tests on preloaded GACs demonstrated that all three target compounds were subject to significantly negative impact from long-term preloading of background NOM, albeit to different extents. Among the three target compounds, naproxen experienced the most severe loss of adsorption affinity, followed by carbamazepine. After an initial reduction within the first three weeks, the adsorption capacity of NP did not substantially decrease for longer preloading times.

6) Compared to other conventional synthetic organic compounds (SOCs) (e.g. atrazine and TCE), which are typically present at relatively higher concentrations in raw water, the reductions of the Freundlich K_F for naproxen and carbamazepine due to preloading were substantially larger. The low concentrations of these compounds in water may contribute to the greater capacity reductions. However, this inference needs to be further confirmed due to the absence of data for the same carbon and the same water matrix.

7) The short fixed bed (SFB) tests on virgin and preloaded GACs indicated that mass transports of all the target compounds significantly decreased due to preloading of NOM. Similar to the impact of preloading on adsorption capacity, naproxen suffered the most deteriorative effect, followed by carbamazepine. The fouling impacts on external and internal mass transports for adsorbing NP were demonstrated to be least pronounced.

8) The decreasing trends of both adsorption capacity and kinetics for the three target compounds were further confirmed by the breakthrough results from the pilot tests performed using PS water. For both F400 and PICA carbon pilot columns, naproxen quickly arrived at more than 70% breakthrough after 79 days' operation. Almost half of the carbamazepine removal capabilities of both pilot adsorbers were exhausted during the same period. Since NP was subject to the least impact from long term preloading on both adsorption capacity and kinetics, it was found to only breakthrough less than 20% in both adsorbers, even though it showed the least adsorbability among the three target compounds on virgin GACs in ultrapure water at low concentrations.

9) The performances on assumed full-scale F400 and PICA adsorbers were predicted using the PSDM in combination with the NOM surface loading associated time variable

approach. Both adsorbers are expected to provide satisfactory performance in achieving 90% removals for carbamazepine and NP. Naproxen was predicted to breakthrough fast in both adsorbers. Comparisons between the carbon usage rate (CUR) values of GAC and the minimum required doses for PAC suggested that PICA PAC and GAC would be recommended for removing naproxen and NP, respectively. Recommendations for carbamazepine removal require more kinetic data on PAC adsorption.

Adsorption Mechanisms

1) Simultaneously performed studies on three target compounds with quite different physicochemical properties revealed that no one generalized mechanism could successfully explain the observed complicated fouling effects. The observations on the markedly different pattern of adsorption capacity reduction for the three target compounds covered all the contradictory observations reported in the literature. The reduced adsorption capacities for the three target compounds might be interpreted as a sequential effect from or a simultaneous interaction among different fouling mechanisms, e.g. non-desorbable adsorption, direct competition, partial pore blockage (restriction), and full pore blockage. Examination of the changing patterns of the Freundlich 1/n and K_F may provide some insight into the possible mechanisms. The changed heterogeneity of carbon in terms of adsorbing naproxen due to long term preloading suggested that some preadsorbed NOM was not replaceable by naproxen. Nevertheless, the preloading for a relatively short time only led to a capacity loss of naproxen most likely due to direct competition and possible pore blockage. In contrast, both direct competition and pore blockage seemed to be the main mechanisms contributing to the loss of adsorption capacity for carbamazepine, thus producing a series of nearly parallel isotherms. The predominant mechanism for the removal of NP in the late preloading phase seemed to be absorption or partition in the NOM matrix on the surface of or inside the carbons.

2) The reductions of the BET surface areas for the two carbons were in agreement with their corresponding DOC breakthrough profiles in the preloading columns. However, inconsistency between reductions of the BET surface areas and of adsorption capacities for the target compounds suggests that the former could not account for the effective surface area for adsorption of micropollutants. A partial pore blockage mechanism was proposed to explain this inconsistency.

3) Film diffusion coefficients (β_L) for the three target compounds were determined by SFB experiments. β_L values on virgin GACs were in disagreement with the values calculated by the Gnielinski correlation. These observations were accordant with the results from previous studies on other SOCs, and could be attributable to the deviations of real GAC particles from the spherical shape assumed in the correlation method. Nevertheless, the extent of the differences between experimentally determined β_L and Gnielinski correlation β_L was found to depend on the specific compound. Among the three target compounds, NP showed the highest film diffusion rate and the largest difference between experimentally determined and Gnielinski correlation β_L. The range in differences (factor 2 – 4) may be attributable to different electrostatic interactions between target compounds and adsorbents.

4) Experimentally determined film diffusion coefficients for the three target compounds on preloaded carbon were found to rapidly decrease during the initial 40-day preloading period, and then slowly decrease with longer preloading times. These results could be explained by the fact that large amounts of background NOM were quickly adsorbed on the carbons and could not penetrate deeply into the carbon particles, and as a result, accumulated on the external surface of carbon. This accumulation would occur intensively during the early preloading stage. Through inspecting the SEM images of virgin and preloaded carbons, it was found that a type of film formed from NOM fouling or biological growth on the surfaces of the preloaded carbons. This observation suggested that the coverage by NOM/bio- film on the surface of preloaded carbon would introduce an additional mass transfer resistance layer and also reduce the uncovered external surface area, thus leading to a reduction in the external diffusion flux. This reduction was compensated for in the calibration processes, thus producing decreasing "apparent film diffusion coefficients" for preloaded carbons.

5) The three target compounds showed different extents for decreasing β_L, which pointed to a mechanism where electrostatic interactions between preloaded carbon and a specific compound might significantly contribute to the reduction of external mass transport. The used carbon may become negatively charged due to the loading of NOM as well as the growth of bacteria.

6) Sensitivity analyses on virgin and preloaded carbons indicated that, under the very low influent concentrations applied in this study, adsorptive capacity and film diffusion

would exert much greater effects on breakthrough profiles than internal diffusions. This could be explained by slow accumulation of adsorbates on the surface of the adsorbents at very low concentration levels. This situation made it difficult to accurately determine internal diffusion coefficients. The sensitivity analyses on the SFB reactors loaded with virgin carbons indicated that, in the cases of naproxen and carbamazepine, pore diffusion influenced the breakthrough profiles only after extremely long running times. With the intermediate preloaded carbons, the sensitivity of SFB breakthrough profiles to the pore diffusion was even less pronounced. Subsequent sensitivity analyses on the pilot columns confirmed that film diffusion contributed most to the breakthrough profiles for carbamazepine and especially for naproxen under the very low concentration conditions investigated in this study. Good agreement between model predictions and measured data for naproxen and carbamazepine in the pilot columns further confirmed this judgement. However, it can be expected that the influence of pore diffusion on carbamazepine breakthrough might become more significant for a deeper bed adsorber run for a longer period of time. Compared to the other target compounds, the breakthrough profiles of NP were significantly and concurrently influenced by surface diffusion and film diffusion.

Adsorption Modeling

1) For the preloading effect, an exponential function (Equation 8.1) was found to best describe the early rapid and late slow decreasing trends of Freundlich K_F, and film diffusion coefficient β_L for the adsorption of all target compounds on the two carbons. Some interpretations were made based on the observations of calibrated parameters. It was also found that the Gompertz model (Equation 8.2) provided the flexibility for time-variable Freundlich 1/n in the cases for naproxen and NP adsorption.

2) In spite of not being able to accurately estimate impedance values (a measure for pore diffusion) in the SFB tests for naproxen and carbamazepine, the time-variable modeling results confirmed that a proposed general function (Equation 8.5) could satisfy the modeling requirements in this study.

3) The satisfactory agreement between the modeling predictions and the measured data from the pilot-scale experiments proved the validity of applying the PSDM in combination with the time-variable approach for the selected compounds at very low

concentration levels. Furthermore, successful applications of this modeling approach to target compounds with diverse physicochemical properties on two different types of carbons demonstrated the reliability of this modeling approach, and it may be used to further predict adsorption of other PhACs and EDCs in GAC adsorbers under the same conditions as employed in this study.

4) Consistent overestimations of removals at the early stages of GAC pilot column operation were observed for all cases when using time-variable PSDM. The subsequent sensitivity analyses suggested that these differences might be attributable to underestimations of the preloading impact on capacity and kinetic parameters. The analyses of DOC breakthrough curves of the preloading columns and of the pilot columns found that the NOM surface loading on the GAC were different between two systems. Therefore, the time-variable approach was adjusted according to the NOM surface loading for the GAC from the preloading columns and from pilot columns. Better agreement was achieved between the new predicted breakthrough profiles and the measured data. This confirmed that the NOM surface loading associated time variable approach could successfully compensate for the differences at the early phase of pilot tests. This finding is significant for the GAC adsorber design if the removal objective is set as 80-90%.

5) In some cases, the improvement of the early phase predictions can only be attribute to the adjustment of film diffusion. Meanwhile, adjusting adsorptive capacity according to overall NOM surface loading led to over-prediction of breakthroughs. Thus, in actual applications, from a conservative perspective, it was recommended only to adjust film diffusion coefficient if early breakthrough prediction is required. Alternatively, breakthroughs could be expressed as an interval encompassing all possible predictions using original and adjusted time-variable approaches.

6) The validated modeling approach was applied for predicting the performances of two hypothetical full-scale GAC adsorbers. Both adsorbers were expected to provide satisfactory performance by achieving 90% removals for carbamazepine and NP at the influent concentration of 0.5 μg/L. Naproxen was predicted to break through quickly in both adsorbers, and thus could be used as an indicator compound for regeneration of GAC in adsorbers. Comparisons between the CUR values of GAC and the minimum required doses for PAC suggested that PICA PAC and GAC would be most appropriate

for achieving 1 log removal of naproxen and NP, respectively. The recommendation for carbamazepine removal requires more kinetic data on PAC adsorption.

Compound Selection and Analytical Method Development

1) Two protocols were set up to screen significant compounds from a wide variety of EDCs and PhACs, since the type of data available for EDCs differed substantially from the ones available for PhACs. The evaluation criteria for the selection of the EDCs considered occurrence of in wastewater effluent, surface, ground, and drinking water, as well as the reported or estimated estrogenicity. The selection process for PhACs focused on the reported environmental occurrence, consumption in Canada, and estimated fish toxicity. Overall, the combination of environmentally occurrence with reported or estimated toxicities/estrogenicities facilitated the choice of the compounds.

2) A multi-residue analytical method based on GC/MS was successfully developed for simultaneous determination of the selected acidic and neutral PhACs and EDCs. The optimal derivatization conditions were determined systematically using a factorial design more specifically, a central composite design. The extraction was optimized in terms of extraction pH, cartridge capacity, and elution solvent type and volume. The statistical experimental design in combination with a concept of total desirability was demonstrated to be an effective tool for improving the multi-residue analytical method.

3) The developed analytical method was successfully applied to Grand River water and tap water from the local area, where pharmaceuticals such as salicylic acid, ibuprofen, gemfibrozil, naproxen and carbamazepine, and EDCs such as E1 and NP1EC were identified as the most common contaminants, and thus should be of more concern.

9.2 Recommendations for Future Research

During the present study, some areas were revealed of significant interest for future research. They are listed as follows:

1) For the first time, this study provided detailed and typical adsorption performances for a new group of emerging contaminants at their environmentally relevant concentration levels. Nevertheless, future research should be directed towards confirming these tendencies by looking at additional PhACs and EDCs.

2) A more fundamental understanding of the markedly different changing patterns of Freundlich K_F and 1/n for the three target compounds on the preloaded carbon is required. Although some mechanisms were suggested to interpret these phenomena in this study, more detailed investigations on mechanisms should be carried out in the future. These investigations should include a comparison between several compounds with different physicochemical properties. The different preloading effects, such as non-desorbable adsorption, direct competition, partial pore blockage, and full pore blockage, may be investigated by using different size fractionated NOM. It is also recommended that the study should be performed on uncrushed GAC because crushing process may influence the deposit of NOM on the surface of GAC.

3) This study found that, at very low SOC concentration levels, the adsorption may be significantly influenced by electrostatic interactions between SOCs and adsorbents. Several previous studies have indicated that uptake of NOM would change the electrostatic properties of the activated carbon. However, more efforts should be invested to evaluate the impact of this change on mass transports and adsorption capacity for adsorbing low concentration SOCs.

4) It has been demonstrated in this study that film diffusion predominantly controlled the mass transport for the target compounds at very low concentrations, especially in the early and intermediate breakthrough phases. Accordingly, these phases of the breakthrough profile are largely dependent on the film diffusion coefficient and the adsorptive capacity parameters. The PSDM could therefore be further simplified by only considering film diffusion for the mass transport. From a conservative perspective, this simplification would be valid when predicting the early breakthrough, and would be significant for GAC adsorber design if the treatment objective is high (80 – 90%). More work should be invested on this model simplification and validation.

5) The large contributions of the film diffusion to the mass transport at very low concentrations increased the difficulty to determine the internal diffusion coefficients using the SFB reactor. Internal diffusion may significantly influence the predictions at the late breakthrough phase, and therefore, future research should improve the experimental approach to facilitate the determination of internal diffusion coefficients at very low concentration levels. It is proposed that the film diffusion coefficient and internal diffusion coefficients could be determined separately using different

experimental approaches. The differential column batch (DCB) reactor would be an option for determining pore diffusion coefficient if it is the main mechanism for the internal mass transport.

6) The results from the NOM surface loading associated time-variable simulations suggested that it might be promising to directly relate the decays of isotherm and kinetic parameters to an overall NOM surface loading amount, thereby possibly improving the accuracy of model predictions. However, to apply this assumption in practical use, the general model describing the relationships between the NOM surface loadings and decaying trends of isotherm and kinetic parameters, and their underlying mechanisms should be better understood.

7) A possible competitive effect from remaining low DOC concentrations in ultrapure water was identified when isotherm tests were performed at very low concentrations. This would introduce some errors in the determined isotherm parameters. Future work should be invested to eliminate this negative influence by using a high purification technology to produce "organic free" ultrapure water, and also assess the impact from this minor competition on the "true" adsorption isotherm in detail.

8) In order to facilitate the study, this research did not consider any biological effect on both adsorbates and adsorbents. However, biological activity is expected in full-scale GAC adsorbers, which are operated for a long time. Therefore, future research should take into consideration biodegradation of adsorbed NOM and its effect on releasing adsorption sites for the target compounds. The possibility of biodegradations of the target compounds at these very low concentrations should be examined. In addition, it would also be interesting to investigate how biomass influences the adsorption of target compounds by changing the surface properties of the GAC.

9) Desorption of adsorbed target compounds was not studied in this research, however, there is the possibility that a GAC adsorber operated for a long time, could serve as a reservoir releasing PhACs and EDCs, especially when influent concentrations fluctuate substantially.

BIBLIOGRAPHY

Abdel-Jabbar, J., S. Al-Asheh, B. Hader, 2001. Modeling, parametric estimation, and sensitivity analysis for copper adsorption with moss packed-bed. *Separ. Sci. Technol.* 36(13), 2811-2833

Adams, C., Y.Wang, K. Loftin, M. Meyer, 2002. Removal of antibiotics from surface and distilled water in conventional water treatment processes. *J. Environ. Engin.-ASCE.* 128(3), 253-260

Ahel, M., W. Giger, M. Koch. 1994. Behaviour of alkylphenol ployethoxylate surfactants in the aquatic environment—I. occurrence and transformation in sewage treatment. *Water Res.* 28(5), 1131-1142

Alda, M. and D. Barcelo, 2001. Determination of steroid sex hormones and related synthetic compounds considered as endocrine disrupters in water by fully automated on-line solid-phase extraction-liquid chromatography-diode array detection. *J. Chromatogr. A.* 911, 203-210

Andreozzi, R., V.Caprio, R. Marotta, A. Radovnikovic, 2003. Ozonation and H_2O_2/UV treatment of clofibric acid in water: a kinetic investigation. *J. Hazardous Materials B.* 103, 233-246

Andrews, R.C., 1990. Removal of low concentrations of chlorination by-products using activated carbon. Ph.D dissertation, University of Alberta, Canada

Balcioglu, I.A. and M. Otker, 2003. Treatment of pharmaceutical wastewater containing antibiotics by O_3 and O_3/H_2O_2 processes. *Chemosphere.* 50, 85-95

Baup, S., C. Jaffre, A. Laplanche, 2000. Adsorption of Pesticides onto granular activated carbon: determination of surface diffusivities using simple batch experiments. *Adsorption.* (6), 219-228

Bautista-Toledo, I., M.A. Ferro-Garcia, J. Rivera-Utrilla, C. Moreno-Castilla, F.J. Vegas Fernandez, 2005. Bisphenol A removal from water by activated carbon: effect of carbon characteristics and solution chemistry. *Environ. Sci. Technol.* 39, 6246-6250

Belfroid, A.C., A.Van der Horst, B. van der Horst, D. Vethaak, 1999. Analysis and occurrence of estrogenic hormones and their glucuronides in surface water and waste water in The Netherlands; *Sci. Total Environ.* 225, 101-108

Bennie, D.T., C.A.Sullivan, H.B. Lee, T.E. Peart, R.J. Maguire, 1997. Occurrence of alkylphenols and alkylphenol mono- and diethoxylates in natural waters of the Laurentian Great Lakes basin and the upper St. Lawrence Reiver. *Sci. Total Environ.* 193, 263-275

Birkett, J.W., 2003. Endocrine Disrupters in Wastewater and Sludge Treatment Sources of Endocrine Disrupters, CRC Press, Boca Raton, FL

Blok, D.J. and I.M.A.D.Wosten, 2000. Source and environmental fate of natural oestrogens, RIWA Research Report. Netherlands.

Bolz U., W.Korner, H. Hagenmaier, 2000. Development and validation of a GC/MS method for determination of phenolic xenoestrogens in aquatic samples. *Chemosphere.* 40, 929-935

Boyd, G.R., H.Reemtsma, D.A. Grimm, S. Mitra, 2003. Pharmaceuticals and personal care products (PPCPs) in surface and treated waters of Louisiana, USA and Ontario, Canada. *Sci. Total Environ.* 311, 135-149

Boyd, G.R., S. Zhang, D.A. Grimm, 2005. Naproxen removal from water by chlorination and biofilm processes. *Water Res.* 39, 668-676

Braun P., M.Moeder, St. Schrader, P. Popp, P. Kuschk, W. Engewald, 2003. Trace analysis of technical nonylphenol, bisphenol A and 17α-ethinylestradiol in wastewater using solid-phase microextraction and gas chromatography-mass spectrometry. *J. Chromatogr. A.* 988, 41-51

Bruce, G.M., R.C. Pleus, S. Snyder, E.M. Snyder, 2006. Toxicological relevance of pharmaceuticals and endocrince disrupting chemicals in water. Proceedings of 5th International Conference on Pharmaceuticals and Endocrine Disrupting Chemicals in Water. March 2006, Costa Mesa, CA, USA.

Bruchet, A., C. Prompsy, G. Filippi, A. Souali, 2002. A broad spectrum analytical scheme for the screening of endocrine disruptor (EDS), pharmaceuticals and personal care products in wastewaters and natural waters. *Water Sci. Technol.* 46 (3), 97-104

Brun, G.L., M. Bernier, R. Losier, K. Deo, P. Jackman, H-B. Lee, 2006. Pharmaceutically active compounds in Atlantic Canadian sewage treatment plant effluents and receiving waters, and potential for environmental effects as measured by acute and chronic aquatic toxicity. *Environ. Toxicol. Chem.* 25(8), 2163-2176

Brunauer, S., P.H. Emmett, E. Teller, 1938. Adsorption of Gases in Multimolecular Layers. *J. Am. Chem. Soc.* 60(2), 309-319

Bucheli, T.D., F.C. Gruebler, S.R. Muller, R.P. Schwarzenbach, 1997. Simultaneous determination of neutral and acidic pesticides in natural waters at the low nanogram per liter level. *Anal. Chem.* 69 (8), 1569-1576

Carter, M.C., W.J. Weber and K.P. Olmstead, 1992. Effect of background dissolved organic matter on TCE adsorption by GAC. *J. Am. Water. Works Assoc.* 84, 81-91

Carter, M.C., 1993. Analysis and modeling of the impacts of background organic matter on TCE adsorption by activated carbon. Ph.D dissertation, University of Michigan, Ann Arbor, Michigan, USA

Carter, M.C. and W.J. Weber, 1994. Modelling adsorption of TCE by activated carbon preloaded by background organic matter. *Environ. Sci. Technol.* 28, 614-623

Carter, M.C., J.E. Kilduff, W.J. Weber, 1995. Site Energy Distribution Analysis of Preloaded Adsorbents. *Environ. Sci. Technol.* 29, 1773-1780

CEPA, 1999. PSL assessment report -- Summary of information critical to assessment of "toxic" under CEPA 1999; http://www.ec.gc.ca/substances/ese/eng/psap/sub18.cfm

CEPA; 1999b. Priority substances list assessment report—Bis (2-ethylhexyl) Phthalate. http://www.ec.gc.ca/substances/ese/eng/psap/sub18.cfm

CEPA, 1999c. Priority substances list II; Nonyphenol and its Ethoxylates (NPES); http://www.ec.gc.ca/substances/ese/eng/psap/sub18.cfm

Chang, S., T.D. Waite, P.E.A. Ong, A.I. Schafer, A.G. Fane, 2004. Assessment of trace estrogenic contaminants removal by coagulant addition, powdered activated carbon adsorption and powdered activated carbon/microfiltration processes. *J. Environ. Eng.-ASCE.* (7), 736-742

Chen, G., B.W. Dussert and I.H. Suffet, 1997. Evaluation of granular activated carbon for removal of methylisoborneol to below odor threshold concentration in drinking water. *Water Res.* 31 (5), 1155-1163

Choi, K.J., S.G. Kim, C.W. Kim, S.H. Kim, 2005. Effects of activated carbon types and service life on removal of endocrine disrupting chemicals: amitrol, nonylphenol, and bisphenol-A. *Chemosphere.* 58(11), 1535-1545

Chu, C.F. and K.M. Ng, 1989. Flow in packed tubes with a small tube to particle diameter ratio. *AIChE Journal* 35(1), 148-158

Clark, R.M. and B.W. Lykins, Jr, 1989. Granular activated carbon: design, operation and cost. Lewis Publishers, Inc. Chelsea, Michigan, USA

Cleuvers, M., 2003. Aquatic ecotoxicity of pharmaceuticals including the assessment of combination effects. *Toxical. Lett.* 142, 185-194

Crittenden, J.C., P. Luft, J. D.W. Hand, J.L. Oravitz, S.W. Loper, M. Arl, 1985. Prediction of multicomponent adsorption equilibrium using ideal adsorbed solution theory. *Environ. Sci. Technol.* 19, 1037-1043

Crittenden, J.C., N.J. Hutzler, and D.G. Geyer, 1986. Transport of organic compounds with saturated groundwater flow: model development and parameter sensitivity. *Water Resour. Res.* 22(3), 271-284

Crittenden, J.C., P.S. Reddy, H. Arora, J. Trynoski, D.W. Hand, D.L. Perram, R.S. Summers, 1991. Prediction of GAC performance with rapid small-scale column test. *J. Am. Water. Works Assoc.* 83, 77-87

Crittenden, J.C., K. Vaitheeswaran, D.W. Hand, E.W. Howe, E. Marco Aieta, C.H. Tate, M.J. McGuire, M.K. Davis, 1993. Removal of dissolved organic carbon using granular activated carbon. *Water Res.* 27(4), 715-721

D'Ascenzo, G., A.DI. Corcia, A. Gentili, R. Mancini, R. Mastropasqus, M. Nazzari, R. Samperi, 2003. Fate of Natural Estrogen Conjugates in Municipal Sewage Transport and Treatment Facilities. *Sci. Total Environ.* 302, 199-209

Daughton, C.G. and T.A.Ternes, 1999. Pharmaceuticals and personal care products in the environment: agents of subtle change? *Environ Health Persp.* 107(11), 907-938

Dastgheib, S.A., T. Karanfil, W. Cheng, 2004. Tailoring activated carbon for enhanced removal of natural organic matter from natural waters. *Carbon.* 24, 547-557

Derylo-Marczewska, A., M. Jaroniec, D. Gelbin, A. Seidel, 1984. Heterogeneity effects in single-solute adsorption from dilute solutions on solids. *Chem. Scr.* 24, 239-246

Deuver, T.A., 2002. Course notes for ChE 622 – Applied statistics in engineering, University of Waterloo, Canada

Diaz A., F.Ventura, 2002. Simultaneous determination of estrogenic short ethoxy chain nonylphenols and their acidic metabolites in water by an in-sample derivatization /solid-phase microextraction method. *Anal. Chem.* 74, 3869-3876

Diaz, A., F. Ventura, M.T. Galceran, 2002. Development of a solid-phase microextraction method for the determination of short-ethoxy-chain nonylphenols and their brominated analogs in raw and treated water. *J. Chromatogr. A.* 963, 159-167

Dierr-MacEwen, N.A. and M.E. Haight, 2006. Expert Stakeholders' views on the management of human pharmaceuticals in the environment. *Environ. Manage.* 38, 853-866

Ding, L., B.J. Marinas, L.C. Schideman, V.L. Snoeyink, Q. Li, 2006. Competitive effects of natural organic matter: parameterization and verification of the three-component adsorption model COMPSORB. *Environ. Sic. Technol.* 40(1), 350-356

Ding, W. and C.Chen, 1999. Analysis of nonylphenol polyethoxycarboxylates and their related metabolotes by on-line derivatization and ion-trap gas chromatography-mass spectrometry. *J. Chromatogr. A.* 862， 113-120

Ebie, K., F. Li, Y. Azuma, A. Yuasa, T. Hafishita, 2001. Pore distribution effect of activated carbon in adsorbing organic micropollutants from natural water. *Water Res.* 35(1), 167-179

Fairey, J.L., G.E. Speitel, L.E. Katz, 2006. Impact of natural organic matter on monochloramine reduction by granular actived carbon: the role of porosity and electrostatic surface properties. *Environ. Sci. Technol.* 40, 4268-4273

Ferrari, B., N.Paxeus, R.L. Giudice, A. Pollio, J. Garric, 2003. Ecotoxicological impact of pharmaceuticals found in treated wastewater: study of carbamazepine, clofibric acid, and diclofenac. *Ecotox. Environ. Safe.* 55, 359-370

Fritz, W. and E.U. Schlunder, 1981. Competitive adsorption of two dissolved organics onto activated carbon –I. *Chem. Eng. Sci.* 36, 721-730

Freundlich, H.M.F., 1906. Over the adsorption in solution. *J. Phys. Chem.* 57, 385-471

Furhacker, M., S. Scharf, H. Weber, 2000. Bisphenol A: emissions from point sources. *Chemosphere.* 41, 751-756

Furlong, E.T., I. Ferrer, S. Glassmeyer, J. effery, D. Cahill, S.D. Zaugg, D.W. Kolpin, 2003. Distributions of organic wastewater concentrations between water and sediment in surface-water samples of the United States. Proceedings of 3rd International Conference on Pharmaceuticals and Endocrine Disrupting Chemicals in Water. March 2003, Minneapolis, Minnesota, USA.

Furuya, E.G., H.T. Chang, Y. Miura, H. Yokomura, S. Tajima, S. Yamashita, K.E. Noll, 1996. Intraparticle mass transport mechanism in activated carbon adsorption of phenols. *J. Environ. Engin-ASCE.* (10), 909-916

Ghijsen, R.T. and W. Hoogenboezem, 2002. Endocrine disrupting compounds in the Rhine and Meuse basin—ocurrence in surface, process and drinking water; RIWA report

Gierke, J.S., N.J. Hutzler, J.C. Crittenden, 1990. Modeling the movement of volatile organic chemicals in columns of unsaturated soil. *Water Resour. Res.* 26(7), 1529-1547

Gillogly, T.E.T., 1998. MIB adsorption in drinking water treatment. Ph.D dissertation, University of Illinois, Urbana, Illinois, USA

Gillogly, T.E.T., V.L. Snoeyink, G. Newcombe, J.R. Elarde, 1999. A simplified method to determine the powdered activated carbon dose required to remove methylisoborneol. *Water Sic. Technol.* 40 (6), 59-64

Graese, S.L., V.L. Snoyink, R.G. Lee, 1987. GAC filter adsorbers. Denver, Colorado: American Water Works Association Research Foundation

Graham, M., Summers, R.S., Simpson, M.R., Macleod, B.W., 2000. Modeling equilibrium adsorption of 2-methylisoborneol and geosmin in natural waters. *Water Res.* 34(8), 2291-2300

Halling-Sorensen, B., S.Nors Nielsen, P.F. Lanzky, F. Ingerslev, H.C. Holten, S.E. Jorgensen, 1998. Occurrence, fate and effects of pharmaceutical substances in the environment- A Review. *Chemosphere.* 36 (2), 357-393

Hand, D.W., J.C. Crittenden, H. Arora, J.M. Miller, B.W. Lykins, 1989. Designing fixed-bed adsorbers to remove mixtures of organics. *J. Am. Water. Works. Assoc.* 81(1), 67-77

Hand, D.W., J.C. Crittenden, D.R. Hokanson, J.L. Bulloch, 1997. Predicting the performance of fixed-bed granular activated carbon adsorbers. *Water Sci. Technol.* 35(7), 235-241

Heberer, T., 2002. Occurrence, fate, and removal of pharmaceutical residues in the aquatic environment: a review of recent research data. *Toxicol. Lett.* 131, 5-17

Heberer, T., K. Reddersen and A. Mechlinski, 2002. From municipal sewage to drinking water: fate and removal of pharmaceutical residues in the aquatic environment in urban areas. *Water Sci. Technol.* 46 (3), 81-88

Helaleh, M.I.H., S. Fujii, T. Korenaga, 2001. Column silylation method for determining endocrine disruptors from environmental water samples by solid phase micro-extraction. *Talanta.* 54, 1039-1047

Hepplewhite, C., G. Newcombe, and D.R.U. Knappe, 2004. NOM and MIB, who wins in the competition for activated carbon adsorption sites? *Water Sci. Technol.* 49 (9): 257-265

Hewitt, M. and M. Servos, 2001. An Overview of Substances Present in Canadian Aquatic Environments Associated with Endocrine Disruption. *Water Qual. Res. J. Canada.* 36 (2)

Hilton, M.J. and K.V.Thomas, 2003. Determination of selected human pharmaceutical compounds in effluent and surface water samples by high-performance liquid chromatography-electrospray tandem mass spectrometry. *J. Chromatogra. A.* 1015, 129-141

Hirsch, R., T.Ternes, K. Haberer, K-L. Kratz, 1999. Occurrence of antibiotics in the aquatic environment. *Sci. Total Environ.* 225, 109-118

Ho, Y., 2004. Selection of optimum sorption isotherm. *Carbon.* 42, 2115-2116

Hoai, P.M., S.Tsunoi, M. Ike, Y. Kuratani, K. Kudou, P.H. Viet, M. Fujita, M. Tanaka, 2003. Simultaneous determination of degradation products of nonylphenol polyethoxylates and their halogenated derivatives by solid-phase extraction and gas chromatography-tandem mass spectrometry after trimethylsilylation. *J. Chromatogra. A.* 1020, 161-171

Hossain, M. and D. Young, 1992. Finite element modeling of single-solute activated carbon adsorption. *J. Environ. Eng.* 118(2), 39

Hu, J.Y., T. Aizawa, Y. Magara, 1997. Evaluation of adsorbability of pesticides in water on powdered activated carbon using octanol-water partition coefficient. *Water Sci. Technol.* 35(7), 219-226

Hu, J.Y., T. Aizawa, Y. Ookubo, T. Morita, Y. Magara, 1998. Adsorptive characteristics of ionogenic aromatic pesticides in water on powdered activated carbon. *Water Res.* 32(9), 2593-2600

Hu, J.Y., G.H. Xie, 2002. Products of aqueous chlorination of 4-nonylphenol and their estrogenic activity. *Environ. Toxicol. Chem.* 21(10), 2034-2039

Hu, J.Y., T.Aizawa and S.Ookubo, 2002b. Products of aqueous chlorination of bisphenol A and their estrogenic activity. *Environ. Sci. Technol.* 36, 1980-1987

Hu, J.Y., S.Cheng, T. Aizawa, Y. Terao, S. Kunikane, 2003. Products of aqueous chlorination of 17β-estradiol and their estrogenic activities. *Environ. Sci. Technol.* 37, 5665-5670

Huber, L., G. Zimmer, and H. Sontheimer, 1989. Powdered or granular activated carbon for micropollutant removal. *J. Water Supply Res. T.* 38, 118-130

Huber, M.M., S. Canonica, G. Park, U. von Gunten, 2003. Oxidation of pharmaceuticals during ozonation and advanced oxidation processes. *Environ. Sci. Technol.* 37, 1016-1024

Huber, M.M., S. Korhonen, T.A. Ternes, U. Von Gunten, 2005. Oxidation of pharmaceuticals during water treatment with chlorine dioxide. *Water Res.* 39, 3607-3617

Huck, P.M., W.B. Anderson, R.C. Andrews, 1993. Chapter 3 – water treatment philosophies and technologies. Water treatment principles and applications: a manual for the production of drinking water. Canadian Water and Wastewater Association, Minister of Supply and Services Canada

Janex, M.L., A.Bruchet, Y. Lèvi, T. Ternes, 2002. Pharmaceutical compounds: occurrence in the environment and fate in drinking water treatment. Proceedings of Water Quality Technology Conference, Nov. 2002. Seattle, Washington, USA

Janex, M.L., A. Bruchet, T.A. Ternes, M. Bonerz, D. McDowell, U.V. Gunten, M. Huber, 2003. Removal of pharmaceuticals in the water cycle- POSEIDON European Project. Proceedings of 3rd International Conference on Pharmaceuticals and Endocrine Disrupting Chemicals in Water. Minneapolis, Minnesota, USA. 2003.3., 19-21

Janex-Habibi, M.L. and A. Bruchet, 2004. Pharmaceuticals and personal care products: occurrence and fate in drinking water treatment. Proceedings of 2004 American Water Works Association Annual Conference, June 2004, Orlando, Florida, USA

Jarvie, M.E., D.W. Hand, S. Bhuvendralingam, J.C. Crittenden, D.R. Hokanson, 2005. Simulating the performance of fixed-bed granular activated carbon adsorbers: removal of synthetic organic chemicals in the presence of background organic matter. *Water Res.* 39, 2407-2421

Jeannot, R., H.Sabik, E. Sauvard, T. Dagnac, K. Dohrendorf, 2002. Determination of endocrine-disrupting compounds in environmental samples using gas and liquid chromatography with mass spectrometry. *J. Chromatogr. A.* 974, 143-159

Jones, O.A., N.Voulvoulis, J.N.Lester, 2002. Aquatic environmental assessment of the top 25 English prescription pharmaceuticals. *Water Res.* 36, 5013-5022

Jones, O.A., J.N. Lester, and N. Voulvoulis, 2005. Pharmaceuticals: a threat to drinking water? *Trends Biotechnol*. 23(4), 163-167

Kang, J.H. and F. Kondo, 2002. Effect of bacterial counts and temperature on the biodegradation of bisphenol A in river water. *Chemosphere.* 49, 493-498

Karanfil, T., S.A. Dastgheib, D. Mauldin, 2006. Exploring molecular sieve capabilities of activated carbon fibers to reduce the impact of NOM preloading on trichloroethylene adsorption. *Environ. Sci. Technol.* 40, 1321-1327

Kelly, C., 2000. Analysis of steroids in environmental water samples using solid-phase extraction and ion-trap gas chromatography-mass spectrometry and gas chromatography-tandem mass spectrometry. *J. Chromatogr. A.* 872, 309-314

Kim, B.R., R.A. Schmitz, V.L. Snoeyink, G.W. Tauxe, 1978. Analysis of models for dichloramine removal by activated carbon in batch and packed-bed reactors using quasilinearization and orthogonal collocation methods. *Water Res.* 12, 317-326

Kim, H., 2004. New insights into the binding site formation and performance of molecularly imprinted polymers. Ph.D dissertation, Louisiana State University

Kim, S.D., J. Cho, I.S. Kim, B.J. Vanderford, S.A. Snyder, 2007. Occurrence and removal of pharmaceuticals and endocrine disruptors in South Korean surface, drinking, and waste water. *Water Res.* 41, 1013-1021

Kimura, K., G. Amy, J.E. Drewes, T. Heberer, T.-U. Kim, Y. Watanabbe, 2003. Rejection of organic micropollutants (disinfection by-products, endocrince disrupting sompounds, and pharmaceutically acitve compounds) by NF/RO membranes. *J. Membr. Sci.* 227, 113-121

Kimura, K., S. Toshima, G. Amy, Y. Watanabe, 2004. Rejection of neutral endocrine disrupting compounds and pharmaceuticals active compounds by RO membranes. *J. Membrane Sci.* 245, 71-78

Kilduff, J.E., T. Karanfil, and W.J.Weber, 1998a. TCE adsorption by GAC preloaded with humic substances. *J. Am. Water Works Assoc.* 90(5), 76-89

Kilduff, J.E., T. Karanfil, and W.J.Weber, 1998b. Competitive effects of nondisplaceable organic compounds on trichloroethylene uptake by activated carbon. II. Model verification and applicability to natural organic matter. *J. Colloid Interf. Sci.* 205, 280-289

Kilduff, J. and A. Wigton, 1999. Sorption of TCE by humic-preloaded activated carbon: incorporating size-exclusion and pore blockage phenomena in a competitive adsorption model. *Envion. Sci. Technol.* 33, 250-256

Knappe, D.R.U., Snoeyink, V.L., Prados, M.J., Bourbigot, M.M., Dagois, G., 1993. Adsorption of atrazine by powdered activated carbon. *Proceedings of the AWWA Annual Conference.* Denver, Colorado

Knappe, D.R.U., 1996. Prediction of the removal of atrazine by powdered and granular activated carbon. Ph.D dissertation, University of Illinois, Urbana, Illinois, USA

Knappe, D.R.U., V.L. Snoeyink, P. Roche, M.J. Prados, M.-M. Bourbigot, 1997. The effect of preloading on rapid small-scale column test predictions of atrazine removal by GAC adsorbers. *Water Res.* 31, 2899-2909

Knappe, D.R.U., Y. Matsui, V.L. Snoeyink, P. Roche, M.J. Prados, M.M. Bourbigot, 1998. Predicting the capacity of powdered activated carbon for trace organic compounds in natural waters. *Environ. Sic. Technol.* 32, 1694-1698

Knappe, D.R.U., V.L.Snoeyink, P. Roche, M.J. Prados, M-M. Bourbigot, 1999. Atrazine removal by preloaded GAC. *J. Am. Water Works Assoc.* 91(10), 97-109

Kolpin, D., E. Furlong, M.T. Meyer, E.M. Thurman, S.D. Zaugg, L.B. Barber, H.T. Buxton, 2002. Pharmaceuticals, hormones, and other organic wasterwater contaminants in U.S. streams, 1999-2000: A National reconnaissance. *Environ. Sci. Technol.* 36(6), 1202-1211

Kormos, J., K. Oakes, M. Servos, 2006. Presence and seasonal variability of pharmaceuticals in Southern Ontario drinking water supplies. Proceedings, the 12th Canadian National Conference & 3rd Policy Forum on Drinking Water. Saint John, NB, Canada, Apr. 1-4, 2006

Koutsouba, V., T.Heberer, B. Fuhrmann, K. Schmidt-Baumler, D. Tsipi, A. Hiskia, 2003. Determination of polar pharmaceuticals in sewage water of Greece by gas chromatography-mass spectrometry. *Chemosphere* 51, 69-75

Kuch, H.M. and K.Ballschmiter, 2001. Determination of endocrine-disrupting phenolic compounds and estrogens in surface and drinking water by HRGC-(NCI)-MS in the Picogran per liter range; *Environ. Sci. Technol.* 35, 3201-3206

Kumar, K.V. and S. Sivanesan, 2005a. Comparison of linear and nonlinear method in estimating the sorption isotherm parameters for safranin onto activated carbon. *J. Hazard. Mater.* 123 (1-3), 288-292

Kumar, K.V. and S. Sivanesan, 2005b. Prediction of optimum sorption isotherm: comparison of linear and nonlinear method. *J. Hazard. Mater.* B126, 198-201

Kwapinski, W., M. Winterberg, E. Tsatsas, D. Mewes, 2004. Modelling of the wall effect in packed bed adsorption. *Chem. Eng. Technol.* 27(11), 1179-1185

Lang, J.S., J.J. Giron, A.T. Hansen, R.R. Trussell, W.E. Hodges Jr., 1993. Investigating filter performance as a function of the ratio of filter size to media size. *J. Am. Water Works Assoc.* 85(10), 122-128

Langmuir, I., 1918. The adsorption of gases on plane surfaces of glass, mica and platinum. *J. Am. Chem. Soc.* 40, 1361-1403

Lee, H.B., T.E. Peart, M.L. Svoboda, 2005. Determination of endocrine-disrupting phenols, acidic pharmaceuticals, and personal-care products in sewage by solid-phase extraction and gas chromatography-mass spectrometry. *J. Chromatogr. A.* 1094, 122-129

Legler, J., CE. Van den Brink, A. Brouwer, AJ. Murk, PT. van der Saag, AD. Vethaak, B. van der Brug, 1999. Development of a stably transfected estrogen receptor-mediated luciferase reporter gene assay in the human T47D breast cancer cell line. *Toxicol. Sci.* 48, 55-66

Lerch, O. and P.Zinm, 2003. Derivatization and gas chromatography- chemical ionisation mass spectrometry of selected synthetic and natural endocrine disruptive chemicals. *J. Chromatogr. A.* 991, 77-97

Li, D., J. Park, J.R. Oh, 2001. Silyl derivatization of alkylphenols, chlorophenols, and bisphenol A for simultaneous GC/MS determination. *Anal. Chem.* 73(13), 3089-3095

Li, Q., P. Quinlivan, D.R.U. Knappe, 2002. Effect of activated carbon surface chemistry and pore structure on the adsorption of organic contaminants from aquaeous solution. *Carbon.* 40, 2085-2100

Li, Q., V.L. Snoeyink, B.J. Mariãas, C. Campos, 2003a. Elucidating competitive adsorption mechanisms of atrazine and NOM using model compounds. *Water Res.* 37, 773-784

Li, Q., V.L. Snoeyink, B.J. Marinas, C. Campos, 2003b. Pore blockage effect of NOM on atrazine adsorption kinetics of PAC: the roles of PAC ore size distribution and NOM molecular weight. *Water Res.* 37, 4863-4872

Li, Q., B.J. Mariãas, V.L. Snoeyink, C. Campos, 2003c. Three-component competitive adsorption model for flow-through PAC system. 1. model development and verification with a PAC/membrane system. *Environ. Sci. Technol.* 37(13), 2997-3004

Liang, S. and W.J. Weber, 1985. Parameter evaluation for modeling multicomponent mass transfer in fixed-bed adsorbers. *Chem. Eng. Commun.* 35, 49-61

Lin, W.C., H.C. Chen, and W.H. Ding, 2005. Determination of pharmaceutical residues in waters by solid-phase extraction and large-volume on-line derivatization with gas chromatography-mass spectrometry. *J. Chromatogra. A.* 1065: 279-285

Lindqvist, N., S.Korhonen, J. Jokela, T. Tuhkanen, 2003. Occurrence of pharmaceuticals and personal care products in Finnish surface waters and their removal by chemical coagulation. Proceedings of 3rd International Conference on Pharmaceuticals and Endocrine Disrupting Chemicals in Water. March 2003, Minneapolis, Minnesota, USA.

Lissemore, L., C. Hao, P. Yang, P.K. Sibley, S. Mabury, K.R. Solomon, 2006. An exposure assessment for selected pharmaceuticals within a watershed in Southern Ontario. *Chemosphere* 64(5), 717-729

Lo, I.M.C. and P.A. Alok, 1996. Computer simulation of activated carbon adsorption for multi-component systems. *Environ. Int.* 22(2), 239-252

Lopez, F.J., J. Beltran, M. Forcada, F. Hernandez, 1998. Comparison of simplified methods for pesticide residue analysis : Use of large-volume injection in capillary gas chromatography. *J. Chromatogr. A.* 823, 25-33

Matsui, Y., D.R.U. Knappe and R. Takagi, 2002. Pesticide adsorption by granular activated carbon adsorbers. 1. effect of natural organic matter preloading on removal rates and model simplification. *Environ. Sci. Technol.* 36, 3426-3431

Matsui, Y., Y. Fukuda, Y. Inoue, T. Matsushita, 2003. Effect of natural organic matter on powdered activated carbon adsorption of trace contaminants: characteristics and mechanism of competitive adsorption. *Water Res.* 37(18), 4413-4424

MathWorks, 2004. Curve fitting toolbox for use with Matlab®, Curve fitting toolbox user's guide. The MathWorks, Inc.

McDowell, D.C., M.M. Huber, M. Wagner, U.V. Gunten, T.A. Ternes, 2005. Ozonation of carbamazepine in drinking water: identification and kinetic study of major oxidation products. *Environ. Sci. Technol.* 39, 8014-8022

Metcalfe, C.D., B.G. Koenig, D.T. Bennie, M. Servos, T.A. Ternes, R. Hirsch, 2003a. Occurrence of neutral and acidic drugs in the effluents of Canadian sewage treatment plants. *Environ. Toxicol. Chem.* 22(12), 2872-2880

Metcalfe, C.D., X.S. Miao, B.G. Koenig, J. Struger, 2003b. Distribution of acidic and neutral drugs in surface waters near sewage treatment plants in the lower Great Lakes, Canada. *Environ. Toxicol. Chem.* 22(12), 2881-2889

Miao, X., B.G. Koenig, C.D. Metcalfe, 2002. Analysis of acidic drugs in the effluents of sewage treatment plants using liquid chromatography-electrospray ionization tandem mass spectrometry. *J. Chromatogr. A.* 952, 139-147

Miao, X., Yang, J., Metcalfe, C.D., 2005. Carbamazepine and its metabolites in wastewater and in biosolids in a municipal wastewater treatment plant. *Environ. Sci. Technol.* 39, 7469-7475

Morris, G. and G. Newcombe, 1993. Granular activated carbon: the variation of surface properties with the adsorption of humic substances. *J. Colloid Interf. Sci.* 159(2), 413-420

Motulsky, H.J., and Christopoulos, A. 2004. Fitting models to biological data using linear and nonlinear regression. A practical guide to curve fitting. New York, NY: Oxford University Press.

Mouatassim-Souali, A., S.L.T.Karolak, D. Perdiz, M. Cargouet, Y. Leve, 2003. Validation of a quantitative assay using GC/MS for trace determination of free and conjugated estrogens in environmental water samples; *J. Sep. Sci.* 26,105-111

Myers, A.L. and J.M. Prausnitz, 1965. Thermodynamics of mixed-gas adsorption. *AIChE Jour*. 11, 121-127

Najm, I.N., V.L. Snoeyink, M.T. Suidan, C.H. Lee, Y. Richard, 1990. Effect of particle size and background natural organics on the adsorption efficiency of PCA. *J. Am. Water. Works Assoc.* 82(1), 65-72

Najm, I.N., Snoeyink, V.L. and Richard, Y. 1991. Effect of initial concentration of a SOC in natural water on its adsorption by activated carbon. *J. Am. Water. Works Assoc.* 83(8), 57-63

Newcombe, G., 1994. Activated carbon and soluble humic substances: adsorption, desorption and surface charge effects. *J. Colloid Interf. Sci.* 164(2), 452-462

Newcombe, G., M. Drikas, S. Assemi, R. Beckett, 1997a. Influence of characterized natural organic material on activated carbon adsorption: I Characterisation of concentrated reservoir water. *Water Res.* 31(5), 965-972

Newcombe, G., M. Drikas and R. Hayes, 1997b. Influence of characterized natural organic material on activated carbon adsorption: II Effect on pore volume distribution and adsorption of 2-Methylisoborneol. *Water Res.* 31(5), 1065-1073

Newcombe, G., J. Morrison, C. Hepplewhite, D.R.U. Knappe, 2002a. Simultaneous adsorption of MIB and NOM onto activated carbon I. Characterisation of the system and NOM adsorption. *Carbon* 40, 2135-2146

Newcombe, G., J. Morrison, C. Hepplewhite, D.R.U. Knappe, 2002b. Simultaneous adsorption of MIB and NOM onto activated carbon II. Competitive effects. *Carbon* 40, 2147-2156

Nghiem, L.D., A.I. Schäfer, M. Elimelech, 2005. Pharmaceutical retention mechanisms by nanofiltration membranes. *Environ. Sci. Technol.* 39, 7698-7705

Öllers, S., H.P.Singer, P. Fassler, S.R. Muller, 2001. Simultaneous quantification of neutral and acidic pharmaceuticals and pesticides at the low ng/L level in surface and wastewater. *J. Chromatogr. A.* 911, 225-234

Olmstead, K.P. and W.J. Weber, 1990. Statistical analysis of mass-transfer parameters for sorption processes and models. *Environ. Sci. Technol.* 24(11), 1693-1700

Oravitz, J.L., 1984. Transport of trace organics with one-dimensional saturated flow: mathematical modeling and parameter sensitivity analysis. MASc thesis, Michigan Technological University, Houghton, Michigan, USA

Parrott, J., M. Wade, 2001. An Overview of Testing Procedures and Approaches for Identifying Endocrine Disrupting Substances. *Water Qual. Res. J. Canada* 36: 273-291

Paterson, S., R.Cordero, S. McCulloch, P. Houldsworth, 2000. Analysis of urine for drugs of abuse using mixed-mode solid-phase extraction and gas chromatography-mass spectrometry. *Ann. Clin. Biochem.* 37, 690-700

Pelekani, C. and V.L. Snoeyink, 1999. Competitive adsorption in natural water: role of activated carbon pore size. *Water Res.* 33(5), 1209-1219

Pelekani, C. and V.L. Snoeyink, 2000. Competitive adsorption between atrazine and methylene blue on activated carbon: the importance of pore size distribution. *Carbon* 38, 1423-1436

Perrich, J.R., 1981. Activated carbon adsorption for wastewater treatment, Boca Raton, Florida, CRC Press Inc.

Petrovic, M., E. Eljarrat, M.J. López de Alda, D. Barceló, 2002. Recent advances in the mass spectrometric analysis related to endocrine disrupting compounds in aquatic environmental sample. *J. Chromatogr.A.* 974, 23-51

Petrovic, M., A.Diaz, F. Ventura, D. Barcelo, 2003. Occurrence and removal of estrogenic short-chain ethoxy nonylphenolic compounds and their halogenated derivatives during drinking water production. *Environ. Sci. Technol.* 37, 4442-4448

Pinkston, K.E. and D.L.Sedlak, 2003. Transformation of pharmaceuticals during chlorination. Proceedings of 3rd International Conference on Pharmaceuticals and Endocrine Disrupting Chemicals in Water. March 2003, Minneapolis, Minnesota, USA.

Pirbazari, M., V. Ravindvan, B.N. Badriyha, S. Craig, M.J. McGuire, 1993. GAC adsorber design protocol for the removal of off-flavors. *Water Res.* 27(7), 1153-1166

Planas, C., J.M. Guadayol, 2002. Degradation of Polyethoxylated Nonylphenols in a Sewage Treatment Plant. Quantitative Analysis by Isotopic Dilution-HRGC/MS; *Water Res.* 36, 982-988

Pomati, F., A.G. Netting, D. Calamari, B. Neilian, 2004. Effects of erythromycin, tetracycline and ibuprofen on the growth of *Synechocystis* sp. And *Lemna minor*. *Aquat. Toxicol.* 67, 387-396

Pomati, F., S. Castiglioni, E. Zuccato, R. Fanelli, D. Vigetti, C. Rossetti, D. Calamari, 2006. Effects of a complex mixture of therapeutic drugs at environmental levels on human embryonic cells. *Environ. Sci. Technol.* 40(7), 2442-2447

Purdom, C.E., Hardiman P.A., Bye V.J., Eno N.C., Tyler C.R., Sumpter J.P., 1994. Estrogenic effects of effluents from sewage treatment works, *Chem. Ecol.*, 8, 275-285

Qi, S., 1992. Evaluation of Activated carbon adsorption for removal of SOCs from natural water. Ph.D dissertation, University of Illinois, Urbana, Illinois, USA

Qi, S., S.S. Adham, V.L. Snoeyink, B.W. Lykins, 1994. Prediction and verification of atrazine adsorption by PAC. *J. Environ. Eng.-ASCE* 120(1), 202-218

Qi, S., L. Schideman, B.J. Mariñas, V.L. Snoeyink, C. Campos, 2007. Simplification of the IAST for activated carbon adsorption of trace organic compounds from natural water. *Water Res.* 41(2), 440-448

Queen's Landing Inn., 2002. Assessment and Management of Pharmaceuticals and Personal Care Products in the Canadian Environment: An interactive CD of the Proceedings of a Multi-Stakeholder Workshop

Quintana, J.B., J.Carpinteiro, I. Rodríguez, R.A. Lorenzo, A.M. Carro, R. Cela, 2004. Determination of natural and synthetic estrogens in water by gas chromatography with mass spectrometric detection. *J. Chromatogr. A.* 1024, 177-185

Radke, C.J. and J.M. Prausnitz, 1972. Thermodynamics of multi-solute adsorption from dilute liquid solutions. *AIChE Jour.* 18, 761-768

Raghavan, N.S. and D.M. Ruthven, 1983. Numerical simulation of a fixed-bed adsorption column by the method of orthogonal collocation. *AIChE Jour.* 29(6), 922-925

Reid, C.R., J.M. Prausnitz, T.K. Sherwood, 1977. The properties of Gases and Liquids (3rd Ed.), McGraw-Hill Book Company, USA

Rivera-Utrilla, J., I. Bautista-Toledo, M.A. Ferro-Garcia, C. Moreno-Castilla, 2003. Bioadsorption of Pb(II), Cd(II), and Cr(VI) on activated carbon from aqueous solutions. *Carbon.* 41, 323-330

Roberts, P.V. and R.S. Summers, 1982. Performance of granular activated carbon for total organic carbon removal. *J. Am. Water Works Assoc.* 74(2), 113-118

Roberts, P.V., P. Cornel, and R.S. Summers, 1985. External mass-transfer rate in fix-bed adsorption. *J. Environ. Eng.-ASCE.* 111(6), 891-904

Rodríguez, I., J.B.Quintana, J. Carpinteiro, A.M. Carro, R.A. Lorenzo, R. Cela, 2003. Determination of acidic drugs in sewage water by gas chromatography-mass spectrometry as tert.-butyldimethysilyl derivatives. *J. Chromatogr. A.* 985, 265-274

Rompa, M., E.Kremer, B. Zygmunt, 2003. Derivatisation in gas chromatographic determination of acidic herbicides in aqueous environmental samples. *Anal. Bioanal. Chem.* 377, 590-599

Rotkowsky, D.A., 1990. Handbook of nonlinear regression models. New York, Marcel Dekker Inc.

Roy, D., G.T. Wang, and D. Adrian, 1993. A simplified solution technique for carbon adsorption model. *Water Res.* 27(6), 1033-1040

Sacher F., F.T.Lange, H.-J Braucn, I. Blankenhorn, 2001. Pharmaceuticals in groundwaters-Analytical methods and results of a monitoring program in Baden-Wurttemberg, germany. *J. Chromatogr. A.* 938, 199-210

Schideman, L.C., B.J. Marinas, V.L. Snoeyink, C. Campos, 2006a. Three-Component competitive adsorption model for fixed-bed and moving-bed granular activated carbon adsorbers. Part I. Model development. *Environ. Sci. Technol.* 40, 6805-6811

Schideman, L.C., B.J. Marinas, V.L. Snoeyink, C. Campos, 2006b. Three-Component competitive adsorption model for fixed-bed and moving-bed granular activated carbon adsorbers. Part II. Model parameterization and verification. *Environ. Sci. Technol.* 40, 6805-6811

Schwab, B.W., E.P. Hayes, J.M. Fiori, F.J. Mastrocco, N.M. Roden, D. Cragin, R.D. Meyerhoff, V.J. D'Aco, P.D. Anderson, 2005. Human pharmaceuticals in US surface waters: a human health risk assessment. *Regul Toxicol. Pharmacol.* 42(3), 296-312

Servos, M.R., T.D.Bennie,M.E. Starodub, J.C. Orr. 2003. Pharmaceuticals and personal care in the environment: a summary of published literature. NWRI Contribution No. 02-309. Technical Report. National Water Research Institute, Environment Canada, Burlington, ON, Canada

Servos, M.R., M. Smith, R. McInnis, K. Burnison, B-H. Lee, P. Seto, S. Backus, 2006. Presence and removal of acidic drugs in drinking water in Ontario, Canada. *Water Qual. Res. J. Can.* Submitted for publication

Shareef, A., C.J. Parnis, M.J. Angove, J.D. Wells, B.B. Johnson, 2004. Suitability of N,O-bis(trimethylsilyl)trifluoroacetamide and N-(tert-butyldimethylsilyl)-N-methyltrifluoroacetamide as derivatization reagents for the determination of the estrogens estrone and 17α-ethinylestradiol by gas chromatography–mass spectrometry. *J. Chromatogr. A.* 1026 (1-2), 295-300

Shareef, A., M.J. Angove, J.D. Wells, 2006. Optimization of silylation using *N*-methyl-*N*-(trimethylsilyl)-trifluoroacetamide, *N*,*O*-bis-(trimethylsilyl)-trifluoroacetamide and *N*-(*tert*-butyldimethylsilyl)-*N*-methyltrifluoroacetamide for the determination of the estrogens estrone and 17α-ethinylestradiol by gas chromatography–mass spectrometry. *J. chromatogr. A.* 1108 (1), 121-128

Smith, E., 1991. Modified solution of homogeneous surface diffusion model for adsorption. *J. Environ. Eng.-ASCE* 117(3), 461

Smith E.H., S. Tseng, and W.J. Weber, 1987. Modeling the adsorption of target compounds by GAC in the presence of background dissolved organic matter. *Environ. Prog.* 6, 18-25

Smith, E.H. and W.J.Weber, 1989. Evaluation of mass transfer parameters for adsorption of organic compounds from complex organic matrices. *Environ. Sci. Technol.* 23, 713-722

Snoeyink, V.L., 1990. Adsorption of organic compounds, In water quality and treatment, 4th ed. McGraw-Hill. Inc. New York, USA

Snyder, S.A., B.Vanderford, 2002. Analytical methods for measuring endocrince disruptors in water. Proceedings of Water Quality Technology Conference, Nov. 2002. Seattle, Washington, USA

Snyder, S.A., P. Westerhoff, Y. Yoon, D.L. Sedlak, 2003. Pharmaceuticals, personal care products, and endocrine disruptors in water: implications for the water industry. *Environ. Eng. Sci.* 20(5), 449-469

Snyder, S.A., S. Adham, A.M. Redding, F.S. Cannon, J. DeCarolis, J. Oppenheimer, E.C. Wert, Y. Yoon., 2007. Role of membranes and activated carbon in the removal of endocrine disruptors and pharmaceuticals. *Desalination.* 202, 156-181

Soliman, M.A., J.A. Pedersen, I.H. Suffet, 2004. Rapid gas chromatography-mass spectrometry screening method for human pharmaceuticals, hormones, antioxidants and plasticizers in water. *J. Chromatogr. A.* 1029, 223-237

Sontheimer, H., J.C. Crittenden, R.S. Summer, 1988. Activated carbon for water treatment. Second edition, DVGW-Forschungsstelle

Souali, A.M., S.L.T. Karolak, D. Perdiz, M. Cargouet, Y. Levi, 2003. Validation of a quantitative assay using GC/MS for trace determination of free and conjugated estrogens in environmental water samples; *J. Sep. Sci.* 26, 105-111

Speth, T.F., 1991. Evaluating capacities of GAC preloaded with natural water. *J. Environ. Eng.-ASCE* 117(1), 66-79

Speth, T.F. and R.J. Miltner, 1989. Effect of preloading on the scale-up of GAC microcolumns. *J. Am. Water Works Assoc.* 81(5), 141-148

Stackelberg, P.E., E.T. Furong, M.T. Meyer, S.D. Zaugg, A.K. Henderson, D.B. Reissman, 2004. Persistence of pharmaceutical compounds and other organic wastewater contaminants in a conventional drinking-water-treatment plant. *Sci. Tol. Environ.* 329, 99-113

Stackelberg, P.E., J. Gibs, E.T. Furlong, M.T. Meyer, S.D. Zaugg, R.L. Lippincott, 2007. Efficiency of conventional drinking-water-treatment processes in removal of pharmaceuticals and other organic compounds. *Sci. Tol. Environ. In press*

Stan, H.J., T Heberer, 1997. Pharmaceuticals in the aquatic environment. *Dossier Water Analysis*. 25(7), M20-23

Staples, C.A., P.B.Dorn, G.M. Klecka, S.T. O'Block, D.R. Branson, L.R. Harris, 2000. Bisphenol A concentrations in receiving waters near US manufacturing and processing facilities. *Chemosphere* 40,521-525

Stuer-Lauridsen, F., M.Birkved, L.P. Hansen, H.-C. Holten Lutzhoft, B. H.-Sorensen, 2000. Environmental risk assessment of human pharmaceuticals in Denmark after normal therapeutic use. *Chemosphere.* 40,783-793

Stumpf, M., T.A. Ternes, K. Heberer, P. Seel, W. Baumann, 1996. Determination of pharmaceuticals in sewage plants and river water. *Vom Wasser.* 86, 291-303

Suffet, IH., 1980. An evaluation of activated carbon for drinking water treatment: a national academy of science report. *J. Am. Water Works Assoc.* 72 (1), 41-50

Summer, R.S. and P.V. Roberts, 1988a. Activated carbon adsorption of humic substances, I heterodisperse mixture and desorption. *J. Colloid Interf. Sci.* 122(2), 367-381

Summer, R.S. and P.V. Roberts, 1988b. Activated carbon adsorption of humic substances, II size exclusion and electrostatic interactions. *J. Colloid Interf. Sci.* 122(2), 382-397

Summers, R.C., B. Haist, J. Koehler, J. Ritz, G. Zimmer, H. Sontheimer, 1989. The influence of background organic matter on GAC adsorption. *J. Am. Water Works Assoc.* 81 (5), 66-74

Sun, L., F. Meuneir, 1991. An improved finite difference method for fixed-bed multicomponent sorption. *AIChE Jour.* 37(6), 244

Tanghe, T. and W.Verstraete, 2001. Adsorption of nonylphenol onto granular activated carbon. *Water, Air, and Soil Pollution.* 131, 61-72

Ternes T.A. 1998. Occurrence of drugs in German sewage treatment plants and rivers; *Water Res.* 32(11), 3245-3260

Ternes, T.A., R. Hirsch, J. Mueller, K. Haberer, J. Fresenius, 1998. Methods for the determination of neutral drugs as well as betablockers and $ß_2$-sympathomimetics in aqueous matrices. *Anal. Chem.* 362, 329-340

Ternes, T.A., M. Stumpf, J. Mueller, 1999. Behaviour and Occurrence of Estrogens in Municipal Sewage Treatment Plants – I. Investigations in Germany, Canada and Brazil. *Sci. Total Environ.* 225, 81-90

Ternes, T.A., 2001. Analytical methods for the determination of pharmaceuticals in aqueous environmental samples. *Trends in Analytical Chemistry.* 20, 419-434

Ternes, T.A., M. Meisenheimer, D. McDowell, F. Sacher, H. Brauch, B. Haist-Gulde, G. Preuss, U. Wilme, N. Zulei-Seibert, 2002. Removal of pharmaceuticals during drinking water treatment. *Environ. Sci. Technol.* 36(17), 3855-3863

Ternes, T.A., J.Stuber, N. Herrmann, D. McDowell, A. Ried, M. Kampmann, B. Teiser, 2003. Ozonation: a tool for removal of pharmaceuticals, contrast media and musk fragrances from wasterwater? *Water Res.* 37, 1976-1982

Tixier, C., H.P. Singer, S. Oellers, S.R. Muller, 2003. Occurrence and fate of carbamzepine, clofibric acid, diclofenac, ibuprofen, ketoprofen, and naproxen in surface waters. *Environ. Sci. Technol.* 37(6), 1061-1068

Trenholm, R.A., B.J. Vanderford, J.C. Holady, D.J. Rexing, S.A. Snyder, 2006. Broad range analysis of endocrine disruptors and pharmaceuticals using gas chromatography and liquid chromatography tandem mass spectrometry. *Chemosphere* 65(11), 1991-1998

USEPA, 2001. Removal of Endocrine Disruptor Chemicals Using Drinking Water Treatment Processes, http://www.epa.gov/ORD/NRMRL/Pubs/2001/edc/625r00015.pdf, latest access on Feb. 8, 2006

US NIST, 2006. Engineering Statistics. NIST Handbook 151. online access http://www.itl.nist.gov/div898/handbook/index.htm, checked by Feb. 2007

Vethaak, A.D., G.B.J.Rijs, el at., 2002. Estrogens and xeno-estrogens in the aquatic environment of the Netherlands—Occurrence, Potency and Biological Effects; Reports from the Dutch National Institute of Inland Water Management and Waster Water Treatment (RIZA) and the Dutch National Institute for Coastal and Marine Management (RIKZ); Feb. 2002

Villadsen, J.V. and M.L. Michelsen, 1978. Solution of differential equation models by polynomial approximation. Pretice-Hall Inc. N.J., USA

Villadsen, J.V. and W.E. Stewart, 1967. Solution of boundary-value problems by orthogonal collocation. *Chem. Eng. Sci.* 22: 1483-1501

Voulvoulis, N. and M. Scrimshaw, 2003. “Methods for the Determination of Endocrine Disrupters” in Endocrine Disrupters in Wastewater and Sludge Treatment. CRC Press, FL, USA

Vogna, D., R.Marotta, R. Andreozzi, A. Napolitano, M. d'Ischia, 2004. Kinetic and chemical assessment of the UV/H2O2 treatment of antiepileptic drug carbamazepine. *Chemosphere* 54, 497-505

Walker, D. 2000. Oestrogenicity and wasterwater recycling: Experience from Essex and Suffolk water. *J. of the chartered institution of water and environmental management.* 14, 427-431

Wang, G.S. and K.T. Alben, 1998. Effect of preadsorbed background organic matter on granular activated carbon adsorption of atrazine. *Sci. Total Environ.* 224, 221-226

Weber, W.J. and K.T. Liu, 1980. Determination of mass transport parameters for fixed-bed adsorbers. *Chem. Eng. Commun.* 6, 49-60

Weber, W.J. and C.K. Wang, 1987. A microscale system for estimation of model parameters for fix-bed adsorbers. *Environ. Sic. Technol.* 21, 1096

Wells, R.J., 1999. Recent advances in non-silylation derivatization techniques for gas chromatography. *J. Chromatogr. A.* 843, 1-18

Westerhoff, P., Y. Yoon, S. Snyder, E. Wert, 2005. Fate of endocrine disruptor, pharmaceutical, and personal care product chemicals during simulated drinking water treatment processes. *Environ. Sci. Technol.* 39(17), 6649-6663

WHO, International Program on Chemical Saftety. 2002. Global Assessment of the State-of-the-Science of Endocrine Disruptors. http://www.who.int/pcs/emerg-site/edc/global_edc_TOC.htm

Winslow, S.D., B.V. Pepich, M.V. Bassett, S.C. Wendelken, 2001. Microbial inhibitors for U.S. EPA drinking water methods for determination of organic compounds. *Environ. Sci. Technol.* 35, 4103-4110

Wintgens, T., M. Gallenkemper, T. Melin, 2002. Endocrine disrupter removal from wasterwater using membrane bioreactor and nanofiltration technology. *Desalination.* 146, 387-391

Wong, Y.C., Y.S. Szeto, W.H. Cheung, G. McKay, 2004. Adsorption of acid dyes on chitosan – equilibrium isotherm analyses. *Process Biochem.* 39, 693-702

Xiao, X., D.V.McCalley, J. McEvoy, 2001. Analysis of estrogens in river water and effluents using solid-phase extraction and gas chromatography-negative chemical ionisation mass spectrometry of the pentafluorobenzoyl derivatives. *J. Chromatogr. A.* 923, 195-204

Yamamoto, T. and A.Yasuhara, 2002. Chlorination of bisphenol A in aqueous media: formation of chlorinated bisphenol A congeners and degradation to chlorinated phenolic compounds. *Chemosphere.* 46, 1215-1223

Ying, G.G., B. Williams, R. Kookana, 2002. Environmental fate of alkylphenols and alkylphenol ethoxylates—a review. *Environ. Int.* 28, 215-226

Ying, G.G., R.S. Kookana, Y.J. Ru. 2002a. Occurrence and fate of hormone steroids in the environment. *Environ. Int.* 28: 545-551

Yoon, Y., P. Westerhoff, S. Snyder, R. Song, B. Levine, 2002. A review on removal of endocrine-disrupting compounds and pharmaceuticals by drinking water treatment processes. Proceedings of Water Quality Technology Conference, Nov. 2002. Seattle, Washington, USA

Yoon, Y, P. Westerhoff, S. Snyder, M. Esparza, 2003. HPLC-fluorescence detection and adsorption of bisphenol A, 17β-estradiol, and 17α-ethynyl estradiol on powdered activated carbon. *Water Res.* 37, 3530-3537

Yu, Z., S. Peldszus, P.M. Huck, W.B. Anderson, 2005. Adsorption of Selected Pharmaceuticals and Endocrine Disrupting Substances by GAC at Low Concentration Levels. *Proceedings of AWWA Water Quality and Technology Conference 2005,* Quebec City, Canada

Yu, Z., S. Peldszus, P.M. Huck, 2007. Optimizing gas chromatographic–mass spectrometric analysis ofselected pharmaceuticals and endocrine-disrupting substancesin water using factorial experimental design. *J. Chromatogr. A.* 1148, 65-77

Zimmer, G., 1988. Untersuchungen zur adsorption organischer spurenstoffe aus natürlichen wässern. Doctoral dissertation, Univsersity of Karlsruhe, Germany

Zhang, Y. and J.L. Zhou, 2005. Removal of estrone and 17β-estradial from water by adsorption. *Water Res.* 39, 3991-4003

Zwiener, C. and F.H.Frimmel, 2000. Oxidative treatment of pharmaceuticals in water. *Water Res.* 34(6), 1881-1885

Zuccato, E., D. Calamari, M. Natangelo, R. Fanelli, 2000. Presence of therapeutic drugs in the environment. *The Lancet.* 335, 1789-1790

Appendix A
Orthogonal Collocation Solution to the PSDM

Equations 2.30 – 2.39 can be solved by the method of orthogonal collocation, which is one of the methods of weighted residuals (Villadsen and Stewart, 1967). This method can solve the differential equations by obtaining the solutions at only a few collocation points, which are located at the roots of the polynomials where the polynomial approximations agree exactly with the true values of the dependent variable. This simplifies the complexity of the solutions compared to the finite element method. The major advantage for choosing this method is that it is very amenable when the parameters in functions are changing with spatial and time factors (Kim, *et al.*, 1978).

In the collocation method, an trial function, $y^{(n)}(x)$, is chosen to approximate the exact solution, u(x), at selected collocation points.

The differential equation is: $$L^V u(x) - g(x) = 0 \qquad \text{A.1}$$

The approximate solution is: $$L^V y^{(n)}(x) - g(x) = R(x) \qquad \text{A.2}$$

in which L is the differential operator, V is the function domain, g(x) is general function, R(x) is the residual.

In this case, $y^{(n)}(x)$ is a polynomial with the highest order ≤ 2n-1. $P_i(x)$ in the following equation is a group of orthogonal polynomials with degree of i in x.

$$y^{(n)}(x) = \sum_{i=1}^{n} a_i^{(n)} P_i(x) \qquad \text{A.3}$$

When an appropriate weight function, $w(x)$, is chosen based on the differential equation and its boundary conditions, and $y^{(n)}(x)$ is adjusted to satisfy the differential equation A.1 at the collocation points, the following residual functions:

$$w_i(x) R_i(x) \qquad \text{A.4}$$

equals zeros or contain a polynomial factor $G_n(x)$, whose zeros are the collocation points. Both $G_n(x)$ and $P_i(x)$ satisfy the orthogonality relationship (Villadsen and Stewart, 1967; Villadsen and Michelsen, 1978):

$$\int_0^1 x^{\alpha}(1-x)^{\beta} P_i(x)P_n(x)dx = C_i\delta_{in} \qquad \text{A.5}$$

Therefore, the collocation points can be selected as the zeros of Jacobi polynomial $P_n^{(\alpha,\beta)}(x)$.

$y^{(n)}(x)$ can be expressed as the form of Lagrange interpolation polynomials:

$$y^{(n)}(x) = y_N = \sum_{i=1}^{N+1} y(x_i)l_i(x) \qquad \text{N = n} \qquad \text{A.6}$$

where $l_i(x)$ is Lagrange interpolation polynomial,

$$l_i = \frac{p_{N+1}(x)}{(x-x_i)P_{N+1}^{(1)}(x_i)} \qquad \text{A.7}$$

where $p_{N+1}(x)$ is the node polynomial, which is also set to satisfy the orthogonality relationship.

$$\frac{d_k(y_N)}{dx^k} = \sum_{i=1}^{N+1} y_i \left[\frac{d^k}{dx^k} l_i(x)\right] \qquad \text{A.8}$$

According to the equations above (A.6 – 8), the derivatives are replaced with the following matrices:

$$\frac{d}{dx}(y_N) = \underline{A}\,\underline{y} \qquad \text{A.9}$$

$$\frac{d^2}{dx^2}(y_N) = \underline{B}\,\underline{y} \qquad \text{A.10}$$

$$\int_0^1 W(x)y_N dx = \sum_{i=1}^{N+1} y_i \left[\int_0^1 W(x)l_i(x)dx\right] = \underline{w}\,\underline{y} \qquad \text{A.11}$$

The key equations A.9 – 11 can substitute the spatial derivatives and integrals in the PSDM equations. Accordingly, the set of PDEs can be transformed into a set of ODEs, which can be solved by some commercially available software toolboxes (e.g. public FORTRAN code LSDOE). More details about the method of orthogonal collocation are given in Villadsen and Stewart (1967) and Villadsen and Michelsen (1978). This method has successfully been applied for solving PDE problems in GAC fixed-bed system by some researchers (e.g. Kim *et al.*, 1978; Raghavan and Ruthven, 1983; Crittenden *et al.*, 1986; Gierke *et al.*, 1990; Roy *et al.*, 1992; Carter, 1993).

In this study, PDEs of the PSDM were discretized as presented by Crittenden *et al.* (1986) and Carter (1993). In the application, MC collocation points and NC collocation points were used for the axial direction and the radial direction, respectively.

Applying the orthogonal collocation points to equations 2.30 – 2.34 yields the following MC ODEs for the axial direction:

$$\frac{d\overline{C}_b(k,T)}{dT} = (D_g+1)\sum_{i=1}^{MC}\left[\frac{B_{i,k}{}^z}{Pe} - A_{i,k}{}^z\right]\overline{C}_b(i,T) - 3(D_g+1)St\left[\overline{C}_b(k,T) - \overline{C}_p(NC,k,T)\right]$$

for k = 2 to MC-1 A.12

Initial condition:

$$\overline{C}_b(k,T=0) = 0 \qquad \text{A.13}$$

Boundary conditions:

$$\frac{d\overline{C}_b(k=1,T)}{dT} =$$

$$\left\{\left[(D_g+1)[\overline{C}_I(T) - \overline{C}_b(MC,T)] - \sum_{k=2}^{MC-1}[(W_k{}^z - W_{MC}{}^z\frac{A_{MC,k}{}^z}{A_{MC,MC}{}^z})\frac{d\overline{C}_b(k,T)}{dT}]\right]\right.$$

$$\left.\cdot\left(W_1{}^z - W_{MC}{}^z\frac{A_{MC,1}{}^z}{A_{MC,MC}{}^z}\right)^{-1}\right\}$$

$$-\left\{3D_g\left(\sum_{k=1}^{MC}W_k{}^z\left(\sum_{j=1}^{NC}W_j{}^r\frac{d\overline{X}(j,k,T)}{dT}\right)\right)\cdot\left(W_1{}^z - W_{MC}{}^z\frac{A_{MC,1}{}^z}{A_{MC,MC}{}^z}\right)^{-1}\right\} \qquad \text{A.14}$$

$$\frac{d\overline{C}_b(MC,T)}{dT} = -\sum_{k=1}^{MC-1}\frac{A_{MC,k}{}^z}{A_{MC,MC}{}^z}\frac{d\overline{C}_b(k,T)}{dT} \qquad \text{A.15}$$

Equations 2.35 – 2.38 can be transformed into the following ODEs at NC collocation points for the radial direction:

$$\frac{d\overline{X}(j,k,T)}{dT} =$$

$$\frac{(D_g+1)}{D_g}\sum_{i=1}^{NC}\left[\left(Ed_p-\frac{D_{gp}}{D_{gs}}Ed_s\right)\cdot {B_{i,j}}^r\overline{C}_p(i,k,T)+\left(Ed_s+\frac{D_{gp}}{D_{gs}}Ed_s\right)\cdot {B_{i,j}}^r\overline{X}(i,k,T)\right]$$

for j = 1 to NC-1 and k = 1 to MC A.16

Initial condition:

$$\overline{X}(j,k,T=0)=0 \qquad \overline{C}_p(j,k,T=0)=0 \qquad \text{A.17}$$

Boundary condition:

$$\frac{d\overline{X}(NC,k,T)}{dT}=\frac{(D_g+1)}{D_g}\frac{St}{{W_{NC}}^r}\left[\overline{C}_b(k,T)-\overline{C}_p(NC,k,T)\right]-\sum_{j=1}^{NC-1}\frac{{W_j}^r}{{W_{NC}}^r}\frac{d\overline{X}(j,k,T)}{dT}$$

for k = 1 to MC A.18

The local equilibrium equation 2.39 can be express as:

$$\overline{X}(j,k,T)=\frac{D_{gp}}{D_g}\overline{C}_p(j,k,T)+\frac{D_{gs}}{D_g}\overline{C}_p(j,k,T)^{1/n} \qquad \text{A.19}$$

${A_{i,k}}^z$, ${B_{i,k}}^z$, and ${W_i}^z$ are the elements in orthogonal collocation matrices and vector in the axial direction. Similarly, ${B_{i,j}}^r$ and ${W_i}^r$ are the elements in orthogonal collocation matrix and vector in the radial direction. Normally, the more collocation points are used in a calculation, the higher the accuracy can be achieved (Villadsen and Michelsen, 1978). Both Raghavan and Ruthven (1983) and Carter (1993) found that seven axial points and three radial points could provide sufficient accuracy of the solution. Therefore, eight axial points and four radial points were used in this study, and corresponding collocation matrices and vectors were obtained from Oravitz (1984).

Appendix B

Supplementary Information for the Analytical Method

Table B-1 Structure of selected target compounds

Compound Name	CAS No.	Structure	Molecular Weight	Log K_{ow}
E1	53-16-7	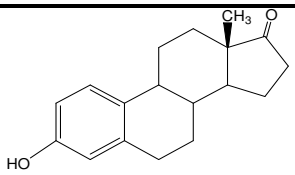	270.4	3.43
EE2	57-63-6	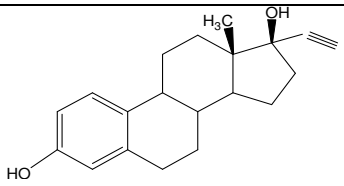	296.4	4.51
4-n-NP	104-40-5	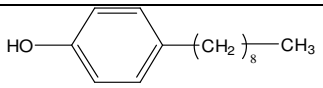	220.36	4.48
NP1EO	27986-36-3	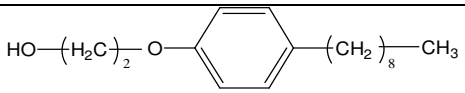	264.44	4.17
NP1EC		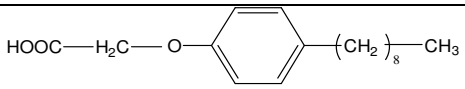	278.42	1.34
4-n-OP	1806-26-4	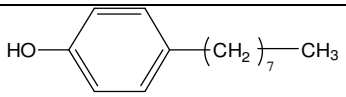	206.33	4.12
Diltiazem	33286-22-5	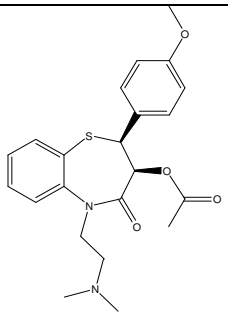	414.52	2.7
Nifedipine	21829-25-4	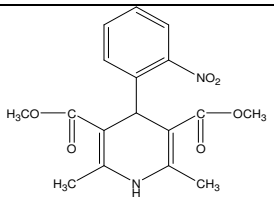	346.34	2.2

Ibuprofen	15687-27-1	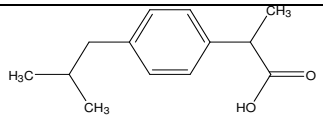	206.29	4.91
Naproxen	22204-53-1	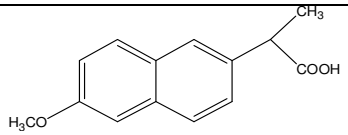	230.27	3.2
Diclofenac	15307-86-5	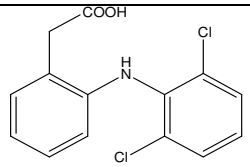	296.15	4.5
Acetaminophen	103-90-2	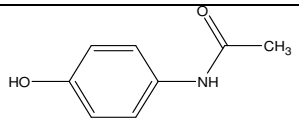	151.17	0.46
Salicylic acid	69-72-7	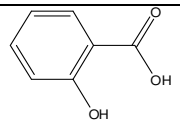	138.12	2.3
Gemfibrozil	25812-30-0	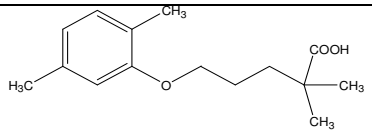	250.34	4.8
Carbamazepine	298-46-4	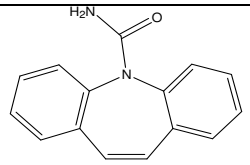	236.28	2.45
Propranolol	318-98-9	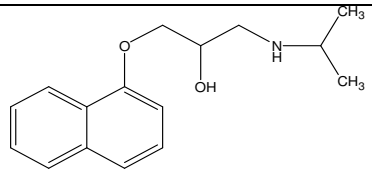	295.81	0.74
Codeine	76-57-3	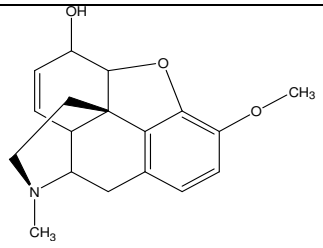	299.37	1.2
Triclosan	3380-34-5	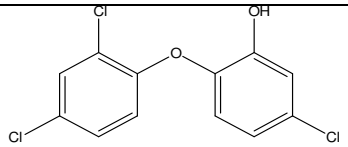	289.55	4.8

Appendix C

Additional Data for Stability Tests

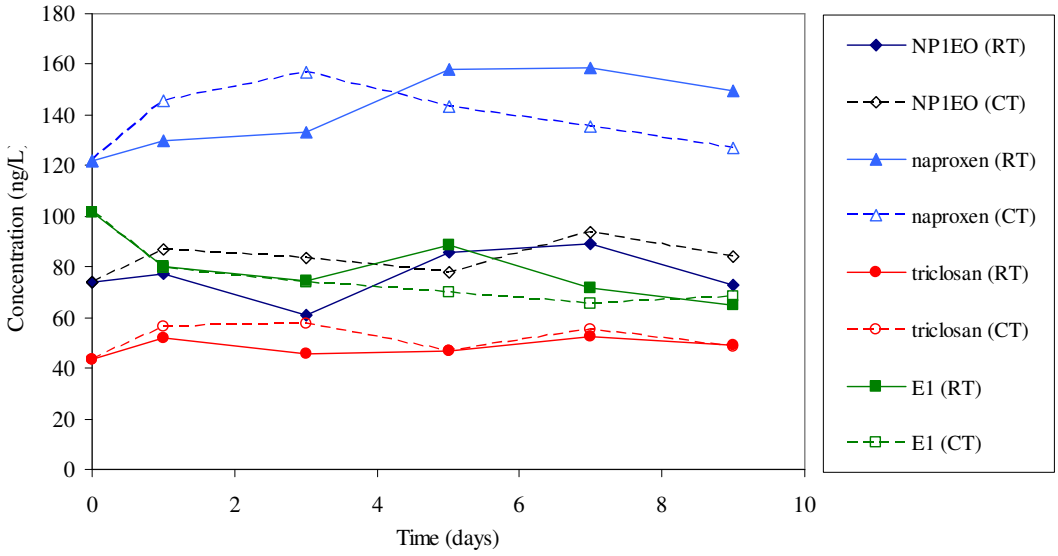

Figure C-1 Comparative stability test at room temperature (RT) and 4 °C (CT) (stable compounds)

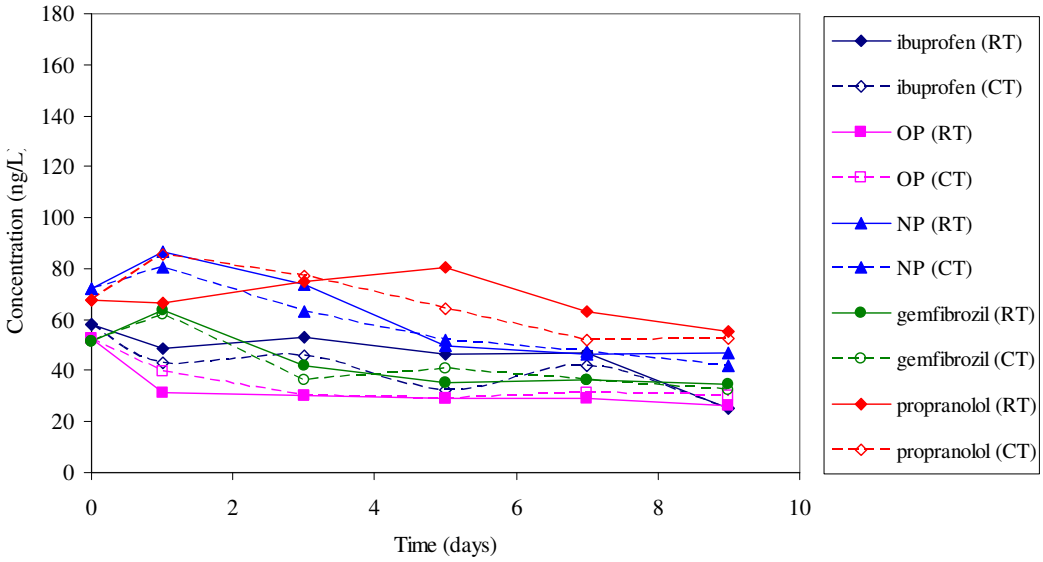

Figure C-2 Comparative stability test at room temperature (RT) and 4 °C (CT) (less stable compounds)

Appendix D
Calculation of Free Diffusivity

The calculations of free diffusivities for the three target compounds were base on Equation 2.44. The molal volume at the normal boiling point (V_b) should first be estimated using the additive-volume increments of Schroeder or Le Bas or from the critical volume (V_c) using the Tyn and Calus method in order to further calculate the D_L. The three approaches were summarized and published by Reid *et al.* (1977), and each tried in the calculations. It was found that the calculation results for a compound using different approaches were different (Table A-1). However, there was no experimental data to validate the estimated data. As a result, only the higher value of two relatively similar values was used further to calculate D_L. In Table A-1, it is marked as bold.

$$D_L = \frac{13.26\times10^{-5}}{\mu_L^{1.14} V_b^{0.589}} \qquad \text{D.1}$$

Table D-1 Estimated molal volumes at normal boiling point and free diffusivities

molal volume at normal boiling point (cm^3/g-mol)	Schroeder	Le Bas	Tyn – Calus	D_L ($x10^{-10}$ m^2/s)
NP	294	303.2	**297.8**	4.618
Naproxen	224	250.1	**259.7**	5.005
Carbamazepine	**238**	236.8	262.6	5.269

Numbers in bold were used for further calculations.

Appendix E
Characterization of Activated Carbons

E.1 Determination of GAC Particle Density and Porosity

This method used water to intrude the pores of the carbon (Sontheimer *et al.*, 1988). The detailed procedures are as follows:

1) Weighted 3 g (M_c) representative carbon sample and put into a beaker.
2) Added an appropriate amount of ultrapure water, and boiled the water with carbon for one hour in order to facilitate thorough wetting of carbon.
3) Filtered the wetted carbon out, and removed the surplus water from the outer surface, then transferred them into a 15 mL (V_p) preweighted pycnometer (M_p).
4) Measured the total weight of wet carbon and pycnometer (M_w), filled ultrapure water into the pycnometer, and measured the total weight (M_T) again.
5) After the all data has been obtained, the calculation could be carried out as follows:

Particle density $$\rho_P = M_c \Big/ \left(V_P - \frac{M_T - M_W}{\rho_{H_2O}} \right)$$

Material density $$\rho_M = M_c \Big/ \left(V_P - \frac{M_T - M_P - M_c}{\rho_{H_2O}} \right)$$

Particle porosity $$\varepsilon_P = 1 - \frac{\rho_P}{\rho_M}$$

E.2 Methodology for Sieve Analysis

U.S. standard mesh sieve numbers 8, 12, 16, 20, 30, and 40 were used, along with a shaker to separate the carbon into various size ranges. These sieves with a bottom pan and a top cover were placed on a shaker. Approximately 200 mL of representative GAC samples were weighed on the balance with a precision of 0.1g, and was placed into the top sieve (No. 8 sieve). The sieve stake was then shaken for ten minutes. Then, each sieve was removed from the stack, and GAC retained on each sieve was transferred into a separate container using a brush. Each fraction of GAC was weighted separately on a balance. A check was conducted on the loss of carbon during sieve analysis. If the total loss was more than 2% of the original total weight, the analysis result was rejected.

The sieve analysis for each type of carbon was repeated four times. The effective mean particle diameter was calculated based on the size distribution plot (Figure B-1). More specifically, it is the sum of the products of weight percentage retained on each sieve and the mean opening of the corresponding sieve.

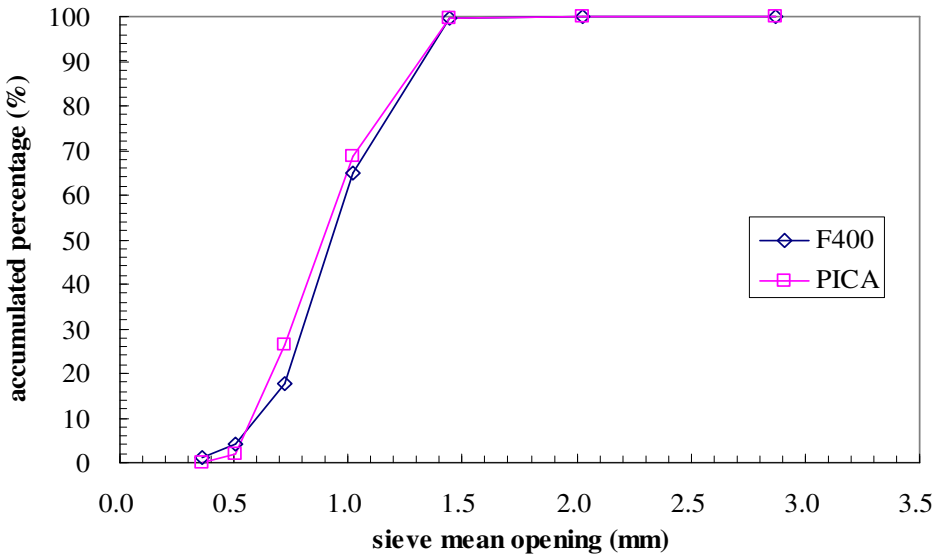

Figure E-1 Typical particle size distribution plot of F400 and PICA carbon

Appendix F

Equilibrium Tests Data on Virgin GAC in Ultra-pure Water

Table F-1 Determined liquid phase concentrations in equilibrium tests

carbon	time (day)	0	0.08	0.25	1	2	3	4	6	9	12	13	15	18
F400 (12 x 40)	naproxen	655	341	ND	399	ND	347	ND	32	82	ND	15	ND	ND
	carbamazepine	760	697	ND	587	ND	382	ND	64	69	ND	53	ND	ND
	NP	800	626	ND	791	ND	373	ND	8	24	ND	16	ND	ND
PICA (12 x 30)	naproxen	655	421	359	354	460	ND	347	188	172	164	ND	41	ND
	carbamazepine	760	703	764	585	462	ND	337	242	146	92	ND	31	ND
	NP	800	698	720	780	654	ND	671	9	6	54	ND	5	ND
PICA (30 x 40)	naproxen	312	ND	ND	302	ND	154	ND	48	28	22	ND	13	9
	carbamazepine	531	ND	ND	326	ND	171	ND	90	49	21	ND	13	8
	NP	413	ND	ND	28	ND	11	ND	5	5	5	ND	12	5

ND: not determined

Appendix G
Additional Isotherms on Virgin GAC in Ultrapure Waters

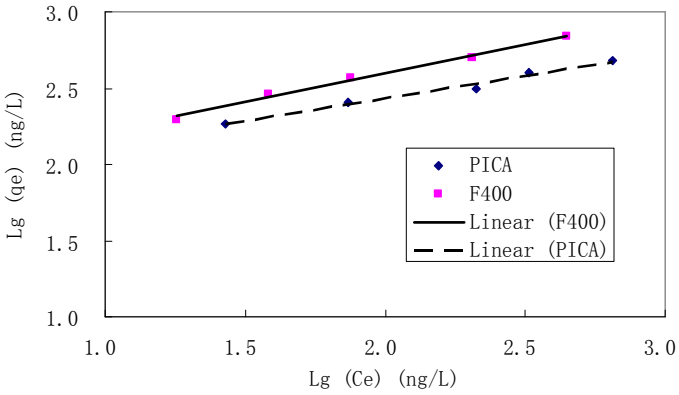

Figure G-1 Linear Freundlich isotherms of naproxen in ASTM type II water

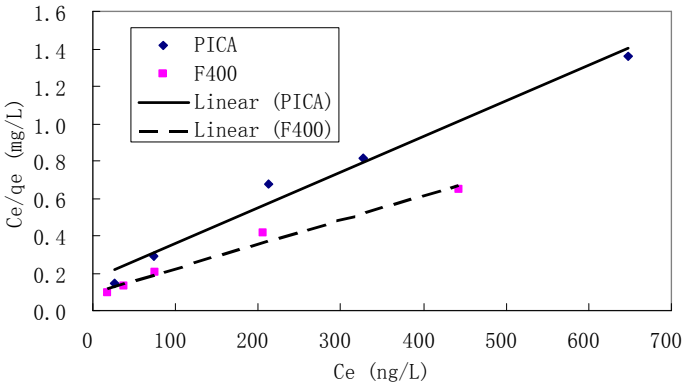

Figure G-2 Linear Langmuir isotherms (Eq. 6.4) of naproxen in ASTM type II water

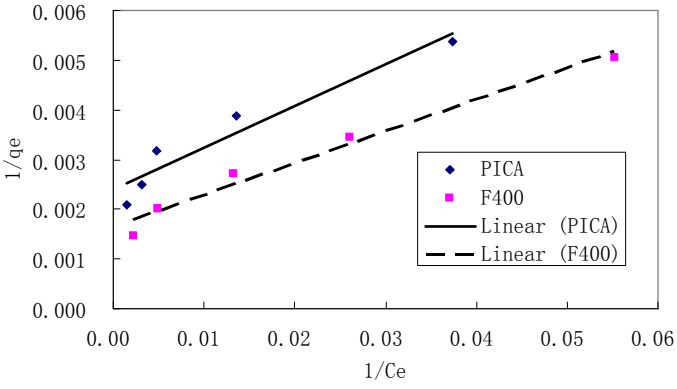

Figure G-3 Linear Langmuir isotherms (Eq. 6.5) of naproxen in ASTM type II water

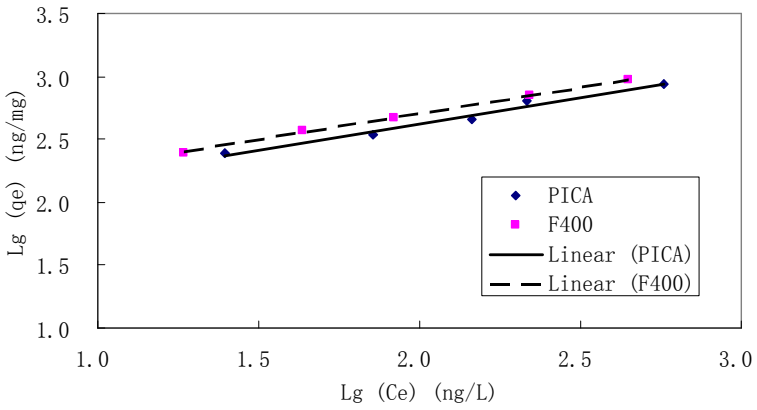

Figure G-4 Linear Freundlich isotherms of carbamazepine in ASTM type II water

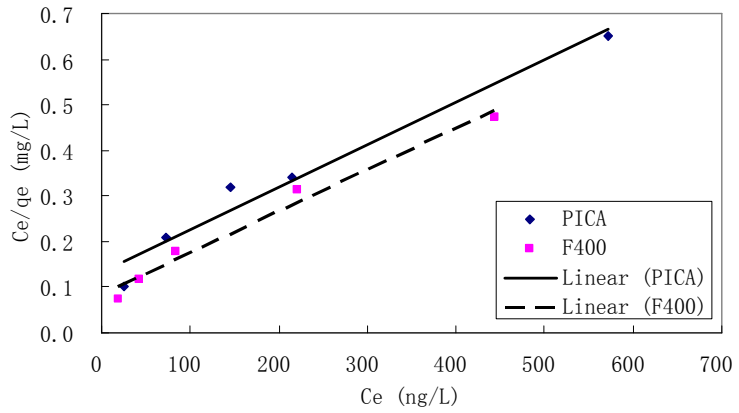

Figure G-5 Linear Langmuir isotherms (Eq. 6.4) of carbamazepine in ASTM type II water

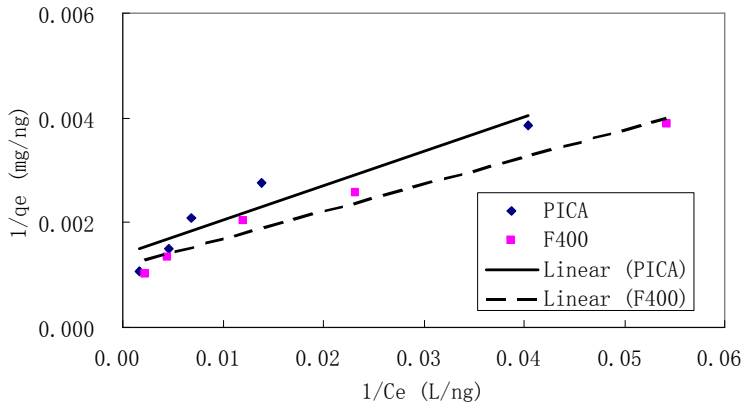

Figure G-6 Linear Langmuir isotherms (Eq. 6.5) of carbamazepine in ASTM type II water

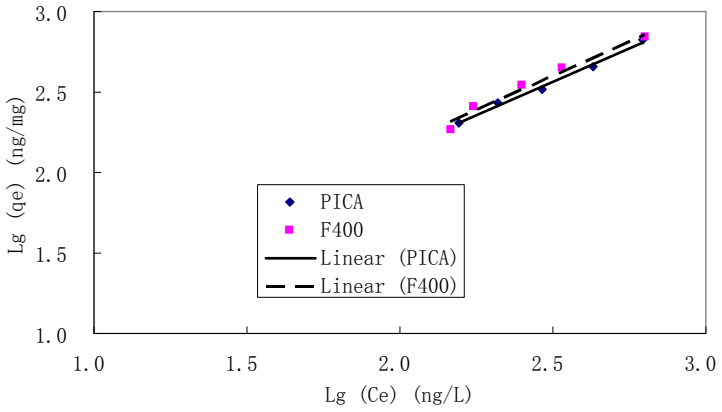

Figure G-7 Linear Freundlich isotherms of NP in ASTM type II water

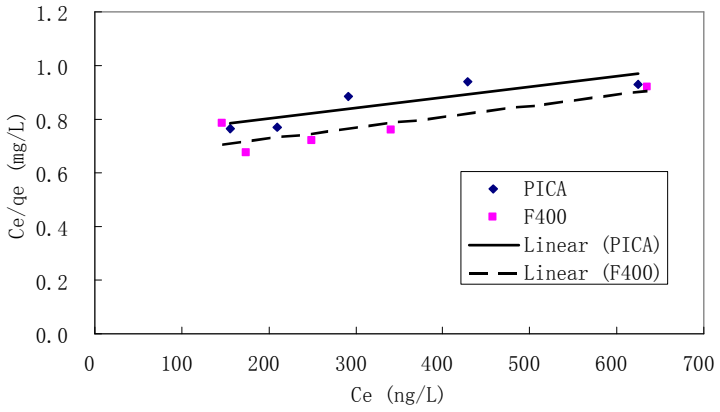

Figure G-8 Linear Langmuir isotherms (Eq. 6.4) of NP in ASTM type II water

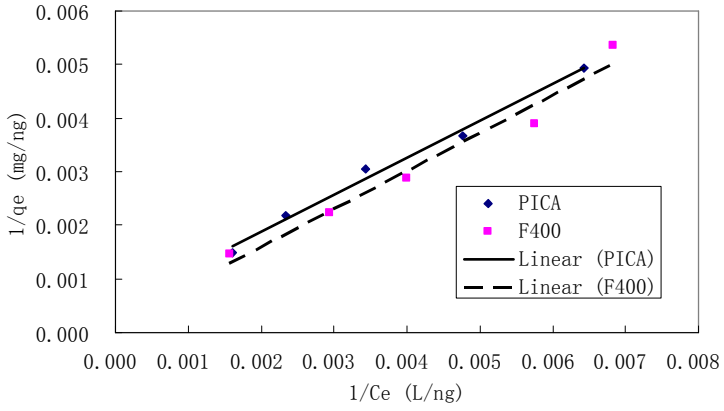

Figure G-9 Linear Langmuir isotherms (Eq. 6.4) of NP in ASTM type II water

Comparisons between Isotherms with Different Initial Concentrations

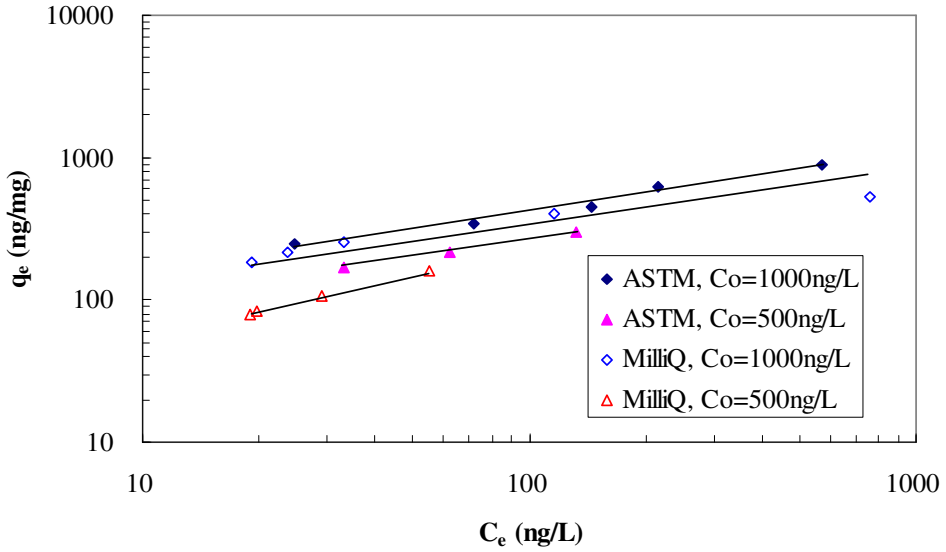

Figure G-10 Carbamazepine adsorption on virgin PICA carbon in Milli-Q and ASTM type II waters

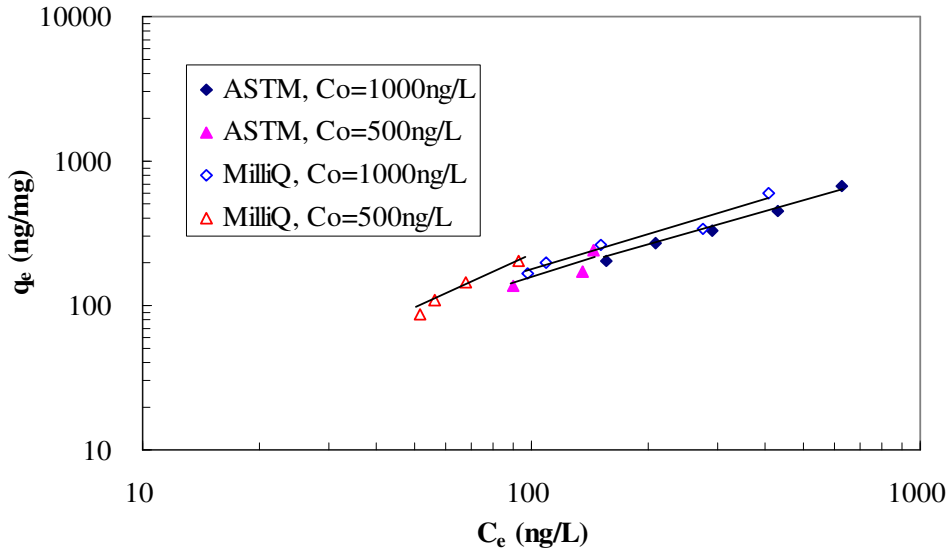

Figure G-11 NP adsorption on virgin PICA carbon in Milli-Q and ASTM type II waters

Appendix H

Isotherms on Preloaded Carbons

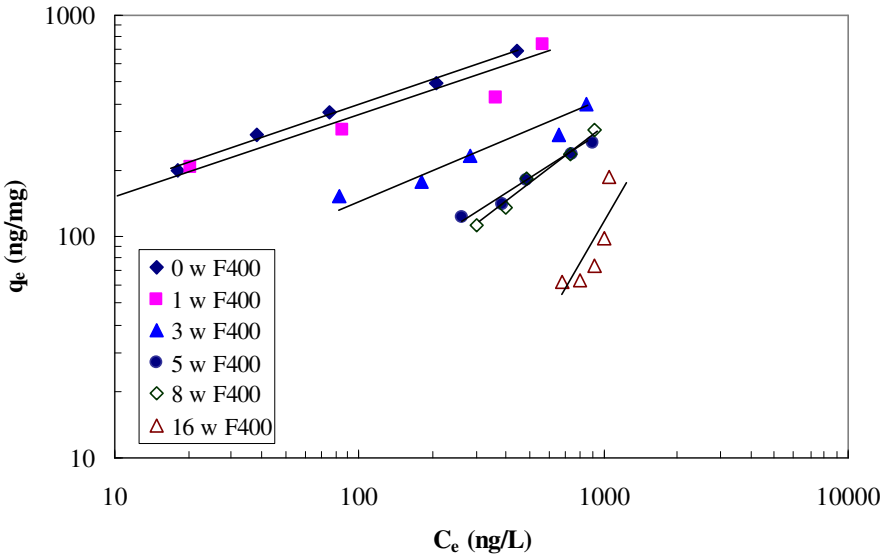

Figure H-1 Naproxen adsorption isotherms on preloaded F400 carbon

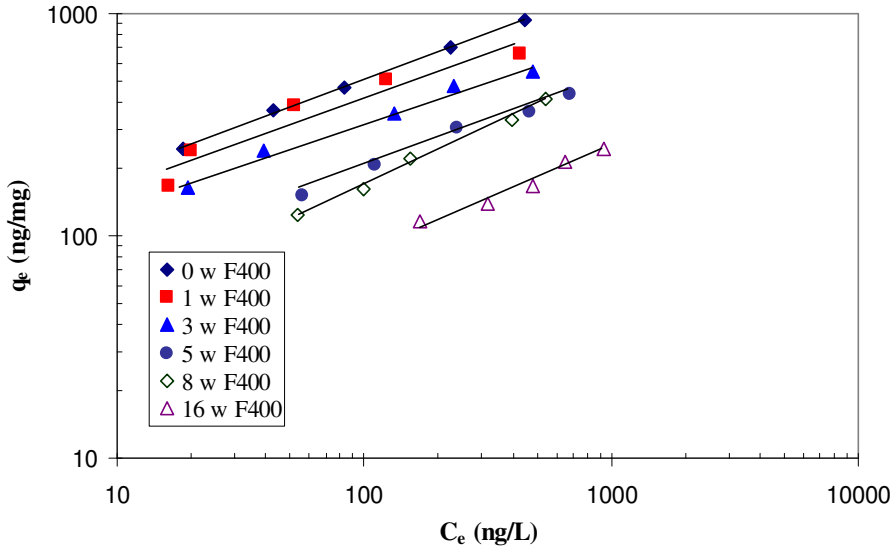

Figure H-2 Carbamazepine adsorption isotherms on preloaded F400 carbon

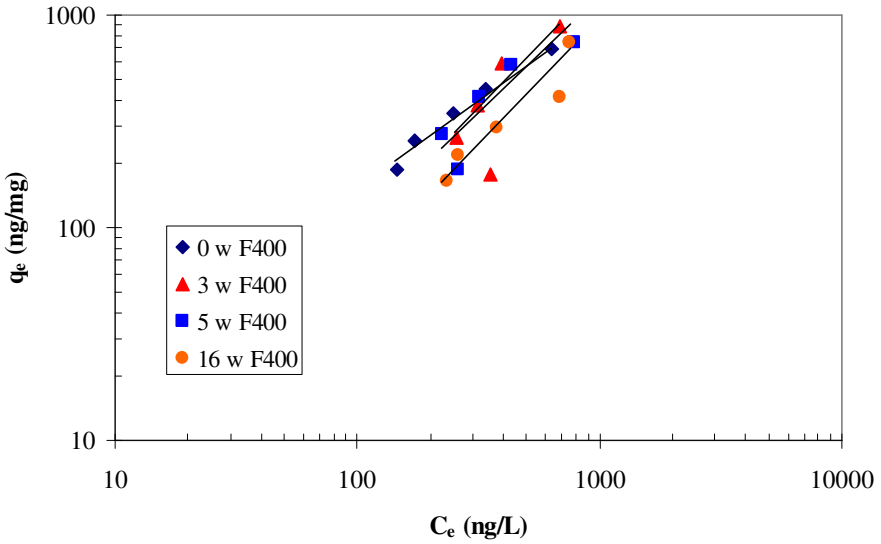

Figure H-3 NP adsorption isotherms on preloaded F400 carbon

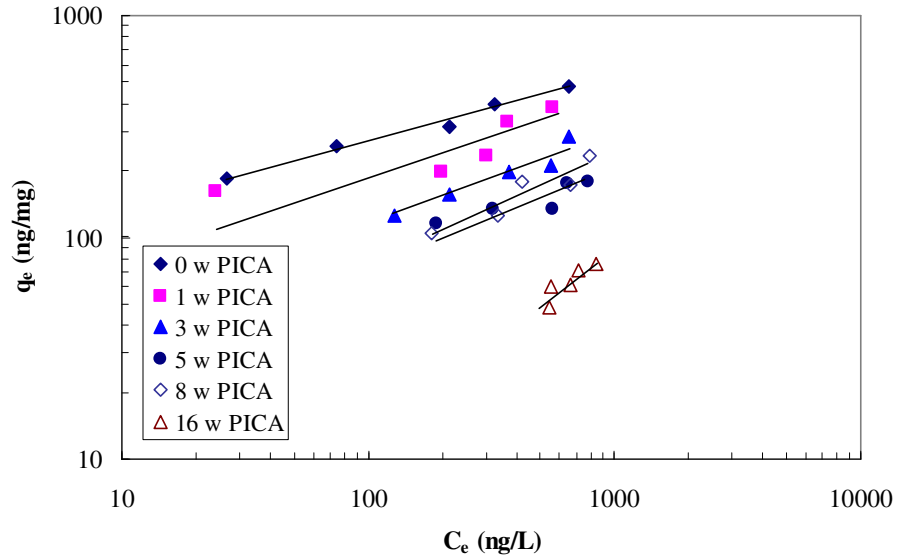

Figure H-4 Naproxen adsorption isotherms on preloaded PICA carbon

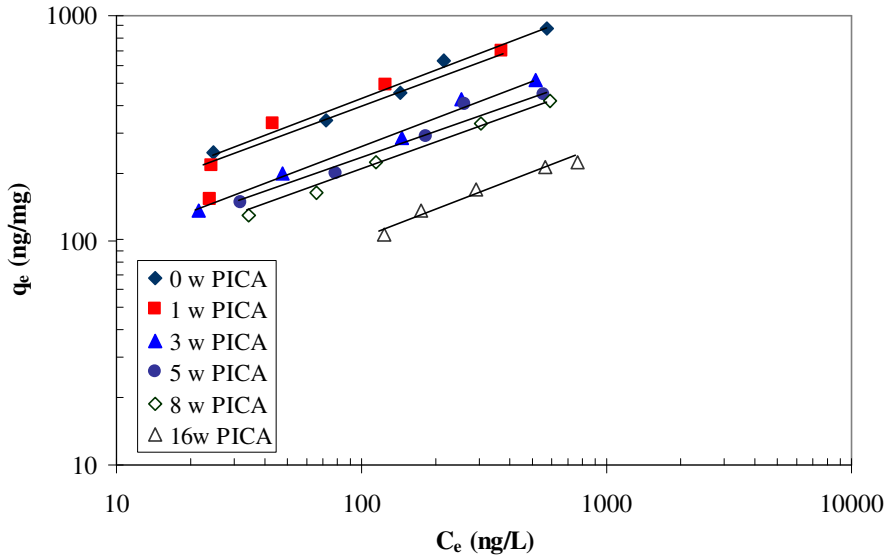

Figure H-5 Carbamazepine adsorption isotherms on preloaded PICA carbon

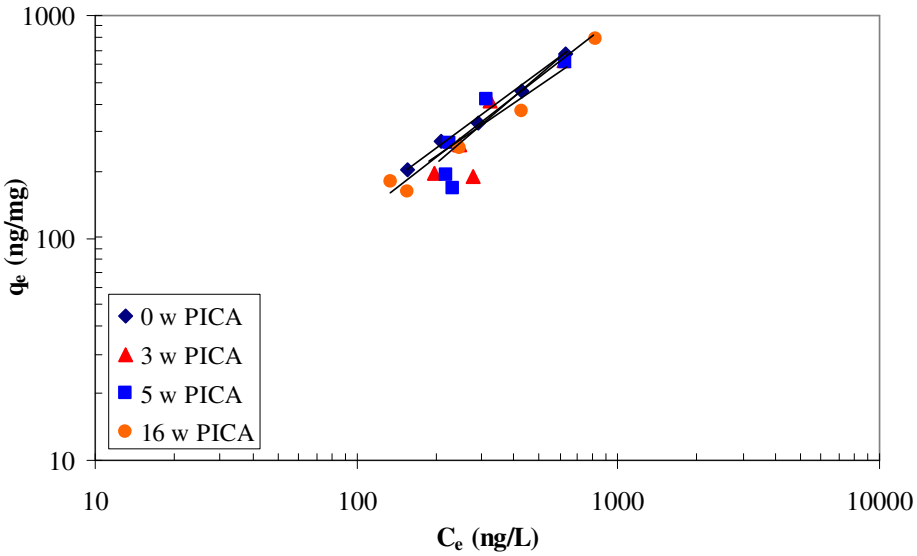

Figure H-6 NP adsorption isotherms on preloaded PICA carbon

Appendix I

Temperature Records for Preloading and Pilot Experiments

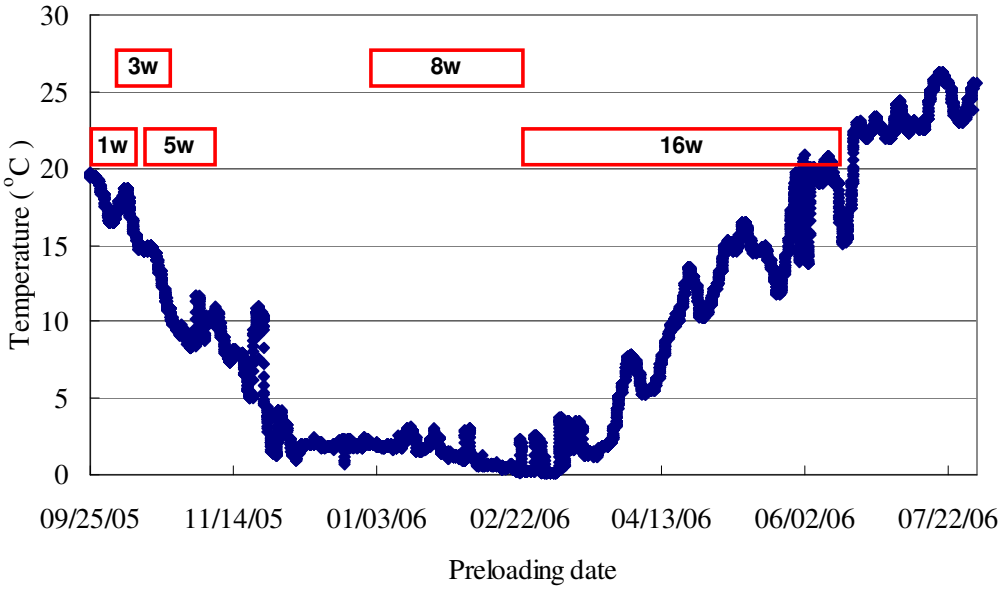

Figure I-1 Temperature trend for carbon preloading period (rectangulars are the differenttime durations)

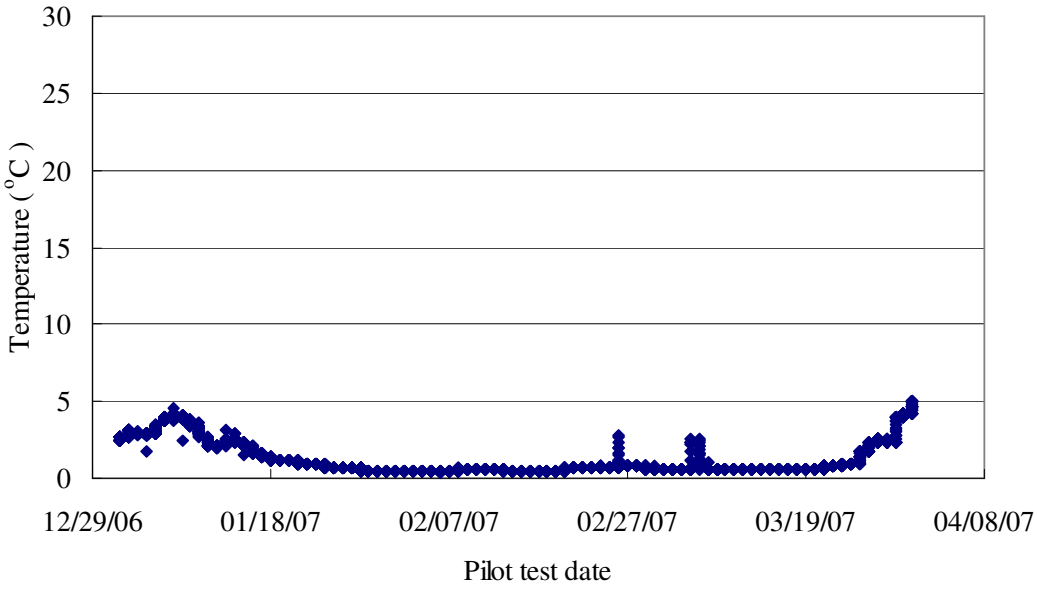

Figure I-2 Temperature trend for pilot-scale test

Appendix J

Supplementary Kinetic Tests Data

This appendix shows the kinetic data sets in which some data were considered as outliners and thus excluded in the calibration processes. Excuded data are marked in *Italic*.

Table H-1 SFB test data for 3-week F400 carbon

		naproxen	carbamazepine	nonylphenol
	average influent concentration (ng/L)	563		324
sample #	sampling time (hrs)	normalized effluent data		
1	0.1	*0.54*		*0.25*
2	0.4	0.62		*0.26*
3	0.8	0.63		*0.17*
4	1.1	0.70		*0.35*
5	1.6	0.65		0.16
6	2.1	0.69		0.13
7	3.1	0.67		0.16
8	4.6	0.68		0.18
9	6.1	0.69		0.22
10	8.1	0.70		0.18
11	10.6	0.66		0.18
12	13.1	0.68		0.18
13	21.3	0.70		0.18
14	23.1	0.71		0.19
15	25.1	0.70		0.19
16	27.1	0.74		0.21

The data in Italic were excluded in the calibration process.

Table H-2 SFB test data for 5-week F400 carbon

		naproxen	carbamazepine	nonylphenol
	average influent concentration (ng/L)	576	703	465
sample #	sampling time (hrs)	normalized effluent data		
1	0.1	*0.71*	*0.45*	0.24
2	0.4	*0.72*	*0.44*	0.26
3	0.8	0.75	0.47	0.21
4	1.1	0.76	0.49	0.23
5	1.6	0.76	0.50	*0.42*
6	2.1	0.76	0.52	0.24
7	3.1	0.76	0.53	0.25
8	4.6	0.76	0.53	0.28
9	6.1	0.78	0.54	0.25
10	8.1	0.80	0.54	0.26
11	10.6	0.80	0.53	0.27
12	13.6	0.79	0.54	0.29
13	21.3	0.78	0.56	0.27
14	23.2	0.79	0.57	0.30
15	25.2	0.80	0.58	0.30
16	27.0	0.79	0.58	0.30

Table H-3 SFB test data for 5-week PICA carbon

		naproxen	carbamazepine	nonylphenol
	average influent concentration (ng/L)	444	613	458
sample #	sampling time (hrs)	normalized effluent data		
1	0.1	0.75	0.44	*0.52*
2	0.4	0.74	0.46	*0.49*
3	0.8	0.74	0.47	0.27
4	1.1	0.79	0.45	0.25
5	1.6	0.77	0.48	*0.39*
6	2.1	0.74	0.49	0.25
7	3.1	0.73	0.46	0.27
8	4.1	0.79	0.49	0.28
9	6.1	0.80	0.48	0.26
10	8.1	0.78	0.49	0.29
11	10.1	0.77	0.48	0.28
12	13.1	0.82	0.50	0.29
13	21.3	0.86	0.50	0.69
14	24.1	0.78	0.50	0.30
15	27.1	0.79	0.49	0.32
16	30.0	0.79	0.50	0.33

Table H-4 SFB test data for 8-week F400 carbon

		naproxen	carbamazepine	nonylphenol
	average influent concentration (ng/L)	580	609	
sample #	sampling time (hrs)	normalized effluent data		
1	0.1	*0.58*	*0.35*	
2	0.4	*0.64*	*0.37*	
3	0.8	0.69	0.39	
4	1.1	0.75	0.42	
5	1.6	0.74	0.42	
6	2.1	0.76	0.45	
7	3.1	0.76	0.46	
8	4.6	0.78	0.48	
9	6.1	0.81	0.49	
10	8.6	0.80	0.50	
11	11.1	0.81	0.50	
12	13.6	0.83	0.51	
13	21.3	0.81	0.53	
14	23.1	0.82	0.53	
15	25.1	0.81	0.54	
16	27.2	0.82	0.53	

Table H-5 SFB test data for 16-week F400 carbon

		naproxen	carbamazepine	nonylphenol
	average influent concentration (ng/L)		558	
sample #	sampling time (hrs)		normalized effluent data	
1	0.2		*0.32*	
2	0.4		*0.34*	
3	0.8		*0.39*	
4	1.1		*0.40*	
5	1.6		0.43	
6	2.1		0.45	
7	3.1		0.45	
8	4.1		0.49	
9	6.1		0.48	
10	8.1		0.50	
11	10.1		0.48	
12	13.1		0.49	
13	21.1		0.49	
14	24.1		0.51	
15	27.1		0.51	

Table H-6 SFB test data for 16-week PICA carbon

		naproxen	carbamazepine	nonylphenol
	average influent concentration (ng/L)	446		518
sample #	sampling time (hrs)	normalized effluent data		
1	0.2	*1.02*		*0.12*
2	0.4	*0.99*		*0.14*
3	0.8	*1.01*		0.18
4	1.1	*0.98*		0.18
5	1.6	*0.96*		0.18
6	2.1	*0.95*		0.19
7	3.1	*0.91*		0.19
8	4.1	0.83		0.18
9	6.1	0.76		0.20
10	8.1	0.77		0.17
11	10.1	0.81		0.21
12	12.1	0.74		0.19
13	14.1	0.85		0.20
14	22.6	0.79		0.25
15	25.1	0.83		0.20
16	28.1	0.82		0.22

Appendix K

JCRplot Program

```
% this program is to plot the joint confidence region of the estimated
% parameters based on Freundlich, Langmuir, Freundlich-Langmuir model.
% input augments x, y, pfinal, jacobian, residuals
% ========================================================================
% method available by Arthur Jutan (The MathWorks MATLAB Digest, 1996)
% program written by Z. Yu
% last modification Jan. 4, 2007
% ========================================================================

function jcrplot(x,y,pfinal,jac,red)

% x - independent variables
% y - dependent variables
% pfinal - estimated parameters
% jac - Jacobian values at Least squares parameter values
% red - vector of residuals

% calculate the predicted dependent variables
ymodel = y+red;

% calculate the best sum of squares
ssmin = red'*red;

% variance of Residuals
n=length(y);
p=length(pfinal);
if (n~=p),varresid=ssmin./(n-p);
else, var=NaN;end

%convert jac to full matrix
jac=full(jac);

xtxinv=inv(jac'*jac);

% calculate variance covariance matrix for parameters
vcm = xtxinv.*varresid;

% calculate standard error of each parameter
std = sqrt(diag(vcm));

choice = input('choose the model: 1 Freundlich; 2 Langmuir; 3 LF model  ');
alpha = input('input confidence level: ');

switch choice
   case 1
      jointcr2p(x,y,pfinal,@SSFreundlich,std,alpha);
   case 2
      jointcr2p(x,y,pfinal,@SSLangmuir,std,alpha);
   otherwise
```

```
    jointcr3p(x,y,pfinal,@SSLF,std,alpha);
end

% ================================================
% plot joint confidence region for two_parameter model
function jointcr2p(x,y,pfinal,func,std,alpha)

n=length(y);

p=length(pfinal);

l = n-p;
% n - number of independent or denpendent variables
% p - number of estimated parameters

ssmin = feval(func,x,y,pfinal); % the mininum sum of squares

% calculate ss contour value conedge
conedge = ssmin.*(1+p./l.*finv(1-alpha,p,l));

% calculate equally spaced plotting values for the estimated parameters
a = 10; % adjustable augument for setting range of SS matrix
b = 200; % adjustable augument for setting mesh of SS matrix
r1 = a*std(1); r2 = a*std(2);
b1s = [linspace((pfinal(1)-r1),(pfinal(1)+r1),b)];
b2s = [linspace((pfinal(2)-r2),(pfinal(2)+r2),b)];

% calculate ss matrix
k = 0;
for ba = b1s
k = k+1;
i = 0;
    for bb = b2s;
    i = i+1;
    a(k,i) = feval(func,x,y,[ba,bb]);
    end
end

% plot contour as joint confidence region
cs = contour(b1s,b2s,a,[conedge conedge],'-b');

hold on

plot(pfinal(1), pfinal(2),'*r');

hold off


% ====================
% calculate sum of squares for regression model by using either best
% estimated parameters or assumed parameters
% ====================
```

```
function q = SSFreundlich(x,y,beta)
pred_y = beta(1).*x.^beta(2);
q=sum((pred_y-y).^2);

% ====================
function q = SSLangmuir(x,y,beta)
pred_y = (beta(1)*beta(2).*x)./(1+beta(2).*x);
q=sum((pred_y-y).^2);
% ====================
function q = SSLF(x,y,beta)
pred_y = (beta(1).*(beta(2).*x).^beta(3))./(1+(beta(2).*x).^beta(3));
q=sum((pred_y-y).^2);
```

Appendix L

IAST-EBC Program

```
!       PROGRAM IAST-EBC
!
!       This program incorporates data from original and competitive isotherms
!       to determine the Freundlich parameters for the EBC.
!       Original code from Gillogly (1998),
!       Modified by Z. Yu
!       ***********************************************************************
        include 'link_f90_static.h'
        IMPLICIT DOUBLE PRECISION (A-H,O-Z)
!
        REAL*8 MWS(10),MCS(10,50)
!
        COMMON PARS(50),QS(10,3,50),CES(10,3,50),&
                & XKS(10),XNS(10),C0(10,10),&
                & MCS,VS(10,50),NDS(10),NCS(10),SSQ,IPS(4),MWS,NDSETS
!
        COMMON/BLOCK2/QD(10,3,50),CD(10,3,50),CMEAN,ERRREL,ITMAX
!
        DIMENSION X(30),XGUESS(30),XSCALE(30),FSCALE(500),&
                & IPARAM(6),RPARAM(7),FVEC(500),FJAC(500,30),FDD(500)
!
        EXTERNAL FCN,LSJAC,DNEQBJ,DU4LSF
        EXTERNAL FS
!
        ERRREL = 0.001
        ITMAX = 100
!
        OPEN(UNIT=1,FILE='EBCIN.txt',STATUS='OLD')
!
!       K = 0
!       K = K+1
!
        NDSETS = 1
        OPEN(NDSETS+1,FILE='EBCOUT.txt')
!
        DO 101 I = 1,4
          IPS(I) = 1
101     CONTINUE
!
        WRITE(NDSETS+1,*) ' INPUT DATA FILE IS: EBCIN.TXT'
        WRITE(NDSETS+1,*) ' OUTPUT DATA FILE IS: EBCOUT.TXT'
!
!        read data from data file
        DO 45 JJ = 1,NDSETS
!
        READ (JJ,*) NDS(JJ),NCS(JJ)
!       NDS: number of dosage
```

```
!       NCS: number of components including EBC and target compounds
        DO 20 I=1,NDS(JJ)
         READ (JJ,*) MCS(JJ,I), VS(JJ,I), (CES(JJ,J,I),J=1,NCS(JJ))
!       MCS: applied doses
!       VS: liquid phase volume
!       CES: observed Ce of EBC and target compounds in natural water
         MCS(JJ,I) = MCS(JJ,I)/1000.0D0  ! change unit from mg to g
         VS(JJ,I)=VS(JJ,I)/1000.0D0  !change unit from mL to L
20      CONTINUE
!
        DO 40 I = 1,NCS(JJ)
         IF(JJ.EQ.1) THEN
          READ (JJ,*) XKS(I),XNS(I),C0(JJ,I),MWS(I)
!       XKS(1), XNS(1): initial guess of EBC's Freundlich parameters
!          C0(1,1): initial guess of EBC concentration
!          MWS(1): assumed molecular weight of EBC
!          XKS(2), XNS(2): original Freundlich parameters of target compound
!          C0(1,2): initial concentration of target compound
!          MWS(2): molecular weight of target compound
          XKS(I) = XKS(I)*(1000.0D0/MWS(I))*MWS(I)**XNS(I)  ! change unit
          XNS(I) = 1.0D0/XNS(I)  ! inverse Freundlich exponent
         ELSE
          READ(JJ,*) DUMXKS,DUMXNS,C0(JJ,I),DUMMWS
         ENDIF
         C0(JJ,I) = C0(JJ,I)/MWS(I)  ! change unit to molarity
         DO 30 J = 1,NDS(JJ)
          CES(JJ,I,J) = CES(JJ,I,J)/MWS(I)  ! change unit to molarity
          QS(JJ,I,J) = (C0(JJ,I)-CES(JJ,I,J))*VS(JJ,J)/MCS(JJ,J)   ! calculate solid loading
          CEQ = CES(JJ,I,J)*MWS(I)
          QEQ = QS(JJ,I,J)*MWS(I)/1000  ! change unit umol/g to mg/g
          WRITE(*,*) CEQ,QEQ
30       CONTINUE
40      CONTINUE
!
45      CONTINUE
!
        I = 2
        NDAT = 0
        CMEAN = 0
        DO 46 JJ = 1,NDSETS
         NDAT = NDAT+NDS(JJ)
         DO 31 J = 1,NDS(JJ)
          CMEAN = CMEAN+CES(JJ,I,J)
31       CONTINUE
46      CONTINUE
        CMEAN = CMEAN/NDAT ! calculate mean of all liquid phase concentrations
!
!       WRITE (NDSETS+1,*) (XKS(I),I=1,NCS(1))
!       WRITE (NDSETS+1,*) (XKS(I),I=1,NCS(2))
!       WRITE (NDSETS+1,*) (QS(1,2,1),I=1,NDS(l))
!       WRITE (NDSETS+1,*) (QS(2,2,1),I=I,NDS(2))
!
!       print initial guess of EBC parameters to output file
```

```
          K = 0
          PARS(1) = XKS(1)
          IF(IPS(1) == 1) THEN
            K = K+1
            XGUESS(K) = PARS(1)
            XGUESS1 = XGUESS(K)/((1000.0/MWS(1))*MWS(1)**(1.0/XNS(1)))
            WRITE(*,*) 'PARAMETER #',K,'=K,','; IG:',XGUESS1
            WRITE(NDSETS+1,*) 'PARAMETER # ',K,'=K ','; IG:',XGUESS1
          ENDIF
!
          PARS(2) = XNS(1)
          IF(IPS(2) == 1) THEN
          K = K+1
          XGUESS(K) = PARS(2)
          XGUESS2 = 1.0/XGUESS(K)
          WRITE(*,*) 'PARAMETER #',K,' = l/n','; IG: ',XGUESS2
          WRITE(NDSETS+1,*) 'PARAMETER #',K,' = l/n','; IG: ',XGUESS2
          ENDIF
!
          PARS(3) = C0(1,1)
          IF(IPS(3) == 1) THEN
          K = K+1
          XGUESS(K) = PARS(3)
          XGUESS3 = XGUESS(K)*MWS(1)
          WRITE(*,*) 'PARAMETER # ',K,' = Co',' ; IG: ',XGUESS3
          WRITE(NDSETS+1,*) 'PARAMETER # ',K,' = Co',' ; IG: ',XGUESS3
          ENDIF
!
      N = K
      M = 0
      DO 70 JJ=1,NDSETS
        M=M+NDS(JJ)
70    CONTINUE
!     WRITE(NDSETS+1,*) (XGUESS(I),I=1,N)
      WRITE(NDSETS+1,*) N,M
      WRITE(*,*) N,M
!     ************************************************************
!     Call to the search routine
!     ************************************************************
      DO 150 I = 1,N
        XSCALE(I) = 1.0D0
150   CONTINUE
      DO 160 J=1,M
        FSCALE(J)=1.0D0
160   CONTINUE
      LDFJAC = M
!
      XGUESS(1) = XGUESS(1)
      XGUESS(2) = XGUESS(2)**2
      XGUESS(3) = XGUESS(3)
!
      CALL DU4LSF(IPARAM,RPARAM)
!     set nondefault values for IPARAM or RPARAM, prepare for DUNLSF
```

```
      IPARAM(3) = 400  ! Max number of iterations, default 100
      IPARAM(4) = 2500  ! Max number of function evaluations, default 400
!
      CALL DUNLSF(FCN,M,N,XGUESS,XSCALE,FSCALE,IPARAM,RPARAM,X,FVEC,FJAC,LDFJAC)
!     use modified Levenberg-Marquardt algorithm and a finite-difference Jacobian
!
      CALL FCN(M,N,X,FDD)
!
!     ************************************************************
!     Send results to output file
!     ************************************************************
      X(1) = ABS(X(1))
      X(2) = (ABS(X(2)))**0.5
      X(3) = ABS(X(3))
!
      WRITE(NDSETS+1,"(A)") 'EBC'
      K = 0
      IF(IPS(1) == 1) THEN
        K = K+1
        XKOUT = X(K)/((1000.0/MWS(1))*MWS(1)**(1.0/XNS(1)))
      ELSE
        XKOUT = PARS(1)/((1000.0/MWS(1))*MWS(1)**(1.0/XNS(1)))
      ENDIF
      WRITE(NDSETS+1,"(1X,'K = ',E17.8,'(mg/g)(ug/L)^-1/n')") XKOUT
!
      IF(IPS(2) == 1) THEN
        K = K+1
        XNOUT = 1.0D0/X(K)
      ELSE
        XNOUT = 1.0D0/PARS(2)
      ENDIF
      WRITE(NDSETS+1,"(1X,'1/n = ',E17.8)") XNOUT
!
      IF(IPS(3) == 1) THEN
        K = K+1
        C0OUT = X(K)*MWS(1)
      ELSE
        C0OUT = PARS(3)*MWS(1)
      ENDIF
      WRITE(NDSETS+1,"(1X,'C0 = ',E17.8,'ug/L')") C0OUT
      WRITE(NDSETS+1,"(1X,'MW = ',E17.8,'g/mol')") MWS(1)
!
      WRITE(NDSETS+1,"(A)") 'TARGET COMPOUND'
      XKOUT2 = XKS(2)/((1000.0/MWS(2))*MWS(2)**(1.0/XNS(2)))
      XNOUT2 = 1.0/XNS(2)
      WRITE(NDSETS+1,"(1X,'K = ',E17.8,'(mg/g)(ug/L)^-1/n')") XKOUT2
      WRITE(NDSETS+1,"(1X,'1/n = ',E17.8)") XNOUT2
      DO 249 JJ = 1,NDSETS
        C0OUT2 = C0(JJ,2)*MWS(2)
        WRITE(NDSETS+1,"(1X,'C0 = ',E17.8,'ug/L')") C0OUT2
249    CONTINUE
      WRITE(NDSETS+1,"(1X,'MW = ',E17.8,'g/mol')") MWS(2)
!
```

```
      WRITE(NDSETS+1,1000)
1000    FORMAT(1X,'No.',8X,'Q-obs', 12X,'Q-cal',15X,'C-obs',12X,'C-cal',12X,'AC-dose')
      DO 250 JJ = 1,NDSETS
        DO 200 J = 1,NDS(JJ)
          Q = QS(JJ,2,J)*MWS(2)/1000.0
          QOUT = QD(JJ,2,J)*MWS(2)/1000.0
          CEQ = CES(JJ,2,J)*MWS(2)
          XMCSJ = MCS(JJ,J)*1000.0
          CEQOUT = CD(JJ,2,J)*MWS(2)
          WRITE(NDSETS+1,1005) J,Q,QOUT,CEQ,CEQOUT,XMCSJ
1005      FORMAT(1X,'Q(',I2,') = ',E10.4,2X,E10.4,'mg/g',2X,E10.4,2X,E10.4,'ug/L',2X,E10.4,'mg/L')
200       CONTINUE
250     CONTINUE
!
       DO 210 I = 1,M
          WRITE (NDSETS+1,"(1X,'F(',I2,') = ',E14.5)") I,FVEC(I)
210   CONTINUE
!
      WRITE(NDSETS+1,"(1X,'Error sum of squares = ',E14.5)") SSQ
!
      STOP 'all done'
      END
!
!     ......................................................................
!     This subroutine evaluates the results of nonlinear regression and calculates SSQ
!     ......................................................................
      SUBROUTINE FCN(M,N,X,F)
!
!     M: corresponding to number of dose
!     N: corresponding to number of estimated parameters
!     X: array of estimated parameters
!     F: array of errors
      IMPLICIT DOUBLE PRECISION (A-H,O-Z)
      REAL*8 MW(10),XMC(10,50)
!
      COMMON PAR(50),Q(10,3,50),CES(10,3,50),XK(10),XN(10),C0(10,10),&
           & XMC,V(10,50),ND(10),NC(10),SSQ,IPS(4),MW,NDSETS
!
      COMMON /BLOCK1/JJ,J,K
      COMMON /BLOCK2/QD(10,3,50),CD(10,3,50),CMEAN,ERRREL,ITMAX
!
      DIMENSION F(M),X(N),XI(10),XIGUESS(10),XIG1(10),XIG2(10)
      DIMENSION QQ(10),QQD(2),FF(2)
!
      DIMENSION XSCALE(2),FSCALE(2),IPARAM(6),RPARAM(5),FVEC(2)
      EXTERNAL FCNIAS,LSJAC,DNEQBJ,DZBREN
      EXTERNAL FS
!
      DATA ICALL/0/
!
!     WRITE(*,*) 'FCN IN DUNLSF'
      ICALL = ICALL+1
!     ......................................................................
```

```
!     If trouble, limit the parameters to the smallest value of 10D-30
!     ...................................................................
!
      X1 = (ABS(X(1)))
      X2 = (ABS(X(2)))**0.5
      X3 = (ABS(X(3)))
!
      IF (X1 < 0.000001) X1 = 0.000001
      IF (X2 < 0.01) X2 = 0.01
      IF (X3 < 0.000001) X3 = 0.000001
!
      IF (IPS(1) == 1) XK(1) = X1
      IF (IPS(2) == 1) XN(1) = X2
      IF (IPS(3) == 1) THEN
      DO 117 JJ = 1,NDSETS
       C0(JJ,1) = X3
117    CONTINUE
      ENDIF
      X11 = X1/((1000.0/MW(1))*MW(1)**(1.0/X2))
      X22 = 1.0/X2
      X33 = X3*MW(1)
      WRITE(*,*) X11,X22,X33
!
      I = 0
      DO 115 JJ = 1,NDSETS
       NN = NC(JJ)
       DO 110 J = 1,ND(JJ)  ! caculate for each dose
        I = I+1
!
        DO 100 K = 1,NN
         QMAX1 = C0(JJ,K)*V(JJ,J)/XMC(JJ,J)
         QMAX2 = XK(K)*C0(JJ,K)**(1.0/XN(K))
         IF(QMAX1 <= QMAX2) THEN
          QMAX = QMAX1
         ELSE
          QMAX = QMAX2
         ENDIF
         QEST = QMAX*1.00001
         QMIN = 0
         EABS = 0
         EREL = 0.002
         MAXFN = 100
!              F1=FS(QMIN)
!              F2=FS(QEST)
!              WRITE(*,*) JJ,J,K,QEST
!                   WRITE(*,*) F1,F2
!              WRITE(*,*) C0(JJ,K),V(JJ,J),XMC(JJ,J)
!              WRITE(*,*) XK(K),XN(K)
         CALL DZBREN(FS,EABS,EREL,QMIN,QEST,MAXFN)
!              WRITE(*,*) JJ,J,K,QEST
         QQ(K) = QEST
100      CONTINUE
!
```

```
!               WRITE(*,*) JJ,J,(QQ(K),K=1,NN),'QQ'
        KMAX = 1000
        PD = 1.1
        MR = 1
        FMAX = 1.0D99
!
        FMIN1 = FMAX
        NFLG = 0
        DO 202 K2 = 1,KMAX
          QQD(2) = QQ(2)/PD**(K2-1)
          FABS = FMAX
          DO 203 K1 = 1,KMAX
          QQD(1) = QQ(1)/PD**(K1-1)
          CALL FCNIAS(NN,QQD,FF)
          FABSB = FABS
          FABS = (FF(1)/C0(JJ,1))**2+(FF(2)/C0(JJ,2))**2
!               FABS=DABS(FF(1))+DABS(FF(2))
          IF(FABS < FMIN1) THEN
            FMIN1 = FABS
            XIG1(1) = QQD(1)
            XIG1(2) = QQD(2)
            K11 = K1
            K22 = K2
            NFLG = 1
          ELSE
            IF(FABS > FABSB) GO TO 205
          ENDIF
203         CONTINUE
205         IF(K2-K22 >= MR.AND.NFLG == 1) GO TO 204
202       CONTINUE
204       CONTINUE
!
       FMIN2 = FMAX
!       GO TO 304
       NFLG = 0
       DO 302 K1 = 1,KMAX
         QQD(1) = QQ(1)/PD**(K1-1)
         FABS = FMAX
         DO 303 K2 = 1,KMAX
         QQD(2) = QQ(2)/PD**(K2-1)
         CALL FCNIAS(NN,QQD,FF)
         FABSB = FABS
         FABS = (FF(1)/C0(JJ,1))**2+(FF(2)/C0(JJ,2))**2
!         FABS=DABS(FF(1))+DABS(FF(2))
         IF(FABS < FMIN2) THEN
           FMIN2 = FABS
           XIG2(1) = QQD(1)
           XIG2(2) = QQD(2)
           K11 = K1
           K22 = K2
           NFLG = 1
         ELSE
           IF(FABS > FABSB) GO TO 305
```

```
          ENDIF
303       CONTINUE
305       IF(K1-K11 >= MR.AND.NFLG == 1) GO TO 304
302       CONTINUE
304       CONTINUE
!
      IF(FMIN1 < FMIN2) THEN
        XIGUESS(1) = XIG1(1)
        XIGUESS(2) = XIG1(2)
      ELSE
        XIGUESS(1) = XIG2(1)
        XIGUESS(2) = XIG2(2)
      ENDIF
!
!     WRITE(*.*) JJ,J,(QQ(K),K=1,NN),'QQ'
!     WRITE(*,*) K11,K22,'k1, k2'
!     WRITE(*,*) JJ,J,(XIGUESS(K),K=1,NN),'XIG'
!
!     CALL DNEQNJ(FCNIAS,LSJAC,ERRREL,NN,ITMAX,XIGUESS,XI,FNORM)
      DO 98 K = 1,NN
        XSCALE(K) = 1.0
        FSCALE(K) = 1.0
98      CONTINUE
      CALL DN4QBJ(IPARAM,RPARAM)
      IPARAM(1) = 0
!     WRITE(*,*) IPARAM(3),RPARAM(1),RPARAM(2)
      IPARAM(3) = 500
      RPARAM(1) = 0.0D0
      RPARAM(2) = 0.0D0
      CALL DNEQBJ(FCNIAS,LSJAC,NN,XIGUESS,XSCALE,FSCALE,IPARAM,RPARAM,XI,FVEC)
!     WRITE(*,*) JJ,J,(XI(K),K= I ,NN)
!
      DO 103 K = 1,NN
        QD(JJ,K,J) = XI(K)
        CD(JJ,K,J) = C0(JJ,K)-XMC(JJ,J)/V(JJ,J)*XI(K)
103     CONTINUE
!
!     QG=Q(JJ,2,J)*MW(2)
!     QDG=QD(JJ,2,J)*MW(2)
!     ebcm 1
!     F(I)=DABS(DLOG(CES(JJ,2,J)-DLOG(CD(JJ,2,J))
!      & +DABS(DLOG(Q(JJ,2,J)-DLOG(QD(JJ,2,J))
!
!     ebcm3
!     F(I)=DLOG(CES(JJ,2,J)-DLOG(CD(JJ,2,J)
!     ebcm4
!     F(I)=(CES(JJ,2,J)-CD(JJ,2,J)/CES(JJ,2,J)**0.5*10
!     ebcm5
!     F(I)=CES(JJ,2,J)-CD(JJ,2,J)
!     ebcm6
!     F(I)=(CES(JJ,2,J)-CD(JJ,2,J)
!      & /(DLOG(C0(JJ,2)/CES(JJ,2,J)))**0.5
!     ebcm 7
```

```
!     F(I)=(CES(JJ,2,J)-CD(JJ,2,J))/CES(JJ,2,J)
!     ebcm8
!     F(I)=DSQRT(DABS(CES(JJ,2,J)-CD(JJ,2,J))
!     ebcm9
!     F(I)=(DABS((CES(JJ,2,J)-CD(JJ,2,J))/CES(JJ,2,J)))
!      & +(DABS((Q(JJ,2,J)-QD(JJ,2,J)/Q(JJ,2,J))
!     ebcm10
!     F(I)=DABS(CES(JJ,2,J)-CD(JJ,2,J)
!      & *(1.0D0/CES(JJ,2,J)+1.0D0/CMEAN)
!     ebcm11
!     F(I)=DSQRT((DLOG(CES(JJ,2,1)-DLOG(CD(JJ,2,J))**2
!      & +(DLOG(Q(JJ,2,J)-DLOG(QD(JJ,2,J))**2)
!     ebcm12
!     F(I)=DSQRT( ((CES(JJ,2,J)-CD(JJ,2,J)/CES(JJ,2,J)**2
!      & + ((Q(JJ,2,J)-QD(JJ,2,J))/Q(JJ,2,J)**2)
!     ebcm13
!     F(I)=DSQRT( (CES(JJ,2,J)-CD(JJ,2,J))**2
!      & *( 1.0D0/CES(JJ,2,J)**2+1.0D0/CMEAN**2) )
!     ebcm14
      F(I)=DSQRT(DABS(CES(JJ,2,J)-CD(JJ,2,J))*(1.0D0/CES(JJ,2,J)+1.0D0/CMEAN))
!     ebcm15
!     F(I)=DSQRT(DABS((CES(JJ,2,J)-CD(JJ,2,J))/CES(JJ,2,J)))
!     ebcm16
!     F(I)=DSQRT(DABS(DLOG(CES(JJ,2,J)-DLOG(CD(JJ,2,J))))
!     ebcm17
!     F(I)=DSQRT(DABS(DLOG(CES(JJ,2,J)-DLOG(CD(JJ,2,J)))
!      & + DABS(DLOG( Q(JJ,2,J)-DLOG(QD(JJ,2,J))))
!     ebcm18
!     F(I)=DSQRT(DABS((CES(JJ,2,J)-CD(JJ,2,J)/CES(JJ,2,J))
!      & + DABS((Q(JJ,2,J)-QD(JJ,2,J))/Q(JJ,2,J)))
!     ebcml9
!     F(I)=DSQRT(DABS(CES(JJ,2,J)-CD(JJ,2,J))
!      & *(1.0D0/CES(JJ,2,J)+1.0D0/CMEAN)
!      & +DABS((Q(JJ,2,J)-QD(JJ,2,J))/Q(JJ,2,J)) )
!     ebcm20
!     F(I)=DABS((Q(JJ,2,J)-QD(JJ,2,J))/Q(JJ,2,J))
!     ebcm21
!     F(I)=DABS(Q(JJ,2,J)-QD(JJ,2,J))
!
!     WRITE(*.*) JJ,J,QG,QDG
!     WRITE(*.*) JJ,J,I,F(I)
110    CONTINUE
115    CONTINUE
!
      SSQ = 0
      DO 120 K = 1,M
       IF(DABS(F(K)) > 1.0D-30) THEN
         IF(DABS(F(K)) < 1.0D30) THEN
           SSQ = SSQ+F(K)**2.0D0
         ENDIF
       ENDIF
120    CONTINUE
      SSQ = SSQ/M
```

```
!
      WRITE (*,1009) ICALL,SSQ
1009    FORMAT(1X,'Iteration No.:',I5,4X,'Error sum of sq. = ',E14.6)
!
      RETURN
      END
!
!     ********************************************************
!     This set up the equations that will be solved by the subroutine DNEQNF
!     The equation is derived from lAST plus Freundlich equations
!     for a target compound and a background compound
!     ********************************************************
!     SUBROUTINE FCNIAS(X,F,N)
      SUBROUTINE FCNIAS(N,X,F)
      IMPLICIT DOUBLE PRECISION (A-H,O-Z)
      REAL*8 MW(10),XMC(10,50)
!
      COMMON PAR(50),Q(10,3,50),CES(10,3,50),XK(10),XN(10),C0(10,10)&
       & ,XMC,V(10,50),ND(10),NC(10),SSQ,IPS(4),MW,NDSETS
!
      COMMON /BLOCK1/JJ,J,KK
!
      DIMENSION X(N),F(N)
      QS = X(1)+X(2)
      QNS = XN(1)*X(1)+XN(2)*X(2)
!
      DO 1000 I = 1,N
        F(I) = C0(JJ,I)-X(I)*XMC(JJ,J)/V(JJ,J)-X(I)/QS*(QNS/XN(I)/XK(I))**XN(I)
!       WRITE(*, *) JJ,I,J,X(I),F(I),F
1000    CONTINUE
!
      RETURN
      END
!     ********************************************************
!     This set up the equations to calculate the Jacobian
!          and that will be solved by the subroutine DNEQNF
!     The equation is derived from lAST plus Freundlich equations
!     for a target compound and a background compound
!     ********************************************************
!     SUBROUTINE LSJAC(N,X,FJAC)
      SUBROUTINE LSJAC(N,X,FJAC,LDFJAC)
!
      IMPLICIT DOUBLE PRECISION (A-H,O-Z)
      REAL*8 MW(10),XMC(10,50)
      INTEGER N,I,J
!
!     DIMENSION X(N),FJAC(N,N)
      DIMENSION X(N),FJAC(LDFJAC,*)
!
      COMMON PAR(50),Q(10,3,50),CES(10,3,50),XK(10),XN(10),C0(10,10),&
          & XMC,V(10,50),ND(10),NC(10),SSQ,IPS(4),MW,NDSETS
!
      COMMON /BLOCK1/JJ,J,KK
```

```
!
      QS = X(1)+X(2)
      QNS = XN(1)*X(1)+XN(2)*X(2)
!
      DO 1000 I = 1,N
        XNI = XN(I)
        XKI = XK(I)
        XI = X(I)
        DO 1100 K = 1,N
          IF(I /= K) THEN
            FJAC(I,K) = XI/QS**2*(QNS/XNI/XKI)**XNI-(XI*XNI*XN(K)/QS)&
            & *QNS**(XNI-1.0)/(XNI*XKI)**XNI
          ELSE
            FJAC(I,K) = -XMC(JJ,J)/V(JJ,J)-1.0/QS*(QNS/XNI/XKI)**XNI&
            & +(XI/QS**2)*(QNS/XNI/XKI)**XNI-(XI*XNI**2/QS)&
            & *QNS**(XNI-1.0)/(XNI*XKI)**XNI
          ENDIF
!         WRITE(*.*) I,J,FJAC(I,K),'JAC'
!         FJAC(I,K)=FJAC(I,K)*0.5
1100      CONTINUE
1000    CONTINUE
!
      RETURN
      END
!
!     ****************************************
      REAL*8 FUNCTION FS(X)
!
      IMPLICIT DOUBLE PRECISION (A-H,O-Z)
      INTEGER JJ,J,KK
      REAL*8 MW(10),XMC(10,50)
!
      COMMON PAR(50),Q(10,3,50),CES(10,3,50),XK(10),XN(10),C0(10,10),&
          & XMC,V(10,50),ND(10),NC(10),SSQ,IPS(4),MW,NDSETS
!
      COMMON /BLOCK1/JJ,J,KK
!
      FS = C0(JJ,KK)-X*XMC(JJ,J)/V(JJ,J)-(X/XK(KK))**XN(KK)
!     WRITE(*,*) JJ,J,FS,'FSINGL'
!
      RETURN
      END
```

Appendix M

IAST Program

```
!       PROGRAM IAST PREDICTION
!
!       This program solves the Freundlich-type ideal adsorbed solution
!       theory for a closed multi-solute equilibrium system, given the
!       single solute isotherm parameters, the carbon dosage, the
!       solution volume.
!       Original code from Gillogly (1998),
!       Modified by Z. Yu
!       ***************************************************************
        include 'link_f90_static.h'
!   Defining variables
        IMPLICIT DOUBLE PRECISION (A-H,O-Z)
        INTEGER ITMAX, N, MAXFN
        REAL*8 ERRREL ! use for DNEQNJ, DNEQNF
        REAL*8 LSJAC, X(10), XGUESS(10), XG1(10), XG2(10)
        EXTERNAL FCNIAS, LSJAC, DNEQNJ, F, DNEQBJ, DZBREN
        INTEGER NC,ND,I
!   NC: number of components, ND: number of dosage
        DIMENSION Q(10,50),C(10,50)
!   Q: matrix of caculated surface loading, C: matrix of calculated liquid concentration
        REAL*8 MW(10),M(50),K(10),V(50),CO(10),XN(10)
!   M: the mass of the adsorbent (mg), V: the volume of the liquid (ml)
!   MW: molecular weight, CO: initial concentration (ug/l)
!   K, XN: Freundlich parameters
        DIMENSION IPARAM(6), RPARAM(5), XSCALE(2), FSCALE(2), FVEC(2)
        REAL*8 QQD(2),FF(2)
        CHARACTER CHAR(10)*80
!   CHAR(1): Dosage, CHAR(2): EBC, CHAR(3): name of target
        COMMON PAR(50)
        COMMON /B1/I
!
!       Open files and read input data
!
        OPEN (9, file = 'DATAIN.txt', status = 'old')
        OPEN (10, file = 'DATAOUT.txt')
        READ (9,*) NC, ND
        DO I = 1,ND
        READ (9,*) M(I), V(I)
        M(I) = M(I)/1000.0D0  ! change the unit mg to g
        V(I) = V(I)/1000.0D0  ! change the unit ml to l
        End DO
        DO I = 1,NC
          READ (9,"(A10)") CHAR(I)
          READ (9,*) K(I),XN(I),CO(I),MW(I)
          WRITE (*,*) K(I),XN(I),CO(I),MW(I)
          K(I) = K(I)*(1000.0/MW(I))*MW(I)**XN(I) ! change unit
          CO(I) = CO(I)/MW(I)  ! change into molarity
```

```
          XN(I) = 1/XN(I)  ! inverse 1/n
        End DO
!
!       Solve each dosage individually
!
        DO J = 1,ND
!       Put 'DATA.IN' into a one dimensional array
!
        IF (J==1) THEN
        DO I = 1,NC
        PAR(I) = K(I)
        PAR(10+I) = XN(I)
        PAR(20+I) = CO(I)
        End DO
        ENDIF
        PAR(30) = M(J)
        PAR(40) = V(J)
!
!       Calcutate initial guesses on surface loadings
!
        DO I = 1,NC
          QMAX2 = K(I)*CO(I)**(1.0/XN(I))
          IF(M(J)>0) THEN
                QMAX1 = CO(I)*V(J)/M(J)
          ELSE
                QMAX1 = QMAX2
          ENDIF
          IF(QMAX1<=QMAX2) THEN
                QMAX = QMAX1
          ELSE
                QMAX = QMAX2
          ENDIF
            QEST = QMAX+1.1
        QMIN = 0
        EABS = 0
        EREL = 0.002
        MAXFN = 100
!       F1 = F(QMIN)
!       F2 = F(QEST)
!       WRITE(*,*) J,I,F1,F2
         CALL DZBREN(F,EABS,EREL,QMIN,QEST,MAXFN)
!     find a zero of IAST function - first estimation of surface loading
        Q(I,J) = QEST
        End DO
!
!       second search for surface loading using opposite direction
!
        KMAX = 1000  ! set maximun iteration
        PD = 1.1
        MR = 1
!
        FMIN1 = 1.0D99
        NFLG = 0
```

```
          DO K2 = 1,KMAX
          QQD(2) = Q(2,J)/PD**(K2-1)
          FABS = 1.0D99
          DO K1 = 1,KMAX
        QQD(1) = Q(1,J)/PD**(K1-1)
        CALL FCNIAS(NC,QQD,FF)  ! setup IAST functions
          FABSB = FABS
!         FABS=DABS(FF(1))/CO(1)+DABS(FF(2))/CO(2)
          FABS = (FF(1)/CO(1))**2+(FF(2)/CO(2))**2
!         FABS=DABS(FF(1))+DABS(FF(2))
!           FABS=(FF(1))**2+(FF(2))**2
              IF(FABS<FMIN1 ) THEN
          FMIN1 = FABS
          XG1(1) = QQD(1)
          XG1(2) = QQD(2)
          K22 = K2
          K11 = K1
          NFLG = 1
        ELSE
          IF(FABS>FABSB) GO TO 205
        ENDIF
          End DO
205       IF(K2-K22>=MR.AND.NFLG==1) GO TO 204
          End DO
204       CONTINUE
!
!         GO TO 304
          FMIN2 = 1.0D99
          NFLG = 0
          DO K1 = 1,KMAX
          QQD(1) = Q(1,J)/PD**(K1-1)
          FABS = 1.0D99
          DO K2 = 1,KMAX
          QQD(2) = Q(2,J)/PD**(K2-1)
          CALL FCNIAS(NC,QQD,FF)  ! setup IAST functions
          FABSB = FABS
!         FABS=DABS(FF(1))/CO(1)+DABS(FF(2))/CO(2)
          FABS = (FF(1)/CO(1))**2+(FF(2)/CO(2))**2
!         FABS=DABS(FF(1))+DABS(FF(2))
!        FABS=(FF(1))**2+(FF(2))**2
              IF(FABS<FMIN2) THEN
          FMIN2 = FABS
          XG2(1) = QQD(1)
          XG2(2) = QQD(2)
          K11 = K1
          K22 = K2
          NFLG = 1
        ELSE
          IF(FABS>FABSB) GO TO 305
        ENDIF
            End Do
305       IF(K1-K11>=MR.AND.NFLG==1) GO TO 304
            End Do
```

```
304       CONTINUE
!
!     choose the better initial guess
!
          IF(FMIN1<FMIN2) THEN
          XGUESS(1) = XG1(1)
          XGUESS(2) = XG1(2)
          ELSE
          XGUESS(1) = XG2(1)
          XGUESS(2) = XG2(2)
          END IF
!
!         QS = Q(1,J)+Q(2,J)
!         QNS = PAR(11)*Q(I,J)+PAR(12)*Q(2,J)
!
!         DO 40 I = 1,NC
!           Q(I,J) = CO(I)/(M(J)/V(J)+(QNS/PAR(I)/PAR(10+I)**PAR(10+I)/QS)
!           XGUESS(I) = Q(I,J)
!           WRITE(*,*) QMAX, QEST
!40       CONTINUE
!
!         Enter the rest of parameters for DNEQNF
!
!         IF (J.EQ.1) THEN
!         READ (9,*) ITMAX,ERRREL
!         ENDIF
          N = NC
!
!         Call DNEQNJ to solve the system of equations
!
!         WRITE(*,*) J,(Q(I,J),I=1,NC)
!         WRITE(*,*) FMIN1,(XG1(I),I=1,NC)
!         WRITE(*,*) FMIN2,(XG2(I),I=1,NC)
          WRITE(*,*) J,(XGUESS(I),I=1,NC)
!
!         CALL DNEQNJ (FCNIAS, LSJAC, ERRREL, N, ITMAX, XGUESS, X, FNORM)
          IPARAM(1) = 0  ! initialization flag
          IPARAM(3) = 500  ! maximun number of iteration when calling DNEQBJ
          DO I = 1,N
          XSCALE(I) = 1
          FSCALE(I) = 1
          End Do
          CALL DNEQBJ(FCNIAS, LSJAC, N, XGUESS, XSCALE, FSCALE, IPARAM, RPARAM, X,
          FVEC)
!         CALL DNEQNF(FCNIAS, ERRREL, N, ITMAX, XGUESS, X, FNORM)
!
!         Store the calculated surface loadings back to Q(I,J)
          QS = 0.0
          QNS = 0.0
          DO I = 1,NC
          Q(I,J) = X(I)
          QS = QS+X(I)  ! sum of q
          QNS = QNS+PAR(10+I)* X(I)  ! sum of q*n
```

```
          End DO
          XMJ = M(J)*1000.0D0
          WRITE(*,*) J,XMJ,' a.c. dose'
          WRITE(*,*) J,(X(I),I=1,NC)
!
!         Calculate the Liquid phase concentrations
!
          DO I = 1,NC
          CD = CO(I)-M(J)/V(J)*Q(I,J)
          C(I,J) = Q(I,J)/QS*(QNS/PAR(I)/PAR(10+I))**PAR(10+I)
!           WRITE(*,*) CD,C(I,J)
          End Do
          End Do
!
!         change units for printing
!
          DO J = 1,ND
          DO I = 1,NC
          Q(I,J) = Q(I,J)*MW(I)/1000.D0  ! change unit from ug/g to mg/g
          C(I,J) = C(I,J)*MW(I)  ! unit ug/l
           End DO
          End DO
!
!         Print out results
!
          WRITE (10,200)
200       FORMAT (//,8X,'PROPERTIES of COMPONENTS')
          WRITE (10,210)
210       FORMAT (/,'COMPONENT',T15,'K (mg/g)(ug/L)**-1/n',T38,'1/n',T45,'CO(ug/l)',3X,'MW(dalton)'/)
          DO I = 1,NC
          XN(I) = 1.0D0/XN(I)  ! change back to 1/n
          CO(I) = CO(I)*MW(I)  ! unit ug/L
           K(I) = K(I)/(( 1000.0/MW(I))*MW(I)**XN(I))  ! change unit (ug/g)(ug/L)**-1/n to (mg/g)(ug/L)**-
          1/n
          WRITE (10,250) CHAR(I),K(I),XN(I),CO(I),MW(I)
250        FORMAT (1X,A10,T20,G11.5,T31,G11.5,T43,G11.5,T55,F10.3/)
          End Do
          WRITE (10,310)
310       FORMAT (//10X,'IAST PREDICTION')
          WRITE (10,320) CHAR(1), CHAR(2), CHAR(3)
320       FORMAT (///,1X,'DOSAGE'T20,A10,T42,A10,T65,A10)
          WRITE (10,330)
330       FORMAT (/2X,'(mg/L)',T14,'C ug/L',T24,'q mg/g',T35,'C ug/L',T45,'q mg/g',/)
          DO J = 1,ND
          M(J) = M(J)/V(J)* 1000.0D0  ! change unit
            WRITE (10,360) M(J),C(1,J),Q(1,J),C(2,J),Q(2,J)
          END DO
!       consider if component more than 2
          IF (NC>2) THEN
          WRITE (10,320) CHAR(4), CHAR(5), CHAR(6)
          WRITE (10,330)
          DO J = 1,ND
          WRITE (10,360) M(J),C(3,J),Q(3,J),C(4,J),Q(4,J)
```

```
          END DO
          ENDIF
!     consider if component more than 6
          IF (NC>6) THEN
          WRITE (10,320) CHAR(7), CHAR(8), CHAR(9)
          WRITE (10,330)
          DO J = 1,ND
          WRITE (10,360) M(J),C(7,J),Q(7,J),C(8,J),Q(8,J),C(9,J),Q(9,J)
          END DO
          ENDIF
360       FORMAT (F6.2,T12,G10.3,T21,G10.3,T32,F10.5,T42,F10.5,/)
!
          DO I = 1,N
            WRITE(*,*) PAR(I),PAR(I+10),PAR(I+20),PAR(30),PAR(40)
          End Do
          STOP
          END
!
!         ***************************************************************
!         subroutine FCNIAS
!         This subroutine will set up the IAST equations that wilL be solved
!         by the subroutine DNEQNF
!
!         SUBROUTINE FCNIAS(X,F,N)
          SUBROUTINE FCNIAS(N,X,F)
          IMPLICIT DOUBLE PRECISION (A-H,O-Z)
          INTEGER N,I
          REAL*8 X(N),F(N),CC
          COMMON PAR(50)
          CC = PAR(30)/PAR(40)
          QS = 0.0D0
          QNS = 0.0D0
          DO 1000 I = 1,N
          IF(X(I)<0) X(I) = 0
          QS = QS+X(I)
          QNS = QNS+PAR(10+I)*X(I)
1000      CONTINUE
          DO 1200 I = 1,N
!           WRITE(* ,*) I,X(I),PAR(I),PAR(10+I),PAR(20+1),CC,QS,QNS
            F(I) = PAR(20+I)-CC*X(I)-X(I)/QS*(QNS/PAR(10+I)/PAR(I))**PAR(10+I)
!           WRITE(*,*) I,F(I)
1200      CONTINUE
          RETURN
          END
!
!     ***************************************************************
!         subroutine LSJAC
!         This subroutine will calculate the Jacobian
!         SUBROUTINE LSJAC(N,X,FJAC)
          SUBROUTINE LSJAC(N,X,FJAC,LDFJAC)
          IMPLICIT DOUBLE PRECISION (A-H,O-Z)
          INTEGER N,I,J
!         REAL*8 X(N),FJAC(N,N),CC
```

```
      REAL*8 X(N),FJAC(LDFJAC,*),CC
      COMMON PAR(50)
      CC = PAR(30)/PAR(40)
      QS = 0.0
      QNS= 0.0
      DO 1000 I = 1,N
        IF(X(I)<0) X(I)=0
      QS = QS+X(I)
      QNS = QNS+PAR(10+I)*X(I)
1000  CONTINUE
      DO 1200 I = 1,N
        DO 1300 J = 1,N
!         WRITE(*,*) I,J
          IF(I/=J) THEN
       FJAC(I,J)=X(I)/QS**2*(QNS/PAR(10+I)/PAR(I))**PAR(10+I)&
                & -(X(I)*PAR(10+I)*PAR(10+J)/QS)&
                & *QNS**(PAR(10+I)-1.0)/(PAR(10+I)*PAR(I))**PAR(10+I)
      ELSE
       FJAC(I,J)=-CC-1.0/QS*(QNS/PAR(10+I)/PAR(I))**PAR(10+I)&
                & +(X(I)/QS**2)*(QNS/PAR(10+I)/PAR(I))**PAR(10+I)&
                & -(X(I)*PAR(10+I)**2/QS)&
                & *QNS**(PAR(10+I)-1.0)/(PAR(10+I)*PAR(I))**PAR(10+I)
      END IF
!       WRITE(*,*) I,J,FJAC(I,J)
!       FJAC(I,J) = FJAC(I,J)*10.0
1300    CONTINUE
1200  CONTINUE
      RETURN
      END
!
      REAL*8 FUNCTION F(X)
      IMPLICIT DOUBLE PRECISION (A-H,O-Z)
      INTEGER I
      COMMON PAR(50)
      COMMON /B1/I
      CC = PAR(30)/PAR(40)
      F = PAR(20+I)-CC*X-(X/PAR(I))** PAR(10+I)  ! IAST equation
!     WRITE(*,*) I,X,F,PAR(20+I)
      RETURN
      END
```

Appendix N

PSDM Program

```
!     PROGRAM PSDM
!
!     ============================================================
!     This program predict breakthrough profile, or estimate kinetic parameters
!     based on the pore and surface diffusion model with constant parameters
!     original code from Carter (1993),
!     modifed by Z. Yu
!     last modification on Nov. 02, 2006
!     ============================================================
!     -List of input viriables-
!
!     -Physical specifications of the GAC bed-
!     DIA column diameter (cm)
!     L bed length (cm)
!     WT mass of carbon in the bed (g)
!     RHOP apparent carbon density (g/cm^3)
!     RAD carbon particle radius (cm)
!     DE dispersion coeficient (cm^2/sec)
!     EPOR particle porosity
!
!     -Experimental conditions-
!     FLRT flow rate to column (ml/min)
!     NCOMP number of compounds(1 as of 5/92)
!     CBO ave. infl. conc. (ug/L) used for normalization
!     DT0 initial time (hr), usually 0
!     DTOL total run time (hr)
!     MW molecular weight of solute
!     FREEDL free liquid diffusivity of solute, used in tortuosity
!     NIN number of infl. data, NIN = 0 for influent=CBO
!     NDATA number of effluent concentration data points
!
!     -solute equilibrium and rate parameters-
!     XK Freundlich KF (ug/mg)*(L/ug)^(1/n)
!     XN Freundlich n
!     KF film transfer coefficient (cm/sec)
!     DS surface diffusivity (cm^2/sec)
!     TORT Tortuosity
!
!     -Numerical modelling specifications-
!     NSERCH search toggle; 0=off, 1=KF, 2=DS, 3=TORT, 4=KF&DS, 5=KF&TORT,
!        6=KF&DS&TORT
!     EPS convergence criteria
!     NTSTEP total number of time steps taken
!     NCOL toggle for printing out collocation points, 0=no
!     NM number of times time step is defined
!     TTIE times at which time steps is changed (hr)
!     TTINC what the time step is changed to at above times (hr)
```

```
!
!      --END OF LIST OF VARIABLES--
!
       INCLUDE 'link_f90_static.h'
       IMPLICIT DOUBLE PRECISION (A-H,O-Z)
       EXTERNAL F,DUMJAC
       DOUBLE PRECISION KF(2),L,MW
       CHARACTER(len=10) DUMMY
       DIMENSION PARVAL(3),PARINC(3),FMIN(2),YPRED(100)

       COMMON/BLOCKX/Y0(300),DS(2),XK(2),CBO(2),DE(2),BIS(2),BIP(2),QE(2),TIE(5),TINC(5),TDAT
       A(1000),DP(2),DGS(2),DGP(2),RWORK(100000),IWORK(320),TTIE(5),TTINC(5),TTDATA(1000)
       COMMON/BLOCKW/KF,L,MW,EPS,RHOP,EBED,EPOR,TAU,RAD,FLRT,AREA,FREEDL,TORT
       COMMON/BLOCKA/DGT,DG(2),ST(2),EDS(2),EDP(2),PE(2),AZ(18,18),BR(7,7),BZ(18,18),WZ(18),D
       (2)
       COMMON/BLOCKB/XNI(2),YM(2),XN(2)
       COMMON/BLOCKC/TP(900),CP(2,900),CD(2,1000),CINT(2,1000),CCD(2,1000)
       COMMON/BLOCKD/CIN(2,1000),TIN(1000),TTIN(1000),CCIN(2,1000)
       COMMON/BLOCKQ/WR(7),NC,N1,MC,NCOMP,NIN,NDATA,NM,NORDER
       COMMON/BLOCKL/ITOL,ITASK,ISTATE,IOPT,LRW,LIW,MF,NSTEPS
       COMMON/BLOCKS/DT0,DTOL,DOUT,DSTEP,D10STP
             COMMON/BLS/NSERCH,NFINSH,NCONF
!
!      -Set parameters for ODE solver-
       ITASK = 1
       ITOL = 1
       ISTATE = 1
       IOPT = 0
       LRW = 100000
       LIW = 320
       NSTEPS = 500
       MF = 22
!      -Read in data from data file-
!      -DUMMYs are to permit comments and blank lines in data file-
       OPEN(UNIT=4,FILE="PSDM_IN.TXT",STATUS="OLD")
       READ(4,*) DUMMY
       READ(4,*) DUMMY
       READ(4,*) DIA, DUMMY
       READ(4,*) L, DUMMY
       READ(4,*) WT, DUMMY
       READ(4,*) RHOP, DUMMY
       READ(4,*) FLRT, DUMMY
       READ(4,*) RAD, DUMMY
       READ(4,*) NCOMP, DUMMY
       READ(4,*) NSERCH, DUMMY
       READ(4,*) KF(1), PARINC(1), DUMMY
       READ(4,*) DS(1), PARINC(2), DUMMY
       READ(4,*) TORT, PARINC(3), DUMMY
       READ(4,*) DE(1), DUMMY
       READ(4,*) (XK(I),I=1,NCOMP), DUMMY
       READ(4,*) (XN(I),I=1,NCOMP), DUMMY
       READ(4,*) MW, DUMMY
       READ(4,*) (CBO(I), I=1,NCOMP), DUMMY
```

```
      READ(4,*) EPS, DUMMY
      READ(4,*) DT0, DUMMY
      READ(4,*) DTOL, DUMMY
      READ(4,*) NTSTEP, DUMMY
      READ(4,*) NM, DUMMY
      READ(4,*) NCOL, DUMMY
      READ(4,*) NDATA, DUMMY
      READ(4,*) NIN, DUMMY
      READ(4,*) EPOR, DUMMY
      READ(4,*) FREEDL, DUMMY
      READ(4,*) (TTIE(I), I=1,NM), DUMMY
      READ(4,*) (TTINC(I), I=1,NM), DUMMY
!
!      read in data and convert times to minutes and convert mass data to
!          molar data. Note that searches are all conducted with 10 timesteps,
!          while the final run is executed with the number specifed in the
!          datafile. For good influent data resolution, this number should
!          be on the order of NIN.
!
      DSTEP = DTOL/DBLE(NTSTEP)        !average time for each step
      D10STP = DTOL/10.D0*60.D0
      DT0 = DT0*60.D0
      DTOL = DTOL*60.D0
      DOUT = DTOL/1000.D0        !calculate the first point (time) output in prediction
      DSTEP = 1.01D0*(DSTEP*60.D0)
!
      DO I = 1,NM
       TTIE(I) = TTIE(I)*60.D0
       TTINC(I) = TTINC(I)*60.D0
      END DO
!
      READ(4,*) DUMMY,DUMMY
      DO J = 1,NIN
       READ(4,*) TTIN(J), (CCIN(I,J), I=1,NCOMP)
         DO I=1,NCOMP
          CCIN(I,J) = CCIN(I,J)/MW        !change to molarity
         END DO
       TTIN(J) = TTIN(J)*60.D0
      END DO
!
      READ(4,*) DUMMY,DUMMY
      DO J = 1,NDATA
       READ(4,*) TTDATA(J), (CCD(I,J), I=1,NCOMP)
       DO I=1,NCOMP
        CCD(I,J) = CCD(I,J)/MW
       END DO
       TTDATA(J) = TTDATA(J)*60.D0
      END DO
!
!      -read in collocadion constants-
!
      OPEN(UNIT=2, FILE="COLLOCATION_MATRICES_IN.TXT", STATUS='OLD')
      READ(2,*) DUMMY
```

```
      READ(2,*) NC        !radial collocation points
      READ(2,*) DUMMY
      READ(2,"(4F20.12)") (WR(I), I=1,NC)
      READ(2,*) DUMMY
      DO I=1,NC
        READ(2,"(4F20.12)") (BR(I,J), J=1,NC)
      END DO
      READ(2,*) DUMMY
      READ(2,*) MC        !axial collocation points
      READ(2,*) DUMMY
      READ(2,"(8F20.12)") (WZ(I), I=1,MC)
      READ(2,*) DUMMY
      DO I=1,MC
        READ(2,"(8F20.12)") (AZ(I,J), J=1,MC)
      END DO
      READ(2,*) DUMMY
      DO I=1,MC
        READ(2,"(8F20.12)") (BZ(I,J), J=1,MC)
      END DO
      NEQ = MC*(NC+1)*NCOMP       !total number of equations to be solved
!
!       -print out collocation constants if NCOL = 1
!       -otherwise skip to statement number 35
!
      OPEN(UNIT=7, FILE="PSDM_OUT.TXT", STATUS='REPLACE')
      IF(NCOL /= 1 ) GOTO 35
      WRITE(7,*) "RADIAL W VECTOR"
      WRITE(7,"(1X,4F20.12)") (WR(I), I=1,NC)
      WRITE(7,*) "RADIAL B MATRIX"
      DO I=1,NC
        WRITE(7,"(1X,4F20.12)") (BR(I,J), J=1,NC)
      END DO
      WRITE(7,*) "AXIAL W VECTOR"
      WRITE(7,"(1X,8F20.12)") (WZ(I), I=1,MC)
      WRITE(7,*) "AXIAL A MATRIX"
      DO I=1,MC
        WRITE(7,"(1X,8F20.12)") (AZ(I,J), J=1,MC)
      END DO
      WRITE(7,*) "AXIAL B MATRIX"
      DO I=1,MC
        WRITE(7,"(1X,8F20.12)") (BZ(I,J), J=1,MC)
      END DO
!
!       -calculate fixed bed parameters and convert mass isotherm parameters to
!             molar isotherm parameters
35    DO I=1,NCOMP
        CBO(I) = CBO(I)/MW
      END DO
      AREA = 3.141592654D0*DIA*DIA/4.0D0
      BEDVOL = L*AREA             !bed volume
      EBED = 1.0D0-WT/(BEDVOL*RHOP)       !bed porosity
      EBCT = BEDVOL/FLRT
      TAU = EBCT*60.0D0*EBED
```

```
      SF = 0.2454238D0*FLRT/AREA        !surface loading
      SF1 = FLRT/AREA
      XK(1) = XK(1)*MW**(XN(1)-1.D0)
!
!      -print out fixed bed parameters-
!
!      WRITE(*,103) NC,MC,NEQ,RAD,WT,RHOP,L,DIA,EBED,EPOR,SF,TAU,EBCT
      WRITE(7,103) NC,MC,NEQ,RAD,WT,RHOP,L,DIA,EBED,EPOR,SF1,TAU,EBCT
!
!      -Run rate parameter search or simulation-
      PARVAL(1) = KF(1)
      PARVAL(2) = DS(1)
      PARVAL(3) = TORT
      NFINSH = 0
      NCONF = 0
!
      IF(NSERCH /= 0) THEN
      SELECT CASE(NSERCH)
                  CASE(1,2,3)
                    NPARAM = 1
                  CASE(4,5)
                    NPARAM = 2
                  CASE(6)
                    NPARAM = 3
            END SELECT
            CALL SERCH(NPARAM,PARVAL,FMIN)
      ELSE
       NFINSH = 1
       CALL BTRUN(NDATA,3,PARVAL,YPRED)
      END IF
!
103    FORMAT(/ &
           &'NUMBER OF RADIAL COLLOCATION POINIS, NC = ',I15/&
           &'NUMBER OF AXIAL COLLOCATION POINTS, MC = ', I15/&
           &'TOTAL NO. OF DIFFERENTIAL EOUATIONS, NEQ = ',I15/&
           &'RADIUS OF ADSORBENT PARTICLE, RAD (CM) = ',D15.5/&
           &'MASS OF ADSORBENT, WT (GRAMS) = ',D15.5/&
           &'APPARENT PARTICLE DENSITY, RHOP (GRAM/CM**3) = ',D15.5/&
           &'LENGTH OF BED, L (CM) = ',D15.5/&
           &'DIAMETER OF BED, DIA (CM) = ',D15.5/&
           &'VOID FRACTION OF BED. EBED = ',D15.5/&
           &'VOID FRACTION OF ADSORBENT, EPOR = ',D15.5/&
           &'SURFACE LOADING RATE, SF (CM/MIN) = ',D15.5/&
           &'PACKED BED CONTACT TIME, TAU (SEC) = ',D15.5/&
           &'EMPTY BED CONTACT TIME, EBCT (MIN) = ',D15.5/)
      END
!
!      -END OF MAIN PROGRAM-
!
!
      SUBROUTINE BTRUN(MM,NN,PARAM,FF)
!      ----------------------------------------------------------------------
!      This subroutine performs one breakthrough run for a given set of
```

```
!             isotherm and kinetic parameters
!      ------------------------------------------------------------------------
!
      IMPLICIT DOUBLE PRECISION (A-H,O-Z)
      EXTERNAL F,DUMJAC
      DOUBLE PRECISION KF(2),L,MW
      DIMENSION PARAM(NN),FF(MM),FMIN(2),CDATA(1000),TPRED(200),PRED(200),RES(2,200)
      COMMON/BLOCKX/Y0(300),DS(2),XK(2),CBO(2),DE(2),BIS(2),BIP(2),QE(2),TIE(5),TINC(5),DATA
      (1000),DP(2),DGS(2),DGP(2),RWORK(100000),IWORK(320),TTIE(5),TTINC(5),TTDATA(1000)
      COMMON/BLOCKW/KF,L,MW,EPS,RHOP,EBED,EPOR,TAU,RAD,FLRT,AREA,FREEDL,TORT
      COMMON/BLOCKA/DGT,DG(2),ST(2),EDS(2),EDP(2),PE(2),AZ(18,18),BR(7,7),BZ(18,18),WZ(18),D
      (2)
      COMMON/BLOCKB/XNI(2),YM(2),XN(2)
      COMMON/BLOCKC/TP(900),CP(2,900),CD(2,1000),CINT(2,1000),CCD(2,1000)
      COMMON/BLOCKD/CIN(2,1000),TIN(1000),TTIN(1000),CCIN(2,1000)
      COMMON/BLOCKQ/WR(7),NC,N1,MC,NCOMP,NIN,NDATA,NM,NORDER
      COMMON/BLOCKL/ITOL,ITASK,ISTATE,IOPT,LRW,LIW,MF,NSTEPS
      COMMON/BLOCKS/DT0,DTOL,DOUT,DSTEP,D10STP
      COMMON/BLS/NSERCH,NFINSH,NCONF
!
            DP(1) = FREEDL/TORT
             IF (NFINSH == 0) THEN                ! Used for changing values in searching routine
             SELECT CASE(NSERCH)
             CASE(1)
               KF(1) = PARAM(1)
             CASE(2)
               DS(1) = PARAM(1)
!              IF (DS(1) < 0.D0) DS(1) = 0.D0
             CASE(3)
               DP(1) = FREEDL/PARAM(1)
             CASE(4)
               KF(1) = PARAM(1)
               DS(1) = PARAM(2)
!              IF (DS(1) < 0.D0) DS(1) = 0.D0
             CASE(5)
               KF(1) = PARAM(1)
               DP(1) = FREEDL/PARAM(2)
             CASE(6)
               KF(1) = PARAM(1)
               DS(1) = PARAM(2)
               DP(1) = FREEDL/PARAM(3)
!              IF (DS(1) < 0.D0) DS(1) = 0.D0
             END SELECT
             ELSE
             KF(1) = PARAM(1)
             DS(1) = PARAM(2)
             DP(1) = FREEDL/PARAM(3)
             END IF

!      Calculate ard print out dimensionless groups
!
       QTE = 0.0
       DO I=1,NCOMP
```

```
        D(I) = DS(I)/DP(I)
        QE(I) = XK(I)*CBO(I)**XN(I)
        QTE = QTE+QE(I)
        DGS(I) = (RHOP*QE(I)*(1.0D0-EBED)*1.0D6)/(EBED*CBO(I))
        DGP(I) = EPOR*(1.0D0-EBED)/EBED
        EDS(I) = DS(I)*DGS(I)*TAU/(RAD**2.0D0)
        EDP(I) = DP(I)*DGP(I)*TAU/(RAD**2.0D0)
        ST(I) = KF(I)*(1.0D0-EBED)*TAU/(EBED*RAD)
        BIS(I) = ST(I)/EDS(I)
        BIP(I) = ST(I)/EDP(I)
        PE(I) = L*FLRT/(60.0D0*AREA*EBED*DE(I))
        DG(I) = DGS(I)+DGP(I)
        XNI(I) = 1.0D0/XN(I)
!       WRITE(*,104) I,CBO(I),XK(I),XN(I),KF(I),ST(I),PE(I),D(I),DS(I),&
!              &DGS(I),BIS(I),EDS(I),DP(I),DGP(I),BIP(I),EDP(I)
         IF (NFINSH == 1 .AND. NCONF == 0) WRITE(7,104)&
         &I,CBO(I),XK(I),XN(I),KF(I),ST(I),PE(I),D(I),DS(I),&
             &DGS(I),BIS(I),EDS(I),DP(I),DGP(I),BIP(I),EDP(I)
       END DO
104          FORMAT(/'PARAMETERS FOR COMPONENT',I1/&
                & 4X,'INITIAL BULK CONCENTRATION, CBO (UMOL/L) = ',D15.5/&
                & 4X,'FREUNDICH ISOTHERM CONSTANT, XK (UMOL/MG)/(L/UMOL)**XN = ',D15.5/&
                & 4X,'FREUNDICH ISOTHERM EXPONENT, XN = ',D15.5/&
                & 4X,'FILM TRANSFER COEFFICIENT, KF (CM/SEC) = ',D15.5/&
                & 4X,'STANTON NUMBER, ST = ',D15.5/&
                & 4X,'PECLET NUMBER BASED ON COLUMN LENGTH, PE = ',D15.5/&
                & 4X,'SURFACE TO PORE DIFFUSIVITY RATIO, D = ',D15.5/&
                & 4X,'SURFACE DIFFUSION COEFFICIENT, DS (CM**2/SEC) = ',D15.5/&
                & 4X,'SURFACE SOLUTE DIST PARAMETER, DGS = ',D15.5/&
                & 4X,'SURFACE BIOT NUMBER, BIS = ',D15.5/&
                & 4X,'SUBFACE DIFFUSION MODULUS, EDS = ',D15.5/&
                & 4X,'PORE DIFFUSION COEFFICIENT, DP (CM**2/SEC) = ',D15.5/&
                & 4X,'PORE SOLUTE DIST PARAMETER, DGP = ',D15.5/&
                & 4X,'PORE BIOT NUMBER, BIP = ',D15.5/&
                & 4X,'PORE DIFFUSION MODULUS, EDP = ',D15.5/)
!          WRITE(*,106) (I,I,I=1,NCOMP)
          IF (NFINSH == 1 .AND. NCONF == 0) WRITE(7,106) (I,I,I=1,NCOMP)
!
106          FORMAT(/1X,'ITP',3X,'TIME(Hrs)',4X,'THROUGHPUT',2X,'REAL BED&
                  &VOL',2X,'BED VOL2',6X,'C(',I1,')/CO(',I1,')'/)
!
!      -total solute dist. parameter and bed volumes fed to column
!
       DGT = 0.0D0
       DO I=1,NCOMP
         DGT = DGT+DG(I)
       END DO
       BVF = EBED*DGT
!
!      -calculate equilibrium adsotbent phase concentration fractions
!      -this is used for IAST calculation
!
       DO I=1,NCOMP
```

```
        YM(I) = QE(I)/QTE
      END DO
!
!     -call subroutine ORTHOG to combine collocation constants and
!        dimensionless groups
!     -and to determine total number of differential equations being solved
!        for by LSODE
!
      CALL ORTHOG(N)
!
!     -convert independent variables to dimensionless form
!     -Note that TAU is in seconds, hence the 60 in TCONV to convert it back
!        to minutes
!
      TCONV = 60.0D0/(TAU*(DGT+1.0D0))
      IF (NFINSH == 1) THEN
        TSTEP = DSTEP*TCONV
      ELSE
        TSTEP = D10STP*TCONV
      ENDIF
      TTOL = DTOL*TCONV
      TOUT = DOUT*TCONV
      T0 = DT0*TCONV
      DO I=1,NM
        TIE(I) = TTIE(I)*TCONV
        TINC(I) = TTINC(I)*TCONV
      END DO
!
!     -convert influent and experimental data to dimensionless form
!
      DO J=1,NDATA
        TDATA(J) = TTDATA(J)*TCONV
        DO I=1,NCOMP
          CD(I,J) = CCD(I,J)/CBO(I)
        END DO
      END DO
      DO J=1,NIN
        TIN(J) = TTIN(J)*TCONV
        DO I=1,NCOMP
          CIN(I,J) = CCIN(I,J)/CBO(I)
        END DO
      END DO
!
!     -initialize dependent variables; Y0 is the solution vector
!      containing solution at all points in one long 1-D vector
!
      DO I=1,N
        Y0(I) = 0.0D0
      END DO
!
!     -Start of loop for calling LSODE to solve ODEs-
!
!     -Set parameters for ODE solver-
```

```
      ITASK = 1   ! output Y0 at TOUT by overshooting and interpolation
      ITOL = 1    ! scalar RTOL and scalar ATOL
      ISTATE = 1  ! set as the first call for the problem
      IOPT = 1    ! change of values allowed in IWORK and RWORK
      LRW = 100000
      LIW = 320
      MF = 22     ! backward differentiation formula method with modified Newton iteration with internally
supplied Jocobian
      IWORK(6) = 1000 ! MAX # OF INTEGRATION STEP
      ITP = 0
      MA = 1
      NMM = NM
65     ITP = ITP+1
      ISTATE = 1
      CALL DLSODE(F,N,Y0,T0,TOUT,ITOL,EPS,EPS,ITASK,ISTATE,IOPT,RWORK,&
                  &LRW,IWORK,LIW,DUMJAC,MF)
!
      DO I=1,NCOMP
!       Y0(N1*I) is the value of liquid-phase concentration at column exit
        CP(I,ITP) = Y0(N1*I)
        PRED(ITP) = CP(I,ITP)
!        the next line sets all negative solution oscillations to zero
        IF (PRED(ITP) < 0.D0) PRED(ITP) = 0.D0
      END DO
      TP(ITP) = TOUT
      TPRED(ITP) = TOUT/TCONV/60.D0        !change back to dimensional data
      BEDVOLAMOUNT = TPRED(ITP)*60/(TAU/60/EBED)
      DUMM = 0.0
      IF (NFINSH == 1 .AND. NCONF == 0) WRITE(7,107) ITP,TPRED(ITP),TOUT,&
                  &BEDVOLAMOUNT,TOUT*BVF,PRED(ITP)
107  FORMAT(1X,I3,2X,D10.5,3X,D10.5,2X,F10.1,5X,D10.5,1X,6(2X,D10.5))
!      WRITE(7,107) ITP,DUMM,TOUT,TOUT*BVF,(Y0(N1*I), I=1,NCOMP)
!107          FORMAT(1X,I3,2X,D10.5,3X,D10.5,2X,D10.5,1X,6(2X,D10.5))
!      IF (NFINSH == 1) WRITE(7,107) ITP,DUMM,DUMM,TPRED(ITP),(Y0(N1*I),I=1,NCOMP)
!
!      -calculate next time point to be input to LSODE
!
      IF (ITP < NSTEPS) THEN
        IF (TOUT < TTOL) THEN
          IF (NMM /= 0 .AND. TOUT >= TIE(MA)) THEN ! judge if time step changed in case of searching
routine
            TSTEP = TINC(MA)
            IF(MA == NMM) THEN
              NMM = 0
            ELSE
              MA = MA+1
            ENDIF
          ENDIF
          TOUT = TOUT+TSTEP
          IF ( TOUT > TTOL) TOUT = TTOL
          GO TO 65
        ENDIF
      ELSE
```

```
        IF ( TOUT < TTOL ) THEN
          WRITE(7,108) NSTEPS, DOUT
          GO TO 85
        ENDIF
      ENDIF
!
108       FORMAT('WARNING MORE STEPS ATTEMPTED THAN NSTEPS; TTOL NOT
REACH:'/6X,'NSTEPS = ',I3,', AND TOUT (MIN) = ',D10.4)
!
!         -END of loop calling LSODE for solving ODEs
!         -if experimental data is given call OBJFUN to determine FMIN for each component and print out
results
!
          IF(NDATA == 0) GOTO 85
          CALL OBJFUN (TDATA,ITP,FMIN)
!
          DO K = 1,NCOMP
            DO J = 1,NDATA
              RES(K,J) = CINT(K,J)-CD(K,J)
              FF(J) = RES(K,J)**2/DBLE(MM)
              WRITE(*,"(2X,'EXP VAL:',F10.5,2X,'PRED VAL:',F10.5,2X,'RESI:',F10.5)")
CD(K,J),CINT(K,J),RES(K,J)
            END DO
          END DO
!
   IF (NFINSH == 1 .AND. NCONF == 0) THEN
     WRITE(7,"(//15X,'MODEL PREDICTION VS DATA',/)")
            DO I=1,NCOMP
              WRITE(7,110) I
              DO J=1,NDATA
                TDATA(J) = TDATA(J)/TCONV/60.D0
                WRITE(7,111) TDATA(J),CD(I,J),CINT(I,J)
                CDATA(J) = CD(I,J)
              END DO
              WRITE(7,112) NDATA, FMIN(I)
            END DO
!           CALL PLOT(NDATA,TDATA,CDATA,ITP,TPRED,PRED)
            CCONV = CBO(1)*MW
!           CALL DOWNLD(NDATA,TDATA,CDATA,ITP,TPRED,PRED,CCONV)
          ENDIF
!
110     FORMAT(/7X,'RESULTS FOR COMPONENT',I3///7X,'TIME (Hrs)',5X,'C/C0(data)',4X,'C/C0(pred)')
111 FORMAT(5X,F10.2,5X,F10.5,5X,F10.5,6X)
112 FORMAT(/5X,'FMIN BASED ON',I4,2X,'DATA POINTS:',3X,'FMIN = ',F10.5)
85        RETURN
          END
!         -END OF SUBROUTINE BTRUN-
!
          SUBROUTINE ORTHOG ( N )
!
!         ---------------------------------------------------------------------------------------------------
!         This subroutine combines the collocation constants and the dimensionless groups calculded in
!         the main program to save computation time, but does not sum them.
```

```
!       ------------------------------------------------------------------------------------------------------
        IMPLICIT DOUBLE PRECISION (A-H,O-Z)
        COMMON/BLOCKA/DGT,DG(2),ST(2),EDS(2),EDP(2),PE(2),AZ(18,18),BR(7,7),BZ(18,18),WZ(1
8),D(2)
        COMMON/BLOCKE/STD(2),BEDS(2,7,7),DGI(2),WY(2,18),WA(18),AA(18),PBA(2,18,18),&
             &BEDP(2,7,7),ND,MD,MND,MNC,DG1
        COMMON/BLOCKQ/WR(7),NC,N1,MC,NCOMP,NIN,NDATA,NM,NORDER
        DIMENSION EDD(2),PEI(2),DG3(2)
!
!       calculation the total number of discretized equations
        ND = NC-1
        MD = MC-1
        MND = MC*ND
        MNC = MC+MND
        N1 = MNC+MC
        N = N1*NCOMP
        AMI = 1.0/AZ(MC,MC)
        DO I=1,NCOMP
          DG1 = 1.0D0+DGT
          DGI(I) = 1.0D0/DG(I)
          DG3(I) = 3.0D0*DG(I)
          STD(I) = ST(I)*DG1
          EDD(I) = DG1*DGI(I)
          PEI(I) = 1.0D0/PE(I)
          DO J=1,ND
            DO K=1,NC
              BEDS(I,J,K) = (EDS(I)+D(I)*EDP(I))*EDD(I)*BR(J,K)
            END DO
          END DO
          DO J=1,ND
            DO K=1,NC
              BEDP(I,J,K) = EDP(I)*(1.0D0-D(I))*EDD(I)*BR(J,K)
            END DO
          END DO
          DO J=2,MD
            DO K=1,MC
              PBA(I,J,K) = DG1*(PEI(I)*BZ(J,K)-AZ(J,K))
            END DO
          END DO
          DO J=1,MD
            WY(I,J) = DG3(I)*WZ(J)
          END DO
          WY(I,MC) = DG3(I)*WZ(MC)
        END DO
        DO J=1,MD
          AA(J) = AZ(MC,J)*AMI
          WA(J) = WZ(J)-WZ(MC)*AA(J)
        END DO
        RETURN
        END
!
!       END OF SUBROUTINE ORTHOG
!
```

```
!
      SUBROUTINE F( N,T,Y0,YDOT)
!
!     ------------------------------------------------------------------------------------------------------------
!     This subroutine is called by LSODE in the integration process.It receives the values of
!      the dependent variables from LSODE, i.e. Y0(T), and returns the values of the derivatives
!     of the dependent variables, i.e. YDOT(T).
!     LSODE then uses the derivatives to calculate Y0(T+ΔT) until total run time is met
!     ------------------------------------------------------------------------------------------------------------
!
      IMPLICIT DOUBLE PRECISION (A-H,O-Z)
      COMMON/BLOCKE/STD(2),BEDS(2,7,7),DGI(2),WY(2,18),WA(18),AA(18),&
            &PBA(2,18,18),BEDP(2,7,7),ND,MD,MND,MNC,DG1
      COMMON/BLOCKB/XNI(2),YM(2),XN(2)
      COMMON/BLOCKQ/WR(7),NC,N1,MC,NCOMP,NIN,NDATA,NM,NORDER
      DIMENSION Y0(N),YDOT(N),Z(2),CPORE(500),Q0(2),BB(7,18),CBS(2,18)
!
! ------Determine CPORE as single solute condition------
! Set parameters for calculating CPORE------
!
!     DOUBLE PRECISION FCPORE
!     EXTERNAL FCPORE
!     COMMON/BLOCKZ/YPARAM
!
!     ERRABS = 0.0
!     ERRREL = 1.0D-16
!
!     ICOUNT = 0
!     DO K = 1,MC
!       DO M = 1,NC
!         ICOUNT = ICOUNT+1
!         IF (Y0(ICOUNT) <= 0) THEN
!           CPORE(ICOUNT) = 0
!         ELSE
! Call DZBREN to calculate CPORE from Y0(I)
!      YPARAM = Y0(ICOUNT)
!      MAXFN = 1000
!      LOWBOUND = 0
!      HIGHBOUND = 1
!      CALL DZBREN(FCPORE,ERRABS,ERRREL,LOWBOUND,HIGHBOUND,MAXFN)
!      CPORE(ICOUNT) = HIGHBOUND
!    ENDIF
!    IF(M < NC-1) THEN
!           ICOUNT = (K-1)*ND+M
!         ELSE
!           ICOUNT = (K-1)+MND
!         ENDIF
!       END DO
!       ICOUNT = ND*K
!     END DO
! ------End of CPORE determination module(single solute)------
!
!     determine CPORE at each radial and axial position within adsorbent particle
```

```
!       using Ideal Adsorbed Solution Theory
!
        II = 0
        JJ = 0
        DO K = 1,MC
          DO M = 1,NC
            QTE = 0.0D0
            YT0 = 0.0D0
            DO I = 1,NCOMP
              II = II + 1
              Z(I) = YM(I)*Y0(II)
              QTE = QTE+Z(I)
              YT0 = YT0+XNI(I)*Z(I)
              II = II+N1-1
            END DO
            DO I = 1,NCOMP
              JJ = JJ+1
              IF( QTE <= 0.0D0 .OR. YT0 <= 0.0D0 ) THEN
                CPORE(JJ) = 0.0D0
              ELSE
                Z(I) = Z(I)/QTE
                Q0(I) = YT0*XN(I)/YM(I)
                IF (XNI(I)*DLOG10(Q0(I)) < -20.0D0 ) THEN
                  CPORE(JJ) = 0.0D0
                ELSE
                  CPORE(JJ) = Z(I)*Q0(I)**XNI(I)
                ENDIF
              ENDIF
              JJ = JJ+N1-1
            END DO
            IF(M < NC-1) THEN
              II = (K-1)*ND+M
              JJ = (K-1)*ND+M
            ELSE
              II = (K-1)+MND
              JJ = (K-1)+MND
            ENDIF
          END DO
          II = ND*K
          JJ = ND*K
        END DO
!       END IAST calculations
!
!       -Mark off key indices in solution vector Y0-
!       Solution vector Y0 contains in order:
!       1->MC: rad. coll. pnt1 @ each ax. pnt.
!       MC+1->2*MC: rad. coll. pnt2 @ each ax.pnt.
!       I*MC+1->(I+1)*MC: rad. coll. pnt.I+1 @ each ax. pnt.
!       ...etc...
!       (NC-1)*MC+1->NC*MC: RAD. COLL. PNT. @ each ax. pnt
!       NC*MC+1->(NC+1)*MC: fluid phase conc. @ each ax. pnt
!       Note that the last two series in vector Y0 are the boundary
!       between the solid surface (starting with Y0(III+1)) and the
```

```
!       bulk liquid phase (starting with Y0(III+1)).
!
        DO I=1,NCOMP
          II = (I-1)*N1
          III = II+MND
          IIII = III+MC
          IF(NIN == 0) THEN       !constant influent conc.
            CINFL = 1.0D0
          ELSE
            CINFL = CINF(I,T)     !changing influent conc.
        ENDIF
!
!       -sink term for fluid phase-
!       -gives CBS=St*(Cb-Cp(NC))-
          WDW = 0.0D0
          DO K = 1,MC
            WW = 0.0D0
            IF (CPORE(III+K) <= 0.0D0 ) THEN
              CBS(I,K) = STD(I)*Y0(IIII+K)
            ELSE
              CBS(I,K) = STD(I)*(Y0(IIII+K)-CPORE(III+K))
            ENDIF
!
!       -solid phase mass balance (excluding boundary)-
!       -gives dX(j,k,T)/dT
!
            KK = II+(K-1)*ND
            DO J=1,ND
              BB(J,K) = 0.0D0
              DO M=1,ND
                BB(J,K) = BB(J,K)+BEDS(I,J,M)*Y0(KK+M)+BEDP(I,J,M)*CPORE(KK+M)
              END DO
              BB(J,K) = BB(J,K)+BEDS(I,J,NC)*Y0(III+K)+BEDP(I,J,NC)*CPORE(III+K)
            END DO
            DO J=1,ND
              JJ = KK+J
              YDOT(JJ) = BB(J,K)
              WW = WW+WR(J)*YDOT(JJ)
            END DO
!
!       -Liquid-Solid Boundary Layer Mass Balance-
!       -gives dX(j=NC,k,T)/dT-
            YDOT(III+K) = (CBS(I,K)*DGI(I)-WW)/WR(NC)
            WW = WW+WR(NC)*YDOT(III+K)
            WDW = WDW+WY(I,K)*WW
          END DO
!
!       -Fluid phase mass balance (excluding boundaries)-
!
!       -gives dCb(k,T)/dT-
!
          WAC = 0.0D0
          AAC = 0.0D0
```

```
            DO K = 2,MD
              PC = 0.0D0
              DO J = 1,MC
                PC = PC+PBA(I,K,J)*Y0(IIII+J)
              END DO
              PC = PC-3.0D0*CBS(I,K)
              YDOT(IIII+K) = PC
              WAC = WAC+WA(K)*PC
              AAC = AAC+AA(K)*PC
            END DO
!
!       -Liquid Phase Mass Balance at Entrance of Column-
!       -use FUNCTION CINF to get influent concentration at each T-
!       -gives dCb(k=1,T)/dT-
!
              YDOT(IIII+1) = (DG1*(CINFL-Y0(IIII+MC))-WAC-WDW)/WA(1)
!
!       -Liquid Phase Mass Balance at Exit of Column-
!       - gives dCb(k=MC,T)/dT-
!
              YDOT(IIII+MC) = -AAC-AA(1)*YDOT(IIII+1)
!
            END DO
            RETURN
            END
!       -END OF SUBROUTINE F-
!
!
            SUBROUTINE OBJFUN(TD,NP,FMIN)
!
!       ----------------------------------------------------------------
!       This suboutine calculates the standard deviation between the predicted
!       concentrations and experimental data, if any is given. If no data is
!       given, this subroutine is ignored.
!       ----------------------------------------------------------------
!
            IMPLICIT DOUBLE PRECISION (A-H,O-Z)
            DIMENSION TD(1000),FMIN(2)
            COMMON/BLOCKC/TP(900),CP(2,900),CD(2,1000),CINT(2,1000),CCD(2,1000)
            COMMON/BLOCKQ/WR(7),NC,N1,MC,NCOMP,NIN,NDATA,NM,NORDER
!
            IF (NORDER == 1) WRITE(*,*) 'OBJFUN'
            DO K = 1,NCOMP
              FMIN(K) = 0.0D0
              NP1 = NP-1
              DO J = 1,NDATA
                DO I = 1,NP1
                  IF( TD(J) < TP(I) .OR. TD(J) > TP(I+1)) GO TO 4
                  CAP = CP(K,I)+((TD(J)-TP(I))/(TP(I+1)-TP(I)))*(CP(K,I+1)-CP(K,I))
!       -next line sets negative oscillations of solutbn to zero
                  IF(CAP < 0.D0) CAP = 0.D0
                  CINT(K,J) = CAP
                  FMIN(K) = FMIN(K)+(CAP-CD(K,J))**2
```

```
              GOTO 10
4             IF(TD(J) < TP(1)) THEN
                CAP = CD(K,J)
!               CAP = (TP(1)-TD(J))/(TP(1))*CP(K,1)
!               IF(CAP < 0.0D0) CAP = 0.0D0
                CINT(K,J) = CAP
                FMIN(K) = FMIN(K)+(CAP-CD(K,J))**2
              ENDIF
            END DO
10        END DO
          END DO
          DO K = 1,NCOMP
            FMIN(K) = DSQRT(FMIN(K)/FLOAT(NDATA))
          END DO
          RETURN
          END
!
!         -END OF SUBROUTINE OBJFUN-
!
!
          DOUBLE PRECISION FUNCTION FCPORE(X)
!
!  ---------------------------------------------------------------------
!  This function expresses dimensionless equilibrium equation, called by
!  D_ZREAL to calculate CPORE based on Y0 at each collocation point
!  ---------------------------------------------------------------------
    IMPLICIT DOUBLE PRECISION (A-H,O-Z)
    COMMON/BLOCKX/Y0(300),DS(2),XK(2),CBO(2),DE(2),BIS(2),BIP(2),QE(2),TIE(5),&
          &TINC(5),TDATA(1000),DP(2),DGS(2),DGP(2),RWORK(100000),IWORK(320),&
          &TTIE(5),TTINC(5),TTDATA(1000)
    COMMON/BLOCKA/DGT,DG(2),ST(2),EDS(2),EDP(2),PE(2),AZ(18,18),BR(7,7),&
          &BZ(18,18),WZ(18),D(2)
   COMMON/BLOCKB/XNI(2),YM(2),XN(2)
   COMMON/BLOCKZ/YPARAM
!
   APARAM = DGS(1)/DG(1)
   BPARAM = DGP(1)/DG(1)
   FCPORE = APARAM*X**XN(1)+BPARAM*X-YPARAM
!
   RETURN
   END
!
!
          FUNCTION CINF(I,T)
!
!         ---------------------------------------------------------------
!         This function calculates the influent concentration to the column for
!         each component at each time interval T. If no, varying influent data
!         is given, this subroutine is ignored.
!         ---------------------------------------------------------------
          IMPLICIT DOUBLE PRECISION (A-H,O-Z)
          COMMON/BLOCKD/CIN(2,1000),TIN(1000),TTIN(1000),CCIN(2,1000)
          COMMON/BLOCKQ/WR(7),NC,N1,MC,NCOMP,NIN,NDATA,NM,NORDER
```

```
!
!          IF(NORDER == 1) WRITE(*,*) 'CINF'
           IF(T <= TIN(1)) THEN
             CINF = CIN(I,1)
           ELSE IF (T >= TIN(NIN)) THEN
             CINF = CIN(I,NIN)
           ELSE
             J = 1
10           J = J+1
     IF (T>=TIN(J-1) .AND. T<=TIN(J)) THEN
       CINF = CIN(I,J-1)
!    The two lines below may be used to calibrate the contineous conc. increment situation
!            IF(T >= 1 .AND. T <= TIN(J)) THEN
!              CINF = CIN(I,J-1)+(CIN(I,J)-CIN(I,J-1))*(T-TIN(J-1))/(TIN(J)-TIN(J-1))
             ELSE IF (J < NIN) THEN
               GOTO 10
             ENDIF
           ENDIF
           RETURN
           END
!
!  -End of Function CINF-
!
!
           SUBROUTINE DUMJAC(N,T,Y,ML,MU,PD,NROWRD)
!
!  ----------------------------------------------------
!          This subroutine is a dummy subprogram used by LSODE
!  ----------------------------------------------------
!
           IMPLICIT DOUBLE PRECISION (A-H,O-Z)
           COMMON/BLOCKQ/WR(7),NC,N1,MC,NCOMP,NIN,NDATA,NM,NORDER
           RETURN
           END
!
!          -END OF SUBROUTINE DUMJAC
!
!
           SUBROUTINE SERCH(NPARAM,PARVAL,FMIN)
!
!          ------------------------------------------------------------------------
!          This subroutine searches on given rate Parameters using external subroutine
!          DNULSF from IMSL. The subroutine then call the subroutine CALCONF to determine
!          the confidence intervals corresponding to the best estimated parameters.
!          ------------------------------------------------------------------------
!
           IMPLICIT DOUBLE PRECISION (A-H,O-Z)
           DIMENSION PARVAL(3),FMIN(2),BOUNDHIGH(3),BOUNDLOW(3)
           DIMENSION X(NPARAM),XGUESS(NPARAM),XSCALE(NPARAM),&
                     &FSCALE(100),IPARAM(6),RPARAM(7),FVEC(100),FJAC(100),FFINAL(100)
           COMMON/BLOCKQ/WR(7),NC,N1,MC,NCOMP,NIN,NDATA,NM,NORDER
           COMMON/BLS/NSERCH,NFINSH,NCONF
           EXTERNAL BTRUN,DU4LSF
```

```
!
!       Set input parameters for DUNLSF
        N = NPARAM
        M = NDATA
        LDFJAC = M
        SELECT CASE(NSERCH)
          CASE(1)
            XGUESS(1) = PARVAL(1)
          CASE(2)
            XGUESS(1) = PARVAL(2)
          CASE(3)
            XGUESS(1) = PARVAL(3)
          CASE(4)
            XGUESS(1) = PARVAL(1)
            XGUESS(2) = PARVAL(2)
          CASE(5)
            XGUESS(1) = PARVAL(1)
            XGUESS(2) = PARVAL(3)
          CASE(6)
            XGUESS(1) = PARVAL(1)
            XGUESS(2) = PARVAL(2)
            XGUESS(3) = PARVAL(3)
        END SELECT
        DO I = 1,N
          XSCALE(I) = 1.0
        END DO
        DO I = 1,M
          FSCALE = 1.0
        END DO
!
        CALL DU4LSF(IPARAM,RPARAM)
        IPARAM(3) = 500
        IPARAM(4) = 3000
        RPARAM(1) = 1.0D-64
        RPARAM(4) = 1.0D-64
        RPARAM(2) = 1.0D-64
        RPARAM(3) = 1.0D-64
!
!       End of setting parameters
!       Start searching parameters
!
        CALL
DUNLSF(BTRUN,M,N,XGUESS,XSCALE,FSCALE,IPARAM,RPARAM,X,FVEC,FJAC,LDFJAC)
!
!  Transfer the estimated parameter(s) into the parameters array
        SELECT CASE(NSERCH)
          CASE(1)
            PARVAL(1) = X(1)
          CASE(2)
            PARVAL(2) = X(1)
          CASE(3)
            PARVAL(3) = X(1)
          CASE(4)
```

```
            PARVAL(1) = X(1)
            PARVAL(2) = X(2)
          CASE(5)
            PARVAL(1) = X(1)
            PARVAL(3) = X(2)
          CASE(6)
            PARVAL(1) = X(1)
            PARVAL(2) = X(2)
            PARVAL(3) = X(3)
        END SELECT
        NFINSH = 1
        CALL BTRUN(M,3,PARVAL,FFINAL)
!
!  Calculate confidence intervals for the estimated parameters
!
  NCONF = 1   ! TURN ON CONFIDENCE INTERVAL SEARCH, TURN OFF PRINT MORE IMMI
DATA
  NPCOUNT = 0
  DO I = 1,3
   BOUNDHIGH(I) = 0.D0
   BOUNDLOW(I) = 0.D0
  END DO
!  Set the parameter to be calculated CI
500 SELECT CASE(NSERCH)
    CASE(1)
     IPCOUNT = 1
    CASE(2)
     IPCOUNT = 2
    CASE(3)
     IPCOUNT = 3
    CASE(4)
     NPCOUNT = NPCOUNT+1
     IF (NPCOUNT == 1) THEN
      IPCOUNT = 1
     ELSEIF (NPCOUNT == 2) THEN
      IPCOUNT = 2
     ELSE
      GOTO 600
     ENDIF
    CASE(5)
     NPCOUNT = NPCOUNT+1
     IF (NPCOUNT == 1) THEN
      IPCOUNT = 1
     ELSEIF (NPCOUNT == 2) THEN
      IPCOUNT = 3
     ELSE
      GOTO 600
     ENDIF
    CASE(6)
     NPCOUNT = NPCOUNT+1
     IF (NPCOUNT <= 3) THEN
      IPCOUNT = NPCOUNT
     ELSE
```

```
        GOTO 600
       ENDIF
   END SELECT
!
   CALL CALCONF(M,N,PARVAL,IPCOUNT,BHIGH,BLOW,FFINAL)
   BOUNDHIGH(IPCOUNT) = BHIGH
   BOUNDLOW(IPCOUNT) = BLOW
   IF (NSERCH >= 4) GOTO 500
!
600 DO I = 1,3
     WRITE(7,601) I,BOUNDLOW(I),BOUNDHIGH(I)
   END DO
!
601 FORMAT('LOWBOUND AND HIGHBOUND OF PARAMETER',I1,1X,'ARE:',1X,D10.5,2X,D10.5)
!
          RETURN
          END
!
!         -END OF SUBROUTINE SERCH-
!
!
   SUBROUTINE CALCONF(M,N,PARVAL,IPCOUNT,BHIGH,BLOW,FFINAL)
!
!  ---------------------------------------------------------------------------------------
!  The program is for calculating confidence interval for single parameter
!  ---------------------------------------------------------------------------------------
!
   IMPLICIT DOUBLE PRECISION (A-H,O-Z)
   DIMENSION PARVAL(3),FFINAL(100),XMSR(100),XPARVAL(3)
   COMMON/BLOCKQ/WR(7),NC,N1,MC,NCOMP,NIN,NDATA,NM,NORDER
   COMMON/BLS/NSERCH,NFINSH,NCONF
!
!  Calculate the minimun mean sum of squared residuals, MSSR
   SSMIN = 0.D0
   DO I = 1,M
     SSMIN = SSMIN+FFINAL(I)
   END DO
!  Calculate the critical MSSR
   WRITE(*,"('INPUT 95% CONF LEVEL F VALUE AT P=',I3,1X,'AND N=',I3)") N,M
   READ(*,*) FVAL
   SSCRI = SSMIN*(1+FVAL*DBLE(N)/DBLE(M-N))
!  Search for confidence edge points
   XSTEP = 100.D0  !Search steps
   NCOUNT = 0      !Search switcher
   NDIREC = 1      !Search direction
210 J = 0
   IF (NCOUNT == 1) NDIREC = -1
   SSTRY = 0.D0
   DO K = 1,3
     XPARVAL(K) = PARVAL(K)
   END DO
   NCOUNT = NCOUNT+1
200 IF (J <= 200 .AND. SSTRY < SSCRI) THEN
```

```
      J = J+1
      XPARVAL(IPCOUNT) = PARVAL(IPCOUNT)*(1.D0+DBLE(NDIREC*J)/XSTEP)
              CALL BTRUN(M,3,XPARVAL,XMSR)
              SSTRY = 0.D0
              DO I = 1,M
                SSTRY = SSTRY+XMSR(I)
              END DO
              GOTO 200
            ELSEIF (J > 200) THEN
      WRITE(*,*) "SEARCH EXCEEDES PRESET BOUNDS!!"
      IF (NCOUNT == 1) THEN
        BHIGH = 0.D0
        GOTO 210
      ELSE
        BLOW = 0.D0
      ENDIF
    ELSEIF (NCOUNT == 1) THEN
      BHIGH = XPARVAL(IPCOUNT)
      GOTO 210
    ELSE
      BLOW = XPARVAL(IPCOUNT)
    ENDIF
!
    RETURN
    END
!   End of subroutine CALCONF
```